FLOOD RISK ASSESSMENT OF OFU RIVER CATCHMENT IN NIGERIA

BY

Meshach IleanwaAlfa
B. Eng. (ABU, 2008), PGDE (UniMaid, 2009), M.Sc. (ABU, 2013)
P14EGWR9002

A THESIS SUBMITTED TO THE SCHOOL OF POSTGRADUATE STUDIES, AHMADU BELLO UNIVERSITY, ZARIA NIGERIA

IN PARTIAL FULFILMENT OF THE REQUIRMENTS FOR THE AWARD OF DOCTOR OF PHILOSOPHY DEGREE IN WATER RESOURCES AND ENVIRONMENTAL ENGINEERING

DEPARTMENT OF WATER RESOURCES AND ENVIRONMENTAL ENGINEERING,
AHMADU BELLO UNIVERSITY, ZARIA
NIGERIA

June, 2018

DECLARATION

I declare that the work in the thesis entitled "Flood Risk Assessment of Ofu River Catchment in Nigeria" has been carried out by me in the Department of Water Resources and Environmental Engineering. The information derived from literature has been duly acknowledged in the text and a list of references provided. No part of this thesis was previously presented for another degree or diploma at this or any other Institution.

Meshach Ileanwa ALFA	_____	_____
Name of Student	Signature	Date

CERTIFICATION

This Thesis entitled “Flood Risk Assessment of Ofu River Catchment in Nigeria” by Meshach Ileanwa ALFA meets the regulations governing the award of the degree of Doctor of Philosophy in Water Resources and Environmental Engineering of Ahmadu Bello University, and is approved for its contribution to knowledge and literary presentation.

Prof. D. B. Adie	_____	_____
Chairman, Supervisory Committee	Signature	Date
Dr. M. A. Ajibike	_____	_____
Member, Supervisory committee	Signature	Date
Prof. O. J. Mudiare	_____	_____
Member, Supervisory committee	Signature	Date
Prof. A. Ismail	_____	
_____		
Head of Department	Signature	Date
Prof. S. Z. Abubakar	_____	_____
Dean, School of Postgraduate Studies	Signature	Date

DEDICATION

To the loving memory of my mother, Madam Mary Alfa and my mother-in-law, Mrs Grace Mayomi Jegede who joined the cloud of witnesses just before this became a reality.

ACKNOWLEDGMENTS

My greatest gratitude goes to the Almighty God, who has demonstrated again that He is my Glory and the 'Lifter up' of my head. Once again I reaffirm my eternal allegiance to You and my commitment to see Your Kingdom come and Your Will be done on earth as it is in heaven.

I humbly acknowledge and sincerely appreciate my supervisory committee-the trio of Prof. D. B. Adie, Dr. M. A. Ajibike and Professor O. J. Mudiare for their thoroughness, dedication, flexibility yet very firm supervision of this work as well as the moral support they provided during this study.

I wish to express my gratitude and appreciation to Apostle Joshua Selman Nimmak for the spiritual covering I enjoyed throughout this study. You have indeed been a great father, mentor, pastor and friend. I love, honour and greatly celebrate you sir. I want to also specially appreciate Professor and Mrs Emmy Unuja Idegu who have been of great support and inspiration to me throughout this study.

My special appreciation goes to the Vice Chancellor of the University of Jos for the approval and sponsorship of this study. I also appreciate the Dean of the Faculty of Engineering, University of Jos, Prof. Stephen J. Mallo for his consistent and tireless motivation throughout this work and all the staff of the Department of Civil Engineering, University Jos for the support I enjoyed throughout this study.

I also thank my Head of Department (Professor Abubakar Ismail), Professor C. A. Okuofu, Professor J. A. Otun for their in-time academic support, encouragement, patience, understanding and push I received during this study. I am grateful to Dr

Sunday Bamidele Igboro for the significant contributions and academic support in all ramifications towards the successful completion of this study. I also acknowledge the immense support and encouragement of Engr. Sani Ismail, Dr. Babatude Adeogun, Dr. (Mrs.) F. B. Ibrahim and all the members of staff of the Department of Water Resources and Environmental Engineering.

Now my words have failed me to appreciate my priceless Jewel, my treasure of inestimable value-Annie Opeyemi Meshach-Alfa for standing by me. I will need to write an entire thesis to attempt to appreciate your sacrifice, love, support and prayers for the success of this study. You are indeed the best thing that happened to me after Christ. I love you eternally. I specially appreciate my dear sons, Jedidiah Ojimaojo Meshach-Alfa and David Omokorede Meshach-Alfa for their sacrifice to see that Daddy completes this study.

I specially appreciate my research assistants - Achema Alfa and Maneju Wada and my Enumerators – Enemali Alfa, Richardson Edimeh, Hope Enemakwu, Iye Okekwu and Isah Chubiyojo for all their effort on the field to make this work a reality. Finally, I will like to appreciate Engr. Ashara, Mr Paul and Mr Aliyu for the GIS tutorials and others too numerous to mention that contributed in one way or the other towards the success of this work, I thank you all.

ABSTRACT

The aim of this study was to carry out a flood risk assessment for Ofu River Catchment in Nigeria. Shuttle Radar Topographic Mission Digital Elevation Model (SRTM DEM) and River Map of Africa were used to delineate the catchment boundaries in ArcGIS 10.2.2 coupled with ArcHydro and HEC-GeoHMS extensions while the stream ordering was done using the spatial analyst hydrology tool in ArcGIS 10.2.2. Stage and discharge measured from February, 2016 to January, 2017 were used to develop the rating curve at Oforachi Hydrometric Station. Key Informant Interviews and household surveys were carried out to ascertain the opinion of the people on flood occurrence and their perceived causes. Assessment of the rainfall characteristics of the catchment was also carried out using the 35 years radar data corrected with data obtained from the Nigeria Meteorological Agency (NiMet). The soil map of the study area was extracted from the digital soil map of the world while Atterberg limits, sieve analysis and infiltration tests were carried out at Oforachi as a confirmatory test. The percentage loss in volume and surface area and loss in flow depth of Ofu River at Oforachi between 2000 and 2011 were also carried out using GIS tools in ArcGIS 10.2.2 while the loss rate was used to estimate the flow depth for 2016. The annual sediment load of Ofu River at Oforachi Hydrometric Station was also estimated. The terrain elevation, slope and proximity were also measured via field measurement and GIS analysis. The landuse/ landcover (LULC) changes between 1987 and 2016 were also examined using the LULC map for 1987, 2001 and 2016. The runoff curve numbers for these years were also estimated. Synthetic stream flow for 1974 to 2016 was generated using the modified Thomas-Fierring's model. Peak discharge for the catchment was also estimated using the Natural Resource Conservation Services Curve Number method and the rational method. The average values for the three were compared with that from field measurement. Flood frequency

analysis was carried out on the 62 years synthetic discharge values (1955-2016) and peak discharge values for 2, 5, 10, 25, 50, 100 and 200 years return periods were estimated. The extent of flood inundation was estimated first by Multi-criteria evaluation in ArcGIS and secondly by hydraulic modelling in HEC-RAS and HEC-GeoRAS/ArcGIS using hydrologically generated stream flow. Flood Hazard, vulnerability and risk analysis were carried out in ArcGIS 10.2.2. The resulted show that Ofu River Catchment covers a total drainage area of 1604.56 km^2 covering 27.02 % of Dekina, 23.48 % of Ofu, 14.06 % of Igalamela/Odolu, 9.25 % of Idah and 14.04 % of Ibaji Local Government Areas in Kogi State and 0.80 % of Uzo-Uwani Local Government Area in Enugu State, Nigeria. A rating curve equation, $Q = 15.54096(H - 55.43192)^{0.69051}$was developed. Ofu River has lost 6.90 m of its flow depth at Oforachi between 2000 and 2016 at a rate of 0.431 m per year which is the major cause of flood within the catchment. The annual sediment load of the river at Oforachi station is 66,824.73 x 10^3 kg. The runoff curve numbers for 1987, 2001 and 2016 were 61.8, 63.3 and 62.8, respectively showing no significant change. The modified Thomas-Fierring Model was effectively used to generate 12 months synthtic stream flow data for Ofu river from 1974 to 2016. The peak discharge values for 2, 5, 10, 25, 50, 100 and 200 years return periods were 444.57 m^3/s, 499.23 m^3/s, 530.35 m^3/s, 565.61 m^3/s, 589.59 m^3/s, 611.96 m^3/s and 633.25 m^3/s, respectively while the peak discharge values for 1995 and 2000 flood scenarios were 448.89 m^3/s and 446.46 m^3/s, respectively. Three hazard, vulnerability and risk zones-High, moderate and low were identified which have put several elements at varying degrees of risk in 1995 and 2000 flood scenarios and other flood events of 100 years and 200-year return periods. An assessment of the open defecation status of Oforachi, the most developed of the communities within Ofu River Floodplain shows that 50.81 % of the population still

defecate in the open field which will pose a serious health risk to the populace in the event of flood, since Ofu River is a major source of household drinking water in the community. The study demonstrated that Modified Thomas-Fierring's model, Remote Sensing, Geographic Information System, HEC-RAS and HEC-GeoRAS could be effective tools for flood risk assessment. Efforts should be made by the government to urgently dredge Ofu River to provide more discharge-carrying capacity.

TABLE OF CONTENTS

Title page - - - - - - - - - i

Declaration - - - - - - - - - ii

Certification - - - - - - - - - iii

Dedication - - - - - - - - - iv

Acknowledgement - - - - - - - - - v

Abstract - - - - - - - - - vii

Table of Contents - - - - - - - - - x

List of Tables - - - - - - - - - xv

List of Figures - - - - - - - - - xix

List of Plates - - - - - - - - - xxiii

List of Appendices - - - - - - - - - xxiv

CHAPTER ONE: INTRODUCTION

1.1 Background of the Study - - - - - - 1

1.2 Statement of the Research Problem - - - - - 5

1.3 Justification of the Study - - - - - - 7

1.4 Aim and Objectives - - - - - - - 8

1.5 Scope of Research - - - - - - - 8

1.6 Limitations of the Research - - - - - - 9

1.7 Description of Study Area - - - - - - 10

1.7.1 Location - - - - - - - - 10

1.7.2 Climate - - - - - - - - 10

1.7.3 Geology - - - - - - - - 12

1.7.4 Topography - - - - - - - - 12

1.7.5 Hydrology - - - - - - - - 12

1.7.6 Agriculture - - - - - - - - 13

CHAPTER TWO: CONCEPTUAL AND THEORETICAL FRAMEWORK AND LITERATURE REVIEW

2.1 Introduction - - - - - - - - 14

2.2 Conceptual Framework - - - - - - 14

2.2.1 Concept of Flood - - - - - - - 14

2.2.2 Concept of Runoff - - - - - - - 25

2.3 Morphologic Characteristics of a River Basin - - - 29

2.3.1 Delineation of watershed boundaries - - - - - 31

2.3.2 Determination of the morphological characteristics of a watershed - 36

2.4 Stream Gauging and Development of Rating Curve - - - 45

2.4.1 Stage Measurement - - - - - - - 46

2.4.2 Discharge Measurement - - - - - - 47

2.4.3 Development, Fitting and Extension of Rating Curve - - 50

2.5 Determination of Soil Characteristics - - - - - 53

2.5.1 Remotely Sensed Soil Data - - - - - - 53

2.5.2 Field Determination of Soil Characteristics - - - - 54

2.6 Evaluation of Landuse/Landcover Characteristics - - - 58

2.6.1 Image Classification - - - - - - - 58

2.6.2 Land Cover Indices - - - - - - - 60

2.7 Runoff Estimation - - - - - - - 62

2.7.1 Extension of Runoff Records using Thomas-Fiering's Model - 62

2.7.2 Rainfall-Runoff Modelling for Unguaged Catchment using Remote Sensing and GIS - - - - - - 64

2.8 Rainfall Data - - - - - - - - 73

2.8.1 Measurement of Rainfall - - - - - - 73

2.8.2 Rainfall Interpolation - - - - - - - 74

2.8.3 Catchment Mean Aerial Rainfall Estimation - - - - 77

2.8.4 Presentation of Rainfall Data - - - - - - 78

2.9 Flood Frequency Analysis - - - - - - 78

2.10 Field Survey and Statistical Analysis - - - - - 80

2.10.1 Descriptive and Inferential Statistics - - - - 80

2.10.2 Population and Sample - - - - - - 81

2.10.3 Sampling Techniques - - - - - - 81

2.11 The Concept of Disaster - - - - - - 83

2.11.1 Flood Hazard and Flood Hazard Assessment - - - 83

2.11.2 Flood Vulnerability and Flood Vulnerability Assessment - - 84

2.11.3 Flood Risk and Flood Risk Assessment - - - - 86

2.11.4 Disaster Risk Management and Disaster Risk Reduction - - 87

2.11.5 Flood Risk Mapping - - - - - - - 88

2.12 Multi Criteria Evaluation in Risk Assessment - - - 90

2.13 Population Estimation- - - - - - - 93

2.14 Application of Remote Sensing and Geographic Information System in Flood Risk Studies - - - - - - 94

2.14.1 Digital Elevation Models used for Flood risk Mapping - - 96

2.14.2 Satellite Images used for Flood Inundation Mapping - - 99

2.15 Software used in Flood Inundation Modelling - - - 101

2.15.1 Hydraulic models used for Flood Inundation Mapping - - 103

2.15.2 Description of Selected Models used in this Study - - - 104

CHAPTER THREE: MATERIALS AND METHODS

3.1 Materials - - - - - - - - 114

3.1.1 Types and Sources of Data - - - - - - 114

3.1.2 Hardware and Software - - - - - - 117

3.2 Methods - - - - - - - - 119

3.2.1 Determination of Morphologic Characteristics of Ofu River Catchment 119

3.2.2 Development of Stage-Discharge Rating Curve for Ofu River - 133

3.2.3 Methods of Identification of Flood Causative Factors in Ofu River Catchment - - - - - - 143

3.2.4 Method of Flood Frequency Analysis- - - - - 170

3.2.5 Production of Flood Inundation Extent and Hazard Map - - 182

3.2.6 Method of Flood Risk Analysis - - - - - 199

CHAPTER FOUR: RESULTS AND DISCUSSION

4.1 Morphologic Analysis of Ofu River Catchment - - - 211

4.1.1 Delineation of Ofu River Catchment Boundaries - - - 211

4.1.2 Morphologic characteristics of Ofu River Catchment - - 211

4.2 Stage-Discharge Rating Curve for Ofu River- - - - 221

4.2.1 Results of the Observation of Ofu River Stage at Oforachi Hydrometric Station - - - - - 221

4.2.2 Ofu River Discharge Measurement Values at Oforachi Hydrometric station - - - - - 221

4.2.3 Results of the Development, fitting and Extension of Ofu River Rating Curve at Oforachi Hydrometric Station - - 223

4.3 Flood Causative Factors - - - - - - 227

4.3.1 Knowledge of Flood Causes within the Catchment Communities - 227

4.3.2 Rainfall Characteristics of Oforachi Catchment (Meteorological Factors) 232

4.3.3 Geomorphologic Flood Causative Factors - - - - 235

4.3.4 Land use/Settlement Causative Factors - - - - 250

4.3.5 Respective Associations of Elevation, Proximity and Slope with Flood Occurrence - - - - - 258

4.4 Flood Frequency Analysis - - - - - - 259

4.4.1 Peak Runoff - - - - - - - 259

4.4.2 Peak Discharge forecast using Log-Pearson Type III Distribution - 264

4.5 Flood Inundation Extent and Hazard Map - - - - 266

4.5.1 Flood Hazard Map by Thematic Integration of Causative Factors (Multi-Criteria Evaluation) in ArcGIS - - - - 266

4.5.2 Hydraulic Modelling for Development of Flood Inundation and Hazard Maps - - - - - 280

4.5.3 Results of the Comparison of Extent of Flood Inundation from both Methods - - - - - 287

4.6 Flood Risk Analysis - - - - - - - 288

4.6.1 Flood Hazard Assessment - - - - - - 288

4.6.2 Flood Vulnerability Assessment - - - - - 292

4.6.3 Derivation of Population Vulnerability Weights - - - 297

4.6.4 Flood Risk Assessment - - - - - - 305

4.7 Strategic Plan for Ofu River Catchment Flood Management - - 328

CHAPTER FIVE: SUMMARY, CONCLUSION AND RECOMMENDATIONS

5.1 Summary - - - - - - - - 330

5.2 Conclusion - - - - - - - - 333

5.3 Recommendations - - - - - - - 335

REFERENCES - - - - - - - - 337

APPENDICES - - - - - - - - 356

LIST OF TABLES

Table 2.1: Chronicles of Historical Flood Events in Nigeria between 1953 and 2012 - - - - - - - 16

Table 2.2: Guidelines for deciding Number of sub-sections of River for Discharge Measurement - - - - 49

Table 2.3: Band Characteristics for Landsat 5, 7 and 8 Imageries - - 59

Table 2.4: Categories of Antecedent Moisture Content - - - 66

Table 2.5: Classification of Hydrological Soil Groups - - - 67

Table 2.6: Comparison of Spatial Interpolation Techniques - - 76

Table 2.7: Correlation between risk, hazard and vulnerability - - 87

Table 3.1: Properties of the Topographic Maps Used in the Study - - 114

Table 3.2: Historical Mean Annual Rainfall Data for Ofu River Catchment Neighbouring Stations - - - - - - 115

Table 3.3: Historical Mean Discharge Record for Ofu River at Oforachi - 116

Table 3.4: Properties of Satellite Data and Relevance - - - 116

Table 3.5: Methods of Estimation of Derived Areal Morphologic Characteristics 130

Table 3.6: Methods of Estimation of Linear Morphologic Characteristics - 132

Table 3.7: Methods of Estimation of Relief Morphologic Characteristics - 133

Table 3.8: Characteristics of Soil within Ofu River Catchment - - 157

Table 3.9: Band Characteristics for NDVI and NDBI Calculation for Ofu River Catchment - - - - 162

Table 3.10: Logarithm of Stream flow, Monthly Mean, Standard Deviation and Correlation coefficient for T-F Model - 174

Table 3.11: Stream flow Estimation for Model Calibration and Validation 175

Table 3.12: Model Validation Parameters - - - - - 175

Table 3.13: Flood Hazard Classification Based on Flood Depths - - 200

Table 3.14: Estimated Population Growth Rates - - - - 202

Table 3.15: Estimation of Percentage of Population with Disability - 203

Table 3.16: Estimation of Percentage Distribution of Population by Age - 203

Table 3.17: Estimation of Percentage Distribution of Population by Gender 205

Table 3.18: Estimation of Ofu River Catchment Population by LGAs - 205

Table 3.19: Flood Vulnerability Classification - - - - 207

Table 3.20: Flood Risk Classification - - - - - 208

Table 4.1: Morphologic Characteristics of Ofu River Catchment (Areal Aspects) 213

Table 4.2: Morphologic Characteristics of Ofu River Catchment (Linear Aspects)216

Table 4.3: Morphologic Characteristics of Ofu River Catchment (Relief Aspects)220

Table 4.4: Estimation of Rating Curve Calibration Coefficients (h, m and K) 223

Table 4.5: Comparison of Monthly Discharge with Historical Discharge - 227

Table 4.6: Socio-demographic Characteristics of Respondents- - - 228

Table 4.7: Flood Experience and Characteristics - - - - 229

Table 4.8: Knowledge of Flood Causes in the Community - - - 231

Table 4.9: Summary Results of Channel Bed Elevations (2000 and 2011), Bed Elevation Loss, Loss Rate and T-test - 240

Table 4.10: Monthly and Annual Sediment Loads of Ofu River at Oforachi Hydrometric Station - - - - - 244

Table 4.11: Soil Classification based on Results of Atterberg Limits Tests Conducted - - - - 246

Table 4.12: Soil Classification based on the Sieve Analysis Results - 246

Table 4.13: Soil Classification based on Saturated Hydraulic Conductivity 247

Table 4.14: Chi Square Results for Association of Elevation, Proximity and Slope with Flood Experience - - - 258

Table 4.15a: Unbiased Statistics of the gauged (1955-1973) and Synthetic (1955-2016) stream flow data - - - - 260

Table 4.15b: Coefficients of Determination, *P*-value, *Critical F*-value and Reliability Index - - - - - - - 260

Table 4.16: Runoff Coefficient for Ofu River Catchment - - - 263

Table 4.17: Rainfall Intensity and Peak Discharge by Rational Method - 263

Table 4.18: Comparison of Average Peak Discharge from the Respective Methods - - - - - - 264

Table 4.19: Results of the Flood Frequency Calculations using log-Pearson Type III Distribution with Annual Maximum Discharge Values (1955-2016) - - - - - - 265

Table 4.20: Discharge Values for Steady Flow Analysis in HEC-RAS - 266

Table 4.21: Criterion Weight for Elevation - - - - - 271

Table 4.22: Criterion Weight for Slope - - - - - 272

Table 4.23 Criterion Weight for Soil - - - - - 272

Table 4.24: Criterion Weight for Corridor - - - - - 273

Table 4.25: Criterion Weight for Causative Factors - - - 278

Table 4.26: Area, Depth and Velocity of Flood Inundated Water - - 282

Table 4.27: Comparison of Flood Inundation Extents by both Methods - 287

Table 4.28: Flood Hazard Zones/extent for 1995, 2000, 100 year and 200 year Floods - - - - - - - 292

Table 4.29: Population at Risk for 1995 and 2000 Flood Scenarios - 292

Table 4.30: Population at Risk for 100-year and 200-year Return Periods - 293

Table 4.31: Population at Risk by Age groups, Poverty level and Gender for 1995 Flood Scenario - - - - - 294

Table 4.32: Population at Risk by Age groups, Poverty level and Gender for 2000 Flood Scenario - - - - - - 294

Table 4.33: Population at Risk by Age groups, Poverty level and Gender for 100 Year Flood - - - - - - - 296

Table 4.34: Population at Risk by Age groups, Poverty level and Gender for 200 Year Flood - - - - - - - 296

Table 4.35: Vulnerability Weights for all Population Categories for 1995 Flood Scenario - - - - - - 298

Table 4.36: Vulnerability Weights for all Population Categories for 2000 Flood Scenario - - - - - - 298

Table 4.37: Vulnerability Weights for all Population Categories for 100 Year Flood - - - - - - - 299

Table 4.38: Vulnerability Weights for all Population Categories for 200 Year Flood - - - - - - - 299

Table 4.39: Overall Weights for All Vulnerability Maps derived by AHP - 300

Table 4.40: Flood Vulnerability Zones/extent for 1995, 2000, 100 year and 200 year Floods - - - - - - 305

Table 4.41: Elements at Risk of 1995 Flood Scenario - - - 310

Table 4.42: Elements at Risk of 2000 Flood Scenario - - - 312

Table 4.43: Elements at Risk of 100 Year Flood - - - - 314

Table 4.47: Elements at Risk of 200 Year Flood - - - - 316

Table 4.45: Inter Profile Characteristics of Soil within the Risk Zones - 320

Table 4.46: Distribution of Household Populations by Toilet Facilities - 326

Table 4.47: Alternative Place of Defecation for those without Toilet Facilities 326

Table 4.48: Distribution of Household Populations by Sources of Drinking Water 327

Table 4.49: Strategic Plan for Ofu River Catchment Flood Management - 329

LIST OF FIGURES

Fig. 1.1: Map of Study Area - - - - - - - 11

Fig. 2.1: Schema of Double Ring Infiltrometer - - - - 57

Fig. 2.2: Process Flow diagram for Image Classification Methods - - 61

Fig. 2.3: Flood risk as a combination of Hazard and vulnerability - - 87

Fig. 2.4: Diagram showing the Terms in the Energy Equation - - 107

Fig. 2.5: HEC-RAS Conveyance Sub-division Method - - - 108

Fig. 2.6: Mean Energy Head Calculation - - - - - 109

Fig. 3.1: Project Point and Project Area for Ofu River Catchment Delineation 125

Fig. 3.2: Schematic Flowchart of the Morphometric Analysis Methodology 134

Fig. 3.3: Ofu River catchment showing location of gage stations - - 137

Fig. 3.4: Schema of the River Cross-section during one of the Discharge Measurements- - - - - - - 138

Fig. 3.5: Schematic Flowchart of the Rating Curve Development Methodology 143

Fig. 3.6a: Triangulated Irregular Network (TIN) surface for 2000 - - 151

Fig. 3.6b: Triangulated Irregular Network (TIN) surface for 2011 - - 152

Fig. 3.7: Location of sections for Ofu River Volume estimation at Oforachi 153

Fig. 3.8: Location of Soil Sample Collection points at Oforachi - - 158

Fig. 3.9a: Normalized Difference Vegetation Index of Ofu River Catchment for 1987 - - - - - - 163

Fig. 3.9b: Normalized Difference Vegetation Index of Ofu River Catchment for 2001 - - - - - 164

Fig. 3.9c: Normalized Difference Vegetation Index of Ofu River Catchment for 2016 - - - - - 165

Fig. 3.10a: Normalized Difference Built-up Index of Ofu River Catchment for 1987 - - - - - 166

Fig. 3.10b: Normalized Difference Built-up Index of Ofu River Catchment for 2001 - - - - - 167

Fig. 3.10c: Normalized Difference Built-up Index of Ofu River Catchment for 2016 - - - - - 168

Fig. 3.11: Screenshot of the RAS Layers created - - - - 191

Fig. 3.12: View of the Geometric data imported from ArcGIS to HEC-RAS 193

Fig. 3.13: Assigning of Manning's n Values in HEC-RAS - - - 194

Fig. 3.14: One of the Cross-sections in HEC-RAS - - - - 195

Fig. 3.15: Akpagidigbo Bridge data showing deck/roadway editor and bridge design editor - - - - - - 196

Fig. 3.16: Oforachi Bridge data showing deck/roadway editor and bridge design editor - - - - - - 196

Fig. 3.17: Steady Flow Data and Boundary Conditions Input in HEC-RAS 197

Fig. 3.18: Exporting HEC-RAS Results to ArcGIS - - - - 198

Fig. 3.19: Schematic Flowchart of the Food Risk Assessment Methodology 210

Fig. 4.1: Areal Morphologic Characteristics of Ofu River Catchment - 212

Fig. 4.2: Strahler's Stream Order of Ofu River Basin - - - 215

Fig. 4.3: Logarithm of Stream Number (Nu) versus Stream Order (U) - 216

Fig. 4.4: Logarithm of Stream Length (Lu) versus Stream Order (U) - 217

Fig. 4.5: Logarithm of Mean Stream Length (Lum) versus Stream Order (U) 217

Fig. 4.6: Digital Elevation Model (DEM) of Ofu River Catchment - 219

Fig. 4.7: Daily Stage Hydrograph of Ofu River at Oforachi Hydrometric Station 222

Fig. 4.8: Fitted Rating Curve for Ofu River at Oforachi Hydrometric station 225

Fig. 4.9: Discharge Hydrograph for Ofu River using fitted Rating Curve - 226

Fig. 4.10: Average Annual Rainfall Characteristics of Ofu River Catchment 232

Fig. 4.11: Annual Rainfall, 5-yr Moving Average and Trend Analysis Plot 233

Fig. 4.12: Annual Maximum Daily Rainfall Depths of Ofu River Catchment- 234

Fig. 4.13: Average Monthly Rainfall Characteristics of Ofu River Catchment 234

Fig. 4.14: Average Annual Rainfall Characteristics of Ofu River Catchment and Neighbours. - - - - - 235

Fig. 4.15: Elevations of Households obtained during the field work at Oforachi - - - - - - - - 236

Fig. 4.16: Slope of Households obtained during the field work at Oforachi 238

Fig. 4.17: Percentage Loss in Ofu River Channel Volume between 2000 and 2011-239

Fig. 4.18: Percentage Loss in River Surface Area between 2000 and 2011 -239

Fig. 4.19: Loss in Ofu River Channel depth between 2000, 2011 and 2016 (estimated) - - - - - - - 241

Fig. 4.20: Ofu River Channel Bed profile for 2000, 2011 and 2016 - 242

Fig. 4.21a: Plot of Suspended Sediment Concentration vs Ofu River Discharge at Oforachi Station - - - - - 242

Fig. 4.21b: Plot of Unmeasured Sediment Discharge vs Ofu River Discharge at Oforachi Station - - - - - 243

Fig. 4.22: Maximum Infiltration Rate, Average Infiltration Rate and Antecedent Moisture Content - - - - - 245

Fig. 4.23: Comparison of Soil Analyses Results with the Digital Soil Map of the World - - - - - - - 249

Fig. 4.24: Proximity of Households to Ofu River - - - - 251

Fig. 4.25a: Ofu River Catchment Landuse/Landcover classifications for 1987 - - - - - - - - 252

Fig. 4.25b: Ofu River Catchment Landuse/Landcover classifications for 2001 - - - - - - - - 253

Fig. 4.25c: Ofu River Catchment Landuse/Landcover classifications for 2016 - - - - - - - - 254

Fig. 4.26a: Area of each Land cover class (km^2) - - - - 255

Fig. 4.26b: Area of each Land cover class (%) - - - - 255

Fig. 4.27: Ofu River Catchment LULC changes from 1987 to 2016- - 256

Fig. 4.28: Ofu River Catchment Runoff Curve Number for 1987, 2001 and 2016 257

Fig. 4.29: Flood Frequency Analysis for Ofu River at Oforachi using Log-Pearson Type III Distribution with Annual Maximum Discharge Values (1955-2016) - - - - - 265

Fig. 4.30: Elevation Layer for Multi-Criteria Evaluation - - - 267

Fig. 4.31: Slope Layer for Multi-Criteria Evaluation - - - 268

Fig. 4.32: Soil Layer for Multi-Criteria Evaluation - - - - 269

Fig. 4.33: Corridor Layer for Multi-Criteria Analysis - - - 270

Fig. 4.34: Reclassified Elevation Layer for Multi-Criteria Evaluation - 274

Fig. 4.35: Reclassified Slope Layer for Multi-Criteria Evaluation - - 275

Fig. 4.36: Reclassified Soil Layer for Multi-Criteria Evaluation - - 276

Fig. 4.37: Reclassified Corridor Layer for Multi-Criteria Evaluation - 277

Fig. 4.38: Flood Hazard Map by Multi-Criteria Evaluation Method - 279

Fig. 4.39: Processed DEM and Bounding Polygon Using HEC-GeoRAS - 280

Fig. 4.40: Water Surface TIN, Water Surface Grid and Velocity Grid - 281

Fig. 4.41a: 1995 Flood Inundation Extent - - - - - 283

Fig. 4.41b: 2000 Flood Inundation Extent - - - - - 284

Fig. 4.41c: 100-Year Flood Inundation Extent - - - - 285

Fig. 4.41d: 200-Year Flood Inundation Extent - - - - 286

Fig. 4.42a: 1995 Flood Hazard Map- - - - - - 288

Fig. 4.42b: 2000 Flood Hazard Map - - - - - 289

Fig. 4.42c: 100 Year Flood Hazard Map - - - - - 290

Fig. 4.42d: 200 Year Flood Hazard Map - - - - - 291

Fig. 4.43a: 1995 Flood Vulnerability Map - - - - - 301

Fig. 4.43b: 2000 Flood Vulnerability Map - - - - - 302

Fig. 4.43c: 100 Year Flood Vulnerability Map - - - - 303

Fig. 4.43d: 200 Year Flood Vulnerability Map - - - - 304

Fig. 4.44a: 1995 Flood Risk Map - - - - - - 306

Fig. 4.44b: 2000 Flood Risk Map - - - - - - 307

Fig. 4.44c: 100 Year Flood Risk Map - - - - - 308

Fig. 4.44d: 200 Year Flood Risk Map - - - - - 309

Fig. 4.45a: Area Covered by the Soil Types within the respective Risk Zones in km^2 - - - - - - - 318

Fig. 4.45b: Percentage Area Covered by the Soil Types within the respective Risk Zones - - - - - - 319

Fig. 4.46: Distribution of Respondents by Experience of 1995/2000 Flood Event 321

Fig. 4.47: Distribution of Respondents by Various Effects of 1995 Flood Event 323

Fig. 4.48: Distribution of Respondents by Various Effects of 2000 Flood Event 324

Fig. 4.49: Distribution of Households by type of Toilet Facility - - 325

Fig. 4.50: Extent of Open Defecation in Oforachi Community - - 326

Fig. 4.51: Distribution of Households by Sources of Drinking Water - 327

LIST OF PLATES

Plate I: Location of the TBM at Oforachi Bridge Hydrometric station - 135

Plate II: Re-establishment of Staff gage at Oforachi Bridge Hydrometric station 136

Plate III: Stream flow Measurement at Oforachi Bridge Hydrometric station 138

Plate IV: Key Informant Interview with the Information Officer of Igalamela/Odolu LGA - - - - - - 146

Plate V: Key Informant Interview with the Oforachi District Head - 147

Plate VI: Key Informant Interview with the Oforachi Village Head - 147

Plate VII: Researcher and Field Assistants Conducting Household Survey 148

Plate VIII: Researcher Carrying out Soil Analysis in the Laboratory - 159

Plate IX: Researcher conducting in situ infiltration test at Oforachi - 159

LIST OF APPENDICES

Appendix I: Topographic Maps of the Study Area - - - - 356

Appendix II: Rainfall Data - - - - - - - 359

Appendix III: Gauged Stream Flow Data - - - - - 361

Appendix IV: Sample Size Estimator - - - - - 362

Appendix V: Data Collection Instruments - - - - - 363

Appendix VI: Stream Discharge Measurements and Calculations - - 366

Appendix VII: Observed Daily Stage for Ofu River at Oforachi - - 377

Appendix VIII: Soil Classification - - - - - - 389

Appendix IX: SCS Runoff Curve Numbers - - - - 392

Appendix X: Normally Distributed Random Numbers - - - 396

Appendix XI: Runoff Computation by Rational Method - - - 398

Appendix XII: Analytical Hierarchical Process Tables - - - 401

Appendix XIII: Results of Soil Analyses - - - - - 402

Appendix XIV: Curve Number Estimation - - - - - 430

Appendix XV: Synthetic Stream Flow Results - - - - 432

Appendix XVI: Results of NRCS-CN Rainfall-Runoff Modelling - - 434

Appendix XVII: Estimation of Runoff Coefficient - - - - 435

Appendix XVIII: Flood Frequency Analysis Results - - - 436

Appendix XIX: Estimation of Flood Vulnerable Population - - 438

Appendix XX: Elements at Risk - - - - - - 442

CHAPTER ONE

INTRODUCTION

1.1 BACKGROUND OF STUDY

The issues relating to hydrological hazards such as flood have increasingly been a major disturbing concern world over. These hydrological trends have been attributed to global warming and climate change occasioned by anthropogenic activities (NHSA, 2015).

Flood is the flow of water above the carrying capacity of a channel (Nwafor, 2006; Olajuyigbe *et al.*, 2012). It refers to a general temporal condition of partial or total inundation of normally dry areas as a result of the overflow of inland or tidal waters or from an unusual and rapid accumulation of runoff (Jeb and Aggarwal, 2008). This accumulation of runoff could be as a result of heavy rainfall.

Among the most widespread natural disasters globally, flood is the one which is caused principally by heavy rainfall and damages human life and social developments (Sarma, 2013; Kandilioti and Makropoulos, 2012). Flood accounts for about 31 % of economic losses globally (Jeb, 2014).

Excessive rainfall and its devastating consequences as a result of increasing climate change remain unforgettable in the lives of many people and the environment as it has resulted in flooding over the years which has claimed lives and properties (Alkema, 2004; Kafle *et al*., 2004; Daffi, 2013; Komolafe *et al.*, 2015). These experiences among others have hindered the developmental drive of many nations of the world. As the world's population increases at an alarming rate with increase in infrastructural development on the rise, more lives and properties are becoming vulnerable to the risk of flood hazards

whenever extreme events occur (Few, 2003; Gaillard, 2010). The United Nation International Strategies for Disaster Reduction (UNISDR, 2005) reported a 35% increase in flood economic risks, driven by the increasing exposure of people and economic assets experienced in the last decades.

Nigeria as a nation is left out of these global hydrological manifestations and scenarios. According to Aderogba (2012) flood is the highest occurring natural hazard in Nigeria with great and devastating consequences on lives and properties. It is fast becoming an annual occurrence in many regions occurring in the form of coastal flood, river flood, flash floods and urban flood (Komolafe *et al.,* 2015).

The encroachment into floodplains in Nigeria is not new. Obansa (2012) and Jeb (2014) in separate studies reported that there was serious encroachment into the floodplains of Kaduna River within Kaduna Metropolis. Daffi (2013) also reported encroachment into the floodplains of the Dep River in North-Central, Nigeria. This encroachment into floodplains is not unconnected with the fact that floodplains are very fertile lands principally due to the alluvial deposits which attract agricultural activities. This usually progresses from mere agricultural to developmental activities within the floodplains (Alkema, 2007). As these activities increase within floodplains and the entire catchment of the River, chances are that the dynamics of the River as well as its hydrologic behaviour could be greatly influenced and modified. For instance, tilling of the soil for cultivation of crops and removal of natural vegetative covers could increase the erodibility of the soil and makes the land susceptible to flooding of varying magnitude (Stabel and Löffler, 2003; Daffi, 2013). It therefore becomes pertinent to carry out flood inundation extent mapping to provide warning for those who stand the risk of being submerged in the event of floods.

Nigeria was hit by the worst flood event in recent history (the worst in the last 40 years) that affected about 35 out of the 37 states (including the Federal Capital Territory) across the geopolitical zones. This flood event which lasted from July to October 2012 resulted in serious damages both to lives and properties with Kogi, Plateau, Taraba, Benue, Edo, Kwara, Delta and Bayelsa as the most affected (UNOCHA, 2012). According to the report, the flood which was caused by heavy rainfall between July and September 2012 and water released from dams, notably the Lagdo dam in Cameroon, affected a population of 7,705,378 persons, 3,870 communities, leaving 363 persons dead.

There is a yearly occurrence of floods of different severity within the Ofu River Basin covering parts of Dekina, Ofu, Igalamela/Odolu, Idah and Ibaji Local Government Areas in Kogi State and parts of Uzo-Uwani LGA in Enugu State. These have resulted in loss of valuable properties, destruction of infrastructure, livestock and crops. Flood depth and velocity affect agricultural activities within the Ofu floodplain including harvest and transportation of crops within the area. During the rainy season, the farms become submerged in floodwater which can be over one meter in depth, sometimes taking several days to recede and resulting in destruction of submerged crops.

In addition, the increased runoff as a result of flooding within the Ofu River Basin has resulted in major gullies across the entire Basin. Some of these gullies have resulted in the relocation of inhabitants of the locations. While efforts are underway to control and correct the challenge of gully erosion within the Basin, a proper assessment of the flood pattern and potential hazard would provide sound footing for a proper erosion control strategy. Though conventional traditional methods can be used for flood hazard assessment, the use of remote sensing and geographic information system techniques have been suggested to provide quick, efficient and effective results as investigated and

documented by Balabanova and Vassilev (2010), Damayanti (2011), Kafle *et al*. (2006), Salimi *et al*. (2008), Ahmad *et al.* (2010) amongst others.

The study of flood frequency and magnitude is highly dependent on the availability of both hydro-meteorological data as well as history of flood events themselves. These data are usually insufficient or nonexistent in most cases in a developing economy like Nigeria. These data scarcity have been a major clog in the wheel of flood related studies as buttressed by Mazvimavi (2003). The case of Ofu River catchment in Kogi State, Nigeria is a direct reflection of this scenario.

According to Eleuterio (2012), all kinds of flood risk management processes expect the reduction of negative consequences of floods by controlling the hazard and/or by reducing the vulnerability of the assets exposed to flood events. It therefore implies that preventive approach to flood risk management is greatly essential in reducing the vulnerability of assets to the events. It is therefore, necessary and possible to prepare for any flood event by carrying out basin-wide flood risk assessment for rivers to determine the extent to which water will overflow stream and river banks as a result of floods of different magnitudes. This assessment will be instrumental in decision making in planning flood disaster management at all stages.

Floodplain mapping has been (and being) carried out in the past via traditional/manual methods. This is very tedious, time consuming and relatively expensive requiring considerable field work and maintenance of long-term river and stream records, which are not readily available for catchments (mostly ungauged) in a large developing country such as Nigeria (Daffi, 2013). The aforementioned challenges to the use of traditional methods could be solved with the use of Remotely Sensed data and Geographic Information System. This method is less tedious and faster, more effective, more efficient,

more reliable and makes immediate assessment of natural resources possible and more accurate although remotely sensed data could be expensive. Since remotely sensed data covers large areas in one synoptic view, its use with GIS techniques can be instrumental at various stages of flood forecasting as well as the flood risk assessment especially in data-scarce areas (Khan *et al.*, 2011) such as Ofu River Catchment.

1.2 STATEMENT OF THE RESEARCH PROBLEM

Flood has been widely considered by researchers to be one of the most devastating and frequently occurring natural hazards in the world (Coto, 2012; Ajin *et al.*, 2013; Obeta, 2014; Komolafe *et al.*, 2015). The case in Nigeria is not any different as flooding is viewed as the most frequent and most widespread natural hazard responsible for more than 30% of all geophysical related hazards, adversely affecting more people than any other natural hazard (Galy and Sanders, 2000; Adebayo and Oruonye, 2013; Obeta, 2014). This pronounced flood scenarios extensively recorded in Nigeria is not unconnected with the overtopping of the natural boundaries of rivers together with the submergence of the low-lying coastal areas (Sarma, 2013; Daffi *et al.*, 2014; Komolafe *et al.*, 2015).

Notwithstanding the various solutions and recommendations developed over the years to curb the far reaching impact of flood in Nigeria, it seems to have become an annual occurrence with increasing frequency and magnitude of occurrence (Adebayo and Oruonye, 2013; Aderoju *et al.*, 2014). This has been the case with Ofu River Catchment in Kogi and Enugu States, Nigeria. The settlements towards the downstream side of the Ofu River especially Oforachi in Kogi State have been bedevilled with flood disasters on annual basis. This disaster has caused colossal loss of properties, farmlands, submerged

routes and highways as well as divers degrees of injuries to a lot of people, yet no investigation has been carried out on the menace beside the routine investigation for the distribution of relief materials. In an interview with the Information Officer of Igalamela/Odolu Local Government Area in Kogi State, the District Head of Oforachi District and the Village head of Oforachi Community, there was a consensus of opinion that the flood disaster of varying severity has been an annual occurrence at Oforachi, a settlement along the Ofu River course with the flood events of 1995 and 2000 being the most severe ones. It was gathered via the interview that some buildings 400 meters away from the river had flood water rising to about 3 meters above the ground submerging many of the buildings. This inundation was accompanied by varying degrees of damages to properties and means of livelihood, although no loss of life was recorded.

Besides this menace at Oforachi in Kogi State, the flooding of some coastal communities in Anambra State by the Anambra River is no longer a hidden news. For instance, it was reported in the national dailies (Vanguard and This Day) on 8th September, 2016, that about six (6) communities in Anambra state were submerged by flood resulting from the Anambra River and were trapped by water hyacinth (www.vanguardngr.com; www.thisdaylive.com). In as much as various stakeholders are making efforts to tackle the problem of the Anambra River flood, neglecting the Ofu River will amount to serious progress in the wrong direction. This is because Ofu River is one of the three (3) major rivers draining into the Anambra River thus a contributor to the flood situation. It is for these reasons that researches such as this one need to be carried out to provide information on flood causes, scenario and possible mitigation, control and management strategies.

1.3 JUSTIFICATION OF THE STUDY

Disasters of all kinds happen when hazards seriously affect communities and households, destroying the livelihood security of their members temporarily or for many years. The United Nations Department of Humanitarian Affair (UNDHA, 1992), stated that adequate assessment entails a survey of a real and/or potential disaster to estimate the actual or expected damage in order to make adequate recommendations for prevention, preparedness and response. There is therefore, a need to prevent avoidable disasters which have resulted in colossal destruction of properties as a result of flood disasters. Rainfall cannot be stopped but hazards of flooding, depending on the type can be contained. There is a need to embark on preventive and mitigation measures that would ensure free flow of runoff into the drainages. With adequate information and proper management strategies, man can still enjoy the benefits that the floodplain provides and yet avoid the hazards that come with such floods. This is achievable once the flood-prone areas for different recurrence intervals have been identified.

In response to the Nigerian President's request in 2010, the Nigeria Erosion and Watershed Management Project (NEWMAP) was established by the World Bank in collaboration with the Federal Government of Nigeria to reduce vulnerability to soil erosion in targeted sub-catchments (www.newmap.gov.ng). According to the information on the NEWMAP website, the Project focuses on watershed management in targeted areas in Kogi State apart from the gully control (http://newmap.gov.ng/partner-states/kogi-state/).

The findings of this study especially the catchment wide morphometric analysis will be very instrumental to the attainment of the NEWMAP objective in Kogi state as it will provide the basis for the desired watershed management flagged off by the Nigerian

Minister of State for Environment on 1st August, 2016 (www.newmap.gov.ng). Furthermore, the results of this study on Ofu River Catchment will provide some vital information for the adequate analysis and management of the Anambra River Watershed where flooding has become a national concern in recent times.

1.4 AIM AND OBJECTIVES OF THE STUDY

This study was aimed at assessing flood risk assessment of Ofu River catchment in Nigeria.

The specific objectives of this research include to:

i. determine the morphologic characteristics of Ofu River Catchment.
ii. develop a stage-discharge relationship or rating curve for Ofu River.
iii. identify flood causative factors within Ofu River Catchment.
iv. analyze flood frequencies and determine the return periods of extreme flood events in the study area.
v. estimate the extent of flood inundation for respective return periods of extreme flood events in the study area.
vi. assess flood risk in the study area.

1.5 SCOPE OF THE RESEARCH

This study was restricted to the Ofu River Catchment spanning across parts of Kogi and Enugu States, Nigeria and the flood hazard, vulnerability and risk assessment was restricted to only the flood prone areas within the flat river valley of the watershed with respect to infrastructure and land uses that were affected. Flash floods within the

catchment were not considered. The study assessed flood hazard, vulnerability and flood risk assessments within the floodplain of the study area. The flood events of 1995 and 2000 respectively were considered in this study as well as floods of different probabilities or return periods between 2 to 200 years were used.

1.6 LIMITATIONS OF THE RESEARCH

This research has the following limitations:

i. Cost: The cost of acquiring high resolution satellite imageries is high which made the researcher to resort to the freely sourced archived satellite imageries made available by the United States Geological Services (USGS). The choice of satellite imageries, digital elevation data and software were also influenced by cost constraints.

ii. Satellite Data availability and Quality: Most of the available satellite data for the dates when the floods occur had challenges of high cloud cover which would make their interpretation difficult. Therefore, available satellites imageries (with minimal cloud cover) of the closest dates to the time of flood occurrence were adopted and used in this study.

iii. Insufficient Hydrological Data: Lack of sufficient hydrological data for the Ofu River Basin necessitated the use of synthetic methods to generate data required for this study and only one year stream discharge data was used to establish a rating curve.

1.7 DESCRIPTION OF STUDY AREA

1.7.1 Location

The Ofu River sub-basin lies between latitudes 6º 46' 48.38'' N and 7º 38' 31.2'' N and longitudes 6º 42' 43.56'' E and 7º 20' 54.6'' E covering parts of Dekina, Ofu, Igalamela/Odolu, Idah and Ibaji Local Government Areas in Kogi State and Uzo-Uwani Local Government Area in Enugu State, Nigeria, within the humid tropical rain forest of Nigeria. It is bounded to the north by Bassa and Omala LGAs in Kogi State, to the east by Ankpa and Olamaboro LGAs in Kogi State and Nsukka, Igbo Eti and Igbo-Eze North and South in Enugu State, to the south by Ezeagu and Udi LGAs in Enugu State and Anambra West and Ayamelum LGAs in Anambra State and to the south by Ajaokuta LGA in Kogi State, Etsako East and Central, and Esan South LGAs in Edo State. It falls within the Lower Benue River Basin Development Authority in North Central Nigeria. Fig. 1.1 shows the map of the study area within Kogi and Enugu States.

1.7.2 Climate

Climatologically, the study area falls within the tropical continental north region. It is characterized by a tropical sub-humid climate with a fairly wide seasonal/ diurnal range of temperature. Rainfall within the catchment is concentrated in one season lasting from April/May to September/October. The overall climatic characteristics of the area are generally determined by the Inter Tropical Convergence Zone (ITCZ) and air mass movements (AR-AR, 2004).

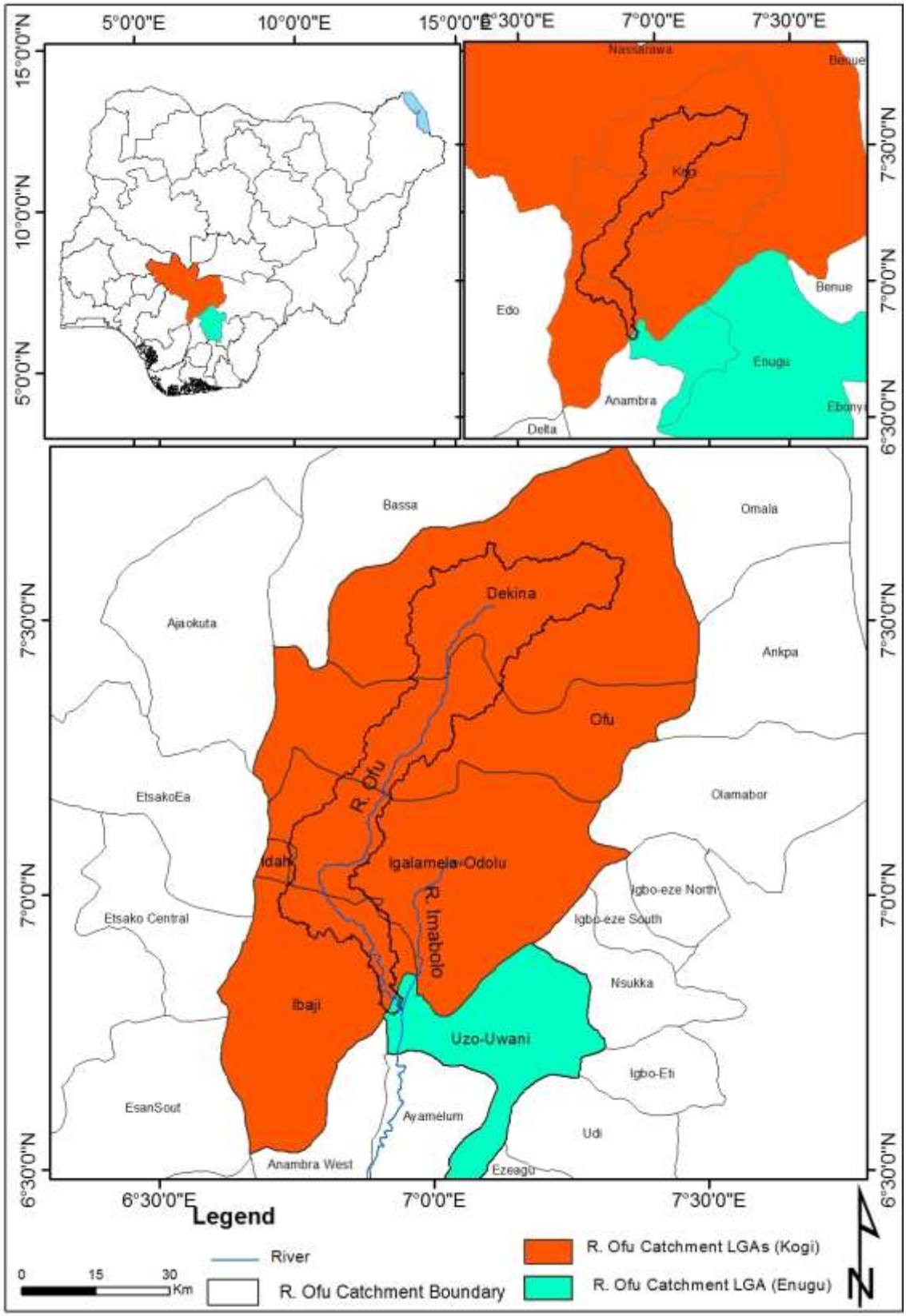


Fig. 1.1: Map of Study Area
Source: Adapted from the Administrative Map of Nigeria, LOC (n.d); http://www.nationsonline.org

1.7.3 Geology

Ofu River catchment is underlain by cretaceous sediments. Basement complex rocks, mainly granites and granitic gneisses are found at the upstream of the river, the outcrops of which appear to be scarce or absent (AR-AR, 2004).

1.7.4 Topography

The area is nearly level to undulating with dominant slopes between 0 to 2% clay plains which are largely subject to seasonal water logging owing to impeded drainage. Rock outcrops of sandstone and volcanic cones occur on the high grounds of the plains (AR-AR, 2004).

1.7.5 Hydrology

The main river within the sub-basin (Ofu River) is perennial and parallel in pattern to Imabolo and Okura Rivers which are close to the study area. Ofu River took its source from Ojofu, in Dekina Local Government Area in Kogi State and flows in the eastward direction with a catchment area amounting to about 1,604 km^2 most of which is covered by dense forest. Okura River joined Imabolo River in Egabada (Kogi State) and further flow southwards before joining the Ofu River and the 'three-in-one' river empties into the famous Anambra River in Anambra State (Gideon *et al.*, 2013). According to the Oforachi Irrigation Project Report by AR-AR (2004), the river is controlled by direct rainfall into the stream channel, surface runoff from the fields around and close to the main rivers and from ground water discharge. The peak flow is obtained during the wet season in the month of September which causes flooding of nearby fields. The report also stated that the catchment is characterized of dry season of about 5 months (November to March) during which the flow in the River Ofu is maintained by ground water outflow. The peak of rainy season (June to October) accounts for 96 % of the total annual flow.

1.7.6 Agriculture

The land within the study area is predominantly used for agriculture. This is becauseOfu River has long been recognized as an extremely valuable water resource in North Central Nigeria, where it is one of very few perennial rivers. Basin wide studies carried out by the Lower Benue River Basin Development Authority have identified the Ofu-Imabolo area as a potential for irrigated agriculture. As a result an irrigation project promoted by the Lower Benue River Basin Development Authority is currently ongoing at Oforachi town along the Idah-Nsukka highway (between longitude 6º 49' E and 6º 57' E and latitude 7º 06' N and 7º 09' N) in Igalamela/Odolu Local Government Area.

CHAPTER TWO

CONCEPTUAL AND THEORETICAL FRAME WORK AND LITERATURE REVIEW

2.1 INTRODUCTION

The review presented herein covers conceptual, theoretical and state-of-the art information on Flood (definition, types, history, the situation in Ofu River Catchment and causes), morphometric analysis of a river basin (boundary delineation and estimation of morphologic characteristics), runoff (definition, factors affecting runoff and methods of estimation) as well as the concept of stream gauging and development of rating curve. Also covered in this review are concepts of rainfall-runoff modelling, generation of synthetic stream flow data, flood frequency analysis, Flood hazard, vulnerability and risk analysis.

2.2 CONCEPTUAL FRAMWORK

2.2.1 Concept of Flood

A flood is an unusual high stage of a river that overflows the natural or man-made banks spreading water to its floodplains that are usually thickly populated due to the obvious advantages of water supply, fertile soil and irrigation (Patra, 2008). Buttressing this, Mustafa and Yusuf (2012) stated that a flood is said to occur when there is an unusual high stage of a stream or river due to runoff from precipitations in quantities too large to be confined in the normal water surface elevations of the streams or river which may result from unusual combination of meteorological factors. Simply put, Nwafor (2006) and Olajuyigbe *et al.* (2012) defined it as the flow of water above the carrying capacity of a channel. Similarly, Chow (1956) defined flood as a relatively high flow which over-

taxes the natural channel provided for it while Ward (1978) sees it as a body of water which rises to overflow land that is not normally submerged.

Generally, flood refers to a temporal condition of partial or total inundation of normally dry areas as a result of the overflow of inland or tidal waters or from unusual and rapid accumulation of runoff (Jeb and Aggarwal, 2008). Similarly, Walesh (1989) defined flooding as temporary inundation of all or part of the floodplain or temporary localized inundation occurring when surface water runoff moves through surface flow, drainages and sewers.

Furthermore, Rossi *et al.* (2012) defined flood from two different perspectives. They first described flood as a condition where an extremely high flow or level of river water inundates floodplains or terrains outside of the water-confined in the major river channels and secondly as a situation when water levels of lakes, ponds, reservoirs, aquifers and estuaries exceed some critical values and inundate the adjacent land, or when the sea surges on coastal lands much above the average sea level.

From the foregoing, it can be seen that different authors have defined flood from different points of view. While some authors defined it in relation to rivers and other water bodies (Chow, 1956; Ward, 1978; Rossi *et al.*, 2012; Patra, 2008; Mustafa and Yusuf, 2012; Nwafor, 2006 and Olajuyigbe *et al,*. 2012), others defined it in relation to general inundation of originally dry land irrespective of the cause (Jeb and Aggarwal, 2008; Walesh, 1989).

2.2.1.1 Historical perspective of flooding in Nigeria

Flood in history have wrought great havocs on humans, destroying settlements, properties and inflicting great sufferings and even death in some cases. As discussed earlier floods are natural occurrences caused by a combination of changes in climatic and

geomorphologic factors, channel characteristics of rivers, and human factors. Some parts of Nigeria have experienced flood on a regular and perennial basis as a result of the interplay of these factors. Akintola and Ikwuyatum (2006) stated that about one-third of the land in Nigeria is at an elevation of less than eight meters above the mean sea level which implies that about 30 percent of the country is often covered with flood water.

The major areas usually affected by flooding in Nigeria include the low-lying areas of southern Nigeria such as the Niger Delta, the floodplains of the large rivers such as Benue, Niger, Gongola, Sokoto, Hadejia, Tedseram, Katsina-Ala, Donga, Taraba, Cross River, Imo, Anambra, Ogun, Kanupe, Gusao, Mada, Shemanker, and the flat and low-lying areas to the south of Lake Chad, which may be flooded during the rainy season usually up to a few weeks later. The Niger Delta area is the largest single area that have experienced the highest number of flooding annually (Akintola and Ikwuyatum, 2006). A brief chronicle of historical flood events with their causes and attendant damages is presented in Table 2.1.

Table 2.1: Chronicles of Historical Flood Events in Nigeria (1953 and 2012)

S/No	Location	Date	Cause	Damage
1.	Ibadan, Oyo State	Sept.3, 1953	Heavy Rainfall	Houses destroyed and Thousands of
2.		1956	Urban induced	people rendered homeless
3.		1960	Urban Induced	
4.		1963	Collapse of Eleye water works	
5.		1973	Urban Induced	
6.		1978	Urban Induced	
7.		1980	Urban Induced	
8.		1982	Urban Induced	
9.		1984	Urban Induced	
10.		1986	Urban Induced	
11.	Edo State	July, 1980	Ojirami dam failure due to heavy rainfall	218 persons rendered homeless; ₦2.2 million worth of properties destroyed
12.	Borno State	1988	Heavy rainfall in Gadaka town	Killed nine persons and destroyed 50 houses
13.	Imo State	1988	Gully erosion	10,000 persons rendered homeless
14.	Kano, Kano State	August, 1988	Bagauda dam failure	206,376 families rendered homeless; 31,147 houses and 14,000 farmlands destroyed
15.	Lagos, Lagos State	June, 1988	Heavy rainfall	3,000 people rendered homeless
16.	Akure, Ondo State	1988	Heavy rainfall	Properties worth millions of naira destroyed

Table 2.1: Chronicles of Historical Flood Events in Nigeria (1953 and 2012) continues

S/No	Location	Date	Cause	Damage
17.	Rivers State	1988	Heavy rainfall in Port-Harcourt	Rendered 6,000 persons homeless and properties worth millions of naira destroyed
18.	Kwara State	1988	Heavy rainfall, dam failure	100 villages destroyed; 10,000 families displaced, 440 hectares of sugarcane plantation destroyed; 72km of farmland destroyed.
19.	Sokoto State	1988	Heavy rainfall	74 villages affected by the flood
20.	Niger State	1988	Kainji lake flooded due to the release of excess water	Affected communities along Jebba to Pategi; 100,000 people displaced; ₦300 million worth of sugarcane destroyed
21.	Lagos, Lagos State	July, 1990	Heavy rainfall	Left many dead and thousands of people were rendered homeless
22.		1991	Heavy Rainfall	Flooded houses, washed off fences and roads
23.	Kano State	Oct, 1992	Tiga dam failure	15 houses destroyed; 162 rendered homeless; 6 hectares of farmland destroyed
24.	Niger State	Sept., 1994	Heavy rainfall; Niger river overflowing banks	50 hectares of farmland destroyed plus 15 deaths
25.	Jos, Plateau State	Aug., 1995	Lamingo dam, heavy rainfall	24 people killed; 50 houses washed away; ₦2 million worth of properties washed away
26.	Osun State	Aug., 1998	Erinle reservoir overfilled due to heavy rainfall	Destroyed farms and roads
27.	Borno State	Nov. 1998	Maga dam. Heavy rainfall	46 houses destroyed; ₦1.5 million worth of farmland destroyed.
28.	Imo State	1999	Heavy rainfall	50 lives lost; submerged farmland and oil installations destroyed
29.	Kogi State	1999	Heavy rainfall, spill over from Shiroro dam	Thousands of people rendered homeless
30.	Niger	1999	Shiroro dam failure due to heavy rainfall	16 people killed; thousands of people rendered homeless
31.	Cross River State	2000	Heavy rainfall	200 houses submerged; damaged and cut off the highway linking Cross River State and Eastern States
32	35 out of 37 states	2012	Heavy rainfall, water release from dams, notably Lagdo dam in Cameroun, Jebba, Kainji and Shiroro dams along the River Niger, increase in water at the Niger and Benue confluence	Affected 7,705.378 persons, 3,879 communities, internally displaced 387,153 persons, left 363 persons dead, damaged 597,476 houses as well as other public infrastructures such as schools, health centers, roads and bridges that were completely destroyed.

Source: Akintola and Ikwuyatum (2006); UNOCHA (2012)

2.2.1.2 Flooding situation in Ofu River Catchment

Flood has been an annual occurrence within Ofu River floodplain especially in Oforachi since 1991 though little or no report exists on the menace. In an interview with the Village head of Oforachi community, Chief Isah Atawodi (Agenyi Atta Igala) on 8th October, 2016, the first flood event in the community happened in 1991 which according to him was the anger of the gods. He stated that, the corpse of a child who drowned in Ofu River was taken away for burial in another village contrary to the demands of the 'gods'. So, in anger that the demand of the gods was violated, the river flooded a major part of the community. This implied that the community generally regarded this flood occurrence as a spiritual phenomenon which would later change with time. He further stated that the next flood after the 1991 event happened in 1995 in a magnitude that was far beyond that of 1991 attributed to the removal of sharp sand from the shores of the river after which the flood has become an annual occurrence. In another interview with the information officer of Igalamela/Odolu Local Government Area (LGA), Mr. Joel Idris Alfa on Monday, 10th October, 2016, the most severe flood within the community happened in 2000, destroying properties and displacing many. He stated that attempt was made to recommend relocation to higher ground for the inhabitants but was met with strong oppositions so that the best they were able to do in conjunction with the State Emergency Management Agency (SEMA) was to distribute relief materials after much oppositions as well. The village head also stated that the flood situation is not only from the river but that some areas of the community, his house being an example, are being flooded by groundwater outflow. This has been so severe that it has destroyed their houses including his palace several times.

2.2.1.3 Types of flood

Broadly speaking, flood has been classified based on the location by some authors while others have classified it based on duration and speed of occurrence (Jeb, 2014).

(A) Classification of flood based on location

Scholars have classified flood based on location into four types. They are Coastal flooding, River (or fluvial) flooding, Groundwater flooding, Arroyos flooding and Pluvial flooding (Jeb, 2014; Nicholas, 2014).

a. Coastal flood:

This type of flood occurs in low-lying coastal areas such as, but not restricted to deltas and estuaries when the land is inundated by brackish or saline water. The flood occurs when the river water spills over the embankment along the coastal reaches. The increase in the high-tide levels in the sea above the normal level by storm surge conditions can greatly intensify this flooding situation (Smith and Ward, 1998). This type of flood occurs in the coastal regions of Nigeria especially in cities such as Calabar, Port Harcourt, Warri, Lagos and other smaller rural communities along the coast.

b. River or Fluvial flood:

This type of flood occurs mostly on floodplains of rivers as a result of flow exceeding the discharge carrying-capacity of the stream channels thereby over spilling the banks. Most river floods result directly or indirectly from climatological factors such as heavy and/or prolonged rainfall (Smith and Ward, 1998; Nicholas, 2014).

c. Groundwater flood:

Macdonald *et al.* (2012) defined groundwater flooding as the emergence of groundwater at the ground surface away from perennial river channels and can also include the rising of groundwater into man-made ground, including basements and other subsurface infrastructure. The British Geological Survey (BGS, nd.) stated that periods of abnormally high rainfall can result in groundwater flooding of basements and the emergence of groundwater at the ground surface, causing damage to property and infrastructure. The challenges of high groundwater levels mainly occur in floodplains or low-lying areas (Nicholas, 2014). Damage due to high groundwater levels occurs if there is a considerable change in the groundwater levels whether sudden, gradual or prolonged. These changes can be attributable to high rate of infiltration into the aquifer either as a result of flooding or heavy rainfall, or reduced abstraction of groundwater (Kreibich and Thieken, 2008).

d. Arroyos Flood:

Jeb (2014) described an arroyo as a river which is usually dry but forms fast moving river along the gullies when there are storms approaching these areas. This can cause severe damages. This type of flood occurs in the northern semi-arid regions of Nigeria such as Sokoto, Katsina, Borno and Jigawa states.

e. Pluvial flood:

Pluvial flood is a type of flood that arises from high intensity extreme rainfall and is typified by overland flow and ponding before the runoff reaches a watercourse or drainage system (www.floodresiliencity.eu; Falconer*et al.*, 2009; Maksimović *et al.*, 2009; Douglas *et al.*, 2010; Chen *et al.*, 2010). Sometimes, the runoff may not be able to enter the stream or drainage channels which probably must have been filled to capacity as a

result of the rain. This type of flood is usually associated with high intensity rainfall with short duration. Depending on the percentage of imperviousness, it can also occur with prolonged lower intensity rainfall (Nicholas, 2014). Pluvial flooding can occur anywhere, even areas at a high elevation well above the river or coastal floodplain, and often in areas which are never expected to have a risk of flooding. This was the case in the summer 2007 floods in England when around two thirds of damage estimated at over 3 billion euro was thought to be due to this type of flooding - much in areas where no flood risk had been identified (www.floodresiliencity.eu). Furthermore, this type of flood is highly influenced by the hydraulic conductivity of the soil and the degree of imperviousness. Soils with low hydraulic conductivity such as saturated surface soils and paved surfaces will increase the flood extent (Cobby *et al.*, 2009).

The hazard associated with pluvial flooding can arise from rapid and sometimes deep ponding or high velocity flows along roads and streets especially those with steep slopes (Douglas *et al.*, 2010). This is aggravated by the fact that it often occurs unexpectedly in locations not obviously prone to flooding and with minimal warning. Since it is not well understood by the general public, it is often termed "invisible hazard" (Houston *et al*., 2011).

Pluvial flood is more likely to occur in urban areas than in rural because of the increase in paved surfaces and built up areas due to urbanisation without adequate drainage systems to handle the resultant runoff (Chen *et al.*, 2010). Urban floods in Nigeria result from human activities such as unplanned urbanization, poor refuse disposal, blocked drainages and siltation of waterways (Jeb, 2014).

(B) Classification of flood based on duration and speed of occurrence

a. Flash Floods

Flash Floods usually occur within minutes or a few hours after a heavy rainfall, tropical storm, failure of dams or levees or releases of ice jams. This usually results in the greatest damages to society. Most Pluvial floods occur as flash floods especially in unplanned urban areas. A recent example of such occurrences in Nigeria is the 2012 flood event in Maraba Gurku in Nasarawa state, near Abuja as a result of prolonged heavy rainfall. In addition, dam failures could also lead to flash floods with fatal consequences. This was the case of Bagauda in Kano state and the Goronyo Dam failure in Sokoto state in 2011 which led to serious flash floods that washed away farmlands and led to loss of several lives (Jeb, 2014)

b. Slow-Onset Floods

Slow-Onset floods usually last for a relatively longer period than the flash flood. It could last for weeks or even months. The damage caused by this kind of flood is gradual but with great magnitude. It could lead to loss of stock, damage to agricultural products, roads and railway lines.

c. Rapid-Onset Floods

Rapid-Onset Floods last for a relatively shorter period than the slow-onset floods but usually longer period than the flash floods. They could last for one or two days only. Although this kind of flood lasts for a shorter period, it can cause more damages and pose a greater risk to life and property as people usually have less time to take preventative action during rapid-onset floods.

2.2.1.4 Causes of flood

Causes of flood tend to vary from one place to another depending on the available protection and management processes (Akintola and Ikwuyatum, 2006). Urbanization and/or the concentration of settlements have continued to increase the flood damage potentials, as human settlements continue to encroach on flood prone areas. In some places, over-reliance on available safety provided by existing flood control infrastructure, such as dikes, levies and reservoirs can also result in flood disaster more severe than the natural ones. For instance, dykes can collapse and cause immense destruction when flood is on a large scale although it was a flood protective structure on a small scale. Losses in this case could and usually exceed those in natural ones. Furthermore, human actions can also cause floods. The insatiable affinity for more fertile lands has usually led to the encroachment on floodplains. Increase in the percentage imperviousness, deforestation and channel interference can also cause floods. Coto (2002) broadly summarized the causes of flood into three factors. These factors are meteorological, geomorphologic and land use/urbanization factors.

(A) Meteorological factors

The meteorological factors refer to the climatic characteristics of the catchment such as rainfall, temperature, relative humidity amongst others. For instance, the meteorological conditions in the Turrialba in Costa Rica induced torrential rainfall caused by the humid winds coming from the Caribbean Sea (Coto, 2002).

(B) Geomorphologic factors

These factors relate with the terrain characteristics such as elevation, soil and drainage characteristics, and slope amongst others.

(C) Land use/urbanization factors

Garba (2015) noted that the type of land use largely affects the surface runoff within the catchment. Land use/Land cover (LULC) changes have been linked with flood occurrence by various researchers (Ndabula, 2006; Nicholas, 2014; Garba, 2015). This is because the land cover type determines the runoff curve number or runoff coefficient which in turn determines the amount of runoff that could be generated from the catchment (Patra, 2008).

2.2.2 Concept of Runoff

Runoff refers to that part of precipitation which is drained from land after all losses such as groundwater and evaporation and makes its way towards the river, stream or ocean (Patra, 2008; Suresh, 2008; Mustafa and Yusuf, 2012).

Rainfall is the primary source of water for runoff generation over the land surface. As rain falls over the earth's surface, a part of it is intercepted by vegetation, buildings and other objects, preventing that part from reaching the ground surface (interception) while another part is stored in surface depressions and may not immediately contribute to the runoff to the stream (depression storage), though this part may eventually infiltrate into the soil or evaporate. When these losses are removed from the total precipitation, the excess is what ends up as runoff to the stream or river (Suresh, 2008; Patra, 2008; Mustafa and Yusuf, 2012).

An adequate knowledge of the runoff volume characteristics of a catchment over a period of time at a particular site is very important for the appropriate and effective planning and management of any water resource project. Patra (2008) emphatically stated that the availability of a long-term runoff data covering a minimum of 30 years is required for appropriate study of the economics of the project and to establish the pattern of demand

from that project. As a result of the foregoing, reliable methods of generating the runoff (stream flow) data should be used to handle complex rainfall-runoff processes which should effectively combine all the loss variables to provide a net output at the desired location in the watershed.

2.2.2.1 Factors affecting runoff

The factors affecting runoff of a basin are broadly classified into three categories-climatic, morphologic and Human (Patra, 2008; Suresh, 2008; Mustafa and Yusuf, 2012). These factors are discussed as follows:

a. Climatic factors:

The principal climatic factors affecting runoff are the precipitation characteristics which include the type, intensity, duration and aerial distribution in addition to other climatic factors.

i. Type of Precipitation:

Precipitation may occur in the form of rainfall, snow, sleet or hail. The type of precipitation has a great effect on the runoff. For instance, while runoff may start immediately for precipitation which occurs as rainfall depending on its intensity and magnitude, snow or hail will not result in runoff immediately as they have to melt first before runoff takes place.

ii. Rainfall intensity:

The intensity of rainfall is directly proportional to the resultant runoff to the stream or river. Rainfall at high intensity causes immediate rise in the discharge of the stream. If rainfall intensity is greater than infiltration rate of the soil, the surface runoff takes place

very shortly while the reverse is the case for intensity less than infiltration rate. Prolonged rainfall therefore will infiltrate and raise the surface of saturation to the ground surface thereby reducing the infiltration capacity to zero and cause sudden increase in surface runoff.

iii. Rainfall duration:

This also has a direct effect on the volume of runoff from a basin. Rainfall of given intensity occurring for longer duration will result to more runoff from a catchment. Keeping the intensity constant, the storm of longer duration will result in gradual rise in the peak discharge of the stream until a maximum and remaining there as the storm lasts. This is due primarily to the mean areal travel of a drop of water in the basin or watershed.

iv. Aerial distribution of Rainfall:

The aerial distribution of the rainfall also affects the runoff of a stream both in magnitude and temporal distribution. Maximum runoff occurs when rainfall from the entire area of a basin contribute to the runoff. A storm moving from upstream to downstream of a catchment at a rate equal to the movement of water in the stream channel will result to a maximum flood peak at the outlet.

v. Other climatic factors:

Other factors such as temperature, wind velocity, relative humidity amongst others will affect the water losses from the watershed area significantly which in turn will affect the runoff within the catchment. The lower the losses, the more the runoff will be.

b. Human factors:

The human factors refer to such effects that result from urbanization, agricultural practices and engineering structures. Urbanization resulting in the construction of roads, pavements, airfields amongst others increases the percentage of imperviousness which often leads to significant increase in the runoff volume. Urbanization is also often accompanied by construction works such as buildings and roads, which can increase the erodibility of the soil. In addition, agricultural practices can also result in a sudden change in catchment characteristics. Activities such as ploughing have been found to reduce runoff by as much as 45% (Mustafa and Yusuf, 2012).

c. Geomorphologic factors:

The morphologic or physiographic factors of a watershed consist of both the characteristics of the catchment and the channel itself such as size, shape, slope and orientation of the catchment, soil characteristics, and land use, amongst others.

i. Size of the catchment

The volume of runoff from a cathment depends on its size amongst other factors. According to Mustafa and Yusuf (2012), runoff increases with the catchment area. The size of the catchment determines to a great extent the extent of the spatial heterogeneity of its hydrological processes. It is expected that large catchments are more heterogeneous than smaller ones. According a report by the Tamil Nadu University of Agriculture, catchment sizes can be broadly classified as follows (http://www.agritech.tnau.ac.in):

1. Small catchment (< 250 km^2)
    a. Mini watersheds (0.01 - 1 km^2)
    b. Micro watersheds (1 - 10 km^2)

c. Milli watersheds (10 - 100 km^2)

d. Sub watersheds (100 - 250 km^2)

2. Medium catchment (250 – 2,500 km^2)

3. Large catchment (> 2,500 km^2)

ii. Shape of the catchment

The runoff peak and duration can be affected by the shape of the catchment (Patra, 2008; Mustafa and Yusuf, 2012). Catchments may have several shapes like square triangular rectangular, oval, palm, and fern leaf shape amongst others. An elongated catchment has lesser peak and longer runoff duration than a fern-shaped catchment of the same area.

iii. Soil characteristics

There is a relationship between the characteristics of soil, runoff and flood occurrence (Vaezi *et al.*, 2010). The soil receives water at the surface after rain, stores it for plant use or slowly releases it for ground water recharge through gravitational flow (Magdolf and Van Es, 2010). The ease with which the soil can do this is dependent on its infiltration capacity. The infiltration capacity of the soil is influenced by the soil type, structure and moisture content at the start of rain (Magdolf and Van Es, 2010). A high infiltration rate will therefore result in lower runoff volumes. This is because runoff is produced when rainfall exceeds a soil's infiltration capacity. An understanding of the soil characteristics is therefore an important pre-requisite to understanding the runoff characteristics and flood risk in a catchment.

iv. Land use/land cover

Land use/ Land cover changes is one of the factors responsible for the non-stationarity in runoff regime. Land use degradation can significantly affect infiltration and surface roughness which could lead to higher flood discharges (Saghafian *et al.*, 2008). In as

much as weather and climate are the major determinants of flood, land cover changes can also influence the occurrence and frequency of floods by changing the responsiveness of river flows to rainfall (Solín *et al.,* 2011). The assessment of land use/ land cover changes is therefore very important in catchment flood studies.

2.3 MORPHOLOGIC CHARACTERISTICS OF A RIVER BASIN

The morphologic characteristics of a river basin are very important factors in watershed hydrology. They reflect the hydrological behaviour of the river basin and are useful in evaluating the hydrologic response of the basin. Morphologic analysis of a river basin refers to the measurement and mathematical evaluation of the surface, shape and dimension of its landform (Agarwal 1998; Obi *et al.*, 2002; Kulkarni, 2015). There are relationships between river basin morphologic parameters and flood potential. For instance, higher drainage density indicates a faster runoff and a more significant degree of channel abrasion for a given quantity of rainfall (Withanage *et al.*, 2014).

According to Horton (1945), rivers and fluvial processes are the most dominant geomorphic systems of earth's surface responsible for morphometric changes in drainage basin or the watershed. According to Sapkale (2013), the geological nature of basin and its landform generally controls the river, influence the channel slope and reveals possibilities of erosion and depositions of the river.

Quantitative morphologic analysis of a river basin facilitates an understanding of the drainage characteristics and development, surface runoff generation, infiltration capacity of the ground as well as groundwater potential (Ibrampurkar, 2012). Raj and Azeez (2012) further stated that baseline morphologic information at a sub basin level is very crucial

for the development of appropriate strategy for sustainable, socially acceptable, ecologically friendly and economically viable development of a river basin. Furthermore, it provides quantitative expression of drainage basins, and is regarded as one important tool in hydraulic analysis that would provide simple and accurate measures to describe the drainage systems (Angillieri, 2008). These factors make the analysis very attractive as it brings out the basic characteristics on the geometrical and mechanical aspects of the river basin which in turn would be helpful in understanding the hydrology, sediment characteristics and landscape evolution of basins.

The morphologic characteristics of the river basins describe the hydrological and geomorphic response of processes such as but not restricted to runoff, variations in river flow, river sedimentation, floods, soil erosion, flow characteristics of the drainage lines and the performance and sustainability of the associated hydraulic structures within the basin (Withanage *et al.*, 2014; Garde, 2005).

River basins are considered as an open system and the basic steps involved in morphologic analysis are defining, measuring and analyzing the quantitative indices related to flow plain geometry and profile, and bed form of river basins (Raj and Azeez, 2012). The morphologic analysis examines the linear, relief and areal aspects of the drainage networks (Waikar and Nilawar, 2014).

Documenting basin characteristics using morphometric techniques became very necessary since the early nineteenth century because of the threat to the world's fresh water flow regime as a result of several anthropogenic pressures and global climate variations. The studies by Horton (1932), Horton (1945), Strahler (1957), Strahler (1964) and Schumm (1956) are considered as pioneers in the field.

2.3.1 Delineation of watershed boundaries

Hydrological modelling of any kind begins with the first step of delineating streams and watersheds (Merwade, 2012a). In other words, the delineation of the catchment boundaries is the first step in the morphometric analysis of a river basin to determine the areal parameters of the basin which are necessary for climate interpolation, runoff calculation as well as other analyses. Basic watershed properties such as area, perimeter, slope, flow length, stream network density, amongst others are also derived in the process.

The drainage basin watershed or catchment of river refers to the part of the earth's surface which is drained by the main stream and its tributaries (Martins and Gadiga, 2015). It is the area of land that drains to a particular point along a stream. Patra (2008) defined it as the area bounded by the highest contour, called ridge line, from where precipitated water is collected by surface and subsurface flows and drains out through the natural river. The ridge line or watershed divide forms a natural barrier dividing one basin or watershed from another. Thus, any drop of water falling outside of the boundary will drain to another watershed. The main element that characterizes the watershed divide is topography (Daffi, 2013).

The process of identifying the drainage area of a point or a set of points on a stream or river network is referred to as watershed delineation. Traditionally, watershed or catchment delineation was and is still being carried out manually using topographic/contour maps (Merwade, 2012a; Daffi, 2013). For instance, Ismail (1989) delineated the catchments of the Kubani and Galma rivers respectively by observing the contour lines on the topographic map of the area. This method was very tedious, time consuming and subject to a high level of human error. These obvious limitations of

manual delineation from topographic map necessitated the shift in recent years to the use of Remote Sensing and Geographic Information System (GIS). This has made the task of catchment delineation faster, less tedious and more efficient depending on the availability of data. According to Merwade (2012a), the availability of Digital Elevation Models (DEM) and GIS tools makes it possible for watershed properties to be extracted by using automated procedures. Daffi (2013) and Jeb (2014) used the Shuttle Radar Topographic Mission Digital Elevation Model (SRTM DEM) to delineate the catchment of Dep River Basin in North-Central Nigeria and 500 meters corridor of River Kaduna in Kaduna Metropolis respectively. Both of them utilized the Integrated Land and Water Information System (ILWIS) GIS software for the delineation.

Watershed delineation can be carried out using various GIS software such as ILWIS 3.7 (Daffi, 2013), Spatial Analyst Hydrology tool in ArcGIS 10 (Merwade, 2012a), HEC GeoHMS extension in ArcGIS 10 (Merwade, 2012b) and ArcHydro Extension in ArcGIS 10 (Merwade, 2012). The processes of watershed delineation using any of the aforementioned software are basically similar. The little variations that may exist may only be a manufacturer's preferences. The basic steps in watershed delineation in GIS include the following, details of which can be obtained from the help menu of the software:

i. Filling Sinks:

This *fill sink* function as the name implies, fills the sinks in a grid. This is important because if higher elevation cells surround a cell, water will be trapped in that cell and will not be able to flow. The Fill Sinks function modifies the elevation value of that particular cell to eliminate this problem. In other words, the fill sink operation is used to clean up the DEM before carrying out Flow Direction Operations. The Fill Sinks Operation

removes both depressions that consist of a single pixel as well as those that consist of multiple pixels

ii. Flow Direction Operation:

This operation computes the flow direction for a given grid. It creates a raster of flow direction from each cell to its steepest down slope neighbour. The value in any given cell of the flow direction grid indicates the direction of the steepest descent from that cell to one of its neighbouring cells using the eight direction pour point (D8) method. It utilizes the output map of the fill sink operation.

iii. Flow Accumulation Operation:

This function uses the flow direction grid to compute the accumulated number of cells that are draining to any particular cell in the DEM. It creates a raster of accumulated flow into each cell.The flow accumulation process represents the amount of water that would flow into each cell assuming all the water became runoff and there was no loss in the form of interception, evapotranspiration or loss to groundwater. Flow Accumulation grid contains a running total of all cells contributing to a given cell. The operation can be used to find the drainage pattern of a terrain.

iv. Stream Network Extraction:

As stated earlier, flow accumulation gives the number of cells (or area) that drain to a particular cell. It can therefore be used to define a stream in the watershed. It is assumed that a stream is formed when a certain area (threshold) drains to a point. This threshold can be defined by using the number of cells in the flow accumulation grid. The stream Network operation extracts a basic drainage network, using the input from the Flow Accumulation Operation. The output raster map will show the basic drainage as pixels with value ‘True’, while other pixels have value ‘False’. A user sets a user-defined *threshold value*, that is, a value for the minimum number of pixels that are supposed to

drain into a pixel to let this pixel remain as a drainage in the output map. The larger the value chosen, the fewer drainages will remain in the output map.The user also sets a user-defined *threshold raster map* that contains variable threshold values. A threshold map can for instance be based on geological units, on height values, or on an internal relief map, amongst others.

v. Stream Link Operation:

This tool assigns a unique number to each link (or segment) in the stream raster. It examines all drainage lines in the Stream network map from the *Stream Network Extraction* Operation, finds the nodes where two or more streams meet, and assigns a unique ID to each stream in between these nodes, as well as to the streams that only have a single node. An attribute table is also created where information on the drainage network can be obtained.

vi. Stream Order:

This tool creates stream order for the stream network.

vii. Catchment Extraction Operation:

This operation uses the Stream Raster obtained from the Stream Network extraction process and the Flow direction raster obtained from the flow direction operation to construct catchment for each stream extracted in the former. As output a raster map, a polygon map and an attribute table are produced.

viii. Catchment Merge Operation:

The Catchment merge operation merges adjacent catchments found from the *Catchment Extraction Operation*. Catchments can be merged in two ways. The first method is carried out by specifying a point map that contains locations of stream outlets within a catchment so that all adjacent catchments that drain into such outlets will be merged while the second method is by simply specifying an ordering value (either Strahler or Shreve) so that all

adjacent catchments that have this or lower order value and which drain into a common catchment will be merged. Either method will produce a new catchment raster map, polygon map and attribute table as output.

While there is a fast growing interest in the use of remote sensing data and GIS techniques, the type of data used as well as the type of software remain the distinguishing factors from one study to the other. There are different sources of digital elevation models used for watershed delineation. As earlier mentioned, Daffi (2013) delineated the Dep River watershed in North-Central Nigeria using Shuttle Radar Topographic Missions Digital Elevation Model (SRTM DEM) with ILWIS 3.7 software. Jeb (2014) used a combination of a DEM generated from topographic map and SRTM DEM to delineate 500 meters corridor of the Kaduna River within Kaduna Metropolis in ILWIS 3.8. Quan (2006) used SRTM data to extract the DEM of the Can Le Catchment in Vietnam after which it was combined with the existing drainage network digitized from the topographic maps to generate a final DEM of the catchment. The Can Le catchment was then delineated from the combined DEM. He noted that the combination of the SRTM DEM with the digitized drainage network optimized the DEM for further hydrological analysis. Similarly, Islam (2004) used two approaches to carry out watershed delineation. The first approach utilized two different types of DEM, one prepared by Australian National University (ANU) model and the other from traditional stereo images. GIS tools in HEC-GeoHMS extension in ArcGIS were used for the delineation. This tool assumes a watershed as a line whose flow accumulation value is zero. The second approach involved hand delineation carried out by observing contour lines and slope where a catchment divide line was indicated with arrows showing opposite directions. After comparing the outcome of both approaches, he noted that differences were observed between them. He

further noted that the ANU DEM provided more accurate delineation than the traditional stereo images. The delineated watersheds were used to simulate rainfall-runoff hydrographs by HEC-HMS using SCS Curve Number method for three small watersheds in the region. This was done to validate the accuracy of the DEM. He observed that the computed and actual hydrographs were quite similar and the computed and observed outflows also matched appreciably. He concluded that although hand delineation was more cumbersome, it was observed not to be less accurate than computer generated delineation.

2.3.2 Determination of the morphologic characteristics of a watershed

The systematic description of the geometry of a river basin and its stream channel requires the measurement of linear aspects of the drainage network, areal aspects of the drainage basin, and relief or gradient aspects of the channel network and contributing ground slopes (Strahler, 1964; Withanage *et al.*, 2014). The various aspects considered in the morphologic description of the river basin are briefly discussed (Horton, 1932; Horton, 1945; Miller, 1953; Schumm, 1956; Melton, 1957; Strahler, 1957; Strahler, 1964; Patra, 2008; Mustafa and Yusuf, 2012; Suresh, 2008; Withanage *et al.*, 2014).

2.3.2.1 Areal aspects

The areal aspects of the river basin are:

i. **Basin area (A):** The area of the basin is defined as the total area projected upon a horizontal plane. Determining the Area of the drainage basin is important because, the size of the basin affect the total volume of rainwater received which in turn determines the total runoff produced and thus the stream discharge. It is measured in km^2.

ii. **Basin Perimeter (P):** Perimeter is the length of the boundary of the basin. In other words, basin perimeter is the length of the watershed boundary that encloses the catchment area. It is measured along the divide between watersheds and may be used as an indicator of watershed size and shape. The basin parameter is used in conjunction with the basin area to give a measure of the departure of the basin from a true circle and in conjunction with relief to give a measure of the general steepness of the basin. It is measured in km.

iii. **Basin Length (L_b):** The length of drainage basin has been defined in different ways by different scientists. While Horton (1932) defined it as the straight-line distance from a basin mouth to the point on the water divide intersected by the projection of the direction of the line through the source of the main stream, Schumm (1956) defined it as the longest dimension of the basin parallel to the principal drainage line. Simply put, the length of the drainage basin is the aerial distance between the watershed outlet and the farthest point on the perimeter of the watershed (Gardiner *et al.,,* 1977). It is measured in km.

iv. **Longest flow path (L_{fp}):** This is the distance between the outlet of the watershed and the remotest part of the watershed along the course of the main stream. It reflects the maximum distance any drop of rain will have to travel to get to the outlet. It is measured in km.

v. **Main Stream Length (S_L):** This is the length of the main stream with maximum length measured along the stream course. The time of concentration is always maximum along the main stream. It is measured in km.

vi. **Basin Centroid (C_b):** This represents the location of the point of weighted center of the watershed. The distance between the centroid and the outlet of the watershed is

approximately half of the basin length (Patra, 2008). This parameter is important when using Snyder's method to synthesize unit hydrograph for an ungauged basin.

vii. **Basin Centroid Longest Flow Path (L_{cfp}):** This is the distance between the watershed outlet and the basin centroid along the course of the main stream. It is measured in km.

viii. **Elongation Ratio (R_e):** Schumm (1956) defined elongation ratio as the ratio of the diameter of a circle of the same area as the basin area to the maximum length of the basin. The value varies between 0.25 and 1.00 over a wide variety of geologic formations. The elongation ratio is equal to 1 for a circular basin and approaches 0 for a straight line. Values in the range of 0.6-0.8 are generally associated with strong relief and steep grounds. The values around 1.00 are typical of regions of very low relief. Elongated basins with high bifurcation ratio yield a low but extended peak flow while circular basins with low bifurcation ratio produce a sharp peak flow.

ix. **Circularity Ratio (R_c):** Miller (1953) defined circulatory ratio as the ratio of the basin area (A) to the area of a circle of perimeter equal to the basin perimeter (P). It is the measure of the degree of circularity of the given basin. A high value of circularity ratio indicates old stage topography. R_c approaching 1 indicates circular shape of the basin and old stage topography. Circularity and elongation ratios are very vital practical parameters useful in predicting certain hydrological characteristics of a drainage basin.

x. **Form Factor (F_f):** Horton (1932) expressed form factor as the ratio of the basin area (A) to the square of the maximum length of the basin (L_b). It varies from 0 to 1. Low form factor indicates elongated basin. Basins with low form factor have flatter peak flow for longer duration while the basins with high form factor have higher peak flows for a shorter duration.

xi. **Compactness Coefficient (C_c):** Strahler (1964) defined compactness coefficient as the ratio of perimeter of the basin (*P*) to the circumference of circle with area equal to the basin area. The value is 1 for perfect circle and increases as the basin length increases. The compactness coefficient therefore, is a direct indicator of the elongated nature of the basin.

xii. **Shape Factor (B_s):** Shape factor of a watershed was proposed by the United States Army Corps of Engineers in 1945 (Patra, 2008). They proposed that the shape factor of a watershed is the ratio of the square of the watershed length to the watershed area. The shape factor of a watershed is often greater than 1.

xiii. **Stream Frequency (F):** According to Horton (1945), stream frequency is the number of stream segments of all orders per unit area of the basin. Stream frequency is a reflection of the distribution of stream network on the watershed. High stream frequency is favoured in regions of impermeable subsoil and steep gradients. The higher the stream frequency, the faster is the surface runoff and therefore less time for infiltration.

xiv. **Drainage Density (D_d):** This is the ratio of the total length of all streams of the catchment to the drainage basin area. It indicates the drainage efficiency of the basin (Patra, 2008). Drainage density was introduced by Horton (1932) as an important indicator of the linear scale of landform elements in stream eroded topography (Withanage *et al.*, 2014). It indicates the closeness of spacing of channels, thus providing a quantitative measure of the average length of stream channels for the whole basin (Horton, 1932). It has been observed from D_d measurements made over a wide range of geologic and climatic types that a low D_d is more likely to occur in regions of highly permeable subsoil material under dense vegetative cover and where relief is low. A high D_d is the resultant of weak or impermeable subsurface material, sparse vegetation and mountainous relief. Low D_d leads to coarse drainage texture while high D_d leads to fine

drainage texture (Strahler, 1964). It is expressed in km/km^2. Drainage density is a useful numerical measure of land dissection and runoff potential (Ibrampurkar, 2013). A study by Krishnamurthy *et al*. (1996) classified drainage density <2 as very coarse, between 2 to 4 as coarse, 4 to 6 as moderate, 6 to 8 as fine and drainage density >8 as very fine.

xv. **Drainage Texture (T):** This is one of the important parameters of geomorphology which describes the relative spacing of drainage lines. It is a factor underlying lithology, infiltration capacity and relief aspect of the terrain. According to Horton (1945), Drainage Texture is the total number of stream segments of all orders per perimeter of the basin. The value of *T* depends upon a number of natural factors such as climate, rainfall, vegetation, rock and soil type, infiltration capacity, relief and stage of development (Smith, 1950). Similar to the drainage density, drainage texture can be classified into very coarse (<2), coarse (2 to 4), moderate (4 to 6), fine (6 to 8) and very fine (>8) (Smith, 1950).

xvi. **Drainage Intensity (I_d):** Drainage intensity refers to the ratio of the stream frequency to the drainage density (Faniran, 1968). The value of I_d reveals the extent of the effect of stream frequency and drainage density on the extent to which the soil surface has been eroded by agents of soil erosion.

xvii. **Constant of Channel Maintenance (C_m):** The constant of channel maintenance (C_m) refers to the area of the basin surface needed to sustain a unit length of stream channel (Horton, 1945; Schumm, 1956). The constant of channel maintenance is a function of ground hydraulic conductivity.

xviii. **Length of Overland Flow (L_o):** According to Horton (1945), the length of overland flow refers to the length of flow of the rain water over the ground surface before it gets concentrated in definite stream channels. In other words, it is the length of the runoff of the rain water. It is measured as the length of non-channel flow path from a

point on the watershed divide to a point on the adjacent stream channel and is computed as one half of the reciprocal of drainage density. The length of overland flow of a drainage basin is an important measure of erodibility affecting hydrologic response and physiographic development of watershed (Horton, 1945). In other words, the smaller the value of length of overland flow, the quicker the surface runoff and lesser erosion and vice-versa.

xix. **Channel Sinuosity (S_c):** Sinuosity is a quantitative index of stream meandering and a distinctive property of channel pattern which is related to the morphological, sedimentological and hydraulic characteristics of stream channels. According to Brice (1984), channel sinuosity is calculated as the ratio of total stream length to valley length (Longest flow path of the basin). A channel sinuosity value of 1 indicates a straight course of the streams, 1 -1.5 indicates a sinuous course and values greater than 1.5 indicate meandering course (Langbein and Leopold, 1964).

xx. **Time of Concentration (T_c):** This is the time required to move the surface runoff from the remotest point of the basin to its outlet. High value of time of concentration will produce low runoff rate.

xxi. Time from Peak to Recession (N): This is the time required for the flood hydrograph to return from peak to minimum. It is estimated as a function of the basin area (Mustafa and Yusuf, 2012).

2.3.2.2 Linear aspects

The Linear aspect of the drainage basin is characterized by the stream links and nodes (Withanage *et al.*, 2015). The Linear aspects of the river basin are briefly described as follows:

i. **Stream Order (U):** Stream order according to Strahler (1964) is defined as a measure of the position of a stream in the hierarchy of tributaries. Furthermore, it is the relative position or rank of a stream channel segment in a drainage network. According to Strahler (1964), the smallest unbranched stream, that is, finger tip stream with no tributaries are designated as the 1^{st} order stream, the one formed by the merging of two such 1^{st} order segments is the 2^{nd} order stream and so on. He further stated that Stream order is a useful indicator of stream size, drainage area and discharge. Furthermore, stream order is inversely proportional to stream frequency.

ii. Stream Number (N_u): Stream number refers to the count of stream channels in a given order. Stream numbering follows Horton's law which states the number of streams of different orders in a given basin tends closely to approximate as inverse geometric series of which the first term is unity and the ratio is the bifurcation ratio (Horton, 1932). Stream number is directly proportional to the size of contributing basin and the channel dimension. The higher the stream number the lower the hydraulic conductivity and infiltration.

iii. **Stream Length (L_u):** Stream length is the total length of stream segment of each of the consecutive order in the basin (Horton, 1945). It is the quantification of hydrological characteristics of bedrock and the drainage extent. When bedrock is of permeable character then only small number of relatively longer streams is formed in a well drained basin area. On the other hand, when the bed rock is less permeable then large number of smaller lengths of streams in the basin is produced (Kulkarni, 2015).

iv. **Mean Stream Length (L_{um}):** Stream length of an order divided by its stream number gives the mean stream length of that order. Mean stream length reveals the size of components of drainage network and its contributing surface. It is directly proportional to the size and topography of the drainage basin (Kulkarni, 2015).

v. **Bifurcation Ratio (R_b):** The ratio of number of streams of any given order (N_u) to the number of streams in the next higher order (N_{u+1}) is called bifurcation ratio (Horton, 1932; Schumm, 1956). It generally ranges between 3 and 5 for natural drainage basins without differential geological controls and only reaches higher values where geological controls favour the development of elongated narrow basins (Strahler, 1964). Elongated basin with high bifurcation ratio yields a low but extended peak flow while a circular basin with low bifurcation ratio produces a sharp peak flow.

vi. **Stream Length Ratio (R_L):** Horton's law of stream lengths states that, there exists a geometric relationship between the average length of streams of a given order and the corresponding order, U. The parameter of this relationship is the Stream Length Ratio, R_L. The stream length ratio is a very important parameter in the study of surface runoff and erosion in a basin (Horton, 1945; Schumm, 1956).

2.3.2.3 Relief aspects

The relief aspects of a drainage basin refer to to the three dimensional features of the basin involving area, volume and altitude of vertical dimension of landforms wherein different morphometric methods are used to analyze terrain characteristics. The basin relief, relief ratio, relative relief and Basin slope are commonly evaluating relief aspects (Horton, 1945; Melton, 1957; Miller, 1953; Schumm, 1956; Strahler, 1964) and are briefly described as follows.

i. **Basin Relief (H):** The basin relief (H) of the watershed is defined as the difference in the elevation between the highest point (Z) and the lowest point (z) on the valley floor (Strahler, 1957).

ii. **Relief Ratio (R_h):** The Relief ratio (R_h) of a watershed can be obtained by dividing the basin relief (H) by the maximum basin length (L_b). Relief ratio is a

dimensionless ratio which is equal to the tangent of the angle formed by two planes intersecting at the mouth of the basin (Schumm, 1956). He further stated that it is a measure of the overall steepness of a river basin and it is an indicator of the intensity of the erosion process operating on the slope of the basin. Furthermore, relief ratio is an indicator of the potential energy available to move water and sediments down the slope. Therefore, high value of relief ratio indicates quick runoff of water resulting in large peaked and steep limbed runoff hydrograph. Low relief ratio is indicative of gentle topography while high relief ratio is characteristic of steep slopes.

iii. **Relative Relief (R_{hp}):** The relative relief (R_{hp}) is an important morphometric variable used for the overall assessment of morphological characteristics of the terrain. According to Melton (1957), relative relief (R_{hp}) is the ratio of the basin relief (H) to its perimeter (P).

iv. **Ruggedness Number (R_N):** It is defined as the product of the Basin relief (H) and the drainage density (D_d). It gives an idea of the overall roughness of a watershed.

v. **Basin Slope (S):** The Basin slope is expressed as the difference in elevation between two points divided by the horizontal difference between them. The slope of the basin affects the velocity of flow in the stream channel as well as the runoff velocity in the entire watershed. This affects the flow carrying capacity at any given location on the stream course or at the outlet (Patra, 2008).

Waikar and Nilawar (2014) carried out morphometric analysis for the drainage basin in Charthana, located in Parbhani district of Maharashtra state in India, to extract linear, areal and relief aspects of the basin characteristics. The parameters estimated include stream length, bifurcation ratio, drainage density, stream frequency, texture ratio, elongation ratio, circularity ratio and form factor ratio amongst others. Similarly, Raj and Azeez (2012) carried out morphometric analysis for Barathapuzha River in Southern

India. Remote sensing and GIS tools were used to study the morphometric characteristics of the basin. They also determined the linear, areal and relief aspects of the watershed characteristics. They noted that the Barathapuzha River, the second longest river in the state of Kerala was a seventh order river formed by several lower order streams resulting to a dentritic flow pattern. Similarly, Withanage *et al.* (2014) carried out morphometric analysis of the Gal Oya River Basin in Sri Lanka to assess its hydrological characteristics and flood potentials based on the morphological characteristics. They utilized spatial data obtained from Geographical Information Systems (GIS) to estimate the linear, areal and relief aspects of the basin characteristics. They noted that the Gal Oya River was a 6^{th} order river network following the Strahler's classification with a dendritic drainage pattern and moderate drainage texture. Martins and Gadiga (2015) also carried out morphometric analysis of upper Yedzaram catchment of Mubi in Adamawa State, Nigeria using Geographic Information System (GIS). The study focused on the hydrological and geometrical analysis with emphasis on the linear and areal morphometric characteristics of the catchment.

2.4 STREAM GAUGING AND DEVELOPMENT OF RATING CURVE

Measurement of surface water flow is an important aspect of hydrology related project such as water quality monitoring, flooding, geomorphology, and aquatic life support amongst others (Meals and Dressing, 2008). Accurate measurement of discharge of a basin therefore is the first and most essential requirement for planning and management of any water resource project including flood forecasting (Patra, 2008; Daffi, 2013). Discharge measurements are usually done once in a day during normal periods and on an hourly basis during floods. This continuous measurement is usually impractical and very expensive, especially in less developed and developing countries such as Nigeria, where

the cost of establishing and maintaining a network of stream gauges is prohibitive (Patra, 2008; WMO, 2010). The rating curve is a most frequently used methodology to overcome this difficulty (Leonard *et al.*, 2000; Patra, 2008) reducing the problem to a simple reading of river stage and then finding the corresponding discharge either from stage-discharge graph or equation established at the site (Meals and Dressing, 2008; Patra, 2008; Sadeghian *et al.*, 2016).

2.4.1 Stage Measurement

The stage of a stream or lake is the height or elevation of the water surface above an established datum plane (Sauer and Turnipseed, 2010). Stream stage is an important parameter of stream flow measurement. While stage itself may be of interest in some cases, such as flood management or the design of structures, it can also be a surrogate for stream cross-sectional area if the stream channel has been surveyed and a component of a stage-discharge relationship used to calculate flow (Meals and Dressing, 2008).

Mustafa and Yusuf (2012) listed the following methods for measuring stage height.

i. Visually observing staff gauges
ii. Manually operated weight or electrical sensors
iii. Float operated stage gauges and
iv. Depth sensor using either electrical resistance or capacitance-resistance or pressure principles.

The further noted that the commonest of them is the float type which moves with the falling or rising of water surface.

2.4.2 Discharge Measurement

Direct stream gauging is the most reliable method of determining surface runoff because it is an accurate and continual study of water flows through rivers and streams over a period of years by actual gauged discharge measurements. The most common methods that could be employed as obtained from Patra (2008), Mustafa and Yusuf (2012) and Mays (2005) are discharge measuring structures, approximate slope-area method, radiotracer method, dilution or dye method, electromagnetic induction method and velocity-area method. The method used for this study is the velocity-area method because it is the most commonly used method for estimating river discharge globally (Herschy 1993).

2.4.2.1 Discharge measurement by Velocity-Area method

This method is based on the continuity equation. It involves the measurement of velocity at the gauging site and the corresponding area to obtain river discharge directly in the field. It involves the measurement of velocity and area.

a. ***Measurement of velocity:*** The velocity of flowing stream can be measured by using floats method, ultrasonic methods and current meter method (Patra, 2008). The method used for measuring velocity in this study is the current meter method. It is a more accurate method for the determination of velocity of flow (Patra, 2008). There are various types of current meters. There is the vertical axis type or price current meter which consists of a horizontal wheel carrying a series of conical cups around a vertical axis, the tail vans to keep it along the direction of flow and the balancing weight at the bottom. There is also the propeller or horizontal axis current meter which has propellers fixed to one end of a horizontal shaft and the other end carrying a set of fins which help to stabilize

it against the velocity of flowing water. The last type of current meter is the optical type which is used as surface floats during high floods. The speed of revolution of the current meter is proportional to the velocity. The number of revolutions in a given time is counted on a digital counter or by use of earphones. Recent current meters give the velocity directly in m/s on the digital counter. Measurement can be done by wading in shallow streams or from a bridge or overhead cableway for big rivers.

b. ***Measurement of Area:*** The velocity of water at any river section varies in all the direction being zero at the river periphery and changes rapidly as one moves from the channel bed. A single velocity-area measurement for the entire section will give highly erroneous results. Therefore, the cross-section of river at the gauging site is divided into a number of subsections by imaginary verticals. The number of such subsections for a stream are decided from the following criteria:

i. Discharge carried by any subsection should be up to 10 % of the total discharge of the entire section.
ii. The width of any subsection should be about 1/15 to 1/20 of the total width of the river at the site.
iii. There should not be any large velocity difference between the adjacent subsections
iv. The discharge variations between adjacent subsections should be between 5 and 10%.

The guidelines for the selecting number and width of subsections for different river channel width are presented in Table 2.2.

Table 2.2: Guidelines for deciding Number of Subsections of River for Discharge Measurement

River or Channel Width (m)	Number of observation sections	Maximum section width (m)
Upto 15	15	1.5
Between 15-90	15	6
Between 90-180	15	15
Over 180	25	To be fixed suitably

Source: Patra (2008)

Computation of area and water depths at various subsections is carried out by any of the following methods:

i. Wading or sounding rod

ii. Lead-line or cable arrangement

iii. Echo sounder

Selecting a measurement section with desirable qualities is the first step in making a conventional current-meter measurement of discharge. The section should meet as many of the following criteria as possible:

i. Cross section lies within a straight reach, and streamlines are parallel to each other.

ii. Velocities are greater than 0.15m/s and depths are greater than 0.15m.

iii. Streambed is relatively uniform and free of numerous boulders and heavy aquatic growth.

iv. Flow is relatively uniform and free of eddies, slack water, and excessive turbulence.

v. Measurement section is relatively close to the gauging-station control to avoid the effect of tributary inflow between the measurement section and control and to

avoid the effect of storage between the measurement section and control during periods of rapidly changing stage.

2.4.3 Development, Fitting and Extension of Rating Curve

The empirical, or theoretical, relationship existing between the water-surface stage (that is, the water level) and the simultaneous flow discharge in an open channel is known as stage-discharge relation or rating curve (Braca, 2008). The rating curve is a very important tool in surface hydrology because the reliability of discharge data values is highly dependent on a satisfactory stage-discharge relationship at the gauging station. It can be used to obtain an estimate of the discharge of a large flood where only the stage data is available, by extension of the rating curve (Patra, 2008; Mustafa and Yusuf, 2012). The preparation of rating curves is an essentially empirical task which requires a wide theoretical background in order to create a reliable tool to transform measured water level to discharge. The rating curve has been and is still an extensively used tool in hydrology to estimate discharge in natural and/or artificial open channels. It has been a common practice to measure the discharge of streams at suitable times, usually by a current meter or other methods since the early 19th century (Rantz, 1982a; ISO 1100-2, 2010). Meanwhile, the corresponding stage is also measured; a curve of discharge against stage can then be built by fitting these data with a power curve. Thus, a traditional and simple way to gather information on current discharge is to measure the water level with gauges and to use the stage-discharge relationship to estimate the flow discharge.

The most commonly used stage-discharge relationship or rating curve treats the discharge as a unique function of the stage which typically follows a power curve of the form

$Q = K(H - h)^m$ in which K, h and m are calibration coefficients (Rantz, 1982b; Herschy, 1995, Braca, 2008; Patra, 2008 and ISO 1100-2, 2010).

The gauging site could be a permanent control when the stage-discharge relationship remains unchanged with time or a shifting control when it changes with time. The rating curve is only valid for a permanent control (ISO 18365, 2013).

ISO 1100-2 (2010) stated that although completely automatic rating analysis using the curve-fitting programmes normally available for computers is technically possible, it is usually discouraged. The reason for this is the fact that computer programmes use least squares fitting technique, but do not allow any judgment as to the quality of individual measurements, especially outliers, and about the hydraulic factors that are related to bends and/or breaks in rating curves. As a result, extrapolation of an automatically fitted curve is generally unsatisfactory. Fitting an equation to a manually drawn curve by inputting selected points from that curve rather than from the observed data to a fitting programme avoids the problem and is advised wherever the equation format is needed. Meanwhile, another way to avoid the problem is by fitting the rating curve by determination of the calibration coefficients via linear regression analysis. The logarithm of both sides of the curve is taken to transform the equation into a linear form.

Patra (2008) outlined the following methods for assessing the efficiency of the fitted curve:

i. **The standard error of estimate (S_e)**: This is the measure of variation of observations made around the computed regression line. It is used to check the accuracy of predictions made with the regression line.

ii. **The correlation coefficient (r):** This is a measure of the strength and direction of the linear relationship between two variables. It is defined as the covariance of the variables divided by the product of their standard deviations. It is an indicator of how well the regression equation truly represents the set of data.

iii. **Coefficient of Determination (R^2):** This is a statistical measure of how well the regression line approximates the real data points. It gives some information about the goodness of fit of a model. It is interpreted as the proportion of the variance in the dependent variable that is predictable from the independent variable. The coefficient of determination ranges from 0 to 1. It is the square of the correlation (r) between *x* and *y* scores. An R^2 of zero means that the dependent variable cannot be predicted from the independent variable while an R^2 of one means the dependent variable can be predicted without error from the independent variable. An R^2 between 0 and 1 indicates the extent to which the dependent variable is predictable (http://www.stattrek.com).

iv. **The Efficiency (η):** This is the overall efficiency of the fitting process as a function of the standard error of estimate and the variance of the observed discharge. Patra (2008) further noted that the closer the efficiency is to 100 % the more efficient the fitted curve.

This approach for the development and fitting of rating curve was used by Maroof *et al.* (2015) to develop a stage-discharge relationship or rating curve for the Ero-Omola falls in Kwara State, Nigeria. They determined the calibration coefficients by method of least square. The ease and efficiency reported by them motivated its adoption in this study.

2.5 DETERMINATION OF SOIL CHARACTERISTICS

Soil characteristics can either be remotely sensed or obtained via field measurement.

2.5.1 Remotely Sensed Soil Data

With the growing application of Remote Sensing and Geographic Information System in various fields, there is a possibility of obtaining soil characteristics for any part of the world without necessarily carrying out a field observation. In recognition of the urgent necessity for improved soil and easily accessible global soil information especially in the context of climate change, the Food and Agriculture Organization of the United Nations (FAO) and the International Institute for Applied Systems Analysis (IIASA) took the initiative of combining the recently collected vast volumes of regional and national updates of soil information into a new comprehensive Harmonized World Soil Databas (Nachtergaele *et al.*, 2009). Consequently, the Harmonized Soil Database of the World was produced as a result of collaboration between the the Food and Agriculture Organization of the United Nations, the International Institute for Applied Systems Analysis (IIASA), the International Soil Reference and Information Center (ISRIC), Institute of Soil Science, Chinese Academy of Science (ISSCAS) and the Joint Research Center of the European Union (JRC).

The Harmonized World Soil Database is a 30 arc-second raster database with over 15,000 different soil mapping units that combines existing regional and national updates of soil information worldwide. The soil information obtained from the Soil Map of the World and the Soil and Terrain, the European Soil Bureau Network and the Soil Geographical Database for Europe, Soil Map of China and Soil parameter data based on the World Inventory of Soil Emission Potential were combined with the information contained

within the 1:5,000,000 scale FAO-UNESCO Soil Map of the World (www.fao.org/soils-portal). The raster database resulting from this collaboration consists of 21,600 rows and 43,200 columns, which are linked to harmonized soil property data. The use of a standardized structure allows for the linkage of the attribute data with the raster map to display or query the composition in terms of soil units and the characterization of selected soil parameters.

2.5.2 Field Determination of Soil Characteristics

The second method of obtaining soil information is by conventional field measurement either in situ or ex situ. Some of the soil properties related to runoff and flood studies as well as their methods of determination are briefly described as follows:

2.5.2.1 Determination of soil index properties

Soil index properties refer to the properties of soil that form the bases for its identification and classification. They include properties such as consistency limits, particle size distribution, specific gravity, and moisture content, amongst others.

a. Consistency Limits

The Swedish soil scientist Albert Atterberg originally defined seven "limits of consistency" to classify fine-grained soils. Recently, only two these limits (the liquid and plastic limits) have been commonly used in recent engineering practices. The Atterberg limits are based on the moisture content of the soil. The plastic limit is the moisture content at which the soil changes from a semi-solid to a plastic (flexible) state. The liquid limit on the other hand is the moisture content at which the soil changes from a plastic to a viscous fluid state. Amongst other applications in geotechnical engineering, these Atterberg limits are used to classify a fine-grained soil according to the American

Association of State Highway and Transportation Officials (AASHTO) and Unified Soil Classification Systems (USCS) soil classification systems.

b. Particle size distribution (Sieve Analysis)

The distribution of different grain sizes affects the engineering properties of soil. Grain size analysis provides the grain size distribution, and it is required in classifying the soil. Sieve analysis is a simple and proven method of separating bulk soil materials into size fractions and to ascertain the particle size distribution. This is done by weighing the single fractions retained on respective sieves. Usually, sieving processes are carried out on dry material. However, when dry sieving cannot produce an adequate degree of separation between the individual fractions, wet sieving is adopted.

c. Specific Gravity

The specific gravity of a soil is the ratio of the mass of a given volume of the material at particular temperature to the mass of an equal volume of water at the same temperature. The specific gravity of a soil is used in relating a weight of soil to its volume and in calculation of phase relationship, that is, the relative volume of solids to water and air in a given volume soil. The specific gravity is also used in the computations of most of the laboratory tests, and is needed in nearly all pressure, settlement, and stability problems in soil engineering.

2.5.2.1 Determination of infiltration capacity and hydraulic conductivity

a. Infiltration Measurement

Water infiltration refers to the process of water movement from the ground surface into the soil. It is an important component of the hydrological cycle (Gana, 2011; Haghiabi *et*

al., 2011). The infiltration capacity of soil is a determinant of the extent of surface runoff and groundwater recharge (Chow et al., 1988).

Infiltration characteristics of soils can be estimated either by direct measurement on the field and/or mathematically fitting field infiltration data to infiltration models (Oku and Aiyelari, 2011). The hydraulic conductivity is of critical importance to infiltration rate since it expresses how easily water flows through soil and is a measure of the soil's resistance to flow. In contrast to the unsaturated hydraulic conductivity, the saturated hydraulic conductivity at full saturation is used as a parameter in many of the infiltration equations, since it is easier to determine than either the unsaturated hydraulic conductivity or the diffusivity.

Generally, Reddy (2008) outlined two approaches to the determination of infiltration rate. One of these approaches estimates the infiltration rates by analyzing the observed rainfall hyetograph and the runoff hydrograph from a small plot or a natural watershed while the other approach uses infiltrometer. There are two types of infiltrometer: the flooding type and the rainfall simulator. The focus of this review is the flooding type which was used in this study.

The flooding type infiltrometer can either be single ring or double ring. In both cases, water is applied in the form of a sheet usually with a constant depth of flooding. The rings are used to delineate the sample area. The one ring type is known as a simple infiltrometer or a tube infiltrometer while the two ring type is known as double ring infiltrometer.

The procedure for infiltration measurement by double-ring infiltrometer has been described by Parr and Bertrand (1960) and Bouwer (1986). The double ring infiltrometer consists of two concentric rings as shown in Fig. 2.1.

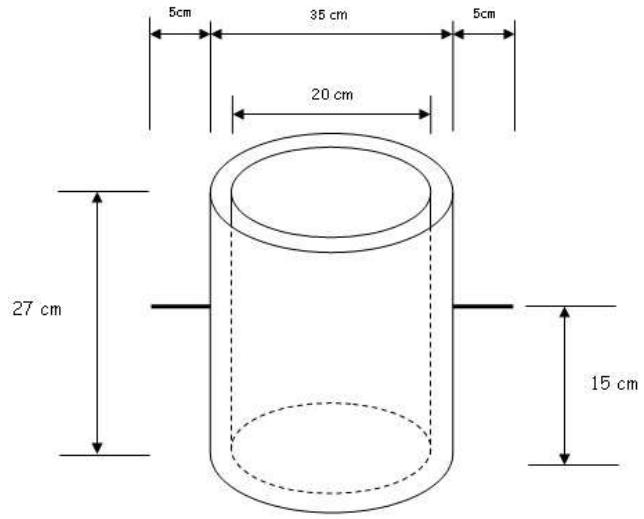


Fig. 2.1: Schema of Double Ring Infiltrometer

The infiltration rate is determined by the amount of water that infiltrates into the soils per surface area per unit time. The purpose of the outer ring is to ensure a one – dimensional flow of water from the inner ring. The two rings are usually made of materials of same thickness and installed to a maximum depth of 15 cm using a hammer and a wood placed across the rings. As a precaution, the installation is done carefully avoiding disturbance of the soil surface as much as possible. The soil surface around the outer surfaces are usually compacted a little to avoid seepage during infiltration test. A Jute bag is wrapped around the surface before pouring water into the rings to avoid scouring of the soil within the rings. The depth of water in the inner ring is usually taken into account immediately marking the beginning of the infiltration measurement. Refilling is done when the water level in the rings has gone down considerably. For every refill of the inner ring, the outer ring is also refilled to the same level with the inner ring. The depth of water that infiltrated into the soil at a given time is considered as the change in depth of the graduated float or meter rule on the surface of water in the inner ring. In situ infiltration measurement such as double infiltration test amongst others have been reported to provide an estimate of infiltration rates that are generally representative of the actual site-specific infiltration rate (Telis, 2001; Philips and Kitch, 2011; Ajayi, 2015).

b. Estimation of Saturated Hydraulic Conductivity

Philip (1957) developed an infinite-series solution to solve the non-linear partial differential Richard's (1931) equation, which describes transient fluid flow in a porous medium for both vertical and horizontal infiltration. Philip's rapidly converging series solves the flow equation for a homogeneous deep soil with uniform initial water content under ponded conditions. The value of saturated hydraulic conductivity, *K* can used to classify the respective soils.

2.6 EVALUATION OF LAND USE/LAND COVER CHARACTERISTICS

The assessment of land use/ land cover changes is very important in catchment flood studies. While imageries from various satellites such as Quickbird, Spot amongst others exist and are very useful in the analysis of land use/land cover, the focus of this review is narrowed to those from the Landsat Thematic Mapper ™ and the Enhanced Thematic plus (ETM+) sensors which are the imageries utilized in this study. The band characteristics of the Landsat 5, 7 and 8 are presented in Table 2.3.

2.6.1 Image Classification

The process of assigning land cover classes to pixels is refered to as Image classification (http://gisgeography.com).

The three main image classification techniques in remote sensing are unsupervised, supervised and object-oriented image classification techniques. Unsupervised and supervised image classification techniques are the two most common approaches but in recent time, the object-based classification has found wide application because of its useful for high-resolution data.

Table 2.3: Band characteristics for Landsat 5, 7 and 8 imageries

Band	Description	Wavelength (μm)	Resolution (m)
	Landsat 5 (TM Sensor)		
1	Blue	0.450 – 0.520	30
2	Green	0.520 – 0.600	30
3	Red	0.630 – 0.690	30
4	Near Infra Red (NIR)	0.760 – 0.900	30
5	Short Wave Infra Red (SWIR)-1	1.550 – 1.750	30
6	Long Wave Infra Red (LWIR)-1	10.40 – 12.50	120
7	Short Wave Infra Red (SWIR)-2	2.080 – 2.350	30
	Landsat 7 (ETM+ Sensor)		
1	Blue	0.450 – 0.515	30
2	Green	0.525 – 0.600	30
3	Red	0.630 – 0.980	30
4	Near Infra Red (NIR)	0.845 – 0.885	30
5	Short Wave Infra Red (SWIR)-1	1.560 – 1.660	30
6	Long Wave Infra Red (LWIR)-1	10.30 – 11.30	100
7	Short Wave Infra Red (SWIR)-2	2.100 – 2.300	30
8	Panchromatic (Pan)	0.500 -0.680	15
	Landsat 8 (ETM+ Sensor)		
1	Coastal/Aerosol		30
2	Blue	0.450 – 0.515	30
3	Green	0.525 – 0.600	30
4	Red	0.630 – 0.980	30
5	Near Infra Red (NIR)	0.845 – 0.885	30
6	Short Wave Infra Red (SWIR)-1	1.560 – 1.660	30
7	Short Wave Infra Red (SWIR)-2	2.100 – 2.300	30
8	Panchromatic (Pan)	0.500 -0.680	15
9	Cirrus	1.360 – 1.390	30
10	Long Wave Infra Red (LWIR)-1	10.30 – 11.30	100
11	Long Wave Infra Red (LWIR)-2	11.50 – 12.50	100

Source: http://web.pdx.edu; NASA (2010)

In the unsupervised classification technique, the pixels are first grouped into "clusters" based on their properties, using image clustering algorithms such as *K*-means and *ISODATA*. The number of groups is specified after the cluster algorithm is selected. The user then manually identifies each cluster with land cover classes and merges related clusters where necessary. It is the most basic image classification technique. It is an easy way to segment and understand an image (http://gisgeography.com). In supervised classification on the other the user selects representative samples called 'training site' for each land cover class. The software then uses these "training sites" and applies them to the entire image. Supervised classification uses the spectral signature defined in the

training set. The common supervised classification algorithms are maximum likelihood and minimum-distance classification.

The last image classification technique is the object-based (or object-oriented) image analysis classification. This technique groups pixels into representative shapes and sizes. This process is multi-resolution segmentation or segment mean shift which produces homogenous image objects by grouping pixels. The classification processes are shown in Fig. 2.2.

2.6.2 Land Cover Indices

Supervised and object-based image classification techniques have been reported to be slowed down by the requirement of selecting training samples for all cover types to be mapped. Therefore, considerable efforts have been made to simplify the process of automatically mapping land covers with the development of indices (Zha *et al.*, 2003). Some of the commonly used indices are Normalized Difference Vegetation Index (NDVI), Normalized Difference Built-up Index (NDBI), Normalized Difference Water Index (NDWI), amongst others. These indices take advantage of the unique shape of the reflectance curve of the respective land cover type such as vegetation. In as much as these indices along cannot be relied upon as the sole land cover classification techniques they can give significant guidance on the development of training sites for supervised classifications.

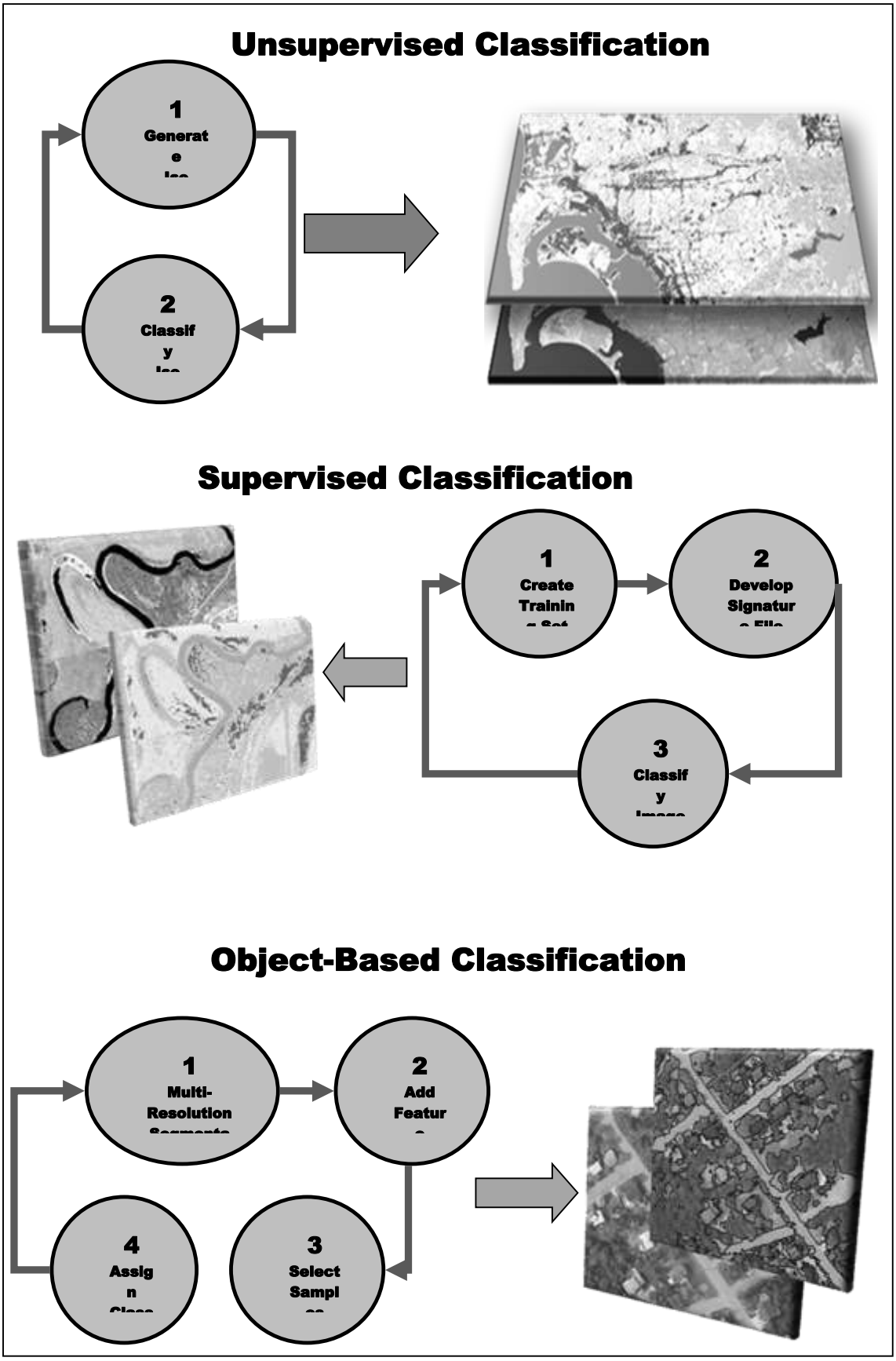


Fig. 2.2: Process Flow diagram for Image Classification Methods
Source: Adapted from http://gisgeography.com

2.7 RUNOFF ESTIMATION

The relationship between rainfall and runoff for a catchment is a very complex one because it is influenced by such factors as the pattern of storm, antecedent moisture condition and basin characteristics (Mustafa and Yusuf, 2012). These complexities and the data scarcity in many developing countries such as Nigeria have necessitated the development of various techniques to estimate runoff from readily available data. It can either be by methods of extension of existing runoff records (such as Thomas-Fiering model (T-F), harmonic analysis model, correlation with adjoining stations, regression techniques, Longbeins methods and flow duration curves), methods of estimation of runoff from rainfall records (such as rainfall-runoff correlation, rainfall-runoff relation of neighbouring sites, empirical relations, runoff equations and runoff simulation models) or rainfall runoff modelling for ungauged catchments (Patra, 2008; Mustafa and Yusuf, 2012; Chow, 1956). The method of extension of existing runoff records by Thomas-Fiering's model and rainfall-runoff modelling for ungauged catchment by Soil Conservation Services Curve Number (SCS-CN) and rational methods were applied and compared in this study.

2.7.1 Extension of Runoff Records using Thomas-Fiering's Model

This method can be used when a runoff series at the site of interest for a period of about 12 years or more is available (Patra, 2008). The Thomas-Fiering model is an Autoregressive Markov model which has been applied successfully to generate sequentially the monthly, 10-daily or weekly volume of discharge from a serially dependent series. The model assumes that a monthly or 10-daily variable is dependent only on the just recent one or two variables involving non-stationarity both in mean and standard deviation.

Harms and Campbell (1967) applied the Thomas-Fierring Model to two representative Pacific Northwest Rivers and concluded that the model provides an authentic representation of stream flow. Stedinger and Taylor (1982) used a range of monthly stream flow models including Thomas-Fiering Model to generate synthetic data for the upper Delaware River basin in New York State. They demonstrated that the model was able to reproduce the basic unbiased statistics of the historical data. More so, Lebbe (1991) used the lognormal Markov model (a modification of the Thomas-Fierring model) to generate synthetic flow data for five reservoirs in Afghanistan and was able to preserve the statistical properties of the historical data used. Similarly, Maroof *et al.* (2015) employed the Thomas-Fierring Model to extend the 12 months discharge data at Ero-Omola falls as a basis to study its hydropower development potential. Celeste *et al.* (2004) also utilized Thomas-Fiering stochastic model for synthetic stream flow generation to determine monthly inflow scenarios for the watershed of the reservoir that supplies the city of Matsuyama, Ehime Prefecture. The scenarios were to be used by a stochastic programming model being developed for the optimal operation of the reservoir. The reason for their choice of this model is that it allows for the non-stationarity of seasonal data. They used 20 years of historical data for calibrating the model parameters and generated a new 20-year synthetic series. They concluded that the model can preserve the characteristics of the historical series and effectively incorporate them into the generated data. Furthermore, Ahmad *et al.* (2001) used the Thomas-Fiering Model alongside Autoregressive Integrated Moving Average (ARIMA) model and deseasonalised model to forecast water quality of river Ganges in India based on the data collected from 1981 to 1990. Similarly, Kurunc *et al.* (2005) evaluated the forecasting performance of two modeling approaches, ARIMA and Thomas–Fiering, for selected water quality constituents and stream flow of the Yeşilırmak River at Durucasu monitoring station

using 13-year (1984–1996) monthly time series records to obtain the best model. They used the two approaches to generate 5-year (1997–2001) data for the river. They concluded based on the root mean square error and mean absolute error calculated for the two approaches that Thomas–Fiering model presented more reliable forecasting of water quality constituents and stream flow than ARIMA model.

2.7.2 Rainfall-Runoff Modelling for Ungauged Catchment using Remote Sensing and GIS

Rainfall-runoff modelling refers to the use of rainfall data to generate runoff data. Establishing a rainfall-runoff relationship is an important aspect of hydrological analysis required to generate stream flow data for data scarce catchments which are ungauged (Makungo *et al*., 2010; Mustafa and Yusuf, 2012).

Conventional models for prediction of river discharge may require considerable hydrological and meteorological data which are expensive and difficult to collect. The use of remotely sensed data and Geographic Information System, however, requires only rainfall data and hydrological soil groups. Remote sensing technology can be used to augment the conventional methods in rainfall-runoff modelling by interpreting satellite data to derive thematic layers of land use, vegetation, drainage amongst others. These combined with conventionally measured climatic parameters such as precipitation, temperature and topographic parameters such as height, contours and slopes provide the necessary inputs to the rainfall-runoff models (Nayak and Jaiswal, 2001).

2.7.2.1 Soil Conservation Service-Curve Number Method

The Soil Conservation Service – Curve Number (SCS-CN) method utilizes Remote Sensing and Geographic Information System for rainfall – runoff modelling. It has been

tested and extensively used for different watersheds in America, where it originated, India and other countries.

The Soil Conservation Services Curve Number (SCS-CN) method was developed by the United States Department of Agricultural Soil Conservation in 1972. It is one of the most popular methods used in computing surface runoff from rainfall by establishing a rainfall-runoff relation for a watershed. It involves the use of simple formulae and easily accessible tables and curves.

For a storm on a watershed, the depth of excess precipitation or direct runoff *'Q'* is always expected to be less than or equal to the depth of actual precipitation *'P'*. Also after runoff begins the additional depth of water retained in the watershed *'F_a'* is less than or equal to the Potential Maximum Retention of the soil, *S*. Some amount of rainfall *'I_a'* is abstracted at the initial stage, before ponding, for which no runoff will occur. Therefore potential runoff is *'$P - I_a$'*. (Mays, 2005).

The method assumes that the ratios of the actual to the potential are equal as expressed by Eq. (2.1).

$$\frac{F_a}{S} = \frac{Q}{P - I_a} \tag{2.1}$$

From continuity, the expression for precipitation is given as:

$$P = Q + I_a + F_a \tag{2.2}$$

Combining the two equations gives the basic equation for computing the depth of direct runoff using the SCS-CN method, expressed by Eq. (2.3).

$$Q = \frac{(P - I_a)^2}{\{(P - I_a) + S)\}} (P \geq I_a \; else \; Q = 0) \tag{2.3}$$

The relationship between *S* and I_a developed from data collected from the study of various small watersheds in U.S.A are as expressed by Eq. (2.4a) to (2.4c) respectively.

$$I_a = 0.3S \; for \; AMCI \tag{2.4a}$$

$$I_a = 0.2S \; for \; AMCII \qquad (2.4b)$$

$$I_a = 0.1S \; for \; AMCIII \qquad (2.4c)$$

The Antecedent Moisture Condition (AMC) is the index of the soil condition with respect to runoff potential before rainfall. The three categories of the AMC are shown in Table 2.4:

Table 2.4: Categories of Antecedent Moisture Content

AMC Class	AMC (mm)	Condition
I	<35	Dry soil but not at the wilting point (Low Moisture)
II	35 – 52.5	Average conditions (Normally used for annual flood estimates)
III	>52.5	Saturated soils; heavy rainfall or light rain over preceding few days

TR-55 (1986)

Empirical studies indicate that the *'S'* value is derived from the Curve Number (*CN*) using the formulae expressed by Eq. (2.5)

$$S = \frac{25400}{CN} - 254 \qquad (2.5)$$

In which *CN* is a runoff curve number that is a function of watershed hydrologic land use / land cover, hydrologic soil groups and antecedent moisture conditions. It is a dimensionless number defined such that $0 \leq CN \leq 100$. $CN < 100$ for natural surfaces except for impervious and water surfaces where it is 100.

Curve Number (CN) can be estimated by combining the soil and land cover characteristics.

The Curve Numbers for all the Hydrologic Soil Groups (HSG) A, B, C and D corresponding to the various landcover classes were obtained from from standard tables (Appendix IX).

The Hydrologic Soil Group classifications based on texture of the distributed soil are described in Table 2.5.

Table 2.5: Classification of Hydrological Soil Groups

Group	Infiltration Rate (mm/hr)		Soil Texture
A	HIGH	>25	Deep sand, deep loess, aggregated silt
B	MODERATE	12.5 – 25	Shallow loess, sandy loam
C	LOW	2.5 – 12.5	Clay Loams, shallow sandy loam, soils low in organic content, and soils usually high in clay
D	VERY LOW	<2.5	Soils that swell significantly when wet, heavy plastic clays, and certain saline soils

TR-55 (1986)

CN values for AMC I and III can be obtained using the formulae expressed by Eqs. (2.6) and (2.7).

$$CNI = \frac{(4.2 * CNII)}{(10 - 0.058 * CNII)} \quad (2.6)$$

$$CNIII = \frac{(23 * CNII)}{(10 + 0.13 * CNII)} \quad (2.7)$$

SCS Dimensionless Unit Hydrograph: Another important empirical formula for determining the quantity of runoff is the SCS dimensionless unit hydrograph. The time to peak and the peak discharge are parameters that are required. The following assumptions are made for the use of this method (de Brouwer, 1997):

i. The duration of excess rainfall is less or equal to 0.133 x the time of concentration
ii. The rainfall duration is not too long (D < 0.2 time to peak)

Hjelmfelt Jr (1991) investigated the curve number procedure of the Soil Conservation Service and established that it is a logically consistent and experimentally verifiable system. Ponce and Hawkins (1996), in a review of the runoff curve number method stated that the method is widely used in the United States and other countries due to the perceived advantages of its simplicity, predictability, stability, reliance on only one

parameter and its responsiveness to major runoff-producing watershed properties such soil type, land use/treatment, surface condition, and antecedent condition. They however pointed out the method's perceived disadvantages of its marked sensitivity to curve number, the absence of clear guidance on how to vary antecedent condition, varying accuracy for different biomes, the absence of an explicit provision for spatial scale effects and the fixing of the initial abstraction ratio at 0.2, pre-empting a regionalization based on geologic and climatic setting. However, Nayak and Jaiswal (2001) carried out rainfall-runoff modelling using Soil Conservation Services Curve number (SCS-CN) method to estimate runoff volume for the Bebas River in Madhya Pradesh, India. They utilized satellite data and GIS for the Bebas River Catchment, and compared the results with actual discharges measured for the river. They calculated monthly correlation coefficients for the estimated and measured runoff volume and found a seasonal correlation coefficient varying between 0.92 and 0.94. Similarly, Pandey *et al*. (2003) carried out a study to estimate runoff for Karso agricultural watershed which is a part of Damodar Barakar Catchment in Hazaribagh District of Jharkhand State using SCS Curve Number method and GIS tools in Arc Info. They estimated the direct runoff from the daily rainfall data for the year 1993 using the SCS-CN method which was then validated by comparing it with the four selected events of monsoon season. The maximum and minimum deviations were observed to be 28.33 and 3.27 per cent respectively. Furthermore, Salau and Daffi (2009) used the SCS-CN method for the rainfall-runoff modelling of Upper River 'Dep' basin in Bokkos Local Government Area of Plateau State. The land use/land cover map and soil map were processed and intersected in ILWIS 3.1 and a cross map produced from which areas of different land use class and soil combinations were obtained and used for the estimation of the runoff curve numbers. They estimated 21 years monthly runoff depths for the watershed from the rainfall data in MS Excel. They

concluded that about 72.51% of total rainfall on the upper river 'Dep' catchment goes into the streams as surface runoff because of the highly clayey nature of the soil and the terrain while the remaining 27.49% is shared between evapotranspiration and infiltration. The same approach was used by Daffi (2013) to estimate the runoff volume contributed by the two major rivers (River Gwayaka and River Dep) that contribute to the Dep River basin based on the rainfall data obtained for 2009. The results obtained showed that without consideration of slope and time of concentration, River Gwayaka and River Dep contributed 72 % and 25 %, respectively to the Dep Basin.

2.7.2.2 Rational Method

The Rational Method is a simplified method of relating the rainfall intensity and catchment characteristics, to obtain an estimate of the design flood. The application of this simplified method is to be limited to catchments up to 12 km^2 (FMW, 2013). For catchments of larger area, adjustments are applied to prevent over estimation of the design flood. The method is widely used for estimation of the peak runoff of ungauged catchments especially in most road drainage designs. For instance, it is the recommended method of peak runoff estimation for drainage design in the Nigerian Highway Manual. In this method the runoff is related to the rainfall intensity in the formula expressed by Eq. (2.8) (Patra, 2008; Mustafa and Yusuf, 2012)

$$Q = 0.278CIA \qquad (\mathbf{2.8})$$

In which, *C* is the composite runoff coefficient of the catchment, *I is the r*ainfall intensity expressed in millimetres per hour for a certain time of concentration and *A* is the catchment area in square kilometres.

The rational method is based on the following assumptions:

i. The peak rate of runoff at any point is a direct function of the average rainfall intensity during the time of concentration to that point.
ii. The frequency of the peak discharge is the same as the frequency of the average rainfall intensity.
iii. The time of concentration is the time required for the runoff to become established and flow from the most remote part of the drainage area to the point under design.
iv. The coefficient of runoff is the same for all storms of all recurrence probabilities.

Although the basic principles of the rational method are applicable to large drainage areas, reported practice generally limits its use to urban areas of up to 12 km^2. For areas larger than this, storage and subsurface drainage flows result in an attenuation of the runoff hydrograph so that rates of flow tend to be overestimated by the rational formula method unless these are taken into account.

For watersheds with an area greater than 12 km^2 a correction factor can be applied. The correction factor is a general approximation that does not take into account specific catchment characteristics therefore, care should be exercised in using the rational formula in such cases where the catchment area greater than 12 km^2. An alternative to the area correction factor is to divide the catchment into smaller sub-catchments of less than 12 km^2 each and aggregate the peak flows from these catchments using hydrologic routing.

The runoff coefficient accounts for abstractions or losses between rainfall and runoff which may vary for a given drainage area as influenced by differing topographical, vegetation and climatological conditions. The estimation of the runoff coefficient is conventionally the most subjective variable of the Rational Method. The selection of the appropriate value of *C* for a particular catchment requires inspection of the site and should be based upon experience and engineering judgement of the prevailing conditions in the

catchment area but with the introduction of GIS and remote sensing, the respective proportions of the catchment required to determine the runoff coefficient can be accurately determined just like the curve number for the SCS-CN method.

The last component of the rational equation is the rainfall intensity which is the rate of rainfall, given in the unit mm/hr. Although rainfall intensity varies during precipitation events, many procedures used to determine intensity assume a constant rainfall intensity to derive peak flow rates.

The determination of rainfall intensity for hydraulic design depends on the following factors (FMW, 2013):

i. Average frequency of occurrence (or return period),
ii. Intensity duration characteristics of rainfall for selected average frequency of occurrence and
iii. Time of concentration of the catchment.

Rainfall intensity can be determined using any of the following methods described in FMW (2013).

a. Intensity Duration Frequency Equation (1973)
b. IDF Curves for Cities
c. Oyebande's Regional Method (IDF Rainfall Maps of Nigeria and Mathematical method)

The mathematical regional method developed by Oyebande (1982) was used in this study.

Oyebande's Regional Mathematical Method

The development of accurate methods for the estimation of design rainfall intensities for a particular city, region or country requires on-going measurement of rainfall using gauges that can measure the rate of rainfall or intensity. Oyebande (1982) developed a method which allows for the calculation of the rainfall intensity at any location in Nigeria for a range of durations and storm frequencies or return periods. He divided the whole country into ten rainfall zones in order to obtain data for design floods of high return period with a good level of confidence. He studied Rainfall intensity-duration-frequency (IDF) using annual extreme rainfall series available for 35 meteorological stations throughout Nigeria on the basis of which the division was done. The IDF estimates were then used to generate curves for the ten different rainfall zones and for individual stations. IDF isohyetal maps for Nigeria were also generated from graphical estimates based on individual stations. The mathematical method is one of the two (2) he developed for determining rainfall intensity. He derived two basic equations for the calculation of rainfall intensity given the rainfall zone, return period and storm duration. They are expressed by Eq. (2.9a and b):

$$y = \propto (I - \beta) \qquad (\mathbf{2.9a})$$

$$y = \ln(T_r) - \frac{1}{(2T_r)} - \frac{1}{\left(24{T_r}^2\right)} - \frac{1}{\left(8{T_r}^3\right)} \qquad (\mathbf{2.9b})$$

In which y is a factor which depends on the scale and location parameters (α and β), I is the rainfall intensity and T_r is the return period or frequency of occurrence.

The rational method has also been extensively used to determine the peak discharge of ungauged catchments for various design purposes especially the design of highway

drainage structures amongst others. For instance, the recommended method by the Nigerian Highway Manual for peak flow estimation in the absence of gauged data is the rational method (FMW, 2013). Nash (1958) noted that although the origin of the method seems obscure, it has been in use as far back as 1851. Hotchkiss and McCallum (1995) analysed six peak flow methods for small watersheds in Nebraska among which are the Statewide regression equations, the Fletcher method and the rational method. They discovered that the peak flows were close for these three methods mentioned. Similarly, Akan (2002) used the rational method to calculate the peak runoff for the sizing of infiltration structures. Furthermore, Chen *et al.* (2007) applied the rational method to estimate the maximum discharge of a landslide-induced debris flow in south-western China.

2.8 RAINFALL DATA

2.8.1 Measurement of Rainfall

Measurement of rainfall can be carried using the following methods (Patra, 2008; Mustafa and Yusuf, 2012):

i. Rain gauges (recording and non-recording)
ii. Totalizers
iii. Automatic or Radio system (radio signal and weather radar)

The rainfall data used for this study were those obtained by weather radar. The choice was inform by its availability and wide application in meteorological studies.

Measurement of rainfall by weather radar is based on the principle that the amount of power returned from hydrometeor (rain drops) target is related to the intensity of rainfall. Impulses from radio-energy are generated by a transmitter and radiated by a narrow beam.

Patra (2008) outlined the advantages of the weather radar over other methods of measurement amongst which are the ease of computation of areal rainfall and stream flow as the data are received directly into the computer and the ability to detect dangerous meteorological phenomena.

There is a growing interest in the use of weather radar-derived data in hydrologic modelling community as a source of input data to hydrologic models. This is because these dataset provide continuous spatial coverage, hence captures the rainfall variability with less uncertainty than simple point data and its derivative interpolated surfaces (Earls and Dixon, 2007). Such data on a global scale have been made available by Waterbase founded by the Institute for Water, Environment and Health (INWEH) and the International Institute for Software Technology both of the United Nations University (UNU) in collaboration with Texas A & M Agrilife Research, Texas A & M University, Cornell University, International Water Management Institute (IWMI), National Oceanic and Atmospheric Administration (NOAA), International Center for Agricultural Research in the Dry Areas (ICARDA) and Virginia Polytechnic Institute and State University (Virginia Tech). This data from 1979 was made freely available on a dedicated site, www.waterbase.org where intending users can specify the coordinate boundaries of their location and the data would be made available by email.

2.8.2 Rainfall Interpolation

Assessment of the spatial variation of rainfall is a major requirement for water resource management, hydrologic and ecologic modelling, groundwater recharge assessment, and irrigation scheduling, amongst others (Hartkamp *et al.,* 1999). The ability to accurately describe variability in rainfall patterns requires a dense network of gauges (Mair and

Fares, 2010). The cost of installation and maintenance of such gauges is prohibitive especially in developing economies such as Nigeria. As such, Hydrologists are often required to estimate point rainfall at unrecorded locations from measurements at surrounding sites using spatial interpolation techniques (Naoum and Tsanis, 2004). A comparison of some of the commonly used rainfall interpolation methods is presented in Table 2.6.

This review focuses on the Kringing interpolation technique that was applied in this study. Wikipedia defines Kriging or Gaussian process regression as a method of interpolation for which the interpolated values are modelled by a Gaussian process governed by prior covariances. Kriging provides a means of interpolating values for points not physically sampled using knowledge about the underlying spatial relationships in a data provided by variograms. It is based on regionalized variable theory which provides an optimal interpolation estimate for a given coordinate location, as well as a variance estimate for the interpolation value. The method involves an interactive investigation of the spatial behaviour of the phenomenon before generating the output surface. It is based on the regionalized variable theory, which assumes that the spatial variation in the phenomenon is statistically homogeneous throughout the surface. In other words, the pattern of variation at all locations on the surface is the same.

The technique is not suitable for data sets known to have spikes or abrupt changes. Naoum and Tsanis (2004) compared 12 interpolation techniques using GIS-based decision support system (DSS) in ArcView GIS Platform. The techniques compared were the Spline (regularized and tension), IDW, Kriging (linear, Gaussian, circular, spherical, exponential, universal 1 and 2), 2nd order polynomial and Thiessen polygons.

Table 2.6: Comparison of Spatial Interpolation Techniques

Method	Deterministic/ Stochastic	Local/global	Transitions (abrupt/gradual)	Exact interpolator?	Limitations of the procedure	Best for	Assumptions of interpolation model
Classification	Deterministic 'soft' information	Global	Abrupt if used alone	No	Delineation of areas and classes may be subjective. Error assessment limited to within-class standard derivations.	Quick assessments when data are sparse. Removing systematic differences before continuous interpolation from data points.	Homogeneity within boundaries
Trend surfaces	Essentially deterministic (empirical)	Global	Gradual	No	Physical meaning of trend may be unclear. Outliers and edge effects may distort surface. Error assessment limited to goodness of fit	Quick assessment and removal of spatial trends	Phenomenological explanation of trend, normally distributed data
Regression Models	Essentially deterministic (empirical-statistical)	Global with Local Refinements	Gradual if inputs have gradual variation	No	Results depend on the fit of the regression model and the quality and detail of the input data surfaces. Error assessment possible if input errors are known.	Simple numerical modelling of expensive data when better methods are not available or budgets are limited	Phenomenological explanation of regression model
Thiessen polygons	Deterministic	Local	Abrupt	Yes	No errors assessment, only one data point per polygon. Tessellation pattern depends on distribution of data.	Nominal data from point observations	Best local predictor is nearest data point
Linear interpolation	Deterministic	Local	Gradual	Yes	No error assessments	Interpolating from point data when data densities are high, as in converting gridded data from one project to another	Data densities are so large that linear approximation is no problem
Inverse distance weighting	Deterministic	Local	Gradual	Not with regular smoothing window, but can be forced	No error assessments. Results depend on size of search window and choice of weighting parameter. Poor choice of window can give artifacts when used with high data densities such as digitized contours	Quick interpolation from sparse data on regular grid or irregularly spaced samples	Underlying surface is smooth
Thin plate splines	Deterministic with local stochastic component	Local	Gradual	Yes, within smoothing limits	Goodness of fit possible, but within the assumption that the fitted surface is perfectly smooth.	Quick interpolation (univariate or multivariate) of digital elevation data and related attributes to create DEMs from moderately detailed data.	Underlying surface is smooth Everywhere
Kriging	Stochastic	Local with local variograms when stratified. Local with global trends	Gradual	Yes	Error assessment depends on variogram and distribution of data points and size of interpolated blocks. Requires care when modelling spatial correlation structures.	When data are sufficient to compute variograms, Kriging provides a good interpolator for sparse data. Binary and nominal data can be interpolated with indicator Kriging. Soft information can also be incorporated as trends or stratification. Multivariate data can be interpolated with co-Kriging.	Interpolated surface is smooth. Statistical stationarity and the intrinsic hypothesis.
Conditional simulation	Stochastic	Local with local variograms when stratified. Local with global trends.	Irregular	No	Understanding of underlying stochastic process and models is necessary.	Provides an excellent estimate of the range of possible values of an attribute at unsampled locations that are necessary for Monte Carlo analysis of numerical models, also for error assessments that do not depend on distribution of the data but on local values.	Statistical stationarity and the intrinsic hypothesis

Source: Adapted from Hartkamp *et al*., 1999

They concluded that Kriging models especially the exponential and universal 1 showed consistent performance and provided reliable estimates regardless of the number of gauges or the cell sizes used in the interpolation. Similarly, Mair and Fares (2010) carried out a comparison of rainfall interpolation methods in the mountainous leeward portion of the island of O'ahu, Hawai'i using data from a total of 21 gauges. They used traditional and geo-statistical interpolation methods, including Thiessen polygon, inverse distance weighting (IDW), linear regression, ordinary kriging (OK), and simple kriging with varying local means (SKlm) to estimate wet and dry season rainfall. They observed that while the Thiessen method produced the highest error, the Ordinary Kriging (OK) produced the lowest error in all but one period. They further reported that OK method produced more accurate predictions than the other methods compared.

2.8.3 Catchment Mean Aerial Rainfall Estimation

Patra (2008) outlined the following methods for estimation of mean aerial rainfall for a catchment:

a. Arithmetic Mean Method
b. Thiessen Polygon Method
c. Isohyetal Method
d. Grid point method
e. Orographic method and
f. Isopercental Method.

The arithmetic mean method was applied in this study. This method is applied to a basin where the gauges are uniformly distributed and the individual gauge catches do not vary much from the mean (Patra, 2008). The method assumes that the basin is reasonably flat. It assumes that all gauges weigh equally. The method gives fairly good results if the

topographic influences on precipitation and aerial representativeness are considered while selecting the gauge site. It is the simplest form in which the average depth of precipitation over the basin is obtained by taking simple arithmetic mean of all the gauged amounts within the basin. This method gives a rough estimate of the average precipitation. It however does not account for the topographic and other influences. For use of this method, no gauge station located outside the boundary of the watershed should be considered.

2.8.4 Presentation of Rainfall Data

Patra (2008) outlined the following methods of presentation of rainfall data.

a. Moving Average Curve
b. Mass Curve
c. Rainfall Hyetograph
d. Intensity-Duration-Frequency Curve

The moving average curve is more commonly used because of its simplicity (Patra, 2008). In hydrologic studies, rainfall data are characteristically plotted chronologically between time on *x*-axis and precipitation on the *y*-axis. A simple moving average of 3 or 5 is used to overcome the randomness associated with rainfall events. It helps to isolate the trend in the rainfall data.

2.9 FLOOD FREQUENCY ANALYSIS

Flood frequency analysis is a form of risk analysis used to extrapolate the return periods of floods beyond the gauged record (Kidson and Richards, 2005; Daffi, 2013). The analysis is based on historical events which are capable of supplying useful predictions

of future probabilities and risks. The primary objectives of flood frequency analysis are to determine the return periods and estimate the magnitudes of events for design return periods beyond the recorded range (Mustafa and Yusuf, 2012). The fitted distribution is used in estimating event magnitudes corresponding to return periods less than or greater than those of the recorded range.

Flood frequency analysis involves using observed annual peak discharges to calculate statistical information such as mean, standard deviations, skewness, and recurrence intervals which are in turn used to construct frequency distributions. Flood frequency distributions are tables and graphs that give information on the likelihood of various discharge values as a function of recurrence interval or exceedence probability (Mays, 2005; Mustafa and Yusuf, 2012).

The frequency distributions can take on different forms according to the equations used to carry out the statistical analyses. Some of these distributions are:

i. Normal Distribution
ii. Log-Normal Distribution
iii. Gumbel Distribution
iv. Pearson Type III Distribution
v. Log-Pearson Type III Distribution

(Chow *et al.,* 1988; Patra, 2008; Mustafa and Yusuf, 2012)

Various researchers have used different distributions to carry out flood frequency analysis. For instance, Salimi *et al.* (2008) carried out flood frequency analysis using Log-Normal, Pearson Type III, Log-Pearson Type III and Gumbel distributions for flow data of 24 years in order to estimate peak flow for 2, 5, 10, 20, 50 and 100 years return periods, respectively. They concluded that the Log-Pearson Type III is the best distribution to

estimate peak flow in different return periods as regards the differences between the observed and estimated peak flows. More so, Daffi (2013) carried out flood frequency analysis for the Dep River using Log-Pearson Type III and Gumbel distributions, respectively for 30 years synthetic flow data to determine its peak discharge for 2, 5, 10, 20, 50, 100, 200, 500 and 1000 years return periods, respectively. She concluded that the Log-Pearson Type III distribution was preferred over the Gumbel distribution reasons being that the values of discharge for the respective return periods were slightly higher for the Log-Pearson Type III and preferred in the prediction of extreme flood events. Besides these, the Log-Pearson Type III distribution is recommended for flood frequency analysis, according to the U.S. Geological Survey (Dalrymple, 1960; Faber, 2010; England Jr., 2017). Patra (2008) also noted that the Log-Pearson Type III distribution is widely used in United States, India and other countries as the standard distribution for flood frequency analysis of annual maximum floods. Benson (1968) cited in Chow *et al.* (1988) also buttressed that the Log-Pearson Type III distribution is the standard distribution for frequency analysis of annual maximum floods in the United States.

2.10 FIELD SURVEY AND STATISTICAL ANALYSIS

2.10.1 Descriptive and Inferential Statistics

As the name implies, descriptive statistics are used to describe the basic characteristics of the data in a survey. They provide simple summaries about the sample and the measures. They form the basis of nearly all quantitative analysis of data. They can sometimes be presented using simple graphics analysis (Liu *et al.*, 1999; Grant *et al.*, 2016; Spriensma and Wijnstok, 2016). Inferential statistics on the other hand are used to make predictions

(inferences) about populations using data drawn from the population (Liu *et al.*, 1999; Spriensma and Wijnstok, 2016)

2.10.2 Population and Sample

According to Frank and Althoen (1995), the universe of potential observations about which some general statement or inference is to be made is called study population or parent population. Depending on the size and accessibility of the parent population, it may be impossible to assess all members of the population. It therefore becomes imperative to make inferences about the distribution in the study population based on a collection of data that constitutes a relatively small fraction of the population called a sample. The process of taking out a predetermined number of observations (sample) from the parent population is refered to as sampling.

2.10.3 Sampling Techniques

There are various sampling techniques. While some set out the probabilities that different subsets of the population may be selected as the sample others are judgmental and not probabilistic. Some of these techniques are briefly described as follows:

i. **Simple random sampling:** This is the simplest form of probability sampling and forms the foundation for nearly all the other sampling techniques. In this technique, every observation in the population has equal probability of being selected. It is the most appropriate technique in situations where little is known about the population being studied (de Leeuw and Dillman, 2008).

ii. **Stratified random sampling:** This technique provides a means of ensuring that the sample contains representation from population subgroups of interest. The population is divided into groups called strata so that each population unit belongs to exactly one

stratum. Simple random sampling can then be applied to the individual groups within the population. This is applicable when different characteristics within the population have to be represented in the sample. The stratified design ensures that the sample will have members from each stratum. In some cases where the sample is expected to reflect the overall characteristics of the population, one can use a stratified design with proportional allocation, in which the same proportion of population units is sampled in each stratum (de Leeuw and Dillman, 2008).

iii. **Cluster sampling:** In this sampling technique, the population is divided into groups called clusters following a clearly defined rule. Each cluster is then treated as a sampling unit. Simple random sampling is applied to select the clusters. All members of the selected clusters are then sampled (Smith *et al.,* 1995; de Leeuw and Dillman, 2008).

iv. **Multistage sampling:** This is a probability sampling technique that involves carrying out the sampling in several stages such that the sample size gets reduced at each stage. Large populations are divided into stages to make the sampling process more practical. The technique combines stratified sampling or cluster sampling with simple random sampling in most cases. The sampling units are usually arranged hierarchically in accordance with the number of stages in the multi- stage sampling design (Shimizu, 1998).

v. **Purposive sampling**: This is a non-probability sampling technique that is most effective when one needs to study a certain characteristic domain with knowledgeable experts within (Tongco, 2007). In other words, the samples are selected based on characteristics of a population and the objective of the study. Purposive sampling is also known as judgmental, selective, or subjective sampling.

2.11 THE CONCEPT OF DISASTER

A disaster is a serious disruption of the functioning of a community or a society causing wide spread human, material, economic or environmental losses which exceed the ability of the affected community or society to cope using its own resources (Baas *et al.*, 2008; ISDR, 2009).

A disaster is a function of the risk process. It results from the combination of hazards, conditions of vulnerability and insufficient capacity or measures to reduce the potential negative consequences of risk.

2.11.1 Flood Hazard and Flood Hazard Assessment

Baas *et al.* (2008) defined hazard as a potentially damaging physical event, phenomenon or human activity that may cause the loss of life or injury, property damage, social and economic disruption or environmental degradation. This can include latent conditions that may represent future threats and can have different origins: natural (geological, hydro-meteorological and biological) or induced by human processes (environmental degradation and technological hazards). Hazards can be single, sequential or combined in their origin and effects. Each hazard is characterized by its location, intensity, frequency and probability.

Alkema and Westen (2005) defined flood hazard as 'the chance that a flood event of a certain magnitude will occur in a given area within a given period of time'. In their opinion, flood hazard assessment seek answers to such questions as 'where does the water come from?', 'where will the water go?' and 'which areas will be inundated?' This implies that catchment flood hazard assessment considers how the different characteristics of the catchment combine and interact to contribute to flooding within the

floodplains (Daffi, 2013). Flood hazard assessment is the identification, quantification and communication of the hazards due to flooding seeking to identify areas subject to particular hazards, such as deep or fast-flowing water, and to assess the likelihood of them occurring both now and in the future (Jeb, 2014).

The South Carolina Emergency Preparedness Division (SCEPD) through Cutter *et al.* (1997) stated that the assessment of any hazard including flood involves identification of the hazard, acquisition of data and calculation of the frequency of occurrence. This provides basis for the determination of the extent of inundation (in the case of flood) either by the multi criteria evaluation method (Garba, 2015) or hydraulic modelling (Daffi, 2013).

2.11.2 Flood Vulnerability and Flood Vulnerability Assessment

Vulnerability has been defined differently by various authors and researchers. International Panel of Climate Change (IPCC) in 1992 defined vulnerability as the degree of incapability to cope with the consequences of climate change and sea-level rise. The panel through Watson *et al.* (1996) redefined it as the extent to which climate change may damage or harm a system depending not only on a system's sensitivity but also on its ability to adapt to new climatic conditions. Meanwhile, Blaikie *et al.* (2014) described it as a measure of a person or a group's exposure to the effects of a natural hazard, including the degree to which they can recover from the impact of that event. Veen & Logtmeijer (2005) expanded the concept of vulnerability beyond just climatic susceptibility and ability to cope to describe flood vulnerability from an economic point of view. The Food and Agricultural Organisation (FAO) through Baas *et al.* (2008) defined vulnerability as the conditions determined by physical, social, economic and environmental factors or

processes, which increase the susceptibility of a community to the impact of hazards. Similarly, ISDR (2004, 2009) defined it as the characteristics and circumstances of a community, system or asset that make it susceptible to the damaging effects of a hazard. Messner and Meyer (2006) and Merz *et al.* (2007), summarized the definition of vulnerability to include elements at risk, the damage potential described by their exposure to the hazard and their degree of susceptibility to loss. Mitchell (2006) on the other hand described vulnerability as a function of exposure, resilience and resistance. Balica *et al.* (2009) considered vulnerability as the extent of harm, which can be expected under certain conditions of exposure, susceptibility and resilience. Specifically, they described flood vulnerability as the extent to which a system is susceptible to floods due to exposure, a perturbation, in conjunction with its capacity/incapacity to be resilient, to cope, recover or adapt.

The South Carolina Emergency Preparedness Division (SCEPD) through Cutter *et al.* (1997) summarized the social descriptors which are most indicative of the population characteristics that may place people at greater risk to include age, gender, income or economic status, amongst others. They outlined the following steps for the determination of the population's vulnerability to any hazard at the county or Local Government Area (LGA) level which makes it most applicable in the present research.

i. Identification of vulnerable population sub-group

The entire population within the hazard zone are sub-divided to know those dependent as well as those with less capacity to cope with a disaster such as flood. The dependent population include persons less than 15 years, persons above 65 years and those living with disabilities (Balica *et al.*, 2009). The economic status is also believed to play a key role in the ability of the populace to cope. Thus, those living in poverty are seen to be

more vulnerable than those above poverty while it is also believed that females are more susceptible than their male counterpart.

ii. Acquisition of population data

Once the vulnerable population subgroups have been identified, the population data is then acquired from relevant agencies.

iii. Calculating social vulnerability scores/index for each LGA in each sub-group

The vulnerability score or index of each LGA for the respective sub-group is calculated for each sub-group on a scale of 0 – 1 which is indicative of the level of vulnerability of each LGA for that sub group.

iv. Calculating Vulnerability weight of each sub-group

The vulnerability weight of each sub-group is calculated as an indication of the contribution of each sub-group to the overall vulnerability to the hazard.

2.11.3 Flood Risk and Flood Risk Assessment

Risk refers to the probability of harmful consequences, or expected losses (deaths, injuries, property, livelihoods, economic activity disrupted or environment damaged) resulting from interactions between natural or human-induced hazards and vulnerable conditions (Baas *et al.,* 2008). Conventionally risk is expressed by the notation Risk = Hazards x Vulnerability (Fig. 2.3).



Fig. 2.3: Flood risk as a combination of Hazard and vulnerability (adapted from Eleuterio, 2012).

A correlation between risk, hazard and vulnerability is presented in Table 2.7.

Table 2.7: Correlation between risk, hazard and vulnerability

Risk	=	Hazard	X	System Vulnerability
The probability of harmful consequences, or expected losses (deaths, injuries, property, livelihoods, economic activity disrupted or environment damaged) resulting from interactions between natural or human induced hazards and vulnerable conditions.		A potentially damaging physical event, phenomenon or human activity that may cause the loss of life or injury, property damage, social and economic disruption or environmental degradation.		The conditions determined by physical, social, economic and environmental factors or processes, which increase the susceptibility of a community to the impact of hazards.

Source: (Jeb, 2014)

2.11.4 Disaster Risk Management and Disaster Risk Reduction

Disaster risk management is the systematic process of using administrative decisions, organization, operational skills and capacities to implement policies, strategies and coping capacities of the society and communities to lessen the impacts of natural hazards and related environmental and technological disasters. This includes all forms of

activities, including structural and non structural measures to avoid (prevention) or to limit (mitigation and preparedness) adverse effects of hazards (Baas *et al.*, 2008).

Disaster risk reduction on the other hand refers to the conceptual framework of elements considered with the possibilities to minimize vulnerabilities and disaster risks throughout a society, to avoid (prevention) or to limit (mitigation and preparedness) the adverse impacts of hazards, within the broad context of sustainable development (Baas *et al.*, 2008). The disaster risk reduction framework is composed of the following fields of actions:

i. Risk awareness and assessment including hazard analysis and vulnerability/capacityanalysis;
ii. Knowledge development including education, training, research and information;
iii. Public commitment and institutional frameworks, including organizational, policy, legislation and community action;
iv. Application of measures including environmental management, land-use and urban planning, protection of critical facilities, application of science and technology, partnership and networking, and financial instruments;
v. Early warning systems including forecasting, dissemination of warnings, preparedness measures and reaction capacities.

2.11.5 Flood Risk Mapping

Flood, like many other natural disasters can neither be totally prevented nor eradicated but the resultant damages can be minimized (Jeb, 2014). Several activities which could be short-term, ameliorative, long-term and preventive are usually carried out to reduce the losses from flooding. These activities include post flood relief and rehabilitation, as well as pre-flood prediction, forecasting, warning, monitoring and regulation. More so,

flood control structures could be built in many countries and regions to prevent water from overflowing its banks (James, 1967; Bird, 1980; e Costa *et al.*, 2004). These efforts are usually made because of the recognition of the inherent socio-economic consequences of flooding. As a result, guidelines for development and utilization of floodplains especially in flood prone areas are developed in form of Master Plans in an effort to reduce significantly the menace of flooding. Information on the nature, extent and severity of the flood problem are baseline information required to produce a flood risk zone map that will give a spatial understanding of the challenge.

Islam *et al.* (2001) considers flood depth as the most important indicator of the intensity of flood hazard. Flood risk maps are therefore prepared based principally on the estimated extent of inundation (Büchele*et al.* 2006).The estimation is commonly derived from various hydrological and remotely sensed data (Sanyal and Lu, 2004).

A flood risk map may be defined as a special thematic map that represents the characteristics of a hypothetical flood graphically from a synthesis of past flood events (Jeb, 2014). With sufficient long term and accurate records, flood extents drawn from the empirical results become very powerful prediction tools because the flood risk map is often a map of more than one flood event, flood risk maps are therefore the basic tools and starting point of regional flood intervention policy (Bhanumurthy*et al.*, 2004). Flood risk maps are very important tool for appropriate land use planning since they provide easily read and readily accessible charts and maps that facilitate the identification and prioritization ofmitigation efforts (Bapalu and Sinha, 2005). Some of the uses of flood risk maps outlined by Bhanumurthy *et al*. (2004) are briefly summarized as follows:

i. Flood hazard maps are used to determine the areas susceptible to flooding when discharge of a stream exceeds the bank-full stage.
ii. They provide basic initial information for land use planning.

iii. Allow correct development plans for new urban areas.

iv. Enable adequate evaluation of costs of flood and flood reduction benefits.

v. They help to identify the worst affected areas or otherwise due to flooding and provide a guide for better planning and rescue operations and allocation of resources.

vi. They provide basis for evaluation of feasibility of non – structural flood control measures such as flood proofing.

vii. They can form the basis of any insurance plan.

viii. They serve as a logical basis for investment planning and priority setting.

ix. They increase the overall public awareness on flood risk and hazards.

2.12 MULTI CRITERIA EVALUATION IN RISK ASSESSMENT

Malczewski (1999) defined multi-criteria evaluation (MCE) as a set of systematic procedures for analyzing complex decision problems which involves dividing the problem into smaller parts that are easily understood, analyzing each part, and integrating the parts in a logical manner to yield a meaningful solution.

Multi-criteria evaluation involves the three major steps described briefly as follows:

i. Problem Definition

The first step in multi-criteria evaluation for decision-making is the identification and definition of the problem. This represents the intelligence phase of decision-making which involves searching the environment for conditions, obtaining, processing and examining the basic information necessary for identification of the problems (Malczewski, 1999).

ii. Evaluation Criteria

The second stage involves specifying a set of objectives that reflects all aspects of the problem and measures for achieving those objectives. Keeney and Raiffa (1976) call them attributes of the problem. Since the evaluation criteria are related to geographic entities and the relationship between them, they are usually presented in the form of maps often referred to as attribute maps (Malczewski, 1999).

iii. Criterion Weights

A criterion weight can be defined as a value assigned to an evaluation criterion which indicates its importance relative to other criteria under consideration (Garba, 2015). Assigning weights of importance to evaluation criteria accounts for the variation of each evaluation criterion and the different relative importance attached to these ranges of variations (Kirkwood, 1997). Commonly employed weighting methods include: Ranking and Pair-wise Comparison (Garba, 2015).

a. The Ranking Method:

The Ranking method which is the simplest method for evaluating the importance of weights involves the ranking of the criteria under consideration in the order of the decision maker's preference. The ranking can be done either inversely or straight on a scale of 1 to n^{th} value where n is the total number of factors being compared. In the inverse ranking, 1 is the least important factor and n is the most important while the straight ranking has n as the least important factor and 1 as the most important factor (Yalcin and Akyurek, 2004). The simplicity of the ranking method makes it very attractive but less appropriate where there are number of criteria to be considered (Murtala, 2014; Garba, 2015).

b. Pair-wise Comparison Method:

The Pair-wise Comparison (PC) method unlike the ranking method allows the comparison of only two criteria at once which often results in a ratio matrix. The PC method is capable of converting subjective assessments of relative importance into a linear set of weights (Heywood *et al*., 1995). It takes pair-wise comparison as inputs and produces relative weights as outputs. The method was developed by Saaty (1980) in the context of a decision-making process known as the Analytical Hierarchy Process (AHP). The method involves development of pair-wise comparison using the Saaty's scale of preference with values ranging from 1 to 9, computation of the weights, and estimating the Consistency Ratio (CR) which is a check to determine if the comparisons are consistent or not. A consistency ratio of $0 \leq CR \leq 0.1$ would be accepted as being consistent but a value greater than 0.1 would require revisiting the comparison. This is a major advantage of the PC method over the ranking method.

Although the multi-criteria evaluation technique is not exactly new, its application in flood risk analysis is quite recent. The technique has found more use in site suitability analysis, but its application in flood risk assessment is receiving fast-growing attention (Meyer *et al.*, 2009). Raaijmakers *et al.* (2008) applied the MCE techniques alongside the quantifiable conventional approach to risk and the taxonomic analysis of perceived risk to assess the flood risk of the 'Ebro Delta' in Spain as part of the European sixth framework project 'Floodsite'. The results of their analysis were applied to a set of scenarios representing both sea-level rise and land subsidence for a time span of 50 years. Wang *et al.* (2011) applied the MCE technique to assess the flood risk in Dungting lake region, Hunan province in Central China. They used a semi-quantitative model and fuzzy analytic hierarchy process in geographic information system (GIS). They used the flood risk index

obtained to classify the study area into very low, low, medium, high and very risks, respectively. Garba (2015) applied the technique to carry vulnerability analysis for Jalingo metropolis using ArcGIS 10.1. Building on the existing deliberative processes, Kenyon (2007) developed a new participant-led multi-criteria method which was used to evaluate flood risk management options in Scotland. The results show that participants preferred regeneration or planting of native woodland to other flood management options, and least preferred building floodwalls and embankments. Meyer *et al.* (2009) carried out flood risk mapping of Mulde River in Germany using a GIS-based multi-criteria approach. Musungu *et al.* (2012) carried out flood risk analysis in Graveyard pond, an informal settlement in South Africa using multi-criteria evaluation and GIS.

2.13 POPULATION ESTIMATION

Population estimation is very importance in vulnerability analysis. Census is seldom carried out on an annual basis. For instance, the last population census in Nigeria was conducted in 2006 (NPC, 2010_a; NPC, 2010_b; NBS 2012). This makes the projection of population for subsequent years very important. Population projection referes to a computational method used for estimating population size and structure at a particular time from population size and structure at another time with particular attention to the rate of changes.

Lin (2007) outlined the following methods for population estimation:

i. Arithmetic growth rate method
ii. Geometric growth rate method
iii. Declining growth rate method and
iv. Logistic curve method

2.14 APPLICATION OF REMOTE SENSING AND GEOGRAPHIC INFORMATION SYSTEM IN FLOOD RISK STUDIES

Flood disaster is a complex phenomenon that requires an integrated approach for the assessment that may lead to the effective management and reduction of the menace. Time dependent information such as latest information on floodplain characteristics, flood occurrence and depth as well as flood duration in addition to intensive fieldwork are often required to prepare flood risk maps using hydrological and hydraulic mathematical formulae and stream geometry. This has traditionally been carried out via manual methods which are often tedious and prone to more error (Daffi, 2013; Jeb, 2014).

Accurate delineation of flood depths and extents within the floodplain is a necessary requirement for the appropriate management of the floodplain (Noman *et al*., 2003). Conventional means of recording hydrological parameters of a flood event often fail to record the extreme event which has made remote sensing technology and GIS an attractive alternative for flood monitoring (Sanyal and Lu, 2004). Furthermore, Hoque *et al*. (2011) were of the opinion that remote sensing could be the most practical method that floodplain managers could effectively use to quantify and adequately map flood impacts especially for large and often inaccessible areas such as major river valleys. In buttressing this assertion, Amini (2007) stated that it is an economical alternative to traditional hydrologic data collection. The growing availability of multi-temporal satellite data has increased opportunities and the applicability of remote sensing in flood risk studies (Smith, 1997; van der Sande *et al*., 2003).

Consequently, various researches have been carried out for flood inundation mapping using different types of satellite images, digital elevation models and diverse kinds of software for hydraulic modelling. Different methods have been used for flood simulation in the GIS environment depending on the available materials used.

Van Western (2001) defined Geographic Information System as a combination of tools and methods for the collection, storage and processing of geo-spatial data and for the dissemination and use of these data and of services based on these data. The implication of this is the development and application of concepts for spatial data modelling, for extraction of information from image data, and for the processing, analysis, dissemination, presentation and use of geo-spatial data on one hand and the development and implementation of concepts for the structuring, organization and management of geo-spatial production processes in an institutional setting on the other hand.

Wikipedia defined remote sensing as the acquisition of information about an object or phenomenon without making physical contact with the object. It is applicable in numerous fields, including geography, land surveying and most earth science disciplines such as hydrology, ecology, oceanography, glaciology, geology amongst others. Remote sensing also has military, intelligence, commercial, economic, planning, and humanitarian applications.

The application of remote sensing and GIS in flood risk mapping has been receiving increasing interest from researchers and stake holders globally (Jeb, 2014). This is because remote sensing provides synoptic data of an area either in real-time or near real-time in different spatial or temporal resolutions for different magnitude of flood so that the flood extent can be related to the flood magnitude. Consequently, the duration and recession of flood waters can be estimated using multiple imageries of the same area over a few days. GIS on the other hand provides platform of storage of large volumes of geospatial data, quick access, retrieval and manipulation. It also provides the environment for the integration of remotely sensed data alongside other spatial datasets to delineate the flood prone areas for different flood scenarios and magnitudes either resulting from

embankment breach or overtopping of unprotected rivers amongst others (Sanyal and Lu, 2004; Sharma, 2004; Forkuo, 2011). In addition, GIS provides the framework within which spatially distributed data are collected and used to prepare model input files and evaluate model results (Miller *et al.*, 2007).

Remote sensing and GIS have played a key role in the field of hydrology and water resources management over the past two decades. GIS has been extensively used to model surface water and flood damage (Smith, 1997; Dewan *et al*., 2007; Merz *et al.*, 2007). GIS is fast emerging as a powerful tool for the assessment of risk and management of natural hazards to delineate flood prone areas (Prahdan, 2010). Such information will provide sound basis for planners and decision-makers to take positive and timely steps with respect to disaster management.

There are various operational satellites which are common source of remotely sensed data relevant to flood risk assessment. Some of these include MODIS Terra/Aqua, RADARST, NOAA/AVHRR, ERS, Landsat TM and ETM+, IRS-1C, SPOT amongst others. Data derived from these satellites are used for deriving inputs for preparation of flood risk zone maps.

2.14.1 Digital Elevation Models used for Flood risk Mapping

A Digital Elevation Model (DEM) is a specialized database that represents the relief of a surface between points of known elevation (www.caliper.com). It is a representation of the elevation values of a surface that change with position It is a continuous grid of regular intervals or sizes and has an elevation specified for each grid cell (Daffi, 2013). In as much as the terms Digital Elevation Model (DEM), Digital Terrain Model (DTM) and Digital Surface Model (DSM) have often been used interchangeably in

scientific literature, it is necessary to distinguish between them. In most cases, DSM represents the earth's surface including all objects on it while the DTM represents the bare ground surface excluding any objects like plants and buildings. DEM is often used as a general term for DSMs and DTMs, only representing height information without any further definition about the surface. A Triangulated Irregular Network (TIN) is a set of adjacent, non-overlapping triangles computed from irregularly spaced points and break lines and stores the topological relationship between triangles and their adjacent neighbour.

A DEM can either be represented as a raster in the form of grids or as a TIN. They can be built using remote sensing techniques or from land surveying. DSM may be useful for landscape modelling, city modelling and visualization applications while a DTM is often required for flood or drainage modelling, land-use studies, geological applications, amongst others. DEMs can be generated using interferometric synthetic aperture radar: two passes of a radar satellite (such as RADARSAT-1 or TerraSAR-X), or a single pass if the satellite is equipped with two antennas as it is the case with the shuttle radar topographic mission (SRTM).

Digital elevation models can be obtained from any of the following sources:

i. GTOPO30 (30 arcsecond resolution, approx. 1 km).
ii. Advanced Spaceborne Thermal Emission and Reflection Radiometer (ASTER) instrument of the Terra satellite (at a 30 meter resolution).
iii. Shuttle Radar Topography Mission (SRTM) data available at high resolution for the United States territory and about 90 meters resolution for the rest of the world

iv. Light Detection and Ranging (LIDAR), a system for gathering digital terrain data using airborne laser systems flown aboard an aircraft equipped with GPS at a resolution of 3m.

The use of digital elevation model in flood risk mapping has received great attention and exploration by researchers. For instance, Webster *et al.* (2006) used the airborne light detection and ranging (LIDAR) DEM to study the flood scenario for a large section of the New Brunswick coast along Northumberland Strait in 2003 and 2004. They generated maps of flood depth for all water levels which were used for socio-economic and ecosystem impact assessment. Flood risk maps were also developed using standard Geographical Information System (GIS) processing routines to determine the spatial extent of inundation for a given water level. They concluded that the high resolution of the LIDAR Digital Elevation Model (DEM) was able to capture embankments such as raised roadbeds that could prevent flooding inland. Similarly, Demirkesen *et al* (2007) carried out coastal flood risk analysis using Landsat-7 ETM+ imagery and SRTM DEM in Izmir, Turkey. They determined the spatial distribution of the coastal inundation hazards of Izmir region using both the land-use and land-cover (LULC) types derived from the maximum likelihood classification of Landsat-7 ETM+ multi-spectral image and the classification of the SRTM-DEM. They came to a conclusion that coastal areas with elevations of 2 and 5 m above mean sea-level vulnerable to inundation covered 2.1 and 3.7% of the study area, respectively. Furthermore, Galy and Sanders (2000) developed a large-scale flood risk assessment model for the River Thames. Zheng *et al*. (2007) also made use of DEM, soil type, landuse, channel network and catchment boundary (spatial data) and inflow discharge (non-spatial data) to develop a grid cell based simplified flood inundation simulation model for large watersheds which was integrated with rainfall-runoff processes in order to obtain temporal-spatial distribution of flood inundation

vulnerability. More so, Daffi (2013) used the SRTM DEM to carry out flood hazard assessment for the Dep sub-basin in North-central Nigeria. The catchment boundaries were delineated from the DEM while the TIN for hydraulic modelling in HEC-RAS was also generated from the DEM. Jeb (2014) combined a DEM obtained from topographic map and SRTM DEM to carry out flood hazard, vulnerability and risk assessment for 500 meter corridor of the river Kaduna within Kaduna metropolis.

2.14.2 Satellite Images used for Flood Inundation Mapping

Satellite imagery consists of photographs of e or other planets made by means of artificial satellites (Wikipedia). A satellite is an object or vehicle manufactured and sent into space to orbit the earth, moon or other celestial body for information gathering.

Satellite imageries in remote sensing have four types of resolution described by Campbell and Wynne (2011) as follows:

i. **Spatial resolution:** This is defined as the pixel size of an image representing the size of the surface area (in square meters) being measured on the ground, determined by the sensors' instantaneous field of view (IFOV). For example Landsat image has a spatial resolution of 30m, the commercial satellite image GeoEye-1 has a resolution of 0.41m in the panchromatic or black and white mode and 1.65m for the multispectral or colour imagery, Nigerian Sat-1 has 31m resolution, SPOT satellites (Spot 2, 4 and 5) have resolutions ranging from 2.5 m to 1 km and so on while Quickbird has 0.3m resolution.

ii. **Spectral resolution:** This is defined by the wavelength interval size (discreet segment of the Electromagnetic Spectrum) and number intervals that the sensor is measuring.

iii. **Temporal resolution:** This is defined by the amount of time (i.e. days) that passes between imagery collection periods. For example Landsat 7 has return period of 16 days.

iv. **Radiometric resolution:** This is defined as the ability of an imaging system to record many levels of brightness.

Satellite imageries have been effective and efficient tools for the determination of flood inundation areas (Brivio *et al.*, 2002; Islam *et al.*, 2009; Khan *et al.*, 2011). With the rapidly increasing availability of multi-temporal satellite data, opportunities for monitoring large rivers from space have increased tremendously (Smith, 1997). Right from the early days of Landsat Multi Spectral Scanner (MSS) with 80 m resolution to Landsat Thematic Mapper (TM) imageries with 30m resolution and then to later stages SPOT multi spectral imageries, satellite images were used for flood delineation with the similar assumption that water has very low reflectance in the near infrared portion of the spectra (Sanyal and Lu, 2004).

Remote sensing data acquired in the visible, near infrared (IR) and short-wave infrared (SWIR) regions have shown encouraging results in providing information on spatial pattern of flood inundation. Where clouds, trees and floating vegetation do not obscure the water surface, passive and active sensors operating in the visible and microwave range can give information for estimating inundation area and delineate flood boundaries (Smith, 1997). However, the use of satellite imagery for flood inundation mapping has the following limitations:

i. Incomplete image coverage of historical flow conditions in satellite imagery archives because of historical gaps in the satellite image coverage
ii. Resolution issues for smaller streams and rivers
iii. Problems of cloud cover which often obscures rivers during major flood events
iv. Excessive vegetation cover for small rivers which makes it difficult to isolate the river during classification.

Satellite images during floods can be used to define the extent of the inundated areas and course of the propagation and are very important for verification and validation of the hydraulic models outputs (Balabanova and Vassilev, 2010). Satellite images can also be used for floodplain delineation but are very difficult to process because of cloud cover during rainy season especially because it is essential to capture the flooded areas during a storm and flood. Islam and Sado (2000b) used the National Oceanographic and Atmospheric Administration - Advanced Very High Resolution Radiometer (NOAA-AVHRR) data, with ground resolution of 1.1km, for evaluation of flooded area and flood hazard assessment in Bangladesh. It was used to analyse historical flood event of 1988 which was a hundred-year flood.

Islam and Sado (2000a) demonstrated a technique to develop a flood hazard map and a land development priority map for countermeasure against flood damage. NOAA-AVHRR data for flood events were incorporated in GIS data of physiography, geology, land cover classification, elevation, drainage network, administrative districts and population density. Flood–affected frequency was carried out to delineate the inundated area into high, medium, low and non-hazard areas and flood depth categories of no-flooding, shallow, medium and deep flooding were estimated using NOAA-AVHRR images.

2.15 SOFTWARE USED IN FLOOD INUNDATION MODELLING

There are various types of software available for flood inundation modelling most of which are from free and open sources. Extensive studies have been going on among researchers globally for ways to effectively apply the software in GIS for flood risk assessment and flood management. For instance, Kafle *et al*. (2007) carried out rainfall-

runoff modelling on the Bagmati Basin in Nepal using the hydrological model HEC-HMS in a GIS environment. The GIS extension HEC-GeoHMS was used in combination with the model to convert excess precipitation to overland flow and channel runoff. The predicted hydrograph was calibrated against the observed one for good simulation. The predicted peak discharge based on point gauge data was fairly accurate but an exact agreement was not achieved for smaller discharges. The peak flow of the derived hydrograph was used as input in HEC-RAS, a hydraulic model, for producing flood maps showing inundation area extent and flood depths. Similarly, Salimi *et al.* (2008) carried out a research by integrating hydraulic simulation model, HEC-RAS and GIS analysis for delineation of flood inundation extents and depths within a selected reach of Zaremroud River in Iran for different return periods. In the research, steady flow was simulated along the 3km end of the river which resulted in the creation of zonation maps which reasonably separated high hazard from low hazard areas within the floodplain. Their conclusion was that the study which made use of GIS for hydraulic simulation has the potential to both improve accuracy and save cost for floodplain and flood hazard mapping. Finally, Ahmad *et al.* (2010) integrated hydrological models with GIS to estimate the flood zone of Nullah Lai in Rawalpindi, Pakistan. The hydrological models, HEC-RAS and HEC-GeoRAS were used to delineate the flood vulnerable areas at different discharge values. GIS technique was also used to delineate the variation of topography and to find the inundation depths at various locations in the study area. Output of the study using HEC-RAS showed that inundated areas and inundation depths were in close approximation with survey based inundation results obtained by Japan International Cooperation Agency (JICA). This confirmed that the integrated modelling approach used in the study worked well to delineate areas vulnerable to flood and also gave good estimation of inundation depths at a specific discharge value.

2.15.1 Hydraulic models used for Flood Inundation Mapping

Flood mapping is a non-structural measure in flood management to reduce flood hazard and improve preparedness and awareness of all people involved in flood situations. Flood inundation maps present the area prone to flooding at one or more floods with given return periods. Flood inundation maps are normally created to get knowledge on the areas that will be flooded corresponding to floods with certain return periods. Estimation of flood depths and extents is necessary to provide information on disaster to deal with contingency and alleviating risk and loss of life and property (Chang *et al.*, 2010). This is used in proposing improved land use planning and emergency preparedness to reduce flood damages.

Before flood inundation mapping can be carried out, hydrological analysis or modelling is needed to calculate lateral inflows and hydraulic models to calculate water levels along the river reach (Lerat *et al.*, 2012) thus requiring flood frequency analysis for the hydrometric station (Balabanova and Vassilev, 2010).

Detailed and complex hydraulic modelling tools available include unsteady flow models, 2D hydraulics models, and 1D gradually varied flow models such as HEC-RAS. Also MIKE 11 hydraulic simulation programme calculates the water surface profiles by running discharges corresponding to flows with different return periods for different scenarios. The output data from hydraulic modelling is then integrated in GIS to convert the water surface to flood map using DEM (Babalanova and Vassilev, 2010). The 2-dimensional hydrodynamic models consider the variation of flow in both the longitudinal and the transverse directions of a river channel and the underlying principle is the solution to the vertically integrated Navier–Stokes equations, also referred to as shallow-water equations (Tarekegn *et al*., 2010).

Some important factors considered in hydraulic calculations are:

Velocity: As water levels rise above the top of bank in the main channel, the mean velocity will continue to rise in addition to the increased flow area, and the design discharge can still be considerably higher than flow at top of bank stage.

Channel slope: Reasonable estimate of channel slope can be obtained from the profiles derived from DEM data.

Roughness parameter: Traditionally the Manning's coefficient is used for hydraulic calculations.

Tarekegn *et al*. (2010) studied the flooding characteristics in the data scarce region of the Lake Tana Basin at the source of the Blue Nile River. The study integrated remote sensing, GIS with a two-dimensional (2D) module of the SOBEK flood model. SOBEK 1D2D was developed with the aim of combining a one-dimensional (1D) channel flow model (Saint-Venant equations) with a two-dimensional (2D) shallow-water equation solver. The model uses the shallow-water equations to simulate flood inundation flows through the conservation of mass and momentum. Digital Elevation Model (DEM) was generated from the Advanced Spaceborne Thermal Emission and Reflection Radiometer (ASTER) image for use in the 2D hydrodynamic model. A GIS model was then developed to reconstruct the river terrain and channel bathymetry.

2.15.2 Description of Selected Models used in this Study

The following were extracted from the software HELP menu of the different methods and models used for the flood inundation modelling:

2.15.2.1 HEC-RAS

HEC-RAS (Hydrological Engineering Center – River Analysis System) is integrated system of software, designed for interactive use in a multitasking, multi-user network environment. The major capabilities of HEC-RAS are the graphical user interface, river analysis components, data storage and management components, the graphics and reporting components and RAS mapper. It performs one-dimensional hydraulic calculations for a full network of natural and constructed channels for steady and unsteady flow, sediment transport-mobile bed simulation and water temperature analysis.

Hydraulic Analysis Components: The HEC-RAS system contains four one-dimensional river analysis components for:

a. Steady flow water surface profile computations
b. Unsteady flow simulation
c. Movable boundary sediment transport computations and
d. Water quality analysis.

All these four components use a common geometric data representation and common geometric and hydraulic computation routines. Other hydraulic design features can be initiated once the basic water surface profiles are computed.

Steady Flow Surface Profile: This component of the modelling system is used for calculation of water surface profiles for steady gradually varied flow and it can handle a single river reach, a dendritic system, or a full network of channels. It can model subcritical, supercritical, and mixed flow regime water surface profiles. The basic computational procedure is based on the solution of the one-dimensional energy equation.

Energy losses are evaluated by friction (Manning's equation) and contraction/expansion (coefficient multiplied by the change in velocity head). The momentum equation is utilized in situations where the water surface profile is rapidly varied. The effects of various obstructions such as bridges, culverts, weirs, and other structures in the flood plain may be considered in the computations. The steady flow system is designed for application in flood plain management and flood insurance studies to evaluate floodway encroachments. Also, capabilities are available for assessing the change in water surface profiles due to channel improvements, and levees.

Theoretical Basis for One-Dimensional Flow Calculation (HEC-RAS): In steady-state modelling, the flows are prescribed by the user and the model calculates water levels at discrete cross-sections. There is essentially one unknown variable (stage) and therefore it uses the energy equation is needed. In unsteady modelling, two variables are calculated (stage and flow), so two equations are needed. Unsteady modelling is also, concerned with how these parameters change with time and distance downstream. This is reflected in the partial differential terms in the equations.

Different fundamental equations used for HEC-RAS algorithm to compute water surface elevations using the standard step method for steady flow analysis are:

Energy Equations: Water surface profiles are computed from one cross-section to the next by solving the Energy Equation with an iterative procedure. Energy equation is based on principle of conservation of energy and it is the sum of the kinetic energy and potential energy at any other cross section plus or minus energy loss or gains between the sections. The energy equation can be written as expressed in Eq. (2.10).

$$Z_2 + Y_2 + \frac{\alpha_2 V_2^2}{2g} = Z_1 + Y_1 + \frac{\alpha_1 V_1^1}{2g} + h_e \qquad (2.10)$$

Where, Z_1, Z_2 = elevation of the main channel inverts

Y_1, Y_2 = depth of water at cross sections

V_1, V_2 = average velocities

α_1, α_2 = velocity weighing coefficients

g = gravitational acceleration

h_e = energy head loss

The diagram showing the terms of the energy equation is shown in Fig. 2.4.

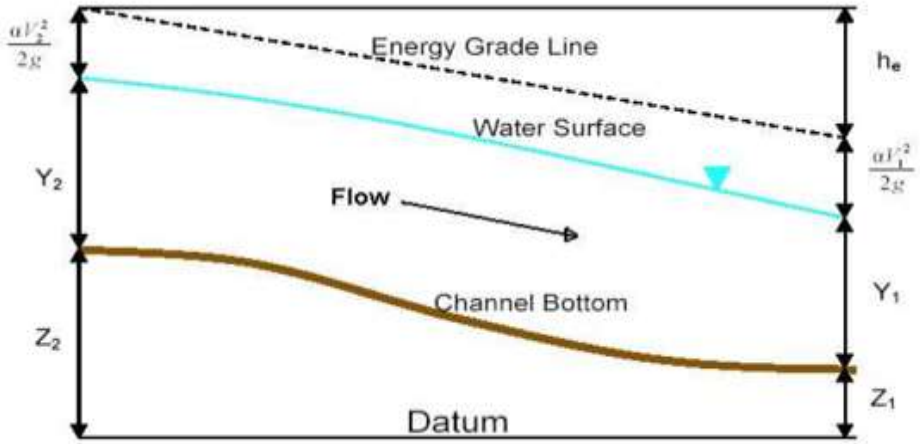


Fig. 2.4: Diagram showing the Terms in the Energy Equation
Source: Bruner (2010)

The energy head loss (h_e) is expressed as shown in Eq. (2.11).

$$h_e = LS_f + C\left|\frac{\alpha_2 V_2^2}{2g} - \frac{\alpha_1 V_1^2}{2g}\right| \quad (2.11)$$

Where: L = distance weighted reach length

S_f = representation friction slope between two sections

C = expansion or contraction loss coefficient

The distance weighted reach length, L, is calculated using Eq. (2.12).

$$L = \frac{(L_{lob}Q_{lob} + L_{ch}Q_{ch} + L_{rob}Q_{rob})}{(Q_{lob} + Q_{ch} + Q_{rob})} \quad (2.12)$$

Where:

$L_{lob}, L_{ch,} L_{rob}$= x-section reach length specified for flow in the left overbank, main channel and right overbank respectively.

Q_{lob}, Q_{ch}, Q_{rob}= arithmetic average of the flows between sections for the left overbank, main channel and right overbank respectively.

Calculation of Conveyance: The determination of total conveyance and the velocity coefficient for a cross-section requires that flow be sub-divided into units for which the velocity is uniformly distributed. The approach used in HEC-RAS is to sub-divide flow in the overbank areas using the input cross-section, n-value break points (location where n-values change) as the basis for sub-division. Conveyance is calculated within each sub-division from the following form of Manning's equation expressed in Eq. (2.13) and (2.14).

$$Q = KS_f^{\frac{1}{2}} \tag{2.13}$$

$$K = \frac{1}{n} AR^{\frac{2}{3}} \tag{2.14}$$

Where: K = conveyance for sub-division

n = Manning's roughness coefficient for sub-division

A = flow area for sub-division

R = hydraulic radius for sub-division

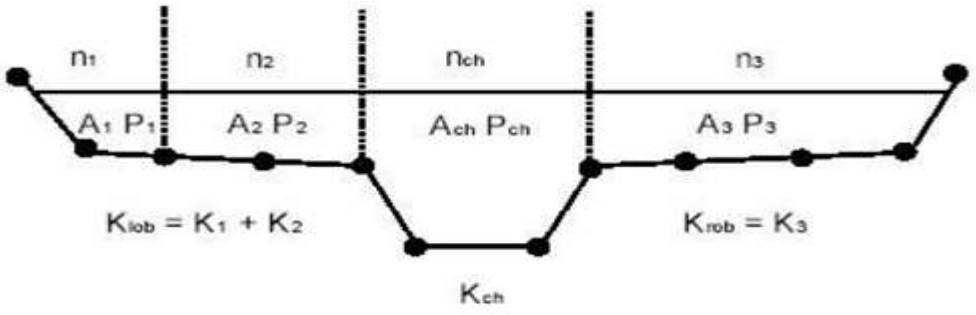


Fig. 2.5: HEC-RAS Conveyance Sub-division Method
Source: Bruner (2010)

All the incremental conveyances in the overbank are summed to obtain a conveyance for the left and the right overbanks and the total conveyance for cross-section is obtained by summing the three sub-division conveyances.

Calculation of Mean Kinetic Energy Head: Mean kinetic energy head for each cross-section is obtained by computing the flow weighted kinetic energy heads for three sub-sections of the cross-sections (Left Overbank, Channel, and Right Overbank). Figure 2.6 illustrates the mean kinetic energy calculation process for a cross-section with a main channel and right overbank.

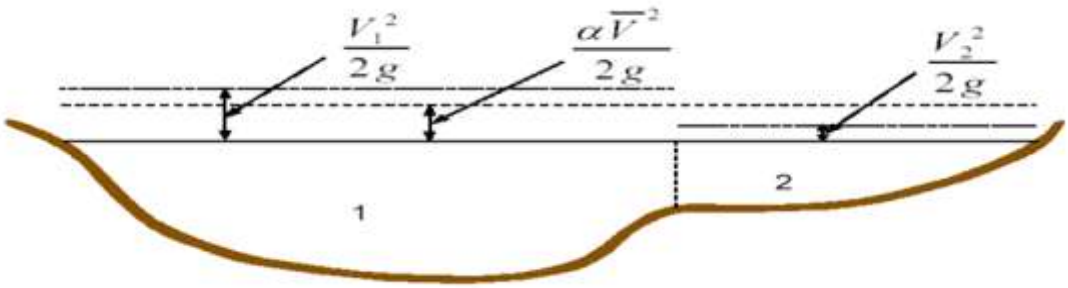


Fig. 2.6: Mean Energy Head Calculation
Source: Bruner (2010)

It is necessary to obtain the velocity head weighting coefficient α in order to compute the mean kinetic energy. α can be calculated using Eq. (2.15).

$$\alpha = \frac{(A_t)^2 \left[\frac{K_{lob}^3}{A_{lob}^2} + \frac{K_{ch}^3}{A_{ch}^2} + \frac{K_{rob}^3}{A_{rob}^2}\right]}{K_t^3} \qquad (2.15)$$

Where, A_t = total flow area of cross-section

A_{lob}, A_{ch}, A_{rob} = flow areas of left overbank, main channel and right overbank

K_t = total conveyance of cross-section

K_{lob}, K_{ch}, K_{rob} = conveyance of left overbank, main channel and right over bank

Unsteady Flow Simulation: The component of the HEC-RAS modelling system is capable of simulating one-dimensional unsteady flow through a full network of open channels. The unsteady flow component was developed primarily for subcritical flow regime calculations but the model can now perform mixed flow regime (subcritical, supercritical, hydraulic jumps, and draw downs) calculations in the unsteady flow computations module. Special features of the unsteady flow component include: Dam break analysis, levee breaching and overtopping, Pumping stations, navigation dam operations and pressurized pipe systems.

Sediment Transport/Movable Boundary Computations: This component of the modelling system is intended for the simulation of one-dimensional sediment transport/movable boundary calculations resulting from scour and deposition over moderate time periods (typically years, although applications to single flood events are possible). This can be used to evaluate deposition in reservoirs, design channel contractions required to maintain navigation depths, predict the influence of dredging on the rate of deposition, estimate maximum possible scour during large flood events, and evaluate sedimentation in fixed channels.

Water Quality Analysis: This component of the modelling system is intended to allow the user to perform riverine water quality analyses. An advection-dispersion module is included in HEC–RAS, adding the capability to model water temperature. This new module uses the QUICKEST-ULTIMATE explicit numerical scheme to solve the one-dimensional advection-dispersion equation using a control volume approach with a fully implemented heat energy budget.

Data Storage and Management: Data Storage is accomplished through the use of "flat" files (ASCII and binary), as well as the HEC-DSS. User input data are stored in flow files under separate categories of project, plan, geometry, steady flow, unsteady flow, and sediment data. Output data is predominantly stored in separate binary files. Data can be transferred between HEC-RAS and other programs by utilizing the HEC-DSS.

Graphics and Reporting: Graphics include X-Y plots of the river system schematic, cross-sections, profiles, rating curves, hydrographs, and many other hydraulic variables. A three-dimensional plot of multiple cross-sections is also provided. Tabular output is available. Users can select from pre-defined tables or develop their own customized tables. All graphical and tabular output can be displayed on the screen, sent directly to a printer (or plotter), or passed through the Windows Clipboard to other software, such as a word-processor or spreadsheet.

RAS Mapper: HEC-RAS has the capability to perform inundation mapping of water surface profile results directly from HEC-RAS. Using the HEC-RAS geometry and computed water surface profiles, inundation depth and floodplain boundary datasets are created through the RAS Mapper. Additional geospatial data can be generated for analysis of velocity, shear stress, stream power, ice thickness, and floodway encroachment data.

2.15.2.2 HEC- GeoRAS

HEC-Geo RAS is an ArcGIS extension specifically designed to process geo-spatial data for use with the Hydrologic Engineering Center Rivers Analysis System (HEC-RAS). The extension allows users to create an HEC-RAS import file containing geometric attribute data from an existing Digital Elevation Model (DEM) and complementary data

sets. Water surface profile processed and exported from HEC-RAS to HEC-GeoRAS can also be processed to visualize inundation depths and boundaries. HEC-GeoRAS extension for ArcGIS used an interface method to provide a direct link to transfer information between the ArcGIS and the HEC-RAS.

HEC-GeoRAS requires ArcGIS with 3D Analyst extensions. Although not a requirement, the availability of the Spatial Analyst extension significantly speeds up post-processing. In summary, HEC-GeoRAS extension provides the user with a set of procedures, tools and utilities for the preparation of GIS data for import into HEC-RAS and generation of GIS data from HEC-RAS output. These tasks are organized as pre-processing (preRAS) and post-processing (postRAS) facilitated by menu and buttons.

Processing to Develop the RAS GIS import file: The RAS GIS Import File is created in HEC-GeoRAS consisting of geometric attribute data necessary to perform hydraulic computations in HEC-RAS. The cross-sectional geometric data is developed from DEM (TIN) of the channel and surrounding land surface, while the cross-sectional attributes are derived from points of intersection of the created RAS layers which include Stream Centerlines, Flow Path Centerlines, Main Channel Banks, and Cross Section Cut Lines. Additional RAS layers that may be created to extract additional geometric data for import in HEC-RAS include Land Use, Levee Alignment, Ineffective Flow Areas, and Storage Areas. Expansion/contraction coefficients, hydraulic structure data such as bridges and culverts are not written to the RAS GIS Import File but are modelled through the RAS interface.

Post – Processing to Generate GIS Data from HEC-RAS Results: Post-processing facilitates the automated floodplain delineation based on the data contained in the RAS-

GIS output file and original terrain TIN. Based on the RAS-GIS export file, cross-sections theme (with water levels for each modelled profile as attributes) and bounding polygon of the likely floodplain can be generated. The water surface TIN is generated using these cross-sections and bounding polygon themes. With the water surface TIN and the original terrain TIN, inundated depth grids and floodplain polygons can be automatically generated. Apart from this, HEC-GeoRAS can also generate the velocity TIN and grid.

2.15.2.3 ArcGIS 10.2.2

ArcGIS 10.2.2 was developed by Environmental Systems Research Institute (ESRI) Inc. (1999 - 2014). It is a very important and easy to use tool that brings GIS to the desktop. ArcGIS 10.2.2 is equipped with excellent graphical user interface (GUI). ArcGIS Desktop includes a suite of integrated applications that allow GIS tasks to be performed, from simple to advanced, including mapping, geographic analysis, data editing and compilation, data management, visualization, and geo-processing.

ArcGIS 10.2.2 is also equipped with a number of extensions designed to perform various tasks. They include spatial analyst which provides spatial analysis tools for use with raster and feature data, 3D analyst which provides tools for surface modelling and 3D visualization, geostatistical analyst which provides a complete set of spatial analytical tools that range from techniques to explore the original data to post-processing, evaluation of data and predictions uncertainties Arcscan which provides support for the creation of vector features from a raster image amongst others. Some extensions, such as the ones mentioned, are bundled with ArcGIS while others such as HEC-GeoHMS, HEC-GeoRAS and ArcHydro are optional and can be added.

CHAPTER THREE

MATERIALS AND METHODS

3.1 MATERIALS

3.1.1 Types and sources of data

The data used in this study were obtained from both primary and secondary sources. The following data were obtained and utilized for the achievement of the stated objectives:

i. Topographic Map:

The topographic maps used in this study are the Nigerian Survey Topographic Map Series of Nigeria. They are Idah N.E. Sheet 267, Idah S. E. Sheet 267 and Ilushi N. E Sheet 286 all on a scale of 1:50,000 (Appendix Ia-c). The Idah N. E. and S. E. sheets were published by the Office of the Surveyor General of the Federation while the Illushi N. E. was published by the defunct Federal Surveys of Nigeria. The summary of the properties of the topographic maps are presented in Table 3.1. They were obtained from the Kogi State Ministry for Land and Urban Development Headquarters, Lokoja.

Table 3.1: Properties of the Topographic Maps Used in the Study

S/No	Title	Sheet No	Coverage		Year Published
			Latitude	Longitude	
1	IDAH NE	267 NE	7º15' - 7º30'	6º45' – 7º	2008
2	IDAH SE	267 SE	7º – 7º15'	6º45' – 7º	2008
3	ILLUSHI NE	286 NE	6º45' – 7º	6º45' – 7º	1964

Source: Kogi State Ministry of Land and Urban Development

The maps were scanned, georeferenced and digitized in ArcGIS 10.2.2 and used to identify features for landuse/land cover classification as well as the flood vulnerability assessment.

ii. Historical Rainfall Data of Neighbouring Towns

Historical rainfall data of towns surrounding the study area were obtained from project reports available at the Library of the Lower Benue River Basin Development Authority

headquarters, Makurdi. The towns for which data were obtained from Literatures are Idah, Onitsha, Nsukka, Adani and Enugu. In addition to these, meteorological data were also obtained from the Nigerian Metrological Agency (NiMet), Tactical Air Command, Makurdi-Airport (1980-2015). The summary of these historical rainfall data are presented in Table 3.2. The details are presented in Appendix II (Table IIa).

iii. Historical Gauged Discharge Data of Ofu River at Oforachi

Discharge data of Ofu River at the Oforachi hydrometric station from 1955 to 1973 were obtained from Kogi State Ministry of Water Resources and Rural Development. The summary is presented in Table 3.3 while the details are presented in Appendix III (Table III).

iv. Soil Map

The digital soil map of the world alongside the attributes was obtained from the Food and Agricultural Organization (FAO)'s website via the following link.

(http://www.fao.org/geonetwork/srv/en/metadata.show?id=14116)

v. Satellite Data

Properties and relevance of the SRTM Digital Elevation Model and other satellite imageries used in this study are presented in Table 3.4. The projection for all the data is the Universal Transverse Mercator (UTM) zone 32 while the datum is WGS84.

Table 3.2: Historical Mean Annual Rainfall for Ofu River Catchment Neighbouring Stations

Station	Latitude (^{0}N)	No. of Years	Mean Annual Rainfall (mm)
Idah	7º06'	32	1517.52
Onitsha	6º23'	55	2243.52
Nsukka	7º52'	21	1930.14
Adani	6º43'	17	1995.00
Enugu	6º27'	54	2163.72
Makurdi	7º41'	30	1165.82

Source: Skoup and Motor Columbus (1980), NiMET (2016)

Table 3.3: Historical Mean Discharge Record for Ofu River at Oforachi

Month	Jan	Feb	Mar	Apr	May	Jun	Jul	Aug	Sep	Oct	Nov	Dec	Total
Ave (m^3/s)	3.86	2.85	2.14	13.31	15.95	44.02	132.45	403.79	432.02	83.01	5.8	3.93	1143.12

Source: Kogi State Ministry of Water Resources and Rural Development

Table 3.4: Properties of Satellite Data and Relevance

Data Type	Resolution	No of Bands	Date of Acquisition	Date of Publication	Source
SRTM DEM V3	30m	1	11/02/2000	26/07/2014	Earthexplorer.usgs.gov
ASTER GDEM2	30m	1	2011	October, 2011	Earthexplorer.usgs.gov
Landsat 8 Imagery of 2016	30m	12	15/03/2016	03/05/2016	Glovis.usgs.gov
Landsat 7 Imagery of 2001	30m	9	09/01/2001	29/11/2014	Glovis.usgs.gov
Landsat 5 Imagery of 1987	30m	7	11/01/1987	18/06/2014	Glovis.usgs.gov
River map of Africa	NA	NA	NA	NA	www.waterbase.org

vi. Meteorological Data

The rainfall data used for this study were obtained from the radar data available on http://www.waterbase.org/download_data.html. They consist of data from 41 stations surrounding the study area. The data covered a 35 year period from January, 1979 to December, 2013. The summary of this data is presented in Appendix II (Tables IIb and IIc).

vii. Information on Previous Flood Occurrence

The information on previous flood experience was gathered with the aid of questionnaires admistered during field survey.

3.1.2 Hardware and software

3.1.2.1 Hardware

i. A High speed memory Lenovo ideapad 100 Intel Pentium Laptop Computer.
ii. A Garmin hand-held Global Positioning System (GPS) receiver model GPSmap 78sc for marking of locations during fieldwork.
iii. An Impeller current meter, Valeport model 0012B Version 4.01
iv. Ring Infiltrometer (Fabricated)
v. Soil Classification Apparatus (Atterberg Limits apparatus, Sieve Analysis Apparatus, Weighing balance and Oven)

3.1.2.2 Software

i. Google Earth Pro 4.2 was used for the identification and extraction of information for landuse/landcover classification.

ii. ArcGIS 10.2.2 is a commercial software developed by Environmental Systems Research Institute (ESRI) that is essentially used for GIS analysis. It has the capability of accepting compatible add-on extensions such as the ArcHydro, HEC-GeoHMS and HEC-GeoRAS. The Spatial analyst and the 3D analyst tools have capabilities that make easy data manipulation, analysis and management with regards to floodplain simulation.

iii. HEC-GeoHMS10.2 is a free software developed by the Hydraulic Engineering Centre (HEC) of the United States Army Corp of Engineers (USACE). It is an extension installed in ArcGIS for GIS analysis with spatial data for catchment delineation and hydrological modelling.

iv. HEC-GeoRAS10.2 is a free software developed by the Hydraulic Engineering Centre (HEC) of the United States Army Corp of Engineers (USACE). It is an extension installed in ArcGIS for GIS analysis with spatial data, flood inundation and water depth simulation. It is normally used in conjunction with HEC-RAS.

v. HEC-RAS 4.1 is also a free software developed by the Hydraulic Engineering Centre (HEC) of the United States Army Corp of Engineers (USACE) for one-dimensional hydraulic modelling. The RAS mapper has the capability of flood inundation mapping. It is normally used in conjunction with HEC-GeoRAS.

vi. Microsoft Office Excel 2007 for river discharge analysis, flood frequency analysis and other statistical analysis and presentation.

vii. Minitab® Release 14.12.0 Statistical Software developed by Minitab Inc. was used alongside Microsoft Excel for statistical analysis.

viii. Stata®/SEversion 13.1 special edition developed by Stata Corp Lp was used alongside Microsoft Excel and Minitab for statistical/data analysis.

3.2 METHODS

3.2.1 Determination of Morphologic Characteristics of Ofu River Catchment

3.2.1.1 Delineation of Ofu River catchment boundaries

The terrain pre-processing of the DEM for the delineation of the catchment boundaries was done using the ArcHydro *terrain preprocessing tool* in ArcHydro extension while the actual delineation was done using the HEC GeoHMS.

(A) Terrain pre-processing using ArcHydro

a. Datasets Preparation

Two datasets were required for the Terrain pre-processing and watershed delineation. The first dataset was the digital elevation model (DEM). The DEM used for this study was obtained from the four tiles of the STRM DEM (Table 3.4). A single DEM was created using the *Mosaic tool* in dataset Management Tool in ArcGIS 10.2.2 by clicking *Dataset management tool>Raster>Raster Dataset>Mosaic* with the four DEMs as input and the first tile chosen as the target raster. On clicking OK, the mosaic process was completed. The other DEMs were removed leaving only the target raster as the raw DEM for the analysis. The mosaicked DEM was projected by clicking *Dataset management tool>Projections and Transformations>Raster>Project Raster* with the mosaicked DEM as the input raster dataset. The output raster dataset was named *ofu_dem* and saved in the working directory. The output coordinate system was defined to *WGS1984 UTM Zone 32*. On clicking Ok, the DEM was projected to the defined coordinate system. The projected DEM was converted to grid using the *raster to other formats* conversion tool by clicking *Conversion>To Raster>Raster to other formats (multiple).*

The second dataset was the streams shapefile. This is a shapefile containing stream network for the study area. This was clipped from the river map of Africa extracted from http://www.waterbase.org/download_data.html. The stream feature was also projected to the same coordinate system as the DEM by clicking *Dataset management tool>Projections and Transformations>Project.*

Both datasets were added to the new map document.

b. Terrain Pre-processing

Terrain Pre-processing in Arc Hydro follows a sequential order. Terrain pre-processing is pre-requisite for the watershed processing and delineation itself thus must be completed first. The processes carried out at this stage are described below:

i. DEM Reconditioning: DEM reconditioning was carried out to modify the elevation data to be more consistent with the input vector stream network. This was done on the assumption that the stream network data are more reliable than the DEM data thus increasing the degree of agreement between stream networks delineated from the DEM and the input vector stream networks.

The DEM reconditioning was carried out by selecting *Terrain Preprocessing >DEM Manipulation> DEM Reconditioning* on ArcHydro Toolbar. The projected *ofu_dem* was selected as input raw DEM while the clipped river of the study area was selected as the input agree Stream feature. The Sharp drop/raise parameter was reduced from its default 1000 to 10 while other fields were left as they were. On clicking Ok, the *AgreeDEM* was produced and added to the map document.

ii. Fill Sinks: The fill sink operation was carried out by selecting *Terrain Preprocessing>Data Manipulation>Fill Sinks* on the ArcHydro toolbar with AgreeDEM as input. The output Hydro DEM was named *ofu_fil*. The other fields were left unchanged. On pressing Ok, the fill sink operation was completed and the *ofu_fil* layer was added to the map document.

iii. Flow Direction: The flow direction operation was carried out by selecting *Terrain Preprocessing>Flow Direction* on the ArcHydro toolbar with *ofu_fil* as the input Hydro DEM. The output grid was named *ofu_fdr*. On pressing Ok, the flow direction operation was completed and the *ofu_fdr* grid was added to the map document.

iv. Flow Accumulation: The flow accumulation operation was carried out by selecting *Terrain Preprocessing>Flow Accumulation* on the ArcHydro toolbar with *ofu_fdr* as the input Flow direction grid. The output grid was named *ofu_fac*. On pressing Ok, the flow accumulation operation was completed and the *ofu_fac* grid was added to the map document.

v. Stream Definition: The definition operation was carried out by selecting *Terrain Preprocessing>stream definition* on the ArcHydro toolbar with *ofu_fac* as the input Flow Accumulation grid. The output grid was named *ofu_str*. A threshold area of 25 km^2 was used in the stream definition. On pressing Ok, the stream definition operation was completed and the *ofu_str* grid was added to the map document.

vi. Stream Segmentation: The segmentation operation was carried out by selecting *Terrain Preprocessing>Stream Segmentation* on the ArcHydro toolbar with *ofu_fdr* and *ofu_str* as the input for Flow direction and stream grids, respectively. The output grid was

named *ofu_str_link.* On pressing Ok, the stream segmentation operation was completed and the *ofu_str_lnk* grid was added to the map document.

vii. Catchment Grid Delineation: The catchment grid delineation operation was carried out by selecting *Terrain Preprocessing>Catchment Grid Delineation* on the ArcHydro toolbar with *ofu_fdr* and *ofu_str_lnk* as the input for Flow direction and stream link grids, respectively. The output Catchment Grid Layer was named *ofu_cat.* On pressing Ok, the catchment grid delineation was completed and the *ofu_cat* grid was added to the map document.

viii. Catchment Polygon Processing: The catchment Polygon processing operation was done to convert the Catchment grid from raster to vector format. This was done by selecting *Terrain Preprocessing >Catchment Polygon Processing* in ArcHydro toolbar with *ofu_cat* as the input Catchment Grid. The output polygon was named *catchment.* On pressing Ok, the catchment grid was converted into a catchment polygon feature class. This was then added to the map document.

ix. Drainage Line Processing: The drainage line processing operation was done to convert the input Stream Link grid into a Drainage Line feature class which would be used for the delineation of the catchments. This was done by selecting *Terrain Preprocessing >Drainage Line Processing* on the ArcHydro toolbar with *ofu_str_lnk* as the input Stream Link and to *ofu_fdr* as the Flow Direction Grid. The default name for the output Drainage Line was accepted as *DrainageLine*. On pressing Ok, the drainage line processing operation was completed and the linear feature class '*DrainageLine*' was added to the map document.

x. **Adjoint Catchment Processing:** The adjoint catchment processing operation was done by selecting *Terrain Preprocessing > Adjoint Catchment Processing* with *DrainageLine* and *Catchment* as inputs while default ouput name was accepted as *AdjointCatchment.*

On pressing Ok, a polygon feature class named *AdjointCatchment* was added to the map document.

(B) Ofu Watershed Processing and Delineation Using HEC GeoHMS

a. Datasets Management

The outputs of the terrain pre-processing in ArcHydro were the inputs for the Watershed processing in HEC GeoHMS project set up. The Datasets were confirmed by clicking *HMS Project Setup>Data Management* on the HEC-GeoHMS Main View toolbar. The corresponding map layers were confirmed as follows:

i. Raw DEM: *ofu_dem*
ii. Hydro DEM: *ofu_fil*
iii. Flow Direction Grid: *ofu_fdr*
iv. Flow Accumulation Grid: *ofu_fac*
v. Stream Grid: *ofu_str*
vi. Stream Link Grid: *ofu_str_lnk*
vii. Catchment: *ofu_cat*
viii. Adjoint Catchment: *AdjointCatchment*

b. Creating Ofu River Project

The first step in catchment delineation in HEC GeoHMS is the Project creation. This involved starting new project, defining the project point and Generating the Project.

i. **Start New Project**

This was done by clicking on *Project Setup>Start New Project*. The default *ProjectArea* and *ProjectPoint* were accepted. Thus, the *ProjectPoint* and *ProjectArea* feature classes were created. The process pops up another dialogue box for defining a new project. The following links fields were required and provided as follows:

Project Name: *OfuRiver*

Description: *HMS model for Ofu River*

Extraction Method: *Original Stream Definition*

Project Data location: *Outside mainview Geodatabase*

Every other field was left as default. On pressing Ok, the process of creating the Ofu River project was completed and the *projectArea and ProjectPoint* feature classes were added to the map document. These feature classes were added to the same geodatabase ofu.gdb

ii. **Define Project Point**

The *Add Project Points* tool on the HEC-GeoHMS toolbar was used to define the outlet of Ofu River just before its confluence with Omabolo River downstream.

A new dialogue box "*Project Point for OfuRiver"* popped up. The defaults point Name and description "*outlet1"* were accepted. Thus, the definition of project point was completed and added to the map document.

iii. **Generating Ofu River Project**

The last step in the Creation of Ofu River project is the generation of the project itself. This was done by selecting *HMS Project Setup>Generate Project*. This created a mesh by delineating watershed for the outlet in Project Point as shown on Fig. 3.1.

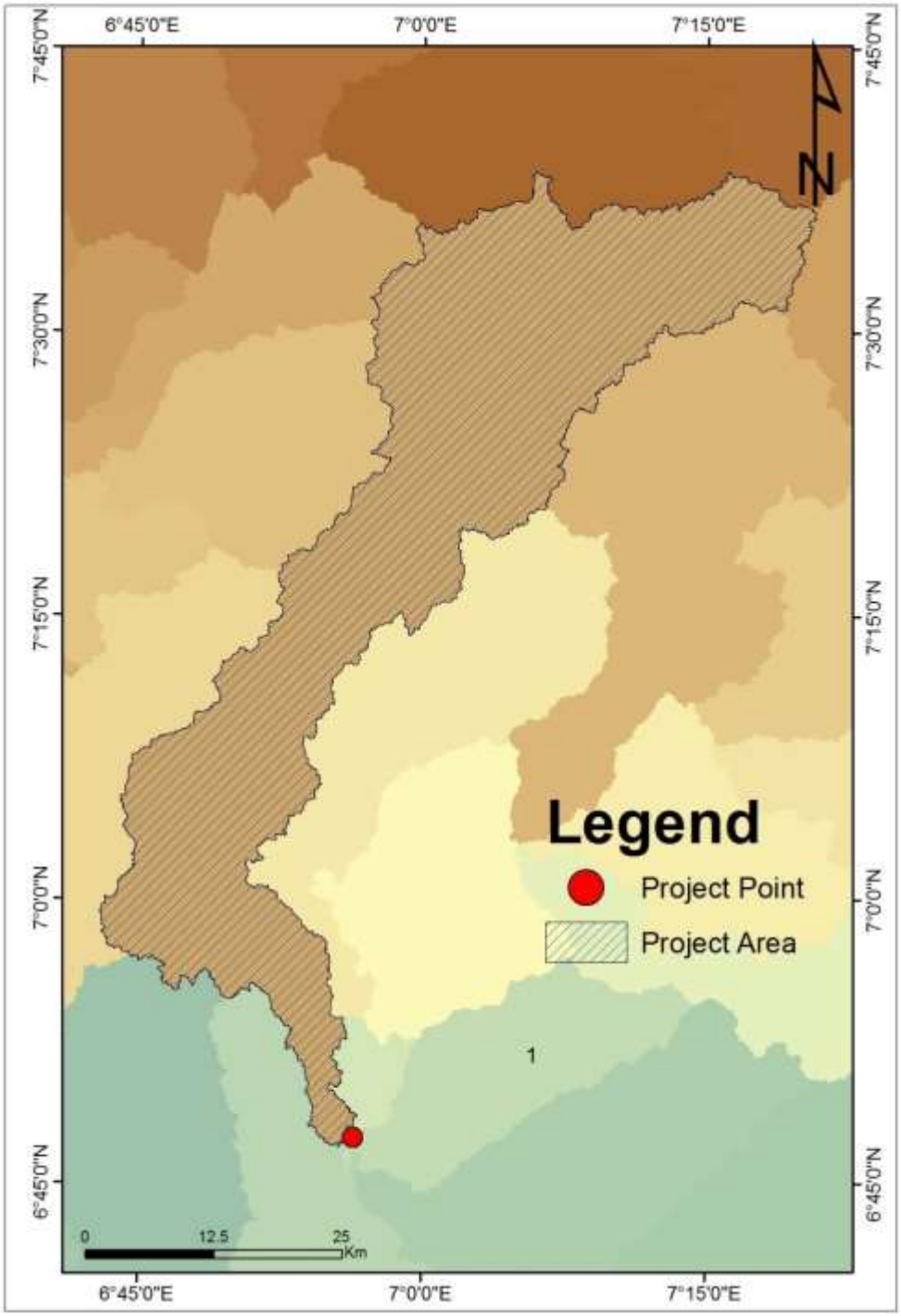


Fig. 3.1: Project Point and Project Area for Ofu River Catchment Delineation

The message box asking if you want to create a project for this hatched area was accepted by clicking 'Yes' on the message box. The layer names for the new project was confirmed while the default names for Subbasin, Project Point, River and BasinHeader were left as they were (*Subbasin 181, ProjectPoint181, River 181*). On clicking Ok, a new folder was created inside the working folder with the name '*OfuRiver'* where all the relevant raster, vector and tabular data were stored. The raster data were stored in a sub folder with the project name (*OfuRiver*) inside *OfuRiver* folder while all vector and tabular data were stored in *OfuRiver.mdb*. At the same time, a new data frame (*OfuRiver*) was added in the map document containing the data for Ofu River.

c. River Profile

The River Profile tool in HEC GeoHMS main toolbar was used to display the profile of selected Ofu river reach. It was observed that there was no significant change in the river slope.

d. Extracting Basin Characteristics

The basin characteristics menu in the HEC-GeoHMS Project was used to extract the physical characteristics of Ofu River (River181) and Ofu Catchment (Subbasin181) into attribute tables.

The properties were extracted via the following methods.

i. River Length: The River length was computed by selecting *Characteristics>River Length* on the HEC GeoHMS toolbar with *River181* (Ofu River) as input River. On pressing Ok, the *RiverLen* field in attribute table was filled with the Length of the main stream.

ii. River Slope: The slope of the River segment was computed by selecting *Characteristics>River Slope* on the HEC GeoHMS toolbar with *River181* (Ofu River) as input River. On pressing Ok, the *Slp* field in attribute table was filled with the slope of the main stream.

iii. Basin Slope: A slope grid was created using Arc Hydro tools by selecting *Terrain Preprocessing > Slope* with *ofu_dem* as input and *percent_rise* as slope type. A slope grid with the default name *WshSlopePct* was produced and added to the map document. This was used as input alongside the subbasin polygon for the computation of average slope for Ofu river basin using HEC geoHMS.

The basin slope computation was done by selecting *Characteristics>Basin Slope* with the *Subbasin181* (Ofu River basin) and *Slope Grid* as input. The Subbasin1 for Ofu River attribute table was instantly filled with the average basin slope of Ofu River watershed.

iv. Longest Flow Path: The longest flow path was computed by selecting *Characteristics>Longest Flow Path* on the HEC GeoHMS toolbar with *ofu_dem* as the input raw DEM, *ofu_fdr* as the input flow direction grid and *Subbasin181* as the input subbasin. On pressing Ok, a new feature class storing longest flow path for the basin was created and added to the map document.

v. Basin Centroid: The Basin centroid was computed by selecting *Characteristics>basin Centroid* on the HEC GeoHMS toolbar with *Subbasin181* as the input subbasin. The default center of gravity method was selected as the centroid method. On pressing Ok, a point feature class showing centroid for each subbasin was added to the map document.

vi. Basin Centroid Elevation: The Basin Centroid Elevation was computed by selecting *Characteristics>Basin Centroid Elevation* on the HEC GeoHMS toolbar with

ofu_dem as the input raw DEM *Centroid181* as the input Centroid. On pressing Ok, the elevation field of the centroid attribute table was populated.

vii. **Centroidal Longest Flow Path:** The Centroidal longest flow path was computed by selecting *Characteristics>Centroidal Longest Flow Path* on the HEC GeoHMS toolbar with *subbasin181* as the input Subbasin, *centroid181* as the input Centroid and *LongestFlowPath181* as the input Longest Flow Path. On pressing Ok, a new feature class storing Centroidal longest flow path for each basin was created and added to the map document.

3.2.1.2 Estimation of morphologic parameters of Ofu River catchment

The morphologic parameters determined for Ofu River catchment were broadly classified into areal, linear and relief aspects, respectively. The following standard methods were followed to determine the morphometric parameters.

(A) Areal Aspects

The basic areal morphologic characteristics of the river basin were determined via the following methods:

i. **Basin area (A):** The basin area was calculated after the delineation of the catchment boundaries. The Attribute table of the Sub-basin was opened in ArcGIS 10.2.2 and a new field was added and named Area. The Calculate Geometry tool was then used to calculate the area of the catchment in km^2 which was done automatically and the required field populated.

ii. **Basin Perimeter (P):** The same procedure followed for the calculation of the basin area was followed for the calculation of the basin perimeter. The Perimeter field was then populated automatically with the perimeter values in km.

iii. **Basin Length (L_b):** The Schumm (1956) definition of basin length was adopted in this study. The basin length was taken as the longest distance between the basin outlet and the remotest part of the watershed divide parallel to the drainage line. This was done using the measurement tool in ArcGIS 10.2.2

iv. **Longest flow path (L_{fp}):** This was extracted from the attribute table of the Longest Flow Path feature class in km.

v. **Main Stream Length (S_L):** This was extracted from the attribute table of the River (*River181)* in km.

vi. **Basin Centroid Longest Flow Path (L_{cfp}):** This was extracted from the *Centroid181* feature class in km.

The methods for the estimation of the derived areal morphologic characteristics of the Catchment are summarized in Table 3.5.

Where A is the Basin area (km^2), L_b is the Basin length (km), P is Basin Perimeter (km), ΣN_u is number of streams of all orders, ΣL_u is total length of streams of all orders (km), L_{fp} is the longest flow path (km) and S is the Basin Slope.

Table 3.5: Methods of Estimation of Derived Areal Morphological Characteristics

S/N	Parameters	Symbol	Equation No.	Reference
vii.	Elongation ratio	$R_e = {2\sqrt{A/\pi}}/{L_b}$	3.1	Schumm (1956)
viii.	Circularity ratio	$R_c = {4\pi A}/{P^2}$	3.2	Miller (1953)
ix.	Form factor	$F_f = {A}/{L_b{}^2}$	3.3	Horton (1932)
x.	Compactness coefficient	$C_c = {0.282038P}/{A^{0.5}}$	3.4	Horton (1945)
xi.	Shape Factor	$B_s = {L_b{}^2}/{A}$	3.5	Horton (1932)
xii.	Stream frequency	$F = {\sum N_u}/{A}$	3.6	Horton (1945)
xiii.	Drainage Density	$D_d = {\sum L_u}/{A}$	3.7	Horton (1932; 1945)
xiv.	Drainage Texture	$D_t = {\sum N_u}/{P}$	3.8	Horton (1945)
xv.	Drainage Intensity	$I_d = {F}/{D_d}$	3.9	Faniran (1968)
xvi.	Constant of Channel Maintenance	$C_m = {1}/{D_d}$	3.10	Strahler (1952)
xvii.	Length of Overland Flow	$L_o = {1}/{2D_d}$	3.11	Langbein & Leopold (1964)
xviii.	Channel Sinuosity	$S_c = {\sum L_u}/{L_{fp}}$	3.12	Le Roux (1992)
xix.	Time of Concentration	$T_c = 0.000323{L_{fp}}^{0.77}S^{-0.385}$	3.13	Kirpich (1940)
xx.	Time from Peak to Recession	$N = 0.84A^{0.2}$	3.14	Mustafa and Yusuf (2012)

(B) Linear Aspects

The Linear aspects of the drainage basin derived in this study are stream order, stream number, stream length, Mean stream length, bifurcation ratio and stream length ratio.

The stream order of Ofu River Catchment was derived using the spatial analyst hydrology tools in ArcGIS 10.2.2. via the following steps using the Ofu River flow accumulation and flow direction rasters obtained from the HEC GeoHMS catchment delineation process as input.

i. **Stream network definition:** In order to extract the stream network, it was assumed that a total of 25km^2 is the required drainage threshold to form a stream (Merwade, 2012). The pixel value of this threshold is calculated as follows:

$$Threshold\ pixels = \frac{25\ \times 10^6}{90 \times 90} = 27{,}778\ pixels$$

The stream network definition was done by creating a raster from the *ofu_fac* such that only cells that have pixel value greater than 27,778 was included. This was done using the raster calculator by selecting *Spatial Analyst Tools>Map Algebra>Raster calculator*. The "setnull" command was used to create a calculation raster where all the cells with value greater than or equal to 27,778 in *ofu_fac* were assigned a value of 1, while all other cells are set to zero. This was done by specifying the command '*SetNull*("*ofu_fac"*<27778,1)' in raster calculator. The output raster was named *stream* and was added to the map document.

ii. **Stream link definition:** The stream link definition tool assigns a unique number to each link (or segment) in the stream raster. This was done by double clicking on Stream Link in spatial analyst hydrology tool providing *stream* as the input surface stream raster and *ofu_fdr* as the flow direction raster. The output raster was named *str_link*.

iii. **Stream order extraction:** The stream order extraction tool was used to stream order for the stream network. This was done by double clicking on stream order in the spatial analyst hydrology tool providing *stream* as the input for stream raster and *ofu_fdr* as the input for flow direction raster. The output raster was named *str_order*. Two methods are available in ArcGIS 10.2.2 for estimating stream order. The Strahler's method was chosen and specified in the 'method of stream ordering' link. On clicking Ok, the process of stream ordering for Ofu River catchment was completed and a new *str_order* raster was added to the map document.

iv. **Conversion of Stream network from raster to feature:** The last step here was the conversion of the stream raster to a polyline feature class (shapefile). This was done by double clicking *Stream to feature* in the spatial analyst hydrology tool providing *stream* as the input for stream raster and *ofu_fdr* as the input for the flow direction raster. The output was saved as *ofu_stream* in the working directory. On clicking Ok, the process of converting the stream raster to ploy line feature class was completed and a shapefile named *ofu_stream* was added to the map document. This same tool was used to convert the *str_order* raster to a polyline feature class named *Stream_oder* using the *str_order* raster instead of the *stream raster.*

The attribute table of the *stream_order* feature class is automatically populated with the stream order (U) of all the defined streams, the number of streams (N_u) in each order and the length of streams (L_u) in each order. These were used to calculate the mean stream length, bifurcation ratio and the stream length ratio as presented in Table 3.6

Table 3.6: Methods of Estimation of Linear Morphological Characteristics

S/N	Parameters	Symbol	Equation No.	Reference
i.	Mean Stream Length	$\boldsymbol{L_{um} = {L_u}/{N_u}}$	3.16	Strahler (1964)
ii.	Bifurcation Ratio	$\boldsymbol{R_b = {N_u}/{N_{u+1}}}$	3.17	Schumm (1956)
iii.	Stream Length Ratio	$\boldsymbol{R_L = {L_u}/{L_{u-1}}}$	3.18	Horton (1945)

Where L_u is length of streams of order U, N_u is the number streams of order U, N_{u+1} is the number of streams of the next higher order U+1 and L_{u-1} is the length of streams of the next lower order U-1.

(C) Relief Aspects

The methods of estimation of the relief characteristics of Ofu River catchment are presented in Table 3.7 except for the basin slope, *S* that was extracted from the sub basin attribute table.

Table 3.7: Methods of Estimation of Relief Morphological Characteristics

S/N	Parameters	Symbol	Equation No.	Reference
i.	Basin Relief	$\boldsymbol{H = Z - z}$	3.18	Strahler (1957)
ii.	Relief Ratio	$\boldsymbol{R_h = {H}/{L_b}}$	3.19	Schumm (1956)
iii.	Relative Relief	$\boldsymbol{R_{hp} = {H}/{P}}$	3.20	Melton (1957)
iv.	Ruggedness Number	$\boldsymbol{R_N = H \times D_d}$	3.21	Patton and Baker (1976)

Where *Z* is the highest elevation (m above seal level), *z* is the lowest elevation (m above sea level), L_b is Basin Length (m), *P* is the Basin Perimeter (m) and D_d is the drainage density.

A schematic flowchart of the morphometric analysis methodology is presented in Fig. 3.2.

3.2.2 Development of Stage-Discharge Rating Curve for Ofu River

Hydrological data such as stream flow and water levels are necessary inputs for hydraulic modelling of a river channel. These data were scarce or inexistent in the case of Ofu River as it is for several ungauged catchments in developing nations thus necessitating field work to generate these data. The detailed description of the methods adopted for the measurement of water levels and discharge of Ofu River as well as the development of the rating curve are presented as follows.

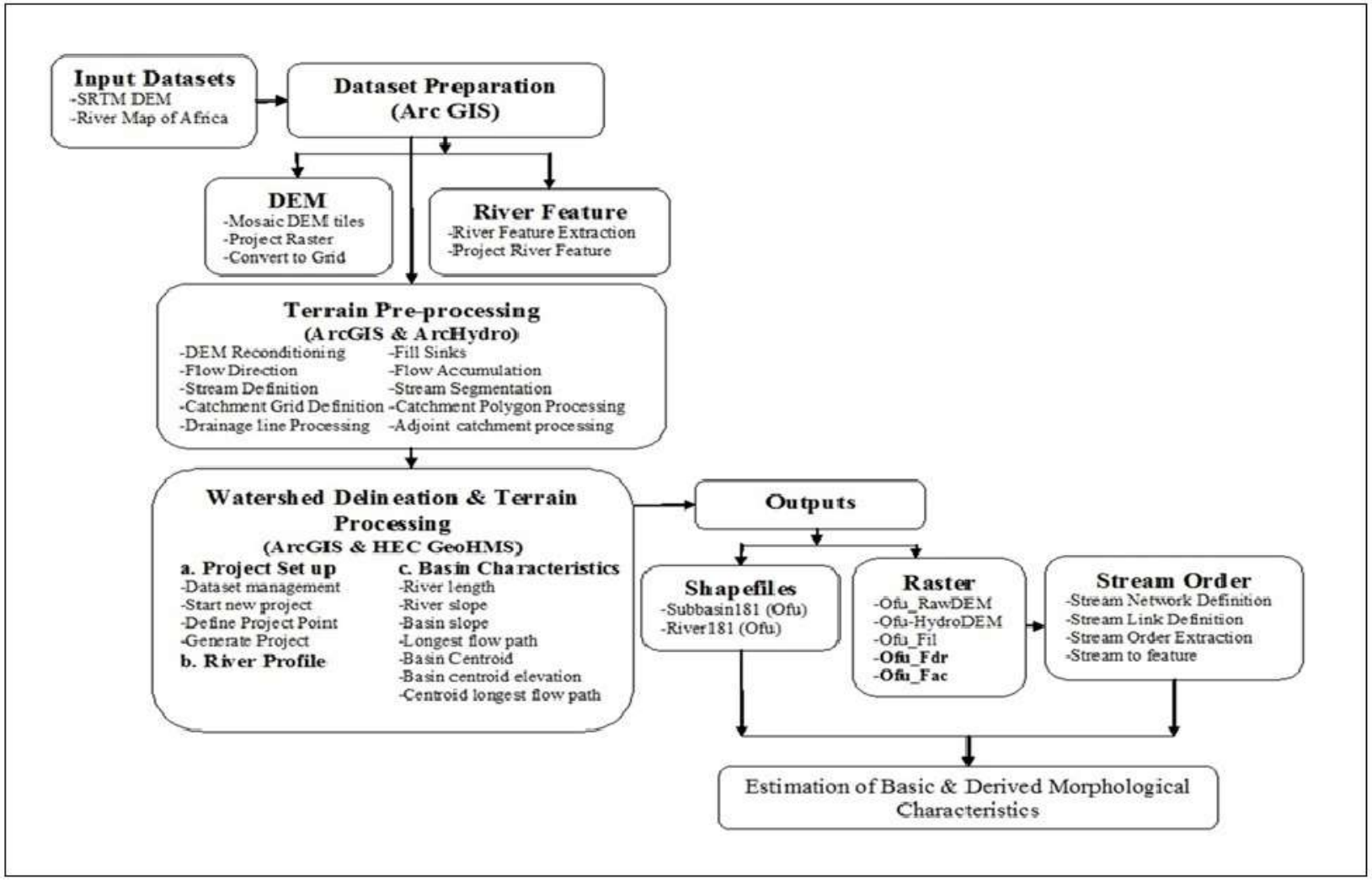


Fig. 3.2: Schematic Flowchart of the Morphometric Analysis Methodology

3.2.2.1 Ofu River stage gauge recalibration and water level measurement

It was observed during the reconnaissance survey that the original staff gauge of the Ofu River at Oforachi Bridge hydrometric station has been washed off by successive flood events that have taken place in the study area which necessitated a recalibration.

The temporary benchmark (TBM) of the area was located (Plate I) and transferred from the bridge to the gauging points on the old Oforachi Bridge where the firm poles of the previous staff gauges were located. This point is firm and satisfies all the criteria for locating a gauging site (Meals and Dressing, 2008; Sauer and Turnipseed, 2010). This was used as a reference for the recalibration of the staff gauge relative to mean sea level.



Plate I: Location of the TBM at Oforachi Bridge Hydrometric station

This transfer was done with the aid of a Total Station. The service of a professional surveyor was employed from the Department of Survey and Geomatics, Federal Polytechnic Idah, Kogi State (Plate II).

Three staff gauges were calibrated and labelled gauge 1, 2 and 3, respectively. These were used to take the water level of Ofu River every morning and evening for twelve (12) months beginning from the February 1, 2016 to January 31, 2017.



Plate II: Re-establishment of Staff gauge at Oforachi Bridge Hydrometric station

The location of the gauge point is shown in Fig. 3.3.

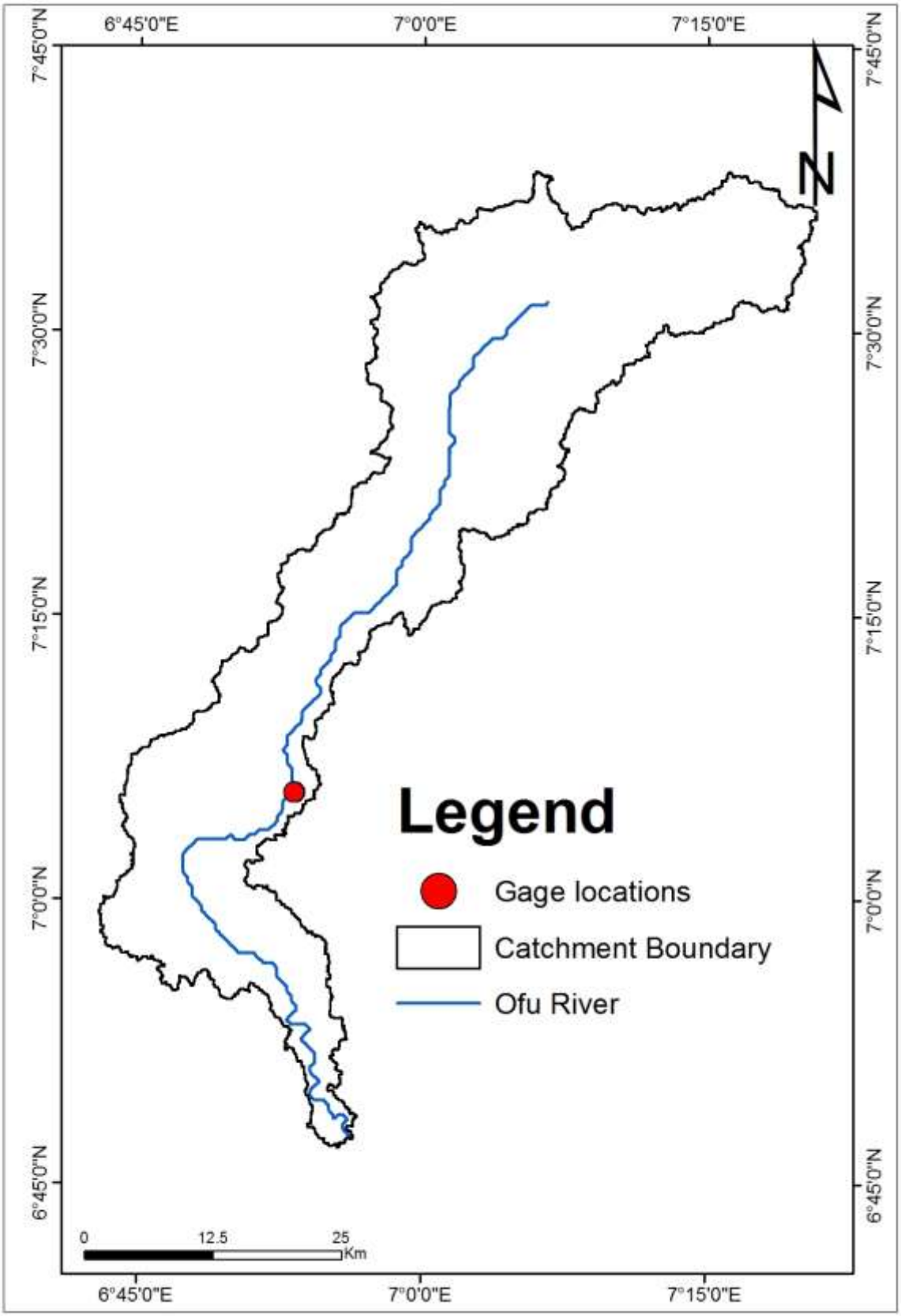


Fig. 3.3: Ofu River catchment showing location of gauge stations

3.2.2.2 Ofu River discharge measurement at Oforachi hydrometric station

The stream flow of Ofu River was measured for 12 months beginning from February 1, 2016 to January 31, 2017 in order to generate data for the development of the rating curve. The discharge measurement carried out in this study adopted the Velocity-Area method (mid section) using a Valeport Impeller current meter model 0012B Version 4.01 (Plate III).

Ofu River is a perennial river whose year round flow depth does not go below 2 meters at the deepest point thus making it difficult to apply the wading method. The bridge suspension method was therefore adopted incorporating some wading techniques to fit into the site peculiarities.



Plate III: Stream flow Measurement at Oforachi Bridge Hydrometric station

The schema of the river cross section is shown in Fig. 3.4.

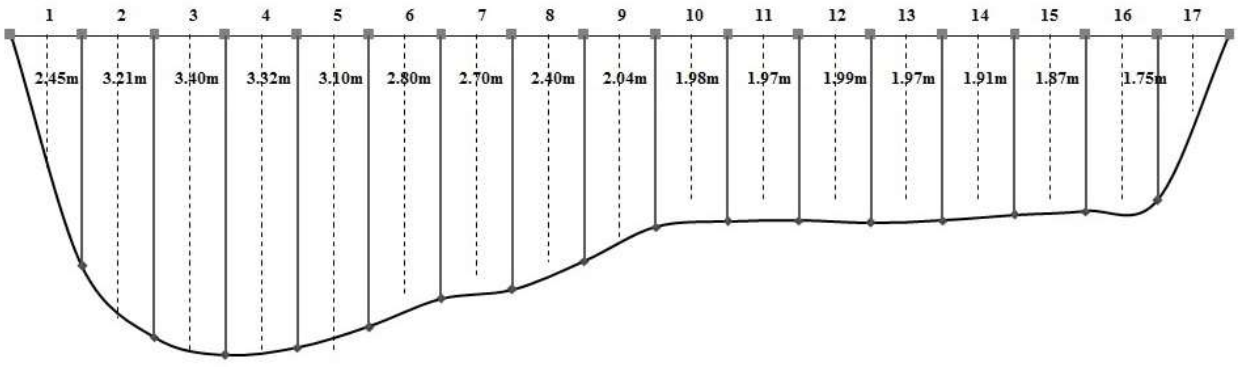


Fig. 3.4: Schema of the River Cross-section during one of the discharge measurements

The number of subsections for the observation was between 12 and 17 spaced 1 m apart throughout the period of observation. The discharge measurement was carried out via the following steps:

Step 1: The depth of water for each subsection was measured using the wading rod and recorded as *d*.

Step 2: A uniform horizontal distance (width of subsections) *w* of 1 m was adopted (Table 2.2). The width was measured from the reference bank along the old bridge beam where the measurement was taken.

Step 3: The area of each subsection was calculated using Eqs. (3.22a) and (3.22b) for the end sections and intermediate sections respectively.

$$a_1 = \frac{d_1}{2}\left(\frac{w_2}{2} + w_1\right) \qquad (3.22a)$$

$$a_2 = d_2\left(\frac{w_2 + w_3}{2}\right) \qquad (3.22b)$$

Step 4: The velocity at the respective sections were measured using the current meter. The one point measurement was done for depths less than 2 m while the two point measurement was done for depths greater than 2 m but less than 3 m as recommended by Mustafa and Yusuf (2012). For the one point measurement, the impeller of the current meter was placed at 0.6*d* from the water surface. The velocity obtained was taken as the average velocity of the section. For the two point measurement on the other hand, the current meter impeller was placed at 0.2*d* and 0.8*d* from the water surface respectively. The average velocity of the section was calculated using the relation expressed Eq. (3.23b).

$$V_i = 0.5(V_{0.2d} + V_{0.8d}) \qquad (3.23)$$

Step 5: The sub-sectional discharge q_i was calculated by multiplying the area of subsection by the average velocity at the sub section. The total discharge of the section was obtained by summing up the discharge for all the sub-sections. Thus the total sectional discharge is calculated using Eq. (3.24) (Patra, 2008; Mustafa and Yusuf, 2012; Daffi, 2013).

$$Q = \sum_{i=1}^{n} v_i y_i \Delta w_i \qquad (3.24)$$

The measured discharge and water levels (stage) for Ofu River are shown in Appendices VI and VII respectively.

3.2.2.3 Method of Development, fitting and extension of Ofu River rating curve at Oforachi hydrometric station

The stage-discharge relationship in this study was treated as a power curve of the form expressed by Eq. 3.25 (Braca, 2008)

$$Q = K(H - h)^m \qquad (3.25)$$

Where:

Q = Discharge (m^3/s)

H = Observed stage (m asl)

h = Gauge height of zero flow (m)

K = Discharge when effective depth of flow (H-h) is equal to 1

m = Slope of the rating curve on a logarithmic paper.

K, *h* and *m* are calibration coefficients for the rating curve.

The value of stage for zero flow, *h* was obtained by trial and error while the value of curve coefficients, *K* and *m* where obtained by the method of least squares for the linear equation obtained by taking logarithm of both sides of Eq. (3.25). The linear equation is expressed by Eq. (3.26). The value of *h* with the lowest standard error of estimate (S_e) was chosen.

$$LogQ = mlog(H - h) + logK \tag{3.26}$$

Which takes the form of a straight line equation, $y = mx + c$ where $y = logQ$ and $x = log(H\text{-}h)$ and $c = logK$.

The coefficient *m* and *K* were calculated using Eqs. (3.27) and (3.28), respectively (Patra, 2008).

$$m = \frac{N(\sum xy) - (\sum x)(\sum y)}{N(\sum x^2) - (\sum x)^2} \tag{3.27}$$

$$K = antilogc = antilog\left(\frac{(\sum y - m\sum x}{N}\right) \tag{3.28}$$

The standard error of estimate, S_e, correlation coefficient, *r*, coefficient of determination, R^2, and efficiency, *I]* were respectively calculated using Eqs. (3.29), (3.30), (3.31) and (3.32).

$$S_e = [\frac{1}{N}\sum(Q_o - Q_c)^2]^{1/2} \tag{3.29}$$

In which Q_o is observed discharge, Q_c is calculated discharge and *N* is number of observations.

$$r = \frac{[\sum xy - (\sum x \sum y)/N]}{[\sum x^2 - (\sum x)^2/N]^{1/2}[\sum y^2 - (\sum y)^2/N]^{1/2}} \tag{3.30}$$

$$R^2 = \{\frac{\left(\frac{1}{N}\right) \times \sum[(x - \bar{x})(y - \bar{y})]}{(\sigma_x \sigma_y)}\}^2 \tag{3.31}$$

In which σ_x and σ_y are the standard deviations of *x* and *y* respectively.

$$\eta = \frac{Variance\ of\ observed\ discharge - {S_e}^2}{Variance\ of\ observed\ discharge} \times 100 \qquad (3.32)$$

The variance used in Eq. (3.32) was calculated using Eq. (3.33).

$$Var = \frac{\sum(Q - \mu)^2}{N} \qquad (3.33)$$

In which μ is mean of observed discharge.

The computations were done using the analysis tool pack of Microsoft Excel 2007.

Thus, the rating curve of Ofu River at Oforachi was developed which followed a power curve of the form expressed by Eq. (3.25).

The graph of the effective depth of flow (*H-h*) was plotted against the calculated discharge as the final rating curve.

3.2.2.4 Estimation of twelve months daily discharge for Ofu River

The rating curve developed was used to estimate the corresponding discharge for the daily stage values obtained from field measurement. The estimation was done for the days that the discharge values were not measured.

The general methodology for the development of the rating curve is shown in Fig. 3.5.

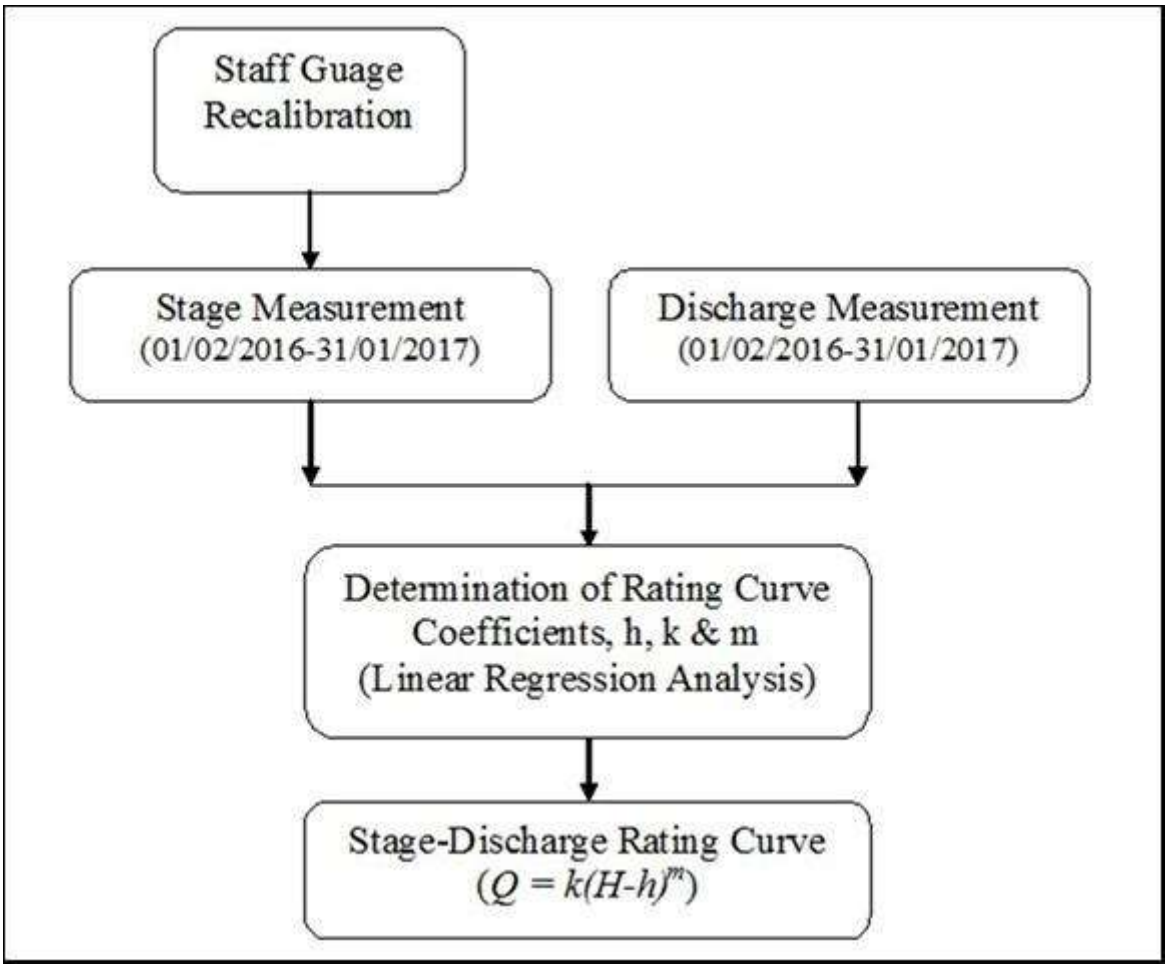


Fig. 3.5: Schematic Flowchart of the Rating Curve Development Methodology

3.2.3 Methods of Identification of Flood Causative Factors in Ofu River Catchment

The assessment of flood causative factors in Ofu River Catchment was carried out as follows:

3.2.3.1 Assessment of knowledge of the causes of flood within Ofu River Catcment communities

The assessment of the local knowledge of the causes of flood was carried out as described in this section.

a. Study Population

The study population comprise of all heads of households or representatives who have lived in Oforachi Community of Igalamela/Odolu Local Government Area (LGA) of Kogi State for a minimum of ten years.

b. Study Design

The study was a cross-sectional study conducted among the household heads in Oforachi Community between September and October, 2016 using quantitative methods of data collection.

c. Inclusion and Exclusion Criteria

The study population included all household heads or the representatives who have been resident within the community for a minimum of ten years and consented to participate in the study. A household was defined as a group of people who live under the same roof and eat from the same pot. All household heads or representative who declined consent and scattered houses within the suburbs such as Fulani settlements were excluded from the study.

d. Determination of sample size

The sample size was estimated using the sample size estimator developed by the Research Advisors (2006) based on the method of Krejcie and Morgan (1970) as expressed by Eq. (3.34).

$$n = \frac{X^2 NP(1-P)}{d^2(N-1) + X^2 P(1-P)} \qquad (3.34)$$

Where:

n	=	Sample Size
X^2	=	the table value of chi-square for 1 degree of freedom at thedesired confidence level.
N	=	the population size.
P	=	the population proportion.
d	=	the degree of accuracy expressed as a proportion.

The sample size estimator is presented in Appendix IV.

The total number of Households in Oforachi Community according to the records available at the Primary Health Care (PHC) centre is 616. A sample size of 320 was estimated at 99% level of confidence and 5% degree of accuracy. A minimum sample size of 325 was used for ease of proportionate distribution among the nine human settlements that make up Oforachi Community.

e. Sampling Technique

A multi-stage sampling technique was used in this study. The first stage was the purposive selection of Oforachi community in Igalamela/Odolu LGA of Kogi State firstly due to its history of being consistently flooded for over 20 years and secondly, on the basis of its accessibility and organisation relative to a few other communities which are quite dispersed, scattered and difficult to access. The number of households sampled from each of the nine (9) human settlements within the community was determined using proportion to size technique (number of households within settlement divided by total number of settlements in the community multiplied by the sample size). This gave 116, 32, 7, 20, 52, 77, 7, 7 and 7 for Oforachi central, Okobu, Caterpillar, Atanegoma, Agwoko, Ojokuta,

Ojoyibo, Ojuwo and Camp respectively. Finally, household listing and enumeration was done to a total of 222, 62, 12, 99, 148, 12, 12 and 12 respectively for Oforachi, Okobu, Caterpillar, Atanegoma, Agwoko, Ojokuta, Ojoyibo, Ojuwo and Camp. Computer generated list of random numbers from Minitab 14.12 statistical software was used to select the respondents for each of the settlements in this study.

f. Data Collection

The first three (3) sections of a five (5) part semi structured interviewer administered questionnaire were used for data collection in this segment of the study. The sections are; socio-demographic characteristics of respondents, historical flood characteristics, and opinions/knowledge of causes of flood. The last two sections were respectively used to assess the specific impacts of the 1995 and 2000 flood scenarios and the open defecation extent/ household sources of drinking water. Reconnaissance visits were paid to the Information Officer of the LGA (Plate IV), the District Head (Plate V) and the Village head of the Community (Plate VI) to intimate them on the research and solicit for their support. They were respectively interviewed as key informants in this study (Appendix Va).



Plate IV: Key Informant Interview with the Information Officer of Igalamela/Odolu LGA



Plate V: Key Informant Interview with the Oforachi District Head



Plate VI: Key Informant Interview with the Oforachi Village Head

A research team consisting of five (5) Field Assistants with the Researcher as the Team Leader was raised for the household survey. The team was made up of two Community Health Extension Workers (CHEW), two teachers with a minimum qualification of National Certificate in Education (NCE) and one National Youth Service Corps (NYSC) member. They were trained by the Researcher in the administration of household survey instruments during the field enumeration (Plate VII). The data collection instruments (Appendix Vb) were pretested in Idah LGA prior to the commencement of the study. Ethical clearance was sought and obtained from the Postgraduate committee of the Department of Water Resources and Environmental Engineering, Ahmadu Bello University, Zaria. Verbal informed consent was obtained from all the respondents with confidentiality and anonymity of their responses assured.



Plate VII: Researcher and Field Assistants Conducting Household Survey

g. Data Management and Analysis

In order to determine the level of knowledge of respondents on the causes of flood, seven questions designed on the five point likert scale was used. The seven causative factors were stated in the positive with the lowest score of 1 for 'strongly disagree' and the highest score of 5 for 'strongly agree'. Any average score less than the average value of 3 was regarded as 'No Knowledge', average scores between 3 to 3.75 as 'Fair Knowledge', average scores between 3.75 to 4.5 as 'Good Knowledge' while average scores greater from greater 4.5 were regarded as excellent knowledge.

3.2.3.2 Assessment of rainfall characteristics in Ofu River catchment (Meteorological factors)

Total monthly rainfall data from the 41 stations for each year were plotted in ArcGIS 10.2.2 and interpolated using the *Ordinary Kriging* interpolation technique in *spatial analyst hydrology* toolbox. The respective rainfall raster surfaces for the catchment were extracted by mask from the interpolated raster surfaces. The average value for the catchment was obtained from the raster statistical tool. The same procedure was carried out with the average annual rainfall data for the 41 stations.

Correction of Radar Rainfall Data with Ground Truth Data

A correction factor was applied to the respective rainfall for the study area interpolated from the rainfall of 41 surrounding stations obtained from radar source. This was necessary because satellite derived rainfall data might not capture localised rainstorms and the seasonality of the rainfall as accurate as the ground-measured data such as the NiMeT rainfall stations would. The correction factor was derived by dividing the 34 years (1980 – 2013) average annual total rainfall of Markurdi by 34 years (1980 – 2013) average annual total rainfall of the study area obtained from radar source. The ground data of Markurdi was used because it falls within the same rainfall Zone (IVa) with the study area. This method was recommended by FMW (2013).

In addition, 5-year moving average and the linear trend were calculated for the annual rainfall values in order to examine the catchment rainfall trend. The annual rainfall, 5-year moving average and the linear trend were plotted on the same graph in Microsoft Excel.

3.2.3.3 Assessment of geomorphologic factors

The geomorphologic factors refer to factors that relate with the earth characteristics such as but not limited to elevation, slope, drainage density, soil type and the discharge capacity of the river channel.

(A) Assessment of the terrain elevation of the flooded areas

In order to collect information of the elevation of the terrain and its relation to flooding, the coordinates and elevations of 325 households surveyed in the course of the field work in this study were taken using the handheld GPS. They were plotted in ArcGIS and used

for the assessment of the relationship between the household elevations and the flood occurrence. This was done by comparing the field elevations with the Ofu River stage (water level) observed for 12 months. The highest elevation obtained for the households flooded by Ofu River with some allowance was set as the limit for highest flood risk class on the elevation raster. These sets of information were used to classify the Shuttle Radar Topographic Mission (SRTM) Digital Elevation Model (DEM) of the study area.

(B) Assessment of the terrain slope of the flooded areas

The slope of the entire catchment was obtained from the DEM of the study area in ArcGIS 10.2.2. The *extract value to point Spatial analyst* tool in ArcGIS 10.2.2 was used to extract the slope for the respective households surveyed.

(C) Assessment of Ofu River channel discharge capacity at Oforachi

The assessment of the change in the carrying capacity of the Ofu River Channel was carried out using the Digital Terrain Model (DTM) of 2000 and 2011. The change in volume, surface area and Channel bed elevation for 29 sections of the river were calculated using the *3D Analyst Tools* in ArcGIS 10.2.2. Although the selection of the sections was random, care was taken to ensure that they were spread around Oforachi where the actual field work was carried out. The steps are described as follows:

Step 1: The DEMs of 2000 and 2011 were respectively converted to triangulated Irregular Network (TIN) surfaces (Fig. 3.6 a and b) using the *3D Analyst Conversion Tool*.

Step 2: Polygon shapefiles for the 29 sections along the river channel were created in ArcCatalogue as shown in Fig. 3.7. They were respectively projected to the same

coordinate as the DTM (WGS_1984_UTM_Zone_32N). These were used as the reference polygons.

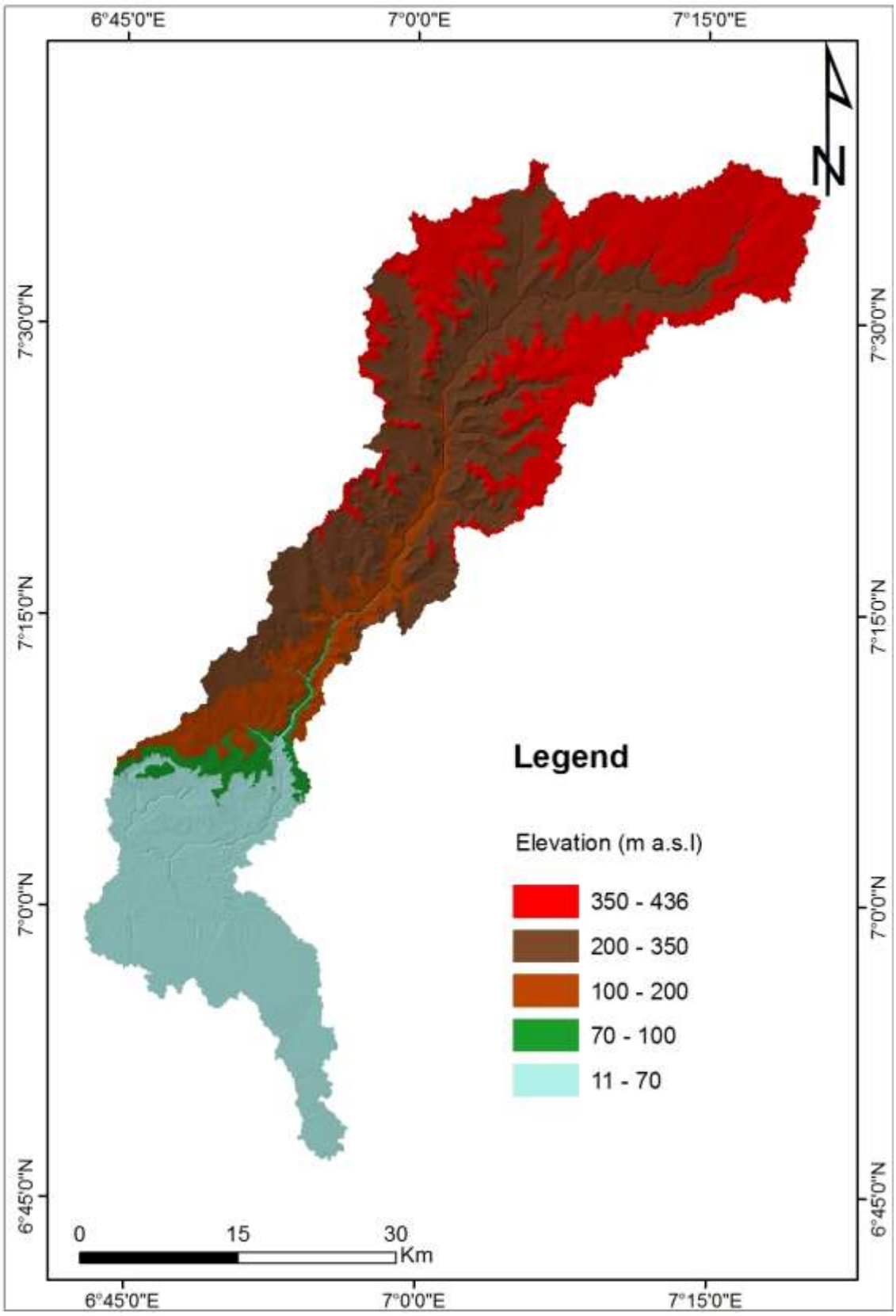


Fig. 3.6a: Triangulated Irregular Network (TIN) surface for Year 2000

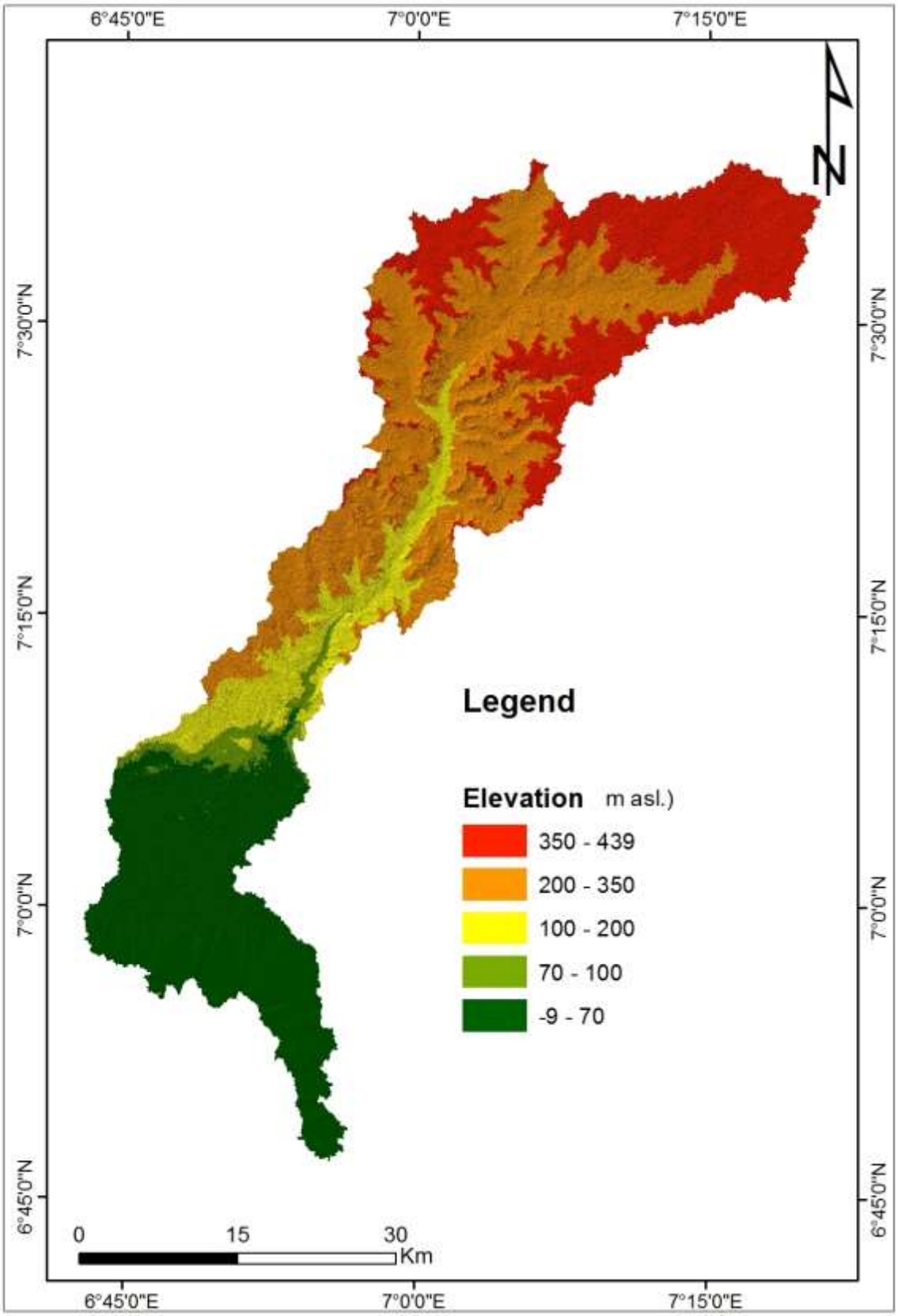


Fig. 3.6b: Triangulated Irregular Network (TIN) surface for Year 2011

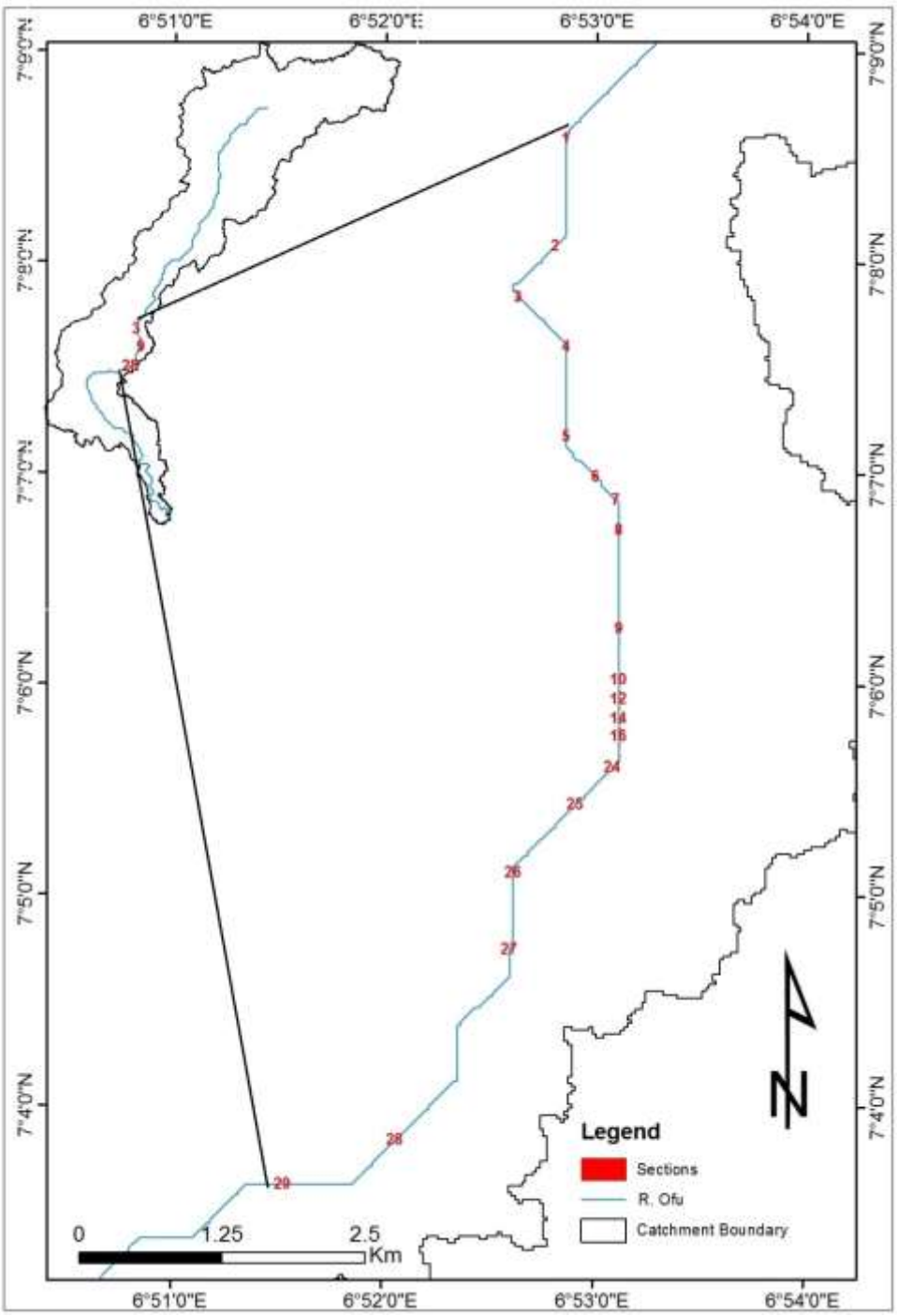


Fig. 3.7: Location of sections for Ofu River Volume estimation at Oforachi

Step 3: The reference height for each of the reference polygons were specified in the respective attribute tables of the reference polygons using the *Editor Extension* tool.

Step 4: The Volume and Surface Area between the reference polygon for each section and the TIN surfaces were calculated using the *3D Analyst Triangulated Surface*

Polygon Volume Tool. The attribute tables of the respective reference polygons were automatically populated with the volume and surface area results for the respective section which were extracted for further analysis. This was carried out for all sections.

Step 5: The process of volume calculation was repeated at different reference heights for all sections until the highest elevation with zero volume and surface area was obtained for that section. This elevation is the channel bed elevation above mean sea level at that section. The average volume and surface area for each section was calculated and recorded.

The steps were followed for both DTMs (2000 and 2011) and the percentage loss in average volume and surface area at the 29 sections for the respective elevations were calculated using Microsoft Office Excel 2007.

In order to calibrate the results obtained for the bed elevations, a relationship of the form a relationship of the form $D = mQ^n$ (where D is maximum depth of flow, Q is discharge and m and n are constants) was developed between the maximum depth of flow and the corresponding discharge obtained during the discharge measurement at Oforachi. The methods described previously for the fitting of the rating curve were followed to estimate the constants m and n. this relationship was used to estimate the maximum flow depth for 2011 based on the extended flow. The value of the maximum depth was respectively added to the 2000 Bed elevation which was used to adjust the bed elevations obtained for 2011. The change in channel bed elevation between 2000 and 2011 (Loss in flow depth), the average annual loss in flow depth as well as estimated bed elevation and loss in flow depth for 2016 were also calculated using Microsoft Office Excel 2007.

(D) Quantification of the Sediment Load of Ofu River at Oforachi Station

The total sediment load for Ofu River at Oforachi was estimated as a combination of the measured and unmeasured sediment loads as recommended by USACE (1995). The measured sediment load is mainly the suspended sediments while the unmeasured loads include some of the unaccounted suspended load, within the lower 0.15m depth portion of a sampled water column and the entire bed load.

In order to measure the suspended sediment load, the river cross-section at Oforachi Bridge Hydrometric Station was divided into three equal verticals of ¼, ½, and ¾ width as recommended by the WMO (1994) after which a standard lightweight hand-held US DH-48 sediment sampler was used to collect samples from these verticals (Otun and Adeogun, 2010). The samples from the three verticals were mixed thoroughly to obtain a representative sample for laboratory analysis to determine the sediment concentration in the sample.

The samples were quickly taken to the Sanitary Chemistry Laboratory of the Department of Water Resources and Environmental Engineering, Ahmadu Bello University Zaria for analysis. Standard method for estimating suspended solids in water was used to estimate the suspended sediment concentration in mg/l (APHA, 2012). The measurement of suspended sediment concentration of Ofu River at Oforachi was done across 12 months beginning from February, 2016 to January 2017. A total of 22 measurements were carried out which were used to develop a suspended sediments versus river discharge rating curve. The rating curve was then used to estimate the suspended sediment concentration for other days of no measurement. The Measured sediment discharge, Q_{ms} (kg/day) was calculated using Eq. (3.35) (USACE, 1995; Ongley, 1996):

$$Q_{ms} = KcQ \quad (3.35)$$

Where Q_{ms} is Measured sediment discharged (kg/day), c is sediment concentration (mg/l), Q is River discharge (m^3/s) and, K= 86.4. The value of c was obtained as the concentration of the sampled sediments using a standard lightweight hand-held US DH-48 sediment sampler, Q was obtained from the stage-discharge relationships for Ofu River at Oforachi Bridge Hydrometric Station described in previuosly.

The Colby's method for estimating unmeasured sediment load described in detail previously by Otun and Adeogun (2010) was used in the study. As a result 22 unmeasured sediment discharges, Q_{us} (tonnes/day) were measured and regressed on the corresponding River discharge values to develop a relation which was used to estimate unmeasured sediment load for the 12 months. The total sediment load Q_{tot} was calculated using Eq. (3.36):

$$Q_{tot} = Q_{ms} + Q_{us} \quad (3.36)$$

Where, Q_{tot} is the total sediment load, Q_{ms} is the measured sediment load and Q_{us} is the unmeasured sediment load.

(E) Assessment of the Soil Characteristics of the flooded areas within the Catchment

The Digital soil map of the World (DSMW) obtained from the FAO's website was added to the map document. The spatial analyst extraction tool was used to extract the soil layer for Ofu River catchment. Four soil layers with distinct characteristics were extracted. A description of the soil types, the area covered and hydrological soil group (HSG) for curve number (CN) generation is presented in Table 3.8

Table 3.8: Characteristics of Soil within Ofu River Catchment

SMU	FAOSoil Symbol	Area (km^2)	Name	Textured Class	HSG
1021	Af13-1a	975.61	Ferric Acrisols	Sandy loam	A
1567	Nd5-1a	259.77	Dystric Nitosols	Loam	B
1193	G2-2/3a	366.61	Gleysols	Clay Loam	D
677	Jd3-2a	2.59	Calcaric Fluvisols	Sandy Clay Loam	C

Source: www.fao.org; Researcher's GIS Analysis (2016)

In addition to the aforementioned, in situ and ex situ soil analysis for determination of index properties and infiltration rates were conducted on soil samples collected from ten (10) locations in Oforachi (Fig. 3.8). This was done to confirm the classifications based on the Digital Soil Map of the world. The classifications were done using the charts and Tables in Appendix VIII.

Apart from the infiltration test and part of the Antecedent Moisture content measurement that were carried out in-situ, the samples were transported to the Geotechnical Engineering Laboratory in The Department of Civil Engineering, Ahmadu Bello University, Zaria for the determination of soil index properties. The tests carried out were Moisture contents, Atterberg limits and Sieve analysis. The tests were carried out according to standard methods for soil analysis and classified according to American Association of State Highway and Transportation Officials (AASHTO) and Unified Soil Classification Systems (USCS) soil classification systems (Appendix VIII).

The double ring infiltrometer method was used for the in-situ infiltration measurement. The infiltrometer consisted of an outer ring of 35 cm diameter and inner ring of 20 cm diameter. The height of both rings was 27 cm. The sizing of the infiltrometer followed the design method described previously by Parr and Bertrand (1960). The fabrication of the rings was made using 1mm mild steel sheets. Both rings were hammered 15 cm into the soil with a plank to protect the surface of the ring from damage during hammering.

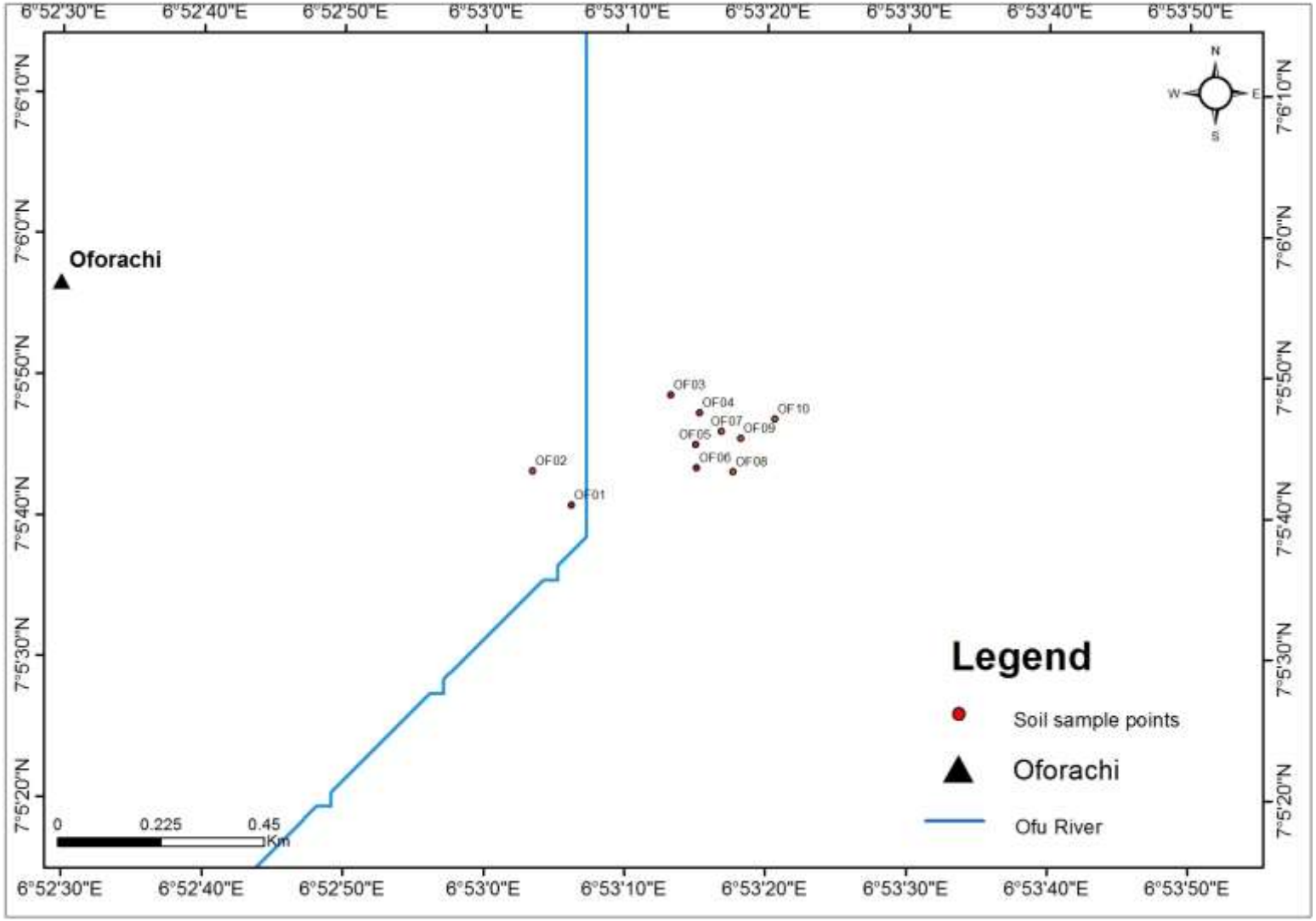


Fig. 3.8: Location of Soil Sample Collection points at Oforachi



Plate VIII: Researcher Carrying out Soil Analysis in the Laboratory



Plate IX: Researcher conducting in situ infiltration test at Oforachi

The test began by pouring water into the inner ring to an appropriate depth and at the same time, adding water to the space between the two rings to the same depth as quickly as possible. The time when the test began was recorded and the water level on the calibration was noted. After two (2) minutes, the drop in water level in the inner ring was

recorded and water added to bring the level back to approximately the original level at the start of the test. The water level outside the ring was maintained similar to the one inside to prevent lateral flow. Each infiltration test lasted four (4) hours with cumulative time intervals; 2, 5, 10, 20, 30, 45, 60, 90, 120, 150, 180, 210 and 240 minutes. The cumulative infiltration depth at the elapsed time was recorded.

Estimation of Saturated Hydraulic Conductivity

The analysis of the field data was done based on Philip's infiltration model expressed in Eq. (3.37) (Philip, 1957).

$$i(t) = St^{1/2} + At \qquad (2.37)$$

Where;

i(t) = Cumulative infiltration at cumulative time *t* (cm)

t = Time (s)

S = Sorptivity (cm/hr$^{1/2}$)

A = Transmisivity or permeability coefficient

Values of cumulative infiltration, *i(t)* and time, *t* were obtained from field measurement while the sorptivity, *S* and permeability coefficient, *A* were determined using the method of least square between the field measured cumulative infiltration and the calculated cumulative infiltration.

The saturated hydraulic conductivity, *K* (ms^{-1}) as a function of the transmisivity or permeability coefficient, *A* and a constant *m* (2/3) was calculated using Eq. (3.38).

$$K = \frac{A}{m} \qquad (2.38)$$

The value of saturated hydraulic conductivity, *K* was used to classify the respective soils based on the CSN 721020 classification table (Appendix VIII).

3.2.3.4 Assessment of Landuse/Settlement Factors

The two causative factors assessed in this category are the proximity of households to Ofu River and the Landuse/Landcover changes. The methods of assessment are discussed as follows:

(A) Assessment of Proximity of Flooded areas to the River channel

It was gathered in the course of the field survey that there were human settlements within the catchment at elevations similar to those of the flooded areas that have never been affected by flood implying that the proximity of the settlements to the river is also a factor to be considered. The coordinates of the 325 surveyed households plotted in ArcGIS were used for the estimation of their distance (corridor) from Ofu River. This was done using the *Near Proximity Analysis tool* in ArcGIS 10.2.2.

(B) Assessment of Landuse/Landcover changes within Ofu River Catchment

The assessment of Landuse/Landcover (LULC) changes within the catchment was carried out using the Landsat 5 Imagery of 1987, Landsat 7 Imagery of 2001 and Landsat 8 Imagery of 2016 (Table 3.4) in ArcGIS 10.2.2. The imageries were atmospherically corrected since the spectral reflectance was the vital component for their classification. The Band composites was created for the respective imageries using the *image analysis* extension after which the *extraction spatial analyst* tool was used to subset the image to

the study area. The Normalized Difference Vegetative Index (NDVI) and the Normalized Difference Built-up Index (NDBI) were respectively calculated for each year to show the extent of vegetative covers and built-up areas. The NDVI and NDBI were both derived using the *Raster Calculator* in *Spatial Analyst Map Algebra* toolbox in ArcGIS 10.2.2 using Eq. (3.39) and (3.40) respectively.

$$NDVI = \frac{NIR - R}{NIR + R} \tag{3.39}$$

$$NDBI = \frac{SWIR - NIR}{SWIR + NIR} \tag{3.40}$$

In which *R, NIR, SWIR* are the Red, Near Infrared and the Short wave Infrared bands respectively.

The details of the bands used for generation of the indices are shown in Table 3.9. The NDVI and NDBI for 1987, 2001 and 2016 are shown in Figs. 3.9 and 3.10.

Table 3.9: Band Characteristics for NDVI and NDBI Calculation for Ofu River Catchment

Year	Satellite	Sensor	Red	NIR	SWIR
1987	Landsat 5	TM	Band 3	Band 4	Band 5
2001	Landsat 7	ETM+	Band 3	Band 4	Band 7
2016	Landsat 8	ETM+	Band 4	Band 5	Band 7

Source: Glovis.usgs.gov

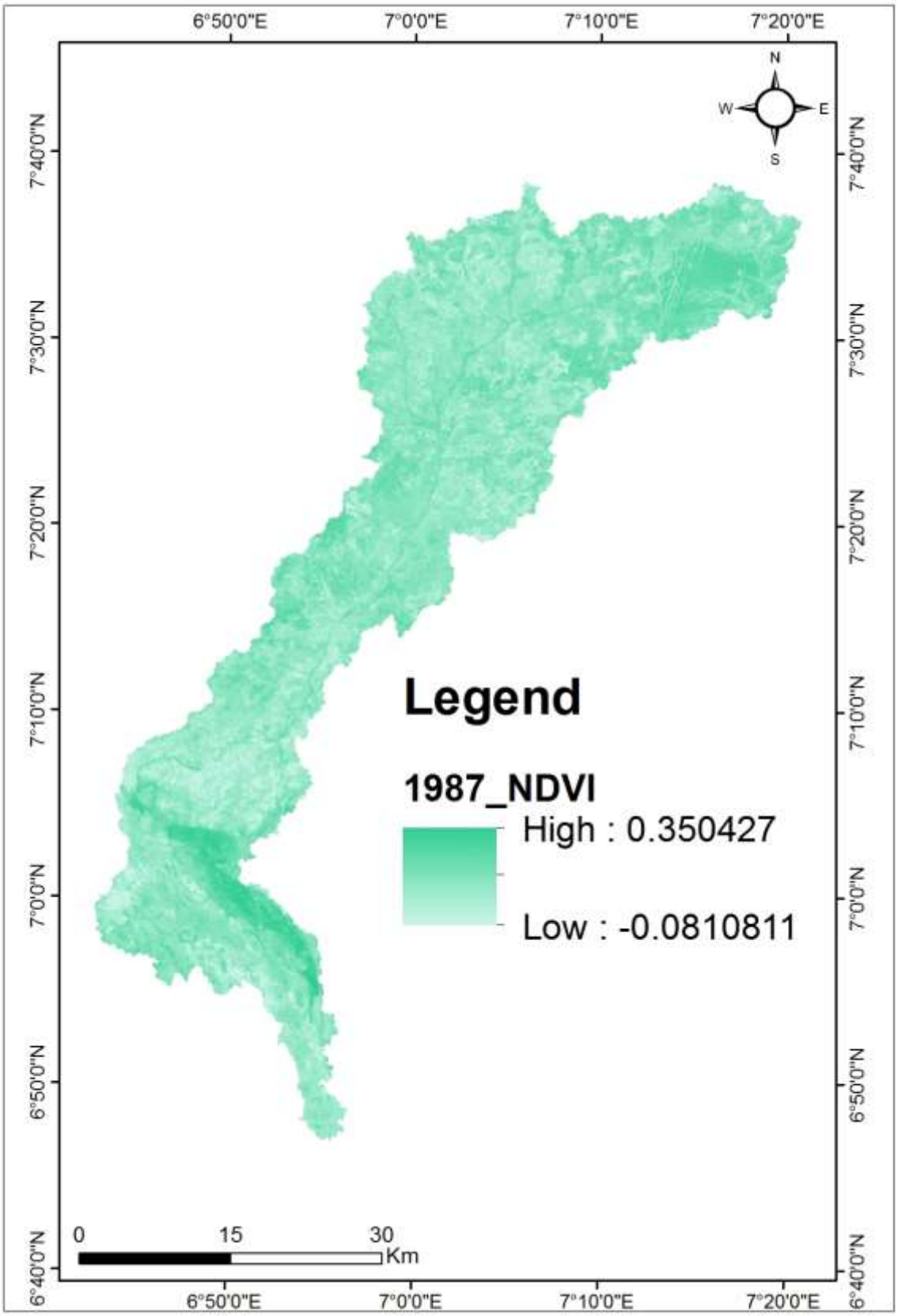


Fig. 3.9a: Normalized Difference Vegetation Index of Ofu River Catchment for 1987

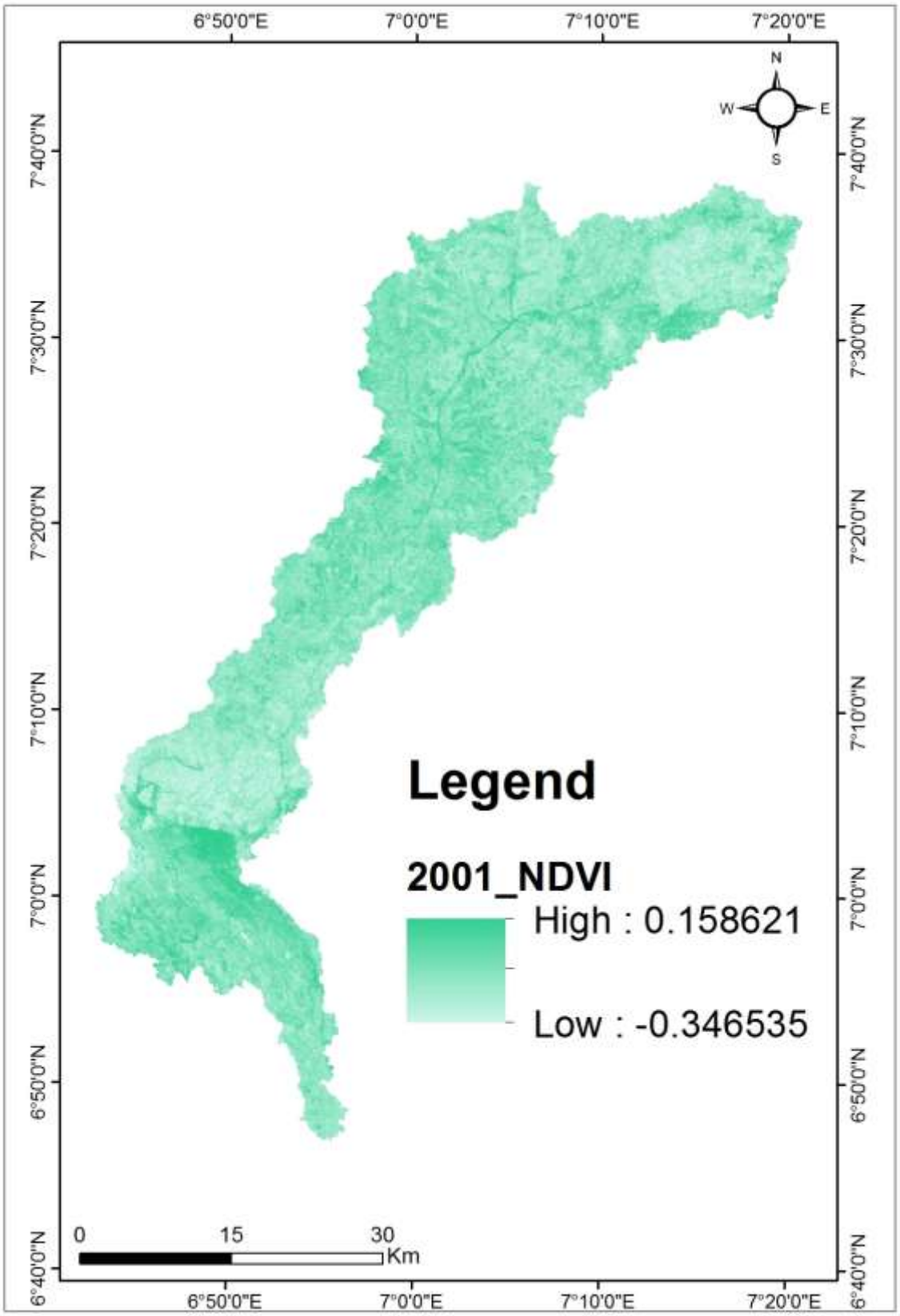


Fig. 3.9b: Normalized Difference Vegetation Index of Ofu River Catchment for 2001

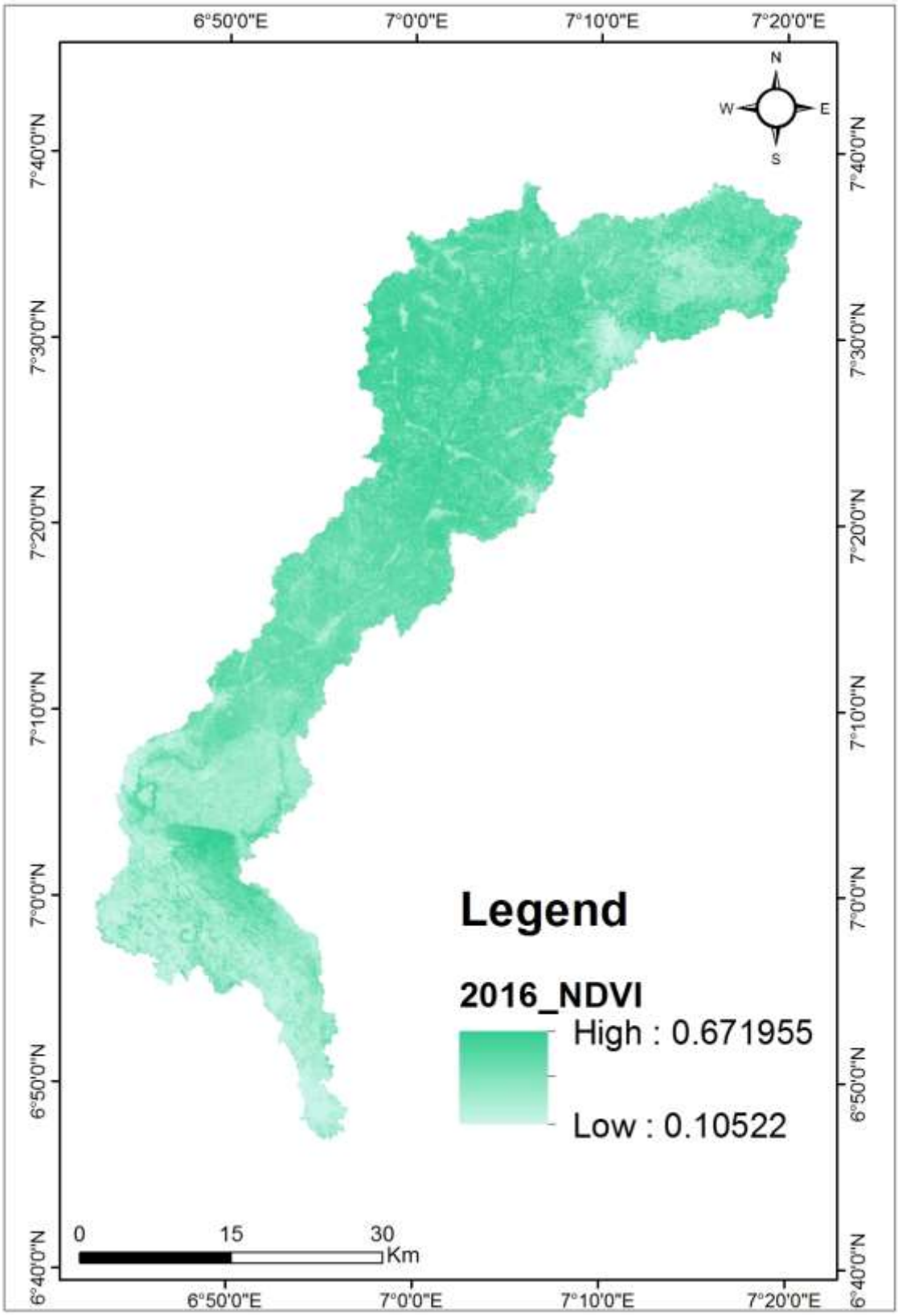


Fig. 3.9c: Normalized Difference Vegetation Index of Ofu River Catchment for 2016

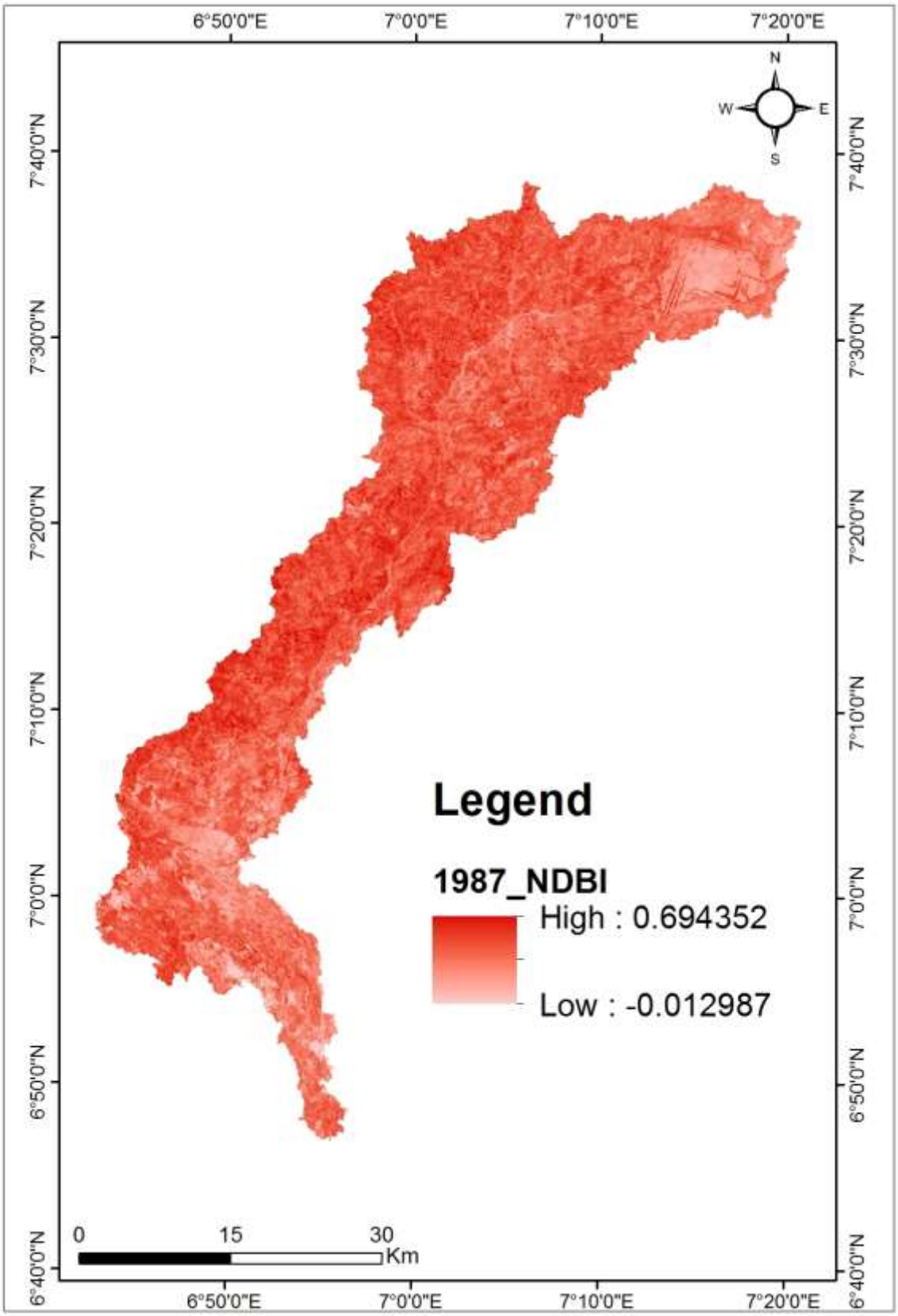


Fig. 3.10a: Normalized Difference Built-up Index of Ofu River Catchment for 1987

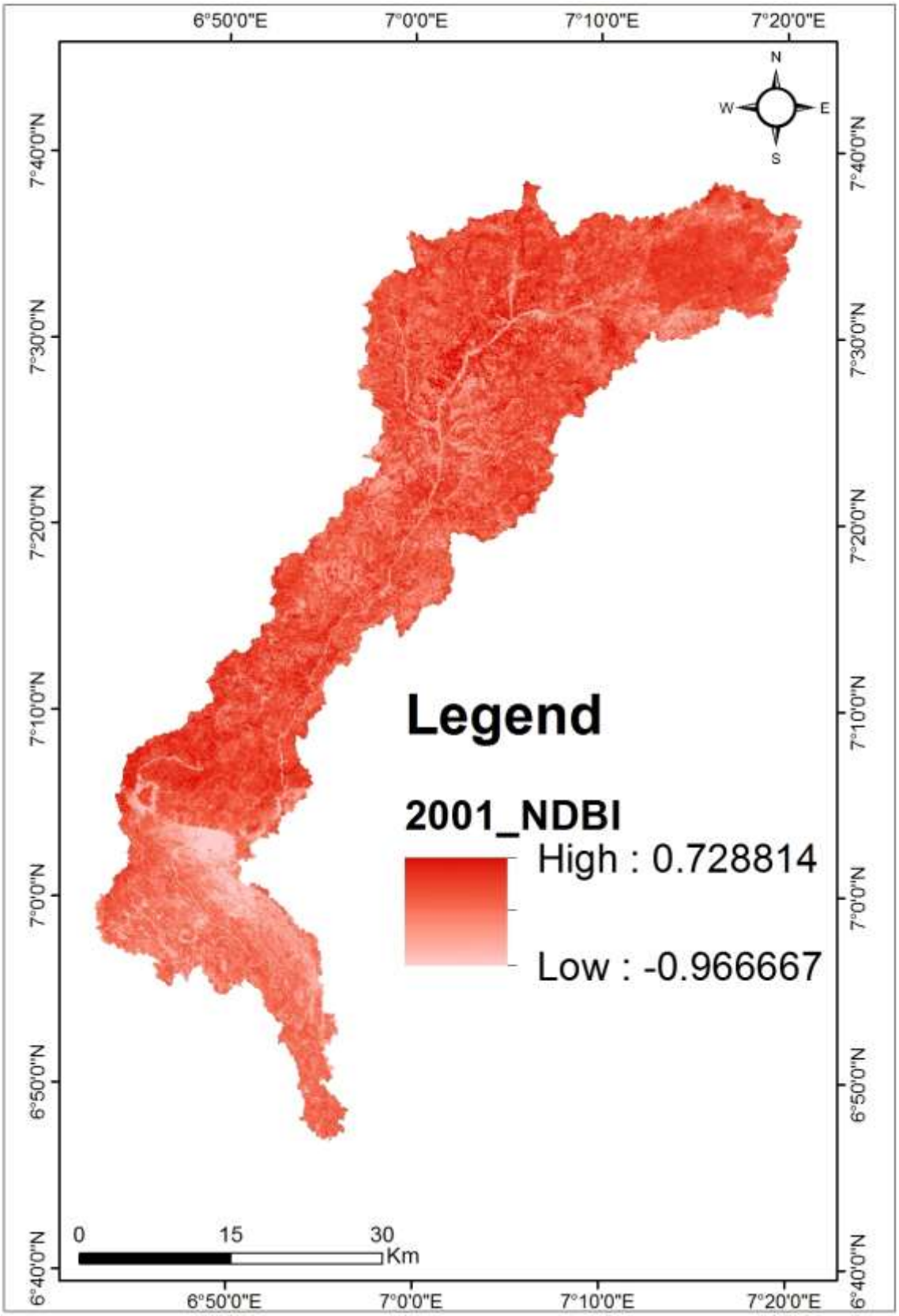


Fig. 3.10b: Normalized Difference Built-up Index of Ofu River Catchment for 2001

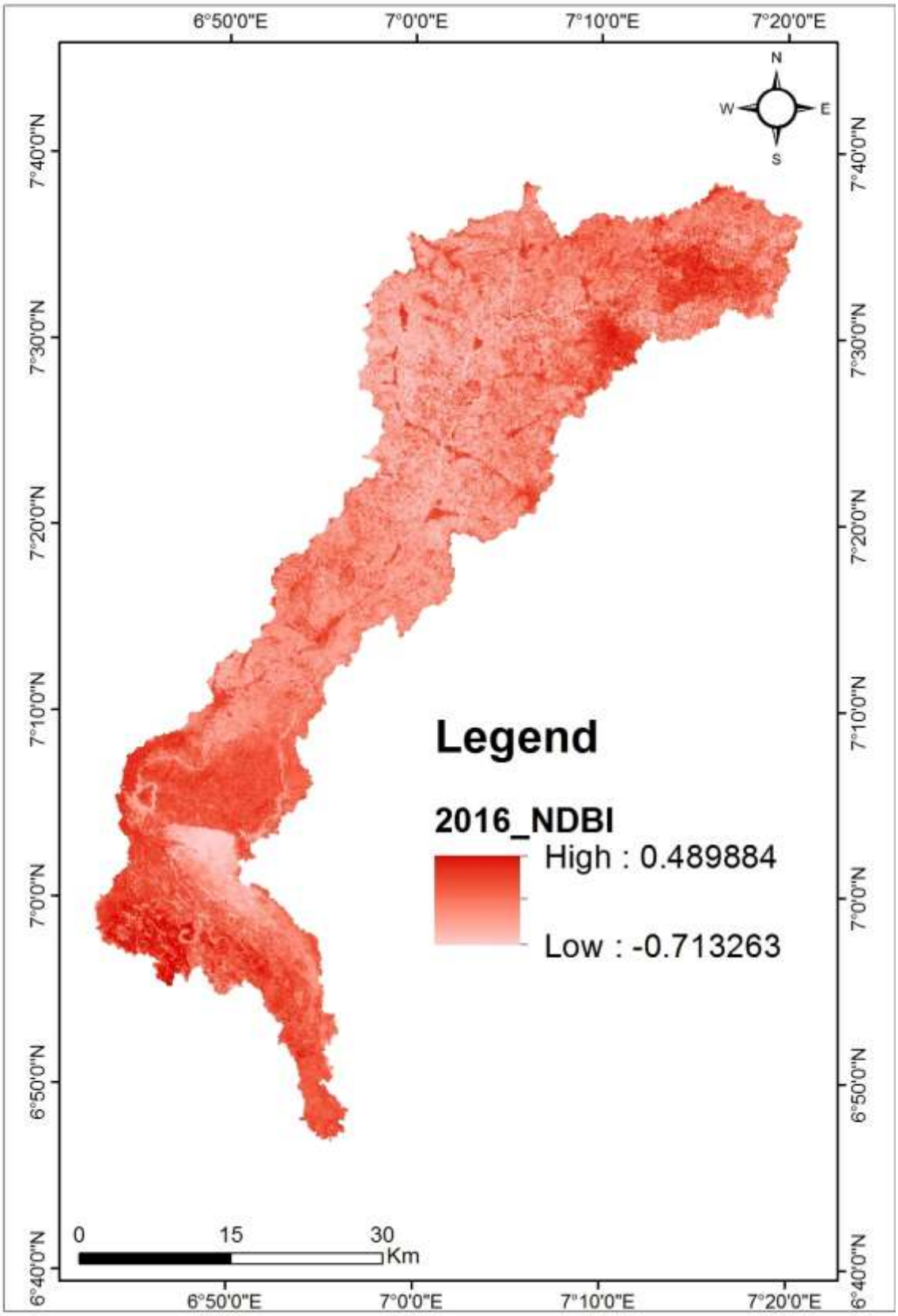


Fig. 3.10c: Normalized Difference Built-up Index of Ofu River Catchment for 2016

The generation of these indices helped in the creation of training signatures for the Maximum likelihood supervised classification of the imageries. This served as an accuracy check for the classified Landuse/Landcovers. In addition, an IsoCluster unsupervised classification was performed in order to have an idea of the maximum number of distinct classes and a general overview of the area which was followed by the maximum likelihood supervised classification for the final land cover classes for 1987, 2001 and 2016.

Ground truthing was embarked upon after the classification of the imageries so as to reaffirm the land use /land cover classes for the 2016 imagery. The area of each land cover class for the respective years were used to evaluate the changes that have happened within the period.

Estimation of Curve Number for Ofu River Catchment

The catchment Curve number for 1987, 2001 and 2016 were estimated using the soil and landuse/Landcover data generated for the respective years. This was done to assess the extent to which the land cover changes might have affected the surface runoff to the streams within the catchment.

The Curve Numbers for all the Hydrologic Soil Groups (HSG) A, B, C and D corresponding to the various landcover classes were obtained from the tables shown in Appendix IX. The Composite Curve number for the respective hydrologic soil group, CN_h was calculated using Eq. (3.41).

$$CN_h = \frac{\sum_{i=1}^{n} A_i CN_i}{\sum_{i=1}^{n} A_i} \tag{3.41}$$

In which A_i = Area of land cover class i, CN_i = Curve number for landcover i and h = HSG

The values of *CN* obtained for the respective *HSG* were used to compute the composite *CN* for the catchment based on the soil classes and their corresponding *HSG* and *CN*. The composite *CN* for the catchment was computed using Eq. (3.42).

$$CN = \frac{\sum_{j=1}^{n} A_j CN_j}{\sum_{j=1}^{n} A_j} \tag{3.42}$$

In which A_j = Area of soil class j, CN_j = Curve number for HSG/Soil class j

3.2.3.5 Assessment of the respective measures of association of Elevation, Proximity and Slope with flood occurrence

Statistical analysis was carried out to determine the respective measures of association of the terrain elevation, household proximity to Ofu River and terrain slope with household flood experience using the Pearson's Chi square in Stata/SE version 13.1 statistical software at 95% confidence level. The Pearson's chi sqaure and the *P*-value were used to determine whether association exist or not.

3.2.4 Method of Flood Frequency Analysis

The estimation of the stream flow for Ofu River was estimated using three methods.

3.2.4.1 Method of estimation of peak runoff

A comparison of three (3) methods for the determination of the peak runoff was made in this section. The methods compared are the extension of stream flow data (Synthetic)

using Modified Thomas-Fiering model, Soil Conservation Services Curve Number (SCS-CN) method and the Rational method.

(A) Generation of synthetic stream flow data

Synthetic stream flow data used in this study were generated from the 19 year gauged stream flow data (Appendix III) using the Modified Thomas-Fierring (T-F) Model. The modification was the incorporation of linear regression to adjust the extended flow data to fit perfectly with the gauged data. The method of generating synthetic discharge values using the T-F model described by Patra (2008) was adopted.

Identification and treatment of outliers was first carried out on the the historical stream flow data for 1955-1973 using boxplot in Minitab 14.12.0 statistical software. The outliers were treated as missing data to prevent excessive skewness of the data.

The logarithm transferred flows method was used to avoid negative flows in the synthetic data. The following steps were followed for the generation of the synthetic stream flow data.

Step 1: The first step was the calculation of the logarithm to base 10 of the gauged stream flow data (1955 – 1973).

Step 2: The second step was the calculation of the mean and standard deviation for each month.

Step 3: The third step was the calculation of the correlation coefficient between all the successive months.

The logarithmic stream flow values, mean, standard deviation and correlation coefficients are presented in Table 3.10.

Step 4: In the fourth step, two sets of normally distributed random numbers with zero mean and unit standard deviation (Appendix X) were generated. The random numbers were generated using the analysis tool park in Microsoft Excel 2007. The number of variables were set as 12 (12 months) in both cases while the number of random numbers were set as 18 and 43 for the respective sets (18 years for which gauged data exist and 43 years of synthetic data respectively).

Step 5: Synthetic stream flow values (logarithm to base 10) were generated using Eq. (3.43).

$$Q_{j+1} = Q_{avj+1} + b_{j,j+1}\left(Q_j - Q_{avj}\right) + Z_j S_{j+1}\sqrt{(1 - {r_{j+1}}^2)} \qquad (3.43)$$

Where:

$j+1$ = month for which synthetic discharge is generated;

j = preceding month;

Q_{j+1} =Discharge during *(j+1)th* month;

Q_j = Discharge during *jth* month;

Q_{avj+1} = mean monthly discharge during *(j+1)th* month;

Q_{avj} = mean monthly discharge during *jth* month;

S_{j+1} = Standard deviation for *(j+1)th* month;

S_j = Standard deviation for *jth* month;

$r_{j,j+1}$ = The correlation coefficient between the months j and (j+1);

Z_j = The random independent variable with zero mean and unit variance while,

$$b_{j,j+1} = r_{j,j+1}\left(\frac{S_{j+1}}{S_j}\right) \quad (3.44)$$

Step 6: The synthetic discharge values for 1956-1973 were obtained by taking the antilogarithm of extended logarithmic values. The values for 1956 – 1970 (15 years) were used for calibration of the model since gauged data exist for these years. The remaining three years (1971 – 1973) were used for model validation.

Linear regression analysis was carried out in Microsoft excel 2007 with the gauged data (1956 -1970) as *'y'* and the generated data (1956 -1970) as '*x'* to obtain linear relationships with slopes and intercepts for the respective months.

Thus 12 linear relationships developed for the 12 months were used to adjust the synthetic discharge values generated for 1971-1973 (Table 3.11) for which gauged data already exist as form of validation.

Step 6: Regression analysis and (student's) paired *t* test (95% confidence interval) were carried out on the gauged data and the adjusted synthetic data (1971 – 1973) using the Analysis Tool Pack of Microsoft Office 2007 to assess the goodness of fit of both data (Table 3.12).

The correlation coefficient (*r*) of 0.9515, coefficient of determination (R^2) of 0.9026 and *P*-value (*P* = 0.1801) obtained show that the adjusted synthetic discharge values fit well with the gauged values thus validating the model which implies that the developed equations could be used to adequately adjust the synthetic data generated for 1974 - 2016.

Table 3.10: Logarithm of Stream flow, Monthly Mean, Standard Deviation and Correlation coefficient for T-F Model

Year	Logarithm of Discharge (m^3/s)											
	Jan	**Feb**	**Mar**	**Apr**	**May**	**Jun**	**Jul**	**Aug**	**Sep**	**Oct**	**Nov**	**Dec**
1955	0.591	0.462	0.322	1.057	0.903	1.270	1.898	2.602	2.359	2.186	0.398	0.122
1956	0.146	-0.046	-0.222	0.851	0.362	1.228	2.270	2.770	2.746	1.811	0.580	-0.222
1957	0.462	0.279	0.114	1.188	0.950	1.453	1.980	2.545	2.639	2.204	0.813	-0.097
1958	0.623	0.447	0.255	1.305	1.193	1.644	2.211	2.580	2.762	1.922	0.653	0.079
1959	0.041	-0.222	-0.222	0.839	1.021	1.272	1.898	2.558	2.559	1.678	0.505	-0.301
1960	0.322	0.176	0.000	0.903	1.068	1.318	2.031	2.513	2.517	1.721	0.568	0.122
1961	0.279	0.114	-0.097	1.340	0.568	1.782	2.352	2.707	2.744	1.932	0.699	-0.222
1962	0.498	0.362	-0.301	1.170	0.613	1.207	1.889	2.762	2.671	2.038	0.699	0.000
1963	0.498	0.400	0.258	1.281	0.950	1.204	1.881	2.464	2.509	2.053	0.857	0.122
1964	0.643	0.531	0.462	0.964	1.093	1.713	2.055	2.789	2.859	1.954	0.716	0.122
1965	0.531	0.342	0.204	1.072	0.690	1.937	2.176	2.687	2.608	1.674	0.690	0.176
1966	0.556	0.462	0.342	1.107	0.950	1.960	1.926	2.475	2.293	1.849	0.301	0.362
1967	-0.301	0.176	0.079	1.265	0.996	1.637	2.195	2.668	2.713	1.956	0.944	0.079
1968	0.724	0.613	0.544	0.602	0.950	1.583	2.094	2.309	2.524	1.619	0.279	0.122
1969	0.114	0.041	0.041	1.365	1.083	1.450	2.125	2.660	2.623	2.210	0.716	0.000
1970	0.519	0.643	0.230	1.049	0.959	1.436	1.833	2.677	2.697	1.714	0.724	0.230
1971	0.623	0.556	0.491	1.124	0.964	1.704	2.189	2.649	2.683	1.732	0.875	0.122
1972	0.724	0.613	0.544	1.033	1.127	1.684	2.119	2.382	2.503	1.601	0.820	0.122
1973	0.672	0.568	0.491	1.124	0.839	1.354	2.197	2.297	2.678	1.775	0.763	0.491
Mean	0.435	0.343	0.186	1.086	0.910	1.518	2.069	2.584	2.615	1.875	0.663	0.075
SD	0.271	0.245	0.268	0.195	0.212	0.243	0.152	0.148	0.141	0.197	0.186	0.192
R	0.534	0.817	0.827	-0.133	0.062	0.152	0.404	0.100	0.534	0.030	0.173	-0.021

Table 3.11: Stream flow Estimation for Model Calibration and Validation

Year	Discharge (m^3/s)											
	Jan	**Feb**	**Mar**	**Apr**	**May**	**Jun**	**Jul**	**Aug**	**Sep**	**Oct**	**Nov**	**Dec**
1971	2.15	1.89	1.15	6.72	4.47	68.25	153.91	511.89	532.32	66.13	2.51	1.14
1972	1.55	2.18	1.82	22.20	11.01	67.33	67.79	330.13	472.22	98.39	3.85	1.66
1973	2.14	3.98	2.66	51.49	2.73	67.92	146.78	300.67	508.97	54.91	3.87	1.06

Table 3.12: Model Validation Parameters

Parameter	Value
Correlation Coefficient, r	0.9515
Coeficient of Determination (Adjusted R^2)	0.9026
P-value	0.1801

Step 7: The synthetic discharge values for 1974-2016 were obtained by taking the antilogarithm of extended logarithmic values for the 1974-2016. The 12 linear equations developed in the preceding steps were then used to adjust the synthetic discharge values for 1974-2016 for the respective months. The mean and standard deviation are principally the determinants of unbiased statistics but since stream flow is a serially dependent phenomenon, the correlation between successive months needs to also be preserved for the generated data to be reliable (Patra, 2008).

The mean, standard deviation and correlation coefficient for the gauged data of 1955-1973 and the synthetic data of 1955-2016 (first, second and third runs) were calculated using the aforementioned statistical software. The reliability assessment was then carried out by comparing these estimates for both datasets using linear regression and One Way Analysis of Variance (ANOVA). The coefficient of determination (R^2), *P*-value, *calculated F* and *Critical F* values at 5% level of significance were used to infer whether there is statistically significant difference or not. $P<0.05$ was taken to be statistically significant.

In order to estimate the reliability index, the average of the three coefficients of determination (R^2) was recorded as the score for R^2, *P*-value greater than 0.05 was given a score of 1 while, *calculated F* less than *Critical F* was given a score of 1. The reliability index was calculated as the ratio of the total score obtained to the total obtainable score.

(B) Runoff Estimation by SCS Curve Number Method

i. Interpolation and extraction of Daily Rainfall layer for Ofu River Catchment

The annual maximum daily rainfall from the 41 stations surrounding the study area obtained from radar source were plotted in ArcGIS 10.2.2 environment and interpolated using the Ordinary Kriging method as discussed earlier. The annual maximum daily rainfall raster surfaces for Ofu River Catchment were respectively extracted and the average values for the catchment were obtained using simple arithmetic mean computed using the raster statistical tool in ArcGIS 10.2.2.

ii. Correction of Radar Rainfall Data with Ground Truth Data

A correction factor was applied to the annual maximum daily rainfall for the study area interpolated from the rainfall of 41 surrounding stations obtained from radar source. This was necessary because satellite derived rainfall data might not capture localised rainstorms and the seasonality of the rainfall as accurate as the ground measured data such as the NiMeT rainfall stations would. The correction factor was derived by dividing the 34 years (1980 – 2013) average annual total rainfall of Markurdi by 34 years (1980 – 2013) average annual total rainfall of the study area obtained from radar source. The ground data of Markurdi was used because it falls within the same rainfall Zone (IVa) with the study area. This method was recommended by FMW (2013).

iii. Estimation of Runoff Depth and Peak Runoff for Ofu River Catchment

The SCS Curve number method was used to estimate the daily runoff from the catchment. The method of estimation of the Curve number for the catchment has been discussed previously.

The method described in the TR-55 (1986) was adopted for the estimation of runoff depth using the rainfall values. The runoff depth, *Q* (mm) was calculated using Eq. (3.45) while Initial abstraction, I_a was calculated using Eq. (3.46) assuming AMC II condition for the watershed.

$$Q = \frac{(P - I_a)^2}{\{(P - I_a) + S)\}} (P \geq I_a else Q = 0) \quad (3.45)$$

$$I_a = 0.2S \quad (3.46)$$

In which *P* is rainfall depth (mm).

The Storage, *S* on the other hand was calculated using Eq. (3.47)

$$S = \frac{25400}{CN} - 254 \quad (3.47)$$

The daily peak runoff Q_p was estimated using the methods described by de Brouwer (1997). It was estimated using Eq. (3.48).

$$Q_p = 2.8 \frac{Q \times A}{t_p} \quad (3.48)$$

Where: Q_p = Peak runoff rate (m^3/s)

Q = Storm runoff or excess rainfall volume (cm)

A = Watershed area (km^2)

t_p = Time to peak (hr)

$= \frac{D}{2} + t_{lag}$ (3.49)

D = Duration of excess rainfall (hr) = $0.133 t_c$

t_c = Time of concentration (hr)

t_{lag} = The lag time of the watershed (hr) = $0.6t_c$

TR-55 (1986) stated clearly that the SCS-CN method was designed for small watershed area. Since Ofu Catchment area falls within the medium size catchment, the area reduction factor developed by FMW (2013) was used to correct the area. This was done to avoid over-estimation.

The area reduction factor, f_A was estimated using Eq. (3.50a) while the corrected area, $A_{corrected}$ was estimated using Eq. (3.50b).

$$f_A = 1/e^{\left(1-\frac{12}{A}\right)} \qquad (3.50a)$$

$$A_{corrected} = A - (f_A \times A) \qquad (3.50b)$$

This corrected area was used in place of the original catchment area.

(C) Rational Method

The rational method described in the Drainage Design of the Highway Manual (FMW, 2013) was adopted in this study. The runoff is related to the rainfall intensity by Eq. (3.51).

$$Q = 0.278CIA \qquad (3.51)$$

In which, *C* is the composite runoff coefficient of the catchment, *I is the r*ainfall intensity expressed in millimetres per hour for a certain time of concentration and *A* is the catchment area in square kilometres.

The steps followed are outlined as follows:

Step 1: The runoff coefficient was calculated based on the recommended guide in Appendix XI (Table XIa and XIb) using Eq. (3.52).

$$C = C_s + C_p + C_v \qquad (3.52)$$

Where:

C = Composite runoff coefficient for the catchment

C_s = Runoff coefficient based on surface slope

C_p = Runoff coefficient based on permeability (soil characteristics)

C_v = Runoff coefficient based on vegetation.

The method described earlier for computation of composite curve number was used to estimate the respective components of the runoff coefficient using the area weighted method.

Step 2: The rainfall intensity was estimated following the regional method developed by Oyebande (1982). The study area falls within the Nigeria Rainfall zone IVa (Appendix XI-Fig. XI). The rainfall intensity was calculated using Eq. (3.53).

$$I = \beta + \left(\frac{1}{\alpha}\right)\left[\ln(T_r) - \frac{1}{(2T_r)} - \frac{1}{\left(24{T_r}^2\right)} - \frac{1}{\left(8{T_r}^3\right)}\right] \qquad (3.53)$$

In which α and β are scale and location parameters, I is the rainfall intensity (mm/hr) and T_r is the return period or frequency of occurrence (years).

The time of concentration-dependent parameters, β and α were derived using Table XId (Appendix XI) for Rainfall zone VIa. The time of concentration has been estimated earlier as part of the areal characteristics of Ofu River Catchment.

Step 3: The area of the catchment had been previously obtained as one of the areal characteristics of Ofu River catchment. Since the area of the catchment is greater than 12 km^2, area correction was carried out to avoid over estimation. The area correction was done using Eqs. (3.50a and b)

Step 4: The last step was the calculation of the Discharge, *Q* using Eq. (3.51).

3.2.4.2 Flood frequency analysis using Log-Pearson Type III Distribution

The flood frequency analysis of synthetic stream flow records for Ofu River at Oforachi Gauge station was carried out using the Log-Pearson Type III distribution (Dalrymple, 1960; Salimi *et al.*, 2008; Daffi, 2013; England Jr., 2017).

The Log Pearson Type III distribution was used to obtain stream flow for 2, 5, 10, 25, 50, 100 and 200-year return periods respectively using the 62 years synthetic discharge data. The method outlined in Patra (2008) and Mustapha and Yusuf (2012) were adopted as follows.

The maximum discharge values for each year from 1955 to 2016 were arranged by year after which they were sorted and ranked in decreasing order from 1 to 62 with 1 being the highest ranked. The logarithm to base 10 of each ranked discharge was obtained and recorded in the respective columns.

The general equation for the Log-Pearson Type III distribution is given by Eq. (3.54):

$$Log\ Q = \overline{Log\ Q} + K\sigma_{Log\ Q} \tag{3.54}$$

Where:

Q = Maximum discharge (m^3/s)

$\overline{Log\ Q}$ = the average of the Logarithm of the maximum discharge values Q

K = frequency factor which is a function of the return period and the Skewness Coefficient and obtained from the frequency factor table

$\sigma_{Log\ Q}$ = standard deviation of the Logarithm of the maximum discharge, Q

The mean, variance, standard deviation and skewness coefficient of the data were calculated using Eqs. (3.55), (3.56), (3.57) and (3.58) respectively:

$$\overline{Log\ Q} = \frac{\sum Log\ Q}{N} \tag{3.55}$$

$$Variance = \frac{\sum(\log Q - \overline{LogQ})^2}{N-1} \tag{3.56}$$

$$\sigma_{LogQ} = \sqrt{\text{Variance}} \tag{3.57}$$

$$C_s = \frac{N\sum(LogQ - \overline{LogQ})^3}{(N-1)(N-2)(\sigma_{LogP})^3} \tag{3.58}$$

The maximum discharge for the respective return periods were obtained by taking the antilog of the value obtained from Eq. (3.54).

3.2.5 Production of Flood Inundation Extent and Hazard Map

The production of flood hazard map for Ofu River catchment was carried out using the Method of Thematic Integration of Causative Factors (Multi-Criteria Evaluation) in ArcGIS and One-dimensional steady flow hydraulic modelling in HEC-RAS (using the hydrologically generated stream flow as input) combined with HEC-GeoRAS extension in ArcGIS. This was to enable a comparison between both methods.

3.2.5.1 Production of flood hazard map by thematic integration of causative factors (Multi-Criteria Evaluation) in ArcGIS

The production of flood hazard map involved the generation of the thematic layers of four causative factors (Elevation, Corridor, slope and soil), derivation of their criterion weight, reclassification based on the derived weights and their final integration. The methods followed are described in the succeeding sections.

(A) Generation of Thematic Layers of Flood Causative Factors

i. Generation of Elevation layer

The Elevation layer was generated using the SRTM DEM of the catchment. The elevation information obtained from the field was compared with the maximum stage obtained for Ofu River which served as a guide for the classification of the SRTM DEM. The DEM was classified into five domain groups based on their respective elevations above sea level (a.s.l.) in ArcGIS 10.2.2 as follows:

0 m a.s.l.	–	70 m a.s.l.	-	Very High Risk (VHR)
70 m a.s.l.	–	100 m a.s.l.	-	High Risk (HR)
100 m a.s.l.	–	200 m a.s.l.	-	Moderate Risk (MR)
200 m a.s.l.	-	350 m a.s.l.	-	Low Risk (LR)
	>	350 m a.s.l.	-	No Risk (NR)

ii. Generation of Slope layer

The catchment slope was obtained in percentage from the sub-mapped SRTM DEM of Ofu River Catchment subjected to spatial analysis by clicking on *Spatial Analyst Tools>Surface>Slope* with *ofu_dem* as the input raster while the output raster was named *ofu_slope*. The slope was then filtered using the filter operation in *spatial analyst*

Neighbourhood tools in ArcGIS 10.2.2 and classified into five domain groups based on Daffi (2013) classification as follows:

0 %	-	2 %	-	Flat (VHR)
2 %	-	8 %	-	Undulating (HR)
8 %	-	16 %	-	Rolling (MR)
16 %	-	30 %	-	Hilly (LR)
	>	30 %	-	Mountainous (NR)

iii. Generation of Soil layer

The soil layer for Ofu River catchment was extracted from the Digital soil map of the World (DSMW) obtained from the FAO's website using the spatial analyst extraction tool in ArcGIS 10.2.2 and was added to the map document. Four soil layers with distinct characteristics were extracted.

iv. Generation of Corridor layer

The DEM of Ofu River Catchment was first converted to point feature class by clicking on *Conversion Tools>From Raster>Raster To Points* on the Arc Toolbox with *ofu_dem* as the input raster while the output point feature class was named *ofu_dem_point.* On clicking Ok, the study area DEM was converted to point feature class. Secondly, the distance of all the points from the main stream (Ofu River) was calculated by clicking on *Analysis Tools>Proximity>Near* on the Arc Toolbox with the point DEM as input and River181 (Ofu River) as the Near feature accepting the default planar method. On clicking

Ok, the distance was calculated in meters and the attribute table of the point DEM was populated accordingly. The corridor layer was classified into five domain groups based on field observations as follows.

0 m	–	500 m	-	Too close (VHR)
500 m	–	1,500 m	-	Very close (HR)
1,500 m	–	6,000 m	-	Close (MR)
6,000 m	–	20,000 m	-	A bit close (LR)
	>	20,000 m	-	Not close (NR)

(B) Derivation of Criterion Weights using the Analytical Hierarchical Process (AHP)

Multi-criteria evaluation (MCE) was carried out to establish a relationship between all the thematic maps of flood causative factors. The relationships between these layers as well as their respective attributes were derived using the Analytical Hierarchical Process (AHP) developed by Saaty (1980).

As stated earlier, four (4) thematic maps were produced for four (4) causative factors (Elevation, slope, soil and corridor). These thematic maps as well as their respective classifications formed the network for the pair-wise comparison in the AHP. The next step was the generation of the Pair-wise Comparison Matrices of the relative important values. This was determined based on Saaty's 1-9 scale shown in Appendix XII (Table XIIa). The respective associations of elevation, proximity (corridor) and slope with flood occurrence were used as a guide for the derivation of relative importance matrix.

The method of Eigenvector estimation was used to estimate respective weights of the various criteria. The pair-wise comparison was checked using the Saaty's Consistency Ratio, *CR*. *CR* was calculated using Eq. (3.59a).

$$CR = \frac{CI}{RI} \qquad (3.59a)$$

Where:

CI = Consistency Index which reflects the consistency of the judgment

RI = Random Inconsistency Index dependent on the sample size

The consistency Index, *CI* was calculated using Eq. (3.59b).

$$CI = \frac{\lambda_{max} - n}{n - 1} \qquad (3.59b)$$

Where, λ is the average of the value of the consistency vector (calculated factor weight).

The Random Inconsistency Indices, *RI* for respective sample sizes are presented in Appendix XII (Table XIIb).

The judgment would be accepted for $0 \leq CR \leq 0.1$ with a value of zero (0) being the most consistent. Any value outside this range would require re-visiting the assignment of the criterion weight.

(C) Reclassification of Thematic Layers

The four (4) thematic layers produced (Elevation, Corridor, Slope and Soil) were subsequently reclassified into appropriate classes based on the criteria weights derived

which in turn were based on the datasets perceived contribution to flood occurrence. This perception was based on field experience and the assessment of their respective measures of association with flood occurence.

(D) Integration of Thematic Layers and production of Hazard Map

All the weighted data sets were integrated in ArcGIS 10.2.2 to produce the flood Hazard map by weighted overlay where each class individual's weight was multiplied by the map scores and the results added.

The flood hazard map produced via the previous operation was then reclassified into five Hazard classes: 'Very High Hazard,' 'High Hazard,' 'Moderate Hazard,' 'Low Hazard' and 'No Hazard. The Very High Hazard zone represents the extent of inundation of flood water.

3.2.5.2 Hydraulic modelling for development of flood inundation and hazard maps

The hydraulic modelling for the development of Ofu River flood inundation and Hazard maps was carried out using HEC-GeoRAS extension in ArcGIS 10.2.2 and HEC-RAS.

(A) Data Preparation

The digital elevation model of Ofu River Catchment was converted from raster format to a Triangulated Irregular Network (TIN) surface using the 3D Analyst Conversion Tools in the ArcToolbox of ArcGIS 10.2.2.

(B) Pre-processing of data in HEC-GeoRAS

The pre-processing was done using the HEC-GeoRAS extension in ArcGIS 10.2.2 following the methods described in Ackerman (2011), Daffi (2013) and Merwade (2016).

The process began with the addition of created TIN surface to the new map document as the terrain data. The *RAS Geometry>Create RAS Layers tool* in HEC-GeoRAS was used to create the required layers. The layers created are:

i. Stream Centreline
ii. Bank Lines
iii. Flow Path Centrelines
iv. XS Cut Lines
v. Bridges/Culverts
vi. Ineffective Flow Areas

A geo-database was created by HEC-GeoRAS in the working directory with the name of the map document where all the created layers were stored.

The respective RAS layers were populated as follows:

i. Creating Stream Centreline: A single feature was digitized for the entire reach of Ofu River by approximately following the centre of the river, aligning in the direction of flow. The stream centreline was created using the Editor Tools. The *Start Editing* tool was selected with *Create New Feature* as *Task* and *River* as the *Target*.

The assigning of the River and Reach name followed the creation of the River centreline feature. This was done using the *Assign RiverCode and ReachCode to River* button.

Ofu River was supplied as the River name and Main Reach as the Reach name.

The remaining attributes (Topology, Lengths/Stations and Elevation) were populated by clicking *RAS Geometry>Stream Centerline Attributes>All***.** These were done to connect the reach using the *FromNode, ToNode,* give the actual length of the reach in map units (ArcLength) and from station to station details (FromSta, ToSta) as well as create the River3D feature with the elevation values.

ii. Creating River Banks: The banks centre lines were created following the same digitization process with the Banks layer as the task. The bank lines were digitized from the upstream end to the downstream end beginning with the left bank looking downstream.

iii. Creating Flow Path Centrelines: The flow path centre lines were created using *RAS Geometry>Create RAS Layers>Flow Path Centerlines***.** The stream centerline was used to create the flowpath centreline and the left and right flow paths were digitized using the sketch tools in the Editor toolbar. This was done by selecting *Create New Feature* as the *Task* and *Flowpaths* as the *Target feature***.** The left and right flowpaths were digitized within the floodplain in the downstream direction by first digitizing the left flowpath followed by the right flowpath for the entire reach looking in the downstream direction.

The *Assign LineType* button on the HEC-GeoRAS toolbar was used to label the flow paths as left, channel and right, respectively looking in the downstream direction

iv. XS Cut Lines: The cross-section cutlines were created by selecting the *Create New Feature* in the Editor Toolbar as the *Task*, and *XSCutlines* as the *Target***.** They were digitized using the sketch tools, making sure that the cross-sections were wide enough to cover the floodplain. The following guidelines were followed in creating cross-section cutlines:

(a) They were digitized perpendicular to the direction of flow;

(b) They spanned over the entire flood extent to be modelled and

(c) They were digitized from left to right, looking in the downstream direction.

One cross-section was defined each on the upstream and downstream of the bridges across Ofu River at Akpagidigbo and Oforachi, respectively.

After digitizing the cross-sections, the next step was to add HEC-RAS attributes to the cutlines. The attributes added were the River/Reach Names, Stationing**,** Bank Stations**,** Downstream Reach Lengths and Elevations. This was done by selecting *RAS Geometry> XS Cut Line Attributes>All* and all these attributes were added automatically to the *XS cutline* feature while a *3D XS cutline* feature was created which contain the Z values.

v. Bridges/Culverts: Two Bridges were identified across the Ofu River at Akpagidigbo and Oforachi. They were defined in the Bridges feature class by selecting *Create New Feature* as the *Task*, and *Bridges* as the *Target*. The sketch tool on the editor toolbar was used to digitize the bridge locations. River/Reach name, stationing and elevations were assigned to the bridge feature by clicking *RAS Geometry>Bridge/Culverts>All.* These attributes were added automatically and a *3D Bridge* feature was added which contain the Z values.

vi. Ineffective Flow Areas: Ineffective flow areas are used to identify non-conveyance areas of the floodplain, that is, areas with water but no flow/zero velocity such as areas behind bridge abutments. One ineffective area was defined at the Oforachi Bridge by selecting *Create New Feature* as the *Task*, and *IneffAreas* as the *Target* in the Editor Toolbar. It was then defined using the sketch tool.

The position and elevation at points where these ineffective areas intersect with cross-sections were extracted using *RAS Geometry>Ineffective Flow Areas>Position.* The attributes of the *IneffectivePositions* table was then opened to view the information stored. *IA2DID* is the HydroID of the ineffective flow area, *XS2DID* is the HydroID of the intersecting cross-section, *BeginFrac* and *EndFrac* are the relative positions of the first and last intersecting points (looking downstream) of the ineffective area with the cross-

section. *BegElev* and *EndElev* are the elevations of the first and last intersecting points of the ineffective area with the cross-section.

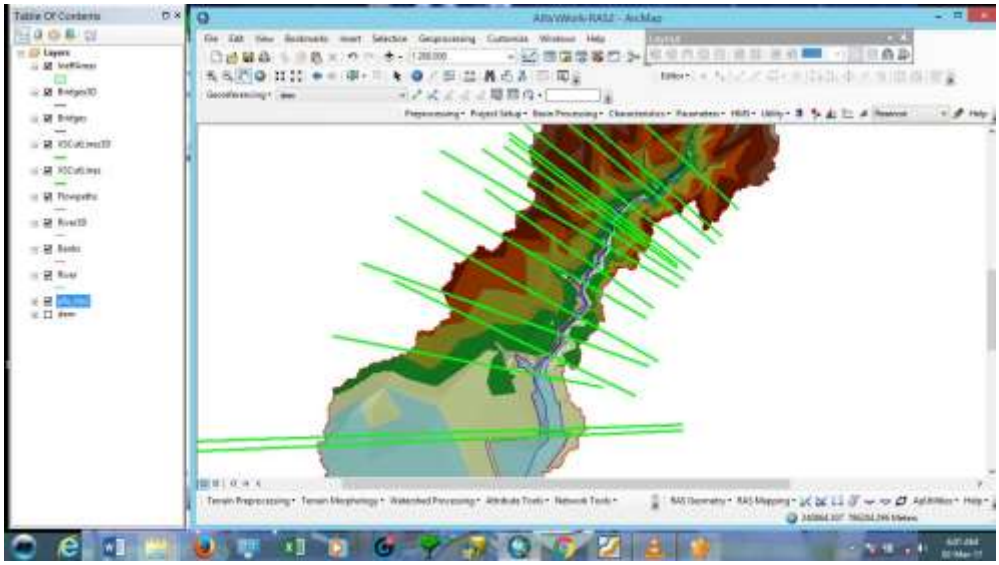


Fig. 3.11: Screenshot of the RAS Layers created

After all the aforementioned layers were created, the *RAS Geometry>Layer Setup* was clicked and the layers in each tab were verified to check if all the layers created are the ones to be exported. After this *RAS Geometry>Export GIS Data* was used to export the RAS layers.

(C) One-Dimensional Hydraulic Modelling in HEC-RAS

The one-dimensional steady state hydraulic modelling was carried out using HEC-RAS and HEC-GeoRAS extension in ArcGIS 10.2.2. HEC-GeoRAS is a GIS-based 2-dimensional hydrodynamic model.

The HEC-RAS software was opened and a new project was created and saved with a new name in the working folder. The Geometric data created in ArcGIS was imported by first opening the Geometric Data editor from the *edit* menu after which the *File>Import Geometry Data>GIS Format* was selected. Thus, the geometric section from HEC-GeoRAS section was imported (Fig. 3.12) while the ArcMap document was left open.

The imported geometric data was saved and some quality checks carried out. Manning's n-values were assigned based on field observation by selecting *Manning's n or k value* from the Table tools. The Manning's n values were assigned shown in Fig. 3.13.

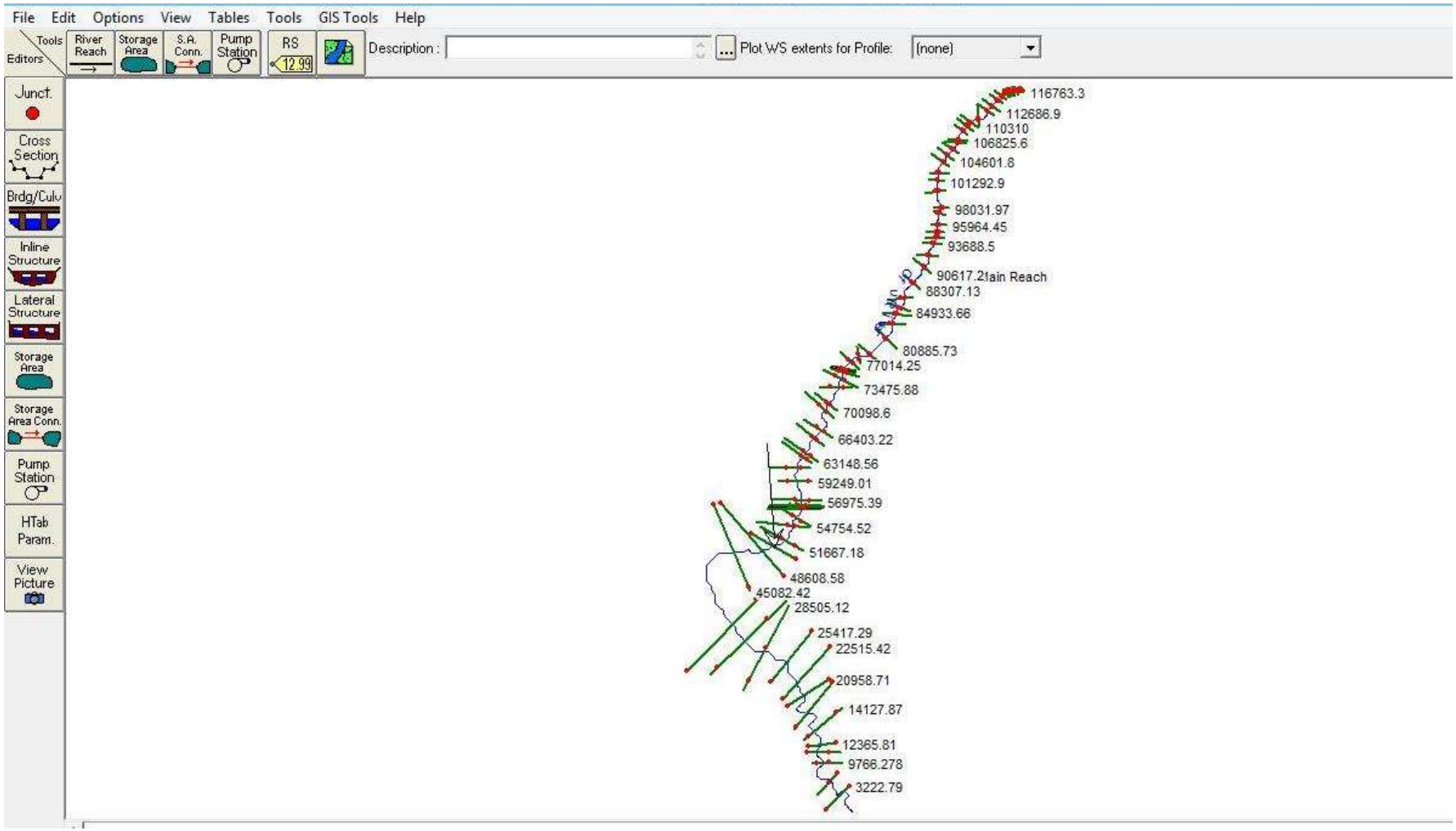
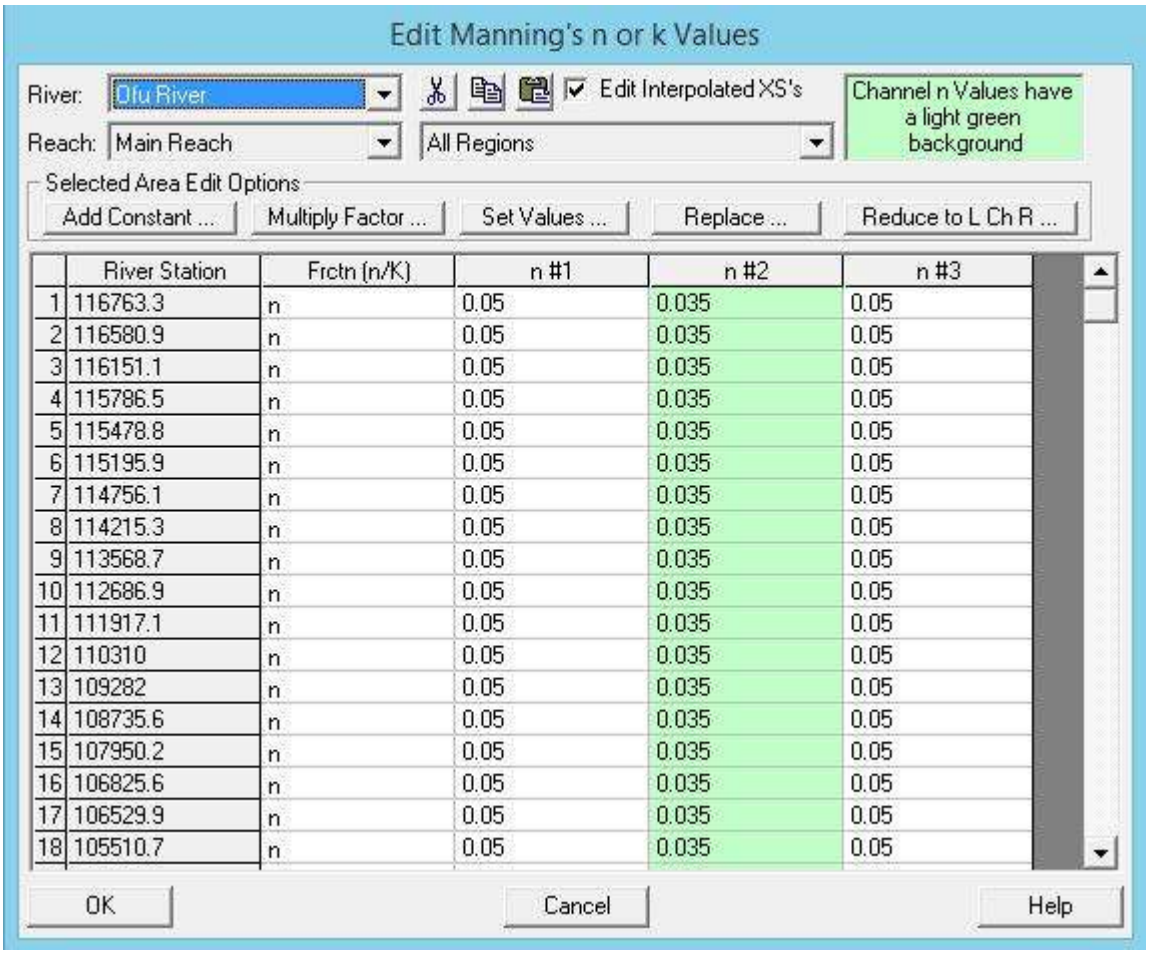


Fig. 3.12: View of the Geometric data imported from ArcGIS to HEC-RAS



	River Station	Frctn (n/K)	n #1	n #2	n #3
1	116763.3	n	0.05	0.035	0.05
2	116580.9	n	0.05	0.035	0.05
3	116151.1	n	0.05	0.035	0.05
4	115786.5	n	0.05	0.035	0.05
5	115478.8	n	0.05	0.035	0.05
6	115195.9	n	0.05	0.035	0.05
7	114756.1	n	0.05	0.035	0.05
8	114215.3	n	0.05	0.035	0.05
9	113568.7	n	0.05	0.035	0.05
10	112686.9	n	0.05	0.035	0.05
11	111917.1	n	0.05	0.035	0.05
12	110310	n	0.05	0.035	0.05
13	109282	n	0.05	0.035	0.05
14	108735.6	n	0.05	0.035	0.05
15	107950.2	n	0.05	0.035	0.05
16	106825.6	n	0.05	0.035	0.05
17	106529.9	n	0.05	0.035	0.05
18	105510.7	n	0.05	0.035	0.05

Fig. 3.13: Assigning of Manning's n Values in HEC-RAS

The cross-section tool in Geometric data Editor window was then used to view the river cross-section after which the *Graphical Cross-section Editor* selected from the Geometric Editor tools was used to edit the cross-sections, The editor was used to adjust the Bank Stations. One of the edited cross sections is shown in Fig. 3.14.

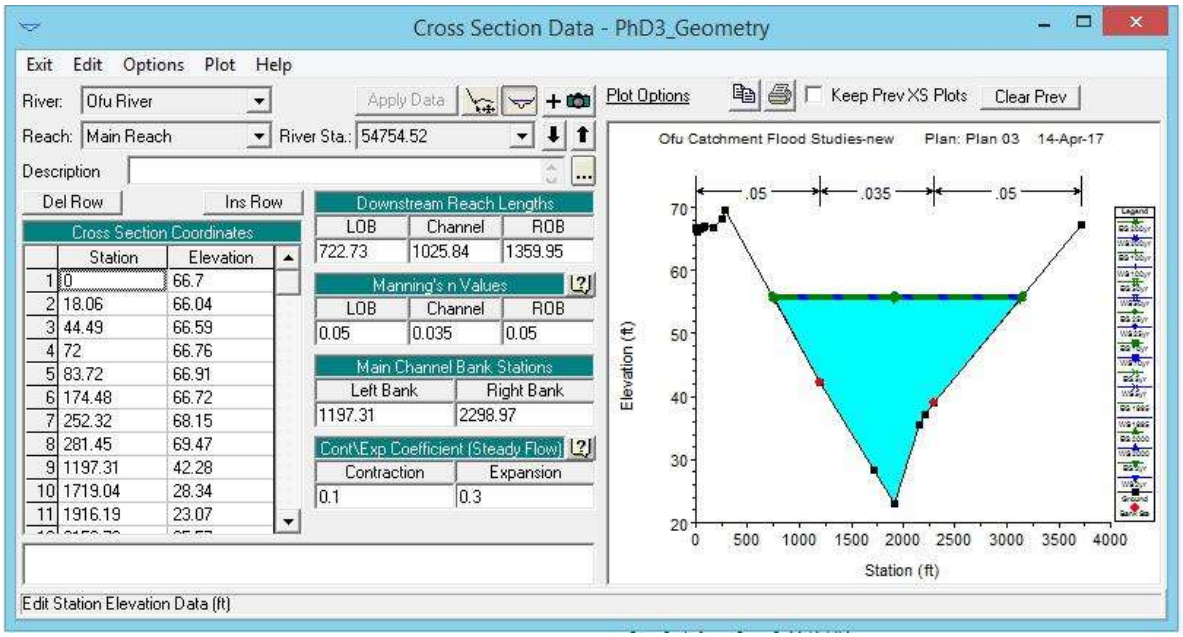


Fig. 3.14: One of the Cross-sections in HEC-RAS

The maximum number of cross-section points in HEC-RAS is 500. Thus, the points were edited and reduced using, *Tools>Cross Section Points Filter*in the Geometric Editor window.

Information on the two bridges was edited using the *Bridge/culvert* editing button in the Geometric Editor window. The width of the bridge at Akpagidigbo was set at 12m while the deck elevations were set at 130 m and 128 m for high and low Chords respectively for both upstream and downstream as shown in Fig. 3.15. The width of the bridge at Oforachi on the other hand was set at 10m while the deck elevations were set at 58.5m and 57m for high and low Chords respectively for both upstream and downstream as shown in Fig. 3.16

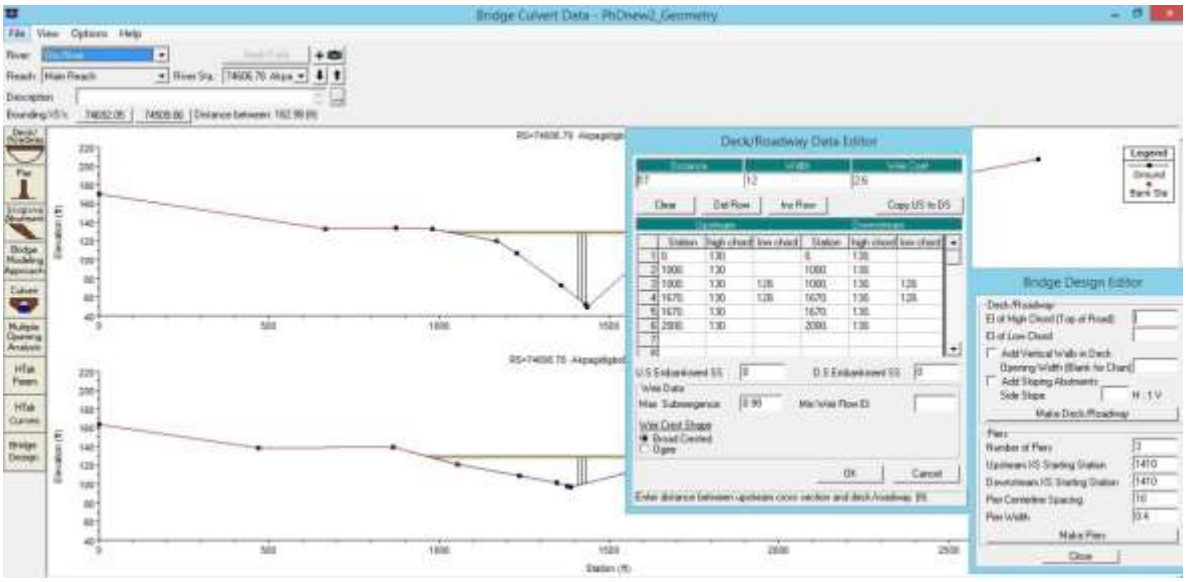


Fig. 3.15: Akpagidigbo Bridge data showing deck/roadway editor and bridge design editor

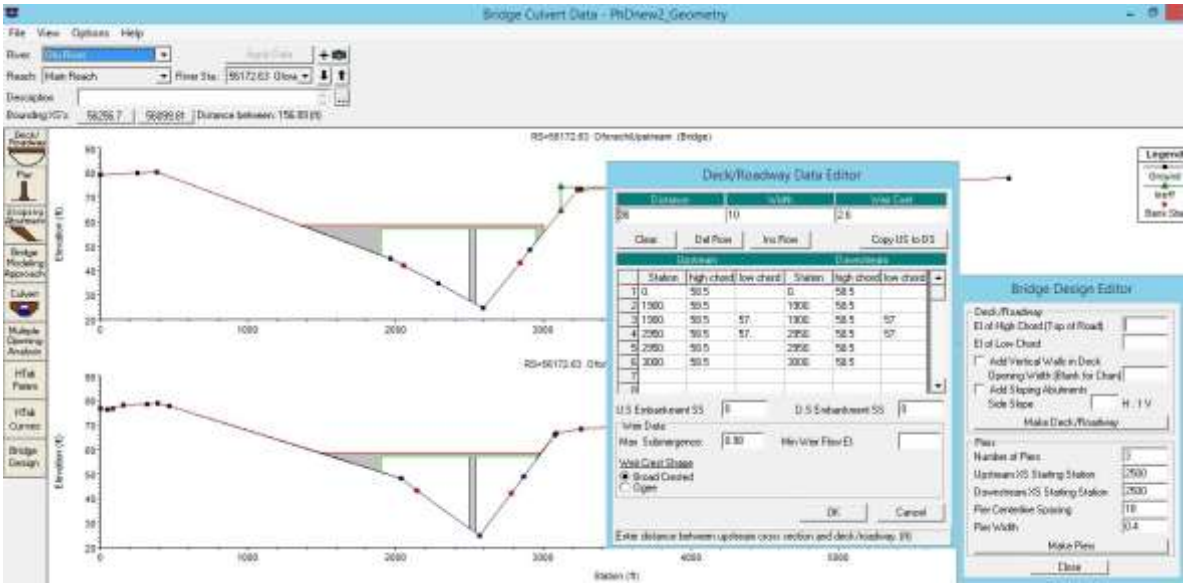


Fig. 3.16: Oforachi Bridge data showing deck/roadway editor and bridge design editor

40 cm diameter pile foundations on three rows (12 per row) were used for both bridges. The pier information was thus edited based on the physical observation of the bridges. While the Akpagidigbo piles were spaced 10 m apart across the bridge length, those of Ofu were space 18 m apart. This information was obtained via a phone interview with one of the Engineers with Setraco Nig Ltd who constructed the Oforachi Bridge and confirmed during the field work. This data were entered in the Bridge Design editor as

shown above for the two bridges (Figs. 3.15 and 3.16). The geometric data was saved and Geometric Editor window exited.

Steady flow information was entered by selecting *Edit>Steady Flow Data* from the HEC-RAS main menu. Nine (9) profiles were created and the estimated flow discharge for Ofu River entered for year 1995, year 2000, 2-yr, 5-yr, 10-yr, 25-yr, 50-yr, 100-yr and 200-yr return periods. Normal Depth was selected and slope of 0.0001 specified as shown in Fig. 3.17.

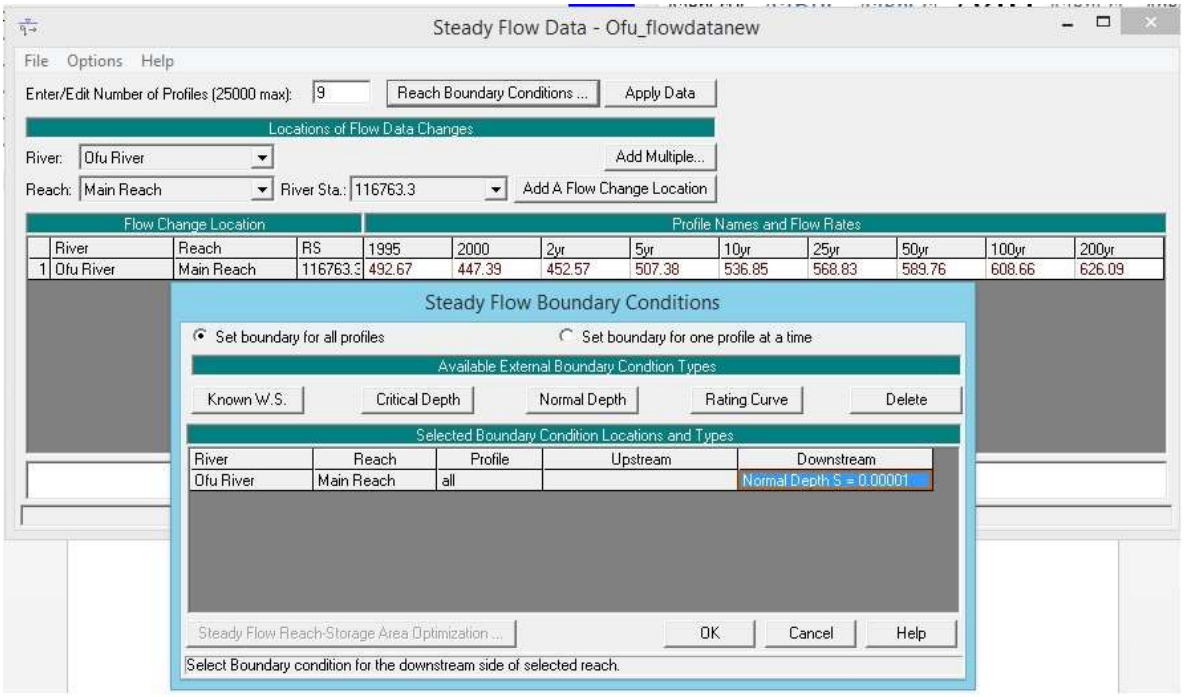


Fig. 3.17: Steady Flow Data and Boundary Conditions Input in HEC-RAS

The flow data was saved and the Steady Flow Data editor exited.

The next step was to run the steady flow analysis. This was done by selecting *Run>Steady Flow Analysis* in the HEC-RAS main window. The HEC-RAS results were then exported to ArcGIS on successful simulation. This was done by selecting *File>Export GIS Data* in the HEC-RAS main window. The results for Water surfaces, water surface extent and velocity for the nine profiles were specified for export as shown in Fig. 3.18.

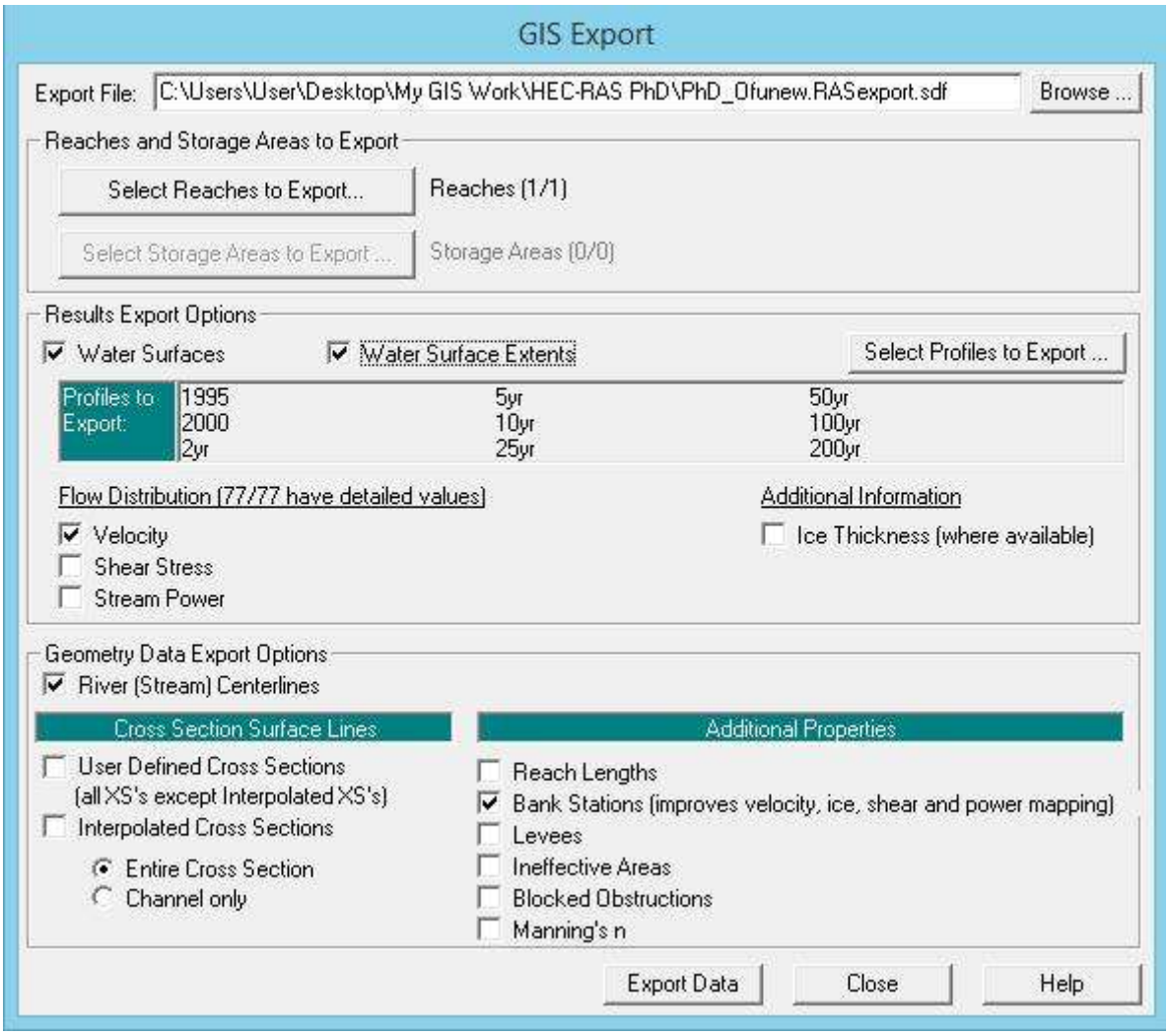


Fig. 3.18: Exporting HEC-RAS Results to ArcGIS

(D) Flood Inundation Mapping

i. *Flood Depths, Inundation Area and Velocity Simulation in HEC-GeoRAS/ArcGIS*

The Import RAS SDF file button ( ) on the HEC-GeoRAS toolbar was selected to convert the RAS output file exported earlier to GIS from the SDF file to XML file. A new analysis layer for HEC-RAS post-processing was set up by selecting *RAS Mapping>Layer Setup* and the required fields were filled. On pressing Ok, the terrain TIN was converted to digital terrain model (DTM). The *RAS Mapping>Import RAS Data* was selected afterwards and the bounding polygon which defines the analysis extent for inundation mapping, by connecting the endpoints of XS Cut Lines, was created and added

to the map layer alongside bank points, velocities, water surface extent, River 2D and XS Cut lines.

The inundation extent mapping was done in two (2) steps. Firstly, *RAS Mapping>Inundation Mapping>Water Surface Generation was selected* on the HEC-GeoRAS toolbar which created a water surface TIN. The second step involved the conversion of the water surface TIN to a GRID and subtracting the DTM grid from the water surface grid. This was done by selecting *RAS Mapping>Inundation Mapping>Floodplain Delineation* on the HEC-GeoRAS toolbar. The area with positive results implied that the water surface is higher than the terrain. These areas are the flood areas which form the flood inundation polygon. HEC-GeoRAS interpolates and expresses model results in two-dimensions on the landscape. Velocity modelling was also carried out by selecting *RAS Mapping>Velocity Mapping* on the HEC-GeoRAS toolbar.

3.2.5.3 Comparison of Extent of Flood Inundation from both Methods

The extents of inundation obtained from the GIS integration of thematic layers and the HEC-RAS hydraulic modelling were compared. The pattern and area extent of inundation were the area of comparison.

3.2.6 Methods of Flood Risk Analysis

3.2.6.1 Method of Flood hazard assessment

Flood hazard analyses were carried out for floods of 1995 and 2000 flood scenarios as well as the 100-year and 200-year flood events. The flood hazard classification was done based on the depth of inundation water only. The velocity was not considered as the average velocity was far less than 1 m/s which is the lowest hazard velocity limit for flood inundation water. Besides, the major flood challenge within Ofu River floodplains has

been that of inundation which probably could be the reason why no loss of live has ever been recorded. Thus the inundation raster maps for the respective events were reclassified into 'High,' 'Moderate' and 'Low' based on Daffi (2013) as shown in Table 3.13.

Table 3.13: Flood Hazard Classification Based on Flood Depths

Flood Depth (m)	Hazard Classification	Indicators
0 – 1	Low Hazard	Minor increase to existing flood levels.
1 – 2	Moderate Hazard	Significant increase in flood levels with respect to crops, roads and buildings.
> 2	High Hazard	Major increase to existing flood levels with respect to crops, roads and buildings.

Source: Daffi (2013)

This implies that the threshold for high hazard was set at 2m depth of flood inundation water.

3.2.6.2 Method of Flood vulnerability assessment

The procedure for determining social vulnerability developed by Cutter *et al*. (1997) for the South Carolina Emergency Preparedness Division was adopted in this study. The method was developed for vulnerability assessment at County level which is equivalent to the LGA system in Nigeria. This makes it suitable for the present study.

(A) Estimation of population within inundated area

i. Estimation of Population Growth Rates Population Figures and Densities

Population figures for 1991 and 2006 census (NPC, 2010_a; NPC, 2010_b; NBS 2012) were obtained from the official websites of the National Populations Commissions and the National Bureau of Statistics. The population growth rates for the respective local

governments were estimated using the geometric growth rate equation expressed by Eq. (3.60).

$$P_E = P_o e^{rn} \qquad (3.60)$$

Where:

P_E = Expected population

P_o = Population of previous year

e = Exponential

r = Growth rate

n = Number of years interval

The population figures of 1991 for each Local Government Area were used as P_o while those of 2006 were used as P_E. The difference in years between 2006 and 1991 was used as n for the estimation of the respective growth rates by LGAs. Igalamela/Odolu and Ibaji LGAs were not created as at the 1991 census thus their population figures were part of their mother LGA-Idah for 1991. The sum of the population figures for Idah, Igalamela/Odolu and Ibaji LGAs was used as P_E for Idah in 2006 for the estimation of the population growth rate for Idah LGA. This growth was eventually used for the three LGAs. The population growth rates estimated are presented in Table 3.14.

The population figures of the respective LGAs for 1995 and 2000 were estimated based on 1991 census figures while those for 2055 (100-year flood) and 2155 (200-Year flood) were estimated based on 2006 census figures. The growth rates estimated previously (Table 2.14) were used for the population projection in both cases.

Table 3.14: Estimated Population Growth Rates

LGA	1991	2006		Growth Rate
Dekina	177513	260968	260968	0.026
Ofu	108095	191480	191480	0.038
Igalamela/Odolu		147048		
Idah	224692	79755	354375	0.030
Ibaji		127572		
Uzo-Uwani	88112	127150	127150	0.024

NBS (2012)

The land area covered by the respective LGAs was obtained from KGS (2012). The population density of the respective LGAs for each year was estimated using Eq. (3.61).

$$P_d = \frac{P_2}{A} \tag{3.61}$$

Where:

P_d = Population density (persons/km^2)

P_2 = Estimated Population for the year

A = Land Area for the LGA (km^2).

ii. Estimation of Affected Population

The polygon of the inundation extent for 1995, 2000, 100-year and 200-year floods were divided using the LGA boundaries so that the area of inundation for each LGA could be extracted. Thus, the population affected for each LGA was estimated using Eq. (3.62).

$$P_A = P_d \times A_i \tag{3.62}$$

Where:

P_A = Affected Population in the LGA

P_d = Population Density for the LGA

A_i = Inundated Area for the LGA

(B) Social Distribution of Affected Population

i. Age and Disability Status

The percentage of the total population for each LGA living with any form of disability was estimated as shown in Table 3.15.

Table 3.15: Estimation of Percentage of Population with Disability

State	LGA	2006	Disabled	
			Population	%
Kogi	Dekina	260968	3825	1.47
	Ofu	191480	2410	1.26
	Igalamela/Odolu	147048	2197	1.49
	Idah	79755	1323	1.66
	Ibaji	127572	1794	1.41
Enugu	Uzo-Uwani	127150	2470	1.94

NPC (2010b)

In addition, the population for each LGA obtained from NPC (2010a) distributed by 5 years interval was divided into three categories. They are under 15 years, 15 – 65 years and above 65 years.

The percentage of the total population for each age category was estimated as shown in Table 3.16.

Table 3.16: Estimation of Percentage Distribution of Population by Age

State	Total	under 15		15 - 65		Above 65	
		Population	%	Population	%	Population	%
Kogi	3314043	1507045	45.47	1715349	51.76	91833	2.77
Enugu	3267837	1163114	35.59	1958088	59.92	146672	4.49

NPC (2010a)

These percentages were used to distribute the affected populations into the three categories (Under 15 years, 15 – 65 years and above 65 years). The population obtained for each category was further divided into those with disabilities (WD) and those with no disabilities (ND) using the percentages obtained in Table 3.14. Thus six (6) categories of population distribution by age were obtained.

ii. Poverty Line

According to NBS (2012), 73.4 % and 69 % of rural population were living in poverty in 2003-04 and 2009-10 respectively. The proportion of affected population living in poverty for 1995 and 2000 were estimated as 73.4 % of the affected population for each LGA while those for the 100-year and 200-year events were estimated as 69 % of the affected population.

iii. Gender

The affected population was distributed according to gender to determine their vulnerability. The population figures for 1991 and 2006 census distributed by gender were used to estimate the percentage for each category as shown in Table 3.17.

These percentages obtained were used to divide the affected population into male and female categories. The percentages obtained for 1991 were used for the 1995 and 2000 scenarios while those for 2006 were used for the 100-year and 200-year events.

Finally, ten (10) social vulnerability groups were obtained and used for further analysis.

(C) Estimation of Vulnerability Weight

The method of estimation of vulnerability weight described previously Cutter *et al*. (1997) for South Carolina Emergency Preparedness Division was adopted for the estimation of vulnerability weight for each category. The population of the entire catchment distributed by the component LGAs was estimated using the population densities and the areas derived previously as shown in Table 3.18.

Table 3.17: Estimation of Percentage Distribution of Population by Gender

LGA	1991					2006				
	Total	Male	%	Female	%	Total	Male	%	Female	%
Dekina	177513	85705	48.28	91808	51.72	260968	131394	50.35	129574	49.65
Ofu	108095	52254	48.34	55841	51.66	191480	96671	50.49	94809	49.51
Igalamela/Odolu	-	-	-	-	-	147048	74489	50.66	72559	49.34
Idah	224692	108777	48.41	115915	51.59	79755	40141	50.33	39614	49.67
Ibaji	-	-	-	-	-	127572	64423	50.50	63149	49.50
Uzo-Uwani	88112	41993	47.66	46119	52.34	127150	63759	50.14	63391	49.86

NBS (2012)

Table 3.18: Estimation of Ofu River Catchment Population by LGAs

LGA	Area	Population within Catchment Portion							
		1995		2000		2055		2155	
		Pop Density	Population	Pop Density	Population	Pop Density	Population	Pop Density	Population
Dekina	672.12	79.18	53219.70	90.17	60608.11	375.07	252089.10	5049.78	3394061.65
Ofu	392.10	75.34	29541.38	91.11	35722.90	737.89	289329.10	32984.67	12933353.62
Igalamela/Odolu	316.50	66.49	21045.30	77.26	24451.15	284.14	89927.46	5707.01	1806241.25
Idah	3.68	66.49	244.62	77.26	284.21	8717.60	32069.95	175097.65	644142.23
Ibaji	213.35	66.49	14186.35	77.26	16482.19	365.20	77914.05	7335.28	1564945.46
Uzo-Uwani	6.82	163.70	1116.15	184.57	1258.46	482.04	3286.71	5313.58	36229.96
	1604.56		119353.50		138807.01		744616.37		20378974.16

The derivation of vulnerability weights was carried out in two steps. The first step was the derivation of the vulnerability proportion. This was done by dividing the population for the vulnerability categories in each LGA by the total population within the catchment. The second step was the estimation of the vulnerability weight. This was done by dividing the vulnerability proportion for each LGA by the maximum vulnerability proportion for that category. Thus, the vulnerability weights were calculated for each category with 1 as the maximum in each case. These weights were multiplied by 100 for ease of reclassification in ArcGIS.

Finally, Saaty's Analytical Hierarchical Process (Saaty, 1980) was used to rank all the vulnerability categories. This method has been previously described. Thus Vulnerability weight was assigned to each category.

(D) Production of Vulnerability Map

i. Production of Vulnerability Maps

A table of estimated populations for the ten categories was produced in Microsoft Excel 2007 and saved in the CSV (Comma delimited) format recognized by ArcGIS. This table was joined to the flood inundation polygon for each event using the *Joins and Relates* tool in ArcGIS. The conversion tool was then used to produce raster maps of each population vulnerability category.

ii. Reclassification of Vulnerability Maps

The Vulnerability weights estimated were used to reclassify the maps produced in the previous process. This was done using the *Reclassify* Spatial Analyst Tool.

iii. Integration of Vulnerability Maps

The reclassified vulnerability maps were then integrated to produce the final flood vulnerability Map for each event/scenario. This was done using the *weighted Sum* tool in the *Spatial Analyst Tools* in ArcGIS 10.2.2. The weights derived for each category was used at this point for the integration. The final Vulnerability Map was first converted to float by dividing by the maximum value using the *Raster Calculator* in Spatial Analyst (Map Algebra) tool. Thus the final Flood Vulnerability Map was produced with 1 as the maximum value. This map was then reclassified into three vulnerability classes as shown in Table 3.19.

Table 3.19: Flood Vulnerability Classification

Vulnerability Index	Vulnerability Classification
0 – 0.1	Low Vulnerability
0.1 – 0.4	Moderate Vulnerability
0.4 – 1	High Vulnerability

Coto (2002)

3.2.6.3 Method of Flood Risk Assessment

(A) Production of Flood Risk Map

The flood Risk map, R_m was produced as a product of the Hazard map, H_m and the Vulnerability map V_m. the multiplication was done using Raster calculator in Map Algebra Spatial Analyst tool in ArcGIS 10.2.2.

Thus, the Flood Risk map for each event was produced and reclassified into three risk zones (‘High,’ ‘Moderate’ and ‘Low’) using Natural breaks as shown in Table 3.20.

Table 3.20: Flood Risk Classification

Vulnerability Index	Risk Classification
1 – 3	Low Risk
4 – 6	Moderate Risk
7 – 9	High Risk

Cutter *et al.* (1997)

(B) Identification of Elements at Risk

The final flood risk map was converted to polygon according the risk classes and used to extract all the elements digitized from the topographic maps obtained for the study area. These features were split into the three risk zones to determine their status.

(C) Assessment of Extent of Damage of the 1995 and 2000 Flood Scenarios

Section D of the household survey questionnaire (Appendix V_b) was used to assess the impacts of the 1995 and 2000 flood events. The scores of the eleven questions were used to assess these flood events which are the most severe in recent history of the community. A total of 22 responses (11 positive and eleven negative) were used. The positive responses were given a score of 1 while the negative ones were given a score of 0. A total score of 0 was regarded as no impact, scores greater than 0 but less than or equal to 2.75 (25%) as low impact, scores greater than 2.75 (25%) but less than 5.5 (50%) as moderate impact, score greater than 5.5 (50%) but less than or equal to 8.25 (75%) as high impact while scores greater than 8.25 (75%) was regarded as very high impact.

(D) Assessment of Environmental Health Implication of Flood

Section E of the household survey questionnaire (Appendix V_b) was used to assess the availability of toilet facilities at household level as well as the type of toilet for those who have. This was done to assess the extent of open defecation within the community. The

assessment also covered the household's source of drinking water. These assessments were carried out to check how much faecal waste are probably washed by floodwater into households and ultimately, Ofu River as well as the extent of dependence of the community on Ofu River as the source of water for household consumption.

The general methodology for the flood risk assessment is shown in Fig. 3.19.

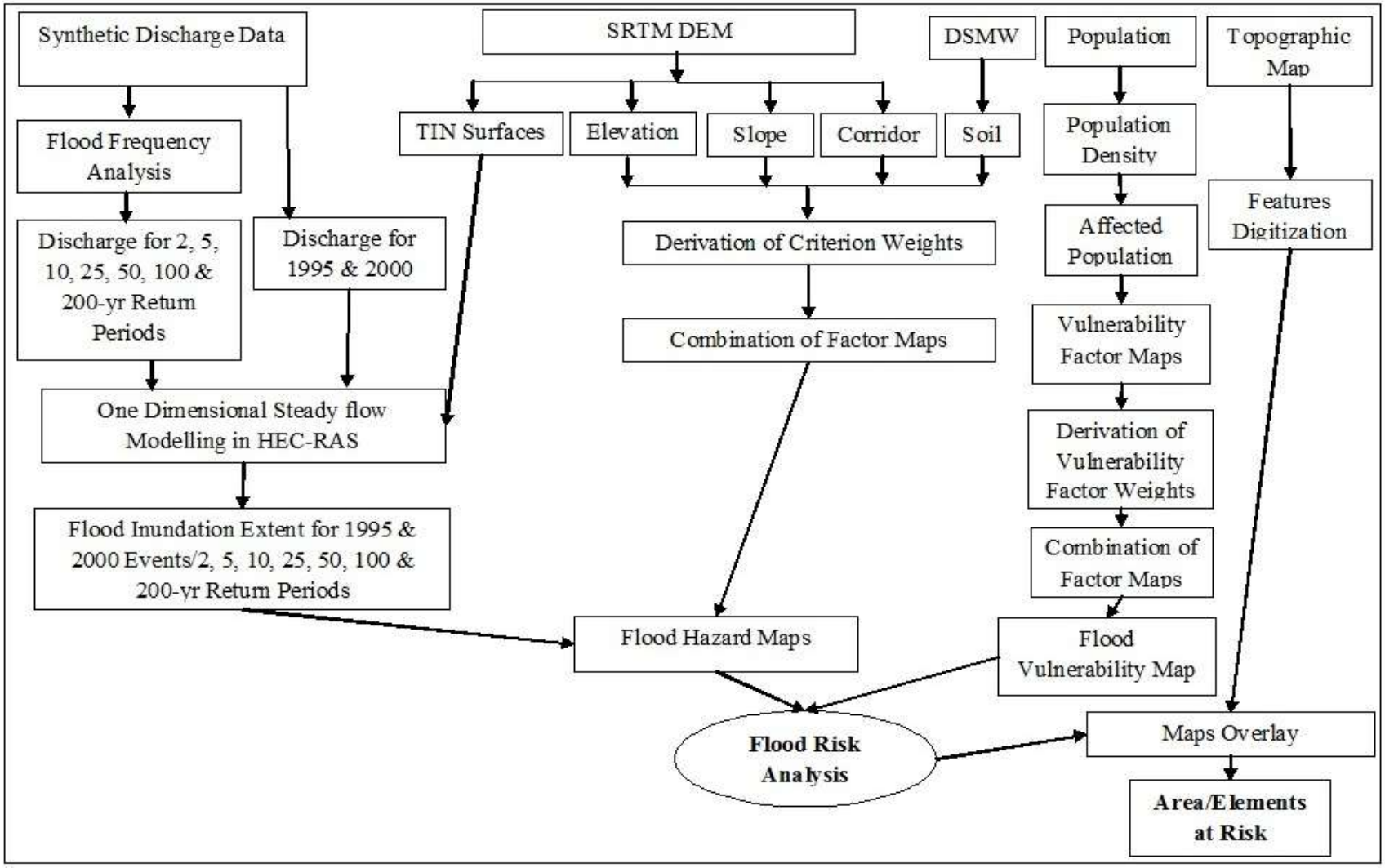


Fig. 3.19: Schematic Flowchart of the Flood Risk Assessment Methodology

CHAPTER FOUR

RESULTS AND DISCUSSION

4.1 MORPHOLOGIC CHARACTERISTICS OF OFU RIVER CATCHMENT

4.1.1 Delineation of Ofu River Catchment Boundaries

The delineation of Ofu River catchment boundaries was carried out using ArcHydro for terrain pre-processing and HEC GeoHMS for the project generation. The physical characteristics of the sub-basin and the Ofu River (main stream) extracted are River length and slope, Basin slope, Longest flow path, Basin centroid, Basin centroid elevation and Centroid longest flow path. The attribute tables of Ofu River and the Ofu River catchment were populated with area, perimeter and average slope of the basin. These data were the basic parameters for the estimation of the areal aspects of the morphometric parameters.

4.1.2 Morphologic Characteristics of Ofu River Catchment

The morphologic characteristics of Ofu River obtained from the morphometric analysis are classified into three categories and presented as follows:

4.1.2.1 Areal characteristics of Ofu River Catchment

The basic areal characteristics of Ofu River Catchment analyzed in this study are shown in Fig. 4.1. This shows the physical characteristics of the river and the catchment extracted during the catchment delineation process.

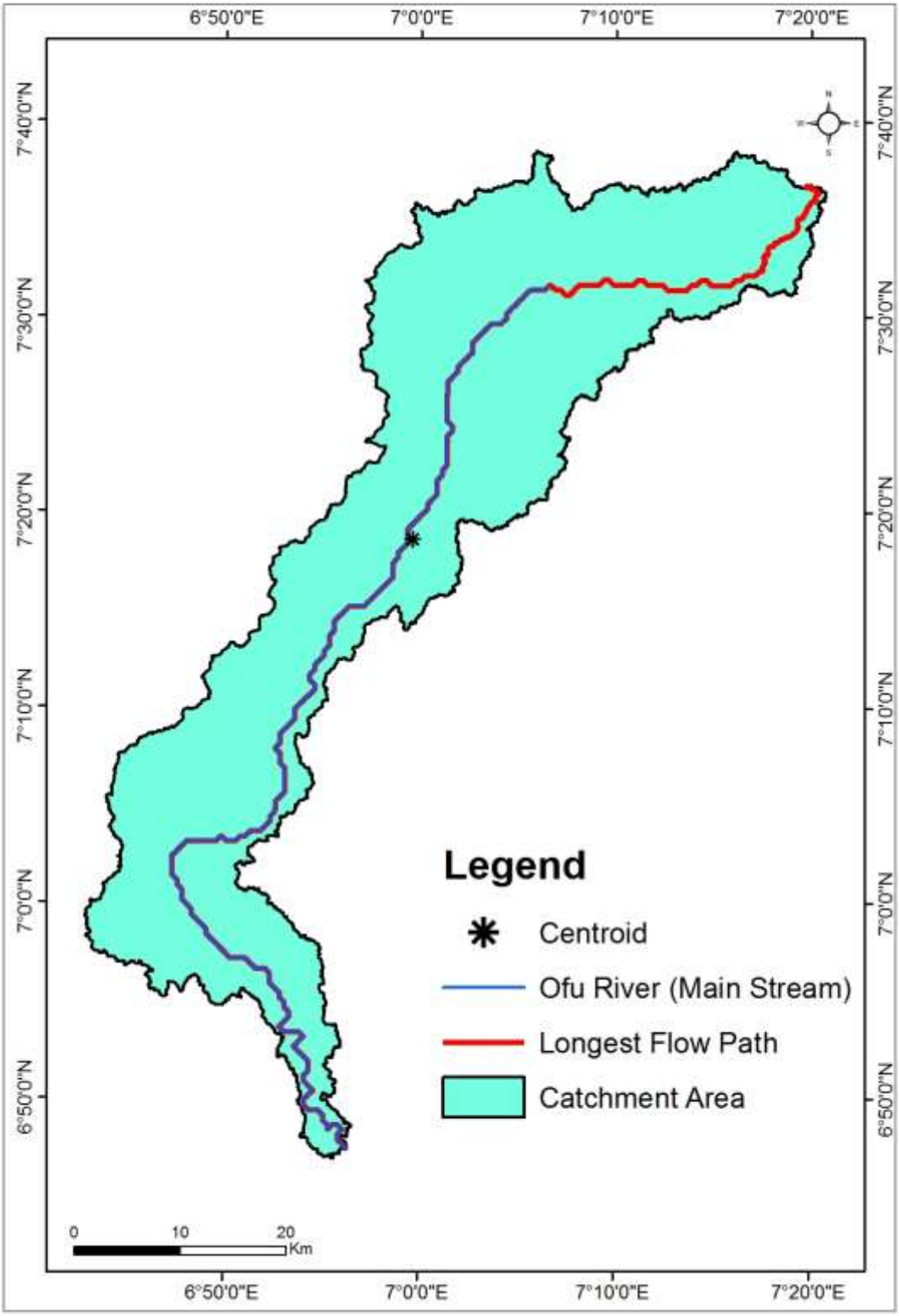


Fig. 4.1: Areal Morphologic Characteristics of Ofu River Catchment

Furthermore, the results of the areal morphological characteristics of Ofu River Catchment estimated are presented in Table 4.1.

Table 4.1: Morphologic Characteristics of Ofu River Catchment (Areal Aspects)

Parameters	Symbol	Unit	Value
Basic Parameters			
Area	A	km^2	1604.56
Perimeter	P	km	556.98
Basin Length	L_b	km	100.93
Longest Flow Path	L_{fp}	km	159.14
Main Stream Length	S_L	km	121.37
Basin Centroid Longest Flow Path	L_{cfp}	km	89.32
Derived Parameters			
Elongation ratio	R_e	-	0.45
Circularity ratio	R_c	-	0.07
Form factor	F_f	-	0.16
Compactness coefficient	C_c	-	3.92
Shape Factor	B_s	-	6.35
Stream frequency	F	km^{-2}	0.11
Drainage Density	D_d	km/km^2	0.26
Drainage Texture	T	km^{-1}	0.31
Drainage Intensity	I_d	km^{-1}	0.42
Constant of Channel Maintenance	C_m	km^2/km	3.90
Length of Overland Flow	L_o	km	1.95
Channel Sinuosity	S_c	-	2.59
Time of Concentration	T_c	Hrs	6.17
Time from peak to Recession	N	Days	3.68

Table 4.1 shows that Ofu River Catchment covers a total area of 1,604.56 km^2 and is bounded by a perimeter of 556.98 km. 41.89 % of this area falls in Dekina LGA, 24.4 % in Ofu LGA, 19.72 % in Igalamela/Odolu LGA, 0.23 % in Idah LGA and 13.30 % in Ibaji LGA all in Kogi State while 0.42 % falls in Uzo-Uwani LGA in Enugu State. In addition, the percentage of each LGA land mass drained by Ofu River are 27.02 %, 23.48 %, 14.06 %, 9.25 %, 14.04 % and 0.80 % for Dekina, Ofu, Igalamela/Odolu, Idah, Ibaji and Uzo-Uwani LGAs respectively. Based on this area, Ofu River Catchment can be classified as medium (Sreedevi *et al.,* 2013). Schumm's basin length of Ofu River Catchment is 100.93 km. The longest flow path is 159.14 km while the length of main stream (Ofu River) is 121.37 km. the basin centroid longest flow path is 89.32 km.

Table 4.1 further shows that the catchment has an elongation ratio of 0.45, circularity ratio of 0.07, form factor of 0.16, compactness coefficient of 3.92 and a shape factor of 6.35. More so, the stream frequency of the catchment is 0.11 km^{-1} while the drainage density is 0.26 km/km^2. The drainage texture is 0.31 km^{-1}, the drainage intensity is 0.42 km^{-1}, while the constant of channel maintenance is 3.90 km^2/km. Finally, the length of overland flow is 1.95 km, and the channel sinuosity is 2.59 while the time of concentration and time from peak to recession were 6.17 hours and 3.68 days respectively. These imply that while it will take a drop of water 6.17 hours to flow from the remotest part of the catchment to get to the outlet, it will take approximately four days for flood water to recede after peak.

The low value of Drainage density (D_d) of 0.26 km/km^2 indicates that the catchment has highly permeable subsoil and thick vegetative cover. In addition, the low Circularity ratio (R_c) of 0.07 obtained also indicates that as the catchment is almost elongated in shape, it has a low discharge rate of runoff and highly permeable subsoil conditions. More so, the low elongation ration (R_e) of 0.45 and Form factor (F_f) of 0.16 confirm that the basin is elongated and thus the basin has a flatter peak with a longer duration. The lower values of Stream frequency (F_s) and Drainage intensity (I_d) values further confirm that the surface runoff is not quickly removed from the river basin. The results reveal that the basin is well capable of absorbing water into the soil and recharging groundwater while reducing the risk of flooding. If such floods happen, they could be managed easily from this type of elongated catchments than from circular basins. The results of the areal morphologic characteristics show that Ofu River Catchment is inherently and morphologically capable of reducing the flood risk but sustainable management plans should be made in advance to cope with the potential floods that can occur due to high rainfalls as has been the case with the low lying flood plains for years.

4.1.2.2 Linear characteristics of Ofu River Catchment

The analyzed drainage network of the Ofu River Catchment is presented in Fig. 4.2.

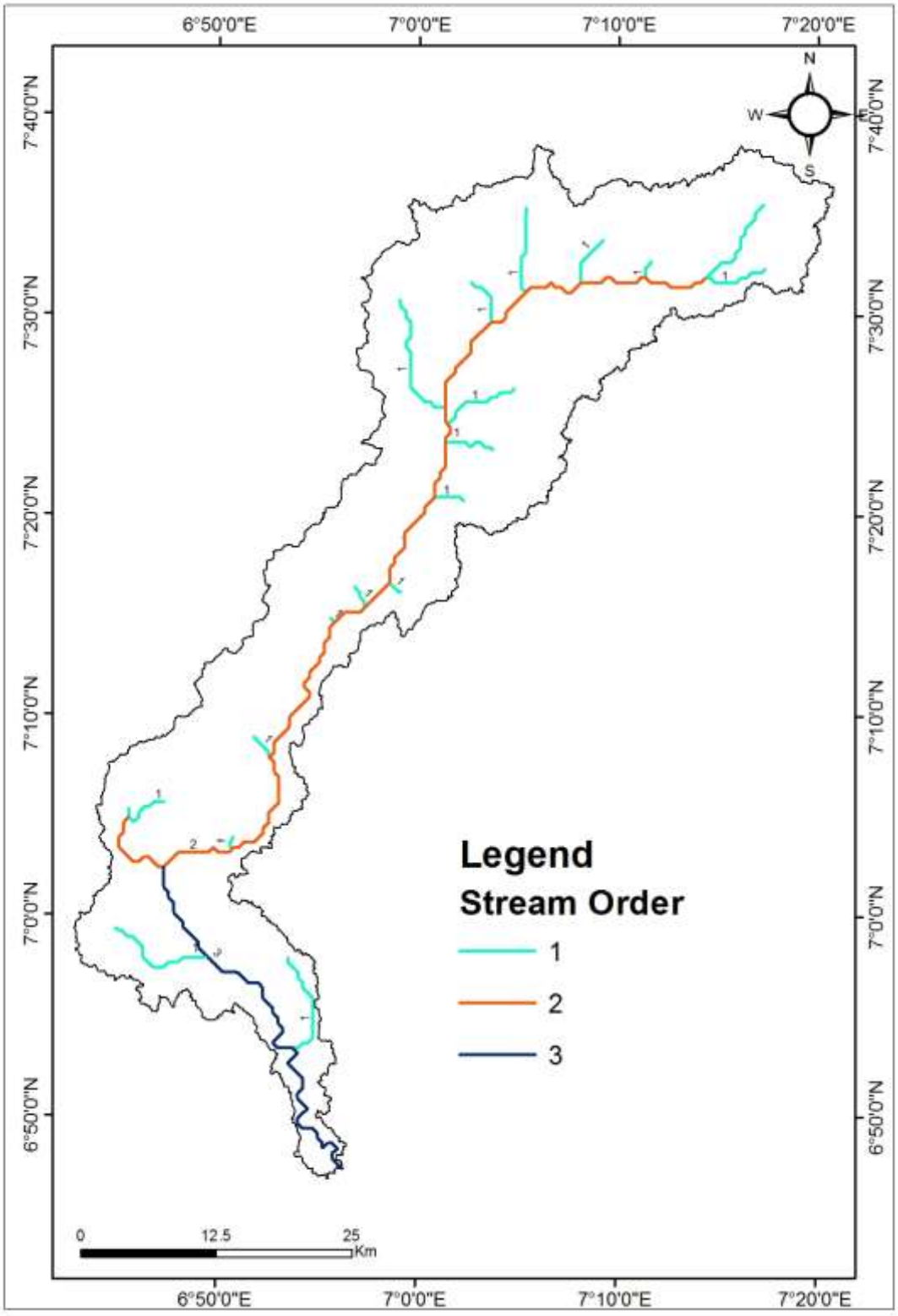


Fig. 4.2: Strahler's Stream Order of Ofu River Basin

The linear aspects of the morphometric analysis conducted for the river network are presented in Table 4.2.

Table 4.2: Morphologic Characteristics of Ofu River Catchment (Linear Aspects)

Stream Order (U)	Stream Number (N_u)	Stream Length (L_u)	Mean Stream Length (L_{um})	Bifurcation Ratio (R_b)	Stream Length Ratio (R_L)
1	20	98.76	4.94	1.25	
2	16	101.17	6.32	5.33	1.02
3	3	41.47	13.82		0.41
	ΣN_u = 39	**ΣL_u =241.40**	**-**	**Av. R_b = 3.29**	**Av. R_L = 0.72**

The results in Table 4.2 reveal that a total of 39 streams are found in Ofu River catchment. These streams are linked up to the 3rd order spreading over an area of 1,604.56 km² (Fig. 4.2). There are a total of 20, 16 and 3 streams of orders 1, 2 and 3, respectively with stream lengths of 98.76 km, 101.17 km and 41.47 km in respective orders. This small number of streams indicates mature topography in the catchment (Zaidi, 2011). The mean stream lengths for order 1, 2 and 3 were, respectively 4.94 km, 6.32 km and 13.82 km. A plot of the respective logarithm of stream number (N_u), stream length (L_u) and mean stream length (L_{um}) versus stream order are presented in Figs. 4.3, 4.4 and 4.5. These were used to describe the relationship between these parameters and the stream order.

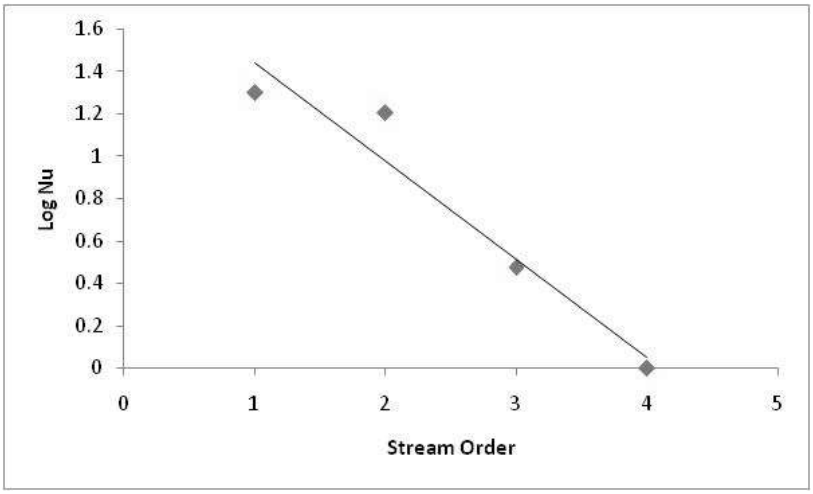


Fig. 4.3: Logarithm of Stream Number (N_u) versus Stream Order (U)

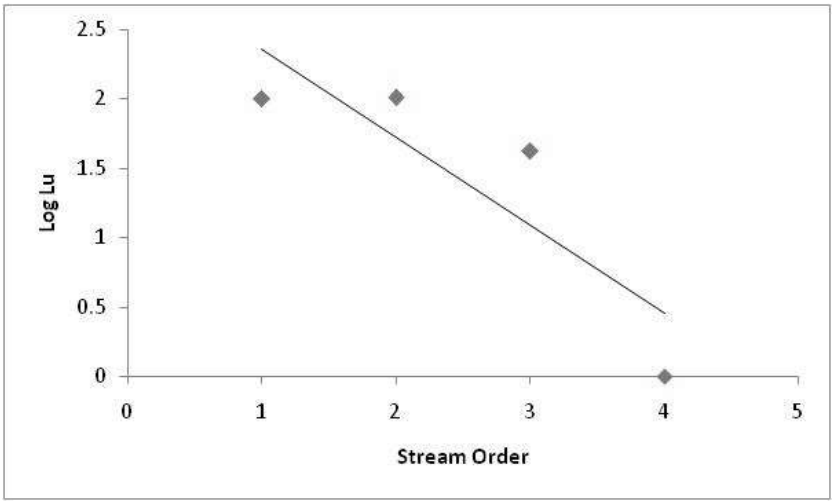


Fig. 4.4: Logarithm of Stream Length (L_u) versus Stream Order (U)

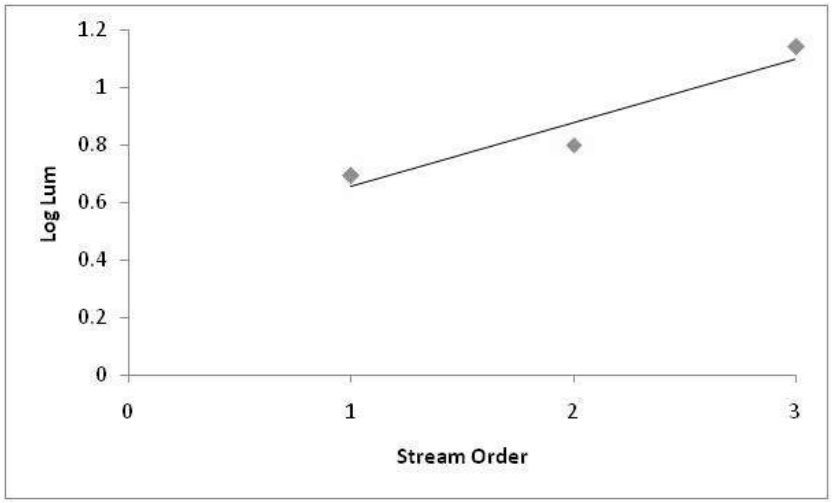


Fig. 4.5: Logarithm of Mean Stream Length (L_{um}) versus Stream Order (U)

Figs. 4.3 and 4.4 show that there was a decrease in stream number and stream length, respectively with increasing order which agrees with Horton (1945). In addition, the mean stream length (L_{um}) showed an increase with increasing order (Fig. 4.5) as explained by Strahler (1964). These results agree with those of previous studies carried out on other similar catchments (Withanage *et al.*, 2014; Waikar and Nilawar, 2014).

Dendritic drainage pattern can be observed in Ofu River basin (Fig. 4.2) which is probably the most common drainage pattern identified in Nigerian river basins and the world at large. This is a randomly developed, treelike pattern composed of branching tributaries

and a main stream characteristic of essentially flat-lying and/or relatively homogeneous rocks and impervious soils (Zernitz, 1932). According to Withanage *et al.* (2014), dendritic patterns develop on rocks of uniform resistance which indicate a complete lack of structural control. It is more likely to be found on nearly horizontal sedimentary rocks or on areas of massive igneous rocks and sometimes on complex metamorphosed rocks (Garde, 2006). Ofu River shares similar geological characteristics with Ankpa which according to Imasuen *et al.* (2011) falls within the Anambra Basin whose genesis has been linked with the development of the Niger Delta Miogeosyncline and the opening of the Benue Trough. According to them, the Benue Trough is underlain by the rocks of Anambra Sedimentary Basin consisting of the Ajali and Mamu formations.

Furthermore, Table 4.2 shows that bifurcation ratios of 1.25 and 5.33 were obtained for Ofu catchment while the average bifurcation ratio is 3.29. According to Horton (1945), bifurcation ratio is an index of reliefs and dissections. The bifurcation ratios were not the same from one order to the next which according to Strahler, (1964) and Withanage *et al.* (2014) is attributable to the geological and lithological development of the drainage basin. Strahler (1964) and Nag (1998) stated that lower values of bifurcation ratios are characteristics of watersheds which have suffered less structural disturbances. The higher bifurcation ratio of 5.33 obtained for order 2 streams in this study indicates that strong structural disturbances have occurred in the basin when the underlying geological structure underwent transformations.

In addition to the forgoing, Chorley *et al.* (1957) noted that bifurcation ratio could be an index of flood risk level. He stated that the lower the bifurcation ratio, the higher the risk of flooding, particularly of parts and not the entire basin. This explains why the flooding within the Ofu River catchments affects only a part of the basin amongst other factors. The values of bifurcation ratio (R_b) obtained in this study (1.25 and 5.33), the high

average of 3.29 together with the elongated shape of Ofu River basin would result in a lower and extended peak flow, which will reduce the risk of flooding within the basin.

4.1.2.3 Relief characteristics of Ofu River Catchment

The Digital Elevation Model (DEM) of Ofu River catchment is shown in Fig. 4.6.

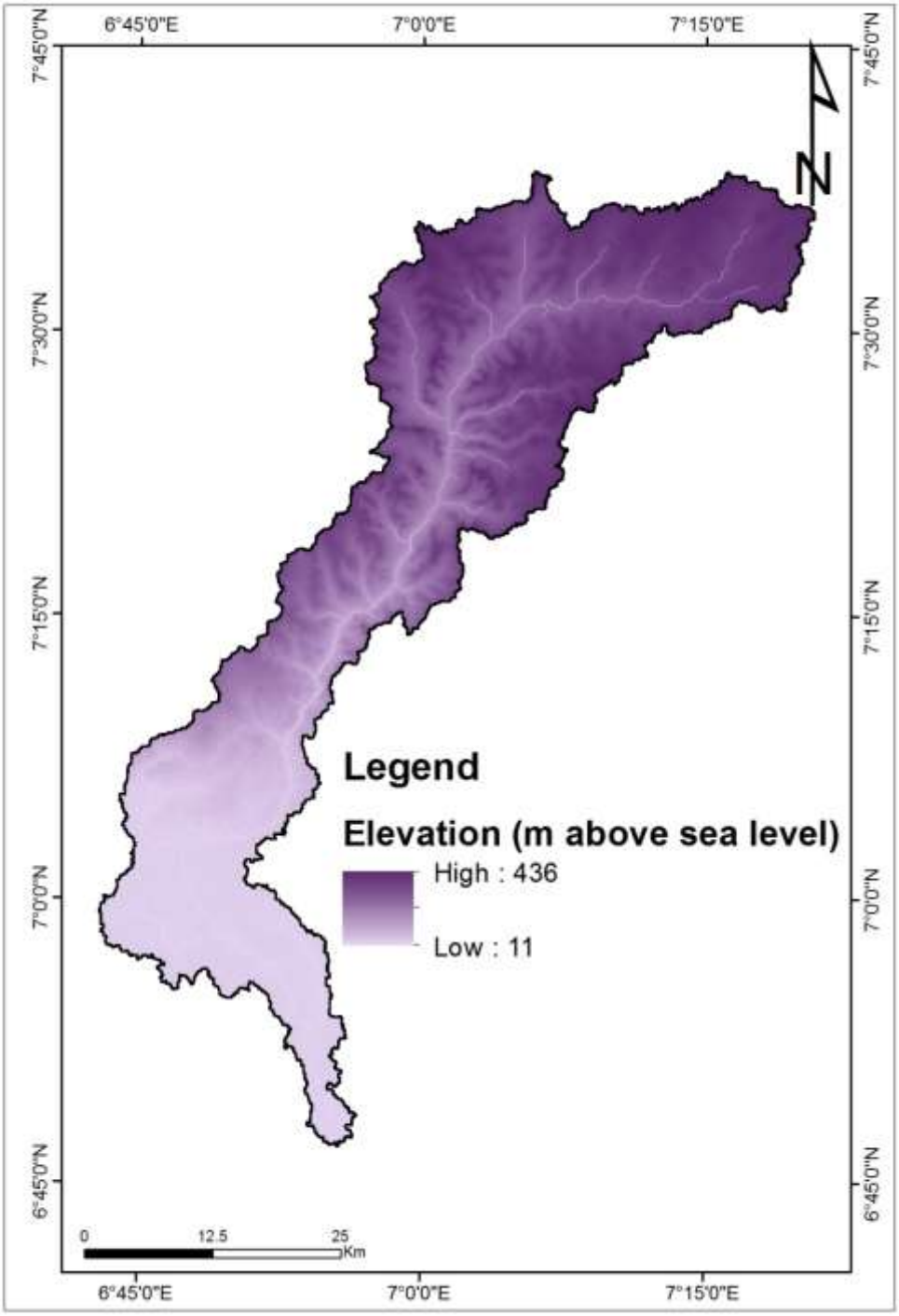


Fig. 4.6: Digital Elevation Model (DEM) of Ofu River Catchment

The relief characteristics of Ofu River Catchment derived using the elevation data obtained from the DEM are presented in Table 4.3.

Table 4.3: Morphologic Characteristics of Ofu River Catchment (Relief Aspects)

Parameters	Symbol	Unit	Value
Highest Elevation	Z	m asl.	436
Lowest Elevation	Z	m asl.	11
Basin Relief	H	M	425
Relief Ratio	R_h	-	0.0042
Relative Relief	R_{hp}	-	0.0008
Ruggedness Number	R_N	-	0.109
Basin Slope	S	-	0.19

The relief aspects of a drainage basin relates to the three dimensional features of the basin involving area, volume and altitude of vertical dimension of landforms wherein different morphometric methods are used to analyze terrain characteristics (Withanage *et al.,* 2014). The results presented in Table 4.3 reveal that the highest and lowest elevations of Ofu River basin are 436 and 11 m above mean sea level (m asl.), respectively. The Basin relief (H), Relief ratio (R_h) and Relative relief (R_{hp}) are 425 m, 0.0042 and 0.0008, respectively while the Ruggedness number and Basin slope are respectively 0.109 and 0.19.

The Relief ratio according to Schumm (1956) is equal to the tangent of the angle formed by two planes intersecting at the mouth of the basin. It is also a measure of the overall steepness of a river basin which is an indicator of the intensity of erosion process operating on the slope of the basin. The R_h value of 0.0042 obtained for Ofu River Basin reveals that the basin is morphometrically less susceptible to severe erosion. From the reconnaissance survey conducted, it was observed that the catchment is not affected by serious erosion characteristic of a major part of Kogi East Senatorial district. The relief

ratio (R_{hp}) is an important morphometric variable used for the overall assessment of morphological characteristics of terrain.

4.2 STAGE-DISCHARGE RATING CURVE OF OFU RIVER

4.2.1 Results of the observation of Ofu River stage at Oforachi Hydrometric Station

The results of the daily stage of Ofu River observed for a period of twelve months at the Oforachi Bridge hydrometric station are presented in Appendix VI. The Daily stage hydrograph developed is shown in Fig. 4.7.

The results show that there are variations in the water levels of Ofu River from morning to evening during the rainy season. This is because the level rises immediately after rainfall and begins to drop gradually. For times of heavy down pour over the night, it is expected that the water level would rise significantly but may not be as high as it was in the morning in the evening as losses are encountered in the process.

The maximum water level observed was 56.39 m above mean sea level (asl) while the minimum value was 55.432 m asl.

4.2.2 Ofu River Discharge Measurement Values at Oforachi Hydrometric Station

The results of the Ofu River discharge measurement at Oforachi hydrometric station are presented in Appendix VII.

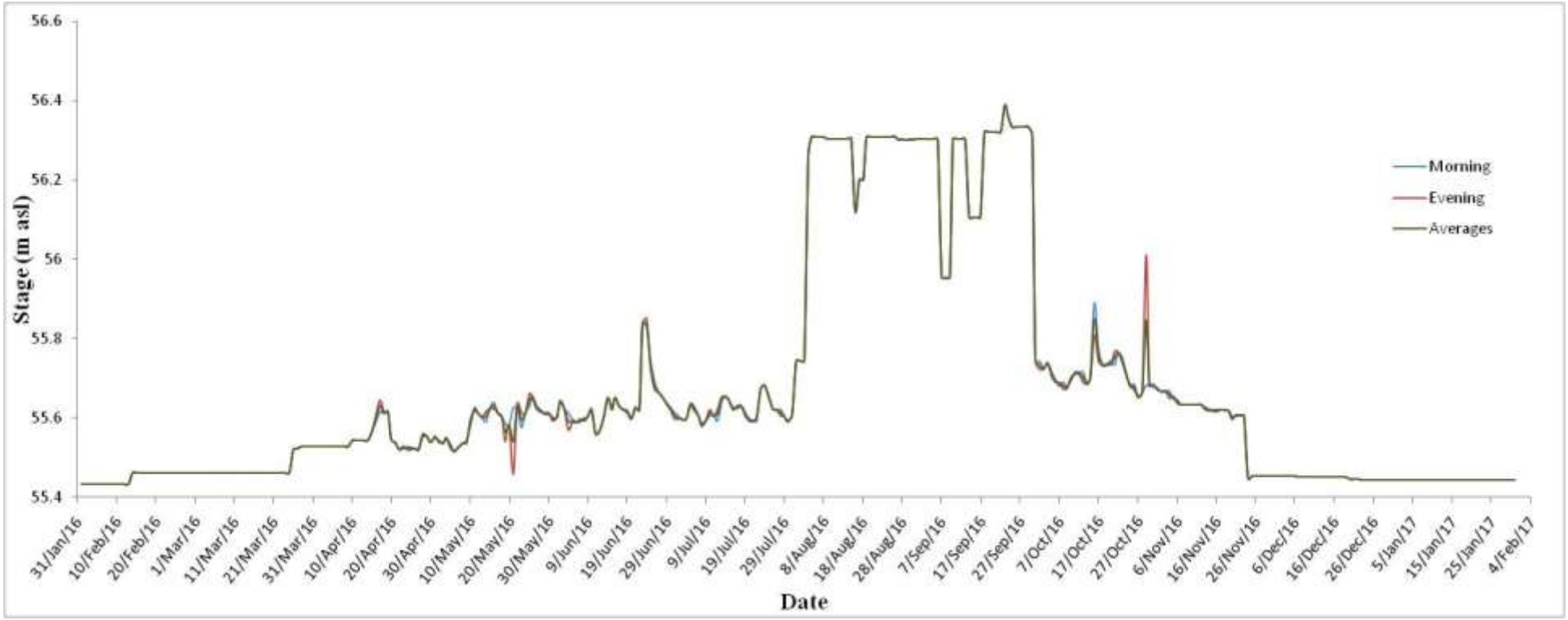


Fig. 4.7: Daily Stage Hydrograph of Ofu River at Oforachi Hydrometric Station

4.2.3 Results of the Development, Fitting and Extension of Ofu River Rating Curve at Oforachi Hydrometric Station

4.2.3.1 Development of stage-discharge rating curve of Ofu River

The result of the stage and discharge measurement from the field observation was used to develop a relationship between the stage and discharge.

The curve follows a power series as a result of the existence of a single permanent control (the Oforachi Bridge).

4.2.3.2 Results of the fitting and extension of stage-discharge rating curve for Ofu River

The results of the linear regression analysis carried out to estimate the calibration coefficients of the rating curve are presented in Table 4.4 with a final trial value of h = 55.43192 m.

Table 4.4: Estimation of Rating Curve Calibration Coefficients (*h, m and K*)

S/No.	H (m asl)	Q_o (m^3/s)	H-h	X (log(H-h))	Y (log Q_o)	X^2	Y^2	XY	$Q_c = K(H-h)^m$	$(Q_o-Q_c)^2$
1	55.432	0.158293	8E-05	-4.09691	-0.80054	16.78467	0.640862	3.279736	0.023042	0.018293
2	55.462	0.268754	0.03008	-1.52172	-0.57065	2.315638	0.325637	0.868364	1.382656	1.240779
3	55.521	4.24297	0.08908	-1.05022	0.62767	1.102962	0.39397	-0.65919	2.926113	1.734112
4	55.523	4.218715	0.09108	-1.04058	0.62518	1.0828	0.39085	-0.65055	2.971321	1.555992
5	55.528	4.38527	0.09608	-1.01737	0.641996	1.035036	0.412159	-0.65315	3.083019	1.695857
6	55.520	4.80537	0.08808	-1.05512	0.681727	1.113284	0.464751	-0.71931	2.903391	3.617522
7	55.556	5.385345	0.12358	-0.90805	0.731214	0.824558	0.534673	-0.66398	3.668254	2.9484
8	55.552	6.651085	0.119747	-0.92174	0.822892	0.849598	0.677152	-0.75849	3.589302	9.374515
9	55.542	6.631095	0.110247	-0.95763	0.821585	0.917064	0.675002	-0.78678	3.390175	10.50356
10	55.663	7.90556	0.23108	-0.63624	0.897933	0.404798	0.806283	-0.5713	5.651318	5.081607
11	55.651	8.64072	0.218747	-0.66006	0.93655	0.435677	0.877126	-0.61818	5.441281	10.23641
12	55.601	6.69484	0.169247	-0.77148	0.82574	0.595181	0.681847	-0.63704	4.557888	4.566562
13	55.597	7.421615	0.164913	-0.78274	0.870498	0.612689	0.757768	-0.68138	4.476984	8.670852
14	56.310	13.43526	0.878267	-0.05637	1.128246	0.003178	1.272939	-0.0636	14.20861	0.598078
15	56.302	13.308	0.869949	-0.06051	1.124113	0.003661	1.26363	-0.06802	14.11555	0.652142
16	56.387	14.61335	0.955272	-0.01987	1.16475	0.000395	1.356642	-0.02315	15.05759	0.197357
17	56.363	14.23846	0.930768	-0.03116	1.153463	0.000971	1.330477	-0.03594	14.78981	0.303993
18	55.653	7.674735	0.220663	-0.65627	0.885063	0.43069	0.783337	-0.58084	5.474158	4.842539
19	55.446	0.209928	0.013802	-1.86006	-0.67793	3.459841	0.45959	1.260995	0.807394	0.356966
20	55.453	0.315042	0.020673	-1.68461	-0.50163	2.837899	0.251634	0.845052	1.067188	0.565724
21	55.444	0.178058	0.011719	-1.93112	-0.74944	3.729238	0.56166	1.447261	0.721138	0.294937
22	55.443	0.168299	0.011081	-1.95543	-0.77392	3.823708	0.59895	1.513344	0.6938	0.276152
	Σ			-23.6753	9.864515	42.36354	15.51694	1.04387		69.33235

The coefficient *m*

$$= \frac{N(\sum xy) - (\sum x)(\sum y)}{N(\sum x^2) - (\sum x)^2}$$

$$= \frac{22 \times (1.04387) - (-23.6753) \times 9.864515}{22 \times 42.36354 - (-23.6753)^2} = 0.69051$$

The coefficient *K*

$$= antilogc = antilog\left(\frac{(\sum y - m\sum x}{N}\right)$$

$$= antilog\left(\frac{9.864515 - 0.69051 \times (-23.6753)}{22}\right) = 15.54096$$

The standard error of estimate, S_e

$$= [\frac{1}{N}\sum (Q_o - Q_c)^2]^{1/2}$$

$$= [\frac{1}{22} \times (69.33235)]^{1/2} = 1.775238$$

The correlation coefficient, *r*

$$= \frac{[\sum xy - (\sum x \sum y)/N]}{[\sum x^2 - (\sum x)^2/N]^{1/2}[\sum y^2 - (\sum y)^2/N]^{1/2}}$$

$$= \frac{[(1.04387) - (-23.6753 \times 9.864515)/22}{[42.36354 - (-23.6753)^2/22]^{1/2}[15.51694 - 9.864515^2/22^{1/2}} = 0.851894$$

The Variance of observed discharge = 22.80335

Thus, the Efficiency, *Ƞ*

$$= \frac{Variance\ of\ observed\ discharge - {S_e}^2}{Variance\ of\ observed\ discharge} \times 100$$

$$= \frac{22.80335 - 1.775238^2}{22.80335} \times 100 = 86.17979 \cong 86.18\%$$

According to Patra (2008), the value of 86.18% obtained shows a good efficiency of the fitted curve. Moreover, the curve shows a very good correlation between the stage and discharge with a coefficient of determination (R^2) of 0.900167 (adjusted R^2 = 0.895175). Thus the Final fitted rating curve for Ofu River at Oforachi bridge hydrometric station is

$$Q = 15.54096(H - 55.43192)^{0.69051} \qquad (\mathbf{4.1})$$

The plot of Effective depth of flow against the calculated discharge using the fitted rating curve is shown in Fig. 4.8

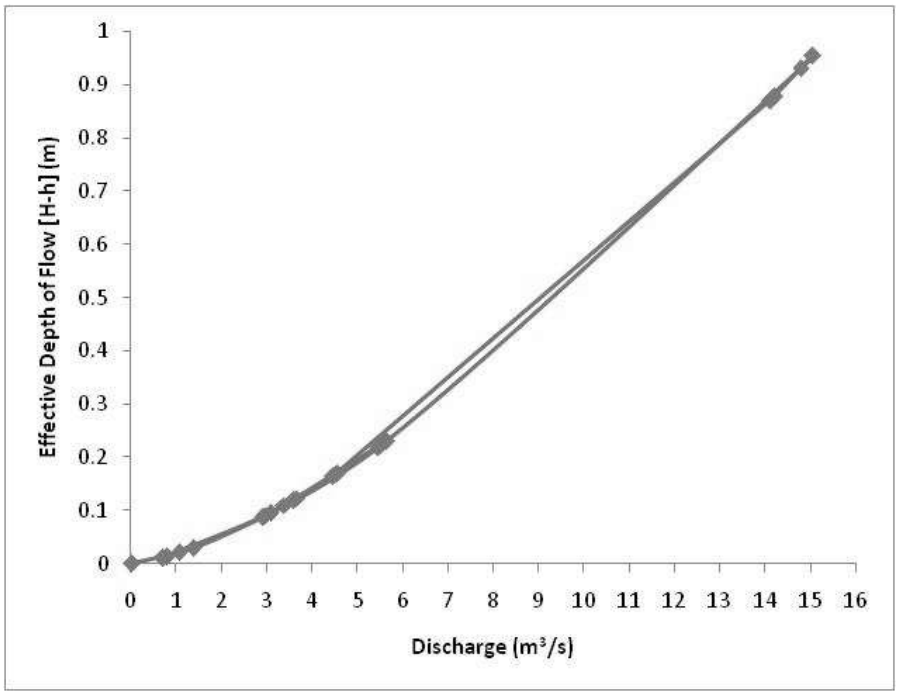


Fig. 4.8: Fitted Rating Curve for Ofu River at Oforachi Hydrometric station

4.2.3.3 Results of the estimation of twelve months daily discharge for Ofu River

The discharge hydrograph obtained is shown in Fig. 4.9.

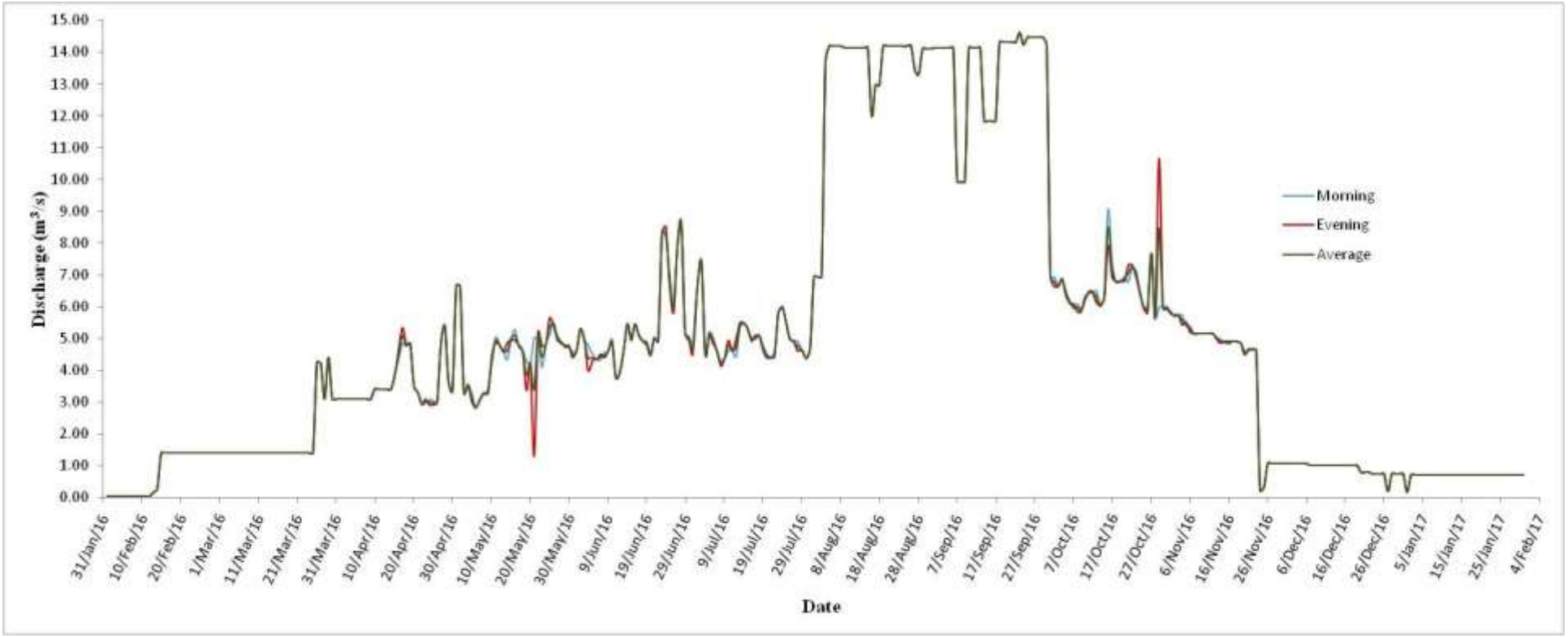


Fig. 4.9: Discharge Hydrograph for Ofu River using fitted Rating Curve

Furthermore, Table 4.5 shows a comparison of total monthly discharge values for 2016/2017 obtained from field measurement and the developed rating curve with the average monthly discharge for 1955 – 1973.

Table 4.5: Comparison of Monthly Discharge with Historical Discharge

	Monthly Discharge (m^3/s)											
	Feb	**Mar**	**Apr**	**May**	**Jun**	**Jul**	**Aug**	**Sep**	**Oct**	**Nov**	**Dec**	**Jan**
2016/2017	21.44	56.66	106.59	138.73	159.88	155.61	410.76	405.60	205.06	123.20	27.93	20.98
Average 1955-1973	2.85	2.14	13.31	15.95	44.02	132.45	403.79	432.02	83.01	5.80	3.93	3.86

The results show that the maximum monthly discharge for Ofu River between February 2016 and January, 2017 is 410.76 m^3/s (August, 2016) contrary to the historical data where a maximum discharge of 432.02 m^3/s was obtained in the month of September. That notwithstanding, the discharge values for August and September for both 2016/2017 and 1955 to 1973 fall within the same range. The closeness of the measured discharge to the historical discharge points to the fact that the flood situation in Ofu River catchment may not be caused by the river discharge alone but by possible inter play of other factors as will be discussed subsequently.

4.3 FLOOD CAUSATIVE FACTORS

4.3.1 Knowledge of Flood Causes within the Catchment Communities

4.3.1.1 Socio-demographic characteristics of respondents

The socio-demographic characteristics of the respondents are presented in Table 4.6.

Majority of respondents in this study 175 (53.85%) were from Oforachi Ward I while the remaining 150 (46.15%) were from Oforachi Ward II. A majority 234 (72%) were males while 91 (28%) were females. This could probably be a factor that could greatly influence the vulnerability of these households to flood disasters (Cutter *et al.*, 1997). The age

distribution shows that 6 respondents (1.85%) were between 26-30 years, 19 (5.85%) between 31-35 years, 54 (16.62%) between 36-40 years while a majority 246 (75.69%) were above 40 years. Furthermore, 279 (85.85%) respondents were married while 7 (2.15%) and 39 (12%) respondents were divorced and widowed respectively.

Table 4.6: Socio-demographic characteristics of respondents

Characteristics	Frequency	Percentage
Ward		
Oforachi I	175	53.85
Oforachi II	150	46.15
Total	325	100.00
Gender		
Male	234	72.00
Female	91	28.00
Total	325	100.00
Age (Years)		
26-30	6	1.85
31-35	19	5.85
36-40	54	16.62
Above 40	246	75.69
Total	325	100.00
Marital Status		
Married	279	85.85
Divorced	7	2.15
Widowed	39	12.00
Total	325	100.00
Highest Education		
Primary	90	27.69
Secondary	86	26.46
Tertiary	59	18.15
Adult Education	90	27.69
Total	325	100.00
Occupation		
Farming	206	63.38
Trading	40	12.31
Civil Servant	58	17.85
Craftsman	14	4.31
Others	7	2.15
Total	325	100.00
Length of Stay in Community (Years)		
11-20	34	10.46
21-30	60	18.46
31-40	125	38.46
Above 40	106	32.62
Total	325	100.00
Household Size	**Minimum**	**Maximum**	**Mean±SD**
	1	30	13±8

SD = Standard Deviation

An equal number of respondents of 90 (27.69%) had primary and adult education respectively, closely followed by secondary education held by 86 (26.46%) respondents

while only 59 (18.15%) respondents proceeded to a tertiary institution. With respect to the occupation of respondents, a majority 206 (63.38%) were farmers, 58 (17.85%) were civil servants, 40 (12.31%) were traders, 14 (4.31%) were craftsmen while a minority 7 (2.15%) were involved in other occupations not listed in the options. More so, a majority 125 (38.46%) respondents had spent between 31-40 years in the community, 106 (32.62%) for more than 40 years, 60 (18.46%) between 21-30 years while 34 (10.46%) had spent 11-20 years. Finally, the minimum household size was one while the maximum and mean sizes were 30 and 13±8.

4.3.1.2 History of flood occurrence

The historical charateristics of flood occurrence for the community surveyed are presented in Table 4.7.

The results show that 197 (60.62%) respondents have ever experienced flood in their households while 128 (39.38%) have never experienced flood in their households.

Out of the 197 (60.62%) respondents that have experienced flood, 104 (52.79%) had their first experience in 1991, 69 (35.03%) in 1995, 5 (2.54%) in 1997, 4 (2.03%) in 1999 while 15 (7.06%) had theirs in 2000. This is implies that the households have been flooded for a minimum of 16 years to a maximum of 22 years with an average of 20.08±2.58 years.

The results on Table 4.7 also show that the maximum depth of flood water at the households ranged from 0.2 m to 3.0 m with an average of 1.158±0.72 m. Furthermore, the Table 4.7 also show that the flood water lasted for a minimum of 1 day to a maximum of 7days with an average of 4.00±1.67 days. This average confirms the time to recession from peak of 3.68 days calculated for Ofu River catchment during the morphometric analysis.

Table 4.7: Flood Experience and Characteristics

Characteristics	Frequency	Percentage
Have you ever experienced flood		
Yes	197	60.62
No	128	39.38
Total	325	100.00
Year of first experience		
1991	104	52.79
1995	69	35.03
1997	5	2.54
1999	4	2.03
2000	15	7.61
Total	197	100.00
How many times have you been flooded? (Years)		
16	55	27.92
21	49	24.87
22	93	47.21
Total	197	100.00
Mean±Standard deviation	20.076±2.58	
Maximum Depth of flood water (m)		
0.2	13	6.60
0.5	47	23.86
1.0	70	35.53
1.5	34	17.26
2.0	18	9.14
3.0	15	7.61
Total	197	100.00
Mean±Standard deviation	1.158±0.72	
Duration of flood (days)		
1	6	3.05
2	35	17.77
3	60	30.46
4	7	3.55
5	44	22.34
6	31	15.74
7	14	7.11
Total	197	100.00
Mean±Standard deviation	4.00±1.67	

The results of the respondents' knowledge of flood causes are presented in Table 4.8. The results further shows the association between the knowledge level and flood experience, ward, education, gender, age, marital status and occupation of respondents respectively.

The results show that 26 (8.00%) had fair knowledge, 263 (80.92%) had good knowledge while, 36 (11.08%) had excellent knowledge of the causes of flood. The results showed that there was no association between the knowledge level and gender (Pearson's $chi^2 = 3.15$; $P = 0.207$). Meanwhile the factors that influenced the knowledge level of the respondents in decreasing order of associations are Age (Pearson's $chi^2 = 44.46$; $P = 0.000$), Education (Pearson's $chi^2 = 44.39$; $P = 0.000$), Occupation (Pearson's $chi^2 = 18.52$; $P = 0.018$), Flood experience (Pearson's $chi^2 =$

17.87; P = 0.000), Marital Status (Pearson's chi^2 = 9.81; P = 0.044) and Ward (Pearson's chi^2 = 9.68; P = 0.008). The closeness of the P-value of the marital status to 0.05 showed that the association between the knowledge level and marital status is actually very weak. The difference in knowledge level between the two wards may not be unconnected to the fact that majority of those affected by flood (69.04%) were from Oforach ward II, while only 30.96 % were from Oforachi ward I. The knowledge of these associating factors will be very instrumental for the development of effective early warning signals and non-structural flood control measures.

Table 4.8: Knowledge of flood causes in the community

Parameter	Knowledge Level			Total	Pearson's chi^2	P-Value
	Fair	Good	Excellent			
Experienced Flood?						
No	20	92	16	128		
Yes	6	171	20	197	17.87	0.000
Total	26	263	36	325		
Ward						
Oforachi I	20	131	24	175		
Oforachi II	6	132	12	150	9.676	0.008
Total	26	263	36	325		
Education						
Primary	0	68	22	90		
Secondary	14	64	8	86		
Tertiary	6	47	6	59	42.3862	0.000
Adult Education	6	84	0	90		
Total	26	263	36	325		
Gender						
Male	20	184	30	234		
Female	6	79	6	81	3.1481	0.207
Total	26	263	36	325		
Age						
26-30	0	6	0	6		
31-35	0	19	0	19		
36-40	13	27	14	54	44.457	0.000
Above 40	13	211	22	246		
Total	26	263	36	325		
Marital Status						
Married	20	223	36	279		
Divorced	0	7	0	7	9.8097	0.044
Widowed	6	33	0	39		
Total	26	263	36	325		
Occupation						
Farming	20	156	30	206		
Trading	0	40	0	40		
Civil Servant	6	46	6	58	18.5246	0.000
Craftsman	0	14	0	14		
Others	0	7	0	7		
Total	26	263	36	325		

4.3.2 Rainfall Characteristics of Oforachi Catchment (Meteorological Factors)

The results of the assessment of the Ofu River Catchment's rainfall characteristics are presented in this section. The average annual rainfall map of the catchment is shown in Fig. 4.10.

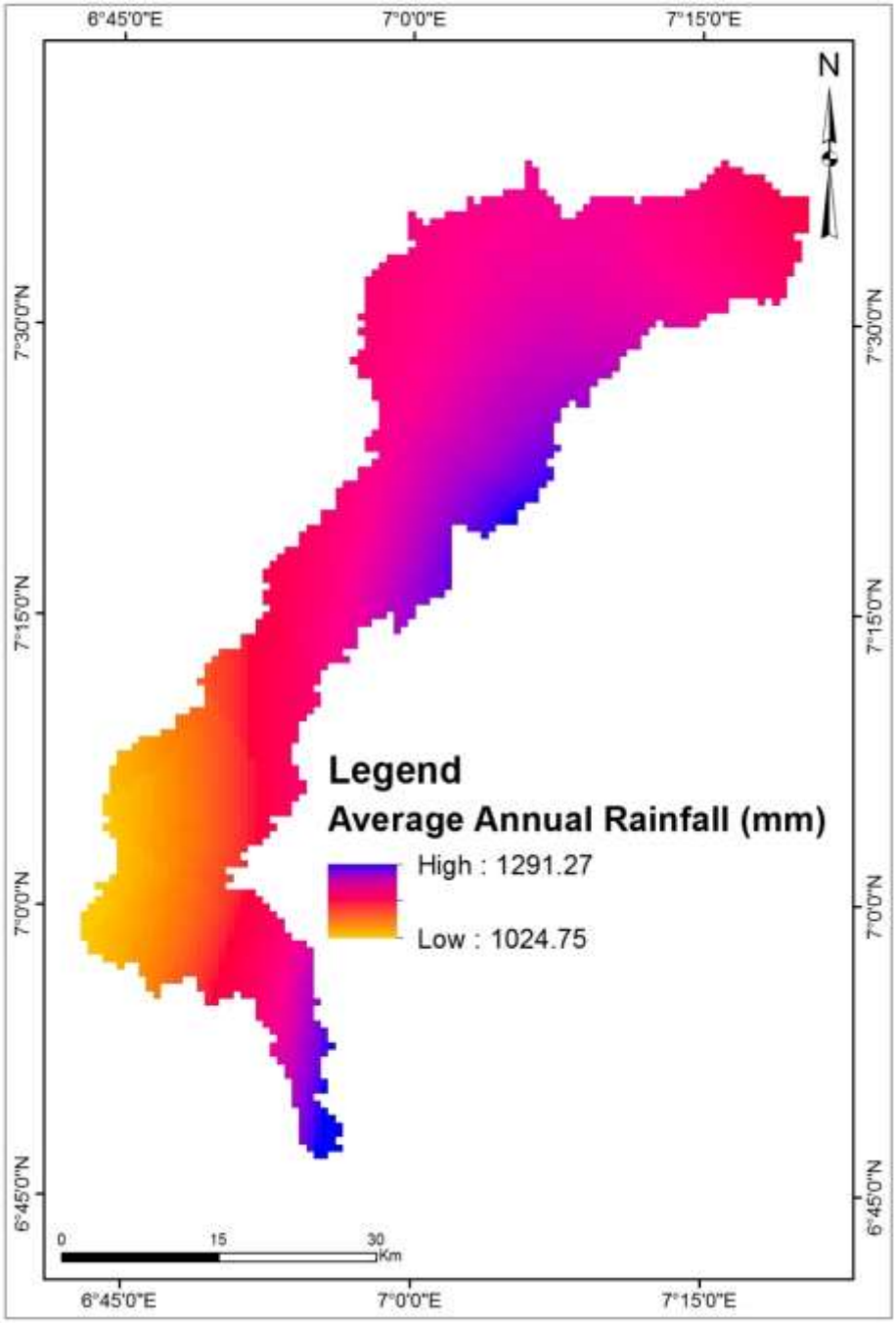


Fig. 4.10: Average Annual Rainfall Depths of Ofu River Catchment

Fig. 4.10 show that the average annual rainfall within the Ofu River catchment ranged from a minimum of 1024.75 mm to a maximum of 1291.27 mm. Meanwhile, the total rainfall for each year, 5-year moving average and the rainfall trend from 1979 to 2013 are presented in Fig. 4.11.

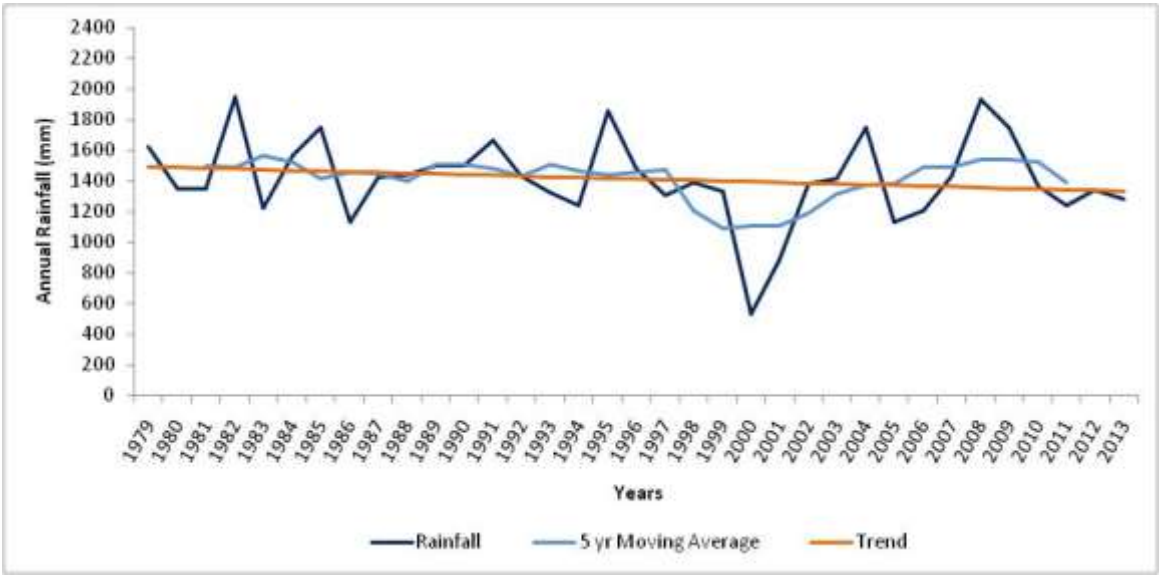


Fig. 4.11: Annual Rainfall, 5-yr Moving Average and Trend Analysis Plot

The results in Fig. 4.11 reveal that the annual rainfall for Ofu River catchment showed a downward trend with 1982 and 2000 recording the highest and lowest annual rainfall of 2298.32 mm and 628.72 mm, respectively. More so, the annual maximum daily rainfall depth for the study area is presented in Fig. 4.12. Figure 4.12 shows that 1985 recorded the highest annual maximum daily rainfall depth of 116.65 mm which closely followed by 2008 with an annual maximum daily rainfall depth of 114.06 mm. the lowest annual maximum daily rainfall depth was recorded in 2000 (20.93 mm) which was closely followed by 2001 with an annual maximum daily rainfall depth of 34.89 mm. The case of year 2000 is very ironical as that year recorded one of the most sever flood events within the catchment in recent history thus implying that rainfall may not be the major factor responsible for flood within Ofu River Catchment.

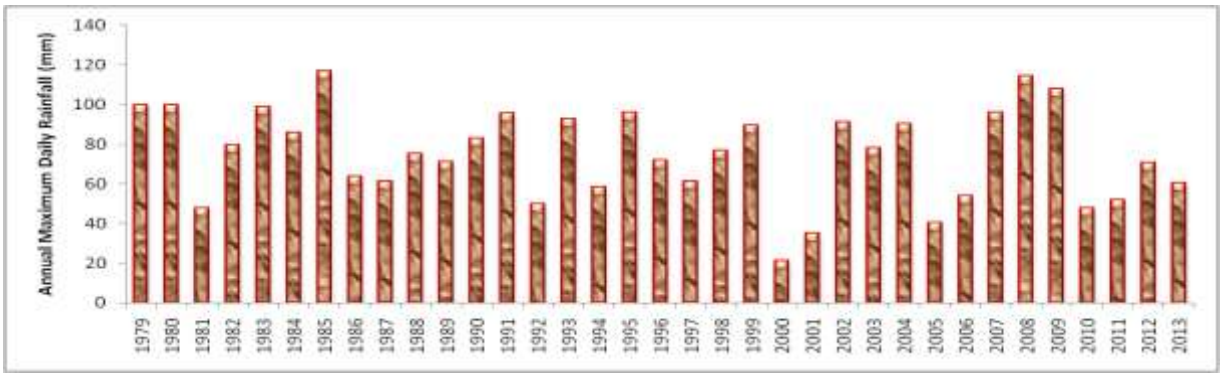


Fig. 4.12: AAnnual Maximum Daily Rainfall Depths of Ofu River Catchment

Furthermore, the average monthly rainfall values (35 year average) for Ofu River Catchment are shown in Fig. 4.13.

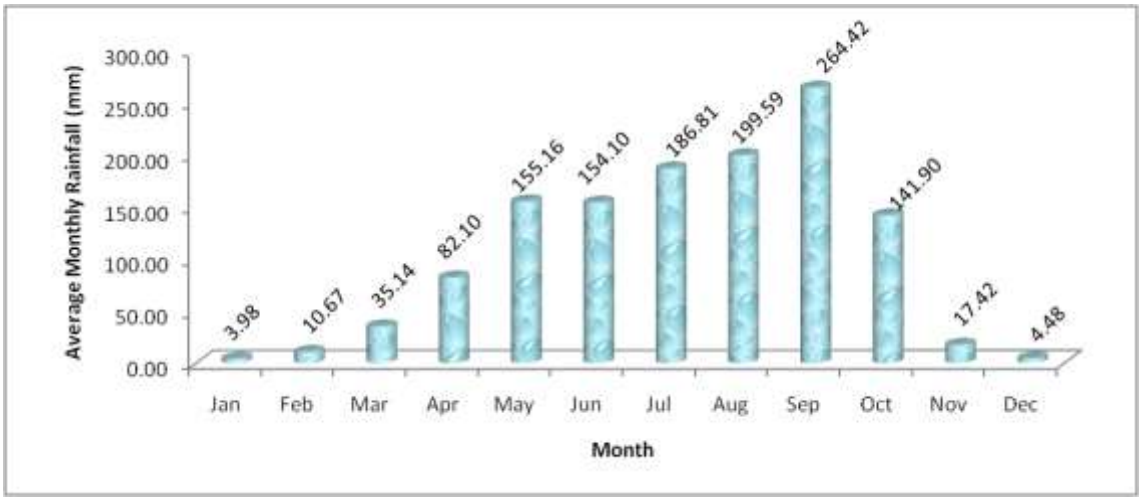


Fig. 4.13: Average Monthly Rainfall Depths of Ofu River Catchment

The results show that September has the highest average monthly rainfall of 312.16 mm which is closely followed by August with an average monthly rainfall of 235.63 mm. Information obtained from the field survey show that the floods experienced by communities within the floodplain often occur between the month of August and September annually. January has the least rainfall of 4.70 mm followed by December with 5.29 mm. The average monthly rainfall for February, March, April, May, June, July, October and November are 12.59 mm, 41.49 mm, 96.93 mm, 183.17 mm, 181.92 mm, 220.54 mm, 167.52 mm and 20.56 mm, respectively. Finally, the average annual Rainfall

for Ofu River Catchment was compared with average annual rainfall of other neighbours with the Rainfall Zone IVa as shown in Fig. 4.14.

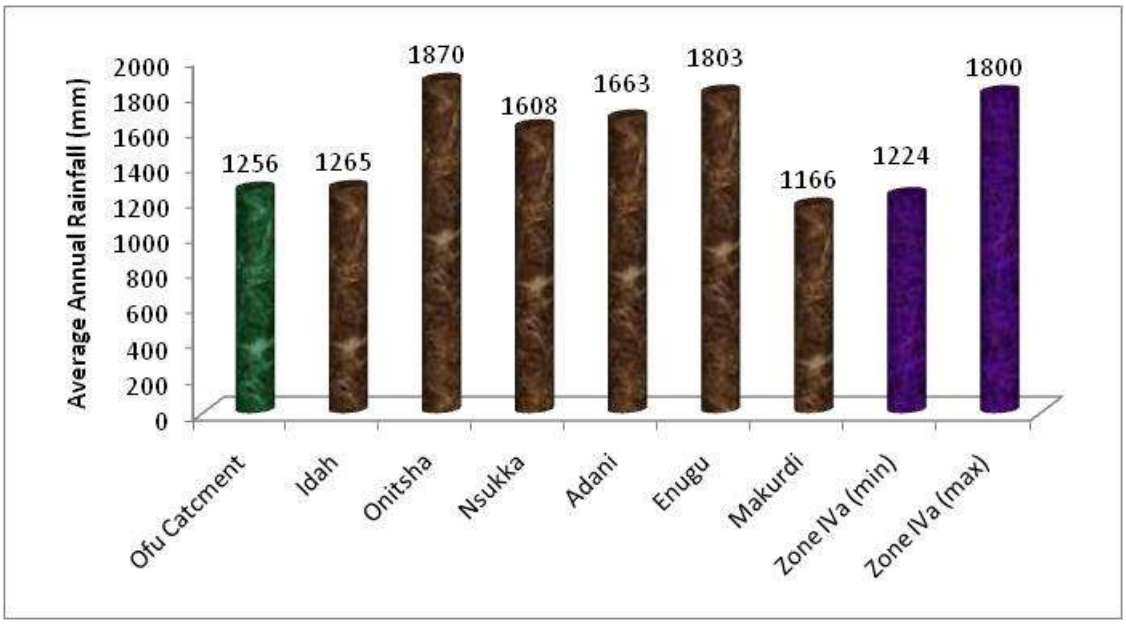


Fig. 4.14: Average Annual Rainfall Characteristics of Ofu River Catchment and Neighbours.
Source: Skoup and Motor Columbus (1980); FMW (2013); NiMeT (2016)

Fig. 4.14 reveals that the average rainfall of Ofu River Catchment is in agreement with the Rainfall pattern of the Nigeria Rainfall Zone IVa where the catchment falls.

4.3.3 Geomorphologic Flood Causative Factors

4.3.3.1 Terrain elevation of the flooded communities

The elevations of households obtained in the course of the field are shown in Fig. 4.15. These elevation data were used for the assessment of the terrain elevations.

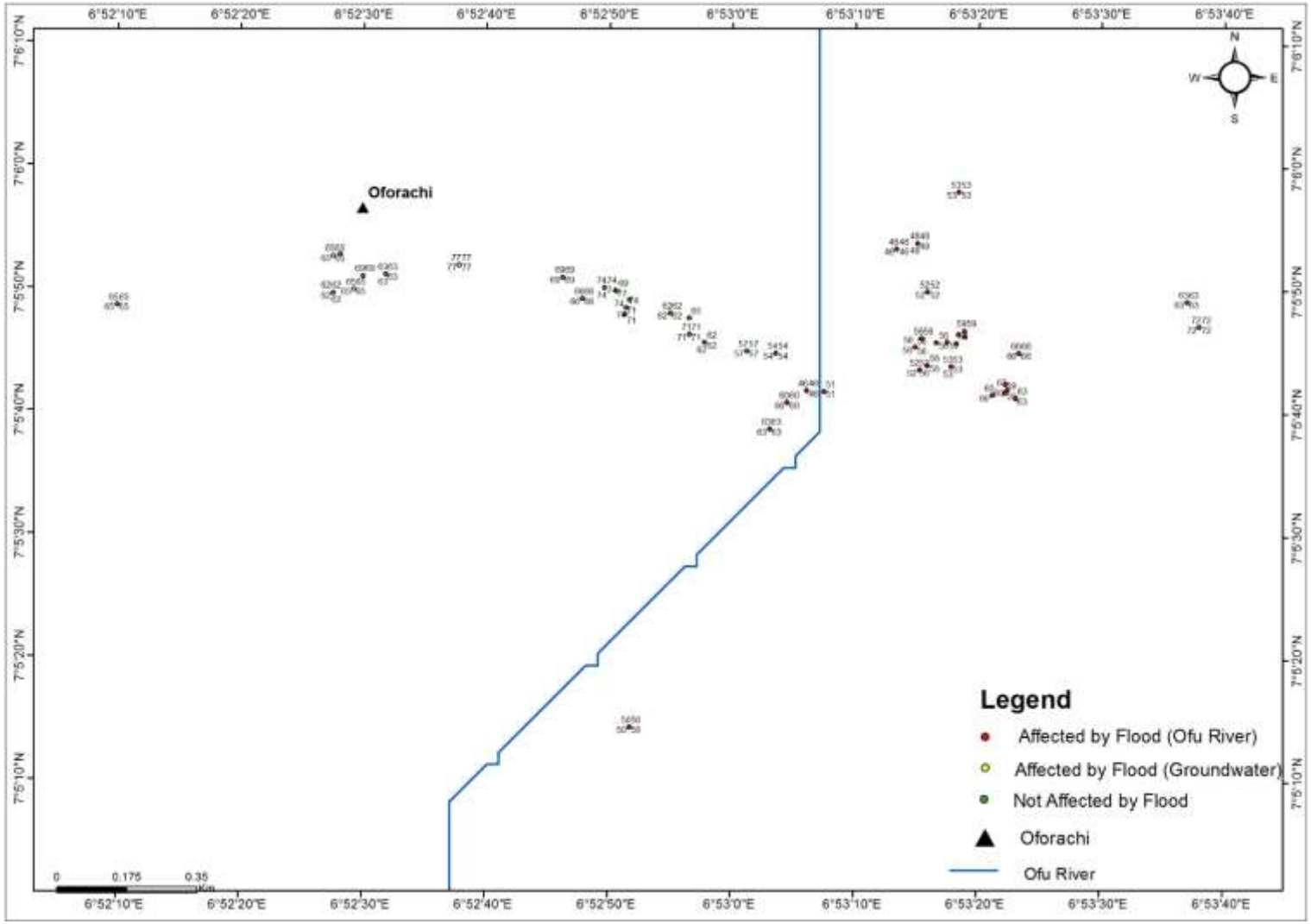


Fig. 4.15: Elevations of Households obtained during the field work at Oforachi

The elevations ranged from 46 m to 67 m above mean sea level for households affected by Ofu River flood, 65 m to 77 m above mean sea level for households affected by groundwater flood and 57 m to 77 m for the households that never experiemced flood. It can be observed that the elevations of some non-flooded households are actually lower than the maximum for the flooded households yet they were not flooded. This could probably be attributed to other factors such as but not limited to their distance from the river.

4.3.3.2 Terrain slope of the flooded communities

The slopes of the surveyed households are shown in Fig. 4.16. The slope ranged from 0.02 % to 8.52% for households affected by Ofu River surface flood, 1.27 % to 1.78 % for households affected by groundwater flood and 0.89 % to 3.89 % for the households that never experiemced flood. The variation of slope with flood occurrence indicates that the contribution of the terrain slope to the occurrence of flood is largely dependent on the elevation and probably the proximity to the river.

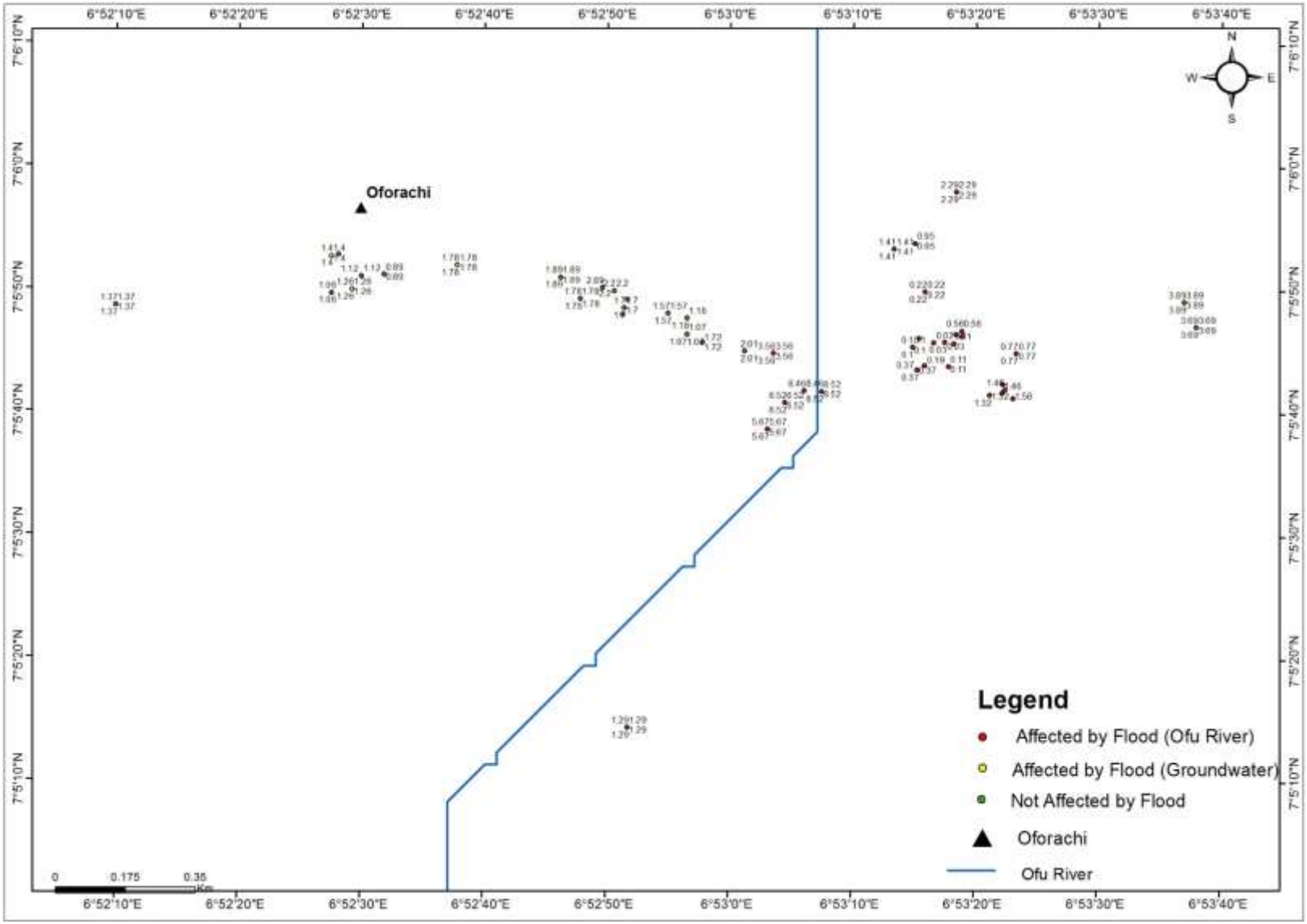


Fig. 4.16: Slope of Households obtained during the field work at Oforachi

4.3.3.3 Ofu River Channel discharge capacity at Oforachi

The results of the percentage loss in volume of Ofu River channel for all sections are presented in Fig. 4.17.

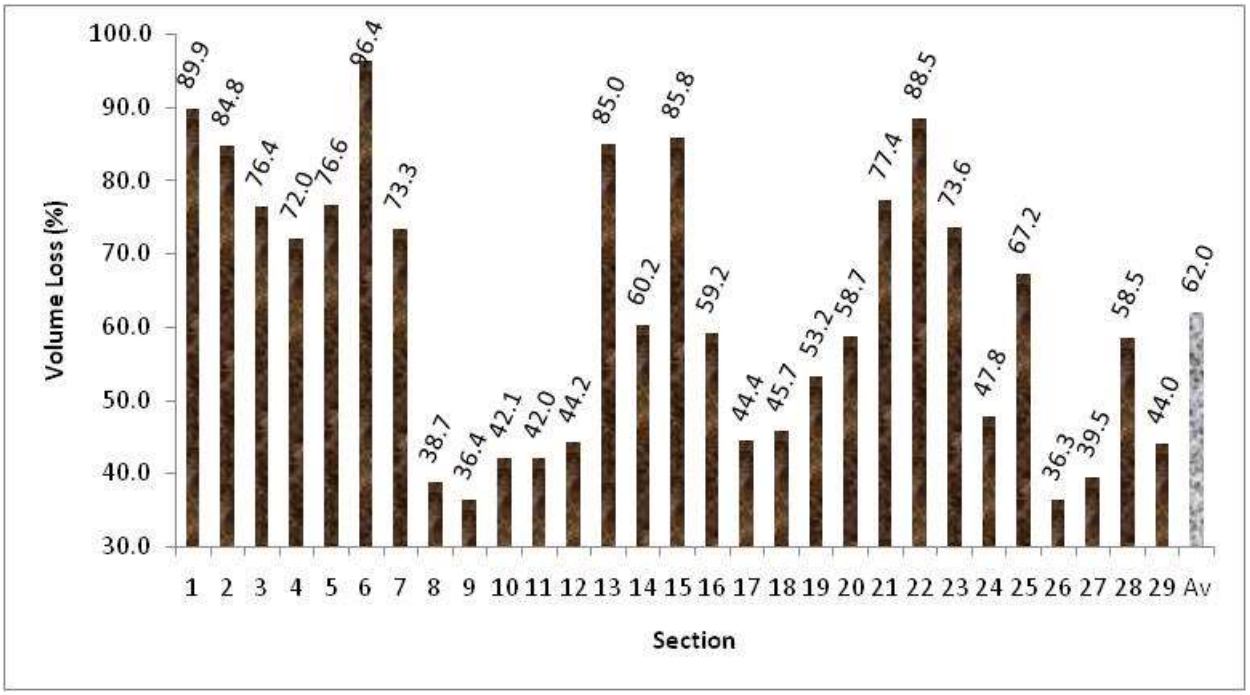


Fig. 4.17: Percentage Loss in Ofu River channel Volume between 2000 and 2011

The percentage loss in volume ranged from a minimum of 36.3 % at section 26 to a maximum of 96.4 % at section 6 with an average of 62±18.9 %. More so, the percentage loss in surface area of Ofu River for the respective sections is presented in Fig. 4.18.

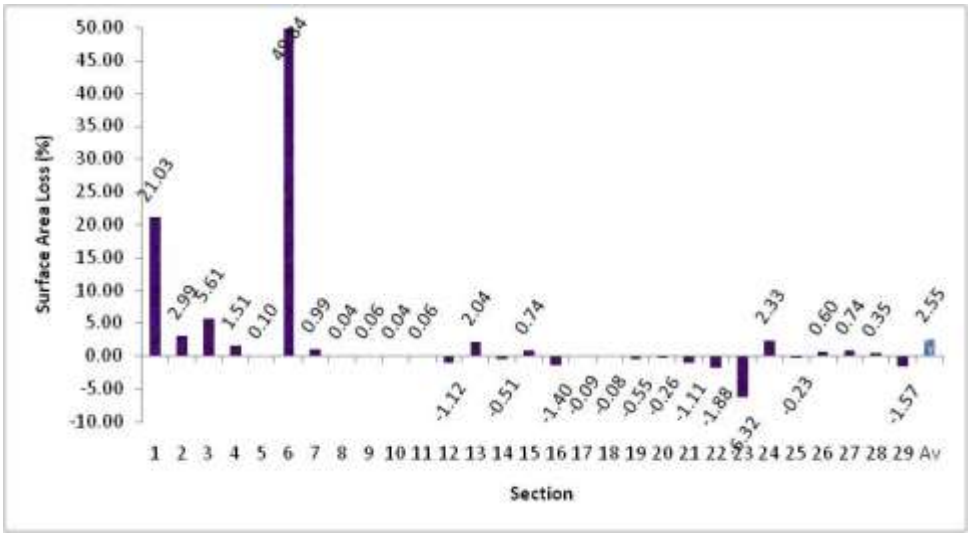


Fig. 4.18: Percentage Loss in River Surface Area between 2000 and 2011

Unlike the volume, the surface area between 2000 and 2011 decreased marginally for 15 sections and significantly for two sections (1 and 6) while marginal increase were observed for 12 sections. The average loss in surface area was 2.55% with a standard deviation of 10.1%. Two outliers were observed at sections 1 and 6 which implies that the percentage loss in surface area for the 29 sections probably did not follow a normal distribution thus could not be adequately described by the means and standard deviation. The skewness of 3.94 calculated also buttresses this assertion. Thus the loss in surface area was better described using the median and interquartile range (0.06% and 1.498% respectively).

The summary of the channel bed elevations for 2000 and 2011, losses and the loss per annum are presented in Table 4.9. The results in Table 4.9 also show the *P*-value and 95% confidence interval obtained from the paired t-test carried out to compare the channel bed elevations for 2000 and 2011.

Table 4.9: Summary Results of Channel Bed Elevations (2000 and 2011), Bed Elevation Loss, Loss Rate and T-test

	Mean ± SD	**Minimum**	**Maximum**	**Median**	**IQR**	***P-Value*& 95% CI**
2000 Bed Elevation (m asl.)	30.248±4.031	21.270	37.240	31.110	7.095	0.000; 2.804, 6.686
2011 Bed Elevation (m asl.)	34.992±3.302	29.427	40.469	34.604	5.679	
Loss (m)	4.745±3.988	-0.297	13.887	4.317	7.391	
Loss/Annum (m/year)	0.431±0.363	-0.027	1.262	0.393	0.672	

SD=Standard deviation; IQR=Inter quartile range; CI=Confidence Interval

The *P*-value and the 95% confidence interval obtained confirm that the difference between the channel bed elevations for 2000 and 2011 were statistically significant at 95 % confidence level. This confirms there is an actual loss in the flow depth of the river over this period. These losses are indicative of possible sedimentation occurring along the river course which could be attributable to the landuse pattern and other anthropogenic activities capable of increasing the erodibility of the soils.

Furthermore, the average bed elevations for 2000 and 2011, bed elevation loss as well as estimated bed elevation and loss for 2016 are presented in Fig. 4.19.

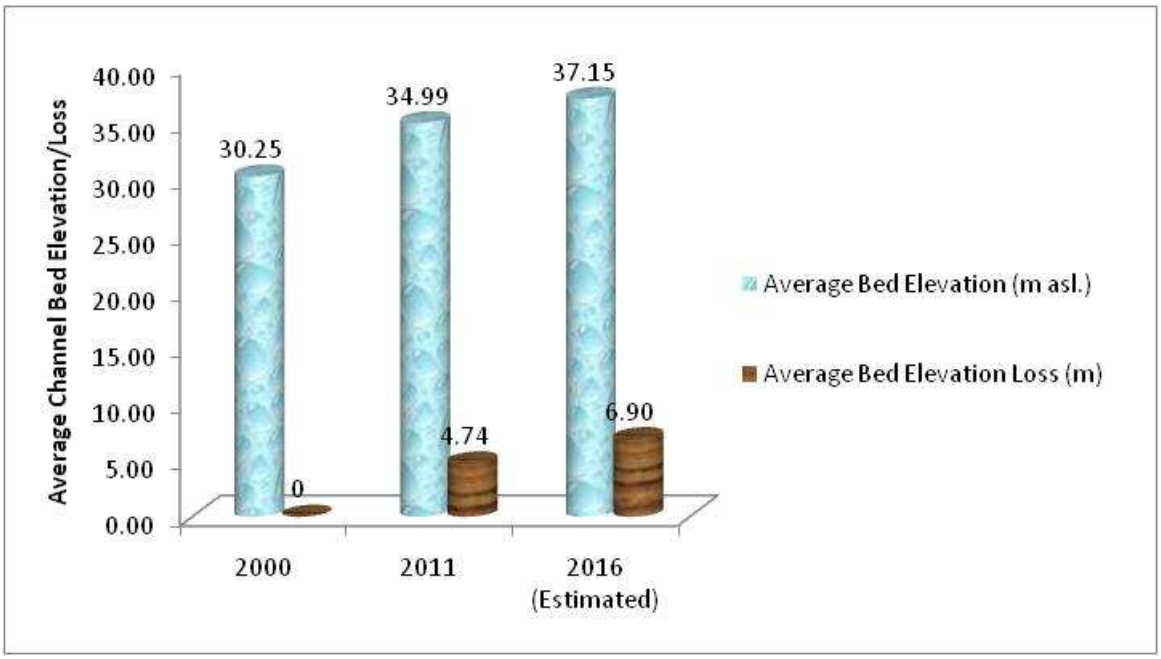


Fig. 4.19: Loss in Ofu River Channel depth between 2000, 2011 and 2016 (estimated).

The Ofu River average bed elevation in 2000 and 2011 were 30.25 m and 34.99 m above mean sea level, respectively. This implied that an average loss in flow depth of 4.74 m had occurred between 2000 and 2011. Based on this, it is projected that the bed elevation would have risen to 37.15 m above mean sea level implying a loss in flow depth of 6.90 m between 2000 and 2016. The Village head confirmed that this extent of loss could actually be true. As stated earlier, this loss in flow depth is indicative of possible sedimention in the river and could be a major factor contributing to the flood situation within the catchment.

The Ofu River channel bed profile for 2000, 2011 and 2016 are presented in Fig. 4.20.

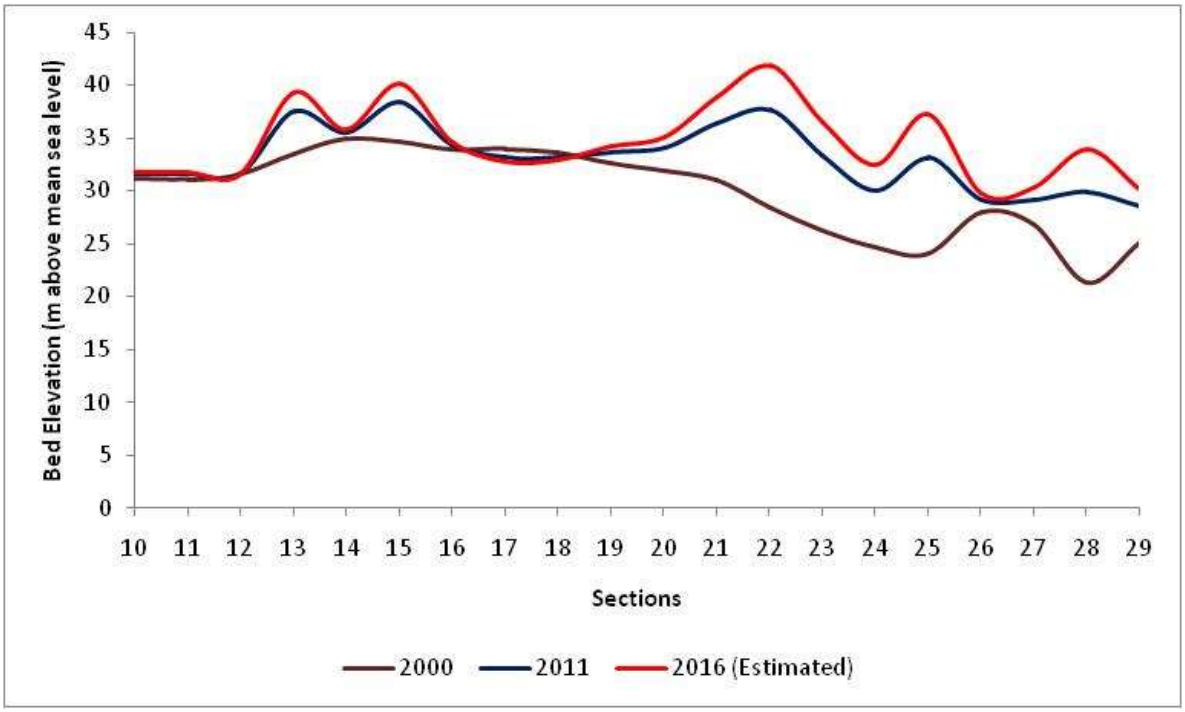


Fig. 4.20: Ofu River Channel Bed profile for 2000, 2011 and 2016

4.3.3.4 Sediment load of Ofu River at Oforachi Station

The respective relationships of the suspended sediment concentrations and unmeasured sediment loads with the river discharges presented in Figs. 4.21a and b follow a power curve in agreement with previous studies (Otun and Adeogun, 2010; Warrick, 2015).

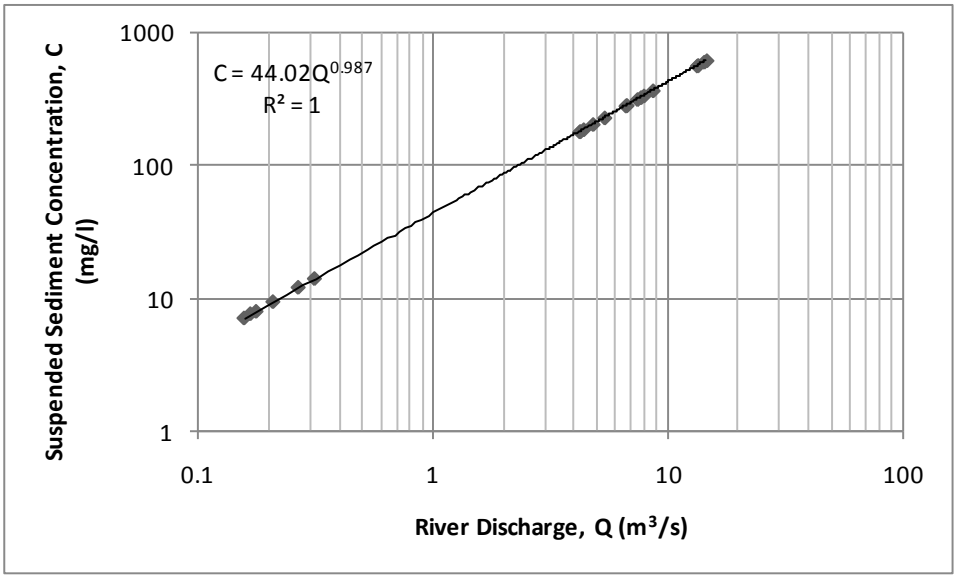


Fig. 4.21a: Plot of Suspended Sediment Concentration vs Ofu River Discharge at Oforachi Station

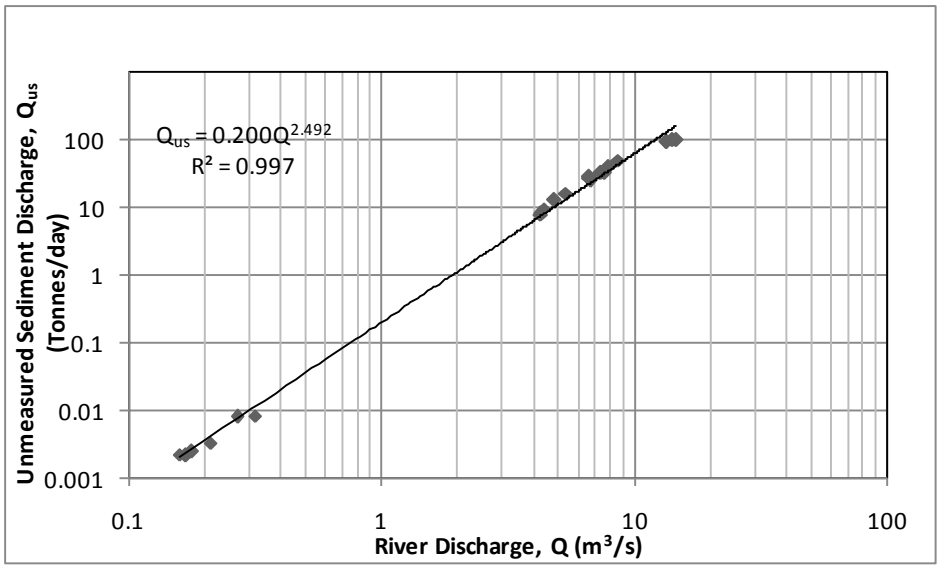


Fig. 4.21b: Plot of Unmeasured Sediment Discharge vs Ofu River Discharge at Oforachi Station

More so, the sediment loads of Ofu River at Oforachi hydrometric station are presented in Table 4.10. Measured sediment loads for Ofu River is 56,747,260 kg/year while the unmeasured sediment loads is 10,077,470 kg/year. While this trend is similar to the results of Otun and Adeogun (2010), the values obtained herein are far higher than the 14,944,000 kg/year and 1,125,000 kg/year obtained respectively for Samaru River. Table 4.10 further shows that January has the lowest total sediment load of 3,030 kg/month while the highest total sediment load of 24,596,840 kg/month was recorded in the month of August. As noted by USACE (1995), the unmeasured sediment loads comprise of the bed load and suspended materials within 0.15 m from the river bed. Thus this unmeasured sediment accounts for the loss in flow depth recorded in this study. However, the annual sediment load of Ofu River at Oforachi bridge hydrometric station was 66,824,730 kg which further confirms not just the loss in flow depth but the fact that it will continue to increase.

The high values of the suspended sediment concentration are indicative of the significant disturbances of nearby fields used for Agricultural activities.

Table 4.10: Monthly and Annual Sediment Loads of Ofu River at Oforachi Hydrometric Station

Month	Measured Sediment Load (x 10^3 kg/Month)	Unmeasured Sediment Load (x 10^3 kg/Month)	Total (x 10^3 kg/Month)
January	2.97	0.06	3.03
February	5.06	0.12	5.19
March	493.38	43.73	537.11
April	1,473.27	152.64	1,625.91
May	2,413.80	280.83	2,694.64
June	3,357.49	434.42	3,791.91
July	2,963.78	358.72	3,322.50
August	20,534.27	4,062.57	24,596.84
September	20,405.29	4,041.63	24,446.92
October	5,088.56	702.50	5,791.06
November	5.87	0.15	6.02
December	3.52	0.08	3.60
Total (x10^3 kg/Annum)	**56,747.26**	**10,077.47**	**66,824.73**

4.3.3.5 Soil and drainage characteristics of the flooded areas within the catchment

The results of the Atterberg-limits tests and sieve analyses as well as their corresponding soil classifications are presented in Tables 4.11 and 4.12, respectively.

Furthermore, a comparison of the infiltration capacities of the soils with their respective antecedent moisture contents (AMC) is presented in Fig. 4.22.

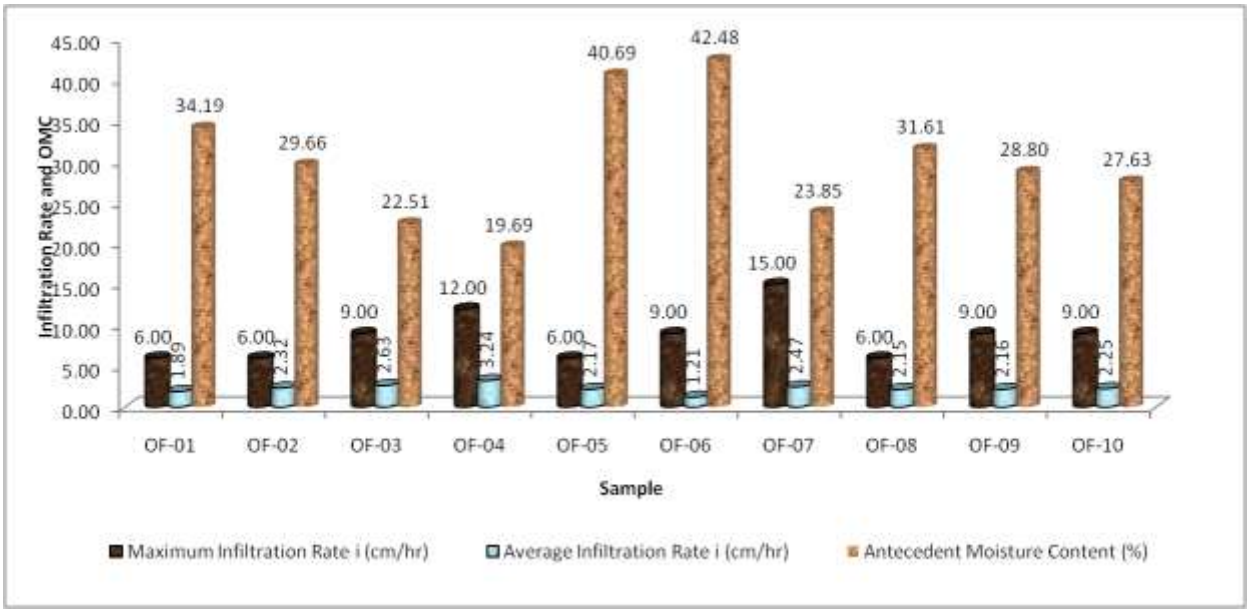


Fig. 4.22: Maximum Infiltration Rate, Average Infiltration Rate and Antecedent Moisture Content

Figure 4.22 shows that OF-03 has the lowest antecedent moisture content of 22.51 (%) while OF-06 has the highest AMC of 42.48 %. This probably explains the low infiltration rates obtained for all the samples. Furthermore, the saturated hydraulic conductivity as well as corresponding classifications is presented in Table 4.13.

Table 4.11: Soil Classification based on Results of Atterberg Limits Tests Conducted

Sample	Atterberg Limits			
	Liquid Limit	Plastic Limit	Plasticity Index	Class
OF-01	28.86	23.87	4.99	ML-Silt
OF-02	26.96	25.14	1.82	ML-Silt
OF-03	31.4	14.07	17.33	CL-Lean Clay
OF-04	Non Liquid	Non Plastic	Non Plastic	-
OF-05	18.54	15.63	2.91	ML-Silt
OF-06	49.84	33.86	15.98	ML-MH (Silt to Elastic silt)
OF-07	Non Liquid	Non Plastic	Non Plastic	-
OF-08	31.52	27.18	4.34	ML-Silt
OF-09	24.82	17.36	7.46	CL-ML-Silty clay
OF-10	27.45	20.16	7.29	CL-ML-Silty clay

Table 4.12: Soil Classification based on the Sieve Analysis Results

Sample	Sieve Analysis Results									Classification	
				Fine sand		Medium sand					
	Cu	Cc	% Fine (Passing #200)	% passing #40	% Fine sand	% passing #10	% Medium sand	% Coarse Sand	% Sand (Total)	USCS	AASHTO
OF-01	5.6	0.86	41.85	86.9	45.05	97.9	11	2.1	58.15	SM - Silty Sand	A-2-4 (Silty sand)
OF-02	31.11	1.07	50.55	84.1	33.55	97	12.9	3	49.45	ML - Sandy silt	A-2-4 (Silty sand)
OF-03	13.08	1.37	37.35	94	56.65	99.6	5.6	0.4	62.65	SC-Clayey Sand	A-2-6 (Clayey sand)
OF-04	11.08	1.66	25	78.5	53.5	98.5	20	1.5	75	SW - Well Graded Sand	A-3 (fine sand)
OF-05	4.59	0.78	32.45	85.2	52.75	99.1	13.9	0.9	67.55	SM-Silty sand	A-2-4 (Silty sand)
OF-06	135	2.67	42.2	71.4	29.2	83	11.6	17	57.8	SM - Silty Sand	A-2-7 (Clayey sand)
OF-07	8.06	1.38	22.4	65.1	42.7	79.5	14.4	20.5	77.6	SW - Well Graded Sand	A-3 (fine sand)
OF-08	25.33	0.63	32.5	71	38.5	96.1	25.1	3.9	67.5	SM-Silty sand	A-2-4 (Silty sand)
OF-09	44.55	7.42	21.55	55.1	33.55	97.2	42.1	2.8	78.45	SC-SM-Silty or clayey sand	A-2-4 (Silty sand)
OF-10	171.43	0.67	44.2	80	35.8	98.2	18.2	1.8	55.8	SC-SM-Silty or clayey sand	A-2-4 (Silty sand)

Table 4.13: Soil Classification based on Saturated Hydraulic Conductivity

Sample	K (m/s)	Description	Classification
OF-01	-2.01136×10^{-06}	Highly Impermeable	Low plasticity soil with Clay characteristics
OF-02	-2.35862×10^{-06}	Highly Impermeable	Low plasticity soil with Clay characteristics
OF-03	-3.30082×10^{-06}	Highly Impermeable	Low plasticity soil with Clay characteristics
OF-04	-3.53072×10^{-06}	Highly Impermeable	Non plastic soil with Clay characteristics
OF-05	6.68813×10^{-07}	Lowly (poorly) Permeable	Low plasticity soil with characteristics of sandy loams, loamy sands or clayey sands
OF-06	-1.47864×10^{-06}	Highly Impermeable	Low plasticity soil with Clay characteristics
OF-07	-2.69122×10^{-06}	Highly Impermeable	Non plastic soil with Clay characteristics
OF-08	-2.16694×10^{-06}	Highly Impermeable	Low plasticity soil with Clay characteristics
OF-09	-1.84564×10^{-06}	Highly Impermeable	Low plasticity soil with Clay characteristics
OF-10	-2.5993×10^{-06}	Highly Impermeable	Low plasticity soil with Clay characteristics

Based on the three classifications shown in Tables 4.11 to 4.13, it can be seen that the soils tested combines silt and clay characteristics. This probably confirms the digital soil map of the world's (DSMW) classification of the soil within the sample locations as sandy loam. The plotted sample locations were overlaid on the DSMW as shown in Fig. 4.23. This shows that the classification based on the DSMW actually reflect the soil characteristics of Ofu River Catchment.

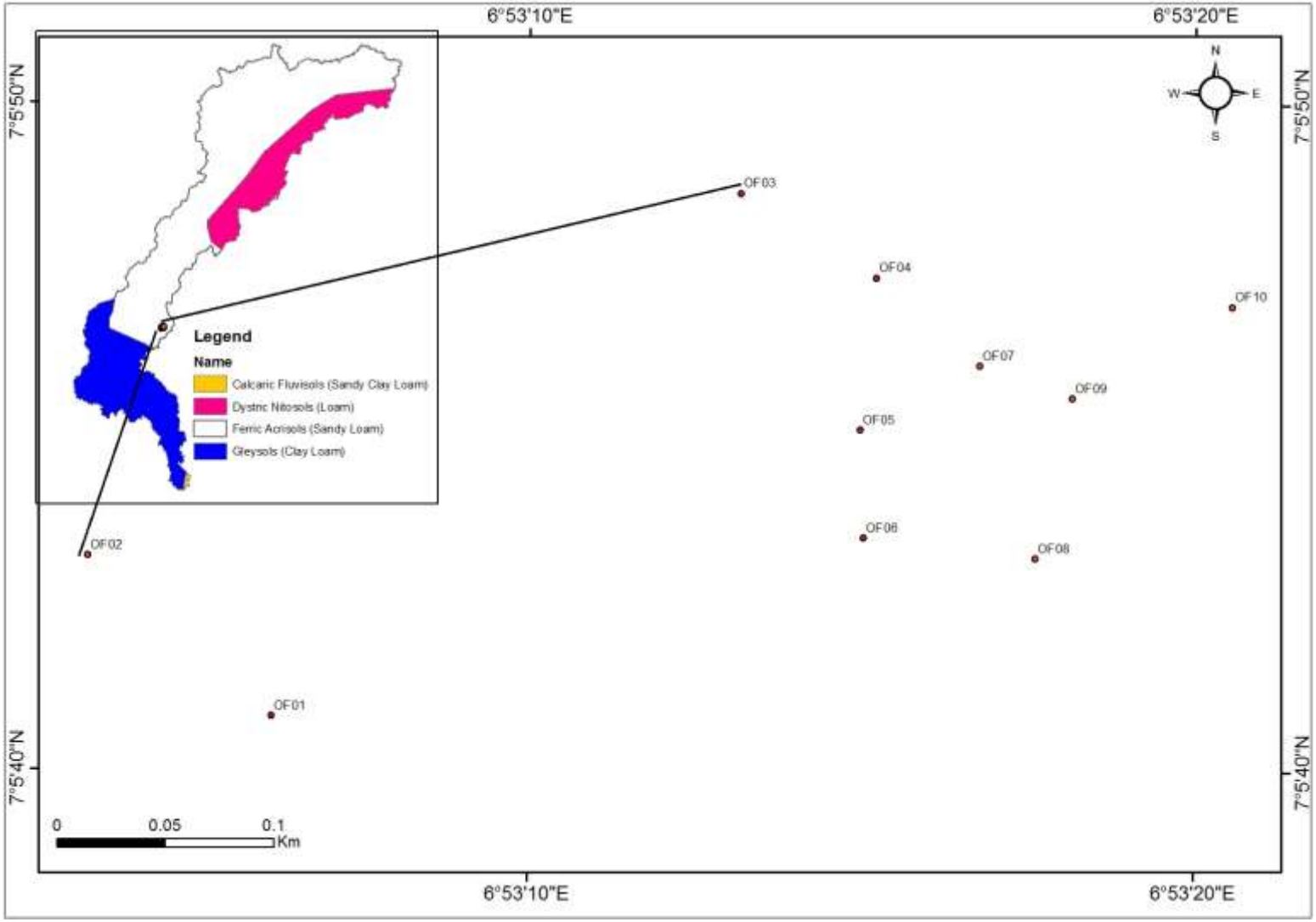


Fig. 4.23: Comparison of Soil Analyses Results with the Digital Soil Map of the World

4.3.4 Landuse/Settlement Causative Factors

4.3.4.1 Proximity of households to Ofu River

The proximity of households to Ofu River obtained in the course of the field are shown in Fig. 4.24. The proximity ranged from 9.08 m to 495.73 m for households affected by Ofu River surface flood, 900.80 m to 1170.57 m for households affected by groundwater flood and 183.51 m to 1466.89 m for the households that never experiemced flood. From the forgoing, it can be deduced that the occurrence of flood within the study area is not exclusively dependent on a single factor but a combination multiple factors. In order words, neither elevation, proximity nor slope can stand alone as a factor that determines whether a household would be flooded or not but a combination of all.

4.3.4.2 Landuse/landcover changes within Ofu River Catchment

The results of the Land use/ Land cover classifications for 1987, 2001 and 2016 are presented in Figs. 4.25 (a – c). The study area is a rural community. They were classified into three classes: Built Up, Vegetation and Bare Surfaces. Furthermore, the areas of the respective land cover for each year as well as their percentage are presented in Fig. 4.26 (a and b) while percentage changes in land use/ land cover is presented in Fig. 4.27.

The results show that vegetation covered a land area of 711.23 km^2 (44.33 %), 651.99 km^2 (40.64 %) and 869.10 km^2 (54.17 %) in 1987, 2001 and 2016, respectively. Meanwhile, the bare surface area was 415.12 km^2 (25.87 %), 402.22 km^2 (25.07 %) and 122.84 km^2 (7.66 %) in 1987, 2001 and 2016, respectively. Finally, the built up areas were 478.15 km^2 (29.80 %), 550.29 km^2 (34.30 %) and 612.56 km2 (38.18 %) in 1987, 2001 and 2016, respectively.

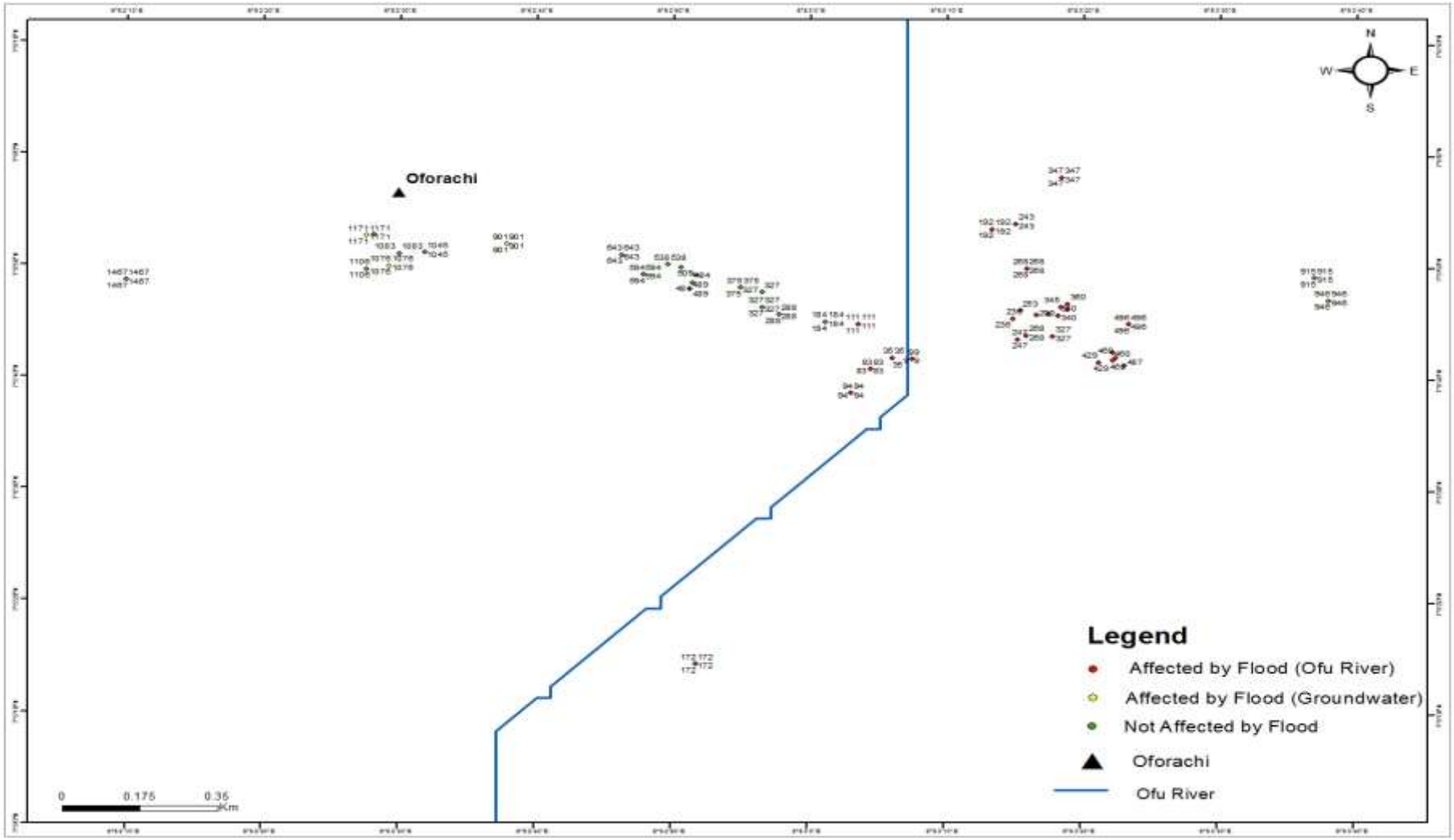


Fig. 4.24: Proximity of Households from Ofu River

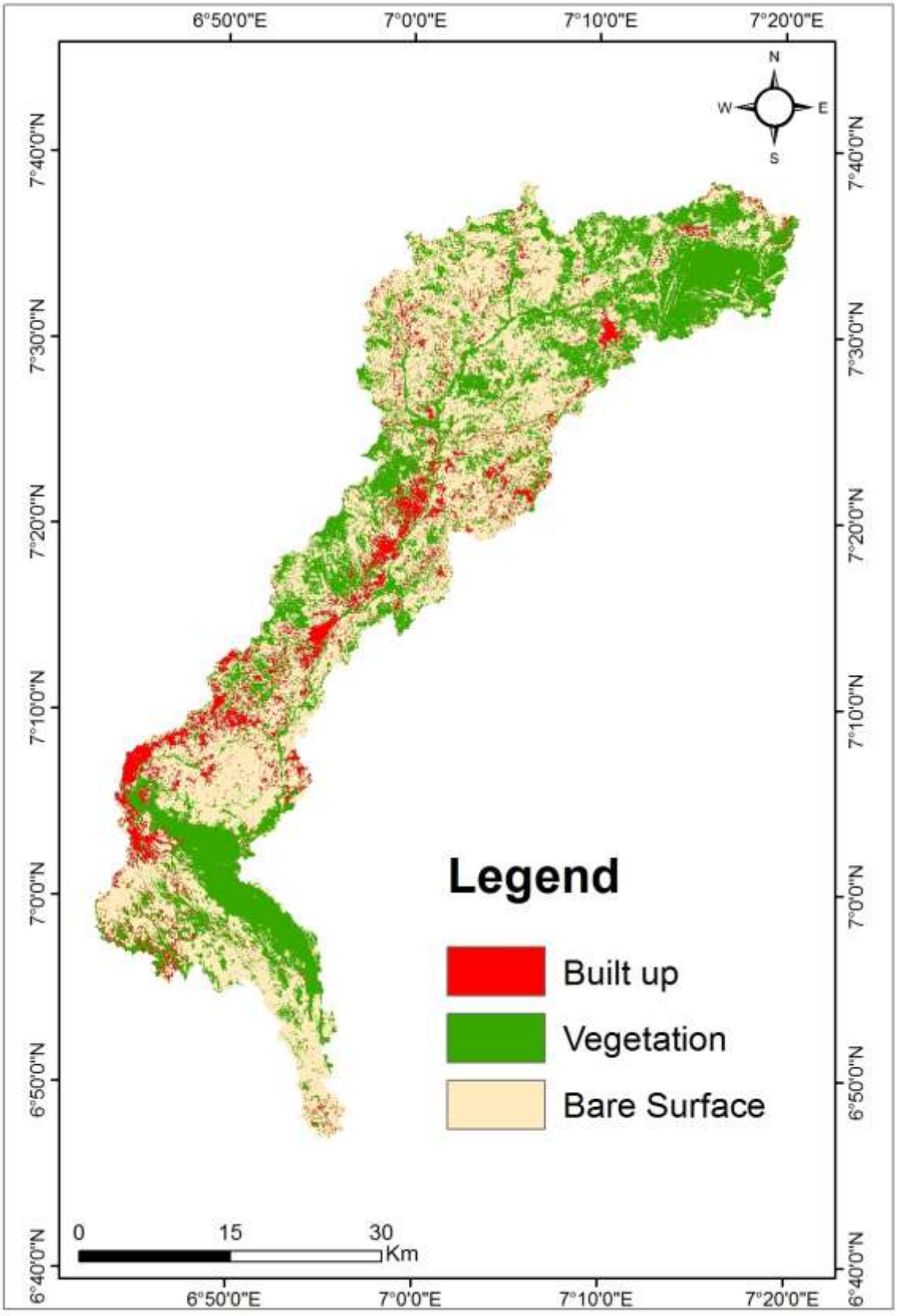


Fig. 4.25a: Ofu River Catchment Land use/Land cover classifications for 1987

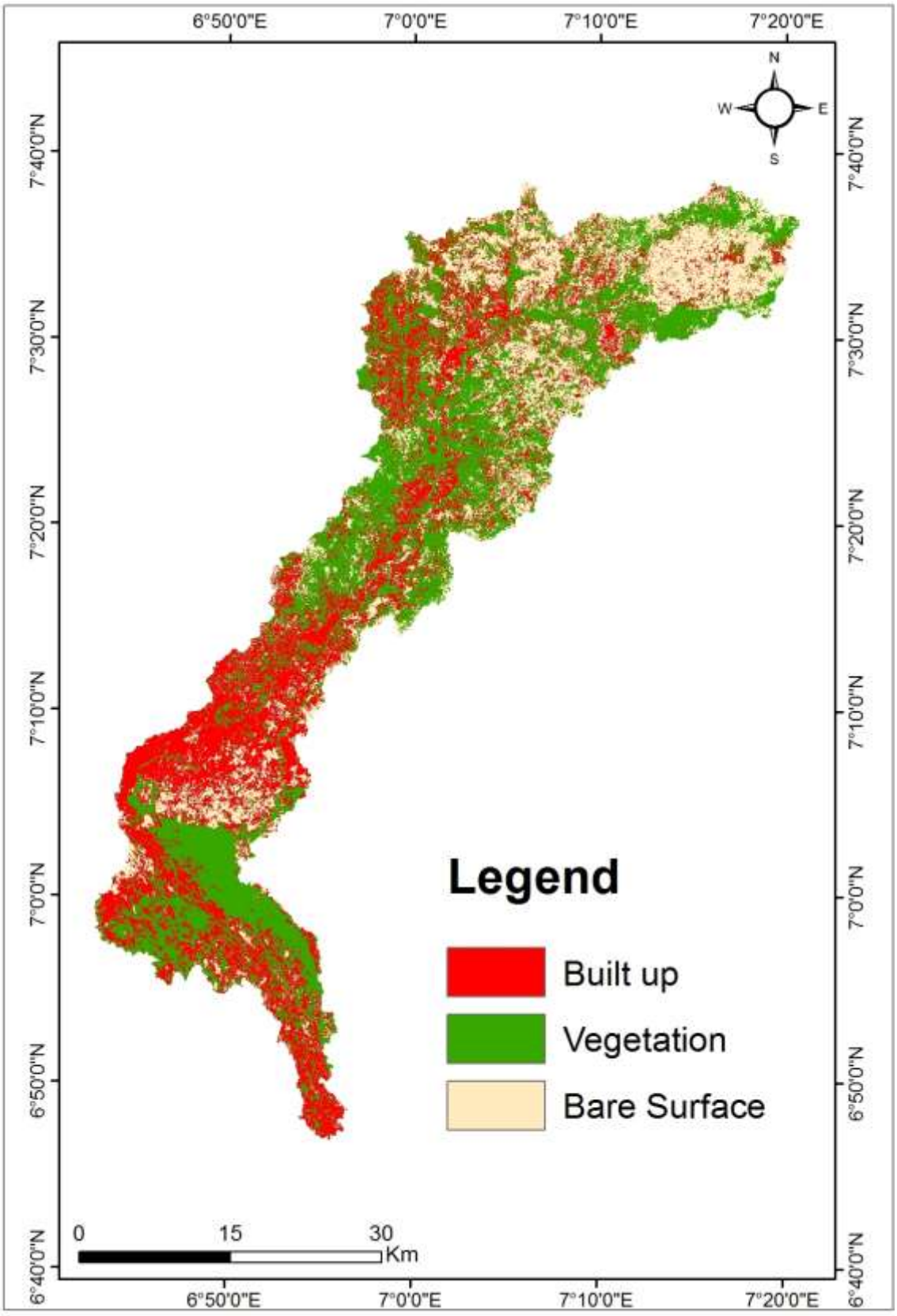


Fig. 4.25b: Ofu River Catchment Land use/Land cover classifications for 2001

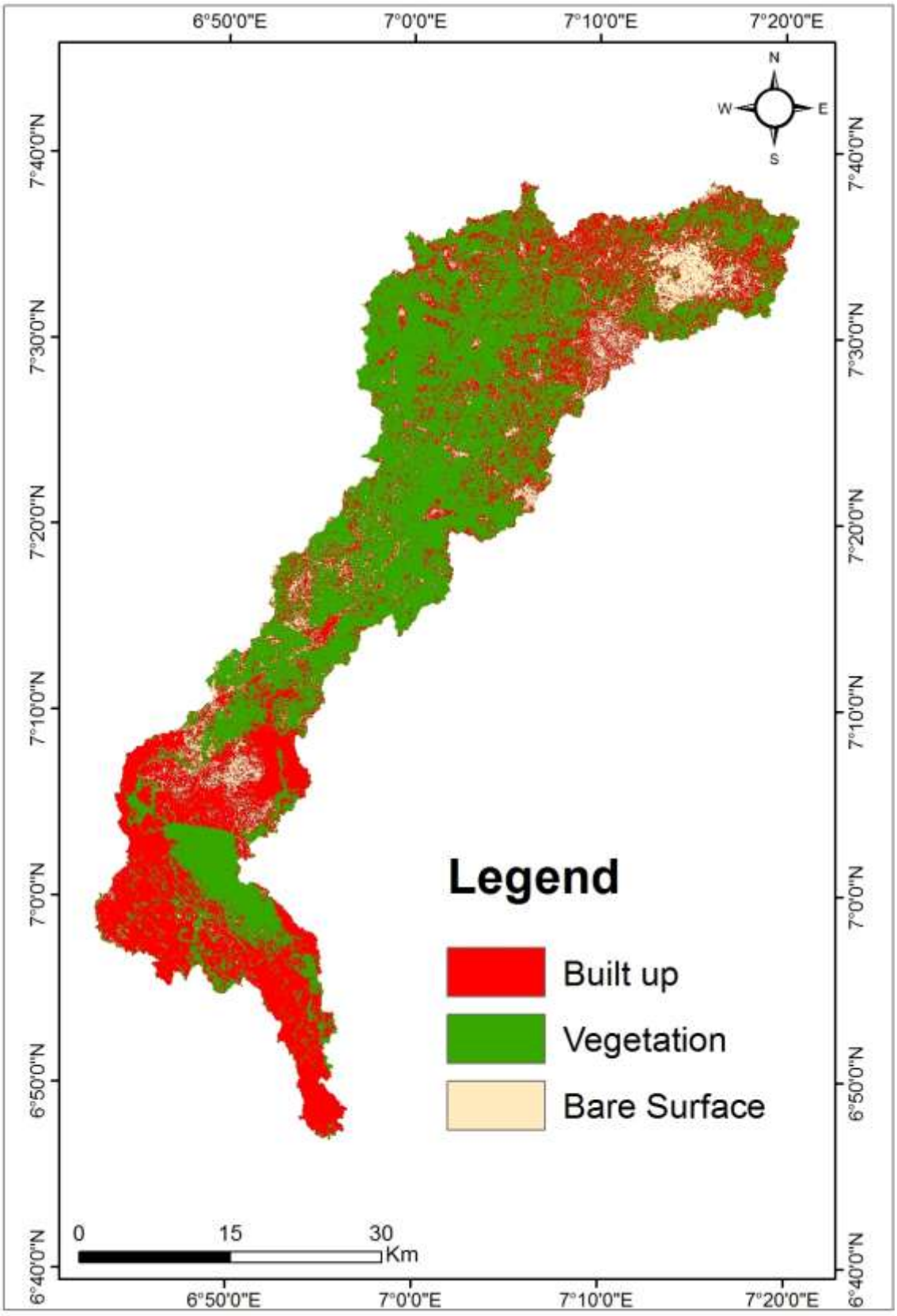


Fig. 4.25c: Ofu River Catchment Land use/Land cover classifications for 2016

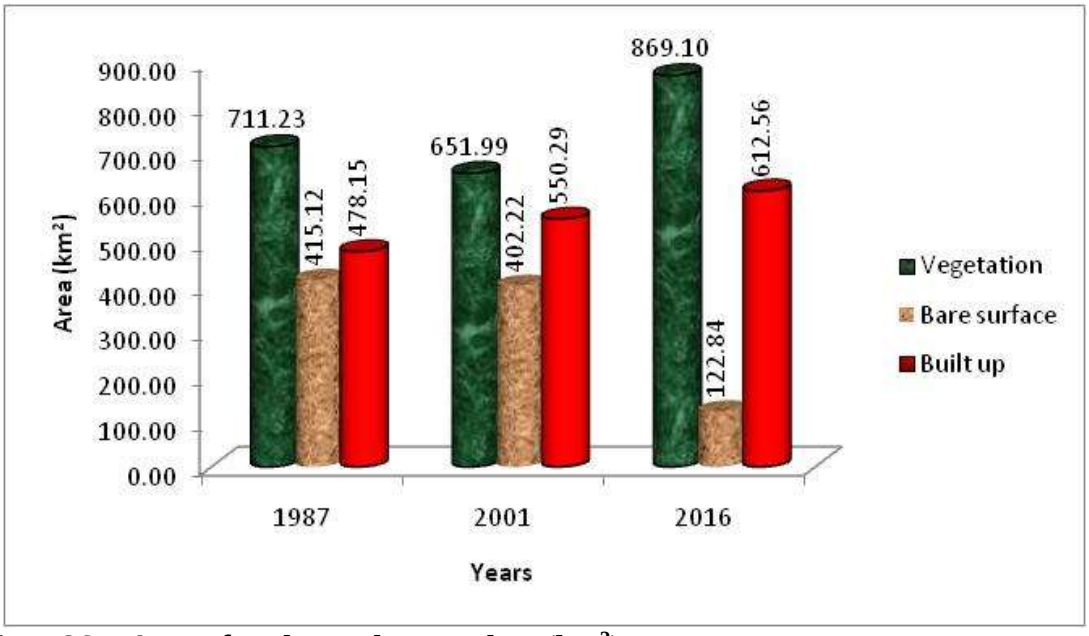


Fig. 4.26a: Area of each Land cover class (km^2)

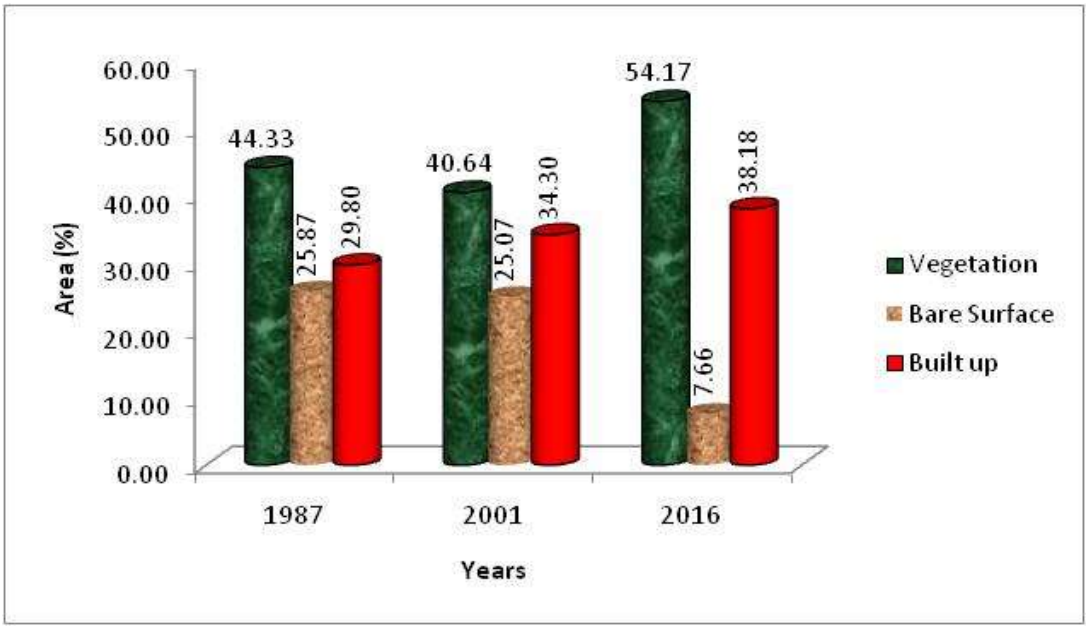


Fig. 4.26b: Area of each Land cover class (%)

Further more, the land use/Land cover changes for Ofu River catcment are presented in Fig. 4.27.

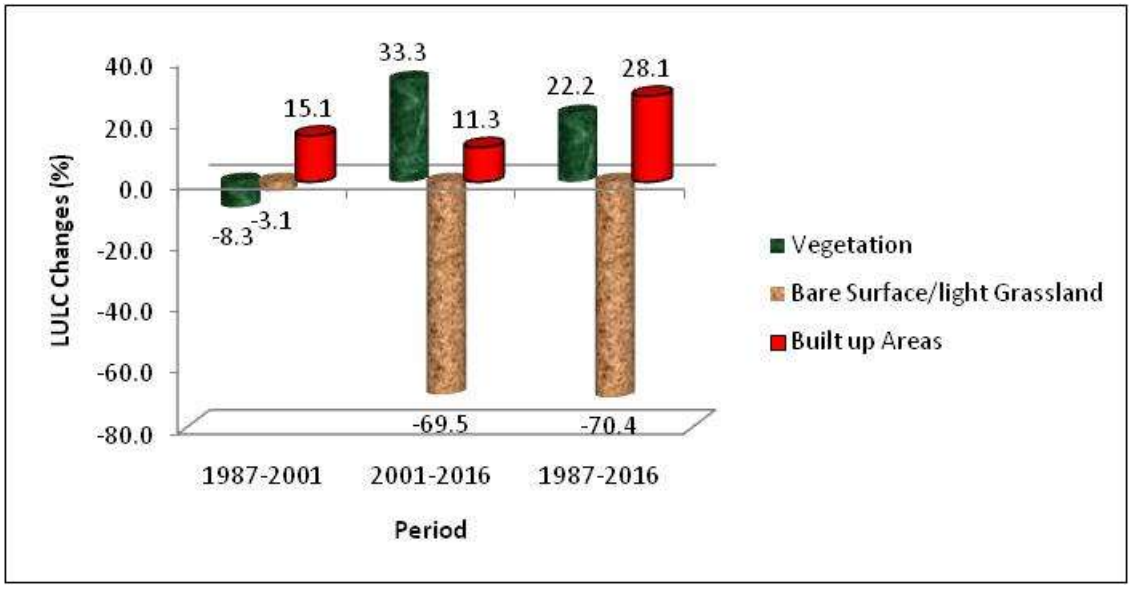


Fig. 4.27: Ofu River Catchment LULC Changes from 1987 to 2016

Figure 4.27 shows that the land area covered by vegetation reduced by 8.3 % between 1987 and 2001 but suddenly increased by 33.3 % between 2001 and 2016. This probably could be a function of the date of acquisitions of the respective satellite imageries. The Imageries for 1987 and 2001 were acquired in January while that of 2016 was acquired in March. The imageries used for the respective years were the ones with minimal cloud cover to allow for easy classification. The monthly rainfall characteristics of the catchment shown in Fig. 4.13 reveal that January is actually the lowest rainfall month with an average monthly rainfall of 3.98 mm while March has slightly higher average monthly rainfall of 35.14 mm which is usually the beginning of the rainy season. This implies that a part of the vegetations in 1987 and 2001 will be so dry and unhealthy that the maximum likelihood may interpret them as bare surfaces while that of 2016 obtained at the onset of the rainy season would appear healthy and rightly interpreted as vegetation. This probably explains the vegetation trend mentioned earlier. Meanwhile the change in vegetation between 1987 and 2016 was found to be 22.2 %. The change in bare surface area showed a downward trend. There was a 3.1 % reduction from 1987 to 2001 and 69.5 % reduction from 2001 to 2016. The change in bare surface area from 1987 to 2016 was

70.4 %. This confirms the explanation given earlier for the vegetation trend. The built up areas on the other hand increased continuously between 1987 and 2016 in agreement with urbanization trend.

4.3.4.3 Runoff curve number for Ofu River Catchment

The runoff curve numbers estimated for 1987, 2001 and 2006 are presented in Fig. 4.28. The details of the calculations are presented in Appendix XIV.

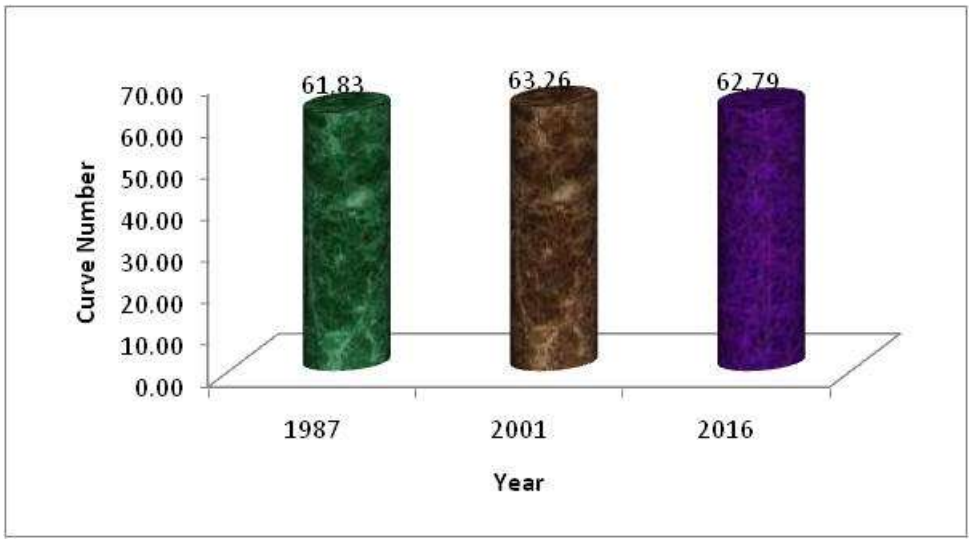


Fig. 4.28: Ofu River Catchment Runoff Curve Number for 1987, 2001 and 2016

The results show there was no major change in the value of the curve numbers for the respective years. This shows that although changes in land covers have happened over the period, the change has not significantly affected the runoff that would be generated from the catchment. This is not excusing other activities that probably have increased the erodibility of the soils.

4.3.5 Respective Associations of Elevation, Proximity and Slope with Flood Occurrence

The results of the Pearson's chi square test carried out to assess the respective association of terrain elevation, proximity of houses to Ofu River and the terrain slope with household flood experience are presented in Table 4.14.

Table 4.14: Chi Square result for Association of Elevation, Proximity and Slope with Household flood experience

Parameter	Flood Experience		Total [Freq. (%)]	Pearson's Chi^2	P-Value
	Affected [Freq. (%)]	Never Affected [Freq. (%)]			
Elevation (m asl)					
> 67	7(3.55)	65(50.78)	72(22.15)		
< 67	190(96.45)	63(49.22)	253(77.85)	100.35	0.000
Total	197 (100)	128(100)	325(100)		
Proximity (m)					
> 495.73	22(11.17)	75(58.59)	97(29.85)		
< 495.73	175(89.83)	53(41.41)	228(70.15)	83.35	0.000
Total	197(100)	128(100)	325(100)		
Slope (%)					
Flat (0 – 2)	14(7.11)	0(0)	14(4.31)		
Undulating (2 - 8)	26(13.20)	39(30.47)	65(20.00)		
Rolling (8 – 30)	157(79.70)	89(69.53)	246(75.69)	21.73	0.000
Total	197(100)	128(100)	325(100)		

The *P*-value of 0.000 obtained in all cases demonstrates that terrain elevations, proximity of households to the river and the terrain slope had varying measures of association with the household experience of flood which implies that they are actually flood causative factors. Meanwhile, Elevation had strongest association with flood occurrence ($chi^2 = 100.35$) followed by proximity ($chi^2 = 83.35$) with slope having the least association ($chi^2 = 21.73$).

4.4 FLOOD FREQUENCY ANALYSIS

4.4.1: Peak Runoff

The results of the estimation of peak runoff by the three methods (Modified Thomas-Fierring Model, SCS Curve Number Method and the Rational Method) are presented and discussed in this section.

4.4.1.1 Generation of synthetic stream flow data using Modified Thomas-Fierring Model

The results of the extension of gauged stream flow data for Ofu River are presented in Appendix XV. The generated synthetic data are presented in Table XVa (Appendix XV) while the adjusted results are presented in Table XV (Appendix XV). Meanwhile, the unbiased statistics of the gauged and synthetic stream flow data are presented in Table 4.15a. Furthermore, the coefficients of determination, *P*-value, *F*-value, *Crtitical F*-value and Reliability Index are presented in Table 4.15b. The coefficients of determination for the comparison of mean and standard deviation were very close to unity which is indicative of a very good fit which agrees with the findings of Dashora *et al.* (2015) who concluded that Thomas-Fiering's model performed very well in the prediction of high stream flows for the Narmada River Basin given by the high coefficient of determination and the Root Mean Square Error. The coefficient of determination for the comparison of correlation coefficient on the other hand is very low (0.677) which shows that only about 67% of the correlation coefficients of the gauged data were preserved in the synthetic data. The *P*-values obtained for the mean, standard deviation and correlation coefficient were all greater that 0.05 which shows that the difference between these parameters were not statistically significant. This was further buttressed by the calculated *F*-value which was less than the critical *F*-value for the three parameters compared.

Table 4.15a: Unbiased Statistics of the gauged (1955-1973) and synthetic (1955-2016) stream flow data

Year	Mean (m^3/s)		Standard Deviation (m^3/s)		Correlation Coefficient	
	Gauged	Synthetic	Gauged	Synthetic	Gauged	Synthetic
January	3.15	3.15	1.43	0.80	0.52	0.43
February	2.51	2.41	1.17	0.66	0.89	0.79
March	1.81	1.75	1.00	0.55	0.85	0.84
April	13.31	13.36	5.34	2.92	-0.28	-0.28
May	8.92	8.91	3.44	1.91	0.09	0.08
June	38.32	37.43	22.60	13.15	0.01	0.01
July	124.31	126.25	43.40	24.70	0.30	0.27
August	403.79	402.81	125.73	73.33	0.20	0.15
September	432.02	444.86	129.61	72.11	0.64	0.59
October	83.01	74.29	39.97	26.98	-0.03	-0.09
November	4.98	5.14	1.87	1.03	0.13	0.07
December	1.30	1.24	0.60	0.38	-0.02	0.00

Table 4.15b: Coefficients of Determination, *P*-value, *F*-value, *Crtitical F*-value and Reliability Index

Parameter	Mean (m^3/s)		Standard Deviation (m^3/s)		Correlation Coefficient	
	Value	Score	Value	Score	Value	Score
R^2	0.998	0.998	0.956	0.956	0.677	0.677
P-Value	1.000	1	0.879	1	0.905	1
F	0.001	1	0.224	1	0.187	1
F-Critical	2.816		2.816		2.817	
Total Score		2.998		2.956		2.677
Reliability Index			0.9590			

The above results are indicative of the fact that the unbiased statistics of the gauged data especially mean and standard deviation were sufficiently preserved in the synthetic data (Stedinger and Taylor, 1982; Lebbe, 1991). Related studies by other researchers (Teymouri and Fathzadeh, 2015; Dashora *et al.*, 2015; Cui et al, 2017; Sathish and Babu, 2017) agree with the findings in this present study in the aspect of the unbiased statistics of the gauged data being preserved in the synthetic data but most concluded that in comparison with other models such as the Autoregressive Intigrated Moving Average (ARIMA) model, the Thomas-Fiering's model has the tendency of over-estimating the stream flow especially for months of low flow. Kurunc *et al.* (2005) however was of a contrary opinion that the Thomas-Fiering's Model is more reliable in stream flow prediction than the ARIMA model.

The overall reliability index obtained was 0.959. This implies that the synthetic stream flow data generated using the modified Thomas Fierring's model is 95.9% reliable.

4.4.1.2 SCS Curve Number method of runoff estimation

The Storage, *S*

$$= \frac{25400}{CN} - 254$$

Curve number for 2016, CN = 62.79

Therefore, Storage, S

$$= \frac{25400}{62.79} - 254 = 150.53\ mm$$

Initial Abstraction, I_a

$$= 0.2S$$

$$= 0.2 \times 150.53 = 30.11\ mm$$

Depth of Runoff, *Q*

$$Q = \frac{(P - I_a)^2}{\{(P - I_a) + S)\}} (P \geq I_a else Q = 0)$$

Duration of excess rainfall, *D*

$$= 0.133 t_c$$

Where time of concentration, t_c = 6.17 hr

Therefore, duration of excess rainfall, *D*

$$= 0.133 \times 6.17 = 0.82 Hr$$

The lag time of the watershed, t_{lag}

$$= 0.6 t_c$$

$$= 0.6 \times 6.17 = 3.70 Hr$$

Time to peak, t_p

$$= \frac{D}{2} + t_{lag}$$

$$= \frac{0.82}{2} + 3.70 = 4.11\ Hr$$

Area reduction factor, f_A

$$= 1/e^{\left(1 - \frac{12}{A}\right)}$$

Area of catchment, A = 1604.56 km^2

Therefore, f_A

$$= 1/e^{\left(1 - \frac{12}{1604.56}\right)} = 0.371$$

Thus, corrected Area, $A_{corrected}$

$$= A - (f_A \times A)$$

$$= 1604.56 - (0.371 \times 1604.56) = 1{,}009.84\ km^2$$

Finally, the peak runoff, Q_p

$$= 2.8 \frac{Q \times A_{corrected}}{t_p}$$

The peak runoff values calculated from the corrected annual maximum daily rainfall for Ofu River Catchment are presented in Table XVIa (Appendix XVI).

4.4.1.3 Rational method of estimation of peak runoff

Estimation of Runoff Coefficient

The results of the estimation of runoff coefficient for Ofu River catchment is summarized in Table 4.16. The details of the calculations are presented in Appendix XVII.

Table 4.16: Runoff Coefficient for Ofu River Catchment

Component	Runoff Coefficient
Surface Slope (C_s)	0.08
Permeability (C_p)	0.14
Vegetation (C_v)	0.15
Composite C	**0.38**

The results in Table 4.16 show that the composite runoff coefficient for Ofu River Catchment is 0.38. Furthermore, the rainfall intensity parameters ($1/\alpha$ and β) for the time of concentration of 6.17 hours, rainfall intensity and peak discharge are presented in Table 4.17.

Table 4.17: Rainfall Intensity and Peak Discharge by Rational Method

$1/\alpha$	β	Rainfall Intensity (mm/hr)	Peak Discharge (m^3/s)
3.00	10.42	8.42	898.34

The results show that the rainfall intensity is 8.42 mm/hr while the peak discharge is 898.34 m^3/s.

4.4.1.4 Comparison of the results from the three methods

A comparison of the peak discharge obtained using Modified Thomas-Fierring's (T-F) model, SCS-CN method and the rational method with the field measured discharge is presented in Table 4.18.

Table 4.18: Comparison of Average Peak Discharge from the Respective Methods

	Synthetic (T-FM)	SCS-CN	Rational	Field Measurement (Rating Curve)
Average Peak Discharge (m^3/s)	448.66	825.95	898.34	410.79

Table 4.18 shows that the average peak discharge for the synthetic stream flow obtained using the Modified Thomas-Fierring's Model was 448.66 m^3/s, while those for the SCS-CN and the rational methods were respectively, 825.95 m^3/s and 898.34 m^3/s. Peak discharge obtained from the twelve month discharge (February, 2016 to January, 2017) derived using the rating curve on the other hand is 410.79 m^3/s. It can be seen that the synthetic data (T-FM) reflects the current discharge characteristics much more than the other methods. Meanwhile, the synthetic discharge values covers a period of 62 years compared to the 35 years of the SCS-CN discharge values. As a result of these factors, the synthetic discharge values were used for the flood frequency analysis.

4.4.2 Peak Discharge Forcast using Log-Pearson Type III Distribution

The results of the flood frequency Analysis using Log-Pearson Type III distribution are presented in Table 4.19.

Table 4.19: Results of the Flood Frequency Calculations using log-Pearson Type III Analysis with Average Annual Maximum Discharge Values (1955-2016)

Return Period (years)	Skew Coefficient K(-0.0104)	Discharge, Q (m^3/s)
2	0.00	444.57
5	0.84	499.23
10	1.28	530.35
25	1.75	565.61
50	2.05	589.59
100	2.32	611.96
200	2.57	633.25

Table 4.19 shows that discharge values of 444.57 m^3/s, 499.23 m^3/s, 530.35 m^3/s, 565.61 m^3/s, 589.59 m^3/s, 611.96 m^3/s and 633.25 m^3/s, respectively were obtained for 2, 5, 10, 25, 50, 100 and 200 years return periods. Flood frequency curve for the respective return periods is shown in Fig. 4.29.

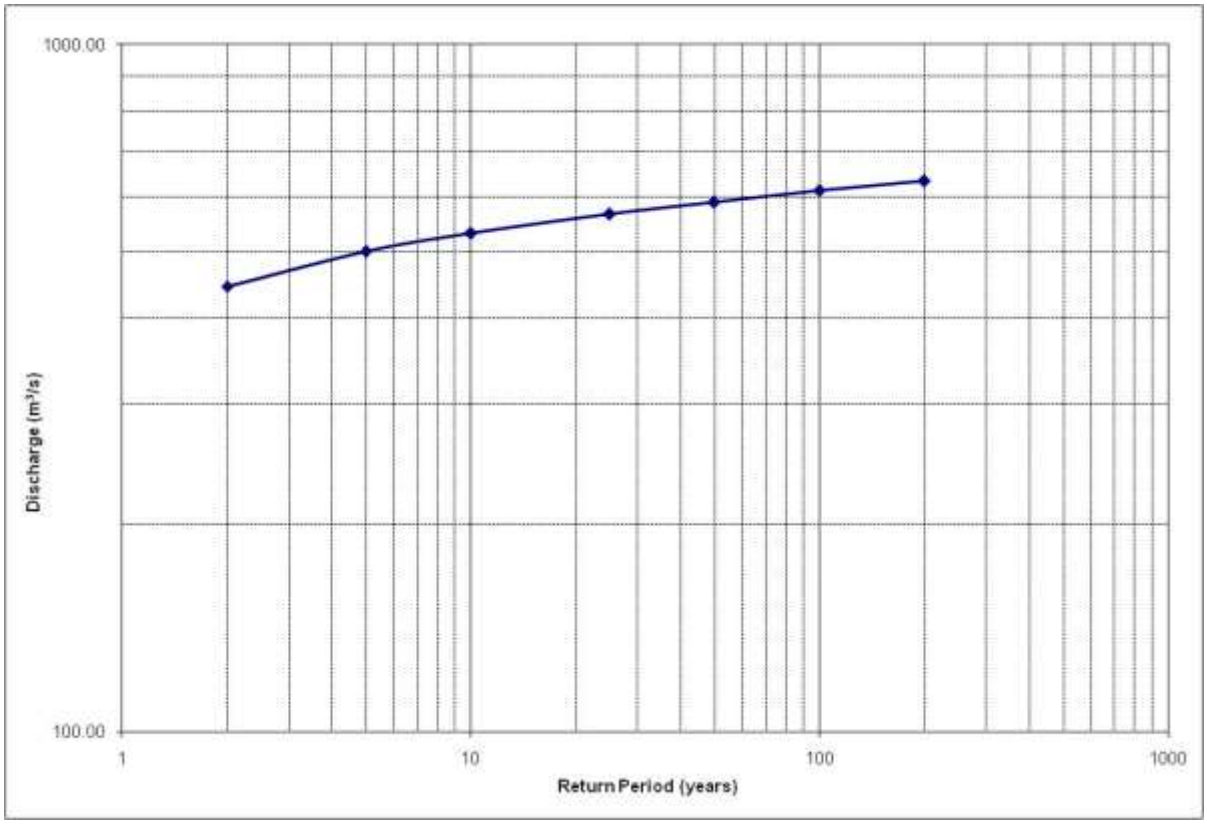


Fig. 4.29: Forecasted Discharge of Ofu River at Oforachi using Log-Pearson Type III Distribution with Annual Maximum Discharge Values (1955-2016).

Furthermore, the discharge values for the 1995 and 2000 flood scenarios as well as for the respective return periods that were used for the Steady flow modelling in HEC-RAS are presented in Table 4.20.

Table 4.20: Discharge Values for Steady Flow Analysis in HEC-RAS

	Flood Events		**Return Periods**						
	1995	**2000**	**2**	**5**	**10**	**25**	**50**	**100**	**200**
Discharge (m^3/s)	448.89	446.46	444.57	499.23	530.35	565.61	589.59	611.96	633.25

4.5 FLOOD INUNDATION EXTENT AND HAZARD MAP

4.5.1 Flood Hazard Map by Thematic Integration of Causative Factors (Multi-Criteria Evaluation) in ArcGIS

The results of the production of flood hazard map by thematic integration of causative factor maps in ArcGIS are presented in this section. The results cover the generation of the thematic layers of four causative factors (Elevation, Corridor, slope and soil), derivation of their criterion weight, reclassification and final integration.

4.5.1.1 Thematic maps of flood causative factors in Ofu River Catchment

(A) Elevation

The elevation layer of the study area was obtained from the DEM of the study area extracted from the SRTM DEM (Table 3.4)**.** The output Elevation layer is shown in Fig. 4.30.

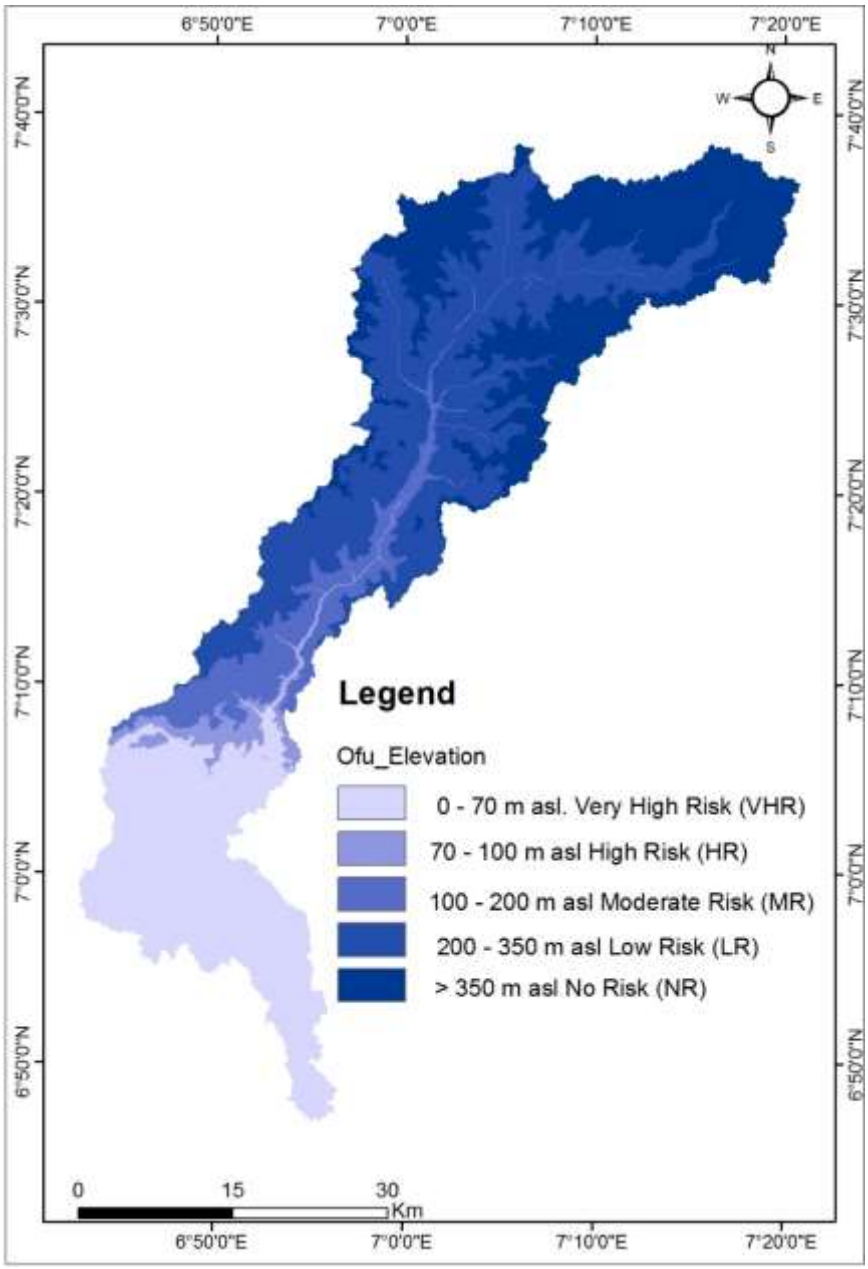


Fig. 4.30: Elevation Layer for Multi-Criteria Evaluation

The elevation was classified into five classes based of field experience. Elevations less than 70 m above mean sea level were categorised as very high risk (VHR). This elevation range characterise the south western part of the catchment towards its outlet. The other ranges are 70 – 100 m, 100 – 200 m, 200 – 300 m and greater than 300 m above sea level which were respectively categorised as high risk (HR), moderate risk (MR), low risk (LR) and no risk (NR).

(B) Slope

The output slope layer is shown in Fig.4.31.

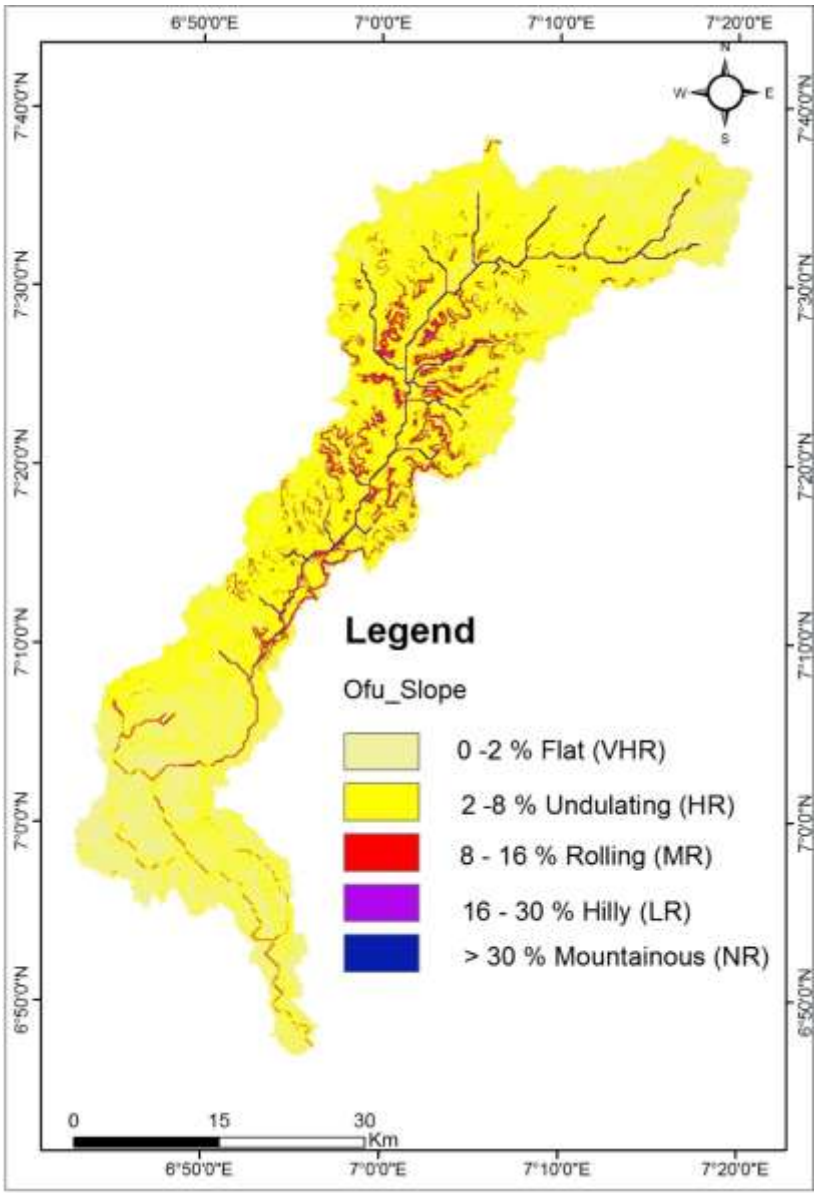


Fig. 4.31: Slope Layer for Multi-Criteria Evaluation

Figure 4.31 shows that the Ofu River Catchment could be said to be predominantly flat to undulating terrain. Similar to the elevation layer, the south western part towards the catchment outlet are relatively flat terrain. While a major part of the catchment northward are relatively undulating which very small portion of rolling, hilly and mountainous terrain.

(C) Soil

The output soil layer for the study area extracted from the digital soil map of the world (DSMW) is shown in Fig.4.32

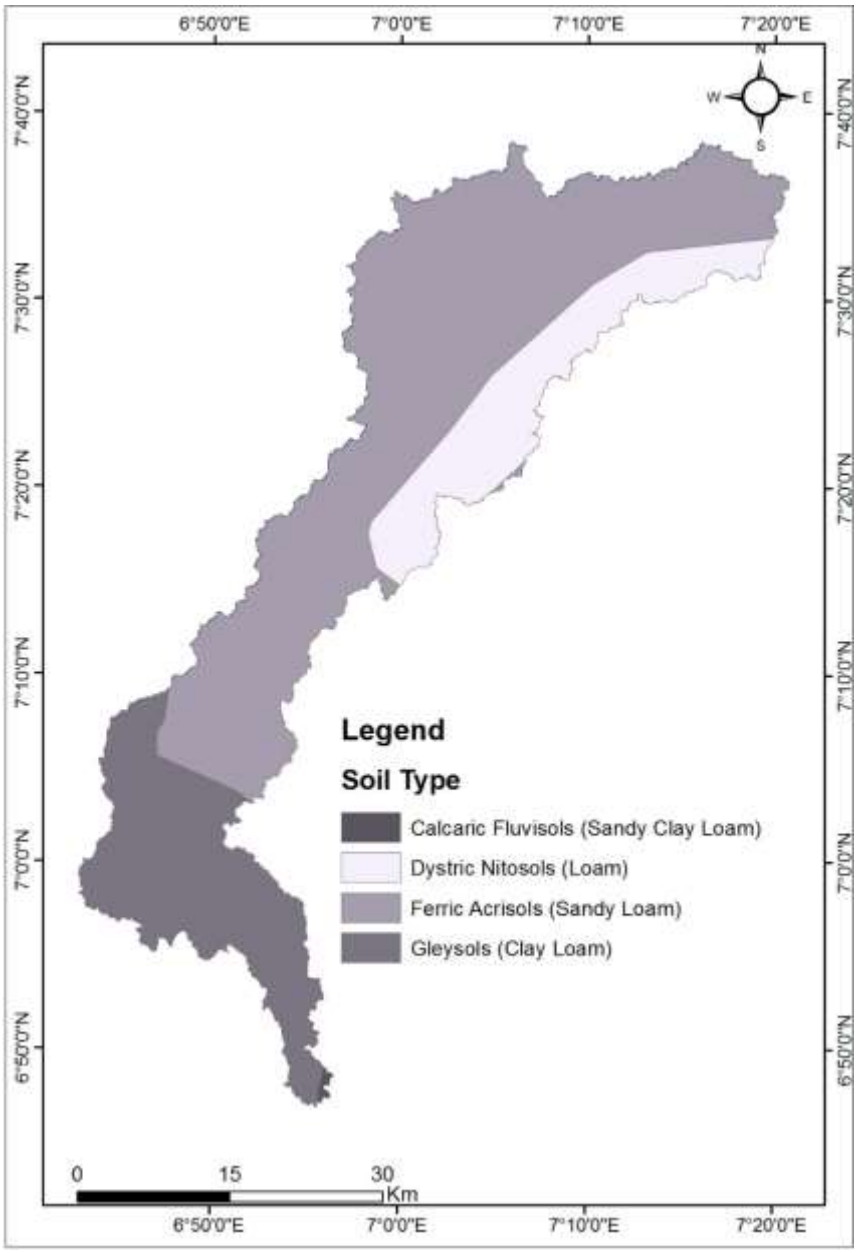


Fig. 4.32: Soil Layer for Multi-Criteria Evaluation

Figure 4.32 shows that the catchment is composed of four distinct types of soil. At the catchment outlet are found Calcaric Fluvisols (Sandy Clay Loam), while Gleysols (Clay loam) are found just before this at the South western part of the catchment. The north

eastern part of the catchment consists of Dysteric Nitosols (Loam) while the extreme north towards the central part of the catchment is composed principally of Ferric Acrisols (Sandy Loam).

(D) Corridor

The corridor layer shows the distance of respective points on the catchment from Ofu River. The output corridor layer is shown in Fig. 4.33.

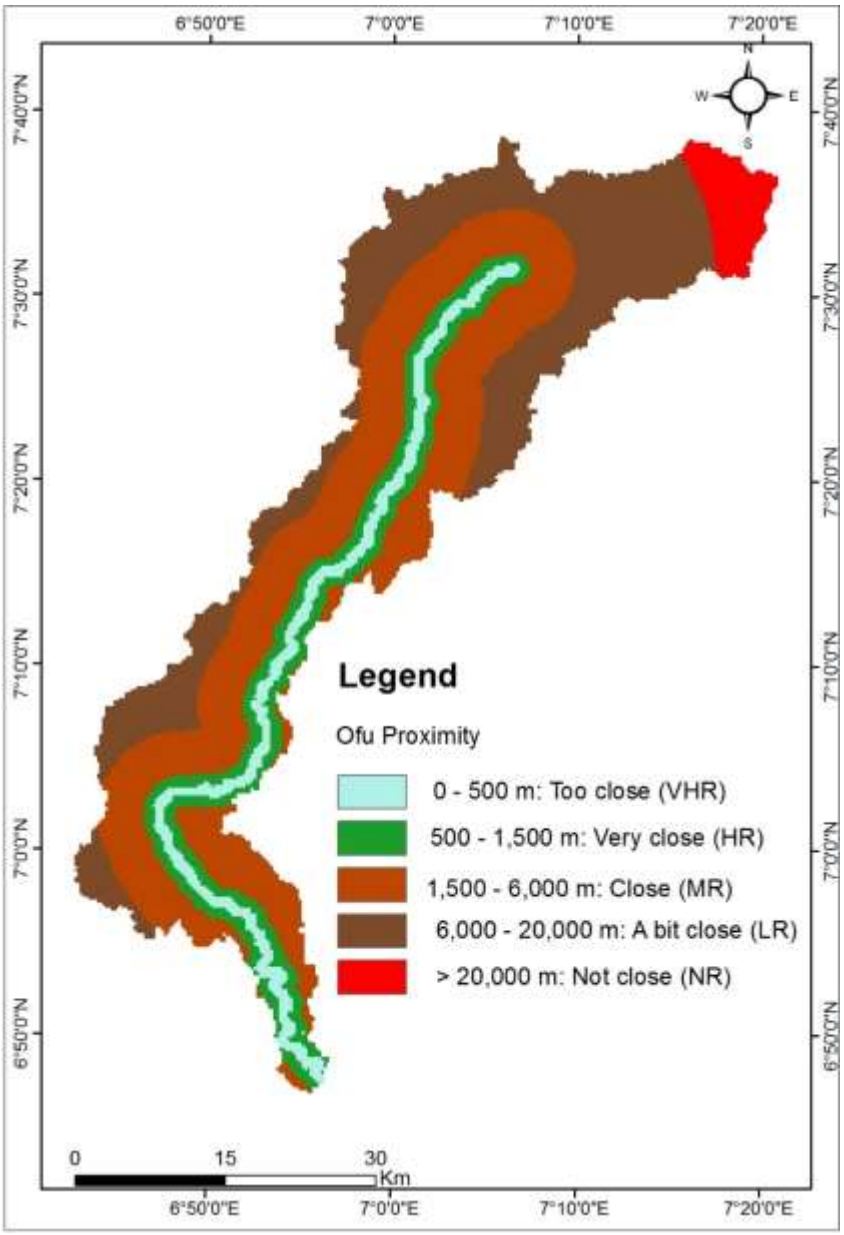


Fig. 4.33: Corridor Layer for Multi-Criteria Analysis

Fig. 4.45 shows that locations with distance less than 500 m from the river was categorised as being too close and constitutes a very high risk of inundation. The other categories are 500 – 1,500 m, 1,500 – 6,000 m, 6,000 – 20, 000 m and greater than 20,000 m categorised as 'Very close', 'Close', 'A bit close' and 'Not close,' respectively.

4.5.1.2 Criterion Weights and Reclassification of Thematic Maps of Causative Factors

(A) Elevation Layer

The results of the pair-wise comparison for elevation carried out using AHP are presented in Table 4.21.

Table 4.21: Criterion Weight for Elevation

	VHR	**HR**	**MR**	**LR**	**NR**	**Weight**	**Weight*100**
VHR	1	9/8	9/5	9/3	9	0.35	35
HR	8/9	1	8/5	8/3	8	0.31	31
MR	5/9	5/8	1	5/3	5	0.19	19
LR	1/3	3/8	3/5	1	3	0.12	12
NR	1/9	1/8	1/5	1/3	1	0.04	4
						1.00	100
						CR =	0.00

The VHR class which is the most susceptible to flood had a weight of 35 while the HR, MR, LR and NR classes had weights of 31, 19, 12 and 4, respectively. The consistency ratio of 0.00 obtained shows the accuracy of the process. The elevation layer was reclassified based on these weights (Fig. 4.34).

(B) Slope Layer

The results of the pair-wise comparison of the slope carried out using the AHP are presented in Table 4.22.

Table 4.22: Criterion Weight for Slope

	Flat	Undulating	Rolling	Hilly	Mountainous	Weight	Weight*100
Flat	1	9/7	9/5	9/3	9	0.36	36
Undulating	7/9	1	7/5	7/3	7	0.28	28
Rolling	5/9	5/7	1	5/3	5	0.20	20
Hilly	1/3	3/7	3/5	1	3	0.12	12
Mountainous	1/9	1/7	1/5	1/3	1	0.04	4
						1.00	100
						CR =	0.00

The results of the pair-wise comparison on slope (Table 4.22) show that flat terrain has the highest weight of 36 which is followed by the undulating terrain with a weight of 28. The rolling, hilly and mountainous terrains respectively have weights of 20, 12 and 4. The consistency ration of 0.00 obtained show that the results can be accepted. The slope layer was reclassified using the derived weights (Fig. 4.35).

Lindsay-Walters (n.d) stated that the slope of the terrain can significantly affect the rate of runoff. He noted that the greater and steeper the angle, the faster the runoff and the lower the tendency for flooding and vice versa (Daffi, 2013; Garba, 2015).

(C) Soil Layer

The results of the pair-wise comparison for the soil layer are presented in Table 4.23.

Table 4.23 Criterion Weight for Soil

	Clay Loam	Sandy Clay Loam	Loam	Sandy Loam	Weight	Weight*100
Clay Loam	1	9/7	9/5	9/3	0.38	38
Sandy Clay Loam	7/9	1	7/5	7/3	0.29	29
Loam	5/9	5/7	1	5/3	0.21	21
Sandy Loam	1/3	3/7	3/5	1	0.13	13
					1.00	100
					CR =	0.00

The ranking was done based on the ability of the soil class to allow water to infiltrate into the ground thereby reducing surface runoff (Garba, 2015). Based on the aforementioned reason, Clay loam with least infiltration rate ranked highest with a weight of 38 while Sandy Clay loam, Loam and Sandy Loam had weights of 29, 21 and 13 respectively. The soil layer was reclassified based on these weights (Fig. 4.36).

(D) Corridor Layer

The results of the pair-wise comparison for corridor layer are presented in Table 4.24.

Table 4.24: Criterion Weight for Corridor

	Too close	Very close	Close	A bit close	Not close	Weight	Weight*100
Too close	1	9/7	9/4	9/2	9	0.39	39
Very close	7/9	1	7/4	7/2	7	0.30	30
Close	4/9	4/7	1	2	4	0.17	17
A bit close	2/9	2/7	½	1	2	0.09	9
Not close	1/9	1/7	¼	½	1	0.04	4
						1.00	100
						CR =	0.00

The ranking was done based on the field experience. Some household with elevations similar to those of the flooded households were not flooded because of their distance from the River. Thus the areas with 500 meters from the river were designated too close and ranked the highest with a weight of 39 while the very close, close, A bit close and Not close categories had weights of 30, 17, 9 and 4 respectively. The consistency ratio of 0.00 obtained shows that the decision was correct. These weights derived were used to reclassify the corridor layer (Fig. 4.37).

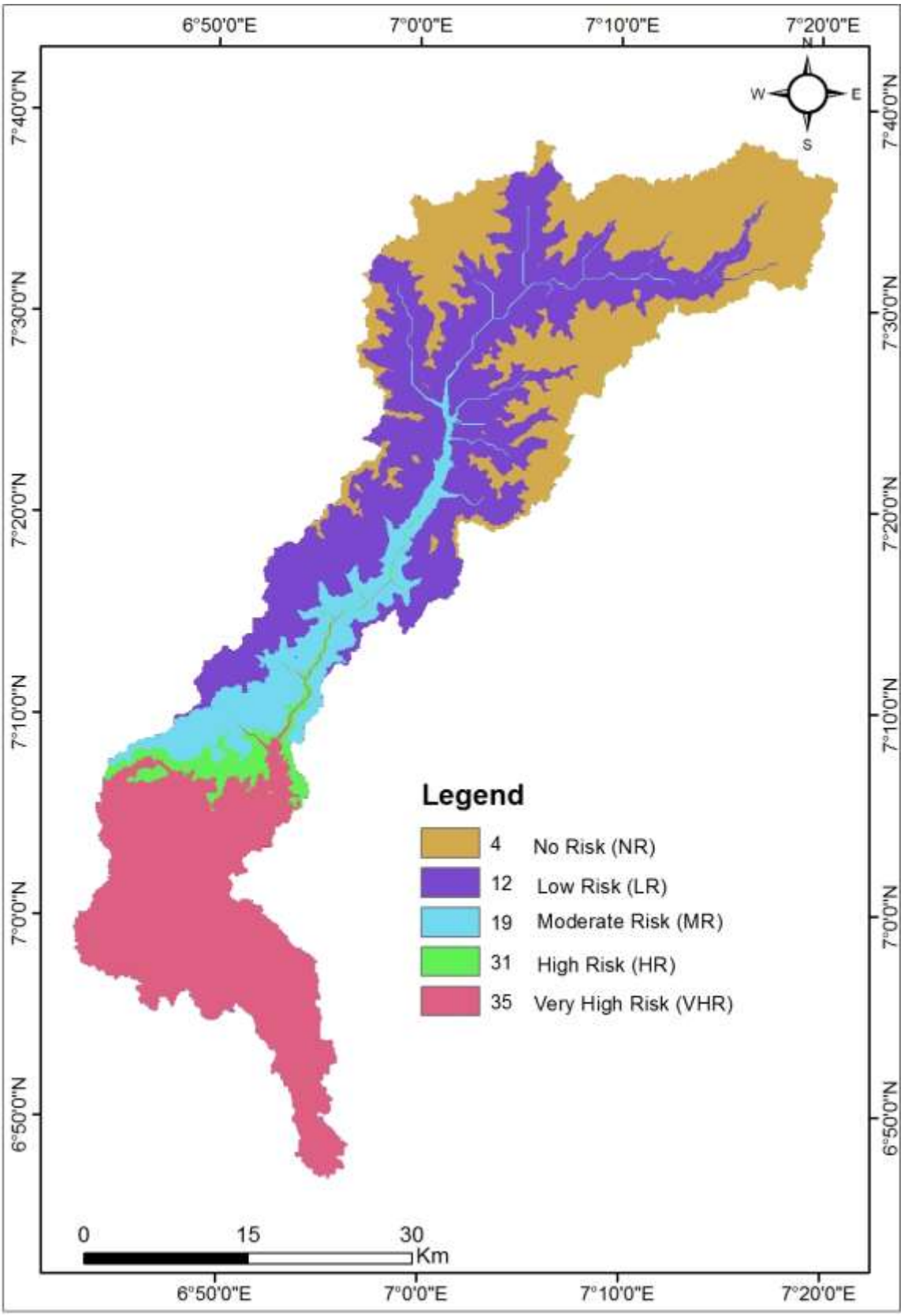


Fig. 4.34: Reclassified Elevation Layer for Multi-Criteria Evaluation

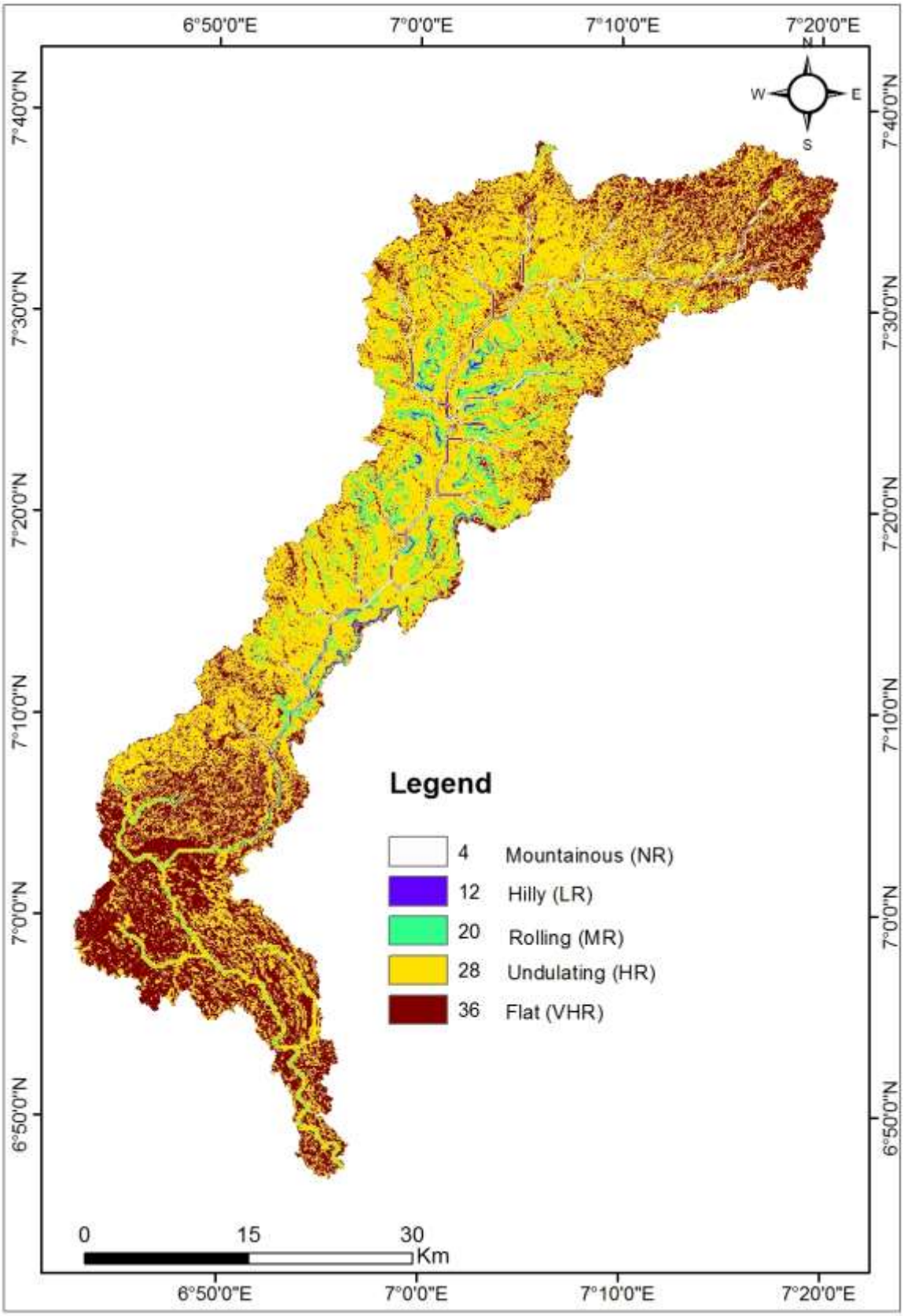


Fig. 4.35: Reclassified Slope Layer for Multi-Criteria Evaluation

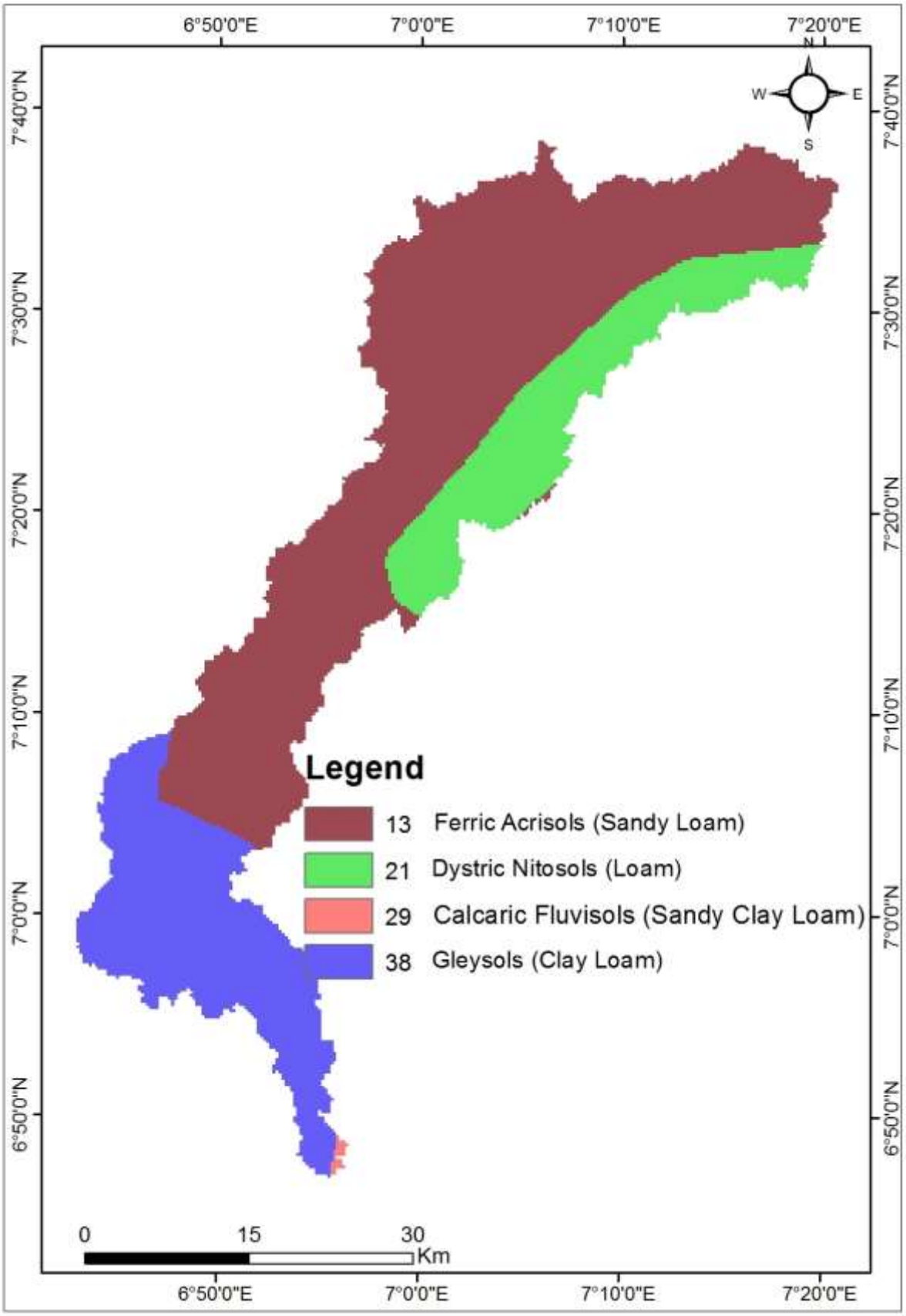


Fig. 4.36: Reclassified Soil Layer for Multi-Criteria Evaluation

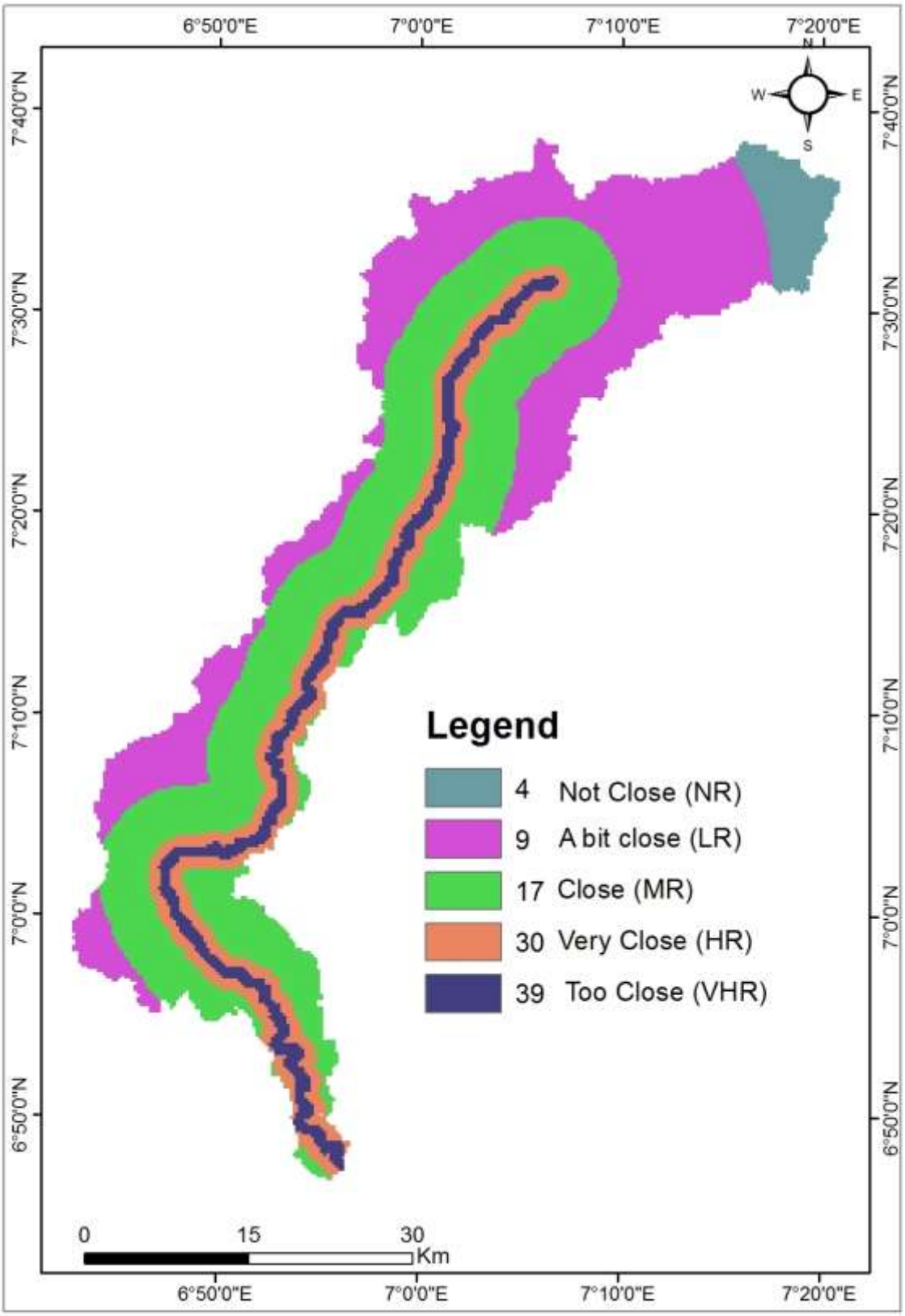


Fig. 4.37: Reclassified Corridor Layer for Multi-Criteria Evaluation

4.5.1.3 Criterion weights of flood causative factors and integration of thematic maps

The results of the comparison of the four flood causative factors using the Analytical Hierarchical Process (AHP) are presented in Table 4.25.

Table 4.25: Criterion Weight for Causative Factors

	Elevation	Corridor	Slope	Soil	Weight	Weight*100
Elevation	1	1	9/8	9/5	0.29	29
Corridor	1	1	9/8	9/5	0.29	29
Slope	8/9	8/9	1	8/5	0.26	26
Soil	5/9	5/9	5/8	1	0.16	16
					1	100
					CR =	0.00

Elevation and corridor ranked equally first with a weight of 29 each followed closely by slope with a weight of 26 while soil ranked least with a weight of 16. A consistency ratio of 0.00 was obtained for the pair-wise comparison which implies that the decision is correct. The thematic maps of flood causative factors were integrated using the criterion weights derived. The output Hazard map is classified as shown in Fig. 4.38.

The output map (Fig. 4.38) was classified into 'High Hazard', 'Moderate Hazard' and 'Low Hazard'. The high hazard class represents the extent of inundation by flood water.

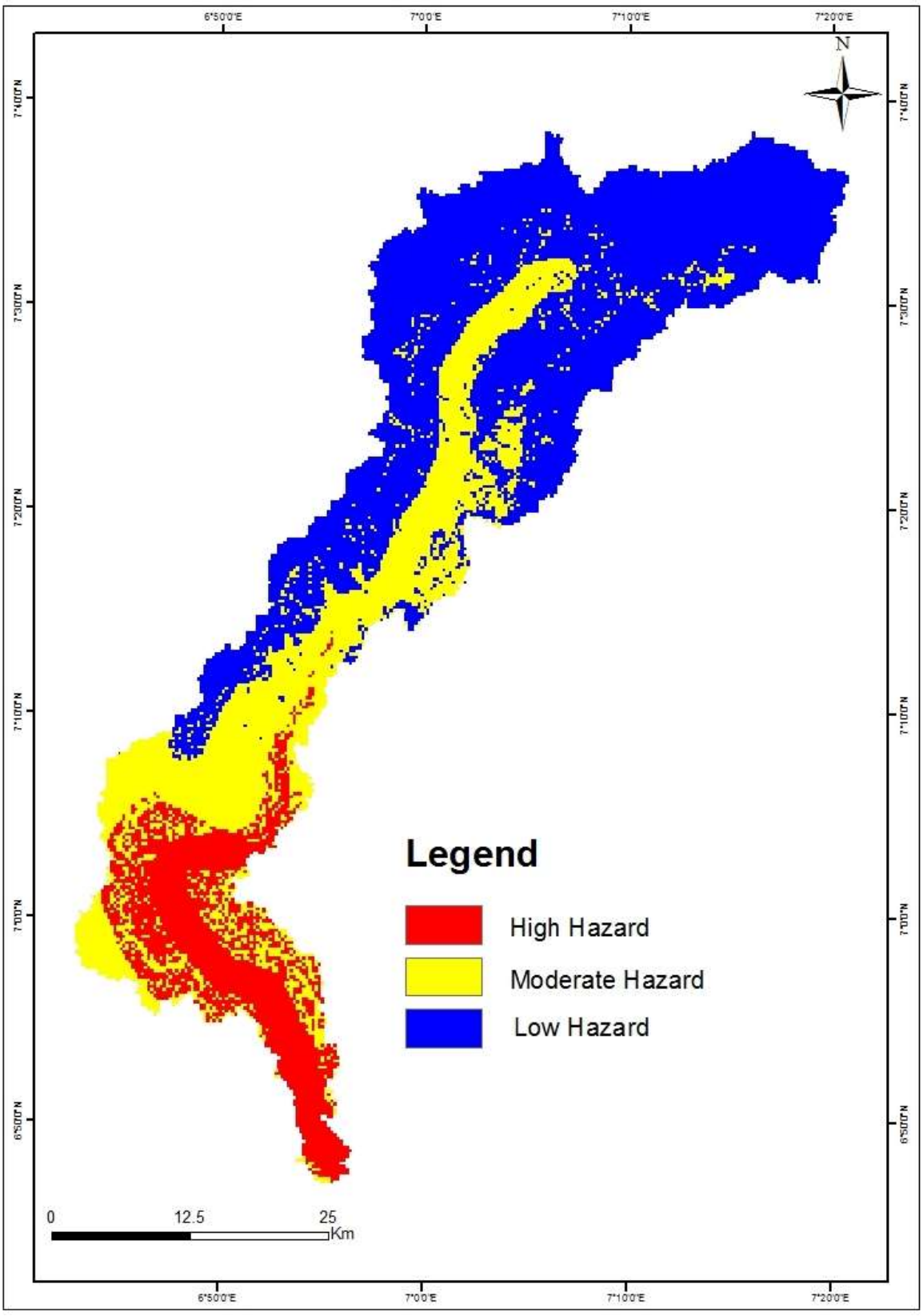


Fig. 4.38: Flood Hazard Map by Multi-Criteria Evaluation Method

4.5.2 Hydraulic Modelling for Development of Flood Inundation and Hazard Maps

4.5.2.1 Flood inundation simulation in HEC-GeoRAS/ArcGIS

The bounding polygon which defines the analysis extent for flood inundation mapping and the digital elevation model (DEM) converted from the terrain triangulated irregular network surface (TIN) are shown in the Fig. 4.39.

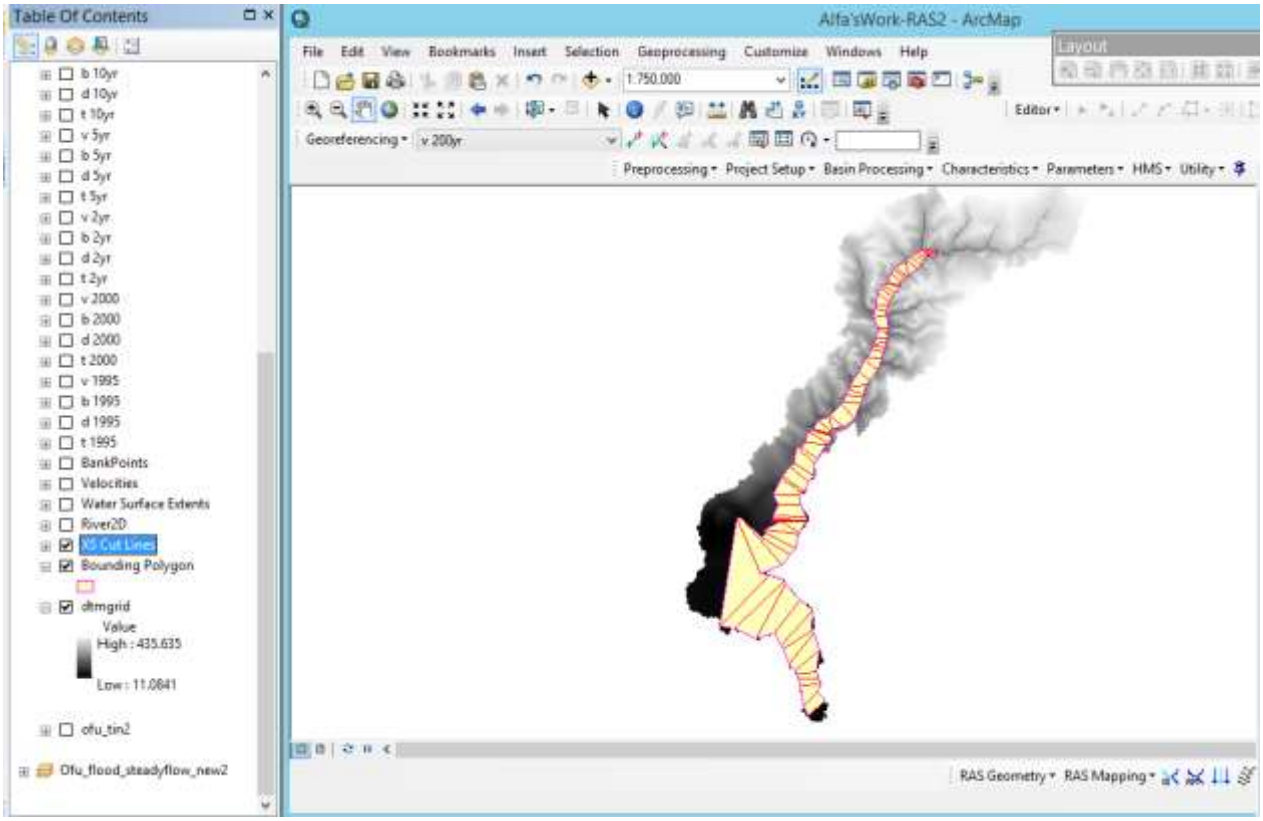


Fig. 4.39: Processed DEM and Bounding Polygon Using HEC-GeoRAS

More so, the water surface TIN, water surface GRID and velocity GRID are shown in Fig. 4.40.

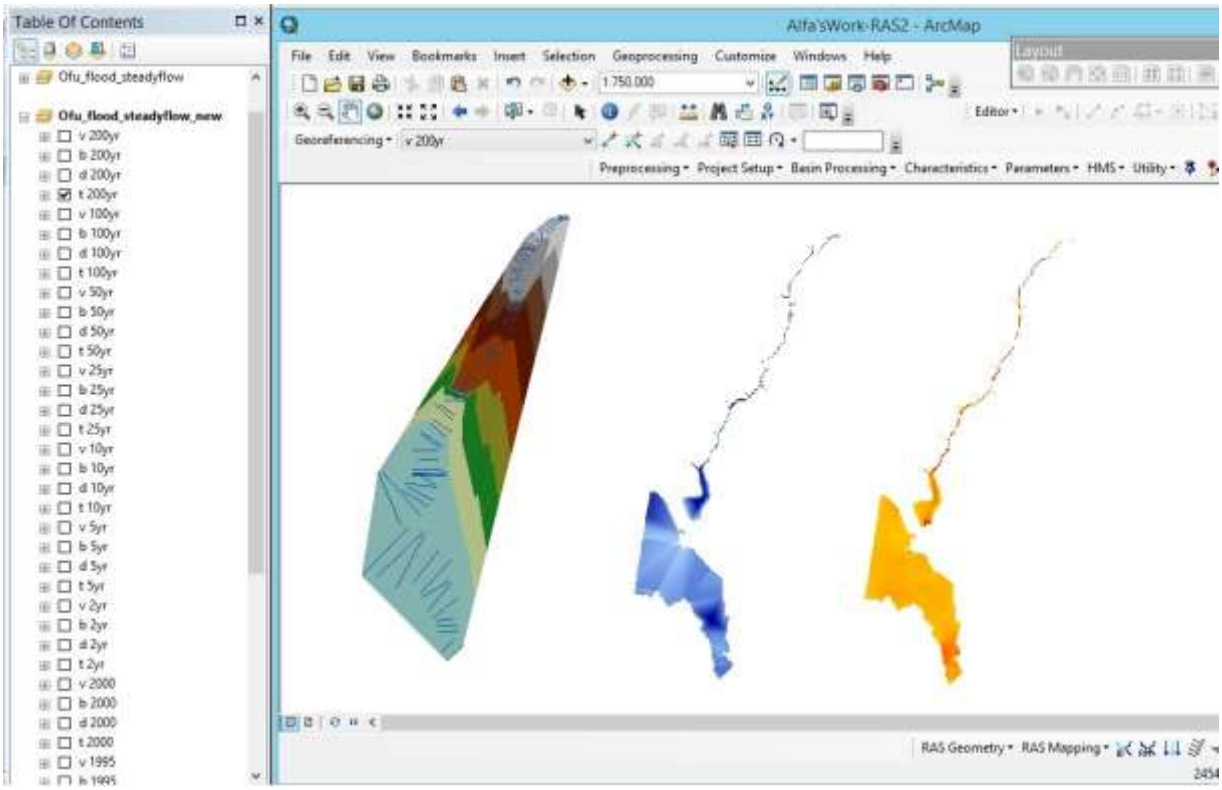


Fig. 4.40: Water Surface TIN, Water Surface Grid and Velocity Grid

The TIN created represent the water surface elevation which includes all the outer points of the bounding polygon. This implies that the TIN takes into account all areas that are within the possible flood inundation extent. The water surface GRID on the other hand is a result of water surface TIN conversion. It is the digital elevation model of the water surface.

The flood inundation depth and extent are determined by subtracting the terrain DEM from the water surface GRID in the Flood delineation process. This process results in the creation of the flood area map. The flood inundation process produced flood maps for the 1995 and 2000 flood events as well as the floods of the inputted return periods of 2, 5, 10, 25, 50, 100 and 200 years.

The flood depths, flood inundation extents and flood velocities obtained from flood inundation mapping in HEC-GoeRAS/ArcGIS are shown in Table 4.26.

Table 4.26: Area, Depth and Velocity of Flood Inundated Water

Return Period/Scenario	Area (km^2)	Depth (m)		Velocity (m/s)	
		Range	Average	Range	Average
200	267.37	0.000092 - 11.76	8.28	0 - 2.75	0.46
100	266.84	0.000015 - 11.70	8.12	0 - 2.62	0.46
50	265.96	0.000023 - 11.63	8.00	0 - 2.60	0.45
25	262.34	0.000008 - 11.56	7.93	0 - 2.57	0.45
10	258.17	0.000034 - 11.01	7.78	0 - 2.53	0.44
5	256.34	0.000011 - 10.91	7.59	0 - 2.50	0.42
2	252.63	0.000004 - 10.72	7.28	0 - 2.42	0.40
2000	251.80	0.000027 - 10.72	7.29	0 - 2.42	0.40
1995	251.98	0.000019 - 10.73	7.30	0 - 2.43	0.40

Table 4.26 shows that average velocity of flood water is less than 1 m/s for the scenarios analysed which implies that the challenge of flood within Ofu River catchment is not actually a function of the velocity but just the inundation. This explains why no death or injury has ever been recorded.

The flood inundation extents for 1995, 2000, 100-year and 200-year floods are shown in Fig. 4.41a –d

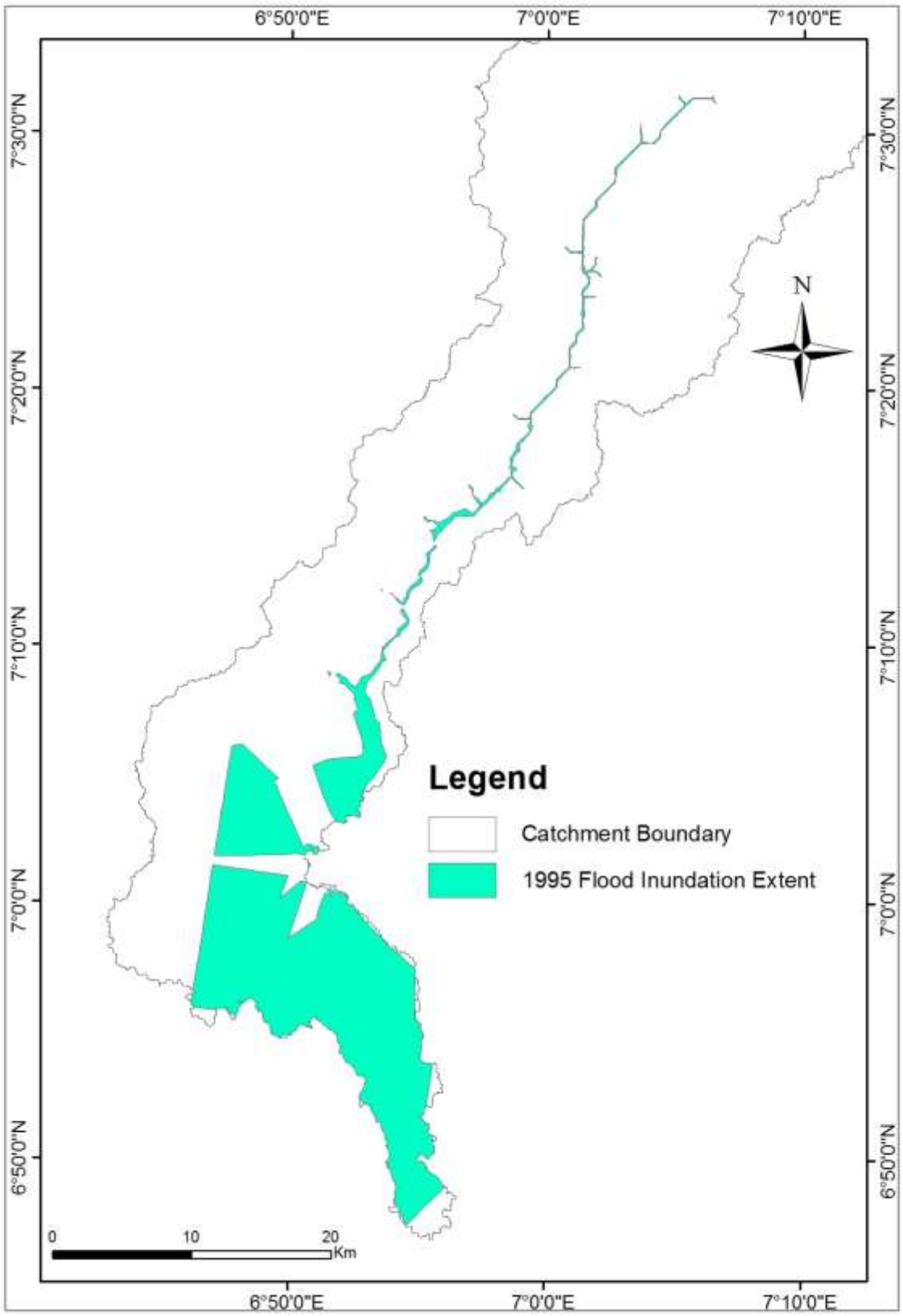


Fig. 4.41a: 1995 Flood Inundation Extent

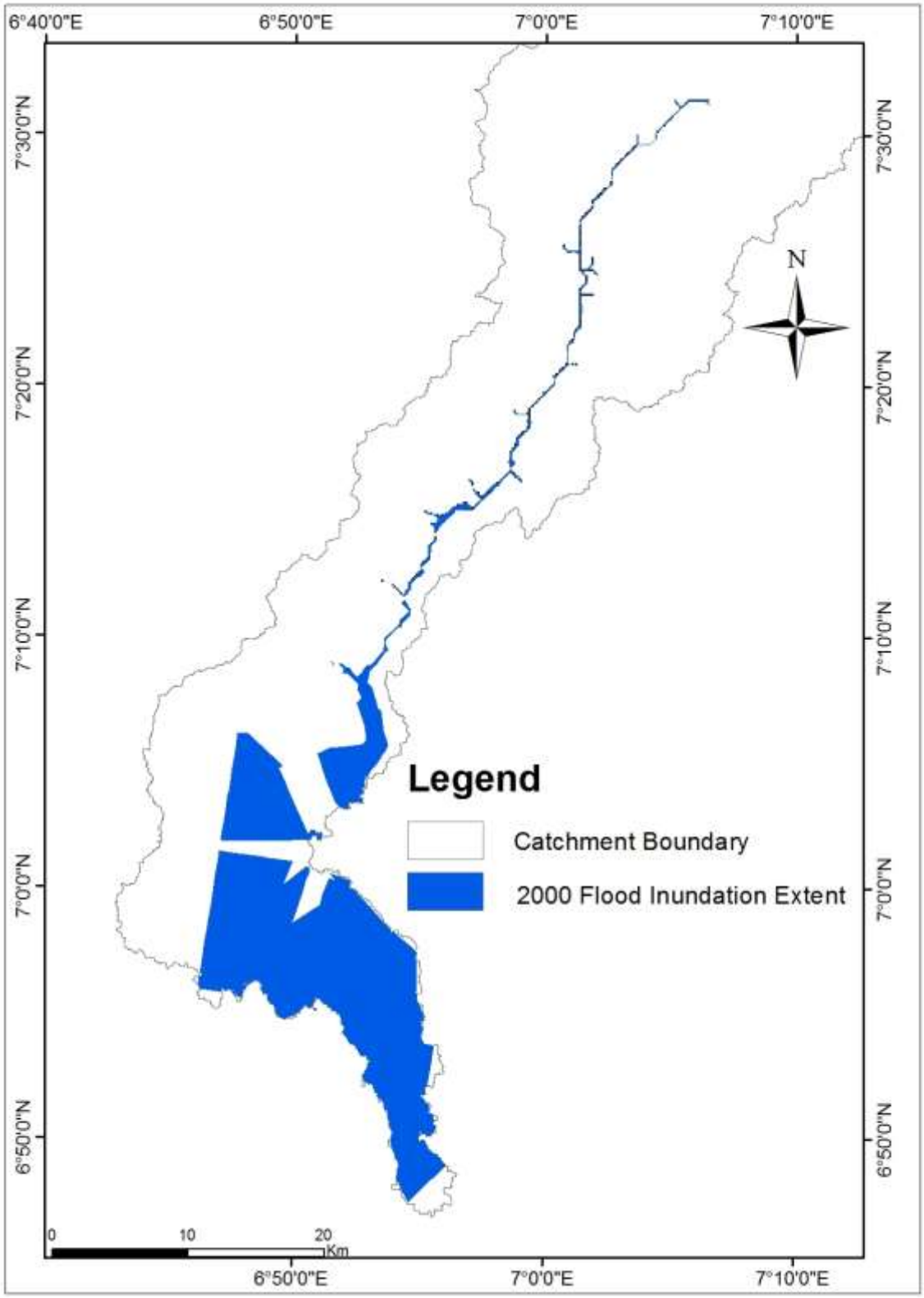


Fig. 4.41b: 2000 Flood Inundation Extent

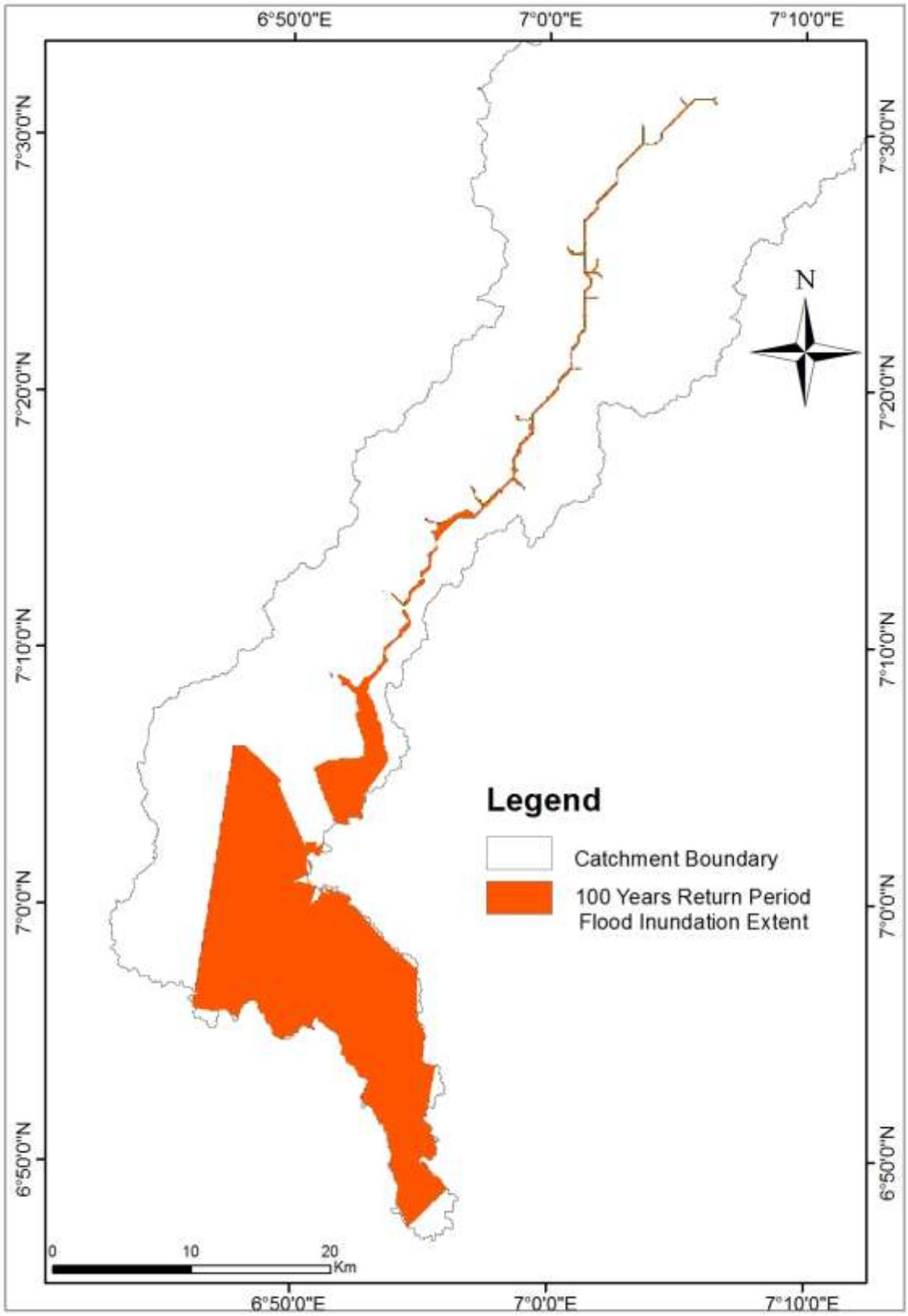


Fig. 4.41c: 100-Year Flood Inundation Extent

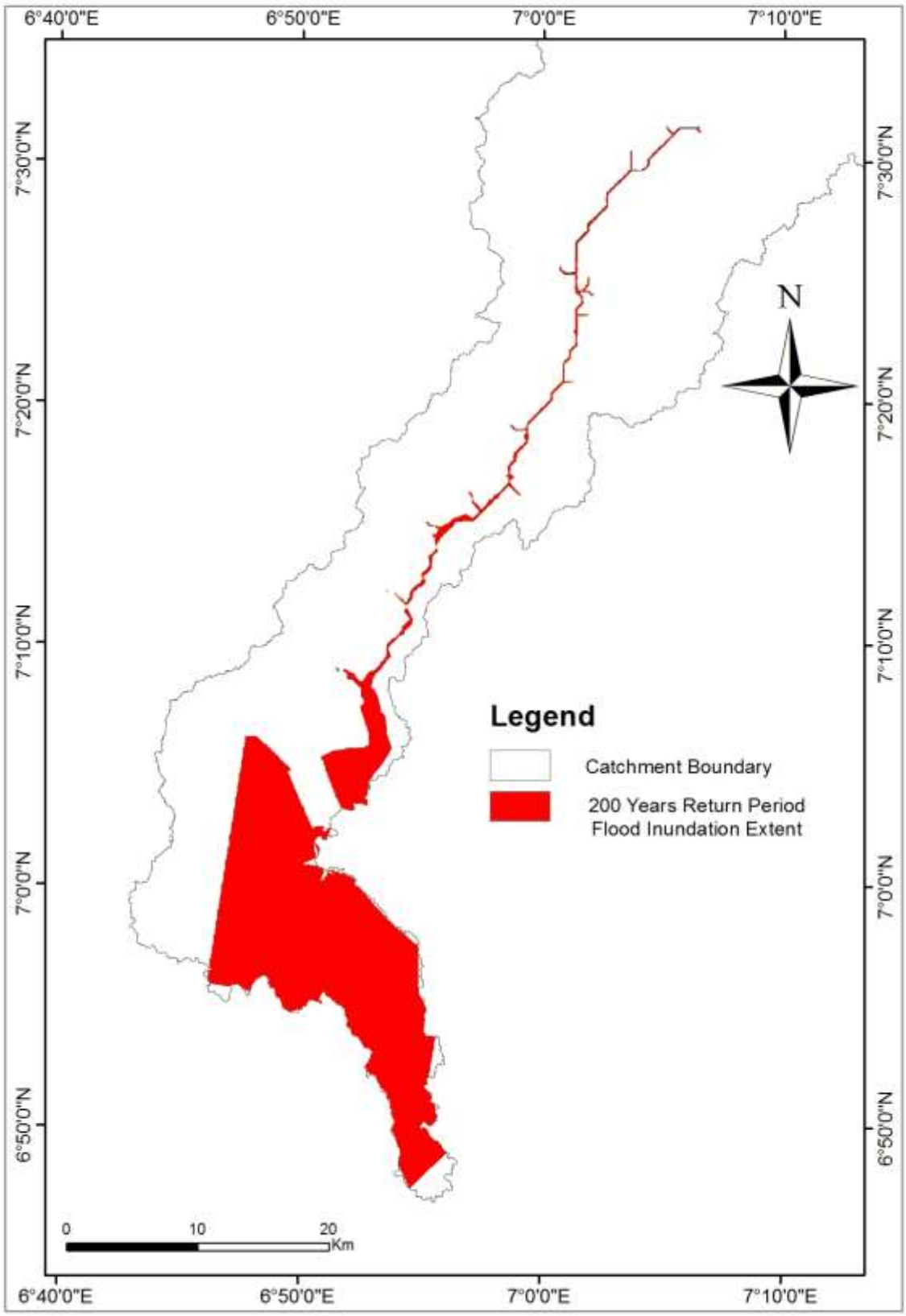


Fig. 4.41d: 200-Year Flood Inundation Extent

4.5.3 Results of the Comparison of Extent of Flood Inundation from both Methods

Table 4.27 shows a comparison between the extents of flood inundation obtained by the method of thematic integration of causative factor maps (multi-criteria evaluation) and the one-dimensional steady flow modelling in HEC-RAS/HEC-GeoRAS.

Table 4.27: Comparison of Flood Inundation Extents by both Methods

Method	Scenario/Return Period	Inundation Area (km^2)
Integration of Thematic Maps	**NA**	257.49
HEC-RAS Modelling	Year 1995	251.98
	Year 2000	251.80
	2 Years	252.63
	5 Years	256.34
	10 Years	258.17
	25 Years	262.34
	50 Years	265.96
	100 Years	266.84
	200 Years	267.37

Table 4.27 shows that the inundation extent for the thematic integration method (multi-criteria evaluation) is 257.49 km^2 while those for the HEC-RAS modelling ranged from 251.80 km^2 (year 2000 flood event) to 267.37 km^2 (200 year flood). The inundation extent obtained through the thematic integration is a bit similar to the 5 years return period (256.34 km^2) and 10 years return period (258.17 km^2) flood inundation extents obtained via HEC-RAS modelling. Since the HEC-RAS model allows for easy use of hydrologically generated stream flow for different flood scenarios and different return periods, the results obtained via the one-dimensional steady flow modelling in HEC-RAS/HEC-GeoRAS was used for the flood hazard, vulnerability and risk analysis.

4.6 FLOOD RISK ANALYSIS

4.6.1 Flood Hazard Assessment

The flood hazard maps for 1995 and 2000 flood events are shown in Fig. 4.42a and b.

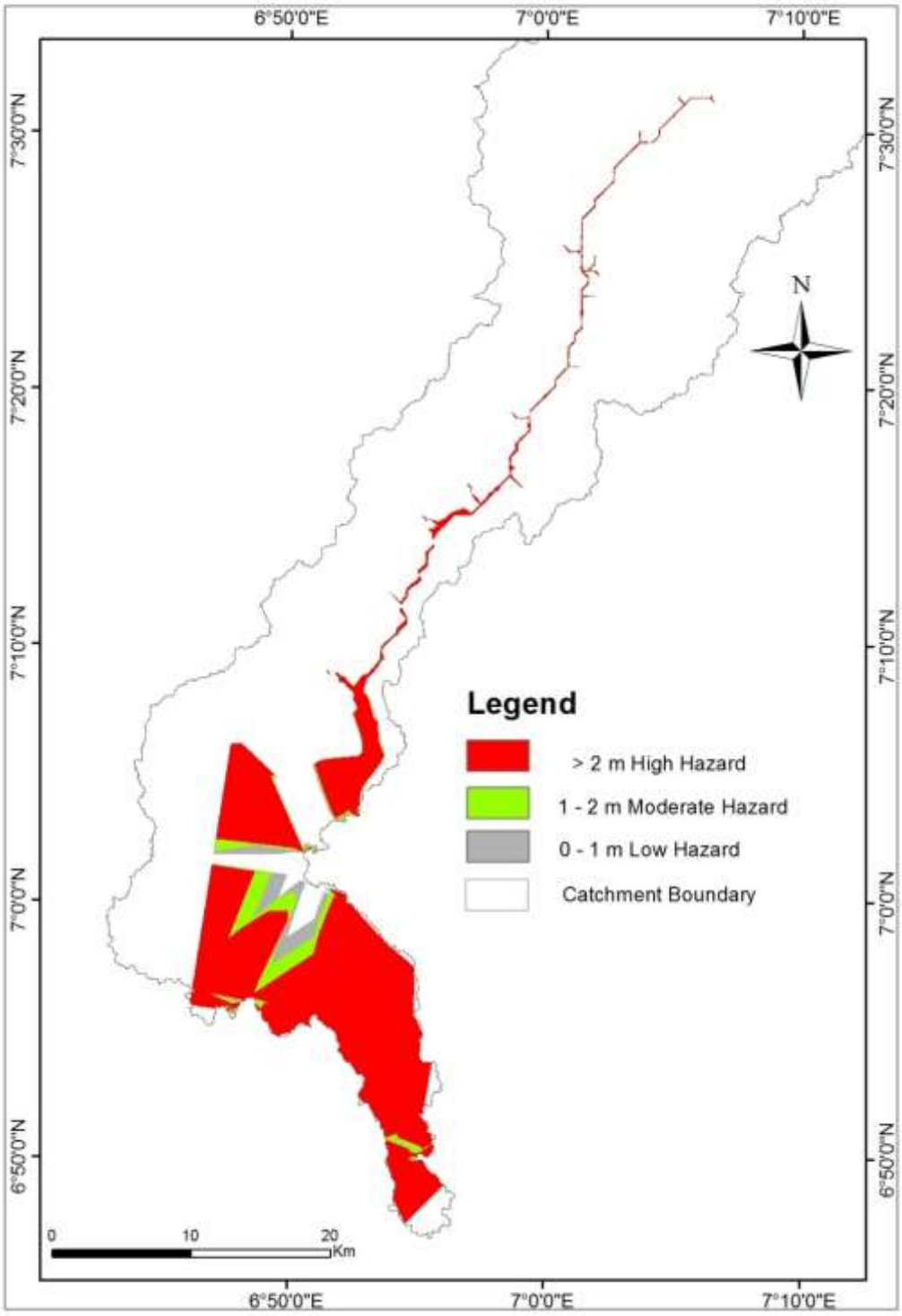


Fig. 4.42a: 1995 Flood Hazard Map

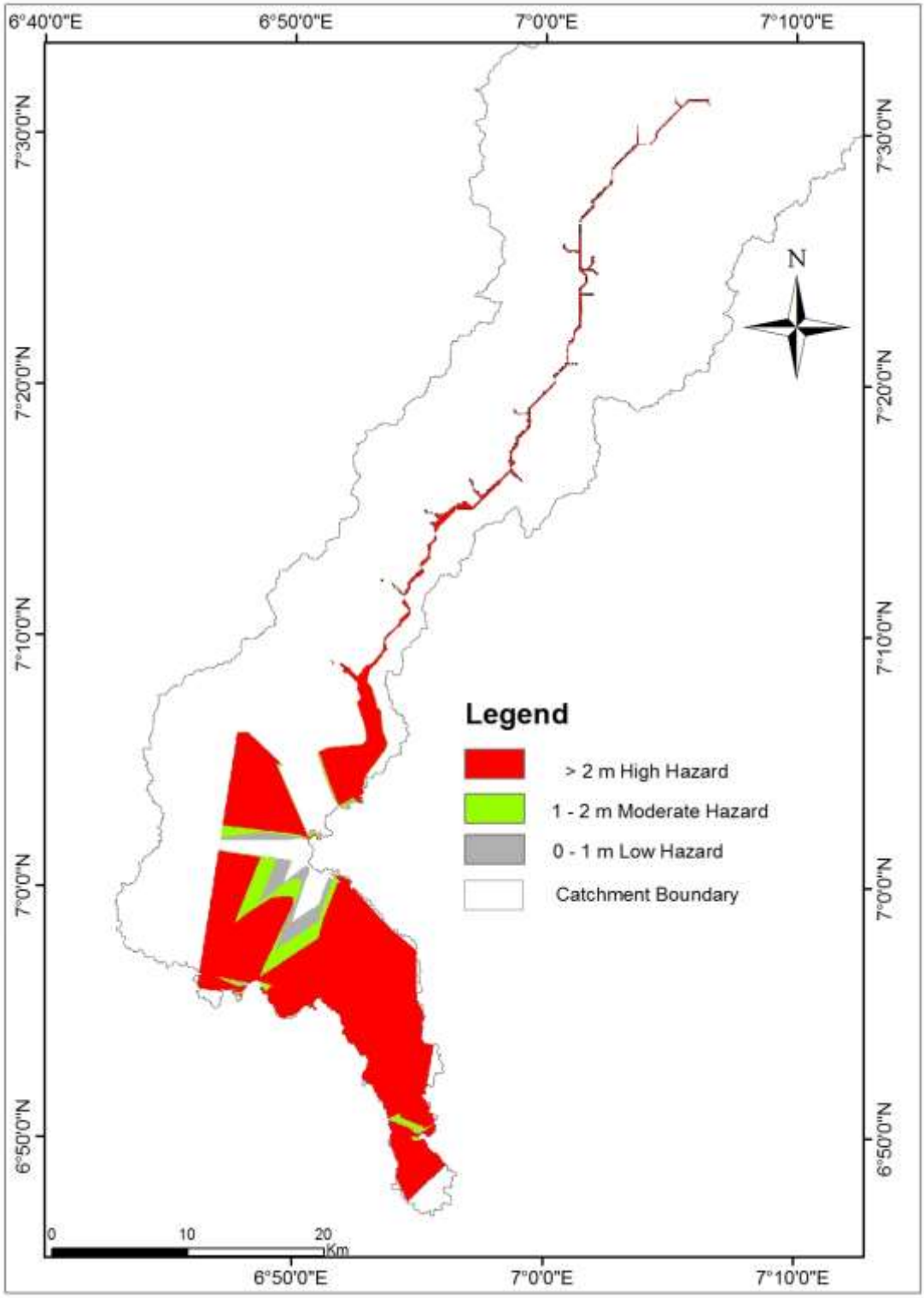


Fig. 4.42b: 2000 Flood Hazard Map

The flood hazard maps for 100 and 200 years return periods are shown in Fig. 4.42c and d.

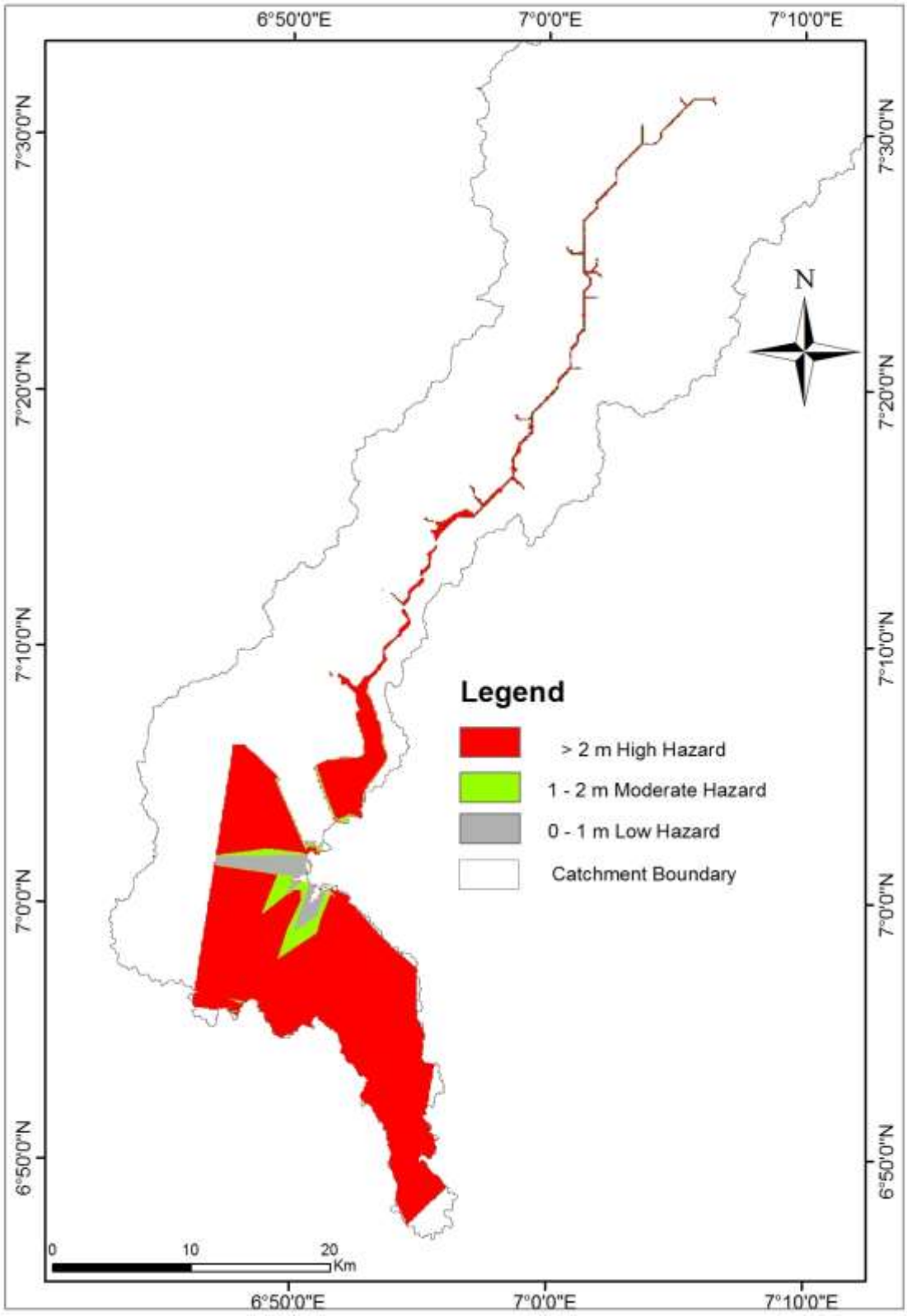


Fig. 4.42c: 100 Year Flood Hazard Map

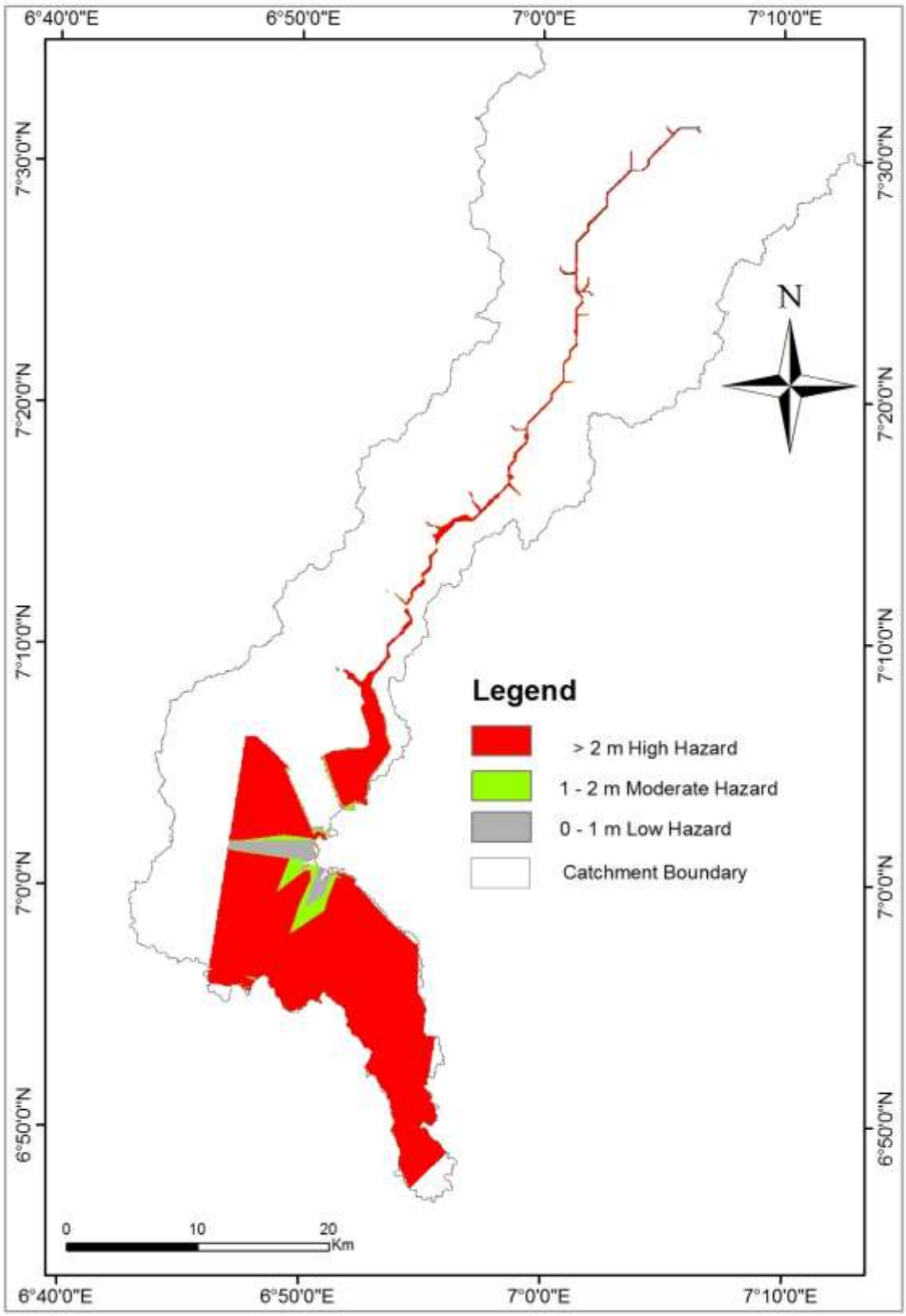


Fig. 4.42d: 200 Year Flood Hazard Map

Details of the classifications and the extent of each class for 1995 and 2000 flood events as well as the 100 and 200 years return periods are presented in Table 4.28.

Table 4.28: Flood Hazard Zones/extent for Year 1995, Year 2000, 100 years and 200 years Return Periods Floods

Scenario/Return Period	Hazard Zone			Total
	High	Moderate	Low	
Year 1995	218.232	20.250	14.481	252.963
Year 2000	217.832	20.331	14.630	252.793
100 Years	242.366	12.711	12.756	267.833
200 Years	244.939	11.496	11.937	268.372

Table 4.28 shows that the High hazard zone covered an area of 218.232 km^2, 217.832 km^2, 242.366 km^2 and 244.939 km^2 for year 1995, year 2000, 100 years and 200 years return periods floods, respectively. The moderate hazard category covered 20.250 km^2, 20.331 km^2, 12.711 km^2 and 11.496 km^2, respectively while the low hazard category covered 14.481 km^2, 14.630 km^2, 12.756 km^2 and 11.937 km^2, respectively.

4.6.2 Flood vulnerability assessment

4.6.2.1 Estimation of population at risk

The total population affected by the 1995, 2000, 100-year and 200-year flood inundations are presented in Table 4.29 and 4.30. Details of the calculations are presented in Table XIXa and b (Appendix XIX).

Table 4.29: Population at Risk for 1995 and 2000 Flood Scenarios

State	LGA	Persons affected	
		1995	2000
Kogi	Dekina	161	183
	Ofu	481	581
	Igalamela/Odolu	5245	6085
	Idah	0	0
	Ibaji	10889	12648
Enugu	Uzo-Uwani	156	176
		16932	19673

The results in Table 4.29 show that a total of 16, 932 and 19,673 persons were affected by the year 1995 and 2000 flood events, respectively.

Table 4.30: Population at Risk for 100-years and 200-years Return Periods

State	LGA	Persons affected	
		100 Years	**200 Years**
	Dekina	828	11269
	Ofu	5147	232184
Kogi	Igalamela/Odolu	26120	527132
	Idah	0	0
	Ibaji	60179	1208741
Enugu	Uzo-Uwani	459	5051
		92733	1984377

The results in Table 4.30 on the other hand show that a total of 92,733 and 1,984,377 persons will be affected by the 100-years and 200-years flood events, respectively.

The affected population for year 1995 flood scenario distributed by age, disability status, poverty level and gender are presented in Table 4.31.

Table 4.31 shows that a total of 111 persons under 15 years with disabilities were affected by the 1995 flood while those under 15 years with no disabilities were 7576 persons. Six (6) persons above 65 years with disabilities were affected while those above 65 years with no disabilities were 469 persons. Furthermore, 126 persons between 15 – 65 years with disabilities were affected while those with no disabilities (15 – 65 years) were 8,644 persons. The results also show that a total of 12,429 persons were in poverty while 4,503 persons were above poverty level. Finally, a total of 8,196 and 8,736 persons were male and female, respectively.

More so, the affected population for the 2000 flood scenario distributed by age, disability status, poverty level and gender are presented in Table 4.32.

Table 4.31: Population at Risk by Age groups, Poverty level and Gender for year 1995 Flood Scenario

State	LGA	Population within Inundated Area (Persons)									
		Under 15 Years		Above 65 Years		15 - 65 Years		Poverty		Gender	
		WD	ND	WD	ND	WD	ND	In Poverty	Above Poverty	Male	Female
Kogi	Dekina	1	73	0	5	1	81	118	43	78	83
	Ofu	3	216	0	14	3	245	353	128	233	248
	Igalamela/Odolu	36	2350	2	144	41	2672	3850	1395	2539	2706
	Ibaji	70	4882	4	298	79	5556	7993	2896	5272	5617
Enugu	Uzo-Uwani	1	55	0	8	2	90	115	41	74	82
Total		111	7576	6	469	126	8644	12429	4503	8196	8736

WD (With Disability); ND (No Disability)

Table 4.32: Population at Risk by Age groups, Poverty level and Gender for 2000 Flood Scenario

State	LGA	Population within Inundated Area (Persons)									
		Under 15 Years		Above 65 Years		15 - 65 Years		Poverty		Gender	
		WD	ND	WD	ND	WD	ND	In Poverty	Above Poverty	Male	Female
Kogi	Dekina	1	83	0	6	1	92	134	49	88	95
	Ofu	3	262	0	17	4	295	426	155	281	300
	Igalamela/Odolu	41	2727	3	166	47	3101	4466	1619	2946	3139
	Ibaji	81	5671	5	346	92	6453	9284	3364	6123	6525
Enugu	Uzo-Uwani	1	62	0	8	2	103	129	47	84	92
Total		128	8804	7	543	146	10044	14440	5233	9522	10151

WD (With Disability); ND (No Disability)

The results in Table 4.32 show that a total of 128 persons under 15 years with disabilities and 8,804 persons with no disabilities were affected by the 2000 flood, while, seven (7) persons above 65 years with disabilities and 543 persons with no disabilities were affected. Furthermore, population of affected persons between 15 – 65 years were 146 persons with disabilities and 10,044 persons with no disabilities. The results further reveal that a total of 14,440 persons and 5,233 were in poverty and above poverty level, respectively while, a total of 9,522 and 10,151 persons were male and female, respectively.

Furthermore, the affected population for the 100-year flood distributed by age, disability status, poverty level and gender are presented in Table 4.33.

The results in Table 4.33 show that a total of 600 persons under 15 years with disabilities and 41,527 persons with no disabilities would be affected by the 100-year flood, while, 37 persons above 65 years with disabilities and 2,542 persons with no disabilities would be affected. More so, population of persons between 15 – 65 years that would be affected are 685 persons with disabilities and 47,342 persons with no disabilities. The results further reveal that a total of 63,986 persons and 28,747 are in poverty and above poverty level, respectively while, a total of 46.867 and 45,866 persons were male and female, respectively.

The affected population for the 200-year flood distributed by age, disability status, poverty level and gender are presented in Table 4.34.

The results in Table 4.34 show that a total of 12,735 persons under 15 years with disabilities and 888,154 persons with no disabilities would be affected by the 200-year flood, while, 779 persons above 65 years with disabilities and 54,297 persons with no disabilities would be affected.

Table 4.33: Population at Risk by Age groups, Poverty level and Gender for 100 Year Flood

State	LGA	Population within Inundated Area (Persons)									
		Under 15 Years		Above 65 Years		15 - 65 Years		Poverty		Gender	
		WD	ND	WD	ND	WD	ND	In Poverty	Above Poverty	Male	Female
Kogi	Dekina	6	371	0	23	6	422	571	257	417	411
	Ofu	29	2312	2	141	34	2629	3551	1596	2599	2548
	Igalamela/Odolu	177	11701	11	713	202	13316	18023	8097	13231	12889
	Ibaji	385	26982	23	1645	438	30706	41524	18655	30390	29789
Enugu	Uzo-Uwani	3	161	0	21	5	269	317	142	230	229
Total		600	41527	37	2542	685	47342	63986	28747	46867	45866

WD (With Disability); ND (No Disability)

Table 4.34: Population at Risk by Age groups, Poverty level and Gender for 200 Year Flood

State	LGA	Population within Inundated Area (Persons)									
		Under 15 Years		Above 65 Years		15 - 65 Years		Poverty		Gender	
		WD	ND	WD	ND	WD	ND	In Poverty	Above Poverty	Male	Female
Kogi	Dekina	75	5050	5	308	85	5746	7776	3493	5674	5595
	Ofu	1329	104256	81	6353	1512	118653	160207	71977	117221	114963
	Igalamela/Odolu	3567	235144	218	14389	4091	269723	363721	163411	267025	260107
	Ibaji	7730	541940	471	33024	8797	616779	834031	374710	610406	598335
Enugu	Uzo-Uwani	35	1763	4	223	59	2967	3485	1566	2533	2518
Total		12735	888154	779	54297	14545	1013867	1369220	615157	1002859	981518

WD (With Disability); ND (No Disability)

Furthermore, population of persons between 15 – 65 years that would be affected are 14,545 persons with disabilities and 1,013,867 persons with no disabilities. The results further reveal that a total of 1,369,220 persons and 615,157 are in poverty and above poverty level, respectively while, a total of 1,002,859 and 981,518 persons are male and female, respectively.

Thus, a total of ten (10) vulnerability groups were created for each flood event. The vulnerability classes are WD15 (under 15 years with disabilities), ND15 (under 15 years with no disabilities, WD65 (above 65 years with disabilities), ND65 (above 65 years with no disabilities), WD15_65 (between 15 - 65 years with disabilities), ND15_65 (between 15 – 65 years with no disabilities), InPov (In poverty), AbPov (Above Poverty level), Male and Female.

Further detailed calculations are presented in Table XIXc-h (Appendix XIX).

4.6.3 Derivation of Population Vulnerability Weights

The weights derived for each LGA under each of the vulnerability classes for 1995 and 2000 flood scenarios as well as 100-year and 200-year flood events are presented in Tables 4.35 - 4.38.

The results in Table 4.39 shows that WD15 and WD65 ranked highest with a weight of 13 each followed by ND15 with a weight of 12, ND65 with weight of 11, while WD15_65, InPov and Female had a weight of 10 respectively. ND15_65, AbPov and Male ranked least with a weight of 7 each. The weights represent the level of vulnerability of each class to flood disaster. The consistency ratio of 0.00 obtained show that the pair-wise comparison is correct and the decision can be accepted. Furthermore, the weights of each vulnerability class in the overall vulnerability analysis are presented in Table 4.39.

Table 4.35: Vulnerability Weights for all Population Categories for 1995 Flood Scenario

State	LGA	Vulnerability Weight *100									
		Under 15 Years		Above 65 Years		15 - 65 Years		Poverty		Gender	
		WD	ND	WD	ND	WD	ND	In Poverty	Above Poverty	Male	Female
Kogi	Dekina	1	1	0	2	1	1	1	1	1	1
	Ofu	4	4	0	5	4	4	4	4	4	4
	Igalamela/Odolu	51	48	50	48	52	48	48	48	48	48
	Ibaji	100	100	100	100	100	100	100	100	100	100
Enugu	Uzo-Uwani	1	1	0	3	3	2	1	1	1	1

WD (With Disability); ND (No Disability)

Table 4.36: Vulnerability Weights for all Population Categories for 2000 Flood Scenario

State	LGA	Vulnerability Weight *100									
		Under 15 Years		Above 65 Years		15 - 65 Years		Poverty		Gender	
		WD	ND	WD	ND	WD	ND	In Poverty	Above Poverty	Male	Female
Kogi	Dekina	2	1	0	2	1	1	1	1	1	1
	Ofu	4	5	0	5	4	5	5	5	5	5
	Igalamela/Odolu	51	48	51	48	51	48	48	48	48	48
	Ibaji	100	100	100	100	100	100	100	100	100	100
Enugu	Uzo-Uwani	2	1	0	2	2	2	1	1	1	1

WD (With Disability); ND (No Disability)

Table 4.37: Vulnerability Weights for all Population Categories for 100 Year Flood

State	LGA	Vulnerability Weight *100									
		Under 15 Years		Above 65 Years		15 - 65 Years		Poverty		Gender	
		WD	ND	WD	ND	WD	ND	In Poverty	Above Poverty	Male	Female
Kogi	Dekina	1	1	1	1	1	1	1	1	1	1
	Ofu	8	9	8	9	8	9	9	9	9	9
	Igalamela/Odolu	46	43	46	43	46	43	43	43	44	43
	Ibaji	100	100	100	100	100	100	100	100	100	100
Enugu	Uzo-Uwani	1	1	2	1	1	1	1	1	1	1

WD (With Disability); ND (No Disability)

Table 4.38: Vulnerability Weights for all Population Categories for 200 Year Flood

State	LGA	Vulnerability Weight *100									
		Under 15 Years		Above 65 Years		15 - 65 Years		Poverty		Gender	
		WD	ND	WD	ND	WD	ND	In Poverty	Above Poverty	Male	Female
Kogi	Dekina	1	1	1	1	1	1	1	1	1	1
	Ofu	17	19	17	19	17	19	19	19	19	19
	Igalamela/Odolu	46	43	46	44	47	44	44	44	44	43
	Ibaji	100	100	100	100	100	100	100	100	100	100
Enugu	Uzo-Uwani	0	0	1	1	1	0	0	0	0	0

WD (With Disability); ND (No Disability)

Table 4.39: Overall Weights for All Vulnerability Maps derived by AHP

	WD15	ND15	WD65	ND65	WD15_65	ND15_65	Inpov	Abpov	Male	Female	Weight	Weight*100
WD15	1	9/8	1	9/8	9/7	9/5	9/7	9/5	9/5	9/7	0.13	13
ND15	8/9	1	8/9	1	8/7	8/5	8/7	8/5	8/5	8/7	0.12	12
WD65	1	9/8	1	9/8	9/7	9/5	9/7	9/5	9/5	9/7	0.13	13
ND65	8/9	1	8/9	1	8/7	8/5	8/7	8/5	8/5	8/7	0.11	11
WD15_65	7/9	7/8	7/9	7/8	1	7/5	1	7/5	7/5	1	0.10	10
ND15_65	5/9	5/8	5/9	5/8	5/7	1	5/7	1	1	5/7	0.07	7
Inpov	7/9	7/8	7/9	7/8	1	7/5	1	7/5	7/5	1	0.10	10
Abpov	5/9	5/8	5/9	5/8	5/7	1	5/7	1	1	5/7	0.07	7
Male	5/9	5/8	5/9	5/8	5/7	1	5/7	1	1	5/7	0.07	7
Female	7/9	7/8	7/9	7/8	1	7/5	1	7/5	7/5	1	0.10	10
											1.00	100
											CR =	0.00

WD (With Disability); ND (No Disability)

The resulting flood vulnerability maps for 1995, 2000, 100-year and 200-year floods are presented in Fig. 4.43a-d.

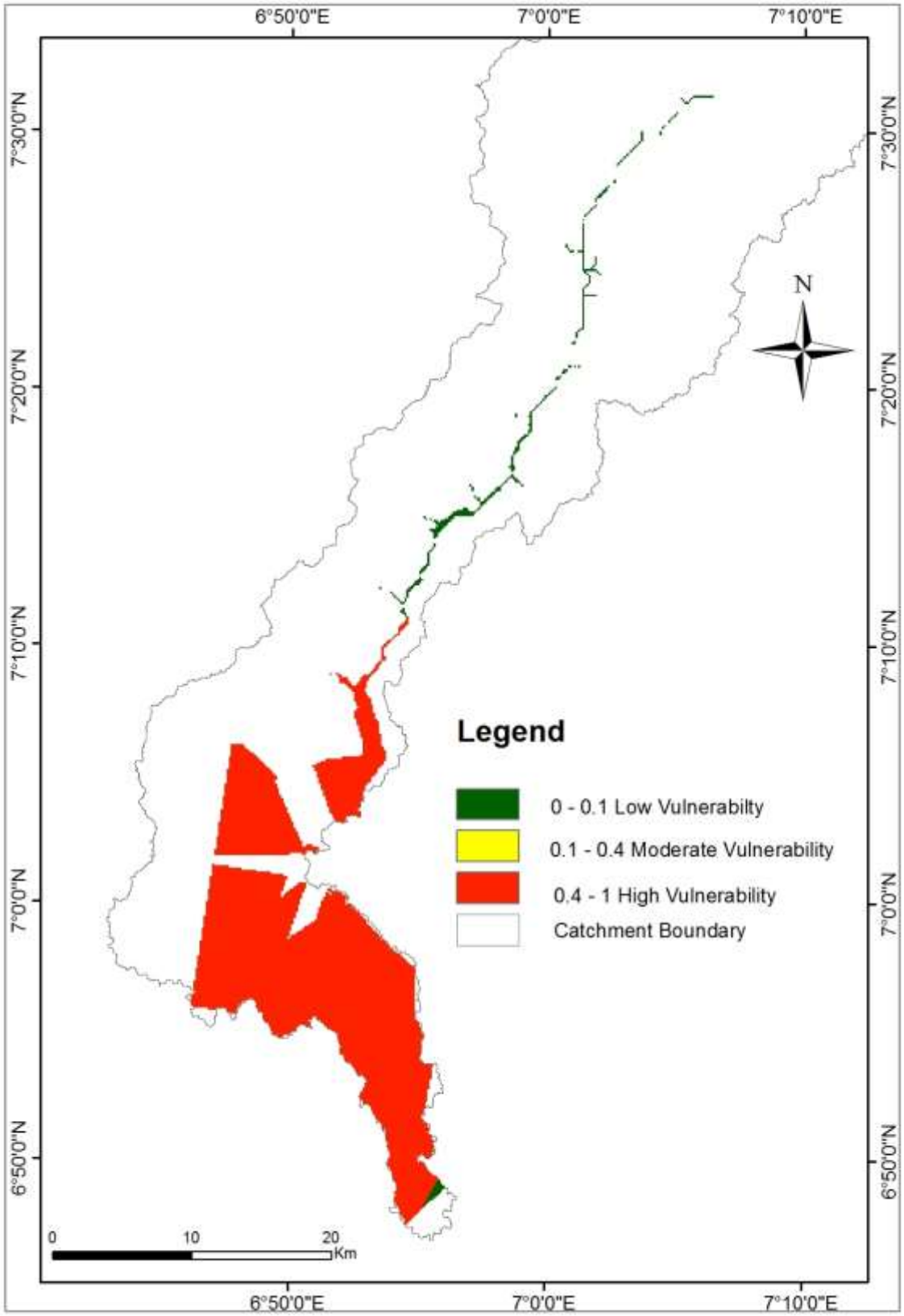


Fig. 4.43a: 1995 Flood Vulnerability Map

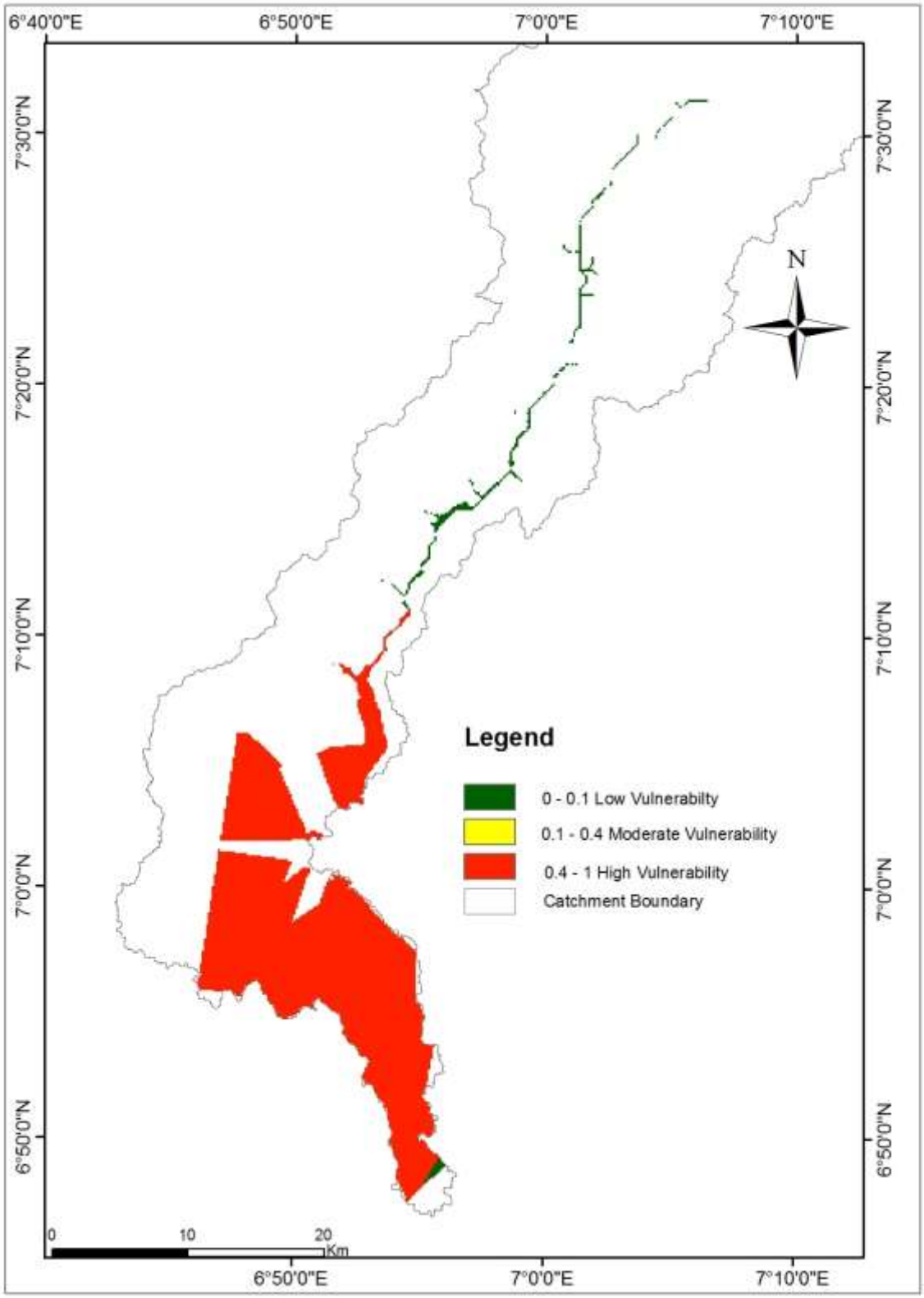


Fig. 4.43b: 2000 Flood Vulnerability Map

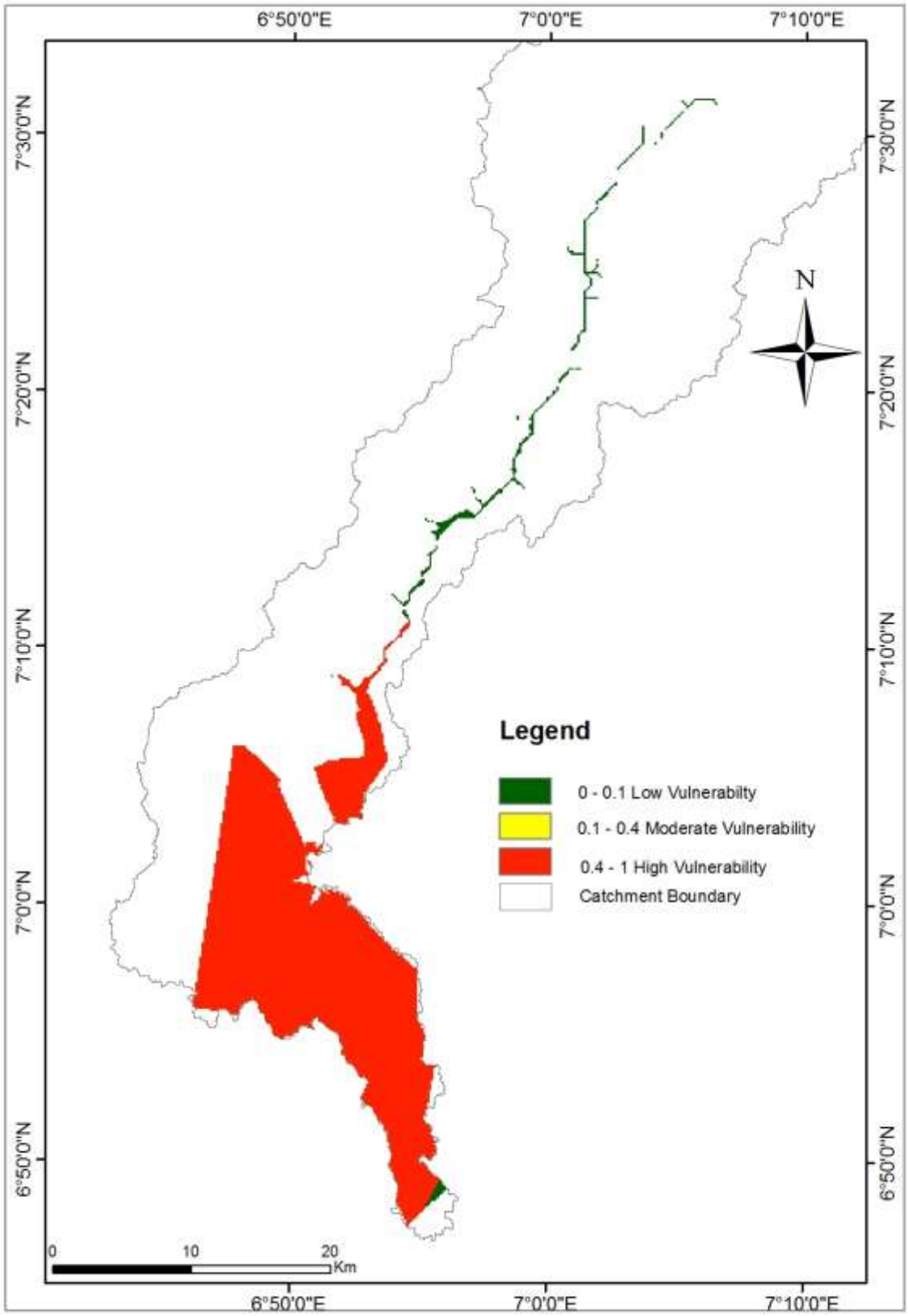


Fig. 4.43c: 100 Year Flood Vulnerability Map

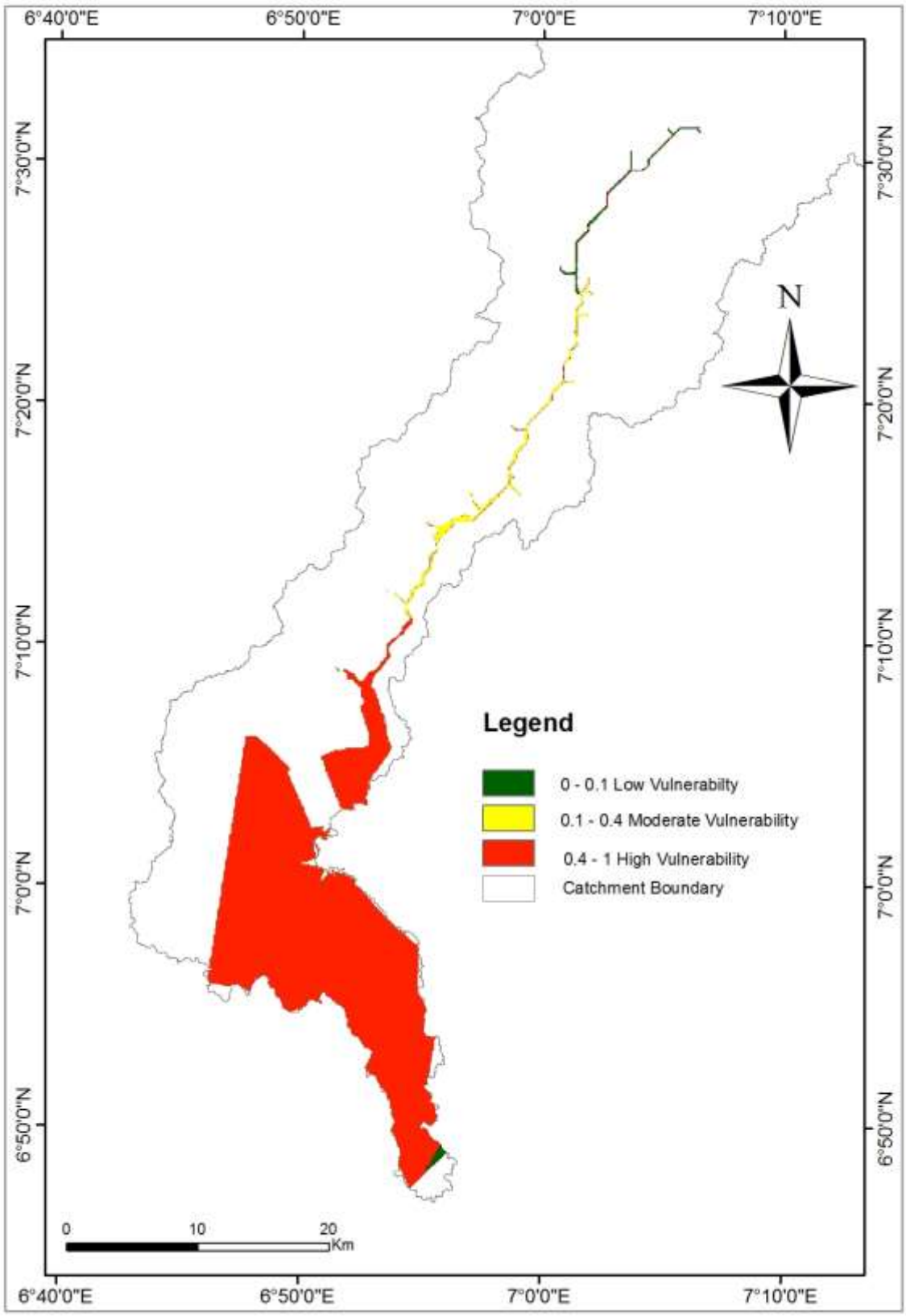


Fig. 4.43d: 200 Year Flood Vulnerability Map

Details of the vulnerability classifications and the extent of each class for 1995 and 2000 flood events as well as the 100 and 200 years return periods are presented in Table 4.40.

Table 4.40: Flood Vulnerability Zones/extent for 1995, 2000, 100 year and 200 year Floods

Scenario/Return Period	Vulnerability Zone			Total
	High	Moderate	Low	
Year 1995	242.413	0.000	9.055	251.468
Year 2000	242.537	0.000	9.009	251.546
100 Years	256.501	0.000	10.164	266.665
200 Years	256.819	6.818	3.361	266.998

Table 4.40 shows that the High vulnerability zone covered an area of 242.413 km^2, 242.537 km^2, 256.501 km^2 and 256.819 km^2 for 1995, 2000, 100 year and 200 year floods, respectively. There was no moderate vulnerability zone for the 1995, 2000 and 100-year floods but covered an area of 6.818 km^2 for the 200-year flood. Lastly, the low vulnerability category covered 9.055 km^2, 9.009 km^2, 10.164 km^2 and 3.361 km^2, respectively.

4.6.4 Flood Risk Assessment

4.6.3.1 Flood risk maps of Ofu River Catchment

The flood risk maps produced as a product of hazard and vulnerability are presented in Fig. 4.44a-d

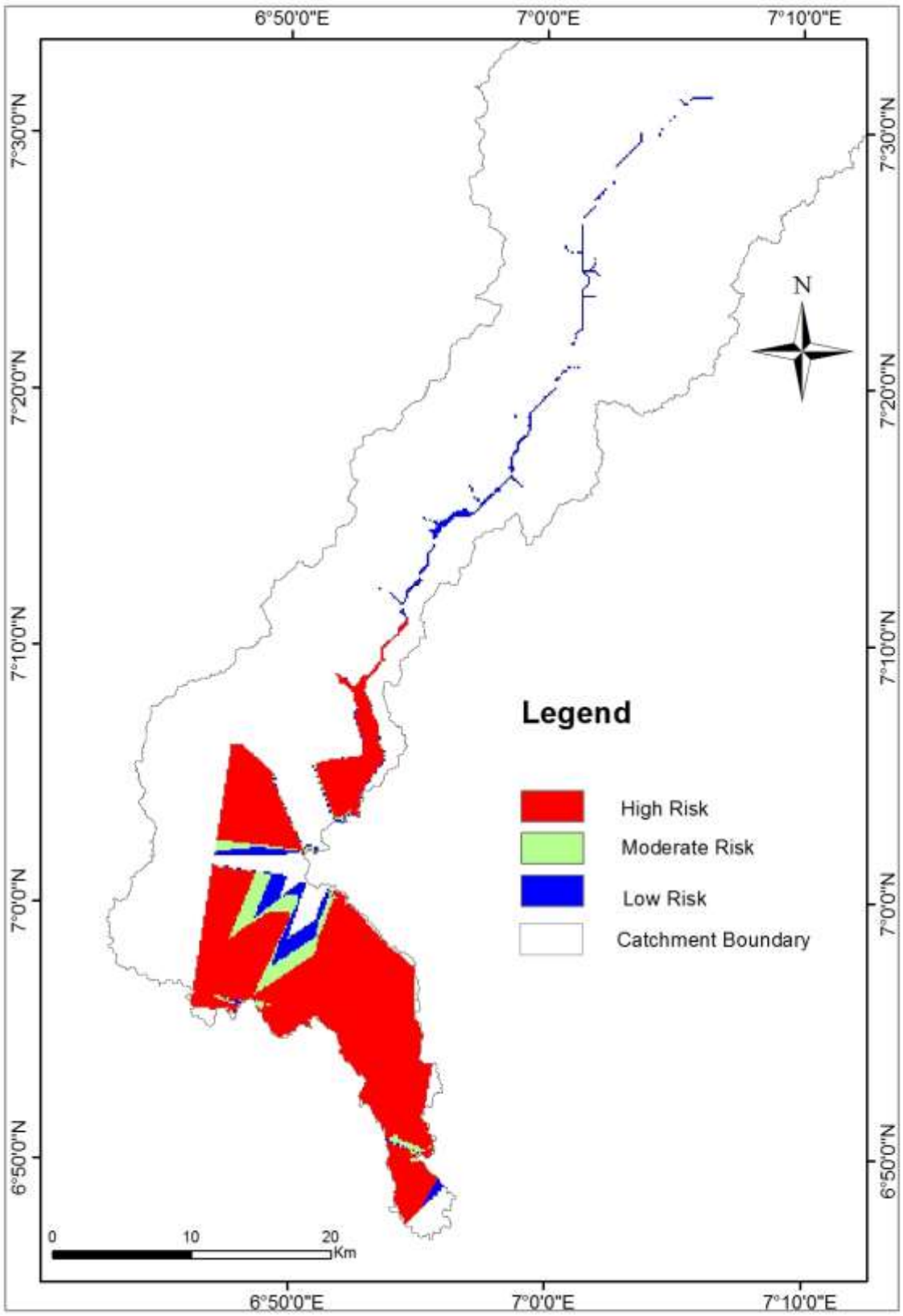


Fig. 4.44a: 1995 Flood Risk Map

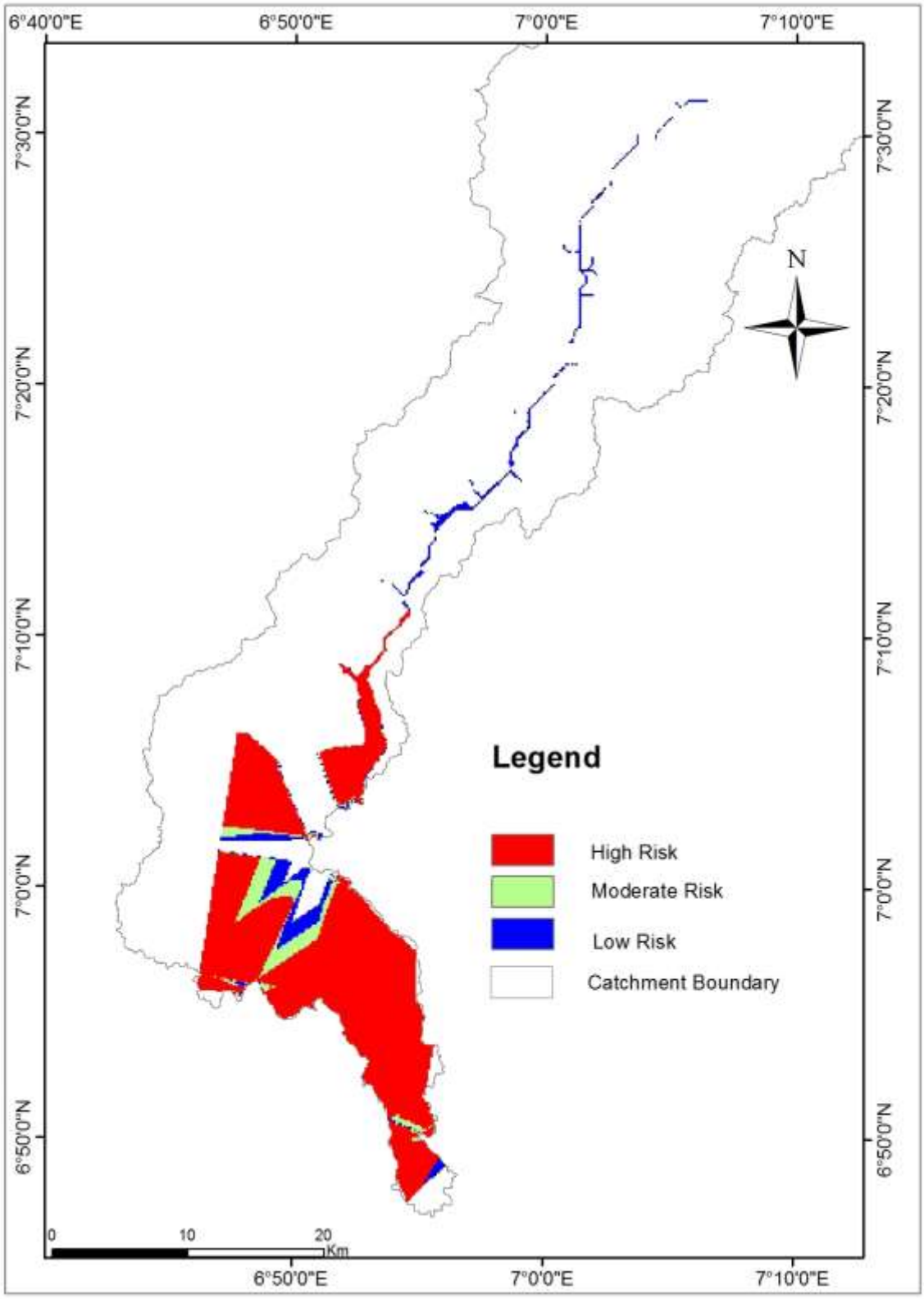


Fig. 4.44b: 2000 Flood Risk Map

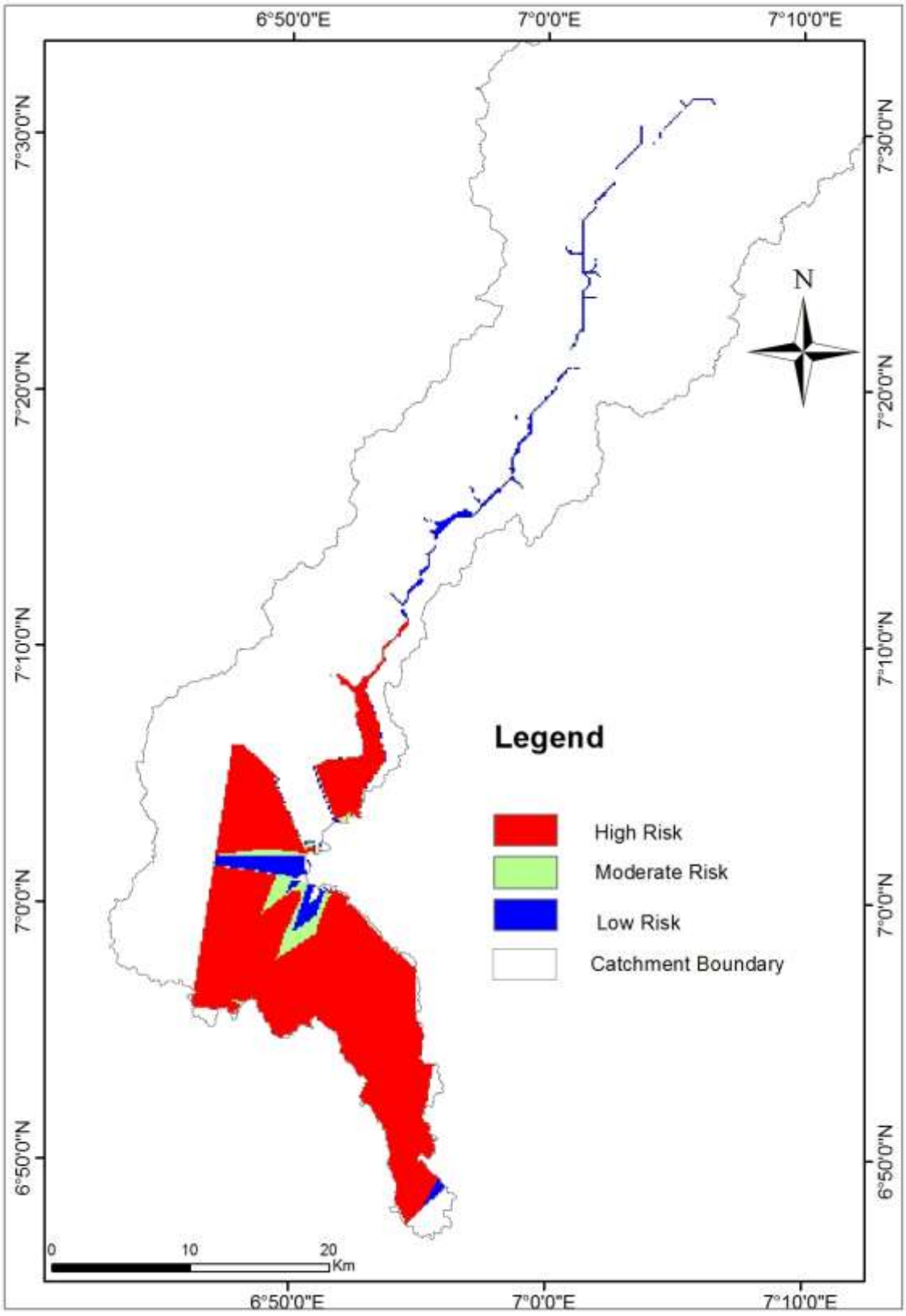


Fig. 4.44c: 100 Year Flood Risk Map

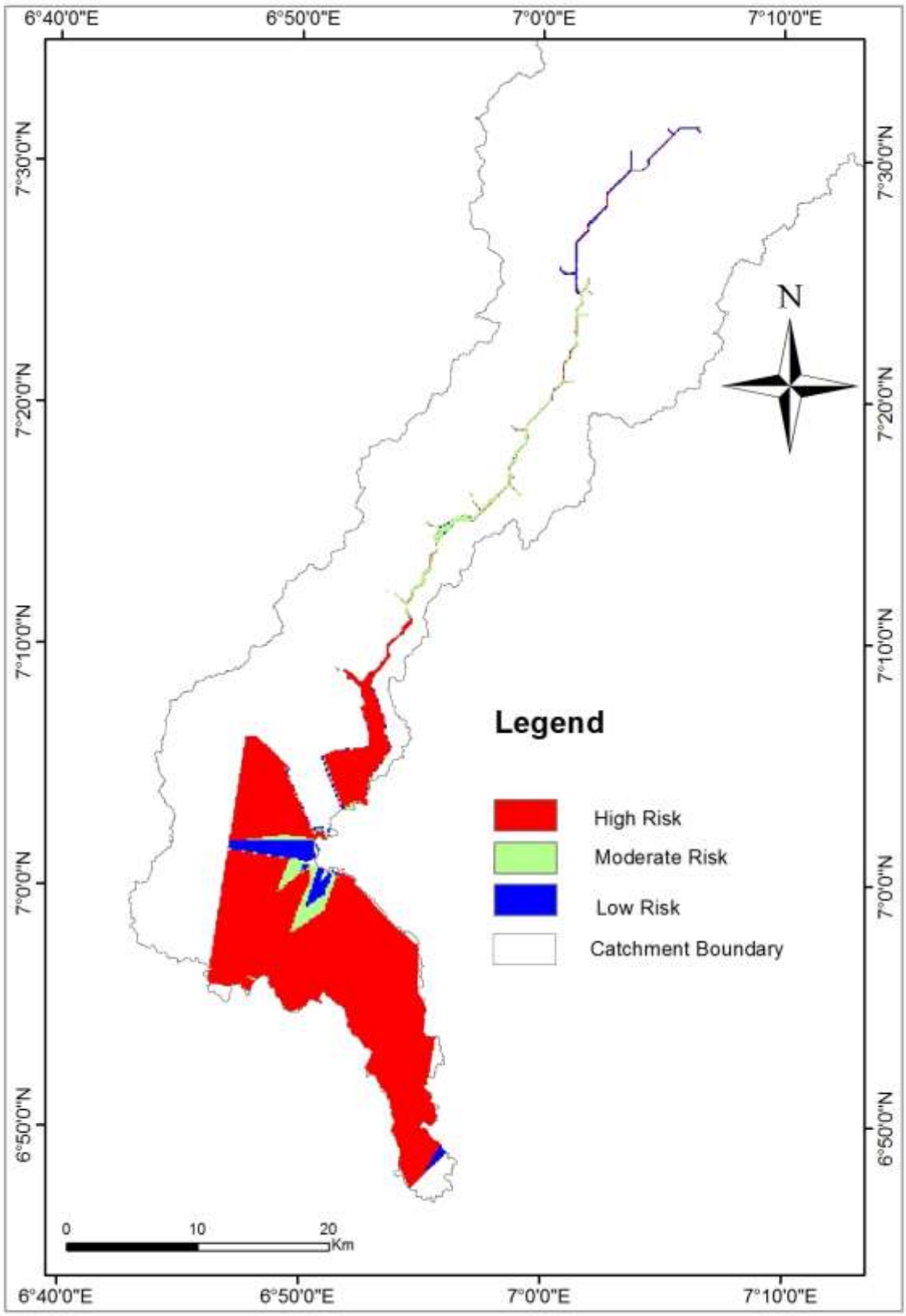


Fig. 4.44d: 200 Year Flood Risk Map

4.6.3.2 Identification of elements at risk

The elements at risk of the 1995 flood events are presented in Table 4.41.

Table 4.41: Elements at Risk of 1995 Flood Scenario

Elements		Risk Zone			Total
		High	Moderate	Low	
Land Surface (km^2)		208.647	19.712	22.457	250.816
Road	Main Road (km)	1.522	0.039	1.646	3.207
	Minor Road (km)	23.170	0.615	0.384	24.169
	Main Path (km)	98.155	9.474	3.398	111.027
Human Settlements	Built Areas (no)	6	0	1	7
	Built Areas (ha)	30.563	0	37.251	67.814
	Scattered (no)		8		8
Agricultural	Forest Reserve (ha)	687.040	27.690	26.220	740.95
	Oil Palm Plantation (ha)	0.132	0	0	0.1324
Others	Church (no)	1	0	0	1
	Mosque (no)	1	0	0	1
	Police Station (no)	1	0	0	1
	PHC (no)	1	0	0	1
	Market (no)	1	0	0	1

Table 4.41 shows that a total land surface of 250.816 km^2 was at risk of the 1995 flood out of which 208.647 km^2, 19.712 km^2 and 22.457 km^2 were in the High, Moderate and Low risk zones, respectively. In addition to this, 3.207 km of main road out of which 1.522 km, 0.039 km and 1.646 km fell in the High, Moderate and Low risk zones, respectively. More so, 24.169 km of minor road (23.170 km, 0.615 km and 0.384 km in High, Moderate and Low risk zones, respectively) was at risk while, 111.027 km of main path (98.155 km, 9.474 km and 3.398 km in High, Moderate and Low risk zones, respectively) was at risk of the 1995 flood. Furthermore, six (6) built areas (30.563 ha) were in the High risk zone while one (1) built area (37.251 ha) was in the Low risk zone making a total of seven (7) built areas (67.814 ha) at risk of the 1995 flood. Closely related to this, eight scattered settlements were at risk of the 1995 flood scattered across the three risk zones. Also at risk is 687.040 ha (High), 27.690 ha (Moderate) and 26.220 ha (Low) of forest reserve comprising principally of Teak and Melina making a total of 740.95 ha of forest reserve. More so, 0.132 ha of oil palm plantation was also identified within the high risk zone. Finally, a church, a mosque, a police station, a Primary Health Care centre and a small village market were also identified within the high risk zones of the 1995 flood event. The flood risk map showing the elements at risk of the 1995 flood scenario is shown in Fig. XXa (Appendix XX).

The elements at risk of the 2000 flood events are presented in Table 4.42.

Table 4.42: Elements at Risk of 2000 Flood Scenario

Elements		Risk Zone			Total
		High	Moderate	Low	
Land Surface (km^2)		208.415	19.725	22.547	250.687
Road	Main Road (km)	1.522	0.039	1.644	3.205
	Minor Road (km)	23.170	0.615	0.384	24.169
	Main Path (km)	98.173	9.463	3.390	111.026
Human Settlements	Built Areas (no)	6	0	1	7
	Built Areas (ha)	30.551	0	37.242	67.793
	Scattered (no)		8		8
Agricultural	Forest Reserve (ha)	687.041	27.690	26.136	740.867
	Oil Palm Plantation (ha)	0.132	0	0	0.1324
Others	Church (no)	1	0	0	1
	Mosque (no)	1	0	0	1
	School (no)	1	0	0	1
	Police Station (no)	1	0	0	1
	PHC (no)	1	0	0	1
	Market (no)	1	0	0	1

The results in Table 4.42 shows that a total of 250.687 km^2 of land surface (208.415 km^2 within High, 19.725 km^2 within Moderate and 22.547 km^2 with Low risk zones) was at risk of the 2000 flood event. 3.025 km of main asphalt overlaid road (1.522 km within High, 0.039 km within Moderate and 1.644 km within Low risk zones) was at risk of the 2000 flood while 24.169 km of minor road (23.170 km within High, 0.615 km within Moderate and 0.384 km within Low risk zones) was at risk. Furthermore, 111.026 km of main path (98.173 km within High, 9.463 km within Moderate, 3.390 km within Low risk zones) was at risk. In addition to these, six (6) built areas (30.551 ha) were in the High risk zone while one (1) built area (37.242 ha) was in the Low risk zone making a total of seven (7) built areas (67.793 ha) at risk of the 2000 flood. Similarly, eight scattered settlements were at risk of the 2000 flood scattered across the three risk zones. Also at risk is 687.041 ha (High), 27.690 ha (Moderate) and 26.136 ha (Low) of forest reserve comprising principally of Teak and Melina making a total of 740.867 ha of forest reserve. More so, 0.132 ha of oil palm plantation was also identified within the high risk zone.

Finally, a primary school, a church, a mosque, a police station, a Primary Health Care centre and a small village market were also identified within the high risk zones of the 2000 flood event. The flood risk map showing the elements at risk of the 2000 flood scenario is shown in Fig. XXb (Appendix XX).

The elements at risk of the 100-year flood events are presented in Table 4.43.

Table 4.43: Elements at Risk of 100 Year Flood

Elements		Risk Zone			Total
		High	Moderate	Low	
Land Surface (km^2)		231.645	12.164	21.627	265.436
Road	Main Road (km)	1.575	1.417	1.760	4.752
	Minor Road (km)	23.539	0.300	0.477	24.316
	Main Path (km)	108.138	1.418	2.167	111.723
Human Settlements	Built Areas (no)	6	0	1	7
	Built Areas (ha)	30.548	0	41.535	72.083
	Scattered (no)		8		8
Agricultural	Forest Reserve (ha)	699.336	37.238	15.711	752.285
	Oil Palm Plantation (ha)	0.132	0	0	0.1324
Others	Church (no)	1	0	0	1
	Mosque (no)	1	0	0	1
	School (no)	1	0	0	1
	Police Station (no)	1	0	0	1
	PHC (no)	1	0	0	1
	Market (no)	1	0	0	1
	Wireless Mast (no)	1	0	0	1

At risk of the 100-year flood are 265.436 km^2 of land surface (231.645 km^2, 12.164 km^2 and 21.627 km^2 within High, Moderate and Low risk zones, respectively), 4.752 km of main asphalt overlaid road (1.575 km, 1.417 km and 1.760 km within the High, Moderate and Low risk zones, respectively), 24.316 km of minor road (23.539 km, 0.3 km and 0.477 km within High, Moderate and Low risk zones respectively) and 111.723 km of main path (108.138 km, 1.418 km, 2.167 km within High, Moderate and Low risk zones, respectively). Also at risk of the 100-year flood are seven (7) built areas (72.083 ha). Six (6) of these built areas (30.548 ha) are within the High risk zone while one (1) built area (37.238 ha) is in the Low risk zone. Similarly, eight scattered settlements are at risk of the 100-year flood scattered across the three risk zones. In addition to these, 699.336 ha (High), 37.238 ha (Moderate) and 15.711 ha (Low) of Teak and Melina forest reserve (A total of 752.285 ha of forest reserve) are at risk of the 100-year flood. Furthermore, 0.132 ha of oil palm plantation was also identified within the high risk zone. Finally, a primary school, a church, a mosque, a police station, a Primary Health Care centre, a small village market and a wireless mast are also at high risk of the 100-year flood event. The flood risk map showing the elements at risk of the 100-year flood scenario is shown in Fig. XXc (Appendix XX).

The elements at risk of the 200-year flood events are presented in Table 4.44.

Table 4.44: Elements at Risk of 200 Year Flood

Elements		Risk Zone			Total
		High	Moderate	Low	
Land Surface (km^2)		234.189	17.021	14.706	265.916
Road	Main Road (km)	1.578	1.555	0.214	3.347
	Minor Road (km)	23.534	0.670	0.101	24.305
	Main Path (km)	108.761	2.024	1.019	111.804
Human Settlements	Built Areas (no)		7		7
	Built Areas (ha)	30.557	38.338	2.954	71.849
	Scattered (no)		8		8
Agricultural	Forest Reserve (ha)	706.197	31.627	15.238	753.062
	Oil Palm Plantation (ha)	0.132	0	0	0.1324
Others	Church (no)	1	0	0	1
	Mosque (no)	1	0	0	1
	School (no)	1	0	0	1
	Police Station (no)	1	0	0	1
	PHC (no)	1	0	0	1
	Market (no)	1	0	0	1
	Wireless Mast (no)	1	0	0	1

At risk of the 200-year flood are 265.916 km^2 of land surface (234.189 km^2, 17.021 km^2 and 14.706 km^2 within High, Moderate and Low risk zones, respectively), 3.347 km of main asphalt overlaid road (1.578 km, 1.555 km and 0.214 km within the High, Moderate and Low risk zones, respectively), 24.305 km of minor road (23.534 km, 0.670 km and 0.101 km within High, Moderate and Low risk zones respectively) and 111.804 km of main path (108.761 km, 2.024 km, 1.019 km within High, Moderate and Low risk zones, respectively). Also at risk of the 200-year flood are seven (7) built areas covering an area of 71.849 ha (30.557 ha within the High risk zone, 38.338 ha within the Moderate risk zone while 2.954 ha are within the Low risk zone). Similarly, eight scattered settlements are at risk of the 200-year flood scattered across the three risk zones. In addition to these, 706.197 ha (High), 31.627 ha (Moderate) and 15.238 ha (Low) of Teak and Melina forest reserve (A total of 753.062 ha of forest reserve) are at risk of the 200-year flood. More so, 0.132 ha of oil palm plantation was also identified within the high risk zone. Finally, a primary school, a church, a mosque, a police station, a Primary Health Care centre, a small village market and a wireless mast are also at high risk of the 200-year flood event. The flood risk map showing the elements at risk of the 200-year flood (2155) scenario is shown in Fig. XXd (Appendix XX).

Furher more, the soil types within the respective risk zones are presented in Figs. 4.45a and b while the inter profile soil characteristics for the respective soil types are presented in Table 4.45.

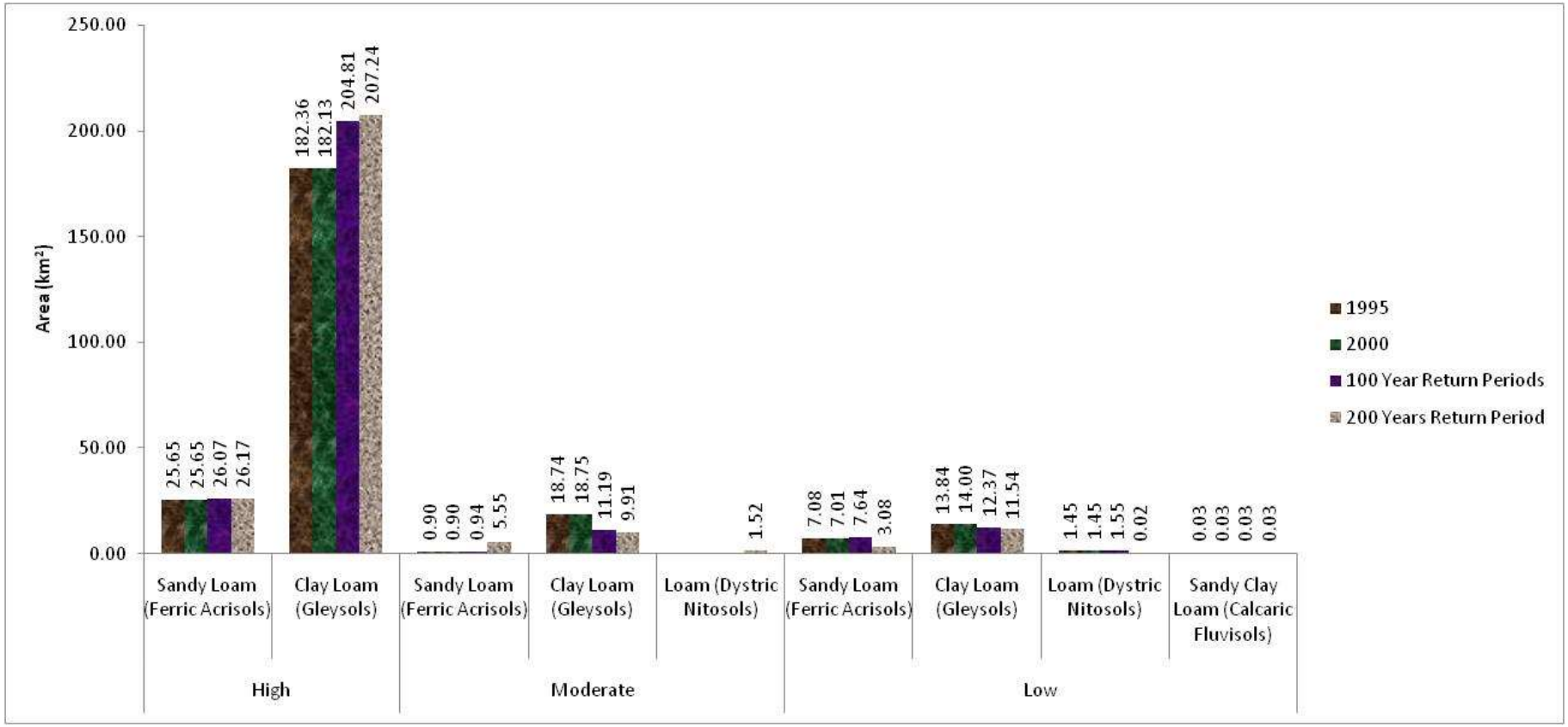


Fig. 4.45a: Area Covered by the Soil Types within the respective Risk Zones in km^2.

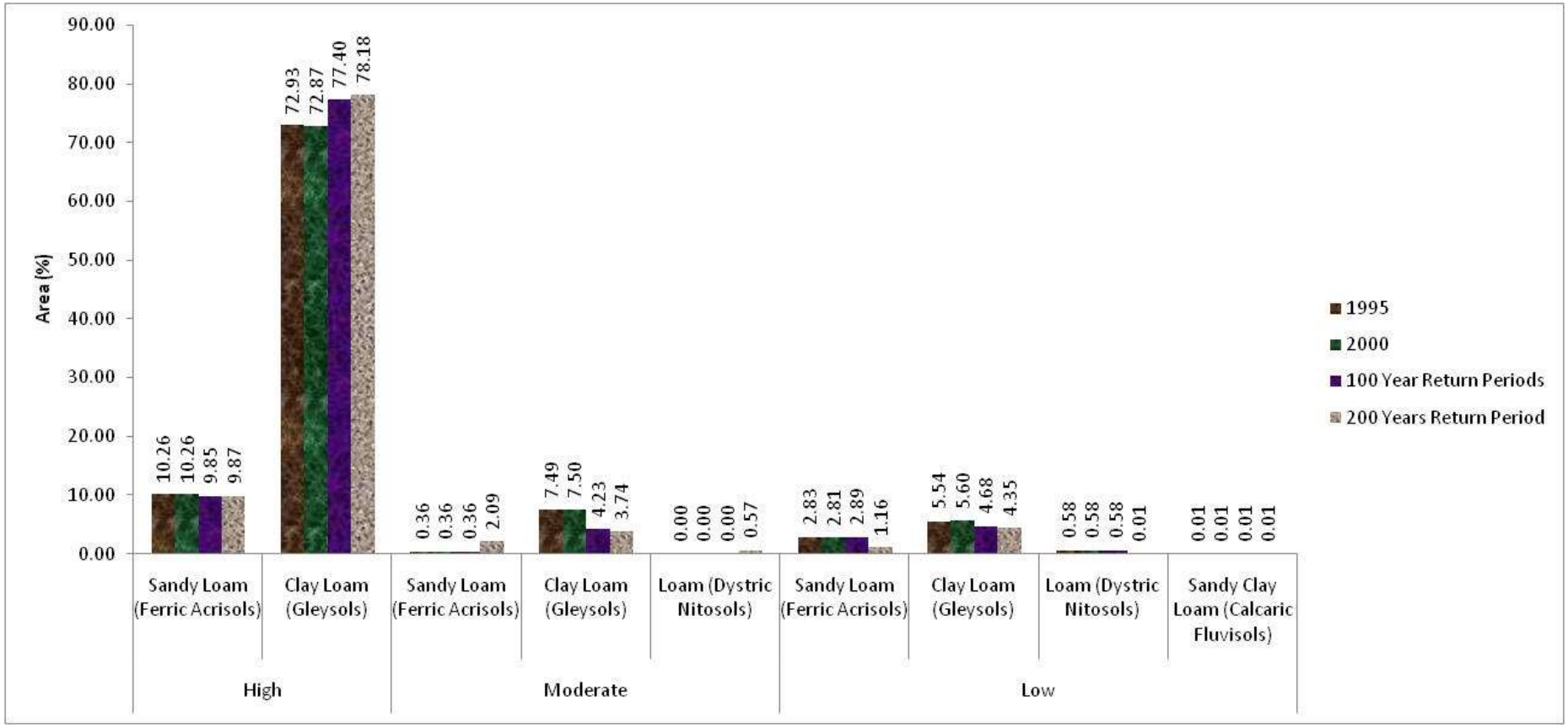


Fig. 4.45b: Percentage Area Covered by the Soil Types within the respective Risk Zones.

Table 4.45: Inter Profile Characteristics of Soil within the Risk Zones

SMU	Name	Share in SMU (%)	Sand Fraction (%)	Silt Fraction (%)	Clay Fraction (%)	Silt+Clay Fraction (%)	Texture	Gravel Content (%)
				Top Soil (0 - 30 cm)				
	Ferric Acrisols (DS)	60	78	12	10	**22**	sandy loam	4
	Lithosols (ASI)	20	43	34	23	**57**	loam	26
	Plinthic Acrisols (ASI)	20	47	30	23	**53**	loam	35
1021	Average		56	25	19	**44**		22
				Sub Soil (30 - 100 cm)				
	Ferric Acrisols (DS)	60	65	12	23	**35**	sandy clay loam	10
	Lithosols (ASI)	20	-	-	-	**-**	-	-
	Plinthic Acrisols (ASI)	20	36	27	37	**64**	clay loam	19
	Average		51	20	30	**50**		15
				Top Soil (0 - 30 cm)				
	Gleysols (DS)	35	38	40	22	**62**	loam	4
	Gleysols (ASI)	35	16	31	53	**84**	clay (light)	7
	Fluvisols (ASI)	30	39	41	20	**61**	loam	4
1193	Average		31	37	32	**69**		5
				Sub Soil (30 - 100 cm)				
	Gleysols (DS)	35	37	35	28	**63**	clay loam	5
	Gleysols (ASI)	35	21	27	52	**79**	clay (light)	1
	Fluvisols (ASI)	30	41	39	20	**59**	loam	8
	Average		33	34	33	**67**		5
				Top Soil (0 - 30 cm)				
	Dystric Nitosols (DS)	60	76	13	11	**24**	sandy loam	4
	Lithosols (ASI)	20	43	34	23	**57**	loam	26
	Orthic Acrisols (ASI)	20	49	27	24	**51**	sandy clay loam	10
1567	Average		56	25	19	**44**		13
				Sub Soil (30 - 100 cm)				
	Dystric Nitosols (DS)	60	62	13	25	**38**	sandy clay loam	4
	Lithosols (ASI)	20	-	-	-	**-**	-	-
	Orthic Acrisols (ASI)	20	40	24	36	**60**	clay loam	10
	Average		51	19	31	**49**		7
				Top Soil (0 - 30 cm)				
	Calcaric Fluvisols (DS)	60	49	32	19	**51**	loam	4
	Dystric Nitosols (ASI)	20	44	33	23	**56**	loam	11
	Plinthic Gleysols (ASI)	20	42	37	21	**58**	loam	7
677	Average		45	34	21	**55**		7
				Sub Soil (30 - 100 cm)				
	Calcaric Fluvisols (DS)	60	52	28	20	**48**	loam	8
	Dystric Nitosols (ASI)	20	35	24	41	**65**	clay (light)	26
	Plinthic Gleysols (ASI)	20	36	30	34	**64**	clay loam	10
	Average		41	27	32	**59**		15

SMU-Soil Mapping Unit; DS-Dorminant soils; ASI-Associated soils with inclusions

Source: Extracted from Harmonised World Soil Database

It can be observed from Fig. 4.45a that the predominant soil type within the high risk zone is Gleysols (Clay loam) covering areas of 182.36 km^2, 182.13 km^2, 204.81 km^2 and 207.24 km^2 for year 1995, year 2000, 100 years return period and 200 years return period respectively. These areas represent 72.93 %, 72.87%, 77. 40 % and 78.18 % of the total flood risk extent for year 1995, year 2000, 100 years return period and 200 years return period respectively (Fig. 4.45b). The inter profile characteristics presented in Table 4.45 shows that the combined fractions of silt and clay in Gleysols are 69 % and 67 % for the top soil and the sub soil respectively. This high clay-silt content explains why the flood risk within that zone is high. It means that the ability of the soil to permit infiltration is low thus resulting in runoff and consequently, flooding.

4.6.3.3 Extent of damage of the 1995 and 2000 flood scenarios

The results of the assessment of the extent of damages of the 1995 and 2000 flood scenarios at Oforachi are presented and discussed in this section. The distribution of households by experience of the 1995/2000 flood events are presented in Fig. 4.46.

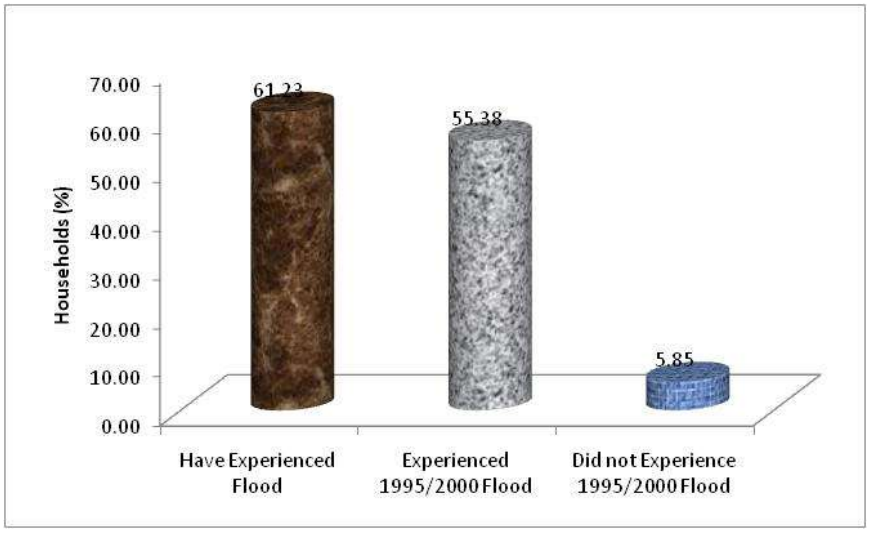


Fig. 4.46: Distribution of Respondents by Experience of 1995/2000 Flood Event

The results in Fig. 4.46 show that out of the 61.23 % households that have experienced flood, 55.38 % experienced either the 1995 flood, 2000 flood or both while 5.85 % did not experience the 1995/2000 flood event.

More so, Fig. 4.47 shows the households' responses on damages/disasters as a result of the 1995 flood event. Figure 4.47 shows that no death or injury was recorded as a result of the 1995 flood event. Although the houses of all those affected by the flood were submerged, the houses of 59 % collapsed. Meanwhile, 81 % had to be evacuated implying that even some households whose building did not collapse had to evacuate their houses because of the depth of floodwater. The crops of 92 % of those affected were destroyed while 48 % lost some goods that were to be sold either in shops or market. As a result of complete inundation of access road, all the students of the affected households and the community at large could not go to school. Furthermore, 41 % of the households lost various livestock ranging from chicken, goats, and sheep, amongst others. Finally, 33 % of affected households experienced outbreak of diseases that could be linked directly to the flood.

Figure 4.48 shows the households' responses on damages/disasters as a result of the 2000 flood event.

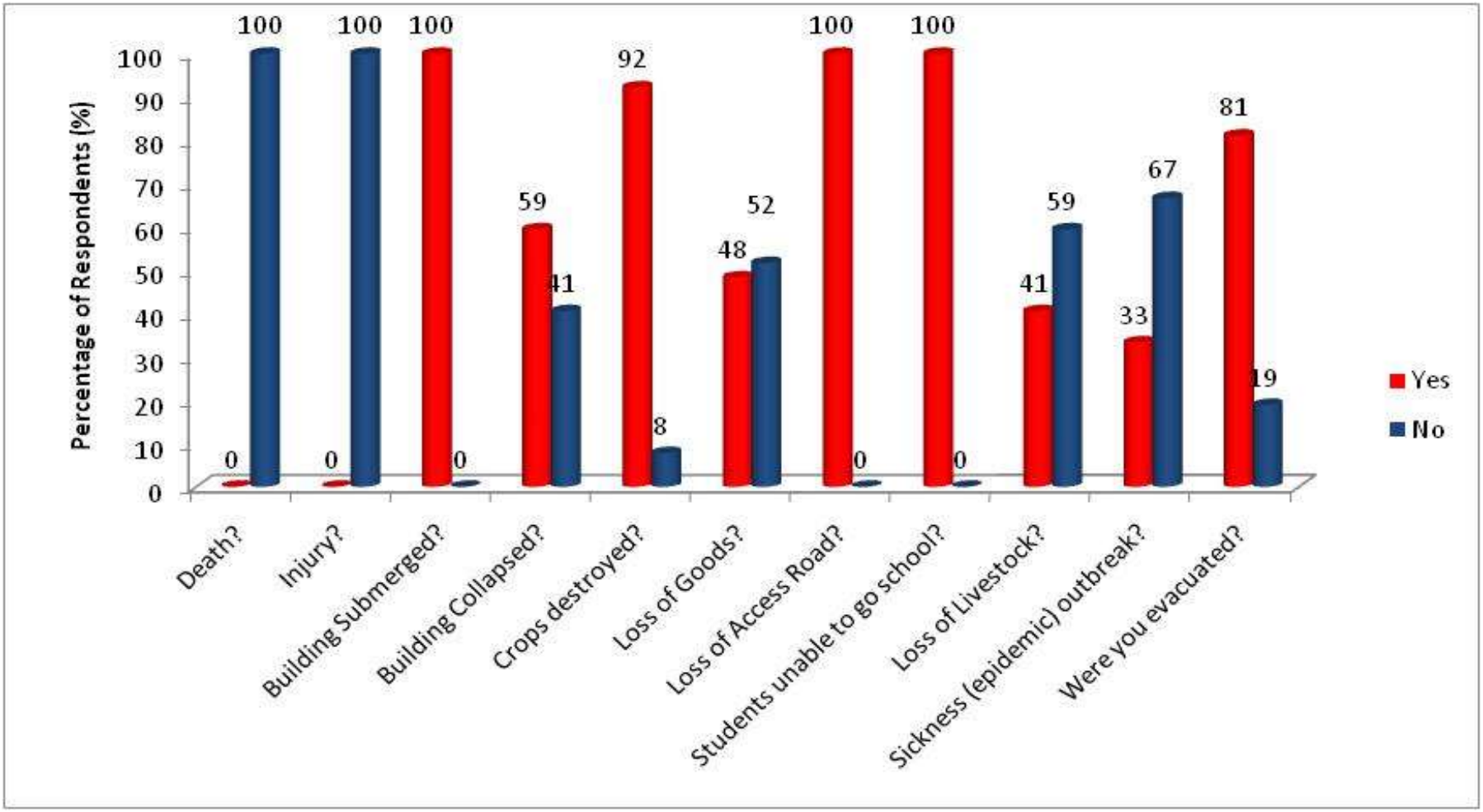


Fig. 4.47: Distribution of Respondents by Various Effects of 1995 Flood Event

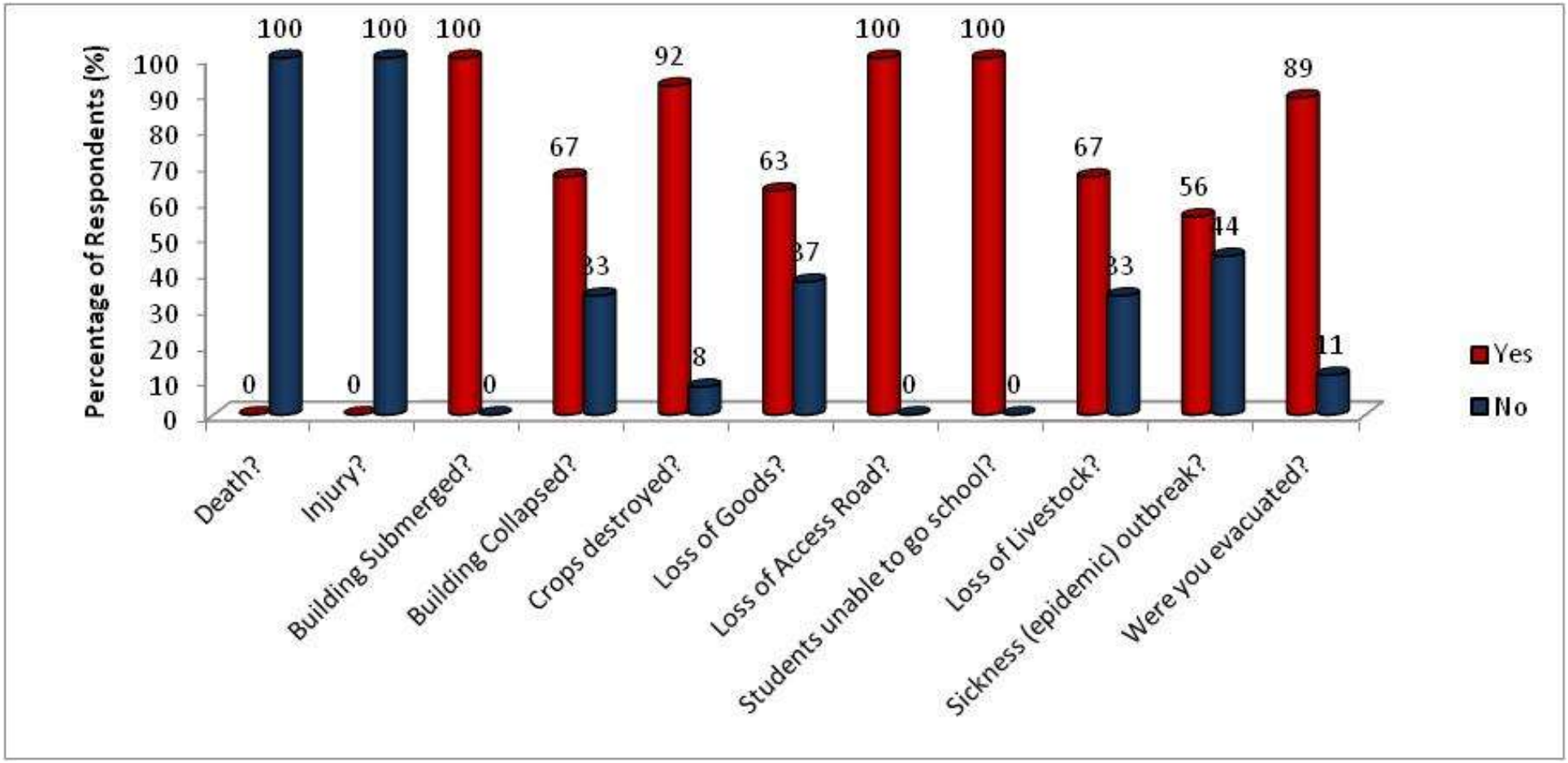


Fig. 4.48: Distribution of Respondents by Various Effects of 2000 Flood Event

The effects of the 2000 flood event seem to be similar to those of 1995 viewing from the response of the respondents. The results in Fig. 4.48 show that no death or injury was recorded as a result of the 1995 flood event, while 100 % of the houses of those affected were submerged. Meanwhile, the houses of 67 % of those affected collapsed while 89 % were evacuated either because of building collapse of because of high floodwater. The results further show that 92 % of respondents lost crops in the farm while 63 % lost some goods either in shops or market. Students of the 100 % of affected households were unable to go to school due to complete inundation of the access roads as well as the challenge of having to manage the flood crisis. More so, 67 % of the households lost various livestock ranging from chicken, goats, and sheep, amongst others. Finally, 56 % of affected households experienced outbreak of diseases that could be linked directly to the flood implying that there were more outbreak of flood related diseases during the 2000 flood event than the 1995 flood event.

4.6.3.4 Environmental health implication of flood

(A) Open Defecation Extent

The results of the assessment of availability of toilet facilities in households as well as the type are presented in Fig. 4.49.

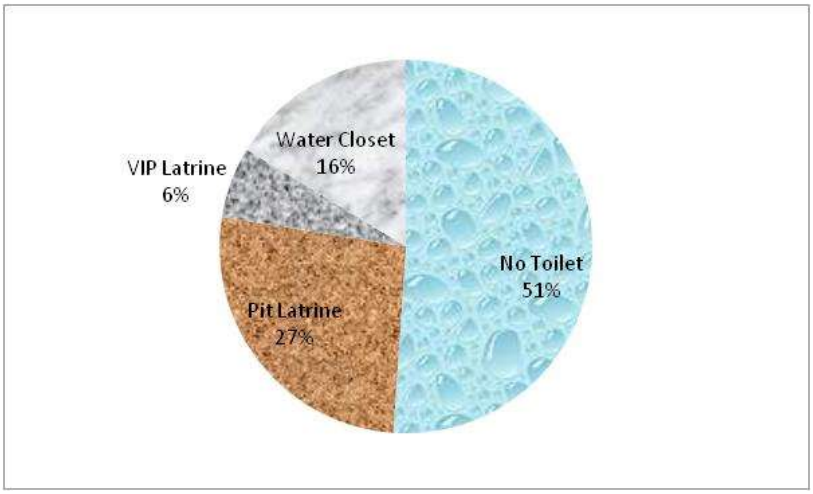


Fig. 4.49: Distribution of Households by type of Toilet Facility

Figure 4.49 shows that 51 % of the households do not have any toilet facility in their households while 27 %, 6 % and 16 % have pit latrine, VIP latrine and water closet, respectively. Furthermore, a projection of the total population represented by the aforementioned percentages is presented in Table 4.46.

Table 4.46: Distribution of Household Populations by Toilet Facilities

Toilet Type	Percentage (%)	Number of Households	Population
No Toilet	51.08	315	4095
Pit Latrine	26.46	163	2119
VIP Latrine	6.15	38	494
Water Closet	16.31	100	1300

Table 4.46 shows that a total of 4,095 persons in Oforachi Community do not have a toilet facility in their houses. On the other hand, 2,119 persons, 494 persons and 1,300 persons have pit latrine, VIP latrine and water closet, respectively in their houses. A further analysis to find out the 4,095 persons without a toilet facility in their houses defecate was carried out. The results are presented in Fig. 4.50 and Table 4.47.

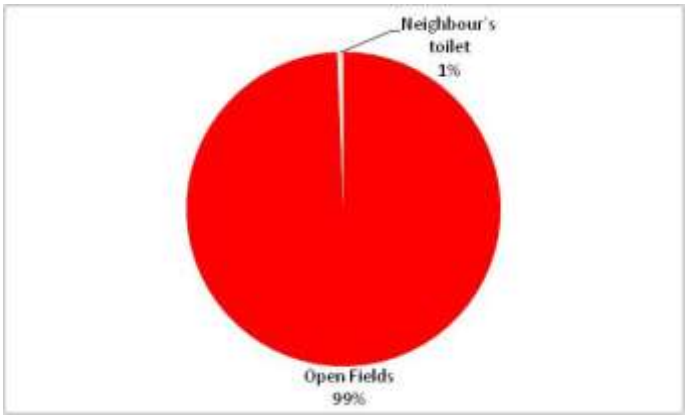


Fig. 4.50: Extent of Open Defecation in Oforachi Community

Table 4.47: Alternative Place of Defecation for those without Toilet Facilities

Point of Defecation	%	Number of Households	Population
Open Fields	99.34	313	4069
Neighbour's toilet	0.66	2	26

The results in Fig. 4.50 and Table 4.47 reveal that only 26 persons representing 0.66% of those without toilet use the facilities in neighbouring households while 4,069 persons representing 99.34 % resort to open defecation in nearby fields. This implies that 4,069 persons representing 50.81 % of the entire community defecate in the open field. The implication of this is that these faeces find their way to the river especially in the event of flood and could possibly lead to an epidemic since a large percentage of the community use the river as their source of drinking water.

(B) Sources of Drinking Water

The community's sources of drinking water and the estimated populations depending on each source are represented in Fig. 4.51 and Table 4.48.

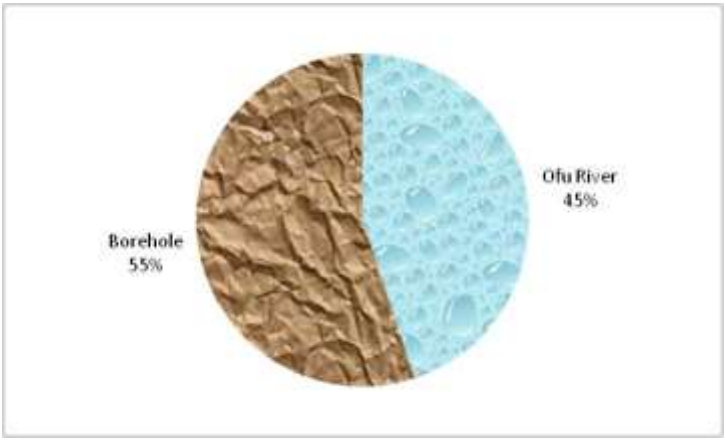


Fig. 4.51: Distribution of Households by Sources of Drinking Water

Table 4.48: Distribution of Household Populations by Sources of Drinking Water

Source of Drinking Water	Percentage (%)	Number of Households	Population
Ofu River	44.92	277	3601
Borehole	55.08	339	4407

The results in Fig. 4.52 and Table 4.48 show that 277 households (3,601 persons) representing 44.92 % of the community depend on Ofu River as their source of drinking water while 339 households (4,407 persons) representing 55.08 % of the community

depend on borehole for their drinking water. The implication is that 3,601 persons are at risk of contacting water borne disease as a result of open defecation and flooding. Since the point of consumption and the point of contamination are the same, there will be insufficient distance for the river to self purify. This probably explains the 33 % and 67 % disease outbreaks during the 1995 and 2000 floods, respectively at Oforachi.

4.7 STRATEGIC PLAN FOR OFU RIVER CATCHMENT FLOOD MANAGEMENT

The foregoing results have clearly shown that Ofu River flood disaster will increase in intensity and the extent of damages to properties of people within the flood plain. In order the effectively manage and prevent the occurrence of flood as well as minimize its impact upon the people, a strategic plan has been developed for sustainable use, maintenance and maximization the benefits of the floodplains. Most flood hazard mitigation measures have shifted from structural approach to non-structural because of the disadvantages associated with the sense of safety the structural measures give to floodplain users. The priority will be given to non-structural measures in this flood management plan. The proposed strategic plan is presented in Table 4.49.

Table 4.49: Strategic Plan for Ofu River Catchment Flood Management

S/N	PLAN	ACTION	RESPONSIBILITY
1.	Ofu River catchment management team	Set up a management team comprising of a representative of LBRBDA, at least one official from each of the component LGAs, the counsellor of component wards and the village heads of communities along the river course or their representatives	LBRBDA, Government, NEWMAP
2.	Channelization of Ofu River to accommodate more flood waters	Dredging and widening of the Ofu River channel	State Government with support from the Federal Government through LBRBDA Headquarters Makurdi
3.	Clearing of Ofu River to accommodate more flood waters	Periodic clearing of excessive vegetative cover on the Ofu River water course	Ofu River catchment Management Team
4.	Increase public awareness of flooding	Public enlightenment campaigns, town hall meetings and stakeholders forum	Information Office of the Respective LGAs in collaboration with the State Ministry responsible for water resources and rural development and Ofu River catchment management team.
5.	Set up an early warning and emergency preparedness scheme	Design and implement emergency and early warning scheme that will involve the community leadership, paying particular attention to ease of understanding of the communities	LBRBDA Headquarters Makurdi State Government, Ofu River Catchment Management Team and the community Leadership
6.	Set up a flood plain management programme	Engage floodplain managers to train people to meet up with current and growing challenges in floodplain management.	LBRBDA Headquarters Makurdi and Ofu River Catchment management team

CHAPTER FIVE

SUMMARY, CONCLUSION AND RECOMMENDATIONS

This chapter highlights the summary of the findings of this work, conclusion drawn from the results of this study and the recommendations made.

5.1 SUMMARY

Flood disaster has become an annual occurrence in the floodplain of Ofu River since 1991 causing varying degree of damages to properties and disrupting the socio-economic live of the residents, yet, no study (to the best of my knowledge) seem to have been carried out to assess the cause and damage extent of this phenomenon that would provide a basis for its mitigation. This is the reason why this study was carried out with the aim of conducting a flood risk assessment for Ofu River Catchment.

The study set out six specific objectives. The first was to determine the morphologic characteristics of Ofu River Catchment, the second was to develop a Stage-Discharge relationship or rating curve for Ofu River, the third was to identify flood causative factors within Ofu River Catchment, the fourth was to analyze flood frequencies and determine the return periods of extreme flood events in the study area, the fifth was to derive the flood hazard maps and determine the extent of inundation for respective return periods of extreme flood events in the study area while the last objective was to carry out a flood risk analysis in the study area.

The major findings of this study are summarized as follows:

1. Ofu River Catchment covers a total drainage area of 1604.56 km^2 covering 27.02 % of Dekina, 23.48 % of Ofu, 14.06 % of Igalamela/Odolu, 9.25 % of Idah and 14.04 %

of Ibaji Local Government Areas in Kogi State and 0.80 % of Uzo-Uwani Local Government Area in Enugu State, Nigeria. The time of concentration for the catchment was 6.17 hours while the time from peak to recession 3.68 days.

2. The rating curve equation (relating discharge Q in m^3/s and stage H in m above mean sea level) for Ofu River at Oforachi Bridge Hydrometric Station is $Q = 15.54096(H - 55.43192)^{0.69051}$ which can be used for the transformation of available stage data into discharge.
3. 8.00% household heads had fair knowledge, 80.92% had good knowledge while, 11.08% had excellent knowledge of the causes of flood. Their knowledge level was influenced by the following factors in decreasing order of associations:Age (Pearson's $chi^2 = 44.46$; P = 0.000), Education (Pearson's $chi^2 = 44.39$; P = 0.000), Occupation (Pearson's $chi^2 = 18.52$; P = 0.018), Flood experience (Pearson's $chi^2 = 17.87$; P = 0.000), Marital Status (Pearson's $chi^2 = 9.81$; P = 0.044) and Ward (Pearson's $chi^2 = 9.68$; P = 0.008).
4. Ofu River has lost an average of 6.90 m of its flow depth at Oforachi between 2000 and 2016 at an average rate of 0.431 m per year which is the major cause of flood as the river overflows its banks with any prolonged rainfall. In addition to this, the Land use/ Land cover changes within Ofu River catchment between 1987 and 2016 has not significantly affected the amount of runoff given by the almost equal runoff curve numbers of 61.8, 63.3 and 62.8 for 1987, 2001 and 2016, respectively.
5. The modified Thomas-Fierring Model was effectively used to generate 12 months synthtic stream flow data for Ofu River from 1974 to 2016 using the gauged data of 1955 to 1973 making the stream flow data cover a total of 62 years (1955 – 2016).
6. The peak discharge values for 2, 5, 10, 25, 50, 100 and 200 years return periods are 444.57 m^3/s, 499.23 m^3/s, 530.35 m^3/s, 565.61 m^3/s, 589.59 m^3/s, 611.96 m^3/s and

633.25 m^3/s, respectively. More so, the peak discharge values for 1995 and 2000 flood scenarios were 448.89 m^3/s and 446.46 m^3/s, respectively.

7. The extent of flood inundation obtain using thematic integration of factor maps (multi-criteria analysis) was 257.49 km^2 while those for the HEC-RAS modelling were 251.98 km^2 and 251.80 km^2 for the 1995 and 2000 flood scenarios, respectively and 252.63 km^2, 256.34 km^2, 258.17 km^2, 262.34 km^2, 266.84 km^2 and 267.37 km^2 for 2, 5, 10, 25, 50, 100 and 200 years return periods, respectively.
8. The high flood hazard zone covered an area of 218.232 km^2, 217.832 km^2, 242.366 km^2 and 244.939 km^2 for year 1995, year 2000, 100 year and 200 year floods, respectively. The moderate flood hazard category covered 20.250 km^2, 20.331 km^2, 12.711 km^2 and 11.496 km^2, respectively while the low hazard category covered 14.481 km^2, 14.630 km^2, 12.756 km^2 and 11.937 km^2, respectively.
9. A total of 242.413 km^2, 242.537 km^2, 256.501 km^2 and 256.819 km^2 were highly vulnerable to year 1995, year 2000, 100 year and 200 year floods, respectively. There was no moderate vulnerability zone for the 1995, 2000 and 100-year floods but covered an area of 6.818 km^2 for the 200-year flood. Lastly, the low vulnerability category covered 9.055 km^2, 9.009 km^2, 10.164 km^2 and 3.361 km^2, respectively.
10. The year 1995 flood event put 250.816 km^2 land area and 16,932 persons at risk while the year 2000 flood event put 250.687 km^2 and 19,673 persons at risk. The 100-year flood will put 265.436 km^2 and 92,733 persons at risk while, the 200-year flood will put 265.916 km^2 and 1,984,377 persons at risk in addition to roads, built and scattered settlements, forest reserve, oil palm plantation, church, mosque, school, police station, primary health clinic, market and wireless mast that will be at risk.
11. The predominant soil type within the high risk zone is Clay loam which could be one of the reasons for the high flood risk.

12. An assessment of the open defecation status of Oforachi, the most developed of the communities within Ofu River floodplain shows that 50.81 % of the population still defecate in the open field. This poses a risk for contamination and outbreak of diseases during flood events.

5.2 CONCLUSION

From the results of the study conducted, the following conclusions were drawn:

1. Ofu River Catchment covers a total drainage area of 1604.56 km^2 covering 27.02 % of Dekina, 23.48 % of Ofu, 14.06 % of Igalamela/Odolu, 9.25 % of Idah and 14.04 % of Ibaji Local Government Areas in Kogi State and 0.80 % of Uzo-Uwani Local Government Area in Enugu State, Nigeria. The time of concentration of 6.17 hours obtained for the catchment implies that it will take a drop of rain approximately 6 hours 10 minutes to flow from the remotest part of the catchment to its outlet, while the time from peak to recession of 3.68 days imply that it would take any flood water an average of approximatley four days to completely recede from the ground surface. The catchment consists of 39 streams up to the third order. It is made up of 20 first order streams of 98.76 km length (4.94 km mean length), 16 second order streams of 101.17 km length (6.32 km mean length) and three (3) third order streams of 41.47 km length (13.82 km mean length).
2. A rating curve equation, $Q = 15.5410(H - 55.4319)^{0.6905}$ (where Q = discharge in m^3/s and H = stage in m above mean sea level) was developed for Ofu River at Oforachi Bridge Hydrometric Station which can be used for the transformation of available stage data into discharge and can therefore serve as a monitoring station for early warning to the inhabitants.

3. The inhabitant's level of knowledge of flood causes was influenced by age (Pearson's $chi^2 = 44.46$; P = 0.000), education (Pearson's $chi^2 = 44.39$; P = 0.000), occupation (Pearson's $chi^2 = 18.52$; P = 0.018), flood experience (Pearson's $chi^2 = 17.87$; P = 0.000), marital status (Pearson's $chi^2 = 9.81$; P = 0.044) and ward (Pearson's $chi^2 = 9.68$; P = 0.008), thus should be considered in the development of early warning schemes. More so, Ofu River has lost an average of 6.90 m of its flow depth at Oforachi between 2000 and 2016 at an average annual rate of 0.431 m due to sediment load accumulation estimated at 66,824.73 x 10^3 kg/annum which makes it overflow its banks with any prolonged rainfall.
4. Ofu River stream flow data for 1955 – 1955 was effectively extended to 2016 using the modified Thomas-Fierring Model coupled with linear regression. Ofu River stream flow values for 2, 5, 10, 25, 50, 100 and 200 years return periods estimated based on these synthetic data were 444.57 m^3/s, 499.23 m^3/s, 530.35 m^3/s, 565.61 m^3/s, 589.59 m^3/s, 611.96 m^3/s and 633.25 m^3/s.
5. Multi-criteria analysis (MCA) via thematic integration of flood causative factor maps in ArcGIS can be effectively used to determine the extent of flood inundation in the absence of stream flow data. More so, HEC-RAS with HEC-Geo-RAS extension in ArcGIS are effective tools for flood inundation mapping using hydrologically generated stream flow which can clearly determine inundation extents, depths and velocity. The flood inundation extent obtained via thematic integration of flood causative factors is 257.49 km^2. The flood inundation extents for year 1995 and year 2000 flood events obtained via steady flow analysis in HEC-RAS/GeoRAS were 251.98 km^2 and 251.80 km^2 respectively while those for floods of 2, 5, 10, 25, 50, 100 and 200 years return periods were respectively 252.63 km^2, 256.34 km^2, 258.17 km^2, 262.34 km^2, 265.96 km^2, 266.84 km^2, 267.37 km^2.

6. The year 1995 flood event put 250.816 km^2 and 16,932 persons at risk while the year 2000 flood event put 250.687 km^2 and 19,673 persons at risk. The 100-year flood will put 265.436 km^2 and 92,733 persons at risk while, the 200-year flood will put 265.916 km^2 and 1,984,377 persons at risk in addition to roads, built and scattered settlements, forest reserve, oil palm plantation, church, mosque, school, police station, Primary Health Clinic, market and wireless mast that will be at risk. The fact that more than 50 % of the community still defecate in the open field makes them at a high risk of an epidemic outbreak in the event of flood disaster since Ofu River is a major source of drinking water for the community.

5.3 RECOMMENDATIONS

The following recommendations are made from the study:

1. The Federal Government of Nigeria should consider dredging Ofu River as a matter of urgency.
2. The State Government in collaboration with the Lower Benue River Basin Development Authority (LBRBDA) and NEWMAP should set up a management team for Ofu River Catchment. The team should comprise of a representative of LBRBDA, one official from each of the component LGAs, the counsellor of component wards and the village heads of communities along the river course or their representatives.
3. The catchment management team should ensure periodic clearing of excessive vegetative cover on the Ofu River water course to provide more discharge capacity for the river.

4. An emergency and early warning scheme should be designed and implemented by the Lower Benue River Basin Development Authority (LBRBDA), involving the community stakeholders for effective implementation.
5. A well planned strategic awareness creation should be made by the management team in the communities within the floodplain, on the danger of living in those places with plans for possible evacuation and resettlement in safer locations.
6. Factors such as age, level of education, occupation and marital status, should be considered by the National Emergency Management Agency (NEMA) in the development of an effective early warning and public enlightenment systems.
7. A monitoring station for early warning be established at Oforachi Bridge Hydrometric Station by the National Emergency Management Agency (NEMA).

REFERENCES

Ackerman C. T. (2011). HEC-GeoRAS GIS Tools for Support of HEC-RAS using ArcGIS® User's Manual, US Army Corps of Engineers Hydrologic Engineering Center. Davis CA.

Adebayo, A. A., and Oruonye, E. D. (2013). *An Assessment of the effects of the 2012 Floods in Taraba State, Nigeria.* Paper presented at the Annual National Conference, organized by the Association Hydrological Science University of Agriculture, Abeokuta, Ogun, state, Nigeria.

Aderogba, K. A. (2012). Global warming and challenges of floods in Lagos metropolis, Nigeria. *Academic Research International*, *2*(1), 448-468.

Aderoju, O. M., Jantiku, J., Fagbemiro, O. A., Aliyu, I., Nwadike, B. K., Ajonye, S. E., and Salman, K. S. (2014). Geospatial assessment of 2012 flood disaster in Kogi State, Nigeria. *J. Environ. Sci. Toxicol. Food Technol*, *8*, 74-84.

Agarwal, C. S. (1998). Study of drainage pattern through aerial data in Naugarh area of Varanasi district, UP. *Journal of the Indian Society of Remote Sensing*, *26*(4), 169-175.

Ahmad, B., Muhammad, S. K., Butt, M. J., and Dahri, Z. H. (2010). Hydrological modelling and flood hazard mapping of Nullah Lai. *Proc Pak Acad Sci*, *47*(4), 215-226.

Ahmad, S., Khan, I. H., and Parida, B. P. (2001). Performance of stochastic approaches for forecasting river water quality. *Water research*, *35*(18), 4261-4266.

Ajayi, S. A. (2015). Performance of Selected Water Infiltration Models in Organic-Amended Soils. Unpublished MSc. Dissertation in the Department of Agricultural Engineering, Ahmadu Bello University, Zaria.

Ajin, R., Krishnamurthy, R., Jayaprakash, M., and Vinod, P. (2013). Flood hazard assessment of Vamanapuram River Basin, Kerala, India: An approach using Remote Sensing & GIS techniques. *Adv Appl Sci Res*, *4*, 263-274.

Akan, A. O. (2002). Modified rational method for sizing infiltration structures. *Canadian Journal of Civil Engineering*, *29*(4), 539-542.

Akintola F. O. and Ikwuyatum G. O. (2006). Sustainable Issues in Flood Management in Nigeria in: Ivbijaro M. F. A., Akintola F. and Okechukwu R. U. (Eds) 2006. Sustainable Environmental Management in Nigeria Ibadan, Mattivi Production.

Alkema, D and Westen, C. (2005). Flood Hazard and Risk Assessment. *Refresher Course on Geo-Information for natural Disaster Reduction in Easter Africa*. Makerere University, 12 – 23 September 2005.

Alkema, D. (2004). Remote Sensing and GIS Applications in Flood Forecasting. *National workshop on Flood Disaster Management – Space Inputs, 3-4 June, 2004. NRSA, Hyderabad. India.*http://www.itc.nl/library/Papers_2004/n_p_conf/alkema.pdf

Alkema, D. (2007). Simulating floods: On the application of a 2D-hydraulic model for flood hazard and risk assessment. ITC dissertation number 147. The Netherlands.

American Public Health Association (2012). Standard Methods for the Examination of Water and Wastewater, 20th ed. Jointly published by American Public Health Association (APHA), American Water Works Association (AWWA) and Water Environment Federation (WEF), Washington, USA.

Amini, J. (2007). Generating floodplain maps using Ikonos image and DTM. *Proceedings of the 4th International Conference on Recent Problems in Geodesy and Related Fields with International Importance*. Sofia, Bulgeria.

Angillieri, M. Y. E. (2008). Morphometric analysis of Colangüil river basin and flash flood hazard, San Juan, Argentina. *Environmental geology*, *55*(1), 107-111.

AR-AR Partnership (2004). Oforachi Irrigation Project Contract Documents Volume III: Main Report Prepared for Lower Benue River Basin Development Authority, Federal Republic of Nigeria (Unpublished).

Baas, S., Ramasamy, S., DePryck, J. D., and Battista, F. (2008). *Disaster risk management systems analysis: A guide book* (Vol. 3). Food and Agriculture Organization of the United Nations.

Balabanova, S., and Vassilev, V. (2010). Creation of flood hazard maps. *Water Observation and Information System for Balkan Countries (BALWOIS).Ohrid*, Republic of Macedonia.

Balica, S. F., Douben, N., and Wright, N. G. (2009). Flood vulnerability indices at varying spatial scales. *Water science and technology*, *60*(10), 2571-2580.

Bapalu, G. V and Sinha, R. (2005). "GIS in Flood Hazard Mapping: A Case Study of Kosi RiverBasin, India". GIS Development Weekly, 1(13), pp 1-3. Accessed fromhttp://www.gisdevelopment.net/application/natural_hazards/floods on 12th March 2009.

Bhanumurthy, V., Manjusree P. and Rao G. S., (2004). Managing Floods: A remote Sensing Approach. ISG Newsletter Vol. 10 No. 1 & 2, March/June, 2004, pp 46-53

Bird, J. F. (1980). Geomorphological implications of flood control measures, Lang Lang River, Victoria. *Australian Geographical Studies*, *18*(2), 169-183.

Blaikie, P., Cannon, T., Davis, I., and Wisner, B. (2014). *At risk: natural hazards, people's vulnerability and disasters*. Abingdon (UK). Routledge.

Bouwer, H. (1986). Intake rate: cylinder infiltrometer. Pp. 825-844 in Klute A (Ed.). Methods of Soil Analysis, Part 1: Physical and Mineralogical Methods, 2nd Ed. Madison: American Society of Agronomy and Soil Science Society of America. 1188 p. ISBN 0-89118-088-5.

Braca, G. (2008). *Stage-discharge relationships in open channels: Practices and problems*. Univ. degliStudi di Trento, Dipartimento di IngegneriaCivile e Ambientale.

Brice, J. C. (1984). Planform properties of meandering rivers. In *River meandering* (p. 15). ASCE available on cedb.asce.org

British Geological Survey (BGS) (nd). Groundwater Flooding. http://www.bgs.ac.uk/research/groundwater/flooding/home.html accessed on 27th March, 2017.

Brivio, P. A., Colombo, R., Maggi, M., and Tomasoni, R. (2002). Integration of remote sensing data and GIS for accurate mapping of flooded areas. *International Journal of Remote Sensing*, *23*(3), 429-441.

Büchele, B., Kreibich, H., Kron, A., Thieken, A., Ihringer, J., Oberle, P., ... and Nestmann, F. (2006). Flood-risk mapping: contributions towards an enhanced assessment of extreme events and associated risks. *Natural Hazards and Earth System Sciences*, *6*(4), 485-503.

Bruner G. W. (2010). HEC-RAS, River Analysis System Hydraulic Reference Manual, US Army Corps of Engineers Hydrologic engineering Center. Davis CA.

Campbell, J. B., & Wynne, R. H. (2011). *Introduction to remote sensing*. New York. Guilford Press.

Celeste, A. B., Suzuki, K., Kadota, A., and de Farias, C. A. (2004). Stochastic Generation of Inflow Scenarios to be used by Optimal Reservoir Operation Models. *Annual Journal of Hydraulic Engineering*, *48*, 451-456.

Chang, L. C., Shen, H. Y., Wang, Y. F., Huang, J. Y., and Lin, Y. T. (2010). Clustering-based hybrid inundation model for forecasting flood inundation depths. *Journal of hydrology*, *385*(1), 257-268.

Chen, A. S., Djordjević, S., Leandro, J., and Savić, D. A. (2010). An analysis of the combined consequences of pluvial and fluvial flooding. *Water Science and Technology*, *62*(7), 1491-1498.

Chen, N. S., Yue, Z. Q., Cui, P., and Li, Z. L. (2007). A rational method for estimating maximum discharge of a landslide-induced debris flow: A case study from southwestern China. *Geomorphology*, *84*(1), 44-58.

Chorley, R. J., Malm, D. E., & Pogorzelski, H. A. (1957). A new standard for estimating drainage basin shape. *American Journal of Science*, *255*(2), 138-141.

Chow, V.T., Maidment, D.R. and Mays, L.W. (1988). Applied Hydrology. *McGraw-Hill Series in Water Resources and Environmental Engineering*. McGraw-Hill: New York. ISBN 0-07-010810-2. xiii, 572 pp.

Chow, V. T. (1956). Hydrologic studies of floods in the United States. *International Association of Hydrological Sciences*, *42*, 134-170.

Cobby, D., Falconer, R., Forbes, G., Smyth, P., Widgery, N., Astle, G., ...and Golding, B. (2009). Potential warning services for groundwater and pluvial flooding.

Coto, E. B. (2002). Flood hazard, vulnerability and risk assessment in the city of Turrialba, Costa Rica. *International Institute for Geo-information Science and Earth Observation (ITC), 1-102*

Cui, Q., Wang, X., Li, C., Cai, Y., and Liang, P. (2016). Improved Thomas–Fiering and wavelet neural network models for cumulative errors reduction in reservoir inflow forecast. *Journal of hydro-environment research*, *13*, 134-143.

Cutter S. L., Mitchell T. T. and Scott M. S. (1997). Handbook for Conducting a GIS-Based Hazard Assessment at the County Level. Prepared for South Carolina Emergency Preparedness Division, Office of the Adjutant General. Accessed 25/01/2016 from https://www.researchgate.net/publication/257343365_Handbook_for_conducting_a_GIS-based_hazards_assessment_at_a_county_level

Daffi R. E. (2013). Flood Hazard Assessment for River Dep Catchment Using Remote Sensing and Geographic Information System Techniques Unpublished PhD Thesis in The Department of Water Resources and Environmental Engineering Ahmadu Bello University, Zaria.

Daffi, R. E., Otun, J. A., & Ismail, A. (2014). Flood hazard assessment of River Dep floodplains in North-Central Nigeria. *Int. J. Water Resour. Environ. Engr*, *6*(2), 67-72.

Dalrymple, T. (1960). Flood-frequency analyses, Manual of Hydrology: Part 3 *Water Supply Paper* (- ed.). A publication of the United State Geological Survey available at https://pubs.er.usgs.gov/publication/wsp1543A (accessed 26/05/2017).

Damayanti, F. (2011). Hydrodynamic Modeling for Flood Hazard Assessment inTelemoyo Catchment Central Java, Indonesia. Unpublished M.Sc Thesis Gadjah Mada University and Faculty of Geo-Information Science and Earth Observation University of Twente.

Dashora, I., Singal, S. K., & Srivastav, D. K. (2015). Software Application for Data Driven Prediction Models for Intermittent Streamflow for Narmada River Basin. *International Journal of Computer Applications*, *113*(10), 9 - 17.

de Brouwer (1997). Determination of Peak Runoffrate in: ILWIS Application Guide, ILWIS Department, International Institute for Aerospace Survey and Earth Sciences, Enschede, The Netherlands.

de Leeuw, E. D., and Dillman, D. A. (Eds.). (2008). *International handbook of survey methodology*. Taylor & Francis.

Demirkesen, A. C., Evrendilek, F., Berberoglu, S., and Kilic, S. (2007). Coastal flood risk analysis using Landsat-7 ETM+ imagery and SRTM DEM: A case study of Izmir, Turkey. *Environmental monitoring and assessment*, *131*(1), 293-300.

Dewan, A. M., Islam, M. M., Kumamoto, T., and Nishigaki, M. (2007). Evaluating flood hazard for land-use planning in Greater Dhaka of Bangladesh using remote sensing and GIS techniques. *Water Resources Management*, *21*(9), 1601.

Douglas, I., Garvin, S., Lawson, N., Richards, J., Tippett, J., and White, I. (2010). Urban pluvial flooding: a qualitative case study of cause, effect and nonstructural mitigation. *Journal of Flood Risk Management*, *3*(2), 112-125.

Earls, J., and Dixon, B. (2007). Spatial interpolation of rainfall data using ArcGIS: A comparative study. In *ESRI User Conference June 2007*.

e Costa, C. A. B., Da Silva, P. A., and Correia, F. N. (2004). Multicriteria evaluation of flood control measures: The case of Ribeira do Livramento. *Water Resources Management*, *18*(3), 263-283.

Eleuterio J. (2012). Flood Risk Analysis: Impact of uncertainty in hazard modelling and vulnerability assessments on damage estimations. PhD thesis at the Augustin Cournot Doctoral School, Water Science and Environmental Economics, Department of Civil Engineering, the University of Strasbourg.

England Jr J. F., Timothy A. Cohn, Beth A. Faber, Jery R. Stedinger, Wilbert O. Thomas Jr., Andrea G., Veilleux, Julie E. Kiang, and Robert R. Mason (2017). Guidelines for Determining Flood FlowFrequencyBulletin17C: Techniques andMethods 4–BXXhttps://acwi.gov/hydrology/Frequency/b17c/Bulletin17C-draft-for-USGS-EditorialReview-10Apr2017.pdf (26/5/2017)

Faber B. (2010). Current Methods for Flood Frequency Analysis. Being a paper presented at the Workshop on Non-Stationarity, Hydrologic Frequency Analysis, and Water Management organized by the Hydraulic Engineering Center of the United States Army Corps of Engineers, January 13, 2010.

Falconer, R. H., Cobby, D., Smyth, P., Astle, G., Dent, J., and Golding, B. (2009). Pluvial flooding: new approaches in flood warning, mapping and risk management. *Journal of Flood Risk Management*, *2*(3), 198-208

Faniran, A. (1968). The index of drainage intensity-A provisional new drainage factor. *Australian Journal of Science*, *31*, 328-330.

Federal Ministry of Works (2013). *Highway Manual Part I-Design Volume IV: Drainage Design.* Abuja. Author

Few, R. (2003). Flooding, vulnerability and coping strategies: local responses to a global threat. *Progress in Development Studies*, *3*(1), 43-58.

Forkuo, E. K. (2011). Flood hazard mapping using Aster image data with GIS. *International journal of Geomatics and Geosciences*, *1*(4), 932-950.

Frank H. and Althoen S. C. (1995). *Statistics: Concepts and Applications*. Cambridge University Press.

Gaillard, J. C. (2010). Vulnerability, capacity and resilience: perspectives for climate and development policy. *Journal of International Development*, *22*(2), 218-232.

Galy, H. M., & Sanders, R. A. (2000). Using SAR imagery for flood modeling. *Englewood, CO. http://www. intermap. ca/PDF/rgs_paper. pdf (22 February 2000)*.

Gana, A. K. (2011). Cow dung: soil amendment agent for the sandy upland sugarcane ecology in Nigeria. *Journal of Agricultural Technology 2011* Vol. 7(2): 497-505

Garba, H. A (2015): Flood Vulnerability Assessment in Jalingo Metropolis, Taraba State, Nigeria. Unpublished M.Sc. Dissertation in the Department of Geography, Ahmadu Bello University, Zaria.

Garde, R.J. (2006). River Morphology, New Age International (Pvt) Ltd. Publishers, New Delhi.

Gardiner, V., Gregory, K. J., and Walling, D. E. (1977). Further notes on the drainage density-basin area relationship. *Area*, 117-121.

Gideon, Y. B., Fatoye, F. B., and Omada, J. I. (2013). Quality Assessment of Physico-Chemical Characteristics of Okura River, Kogi State, Nigeria. *International Journal of Science and Technology*, *2*(12), 891-899.

Grant, A., Ries, R., and Thompson, C. (2016). Quantitative approaches in life cycle assessment—part 1—descriptive statistics and factor analysis. *The International Journal of Life Cycle Assessment*, *21*(6), 903-911.

Haghiabi, A. H., Heidarpourand M. and Habili, J. (2011). A new method for estimating the parameters of Kostiakov and modified Kostiakov infiltration equations. *World Applied Sciences Journal*. 15(1): 129 –135.

Harms, A. A., and Campbell, T. H. (1967). An extension to the Thomas-Fiering Model for the sequential generation of streamflow. *Water Resources Research*, *3*(3), 653-661.

Hartkamp, A. D., De Beurs, K., Stein, A., and White, J. W. (1999). *Interpolation techniques for climate variables*.NRG-GIS Series 99-01. Mexico, D.F.: CIMMYT

Herschy, R. (1993). The velocity-area method. *Flow measurement and instrumentation*, *4*(1), 7-10.

Herschy R. W. (1995). Stream flow Measurement, Chapman & Hall, Second Edition.

Heywood, I., Oliver, J., and Tomlinson, S. (1995). Building an exploratory multi-criteria modelling environment for spatial decision support. *Innovations in GIS*, *2*, 127-136.

Hjelmfelt Jr, A. T. (1991). Investigation of curve number procedure. *Journal of Hydraulic Engineering*, *117*(6), 725-737.

Hoque, R., Nakayama, D., Matsuyama, H., and Matsumoto, J. (2011). Flood monitoring, mapping and assessing capabilities using RADARSAT remote sensing, GIS and ground data for Bangladesh. *Natural Hazards*, *57*(2), 525-548.

Horton, R. E. (1932). Drainage-basin characteristics. *Eos, Transactions American Geophysical Union*, *13*(1), 350-361.

Horton, R. E. (1945). Erosional development of streams and their drainage basins; hydrophysical approach to quantitative morphology. *Geological society of America bulletin*, *56*(3), 275-370.

Hotchkiss, R. H., and McCallum, B. E. (1995). Peak discharge for small agricultural watersheds. *Journal of Hydraulic Engineering*, *121*(1), 36-48.

Houston, D., Werritty, A., Bassett, D., Geddes, A., Hoolachan, A., and McMillan, M. (2011). Pluvial (rain-related) flooding in urban areas: the invisible hazard. *Joseph Rowntree Foundation*.

http://www.agritech.tnau.ac.in/agriculture/agri_majorareas_watershed_watershedmgt.html

http://www.caliper.com/glossary/what-is-a-digital-elevation-model-dem.htm

http://www.fao.org/soils-portal/soil-survey/soil-maps-and-databases/harmonized-world-soil-database-v12/en/

http://www.floodresiliencity.eu/frc-output/153/t/3-understanding-pluvial-flooding

http://gisgeography.com/image-classification-techniques-remote-sensing/

http://www.nationsonline.org/oneworld/map/nigeria-administrative-map.htm

http://newmap.gov.ng/partner-states/kogi-state/

http://www.stattrek.com/statistics/dictionary.aspx?definition=coefficient_of_determination.

https://www.thisdaylive.com/index.php/2016/09/08/five-communities-in-anambra-submerged-by-flood/

http://www.waterbase.org/download_data.html

http://web.pdx.edu/~emch/ip1/bandcombinations.html

http://www.vanguardngr.com/2016/09/flood-water-hyacinth-traps-6-communities-anambra/

Ibrampurkar, M. M. (2012). *Hydrological and hydrogeological evaluation of Mhadei river watershed-in Goa and Karnataka* (Doctoral dissertation, Goa University).

Imasuen, O., Omali, A., and Ibrahim, I. (2011). Assessment of environmental impacts and remedies for gully erosion in Ankpa Metropolis and environs, Kogi State, Nigeria. *Adv. Applied Sci. Res*, *2*, 372-384.

International Strategy for Disaster Reduction (2004), Living with Risk. UNISDR, UN, Geneva (http://www.unisdr.org/eng/about_isdr/bd-lwr-2004-eng.htm)

International Strategy for Disaster Reduction (2009).United Nations International Strategy for Disaster Risk Reduction (UNISDR) Terminology on Disaster Risk Reduction. UNISDR, UN, Geneva

Islam, A. S., Bala, S. K.and Haque, A. (2009). Flood Inundation Map Of Bangladesh Using Modis Surface Reflectance Data. *Proc. Of 2nd International Conference on Water & Flood Management.*

Islam, M. R. (2004). A review on watershed delineation using GIS tools. *Dept. of Civil Engineering, University of Manitoba, Winnipeg from http://www. wrrc. dpri. kyoto-u. ac. jp*.

Islam, M. M., and Sado, K. (2000a). Development of flood hazard maps of Bangladesh using NOAA-AVHRR images with GIS. *Hydrological Sciences Journal*, *45*(3), 337-355.

Islam, M. M, and Sado, K. (2000b). Flood hazard assessment in Bangladesh using NOAA AVHRR data with geographical information system. *Hydrological Processes*, *14*(3), 605-620.

Islam, M. M., Sado, K. I. M. I. T. E. R. U., Owe, M., Brubaker, K., Ritchie, J., and Rango, A. (2001). Flood damage and management modelling using satellite remote sensing data with GIS: case study of Bangladesh. *IAHS PUBLICATION*, 455-457.

Ismail A. (1989). Basin Characteristics of Galma and Kubanni Catchments. A Final year Undergraduate project in the Department of Water Resources and Environmental Engineering, Ahmadu Bello University, Zaria.

ISO 18365: (2013). Hydrometry -- Selection, establishment and operation of a gauging station. https://www.iso.org/standard/62267.html

ISO 1100-2: (2010). Hydrometry -- Measurement of liquid flow in open channels -- Part 2: Determination of the stage-discharge relationship. A publication of the International Organization for standardization. Geva. Available online at https://www.iso.org/standard/42207.html

James, L. D. (1967). Economic analysis of alternative flood control measures. *Water Resources Research*, *3*(2), 333-343.

Jeb, D. N and Aggarwal, S.P (2008), "Flood inundation hazard modeling of the River Kaduna using Remote Sensing and Geographic Information Systems", *Journal of Applied Sciences Research*, 4 (12). 1822-1833

Jeb D. N. (2014). Flood Risk Analysis in Kaduna Metropolis, Kaduna State, Nigeria Using Geo-Information Science. Unpublished PhD Thesis in the Department of Geography, Ahmadu Bello University, Zaria.

Kafle,T. P., Hazarika, M. K., Shrestha, K. G., Prathumchai, K. and Samarakoon, L. (2006). Integration of remote sensing and Gis with flood simulation model for flood hazard mapping in the Bagmati River, Nepal. *New Technologies for Urban Safety of Mega Cities in Asia.* 257 – 267.

Kafle, T. P., Hazarika, M. K., Karki, S., Shrestha, R. M., Sharma, S., and Samarakoon, L. (2007). Basin scale rainfall-runoff modelling for flood forecasts. In *Proceedings of the 5th Annual Mekong Flood Forum, Ho Chi Minh City, Vietnam* (pp. 17-18).

Kandilioti, G. and Makropoulos, C. (2012). Preliminary Flood Risk Assessment: The Case of Athens. *Natural Hazards,* **61,** 441-468

Keeney, R.L. and Raiffa, H. (1976). *Decision with Multicriteria Objectives: Preferences and Value Tradeoffs*. New York.Wiley.

Kenyon, W. (2007). Evaluating flood risk management options in Scotland: A participant-led multi-criteria approach. *Ecological Economics*, *64*(1), 70-81.

Khan, S. I., Hong, Y., Wang, J., Yilmaz, K. K., Gourley, J. J., Adler, R. F., ... and Irwin, D. (2011). Satellite remote sensing and hydrologic modeling for flood inundation mapping in Lake Victoria basin: Implications for hydrologic prediction in ungauged basins. *IEEE Transactions on Geoscience and Remote Sensing*, *49*(1), 85-95.

Kirkwood, C. W. (1997). Strategic Decision Making: Multi-objective Decision Making with Spreadsheets. Belmont, Duxbury Press.

Kidson, R., and Richards, K. S. (2005). Flood frequency analysis: assumptions and alternatives. *Progress in Physical Geography*, *29*(3), 392-410.

Kirpich, Z. P. (1940). Time of concentration of small agricultural watersheds. *Civil Engineering*, *10*(6), 362.

Kogi State Government (2012). Blueprint for the Transformation of Kogi State (2012 – 2016) Volume I.

Komolafe, A. A., Adegboyega, S. A.-A., and Akinluyi, F. O. (2015). A Review of Flood Risk Analysis in Nigeria. *American Journal of Environmental Sciences*, *11*(3), 157-166.

Kreibich, H., and Thieken, A. H. (2008). Assessment of damage caused by high groundwater inundation. *Water Resources Research*, *44*(9).

Krejcie R. V. and Morgan D. W (1970) "Determining Sample Size for Research Activities". *Educational and Psychological Measurement*, #30, pp. 607-610

Krishnamurthy, J., Venkatesa Kumar, N., Jayaraman, V., and Manivel, M. (1996). An approach to demarcate ground water potential zones through remote sensing and a

geographical information system. *International Journal of Remote Sensing*, *17*(10), 1867-1884.

Kulkarni, M. D. (2015) The Basic Concept to Study Morphometric Analysis of River Drainage Basin: A Review.*International Journal of Science and Research*, 4(7), 2277-2280.

Kurunç, A., Yürekli, K., and Çevik, O. (2005). Performance of two stochastic approaches for forecasting water quality and streamflow data from Yeşilırmak River, Turkey. *Environmental Modelling & Software*, *20*(9), 1195-1200.

Langbein, W. B., and Leopold, L. B. (1964). Quasi-equilibrium states in channel morphology. *American Journal of Science*, *262*(6), 782-794.

Lebbe, J. M. E. (1991). Reliability Studies of Multi-Reservoir System Using Stochastic Approach. An M.Sc. Civil Engineering at King Fahd University of Petroleum & Minerals, Dhahran, Saudi Arabia.

Léonard, J., Mietton, M., Najib, H., and Gourbesville, P. (2000). Rating curve modelling with Manning's equation to manage instability and improve extrapolation. *Hydrological Sciences Journal*, *45*(5), 739-750.

Lerat, J., Perrin, C., Andréassian, V., Loumagne, C., and Ribstein, P. (2012). Towards robust methods to couple lumped rainfall–runoff models and hydraulic models: A sensitivity analysis on the Illinois River.*Journal of Hydrology*, *418*, 123-135.

Le Roux, J. P. (1992). Determining the channel sinuosity of ancient fluvial systems from paleocurrent data. *Journal of Sedimentary Research*, *62*(2) 283-29

Library of Congress (n.d). Administrative Map of Nigeria. Available at https://www.loc.gov/item/2010592721/. Accessed 08/06/2017)

Lindsay-Walters, A. (n.d). The chances of a river flooding after a period of rain are determined by natural factors. Available online on http://www.markedbyteachers.com/international-baccalaureate/geography/the-chances-of-a-river-flooding-after-a-period-of-rain-are-determined-by-natural-factors-do-you-agree.html. Accessed 5th May, 2016

Lin S. D. (2007). Water and Wastewater Calculations Manual, 2nd Ed. New York. McGraw-Hill

Liu, R. Y., Parelius, J. M., and Singh, K. (1999). Multivariate analysis by data depth: descriptive statistics, graphics and inference,(with discussion and a rejoinder by Liu and Singh). *The annals of statistics*, *27*(3), 783-858.

Macdonald, D., Dixon, A., Newell, A., and Hallaways, A. (2012). Groundwater flooding within an urbanised flood plain. *Journal of Flood Risk Management*, *5*(1), 68-80.

Magdoff, F., and Van Es, H. (2000). *Building soils for better crops* (No. 631.584/M188b). Beltsville: Sustainable Agriculture Research and Education (SARE). Available online at

http://www.sare.org/Learning-Center/Books/Building-Soils-for-Better-Crops-3rd-Edition/Text-Version (29/11/2017)

Mair, A., and Fares, A. (2010). Comparison of rainfall interpolation methods in a mountainous region of a tropical island. *Journal of Hydrologic Engineering*, *16*(4), 371-383.

Maksimović, Č., Prodanović, D., Boonya-Aroonnet, S., Leitão, J. P., Djordjević, S., and Allitt, R. (2009). Overland flow and pathway analysis for modelling of urban pluvial flooding. *Journal of Hydraulic Research*, *47*(4), 512-523.

Makungo, R., Odiyo, J. O., Ndiritu, J. G. and Mwaka, B. (2010). Rainfall-runoff modeling approach for ungauged catchments: A case study of Nzhelele River sub-quaternary catchment. *Physics and Chemistry of the Earth*. 35; 596 – 607

MalczewskI, J. (1999). *GIS and Multicriteria Decision Analysis*. New York: JohnWiley.

Maroof, L. K., Sule, B. F., and Ogunlela, O. A. (2015). Economic Sustainability of Integrated Hydropower Development of Ero-Omola Falls, Kwara State, Nigeria. In *Decision Making and Knowledge Decision Support Systems* (pp. 143-164). Springer International Publishing.

Martins, A. K., and Gadiga, B. L. (2015). Hydrological and Morphometric Analysis of Upper Yedzaram Catchment of Mubi in Adamawa State, Nigeria. Using Geographic Information System (GIS). *World Environment*, *5*(2), 63-69.

Mays, L. W. (2005). Water Resources Engineering. John Wiley & Sons Inc. NewJersey.

Mazvimavi, D. (2003). Estimation of Flow Characteristics of Ungauged Catchments: Case Study in Zimbabwe. Unpublished PhD Thesis. Wageningen University, The Netherlands.

Meals D. W. and Dressing S. A. (2008). Surface water flow measurement for water quality monitoring projects, Tech Notes 3, March 2008. Developed for U.S. Environmental Protection Agency by Tetra Tech, Inc., Fairfax, VA, 16 p. Available online at www.bae.ncsu.edu/programs/extension/wqg/319monitoring/tech_notes.htm.

Melton, M. A. (1957). *An analysis of the relations among elements of climate, surface properties, and geomorphology* (No. CU-TR-11). COLUMBIA UNIV NEW YORK.

Merwade, V. (2012a). Stream network and watershed delineation using spatial analyst hydrology tools. *School of Civil Engineering, Purdue University* available at ics.purdue.edu

Merwade, V. (2012b). Terrain Processing and HMS-Model Development using GeoHMS. *Lafayette, Indiana*.

Merwade, V. (2016). Tutorial on using HEC-GeoRAS with ArcGIS 10 and HECRAS Modeling. *School of Civil Engineering, Purdue University, Indiana*.

Merz, B., Thieken, A. H., and Gocht, M. (2007). Flood risk mapping at the local scale: concepts and challenges. In *Flood risk management in Europe* (pp. 231-251). Springer Netherlands.
Messner, F., and Meyer, V. (2006). Flood damage, vulnerability and risk perception–challenges for flood damage research. *Flood risk management: hazards, vulnerability and mitigation measures*, 149-167.

Meyer, V., Scheuer, S., and Haase, D. (2009). A multicriteria approach for flood risk mapping exemplified at the Mulde river, Germany. *Natural hazards*, *48*(1), 17-39.

Miller, S. N., Semmens, D. J., Goodrich, D. C., Hernandez, M., Miller, R. C., Kepner, W. G., and Guertin, D. P. (2007). The automated geospatial watershed assessment tool. *Environmental Modelling & Software*, *22*(3), 365-377.

Miller, V. C. (1953). *A quantitative geomorphic study of drainage basin characteristics in the clinch mountain area virginia and tennessee* (No. CU-TR-3). Columbia University New York.

Mitchell, J. K. (2006). Urban disasters as indicators of global environmental change: assessing functional varieties of vulnerability. In *Earth System Science in the Anthropocene* (pp. 135-152). Springer Berlin Heidelberg.

Murtala, H. A. (2014).The use of Gegraphic Information System in Landfill sites Selection in Jos North, Plateau State Nigeria. Unpublished M.Sc. Dissertation in the Department of Geography, Ahmadu Bello University, Zaria.

Mustafa S. and Yusuf M. I. (2012). *A Textbook of Hydrology and Water Resources, Revised Edition.* Abuja. Topsmerit Page Publishing Company.

Musungu, K., Motala, S., and Smit, J. (2012). Using multi-criteria evaluation and GIS for flood risk analysis in informal settlements of Cape Town: the case of Graveyard Pond. *South African Journal of Geomatics*, *1*(1), 92-108.

Nachtergaele, F., van Velthuizen, H., Verelst, L., Batjes, N., Dijkshoorn, K., van Engelen, V., ... and Prieler, S. (2009). Harmonized world soil database. *Wageningen: ISRIC*.

Nag, S. K. (1998). Morphometric analysis using remote sensing techniques in the Chaka sub-basin, Purulia district, West Bengal. *Journal of the Indian society of remote sensing*, *26*(1), 69-76.

Naoum, S., and Tsanis, I. K. (2004). Ranking spatial interpolation techniques using a GIS-based DSS. *Global Nest*, *6*(1), 1-20.

NASA (2010). Landsat Data Continuity Brochure. Available online at landsat.gsfc.nasa.gov/pdf_archive/20101119_LDCMbrochure.pdf Accessed 29/11/2017.

Nash, J. E. (1958). *Determining run-off from rainfall*. Institution of Civil Engineers.

National Population Commission (2010b). 2006 Population and Housing Census Priority Table Volume XI: Population Distribution by Age, Sex and Disability Status (State & Local Government Area) available at www.population.gov.ng. Accessed 28/3/2017

National Population Commission (2010a). 2006 Population and Housing Census Priority Table Volume IV: Population Distribution by Age & Sex (State & Local Government Area) available at www.population.gov.ng. Accessed 28/3/2017

National Bureau of Statistics (2012). Annual Abstract of Statistics, 2012. Available at www.nigerianstat.gov.ng. accessed 17/4/2017

Nayak, T. R and Jaiswal, R. K. (2001). Rainfall-Runoff modeling using satellite data and GIS for Bebas River in Madhya Pradesh.

Ndabalu C. (2006): Assessment of landuse/landcover changes in Kaduna metropolitan area using remote sensing and geographic information system techniques . Unpublished M.Sc. Dissertation in the Department of Geography, Ahmadu Bello University, Zaria

Nicholas J. E. (2014). Assessment of the 2012 flooding in Mararabakaru Local Government Area of Nasarawa state, Nigeria. Unpublished M.Sc. Dissertation in the Department of Geography, Ahmadu Bello University, Zaria.

Nigeria Hydrological Services Agency (2015). *Annual Flood Outlook*. Abuja. Nigeria Hydrological Services Agency.

Migeria Meteorological Agency (2016). Daily Rainfall Data for Makurdi from 1980 – 2015 (unpublished)

Noman, N. S., Nelson, E. J., and Zundel, A. K. (2003). Improved process for floodplain delineation from digital terrain models. *Journal of water resources planning and management*, *129*(5), 427-436.

Nwafor, J. C. (2006). *Environmental impact assessment for sustainable development: the Nigerian perspective*. Environment and Development Policy Centre for Africa (EDPCA).

Obansa Y. M. (2012). Temporal Changes in Floodplains of River Kaduna, Nigeria. Unpublished PhD Thesis in the Department of Geography, Bayero University, Kano

Obeta, M. C. (2014). Institutional Approach to Flood Disaster Management in Nigeria: Need for a Preparedness Plan. *British Journal of Applied Science & Technology, 4*(33), 4575-4590.

Obi Reddy, G. E., Maji, A. K., and Gajbhiye, K. S. (2002). GIS for morphometric analysis of drainage basins. *GIS lndia, 11*(4), 9-14

Oku, E. and Aiyelari, A. (2011). Predictability of Philip and Kostiakov infiltration model under inceptisols in the Humid Forest Zone, Nigeria. *Kasetsart Journal (Natural Science), 45: 594 -602.*

Olajuyigbe, A. E., Rotowa, O. O., and Durojaye, E. (2012). An assessment of flood hazard in Nigeria: The case of mile 12, Lagos. *Mediterranean Journal of Social Sciences*, ***3***(2), 367-375.

Ongley, E. (1996). Sediment Measurement in Water Monitoring- A Practical Guide to the Design and Implementation of Freshwater Quality Studies and Monitoring Programmes Ed. Jamie B. & Richard B. United Nation Environment Programme and The World Health Organisation.

Otun, J. A., and Adeogun, B. K. (2010). Analysis of Fluvial Sediment Discharges into Kubanni Reservoir. *Nigerian Journal of Technology*, *29*(2), 64-75.

Oyebande, L. (1982). Deriving rainfall intensity-duration-frequency relationships and estimates for regions with inadequate data. *Hydrological Sciences Journal*, *27*(3), 353-367.

Pandey, A., Chowdary, V. M., Mal, B. C., and Dabral, P. P. (2003). Estimation of runoff for agricultural watershed using SCS Curve Number and Geographic Information System. *Map India. Online. URL: http://www. gisdevelopment. net/application/agriculture/soil/pdf/48. pdf (Issue: March 2007)*.

Parr, J.R. and Bertrand, A.R. (1960) Water infiltration into soils. *Advances in Agronomy*, 12, 311-363.

Patra, K. C. (2008). *Hydrology and Water Resources Engineering, Second Edition.* New Delhi. Narosa Publishing House.

Patton, P. C., and Baker, V. R. (1976). Morphometry and floods in small drainage basins subject to diverse hydrogeomorphic controls. *Water Resources Research*, *12*(5), 941-952

Philips, C.E. and Kitch, W. A. (2011). *A review of methods for characterization of site infiltration with design recommendation*.Proceedings 43rd Symposium on Engineering Geology and Geotechnical Engineering (University of Las Vegas, Nevada) pg 130 – 140.

Philip, J. R. (1957). The theory of infiltration: 4. Sorptivity and algebraic infiltration equations. *Soil science*, *84*(3), 257-264.

Ponce, V. M., and Hawkins, R. H. (1996). Runoff curve number: Has it reached maturity?.*Journal of hydrologic engineering*, *1*(1), 11-19.

Pradhan, B. (2010). Flood susceptible mapping and risk area delineation using logistic regression, GIS and remote sensing. *Journal of Spatial Hydrology*, *9*(2).

Quan, N. H. (2006). Rainfall-Runoff Modelling in the Ungauged Can Le Catchment, Saigon Basin, an Unpublished M.Sc. Thesis at the International Institute for Geo-Information Science and Earth Observation, Enschede, The Netherlands.

Raaijmakers, R., Krywkow, J., and van der Veen, A. (2008). Flood risk perceptions and spatial multi-criteria analysis: an exploratory research for hazard mitigation. *Natural hazards*, *46*(3), 307-322.

Raj, P. N., and Azeez, P. A. (2012). Morphometric analysis of a tropical medium river system: a case from Bharathapuzha River southern India.*Open Journal of Modern Hydrology*, 2, 91-98.

Rantz S.E. (1982a). Measurement and computation of streamflow, Volume1 Measurement of Stage and Discharge U.S. Geological Survey Water Supply Paper2175

Rantz S.E. (1982b). Measurement and computation of streamflow, Volume2 Computation of Discharge, U.S.Geological Survey Water Supply Paper2175

Reddy, P. J. R. (2008). *A textbook of hydrology*. University Science Press Publishers Bangalore India.

Research Advisors (2006): Sample Size Table. http://research-advisors.com

Richards, L. A. (1931). Capillary conduction through porous mediums. *Physics 1:* 313-318.

Rossi, G., Harmancioglu, N. B., and Yevjevich, V. (Eds.). (2012). *Coping with floods* (Vol. 257). Springer Science & Business Media.

Saaty, T.(1980). *The Analytical Hierachy Process*.New York. McGraw Hill.

Sadeghian, M. S., Salarijazi, M., Ahmadianfar, I., and Heydari, M. (2016). Stage-Discharge Relationship in Tidal Rivers for Tidal Flood Condition. *Feb-Fresenius Environmental Bulletin*, 25(10). 4111-4117.

Saghafian, B., Farazjoo, H., Bozorgy, B., and Yazdandoost, F. (2008). Flood intensification due to changes in land use. *Water resources management*, 22(8), 1051-1067.

Salau, O.B.E. and Daffi, R.E. (2009). Rainfall-Runoff Modelling using remote sensing and geographic information system. *Nigerian Journal of Engineering Management*. 10(2). 42–51.

Salimi, S., Ghanbarpour, M. R., Solaimani, K. and Ahmadi, M. Z. (2008). Floodplain mapping using hydraulic simulation model in GIS. *Journal of Applied Sciences 8 (4)*. 660-665.

Sanyal, J., and Lu, X. X. (2004). Application of remote sensing in flood management with special reference to monsoon Asia: a review. *Natural Hazards*, *33*(2), 283-301.

Sapkale, J. B. (2013). Cross Sectional and Morphological Changes after a Flood in Bhogawati Channel of Kolhapur, Maharashtra. *Indian Geographical Quest, 2*, 68-78.

Sarma, D. (2013). *Rural Risk Assessment due to Flooding and Riverbank Erosion in Majuli, Assam, India. Master's thesis,* in the Faculty of Geo-Information Science and Earth Observation, *University of Twente.*

Sathish, S. and Babu, S. K. (2017, November). Stochastic time series analysis of hydrology data for water resources. In *IOP Conference Series: Materials Science and Engineering*, 263(4), p. 042140). IOP Publishing.

Sauer, V.B., and Turnipseed, D.P. (2010). Stage measurement at gaging stations: U.S. Geological Survey Techniques and Methods book 3, chap. A7, 45 p. (Also available at http://pubs.usgs.gov/tm/tm3-a7/.)

Schumm, S. A. (1956). Evolution of drainage systems and slopes in badlands at Perth Amboy, New Jersey. *Geological society of America bulletin*, *67*(5), 597-646.

Sharma, P. (2004) Flood risk zone mapping of Dikrong Sub-Basin in Assam. *A paper presented at the Map Asia Conference*, 2004 at Beijing International Convention Centre, Beijing, China.

Shimizu, I. (1998). Multistage Sampling. *Wiley StatsRef: Statistics Reference Online*.

Skoup and Co. Ltd and Motor Columbus Inc. Switzerland (1980). Ayangba Project Area Feasibility Study Volume II: Project Report, prepared for the Anambra-Imo River Basin Development Authority, Federal Republic of Nigeria.

Smith, D. R., Conroy, M. J., and Brakhage, D. H. (1995). Efficiency of adaptive cluster sampling for estimating density of wintering waterfowl. *Biometrics*, 777-788.

Smith, K., and Ward, R. (1998). *Floods: physical processes and human impacts*. West-Sussex. John Wiley and Sons Ltd.

Smith, K. G. (1950). Standards for grading texture of erosional topography. *American Journal of Science*, *248*(9), 655-668.

Smith, L. C. (1997). Satellite remote sensing of river inundation area, stage, and discharge: A review. *Hydrological processes*, *11*(10), 1427-1439.

Solín, Ľ., Feranec, J., and Nováček, J. (2011). Land cover changes in small catchments in Slovakia during 1990–2006 and their effects on frequency of flood events. *Natural hazards*, *56*(1), 195-214.

Spriensma, A., and Wijnstok, N. (2016). Randomized controlled trials: how to describe your study population. *Journal of Endourology*, *30*(1), 1-4. DOI: 10.1089/end.2015.29007.cro

Sreedevi, P. D., Sreekanth, P. D., Khan, H. H., and Ahmed, S. (2013). Drainage morphometry and its influence on hydrology in a semi arid region: using SRTM data and GIS. *Environmental earth sciences*, *70*(2), 839-848.

Stabel, E. and Löffler, E. (2003). Optimised Mapping Of Flood Extent And Floodplain Structures By Radar Eo-Methods. *Proc. of FRINGE 2003 Workshop, Frascati, Italy.*

Stedinger, J. R., and Taylor, M. R. (1982). Synthetic streamflow generation: 1. Model verification and validation. *Water Resources Research*, *18*(4), 909-918.

Strahler, A. N. (1952). Hypsometric (area-altitude) analysis of erosional topography. *Geological Society of America Bulletin*, *63*(11), 1117-1142.

Strahler, A. N. (1957). Quantitative analysis of watershed geomorphology. *Eos, Transactions American Geophysical Union*, *38*(6), 913-920.

Strahler, A. N. (1964). Quantitative geomorphology of drainage basin and channel networks. *Handbook of applied hydrology*, Ed. Ven TeChow, 04, 9 - 76.

Suresh R. (2008). Land and Water Management Principles. Delhi. Standard Publishers Distributors.

Tarekegn, T. H., Haile, A. T., Rientjes, T., Reggiani, P., and Alkema, D. (2010). Assessment of an ASTER-generated DEM for 2D hydrodynamic flood modeling. *International Journal of Applied Earth Observation and Geoinformation*, *12*(6), 457-465.

Telis, P. A. (2001). *Estimation of infiltration rates of saturated soils at selected sites in the Caloosahatchee River basin, southwestern Florida* (No. USGS-OFR-01-65). GEOLOGICAL SURVEY RESTON VA.

Teymouri, M., and Fathzadeh, A. (2015). Stochastic modeling of monthly river flow forecasting (Case study: Atrak River Basin, Iran). *Journal of Selçuk University Natural and Applied Science*, *4*(2), 38-48.

Tongco, M. D. C. (2007). Purposive sampling as a tool for informant selection. *Ethnobotany Research and Applications*, *5*, 147-158.

TR-55 (1986). *Urban Hydrology for Small Watersheds, Technical Release 55*. United States Department of Agriculture, Natural Resources Conservation Services and Conservative Engineering Division.

United Nations Department of Humanitarian Affair (UNDHA) (1992). Internationally agreed glossary of basic terms related in disaster management, Geneva

United Nations International Strategy for Disaster Risk Reduction (UNISDR) (2005). Hyogo Framework for 2005-2015: Building the Resilience of Nations and Communities to Disasters. Available at http://www.unisdr.org/wcdr/intergover/official-doc/Ldocs/Hyogo-framework-foraction-english.pdf.

United Nations Office for the Coordination of Humanitarian affairs (2012). Nigeria: Humanitarian Dashboard - Floods (as of 26 Nov. 2012) available at http://reliefweb.int/report/nigeria/nigeria-humanitarian-dashboard-floods-26-nov-2012 (accessed 17/02/2017)

U.S. Army Corps of Engineers (1995). Sediment Measurement Techniques (Em 1110-2-4000; Ch 8). www.usace army.mil

Vaezi, A. R., Bahrami, H. A., Sadeghi, S. H. R., and Mahdian, M. H. (2010). Modeling relationship between runoff and soil properties in dry-farming lands, NW Iran. *Hydrology and Earth System Sciences Discussions*, *7*(2), 2577-2607.

van der Sande, C. J., De Jong, S. M., and De Roo, A. P. J. (2003). A segmentation and classification approach of IKONOS-2 imagery for land cover mapping to assist flood risk and flood damage assessment. *International Journal of applied earth observation and geoinformation*, *4*(3), 217-229.

VanWesten, C., (2001). Geoinformation Science and Earth Observation for municipal risk management : The SLARIM project. In: I. International Instititute for Geoinformation Science and Earth Observation (Editor), Risk management. ITC, Enschede. Accessed 02-02-2009

Veen, A. V. D., and Logtmeijer, C. (2005). Economic hotspots: visualizing vulnerability to flooding. *Natural Hazards*, *36*(1), 65-80.

Waikar, M. L., and Nilawar, A. P. (2014). Morphometric analysis of a drainage basin using geographical information system: a case study. *Int J Multidiscip Curr Res*, *2*, 179-184

Walesh, S. G. (1989). *Urban surface water management*. John Wiley & Sons.

Wang, Y., Li, Z., Tang, Z., and Zeng, G. (2011). A GIS-based spatial multi-criteria approach for flood risk assessment in the Dongting Lake Region, Hunan, Central China. *Water resources management*, *25*(13), 3465-3484.

Ward, R.C. (1978). Floods – A Geographical Perspective. London (UK). Macmillan.

Warrick, J. A. (2015). Trend analyses with river sediment rating curves. *Hydrological processes*, *29*(6), 936-949.

Watson, R. T., Zinyowera, M. C., and Moss, R. H. (1996). *Climate Change 1995 impacts, adaptations and mitigation of climate change: Scientific-technical analysis*. Cambridge University Press.

Webster, T. L., Forbes, D. L., MacKinnon, E., & Roberts, D. (2006). Flood-risk mapping for storm-surge events and sea-level rise using lidar for southeast New Brunswick. *Canadian Journal of Remote Sensing*, *32*(2), 194-211.

Withanage, N. S., Dayawansa, N. D. K., and De Silva, R. P. (2014). Morphometric analysis of the Gal Oya River basin using spatial data derived from GIS. *Tropical Agricultural Research*, *26*(1), 175-188

World Meteorological Organisation (1994). Guide to Hydrological Practices. Fifth Edition, WMO-No. 168, Geneva.

World Meteorological Organization (2010). Manual on Stream Gauging. wmo.int/pages/prog/hwrp/publications/stream_gauging/1044_vol_II_en.pdf

Yalcin, G. and Akyurek, Z. (2004). Analyzing Flood Vulnerable Areas with Multi-criteria Evaluation. *20th ISPRS Congress*, Istanbul, Turkey.

Zaidi, F. K. (2011). Drainage basin morphometry for identifying zones for artificial recharge: A case study from the Gagas River Basin, India. *Journal of the Geological Society of India*, *77*(2), 160-166.

Zernitz, E. R. (1932). Drainage patterns and their significance. *The Journal of Geology*, 498-521.

Zha, Y., Gao, J., and Ni, S. (2003). Use of normalized difference built-up index in automatically mapping urban areas from TM imagery. *International Journal of Remote Sensing*, *24*(3), 583-594.

Zheng, N., Tachikawa, Y. and Takara, K. (2007). Simplified flood inundation model integrating with rainfall-runoff processes. *Annals of Disaster Prevention Research Institute. Kyoto University*. № 50B. Pp75-78.

APPENDIX I: TOPOGRAPHIC MAPS OF THE STUDY AREA

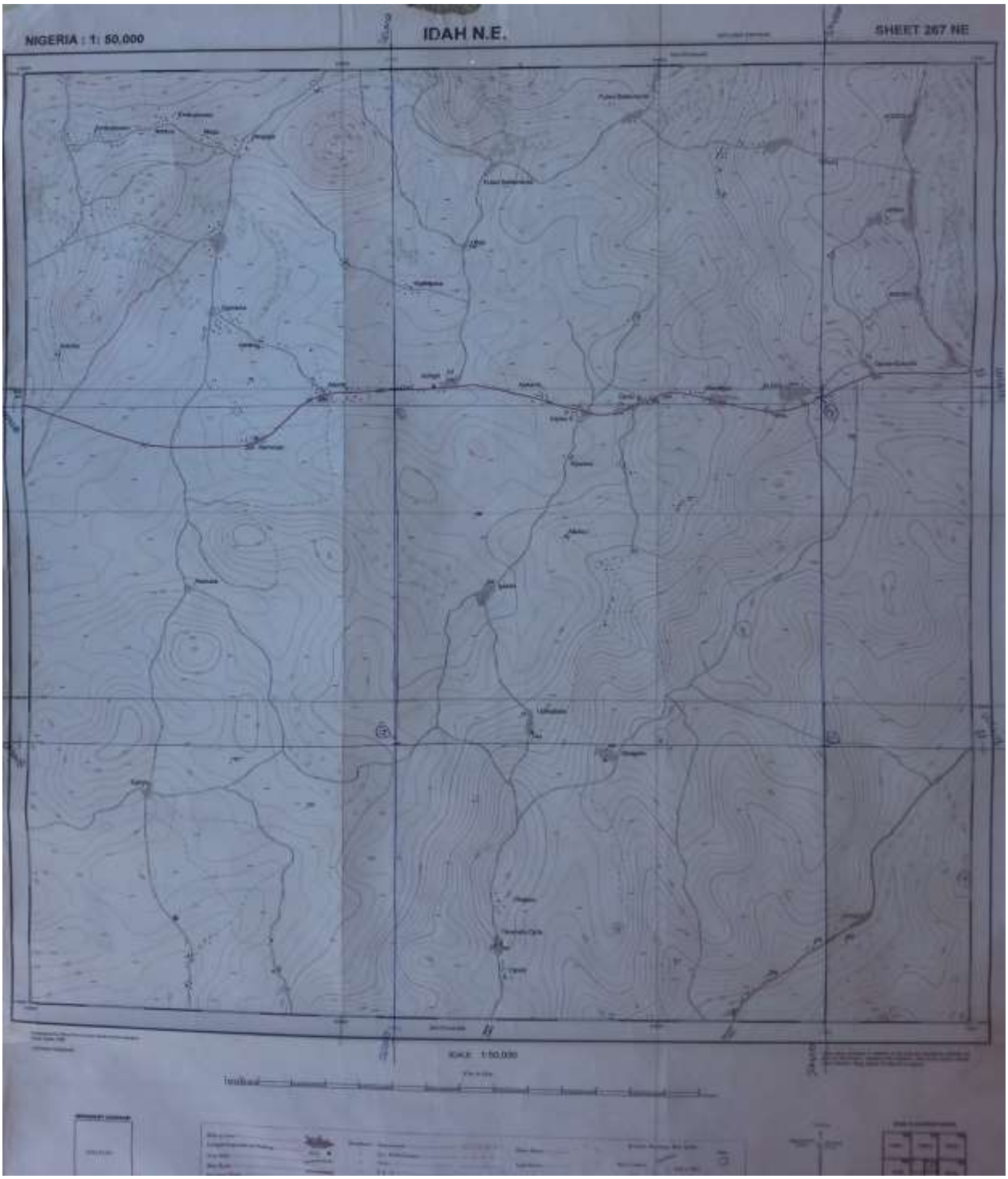


Fig Ia: Topographic Map of Idah sheet 267 NE



Fig Ib: Topographic Map of Idah sheet 267 SE

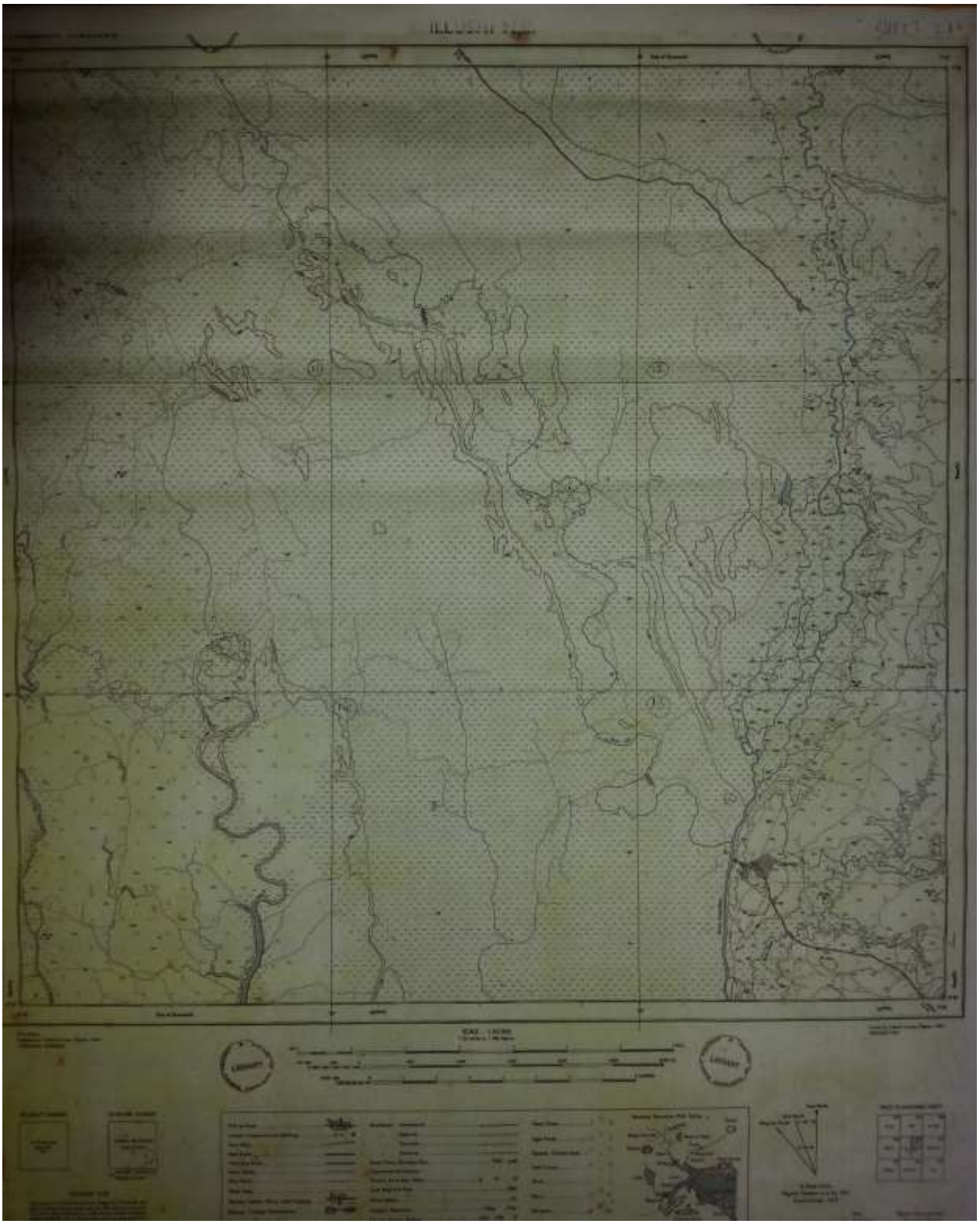


Fig Ic: Topographic Map of Illushi sheet 286 NE

APPENDIX II: RAINFALL DATA

Table IIa: Summary of Rainfall Data Used in this Study (1979 -2013)

Station ID	Coordinates		Average Rainfall (mm)												
	Latitude (ºN)	Longitude (ºE)	Jan	Feb	Mar	Apr	May	Jun	Jul	Aug	Sep	Oct	Nov	Dec	Annual
6163	6.09	6.25	35.44	75.74	166.07	229.67	287.08	318.59	314.83	278.50	388.22	295.88	88.11	35.06	2935.18
6166	6.09	6.56	22.62	48.97	124.07	179.58	232.55	246.37	244.96	222.49	319.20	235.26	61.63	22.43	2312.03
6169	6.09	6.88	17.92	40.20	115.42	178.52	240.40	253.86	251.45	234.88	330.93	248.65	61.29	19.81	2363.21
6172	6.09	7.19	16.95	42.24	128.21	203.46	271.19	287.40	284.06	277.97	384.19	292.43	73.33	23.76	2710.93
6175	6.09	7.50	15.95	41.60	133.75	208.99	273.68	288.47	284.24	288.58	399.02	310.63	68.48	23.55	2785.99
6178	6.09	7.81	14.92	40.94	125.06	192.39	250.65	269.84	288.56	314.82	407.09	297.90	50.33	21.27	2731.55
6463	6.40	6.25	24.38	52.65	118.12	180.02	240.57	258.85	271.39	245.35	351.95	242.71	63.50	26.39	2457.94
6466	6.40	6.56	12.18	26.75	76.32	133.36	186.97	187.20	190.78	176.81	271.24	184.89	38.59	14.56	1802.82
6469	6.40	6.88	9.79	21.02	71.33	130.67	195.91	199.08	209.50	200.95	293.41	190.19	31.78	10.00	1888.21
6472	6.40	7.19	11.89	26.59	90.21	166.77	247.61	258.31	285.42	283.11	382.14	252.53	45.76	14.93	2482.61
6475	6.40	7.50	11.46	30.09	92.53	173.49	252.77	249.75	254.36	260.02	371.56	261.40	49.20	15.87	2431.14
6478	6.40	7.81	8.98	25.57	79.22	152.42	220.18	213.46	229.02	249.20	342.42	224.75	27.91	12.50	2166.53
6763	6.71	6.25	12.78	29.70	72.27	136.38	194.01	190.78	206.41	196.35	298.30	187.19	42.53	16.90	1910.65
6766	6.71	6.56	6.07	15.37	44.31	101.70	159.16	148.27	156.80	153.09	244.98	149.47	23.33	9.69	1489.46
6769	6.71	6.88	5.92	12.95	45.27	103.19	174.06	176.40	197.55	197.46	282.41	160.48	18.72	7.14	1695.71
6772	6.71	7.19	9.69	19.88	62.77	140.76	238.39	256.89	305.11	305.65	395.99	236.32	35.15	11.50	2447.15
6775	6.71	7.50	9.75	22.17	68.03	145.30	251.00	252.03	259.47	267.41	379.16	254.56	42.00	12.83	2369.65
6778	6.71	7.81	6.87	16.84	55.13	126.72	214.69	206.25	220.35	240.15	332.92	206.66	23.34	8.33	2021.14
7063	7.03	6.25	7.57	17.31	46.89	112.01	163.73	161.07	181.68	183.54	274.17	154.76	27.30	9.76	1640.34
7066	7.03	6.56	4.38	10.63	33.14	87.54	139.22	134.21	152.25	156.04	239.15	125.00	15.31	5.22	1367.03
7069	7.03	6.88	4.51	11.11	35.90	89.89	160.33	162.26	195.46	206.64	281.98	139.96	14.43	4.57	1614.24
7072	7.03	7.19	7.47	17.35	49.12	116.83	212.55	222.78	265.42	280.70	368.29	210.16	30.02	8.51	2181.75
7075	7.03	7.50	7.07	17.45	53.54	114.52	225.58	226.16	244.01	262.16	362.21	230.47	35.72	8.99	2175.72
7078	7.03	7.81	4.72	11.57	43.42	106.80	208.64	198.67	218.64	239.77	319.18	197.35	21.19	5.65	1930.81

7363	7.34	6.25	6.87	13.74	40.99	113.05	168.35	169.08	198.03	207.65	293.88	151.16	22.94	6.82	1711.77
7366	7.34	6.56	3.77	8.00	29.27	87.51	140.76	138.58	170.11	180.84	251.30	116.12	12.00	3.26	1421.52
7369	7.34	6.88	4.08	9.69	33.97	86.13	155.88	160.09	206.18	219.57	286.58	127.47	13.48	3.52	1623.84
7372	7.34	7.19	4.59	12.79	42.02	94.15	181.26	185.99	218.63	237.87	318.93	164.75	21.20	4.93	1832.83
7375	7.34	7.50	3.75	11.74	40.32	87.76	176.74	171.61	195.51	218.88	298.70	166.17	19.93	4.30	1719.73
7378	7.34	7.81	2.53	7.69	31.25	79.96	172.49	158.71	189.44	213.88	278.22	149.76	14.25	2.95	1617.42
7663	7.65	6.25	4.23	10.60	37.85	127.68	191.77	190.75	224.10	245.57	310.34	154.05	19.79	3.71	1860.23
7666	7.65	6.56	2.80	6.23	28.51	97.00	152.79	146.71	197.66	217.85	258.10	108.70	10.00	2.65	1520.21
7669	7.65	6.88	3.13	7.77	31.80	92.21	158.28	155.62	225.17	243.16	280.00	114.74	9.82	2.85	1644.99
7672	7.65	7.19	3.59	9.44	37.45	92.29	173.91	162.50	215.12	228.92	291.56	137.74	13.66	3.32	1693.40
7675	7.65	7.50	2.33	8.23	33.25	79.62	153.33	135.17	176.47	193.52	256.44	126.59	10.83	2.92	1467.91
8063	7.96	6.25	1.89	6.15	28.25	130.61	199.57	197.82	245.57	272.44	302.56	136.71	11.20	1.45	1885.93
8066	7.96	6.56	1.67	4.71	24.41	105.74	161.46	155.37	213.69	245.64	252.57	100.44	6.50	1.07	1581.16
8069	7.96	6.88	2.56	5.29	31.00	105.33	165.20	165.72	246.95	275.81	278.69	110.74	7.58	1.93	1739.53
8072	7.96	7.19	3.44	6.95	35.82	105.03	181.61	177.30	245.46	264.15	303.59	138.76	10.87	2.71	1822.63
8075	7.96	7.50	2.74	7.23	33.28	95.90	169.07	153.39	210.79	227.02	275.87	129.10	9.45	2.54	1634.83
8078	7.96	7.81	2.32	6.78	31.24	90.47	168.22	160.10	235.60	253.67	291.14	124.23	8.07	2.42	1719.39

Table IIb: Detailed Historical Rainfall Data for some Towns within Hydrological Zone IVa

Stations	Latitude (N)	Duration	Jan	Feb	Mar	Apr	May	Jun	Jul	Aug	Sep	Oct	Nov	Dec	Total
Idah	7º06’	32	8.60	14.00	36.50	112.90	153.60	185.90	177.60	168.80	227.90	148.50	26.40	3.90	1264.60
Onitsha	6º23’	55	18.10	28.10	72.20	155.90	206.10	248.20	282.40	228.90	322.00	241.70	51.00	15.00	1869.60
Nsukka	7º52’	21	14.00	20.15	75.65	144.15	187.40	178.75	231.10	173.60	307.00	213.65	47.65	15.35	1608.45
Adani	6º43’	17	14.30	16.70	65.30	141.50	186.40	246.50	275.30	197.10	293.80	177.60	31.20	16.80	1662.50
Enugu	6º27’	54	21.50	24.00	75.80	149.00	253.20	288.60	204.80	178.40	317.90	233.70	43.60	12.60	1803.10
Makurdi	7º41’	30	3.70	3.65	18.75	81.83	135.36	169.20	186.53	234.13	205.88	118.39	7.25	1.14	1165.82

APPENDIX III: GAUGED STREAM FLOW DATA

Table III: Detailed Historical Discharge Record for Ofu River at Oforachi

Year	Jan	Feb	Mar	Apr	May	Jun	Jul	Aug	Sep	Oct	Nov	Dec
1955	3.90	2.90	2.10	11.40	8.00	18.60	79.00	399.90	228.60	153.60	2.50	3.90
1956	1.40	0.90	0.60	7.10	2.30	16.90	186.20	588.40	557.30	64.70	3.80	0.60
1957	2.9	1.90	1.30	15.40	36.80	28.40	95.60	350.80	435.50	160.10	6.50	0.80
1958	4.2	2.80	1.80	20.20	15.60	44.10	162.50	380.40	578.70	83.60	4.50	1.20
1959	1.1	0.60	0.60	6.90	10.50	18.70	79.00	361.20	362.10	47.60	3.20	0.50
1960	2.10	1.50	1.00	8.00	11.70	20.80	107.40	326.20	328.50	52.60	3.70	3.30
1961	1.90	1.30	0.80	21.90	3.70	60.60	225.10	508.80	555.10	85.50	13.40	0.60
1962	9.30	2.30	0.50	14.80	4.10	16.10	77.50	578.10	469.00	109.20	12.20	1.00
1963	10.50	9.00	8.10	19.10	43.20	16.00	76.00	290.90	322.90	113.10	7.20	17.20
1964	4.40	3.40	2.90	9.20	12.40	51.60	113.50	615.70	723.30	90.00	5.20	9.10
1965	3.40	2.20	1.60	11.80	4.90	86.50	150.10	486.00	405.70	47.20	4.90	1.50
1966	3.60	2.90	2.20	12.80	54.80	91.10	84.30	298.80	196.50	70.70	2.00	2.30
1967	0.50	1.50	1.20	18.40	9.90	43.40	156.70	466.00	516.90	90.40	8.80	1.20
1968	5.30	4.10	3.50	4.00	34.50	146.50	279.00	203.70	334.10	41.60	1.90	6.80
1969	1.30	1.10	1.10	23.20	12.10	28.20	133.30	457.30	419.60	162.00	5.20	1.00
1970	3.30	4.40	1.70	11.20	9.10	27.30	68.10	474.90	498.10	51.80	5.30	1.70
1971	4.20	3.60	3.10	13.30	9.20	50.60	154.50	445.90	482.00	54.00	7.50	4.70
1972	5.30	4.10	3.50	10.80	13.40	48.30	131.40	241.10	318.20	39.90	6.60	14.10
1973	4.70	3.70	3.10	13.30	6.90	22.60	157.30	198.00	476.30	59.50	5.80	3.10

Source: Kogi State Ministry of Water Resources and Rural Development

APPENDIX IV: SAMPLE SIZE ESTIMATOR

Required Sample Size†

from: The Research Advisors

Population Size	Confidence = 95.0% — Degree of Accuracy/Margin of Error				Confidence = 99.0% — Degree of Accuracy/Margin of Error			
	0.05	0.035	0.025	0.01	0.05	0.035	0.025	0.01
10	10	10	10	10	10	10	10	10
20	19	20	20	20	19	20	20	20
30	28	29	29	30	29	29	30	30
50	44	47	48	50	47	48	49	50
75	63	69	72	74	67	71	73	75
100	80	89	94	99	87	93	96	99
150	108	126	137	148	122	135	142	149
200	132	160	177	196	154	174	186	198
250	152	190	215	244	182	211	229	246
300	169	217	251	291	207	246	270	295
400	196	265	318	384	250	309	348	391
500	217	306	377	475	285	365	421	485
600	234	340	432	565	315	416	490	579
700	248	370	481	653	341	462	554	672
800	260	396	526	739	363	503	615	763
900	269	419	568	823	382	541	672	854
1,000	278	440	606	906	399	575	727	943
1,200	291	474	674	1067	427	636	827	1119
1,500	306	515	759	1297	460	712	959	1376
2,000	322	563	869	1655	498	808	1141	1785
2,500	333	597	952	1984	524	879	1288	2173
3,500	346	641	1068	2565	558	977	1510	2890
5,000	357	678	1176	3288	586	1066	1734	3842
7,500	365	710	1275	4211	610	1147	1960	5165
10,000	370	727	1332	4899	622	1193	2098	6239
25,000	378	760	1448	6939	646	1285	2399	9972
50,000	381	772	1491	8056	655	1318	2520	12455
75,000	382	776	1506	8514	658	1330	2563	13583
100,000	383	778	1513	8762	659	1336	2585	14227
250,000	384	782	1527	9248	662	1347	2626	15555
500,000	384	783	1532	9423	663	1350	2640	16055
1,000,000	384	783	1534	9512	663	1352	2647	16317
2,500,000	384	784	1536	9567	663	1353	2651	16478
10,000,000	384	784	1536	9594	663	1354	2653	16560
100,000,000	384	784	1537	9603	663	1354	2654	16584
264,000,000	384	784	1537	9603	663	1354	2654	16586

Source: The Research Advisors (2006)

APPENDIX V: DATA COLLECTION INSTRUMENTS

Appendix Va: Key Informants Interview (KII)

FLOOD HAZARD VULNERABILITY AND RISK ASSESSMENT FOR OFU RIVER FLOOD PLAIN IN KOGI STATE, NORTHCENTRAL NIGERIA

Being a Ph.D Research Survey

KEY INFORMANTS INTERVIEW QUESTIONNAIRE **ID:**

1. Name of Community: _____ 2. Ward: _____

3. LGA: _____ 4. Constituency: _____

Respondent's Personal Information

5. Name:_____ 6. Position: _____7. Sex: Male [ ] Female [ ]

8. Age: 20-25 [ ] 26-30 [ ] 31-35 [ ] 36-40 [ ] above 40 [ ]

9. Marital Status: Single [ ] Married [ ] Divorced [ ] Separated [ ] Widowed [ ]

10. Highest Educational Level: Primary [ ] Secondary [ ] Tertiary [ ] Others (specify)_____

11. Occupation_____ 12. Family size_____

13. How long have you lived in the Community? _____ years

Flood History

14. What year did you start experiencing flood in this community? _____

15. Was there any change in the magnitude? Yes [ ] No [ ]

16. If yes what year did you observe this change? Yes [ ] No [ ]

17. What year was the Idah-Nsukka highway constructed? _____

18. What year was the new Oforachi bridge constructed? _____

19. Do you think there is a relationship between the construction and the flood? Yes [ ] No [ ]

20. What do you think are the causes of flood in this community (Probe for all possible causes)?

21. Have you had any loss of live as a result of flood? Yes [ ] No [ ]

22. Has there been any case of injuries? Yes [ ] No [ ]

Has any of the following happened as a result of flood?

23. Building submerged? Yes [ ] No [ ]

24. Building collapsed? Yes [ ] No [ ]

25. Crops destroyed? Yes [ ] No [ ]

26. Goods in shop/market affected? Yes [ ] No [ ]

27. Access road submerged? Yes [ ] No [ ]

28. Children unable to go to school? Yes [ ] No [ ]

29. Loss of livestock? Yes [ ] No [ ]

30. Sickness (Epidemic outbreak)? Yes [ ] No [ ]

31. Did you have to evacuate people from their houses? Yes [ ] No [ ]

_____ _____

Name of Enumerator **Signature & Date**

Appendix Vb: Household Survey

FLOOD HAZARD VULNERABILITY AND RISK ASSESSMENT FOR OFU RIVER FLOOD PLAIN IN KOGI STATE, NORTHCENTRAL NIGERIA

Being a Ph.D Research Survey

HOUSEHOLD QUESTIONNAIRE **ID:**

1. Name of Community: _____ 2. Ward: _____

3. LGA: _____

Section A: Respondent's Personal Information

4. Name:_____ 5. Position:_____

6. Sex: Male [ ] Female [ ]

7. Age: 20-25 [ ] 26-30 [ ] 31-35 [ ] 36-40 [ ] above 40 [ ]

8. Marital Status: Single [ ] Married [ ] Divorced [ ] Separated [ ] Widowed [ ]

9. Educational Level: Primary [ ] Secondary [ ] Tertiary [ ] Adult Education [ ] Others specify)___

10. Occupation: Farming [ ] Trading [ ] Civil Servant [ ] Craftsman [ ] Others [ ]

11. Family size_____

12. How long have you lived in the Community? 1-10 [ ] 11-20 [ ] 21-30 [ ] 31-40 [ ] above 40[ ]

Section B: Respondent's opinion on Flood occurrence

13. Have you ever experienced flood in your house? Yes [ ] No [ ]

14. If yes, what year did you start experiencing flood? _____

15. How often is your house flooded?

Max. Depth	How often	Maximum Duration (days)
Ankle		
Knee		
Waist		
Breast		
First floor		

Section C: Respondent's opinion on causes of Flood (For Respondents who answered yes to 13)
(Tick any of the options as it applies to your opinion on causes of flood at Oforachi)

		Strongly Agree	Agree	Indifferent	Disagree	Strongly Disagree
16.	The Construction of the Idah-Nsukka highway is one of the factors responsible for flood					
17.	Prolonged rainfall is one of the causes of flood					
18.	Heavy rainfall upstream sometimes result in flood at Oforachi					
19.	Embankment breach by individuals contributes to the flood					
20.	There is a significant loss in the flow depth of Ofu river at Oforachi					

Section D: Respondents' opinion on the Impact of 1995 and 2000 Flood Event
(For Respondents who answered yes to 13)

		1995	2000
34.	Where you affected by the 1995 and/or 2000 flood?	Yes [ ] No [ ]	Yes [ ] No [ ]

Did you experience any of the following as a result of the 1995 and/or 2000 flood event? Tick appropriately

35.	Loss of lives?	Yes [ ] No [ ]	Yes [ ] No [ ]
36.	Injuries to members of your household?	Yes [ ] No [ ]	Yes [ ] No [ ]
37.	Building submerged?	Yes [ ] No [ ]	Yes [ ] No [ ]
38.	Building collapsed?	Yes [ ] No [ ]	Yes [ ] No [ ]
39.	Crops destroyed?	Yes [ ] No [ ]	Yes [ ] No [ ]
40.	Goods in shop/market affected?	Yes [ ] No [ ]	Yes [ ] No [ ]
41.	Access road submerged?	Yes [ ] No [ ]	Yes [ ] No [ ]
42.	Children unable to go to school?	Yes [ ] No [ ]	Yes [ ] No [ ]
43.	Loss of livestock?	Yes [ ] No [ ]	Yes [ ] No [ ]
44.	Sickness (Epidemic outbreak)?	Yes [ ] No [ ]	Yes [ ] No [ ]
45.	Were you evacuated from your house?	Yes [ ] No [ ]	Yes [ ] No [ ]

Section E: Respondents' opinion on the Availability of Toilet Facility and Household source of drinking water

46. Do you have a toilet facility in your house? Yes [ ] No [ ]
47. If yes to 47, what type? Pit Latrine [ ] VIP Latrine [ ] Water closet [ ]
48. If No to 47, where do you defecate? Open Field [ ] Neighbour's house [ ] Others_____
49. Where do you get drinking water from? Ofu River [ ] Borehole [ ]

_____ _____

Name of Enumerator **Signature & Date**

APPENDIX VI: STREAM DISCHARGE MEASUREMENTS AND CALCULATIONS

RIVER DISCHARGE MEASUREMENT											
River: Ofu					**Gage Height:** 55.432			**Date:** 13-02-2016		**Start Time:** 13:48	
River Basin: Ofu-Imabolo										**End Time:** 15:39	
Location/Station: Oforachi					**Coordinates:**						
Distance from Origin (m)	Width (m)	Depth of Observation (m)			Ave Depth (m)	Sectional Area (m^2)	Time (s)	Velocity (m/s)		Av. Vel (m/s)	Sectional Discharge
		0.2d	0.6d	0.8d				0.2d	0.8d		
1	1		1.192		1.986	1.986	20			0.006	0.011916
2	1	0.4572		1.8288	2.286	2.286	20	0.007	0.005	0.006	0.013716
3	1	0.4752		1.9008	2.376	2.376	20	0.011	0.0091	0.01005	0.0238788
4	1	0.4652		1.8608	2.326	2.326	20	0.012	0.01	0.011	0.025586
5	1		1.18		1.966	1.966	20			0.016	0.031456
6	1		0.966		1.61	1.61	20			0.015	0.02415
7	1		0.924		1.54	1.54	20			0.006	0.00924
8	1		0.804		1.34	1.34	20			0.004	0.00536
9	1		0.648		1.08	1.08	20			0.0035	0.00378
10	1		0.72		1.2	1.2	20			0.003	0.0036
11	1		0.684		1.14	1.14	20			0.003	0.00342
12	1		0.657		1.095	1.095	20			0.002	0.00219
											0.1582928

RIVER DISCHARGE MEASUREMENT											
River: Ofu					**Gage Height:** 55.462			**Date:** 14-02-2016		**Start Time:** 16:42	
River Basin: Ofu-Imabolo										**End Time:** 18:14	
Location/Station: Oforachi					**Coordinates:**						
Distance from Origin (m)	Width (m)	Depth of Observation (m)			Ave Depth (m)	Sectional Area (m^2)	Time (s)	Velocity (m/s)		Av. Vel (m/s)	Sectional Discharge (m^3/s)
		0.2d	0.6d	0.8d				0.2d	0.8d		
1	1		1.068		1.78	1.78	20	0.003	0.001	0.002	0.00356
2	1	0.4632		1.8528	2.316	2.316	20	0.033	0.024	0.0285	0.066006
3	1	0.4812		1.9248	2.406	2.406	20	0.028	0.011	0.0195	0.046917
4	1	0.4714		1.8856	2.357	2.357	20	0.012	0.011	0.0115	0.0271055
5	1		1.198		1.996	1.996	20			0.021	0.041916
6	1		1.064		1.774	1.774	20			0.012	0.021288
7	1		0.98		1.634	1.634	20			0.011	0.017974
8	1		0.928		1.546	1.546	20			0.01	0.01546
9	1		0.881		1.469	1.469	20			0.009	0.013221
10	1		0.868		1.446	1.446	20			0.005	0.00723
11	1		0.841		1.402	1.402	20			0.004	0.005608
12	1		0.74		1.234	1.234	20			0.002	0.002468
											0.2687535

RIVER DISCHARGE MEASUREMENT											
River: Ofu					**Gage Height:** 55.521			**Date:** 26-03-2016		**Start Time:** 07:00	
River Basin: Ofu-Imabolo										**End Time:** 09:25	
Location/Station: Oforachi					**Coordinates:**						
Distance from Origin (m)	Width (m)	Depth of Observation (m)			Ave Depth (m)	Sectional Area (m^2)	Time (s)	Velocity (m/s)		Av. Vel (m/s)	Sectional Discharge (m^3/s)
		0.2d	0.6d	0.8d				0.2d	0.8d		
1	1	0.414		1.656	2.07	2.07	20	0.247	0.223	0.235	0.48645
2	1	0.47		1.88	2.35	2.35	20	0.3255	0.3197	0.3226	0.75811
3	1	0.512		2.048	2.56	2.56	20	0.3611	0.36	0.36055	0.923008
4	1	0.496		1.984	2.48	2.48	20	0.2812	0.2801	0.28065	0.696012
5	1	0.414		1.656	2.07	2.07	20			0.234	0.48438
6	1		0.996		1.66	1.66	20			0.221	0.36686
7	1		0.984		1.64	1.64	20			0.061	0.10004
8	1		0.954		1.59	1.59	20			0.059	0.09381
9	1		0.936		1.56	1.56	20			0.055	0.0858
10	1		0.876		1.46	1.46	20			0.051	0.07446
11	1		0.852		1.42	1.42	20			0.046	0.06532
12	1		0.84		1.4	1.4	20			0.042	0.0588
13	1		0.768		1.28	1.28	20			0.039	0.04992
											4.24297

RIVER DISCHARGE MEASUREMENT											
River: Ofu					**Gage Height:** 55.523			**Date:** 27-03-2016		**Start Time:** 13:30	
River Basin: Ofu-Imabolo										**End Time:** 15:52	
Location/Station: Oforachi					**Coordinates:**						
Distance from Origin (m)	Width (m)	Depth of Observation (m)			Ave Depth (m)	Sectional Area (m^2)	Time (s)	Velocity (m/s)		Av. Vel (m/s)	Sectional Discharge (m^3/s)
		0.2d	0.6d	0.8d				0.2d	0.8d		
1	1	0.412		1.648	2.06	2.06	20	0.212	0.208	0.21	0.4326
2	1	0.472		1.888	2.36	2.36	20	0.297	0.295	0.296	0.69856
3	1	0.49		1.96	2.45	2.45	20	0.322	0.319	0.3205	0.785225
4	1	0.48		1.92	2.4	2.4	20	0.255	0.253	0.254	0.6096
5	1	0.408		1.632	2.04	2.04	20			0.298	0.60792
6	1		1.014		1.69	1.69	20			0.287	0.48503
7	1		0.99		1.65	1.65	20			0.069	0.11385
8	1		0.954		1.59	1.59	20			0.062	0.09858
9	1		0.93		1.55	1.55	20			0.059	0.09145
10	1		0.882		1.47	1.47	20			0.055	0.08085
11	1		0.876		1.46	1.46	20			0.053	0.07738
12	1		0.876		1.46	1.46	20			0.051	0.07446
13	1		0.774		1.29	1.29	20			0.049	0.06321
											4.218715

RIVER DISCHARGE MEASUREMENT											
River: Ofu					**Gage Height:** 55.528			**Date:** 29-03-2016		**Start Time:** 07:38	
River Basin: Ofu-Imabolo										**End Time:** 09:32	
Location/Station: Oforachi					**Coordinates:**						
Distance from Origin (m)	Width (m)	Depth of Observation (m)			Ave Depth (m)	Sectional Area (m^2)	Time (s)	Velocity (m/s)		Av. Vel (m/s)	Sectional Discharge (m^3/s)
		0.2d	0.6d	0.8d				0.2d	0.8d		
1	1	0.428		1.712	2.14	2.14	20	0.227	0.172	0.1995	0.42693
2	1	0.426		1.704	2.13	2.13	20	0.277	0.222	0.2495	0.531435
3	1	0.492		1.968	2.46	2.46	20	0.31	0.294	0.302	0.74292
4	1	0.462		1.848	2.31	2.31	20	0.305	0.32	0.3125	0.721875
5	1		1.182		1.97	1.97	20			0.388	0.76436
6	1		1.026		1.71	1.71	20			0.294	0.50274
7	1		1.008		1.68	1.68	20			0.071	0.11928
8	1		0.972		1.62	1.62	20			0.069	0.11178
9	1		0.954		1.59	1.59	20			0.066	0.10494
10	1		0.918		1.53	1.53	20			0.064	0.09792
11	1		0.894		1.49	1.49	20			0.062	0.09238
12	1		0.876		1.46	1.46	20			0.061	0.08906
13	1		0.81		1.35	1.35	20			0.059	0.07965
											4.38527

RIVER DISCHARGE MEASUREMENT											
River: Ofu					**Gage Height:** 55.520			**Date:** 27-04-2016		**Start Time:** 07:19	
River Basin: Ofu-Imabolo										**End Time:** 09:37	
Location/Station: Oforachi					**Coordinates:**						
Distance from Origin (m)	Width (m)	Depth of Observation (m)			Ave Depth (m)	Sectional Area (m^2)	Time (s)	Velocity (m/s)		Av. Vel (m/s)	Sectional Discharge (m^3/s)
		0.2d	0.6d	0.8d				0.2d	0.8d		
1	1		1.122		1.87	1.87	20			0.222	0.41514
2	1	0.434		1.736	2.17	2.17	20	0.337	0.231	0.284	0.61628
3	1	0.486		1.944	2.43	2.43	20	0.351	0.241	0.296	0.71928
4	1	0.464		1.856	2.32	2.32	20	0.358	0.245	0.3015	0.69948
5	1	0.426		1.704	2.13	2.13	20	0.365	0.251	0.308	0.65604
6	1		1.068		1.78	1.78	20			0.305	0.5429
7	1		0.864		1.44	1.44	20			0.273	0.39312
8	1		1.032		1.72	1.72	20			0.132	0.22704
9	1		0.954		1.59	1.59	20			0.114	0.18126
10	1		0.96		1.6	1.6	20			0.064	0.1024
11	1		0.846		1.41	1.41	20			0.062	0.08742
12	1		0.828		1.38	1.38	20			0.061	0.08418
13	1		0.822		1.37	1.37	20			0.059	0.08083
											4.80537

RIVER DISCHARGE MEASUREMENT											
River: Ofu					**Gage Height:** 55.556			**Date:** 28-04-2016		**Start Time:** 06:59	
River Basin: Ofu-Imabolo										**End Time:** 09:43	
Location/Station: Oforachi					**Coordinates:**						
Distance from Origin (m)	Width (m)	Depth of Observation (m)			Ave Depth (m)	Sectional Area (m^2)	Time (s)	Velocity (m/s)		Av. Vel (m/s)	Sectional Discharge (m^3/s)
		0.2d	0.6d	0.8d				0.2d	0.8d		
1	1		1.17		1.95	1.95	20			0.222	0.4329
2	1	0.446		1.784	2.23	2.23	20	0.345	0.236	0.2905	0.647815
3	1	0.474		1.896	2.37	2.37	20	0.323	0.221	0.272	0.64464
4	1	0.482		1.928	2.41	2.41	20	0.367	0.251	0.309	0.74469
5	1	0.42		1.68	2.1	2.1	20	0.309	0.212	0.2605	0.54705
6	1		1.05		1.75	1.75	20			0.375	0.65625
7	1		1.008		1.68	1.68	20			0.322	0.54096
8	1		1.026		1.71	1.71	20			0.172	0.29412
9	1		0.978		1.63	1.63	20			0.168	0.27384
10	1		0.954		1.59	1.59	20			0.166	0.26394
11	1		0.942		1.57	1.57	20			0.062	0.09734
12	1		0.894		1.49	1.49	20			0.061	0.09089
13	1		0.852		1.42	1.42	20			0.059	0.08378
14	1		0.822		1.37	1.37	20			0.049	0.06713
											5.385345

RIVER DISCHARGE MEASUREMENT											
River: Ofu					**Gage Height:** 55.552			**Date: 01**-05-2016		**Start Time:** 06:41	
River Basin: Ofu-Imabolo										**End Time:** 08:45	
Location/Station: Oforachi					**Coordinates:**						
Distance from Origin (m)	Width (m)	Depth of Observation (m)			Ave Depth (m)	Sectional Area (m^2)	Time (s)	Velocity (m/s)		Av. Vel (m/s)	Sectional Discharge (m^3/s)
		0.2d	0.6d	0.8d				0.2d	0.8d		
1	1	0.422		1.688	2.11	2.11	20	0.268	0.183	0.2255	0.475805
2	1	0.428		1.712	2.14	2.14	20	0.323	0.221	0.272	0.58208
3	1	0.478		1.912	2.39	2.39	20	0.351	0.241	0.296	0.70744
4	1	0.49		1.96	2.45	2.45	20	0.365	0.25	0.3075	0.753375
5	1	0.482		1.928	2.41	2.41	20	0.456	0.312	0.384	0.92544
6	1		1.062		1.77	1.77	20			0.377	0.66729
7	1		1.032		1.72	1.72	20			0.343	0.58996
8	1		0.975		1.625	1.625	20			0.343	0.557375
9	1		0.957		1.595	1.595	20			0.244	0.38918
10	1		0.942		1.57	1.57	20			0.222	0.34854
11	1		0.936		1.56	1.56	20			0.217	0.33852
12	1		0.918		1.53	1.53	20			0.079	0.12087
13	1		0.906		1.51	1.51	20			0.066	0.09966
14	1		0.882		1.47	1.47	20			0.065	0.09555
											6.651085

RIVER DISCHARGE MEASUREMENT											
River: Ofu					**Gage Height:** 55.542			**Date: 02**-05-2016		**Start Time:** 06:30	
River Basin: Ofu-Imabolo										**End Time:** 07:54	
Location/Station: Oforachi					**Coordinates:**						
Distance from Origin (m)	Width (m)	Depth of Observation (m)			Ave Depth (m)	Sectional Area (m^2)	Time (s)	Velocity (m/s)		Av. Vel (m/s)	Sectional Discharge (m^3/s)
		0.2d	0.6d	0.8d				0.2d	0.8d		
1	1	0.428		1.712	2.14	2.14	20	0.282	0.193	0.2375	0.50825
2	1	0.434		1.736	2.17	2.17	20	0.337	0.231	0.284	0.61628
3	1	0.468		1.872	2.34	2.34	20	0.317	0.217	0.267	0.62478
4	1	0.482		1.928	2.41	2.41	20	0.365	0.25	0.3075	0.741075
5	1	0.418		1.672	2.09	2.09	20	0.47	0.322	0.396	0.82764
6	1		1.056		1.76	1.76	20			0.332	0.58432
7	1		0.996		1.66	1.66	20			0.343	0.56938
8	1		0.924		1.54	1.54	20			0.332	0.51128
9	1		0.984		1.64	1.64	20			0.299	0.49036
10	1		1.128		1.88	1.88	20			0.25	0.47
11	1		0.942		1.57	1.57	20			0.221	0.34697
12	1		0.924		1.54	1.54	20			0.081	0.12474
13	1		0.906		1.51	1.51	20			0.073	0.11023
14	1		0.894		1.49	1.49	20			0.071	0.10579
											6.631095

RIVER DISCHARGE MEASUREMENT											
River: Ofu					**Gage Height:** 55.663			**Date: 27**-06-2016		**Start Time:** 06:30	
River Basin: Ofu-Imabolo										**End Time:** 07:54	
Location/Station: Oforachi					**Coordinates:**						
Distance from Origin (m)	Width (m)	Depth of Observation (m)			Ave Depth (m)	Sectional Area (m^2)	Time (s)	Velocity (m/s)		Av. Vel (m/s)	Sectional Discharge (m^3/s)
		0.2d	0.6d	0.8d				0.2d	0.8d		
1	1		1.068		1.78	1.78	20			0.198	0.35244
2	1	0.464		1.856	2.32	2.32	20	0.227	0.187	0.207	0.48024
3	1	0.498		1.992	2.49	2.49	20	0.277	0.213	0.245	0.61005
4	1	0.5		2	2.5	2.5	20	0.366	0.301	0.3335	0.83375
5	1	0.458		1.832	2.29	2.29	20	0.343	0.279	0.311	0.71219
6	1		1.068		1.78	1.78	20			0.349	0.62122
7	1		1.08		1.8	1.8	20			0.371	0.6678
8	1		1.068		1.78	1.78	20			0.338	0.60164
9	1		1.05		1.75	1.75	20			0.294	0.5145
10	1		1.032		1.72	1.72	20			0.251	0.43172
11	1		1.038		1.73	1.73	20			0.232	0.40136
12	1		0.984		1.64	1.64	20			0.104	0.17056
13	1		0.972		1.62	1.62	20			0.091	0.14742
14	1		0.942		1.57	1.57	20			0.082	0.12874
15	1		0.93		1.55	1.55	20			0.74	1.147
16	1		0.894		1.49	1.49	20			0.057	0.08493
											7.90556

RIVER DISCHARGE MEASUREMENT											
River: Ofu					**Gage Height:** 55.651			**Date: 28**-06-2016		**Start Time:** 06:30	
River Basin: Ofu-Imabolo										**End Time:** 07:54	
Location/Station: Oforachi					**Coordinates:**						
Distance from Origin (m)	Width (m)	Depth of Observation (m)			Ave Depth (m)	Sectional Area (m^2)	Time (s)	Velocity (m/s)		Av. Vel (m/s)	Sectional Discharge (m^3/s)
		0.2d	0.6d	0.8d				0.2d	0.8d		
1	1		1.068		1.78	1.78	20			0.223	0.39694
2	1	0.464		1.856	2.32	2.32	20	0.249	0.224	0.2365	0.54868
3	1	0.498		1.992	2.49	2.49	20	0.293	0.268	0.2805	0.698445
4	1	0.5		2	2.5	2.5	20	0.3755	0.3505	0.363	0.9075
5	1	0.458		1.832	2.29	2.29	20	0.345	0.32	0.3325	0.761425
6	1		1.068		1.78	1.78	20			0.372	0.66216
7	1		1.08		1.8	1.8	20			0.395	0.711
8	1		1.068		1.78	1.78	20			0.36	0.6408
9	1		1.05		1.75	1.75	20			0.316	0.553
10	1		1.032		1.72	1.72	20			0.273	0.46956
11	1		1.038		1.73	1.73	20			0.254	0.43942
12	1		0.984		1.64	1.64	20			0.126	0.20664
13	1		0.972		1.62	1.62	20			0.113	0.18306
14	1		0.942		1.57	1.57	20			0.104	0.16328
15	1		0.93		1.55	1.55	20			0.762	1.1811
16	1		0.894		1.49	1.49	20			0.079	0.11771
											8.64072

RIVER DISCHARGE MEASUREMENT											
River: Ofu					**Gage Height:** 55.601			**Date: 02**-07-2016		**Start Time:** 06:30	
River Basin: Ofu-Imabolo										**End Time:** 07:54	
Location/Station: Oforachi					**Coordinates:**						
Distance from Origin (m)	Width (m)	Depth of Observation (m)			Ave Depth (m)	Sectional Area (m^2)	Time (s)	Velocity (m/s)		Av. Vel (m/s)	Sectional Discharge (m^3/s)
		0.2d	0.6d	0.8d				0.2d	0.8d		
1	1		1.176		1.96	1.96	20			0.198	0.38808
2	1	0.43		1.72	2.15	2.15	20	0.227	0.187	0.207	0.44505
3	1	0.51		2.04	2.55	2.55	20	0.272	0.213	0.2425	0.618375
4	1	0.5		2	2.5	2.5	20	0.31	0.301	0.3055	0.76375
5	1	0.442		1.768	2.21	2.21	20	0.366	0.279	0.3225	0.712725
6	1		1.14		1.9	1.9	20			0.299	0.5681
7	1		1.134		1.89	1.89	20			0.36	0.6804
8	1		0.99		1.65	1.65	20			0.288	0.4752
9	1		1.008		1.68	1.68	20			0.291	0.48888
10	1		0.972		1.62	1.62	20			0.277	0.44874
11	1		0.966		1.61	1.61	20			0.252	0.40572
12	1		0.978		1.63	1.63	20			0.179	0.29177
13	1		0.966		1.61	1.61	20			0.088	0.14168
14	1		0.93		1.55	1.55	20			0.064	0.0992
15	1		0.906		1.51	1.51	20			0.061	0.09211
16	1		0.834		1.39	1.39	20			0.054	0.07506
											6.69484

RIVER DISCHARGE MEASUREMENT											
River: Ofu					**Gage Height:** 55.597			**Date: 03**-07-2016		**Start Time:** 06:30	
River Basin: Ofu-Imabolo										**End Time:** 07:54	
Location/Station: Oforachi					**Coordinates:**						
Distance from Origin (m)	Width (m)	Depth of Observation (m)			Ave Depth (m)	Sectional Area (m^2)	Time (s)	Velocity (m/s)		Av. Vel (m/s)	Sectional Discharge (m^3/s)
		0.2d	0.6d	0.8d				0.2d	0.8d		
1	1		1.176		1.96	1.96	20			0.223	0.43708
2	1	0.43		1.72	2.15	2.15	20	0.249	0.224	0.2365	0.508475
3	1	0.51		2.04	2.55	2.55	20	0.2905	0.2655	0.278	0.7089
4	1	0.5		2	2.5	2.5	20	0.3475	0.3225	0.335	0.8375
5	1	0.442		1.768	2.21	2.21	20	0.3565	0.3315	0.344	0.76024
6	1		1.14		1.9	1.9	20			0.322	0.6118
7	1		1.134		1.89	1.89	20			0.384	0.72576
8	1		0.99		1.65	1.65	20			0.31	0.5115
9	1		1.008		1.68	1.68	20			0.313	0.52584
10	1		0.972		1.62	1.62	20			0.299	0.48438
11	1		0.966		1.61	1.61	20			0.274	0.44114
12	1		0.978		1.63	1.63	20			0.201	0.32763
13	1		0.966		1.61	1.61	20			0.11	0.1771
14	1		0.93		1.55	1.55	20			0.086	0.1333
15	1		0.906		1.51	1.51	20			0.083	0.12533
16	1		0.834		1.39	1.39	20			0.076	0.10564
											7.421615

RIVER DISCHARGE MEASUREMENT											
River: Ofu					**Gage Height:** 56.310			**Date: 26**-08-2016		**Start Time: 15**:21	
River Basin: Ofu-Imabolo										**End Time: 16**:45	
Location/Station: Oforachi					**Coordinates:**						
Distance from Origin (m)	Width (m)	Depth of Observation (m)			Ave Depth (m)	Sectional Area (m^2)	Time (s)	Velocity (m/s)		Av. Vel (m/s)	Sectional Discharge (m^3/s)
		0.2d	0.6d	0.8d				0.2d	0.8d		
1	1	0.49		1.96	2.45	2.45	20	0.266	0.241	0.2535	0.621075
2	1	0.642		2.568	3.21	3.21	20	0.283	0.259	0.271	0.86991
3	1	0.68		2.72	3.4	3.4	20	0.502	0.479	0.4905	1.6677
4	1	0.664		2.656	3.32	3.32	20	0.339	0.314	0.3265	1.08398
5	1	0.62		2.48	3.1	3.1	20	0.369	0.344	0.3565	1.10515
6	1	0.56		2.24	2.8	2.8	20	0.519	0.494	0.5065	1.4182
7	1	0.54		2.16	2.7	2.7	20	0.468	0.444	0.456	1.2312
8	1	0.48		1.92	2.4	2.4	20	0.453	0.428	0.4405	1.0572
9	1	0.408		1.632	2.04	2.04	20	0.457	0.432	0.4445	0.90678
10	1		1.188		1.98	1.98	20			0.408	0.80784
11	1		1.182		1.97	1.97	20			0.389	0.76633
12	1		1.194		1.99	1.99	20			0.357	0.71043
13	1		1.182		1.97	1.97	20			0.262	0.51614
14	1		1.146		1.91	1.91	20			0.143	0.27313
15	1		1.122		1.87	1.87	20			0.112	0.20944
16	1		1.05		1.75	1.75	20			0.109	0.19075
											13.435255

RIVER DISCHARGE MEASUREMENT											
River: Ofu					**Gage Height:** 56.302			**Date: 27**-08-2016		**Start Time: 08**:25	
River Basin: Ofu-Imabolo										**End Time: 10**:04	
Location/Station: Oforachi					**Coordinates:**						
Distance from Origin (m)	Width (m)	Depth of Observation (m)			Ave Depth (m)	Sectional Area (m^2)	Time (s)	Velocity (m/s)		Av. Vel (m/s)	Sectional Discharge (m^3/s)
		0.2d	0.6d	0.8d				0.2d	0.8d		
1	1	0.5		2	2.5	2.5	20	0.265	0.241	0.253	0.6325
2	1	0.62		2.48	3.1	3.1	20	0.284	0.259	0.2715	0.84165
3	1	0.67		2.68	3.35	3.35	20	0.503	0.479	0.491	1.64485
4	1	0.66		2.64	3.3	3.3	20	0.339	0.314	0.3265	1.07745
5	1	0.62		2.48	3.1	3.1	20	0.369	0.344	0.3565	1.10515
6	1	0.546		2.184	2.73	2.73	20	0.519	0.494	0.5065	1.382745
7	1	0.52		2.08	2.6	2.6	20	0.468	0.444	0.456	1.1856
8	1	0.48		1.92	2.4	2.4	20	0.453	0.428	0.4405	1.0572
9	1	0.408		1.632	2.04	2.04	20	0.457	0.432	0.4445	0.90678
10	1		1.188		1.98	1.98	20			0.408	0.80784
11	1		1.182		1.97	1.97	20			0.389	0.76633
12	1		1.194		1.99	1.99	20			0.357	0.71043
13	1		1.182		1.97	1.97	20			0.262	0.51614
14	1		1.146		1.91	1.91	20			0.143	0.27313
15	1		1.122		1.87	1.87	20			0.112	0.20944
16	1		1.05		1.75	1.75	20			0.109	0.19075
											13.307985

RIVER DISCHARGE MEASUREMENT											
River: Ofu					**Gage Height:** 56.387			**Date: 23**-09-2016		**Start Time: 15**:06	
River Basin: Ofu-Imabolo										**End Time: 16**:45	
Location/Station: Oforachi					**Coordinates:**						
Distance from Origin (m)	Width (m)	Depth of Observation (m)			Ave Depth (m)	Sectional Area (m^2)	Time (s)	Velocity (m/s)		Av. Vel (m/s)	Sectional Discharge (m^3/s)
		0.2d	0.6d	0.8d				0.2d	0.8d		
1	1	0.5		2	2.5	2.5	20	0.311	0.299	0.305	0.7625
2	1	0.664		2.656	3.32	3.32	20	0.301	0.287	0.294	0.97608
3	1	0.676		2.704	3.38	3.38	20	0.51	0.477	0.4935	1.66803
4	1	0.674		2.696	3.37	3.37	20	0.36	0.342	0.351	1.18287
5	1	0.664		2.656	3.32	3.32	20	0.37	0.345	0.3575	1.1869
6	1	0.642		2.568	3.21	3.21	20	0.53	0.502	0.516	1.65636
7	1	0.602		2.408	3.01	3.01	20	0.478	0.451	0.4645	1.398145
8	1	0.54		2.16	2.7	2.7	20	0.473	0.443	0.458	1.2366
9	1	0.5		2	2.5	2.5	20	0.432	0.421	0.4265	1.06625
10	1		1.194		1.99	1.99	20			0.411	0.81789
11	1		1.188		1.98	1.98	20			0.401	0.79398
12	1		1.182		1.97	1.97	20			0.365	0.71905
13	1		1.182		1.97	1.97	20			0.262	0.51614
14	1		1.146		1.91	1.91	20			0.123	0.23493
15	1		1.122		1.87	1.87	20			0.111	0.20757
16	1		1.086		1.81	1.81	20			0.105	0.19005
											14.613345

RIVER DISCHARGE MEASUREMENT											
River: Ofu					**Gage Height:** 56.363			**Date: 24**-09-2016		**Start Time: 07**:41	
River Basin: Ofu-Imabolo										**End Time: 09**:05	
Location/Station: Oforachi					**Coordinates:**						
Distance from Origin (m)	Width (m)	Depth of Observation (m)			Ave Depth (m)	Sectional Area (m^2)	Time (s)	Velocity (m/s)		Av. Vel (m/s)	Sectional Discharge (m^3/s)
		0.2d	0.6d	0.8d				0.2d	0.8d		
1	1	0.502		2.008	2.51	2.51	20	0.301	0.278	0.2895	0.726645
2	1	0.644		2.576	3.22	3.22	20	0.29	0.26	0.275	0.8855
3	1	0.686		2.744	3.43	3.43	20	0.51	0.481	0.4955	1.699565
4	1	0.67		2.68	3.35	3.35	20	0.361	0.332	0.3465	1.160775
5	1	0.66		2.64	3.3	3.3	20	0.37	0.345	0.3575	1.17975
6	1	0.6		2.4	3	3	20	0.53	0.5	0.515	1.545
7	1	0.58		2.32	2.9	2.9	20	0.48	0.451	0.4655	1.34995
8	1	0.52		2.08	2.6	2.6	20	0.473	0.443	0.458	1.1908
9	1	0.46		1.84	2.3	2.3	20	0.445	0.439	0.442	1.0166
10	1		1.188		1.98	1.98	20			0.408	0.80784
11	1		1.182		1.97	1.97	20			0.389	0.76633
12	1		1.194		1.99	1.99	20			0.357	0.71043
13	1		1.182		1.97	1.97	20			0.262	0.51614
14	1		1.146		1.91	1.91	20			0.143	0.27313
15	1		1.122		1.87	1.87	20			0.112	0.20944
16	1		1.104		1.84	1.84	20			0.109	0.20056
											14.238455

RIVER DISCHARGE MEASUREMENT											
River: Ofu					**Gage Height:** 55.653			**Date: 27**-10-2016		**Start Time: 06**:45	
River Basin: Ofu-Imabolo										**End Time: 08**:15	
Location/Station: Oforachi					**Coordinates:**						
Distance from Origin (m)	Width (m)	Depth of Observation (m)			Ave Depth (m)	Sectional Area (m^2)	Time (s)	Velocity (m/s)		Av. Vel (m/s)	Sectional Discharge (m^3/s)
		0.2d	0.6d	0.8d				0.2d	0.8d		
1	1	0.43		1.72	2.15	2.15	20	0.213	0.188	0.2005	0.431075
2	1	0.466		1.864	2.33	2.33	20	0.246	0.221	0.2335	0.544055
3	1	0.49		1.96	2.45	2.45	20	0.251	0.226	0.2385	0.584325
4	1	0.52		2.08	2.6	2.6	20	0.323	0.298	0.3105	0.8073
5	1	0.42		1.68	2.1	2.1	20	0.368	0.343	0.3555	0.74655
6	1	0.4		1.6	2	2	20	0.362	0.337	0.3495	0.699
7	1		1.14		1.9	1.9	20			0.388	0.7372
8	1		1.17		1.95	1.95	20			0.355	0.69225
9	1		1.074		1.79	1.79	20			0.304	0.54416
10	1		1.032		1.72	1.72	20			0.296	0.50912
11	1		1.026		1.71	1.71	20			0.199	0.34029
12	1		1.044		1.74	1.74	20			0.198	0.34452
13	1		1.038		1.73	1.73	20			0.151	0.26123
14	1		1.002		1.67	1.67	20			0.097	0.16199
15	1		0.978		1.63	1.63	20			0.087	0.14181
16	1		0.906		1.51	1.51	20			0.086	0.12986
											7.674735

RIVER DISCHARGE MEASUREMENT											
River: Ofu					**Gage Height:** 55.446			**Date: 24**-11-2016		**Start Time: 15**:28	
River Basin: Ofu-Imabolo										**End Time: 17**:15	
Location/Station: Oforachi					**Coordinates:**						
Distance from Origin (m)	Width (m)	Depth of Observation (m)			Ave Depth (m)	Sectional Area (m^2)	Time (s)	Velocity (m/s)		Av. Vel (m/s)	Sectional Discharge (m^3/s)
		0.2d	0.6d	0.8d				0.2d	0.8d		
1	1	0.416		1.664	2.08	2.08	20	0.008	0.0059	0.00695	0.014456
2	1	0.43		1.72	2.15	2.15	20	0.0085	0.006	0.00725	0.0155875
3	1	0.474		1.896	2.37	2.37	20	0.012	0.01	0.011	0.02607
4	1	0.5		2	2.5	2.5	20	0.02	0.011	0.0155	0.03875
5	1	0.446		1.784	2.23	2.23	20	0.011	0.008	0.0095	0.021185
6	1	0.4		1.6	2	2	20	0.007	0.005	0.006	0.012
7	1		1.116		1.86	1.86	20			0.008	0.01488
8	1		0.99		1.65	1.65	20			0.011	0.01815
9	1		0.96		1.6	1.6	20			0.009	0.0144
10	1		0.936		1.56	1.56	20			0.0079	0.012324
11	1		0.93		1.55	1.55	20			0.0054	0.00837
12	1		0.912		1.52	1.52	20			0.0033	0.005016
13	1		0.9		1.5	1.5	20			0.0025	0.00375
14	1		0.894		1.49	1.49	20			0.0023	0.003427
15	1		0.852		1.42	1.42	20			0.0011	0.001562
											0.2099275

RIVER DISCHARGE MEASUREMENT											
River: Ofu					**Gage Height:** 55.453			**Date: 25**-11-2016		**Start Time: 05**:42	
River Basin: Ofu-Imabolo										**End Time: 07**:15	
Location/Station: Oforachi					**Coordinates:**						
Distance from Origin (m)	Width (m)	Depth of Observation (m)			Ave Depth (m)	Sectional Area (m^2)	Time (s)	Velocity (m/s)		Av. Vel (m/s)	Sectional Discharge (m^3/s)
		0.2d	0.6d	0.8d				0.2d	0.8d		
1	1	0.418		1.672	2.09	2.09	20	0.008	0.006	0.007	0.01463
2	1	0.436		1.744	2.18	2.18	20	0.009	0.007	0.008	0.01744
3	1	0.478		1.912	2.39	2.39	20	0.012	0.091	0.0515	0.123085
4	1	0.504		2.016	2.52	2.52	20	0.023	0.012	0.0175	0.0441
5	1	0.45		1.8	2.25	2.25	20	0.011	0.007	0.009	0.02025
6	1	0.404		1.616	2.02	2.02	20	0.008	0.005	0.0065	0.01313
7	1		1.134		1.89	1.89	20			0.008	0.01512
8	1		1.002		1.67	1.67	20			0.011	0.01837
9	1		0.966		1.61	1.61	20			0.009	0.01449
10	1		0.936		1.56	1.56	20			0.0079	0.012324
11	1		0.93		1.55	1.55	20			0.0054	0.00837
12	1		0.906		1.51	1.51	20			0.0033	0.004983
13	1		0.9		1.5	1.5	20			0.0025	0.00375
14	1		0.894		1.49	1.49	20			0.0023	0.003427
15	1		0.858		1.43	1.43	20			0.0011	0.001573
											0.315042

RIVER DISCHARGE MEASUREMENT											
River: Ofu					**Gage Height:** 55.444			**Date: 27**-12-2016		**Start Time: 05**:55	
River Basin: Ofu-Imabolo										**End Time: 07**:35	
Location/Station: Oforachi					**Coordinates:**						
Distance from Origin (m)	Width (m)	Depth of Observation (m)			Ave Depth (m)	Sectional Area (m^2)	Time (s)	Velocity (m/s)		Av. Vel (m/s)	Sectional Discharge (m^3/s)
		0.2d	0.6d	0.8d				0.2d	0.8d		
1	1	0.406		1.624	2.03	2.03	20	0.007	0.005	0.006	0.01218
2	1	0.442		1.768	2.21	2.21	20	0.009	0.008	0.0085	0.018785
3	1	0.472		1.888	2.36	2.36	20	0.013	0.009	0.011	0.02596
4	1	0.47		1.88	2.35	2.35	20	0.015	0.0095	0.01225	0.0287875
5	1	0.432		1.728	2.16	2.16	20	0.009	0.008	0.0085	0.01836
6	1		1.104		1.84	1.84	20			0.006	0.01104
7	1		1.074		1.79	1.79	20			0.009	0.01611
8	1		0.966		1.61	1.61	20			0.0095	0.015295
9	1		0.93		1.55	1.55	20			0.009	0.01395
10	1		0.87		1.45	1.45	20			0.0052	0.00754
11	1		0.84		1.4	1.4	20			0.0028	0.00392
12	1		0.828		1.38	1.38	20			0.0025	0.00345
13	1		0.81		1.35	1.35	20			0.001	0.00135
14	1		0.798		1.33	1.33	20			0.001	0.00133
											0.1780575

RIVER DISCHARGE MEASUREMENT											
River: Ofu					**Gage Height:** 55.443			**Date: 01**-01-2017		**Start Time: 16**:16	
River Basin: Ofu-Imabolo										**End Time: 18**:05	
Location/Station: Oforachi					**Coordinates:**						
Distance from Origin (m)	Width (m)	Depth of Observation (m)			Ave Depth (m)	Sectional Area (m^2)	Time (s)	Velocity (m/s)		Av. Vel (m/s)	Sectional Discharge (m^3/s)
		0.2d	0.6d	0.8d				0.2d	0.8d		
1	1	0.404		1.616	2.02	2.02	20	0.007	0.005	0.006	0.01212
2	1	0.448		1.792	2.24	2.24	20	0.008	0.006	0.007	0.01568
3	1	0.466		1.864	2.33	2.33	20	0.009	0.005	0.007	0.01631
4	1	0.48		1.92	2.4	2.4	20	0.013	0.009	0.011	0.0264
5	1	0.458		1.832	2.29	2.29	20	0.009	0.007	0.008	0.01832
6	1	0.41		1.64	2.05	2.05	20	0.007	0.005	0.006	0.0123
7	1		1.044		1.74	1.74	20			0.006	0.01044
8	1		0.99		1.65	1.65	20			0.009	0.01485
9	1		0.93		1.55	1.55	20			0.0091	0.014105
10	1		0.876		1.46	1.46	20			0.008	0.01168
11	1		0.84		1.4	1.4	20			0.005	0.007
12	1		0.822		1.37	1.37	20			0.003	0.00411
13	1		0.816		1.36	1.36	20			0.0025	0.0034
14	1		0.792		1.32	1.32	20			0.0012	0.001584
											0.168299

APPENDIX VII: OBSERVED DAILY STAGE FOR OFU RIVER AT OFORACHI

DAILY STAGE MEASUREMENT FOR OFU RIVER									
Location: Oforachi Bridge			Gage Locations:		Gage1:				
Gage2:					Gage3:				
Date	Morning				Evening				Stage (m) asl
	Gage1	Gage2	Gage3	Average (m)	Gage1	Gage2	Gage3	Average (m)	
01/02/16	55.432	55.432	55.432	55.432	55.432	55.432	55.432	55.432	55.432
02/02/16	55.432	55.432	55.432	55.432	55.432	55.432	55.432	55.432	55.432
03/02/16	55.432	55.432	55.432	55.432	55.432	55.432	55.432	55.432	55.432
04/02/16	55.432	55.432	55.432	55.432	55.432	55.432	55.432	55.432	55.432
05/02/16	55.432	55.432	55.432	55.432	55.432	55.432	55.432	55.432	55.432
06/02/16	55.432	55.432	55.432	55.432	55.432	55.432	55.432	55.432	55.432
07/02/16	55.432	55.432	55.432	55.432	55.432	55.432	55.432	55.432	55.432
08/02/16	55.432	55.432	55.432	55.432	55.432	55.432	55.432	55.432	55.432
09/02/16	55.432	55.432	55.432	55.432	55.432	55.432	55.432	55.432	55.432
10/02/16	55.432	55.432	55.432	55.432	55.432	55.432	55.432	55.432	55.432
11/02/16	55.432	55.432	55.432	55.432	55.432	55.432	55.432	55.432	55.432
12/02/16	55.432	55.432	55.432	55.432	55.432	55.432	55.432	55.432	55.432
13/02/16	55.432	55.432	55.432	55.432	55.432	55.432	55.432	55.432	55.432
14/02/16	55.462	55.462	55.462	55.462	55.462	55.462	55.462	55.462	55.462
15/02/16	55.462	55.462	55.462	55.462	55.462	55.462	55.462	55.462	55.462
16/02/16	55.462	55.462	55.462	55.462	55.462	55.462	55.462	55.462	55.462
17/02/16	55.462	55.462	55.462	55.462	55.462	55.462	55.462	55.462	55.462
18/02/16	55.462	55.462	55.462	55.462	55.462	55.462	55.462	55.462	55.462
19/02/16	55.462	55.462	55.462	55.462	55.462	55.462	55.462	55.462	55.462
20/02/16	55.462	55.462	55.462	55.462	55.462	55.462	55.462	55.462	55.462
21/02/16	55.462	55.462	55.462	55.462	55.462	55.462	55.462	55.462	55.462
22/02/16	55.462	55.462	55.462	55.462	55.462	55.462	55.462	55.462	55.462
23/02/16	55.462	55.462	55.462	55.462	55.462	55.462	55.462	55.462	55.462
24/02/16	55.462	55.462	55.462	55.462	55.462	55.462	55.462	55.462	55.462
25/02/16	55.462	55.462	55.462	55.462	55.462	55.462	55.462	55.462	55.462
26/02/16	55.462	55.462	55.462	55.462	55.462	55.462	55.462	55.462	55.462
27/02/16	55.462	55.462	55.462	55.462	55.462	55.462	55.462	55.462	55.462
28/02/16	55.462	55.462	55.462	55.462	55.462	55.462	55.462	55.462	55.462
29/02/16	55.462	55.462	55.462	55.462	55.462	55.462	55.462	55.462	55.462

DAILY STAGE MEASUREMENT FOR OFU RIVER									
Location: Oforachi Bridge			Gage Locations:		Gage1: Gage3:				
Gage2:									
Date	Morning				Evening				Stage (m) asl
	Gage1	Gage2	Gage3	Average (m)	Gage1	Gage2	Gage3	Average (m)	
01/03/16	55.462	55.462	55.462	55.462	55.462	55.462	55.462	55.462	55.462
02/03/16	55.462	55.462	55.462	55.462	55.462	55.462	55.462	55.462	55.462
03/03/16	55.462	55.462	55.462	55.462	55.462	55.462	55.462	55.462	55.462
04/03/16	55.462	55.462	55.462	55.462	55.462	55.462	55.462	55.462	55.462
05/03/16	55.462	55.462	55.462	55.462	55.462	55.462	55.462	55.462	55.462
06/03/16	55.462	55.462	55.462	55.462	55.462	55.462	55.462	55.462	55.462
07/03/16	55.462	55.462	55.462	55.462	55.462	55.462	55.462	55.462	55.462
08/03/16	55.462	55.462	55.462	55.462	55.462	55.462	55.462	55.462	55.462
09/03/16	55.462	55.462	55.462	55.462	55.462	55.462	55.462	55.462	55.462
10/03/16	55.462	55.462	55.462	55.462	55.462	55.462	55.462	55.462	55.462
11/03/16	55.462	55.462	55.462	55.462	55.462	55.462	55.462	55.462	55.462
12/03/16	55.462	55.462	55.462	55.462	55.462	55.462	55.462	55.462	55.462
13/03/16	55.462	55.462	55.462	55.462	55.462	55.462	55.462	55.462	55.462
14/03/16	55.462	55.462	55.462	55.462	55.462	55.462	55.462	55.462	55.462
15/03/16	55.462	55.462	55.462	55.462	55.462	55.462	55.462	55.462	55.462
16/03/16	55.462	55.462	55.462	55.462	55.462	55.462	55.462	55.462	55.462
17/03/16	55.462	55.462	55.462	55.462	55.462	55.462	55.462	55.462	55.462
18/03/16	55.462	55.462	55.462	55.462	55.462	55.462	55.462	55.462	55.462
19/03/16	55.462	55.462	55.462	55.462	55.462	55.462	55.462	55.462	55.462
20/03/16	55.462	55.462	55.462	55.462	55.462	55.462	55.462	55.462	55.462
21/03/16	55.462	55.462	55.462	55.462	55.462	55.462	55.462	55.462	55.462
22/03/16	55.462	55.462	55.462	55.462	55.462	55.462	55.462	55.462	55.462
23/03/16	55.462	55.462	55.462	55.462	55.462	55.462	55.462	55.462	55.462
24/03/16	55.462	55.462	55.462	55.462	55.462	55.462	55.462	55.462	55.462
25/03/16	55.462	55.462	55.462	55.462	55.462	55.462	55.462	55.462	55.462
26/03/16	55.521	55.521	55.521	55.521	55.521	55.521	55.521	55.521	55.521
27/03/16	55.523	55.523	55.523	55.523	55.523	55.523	55.523	55.523	55.523
28/03/16	55.528	55.528	55.528	55.528	55.528	55.528	55.528	55.528	55.528
29/03/16	55.528	55.528	55.528	55.528	55.528	55.528	55.528	55.528	55.528
30/03/16	55.528	55.528	55.528	55.528	55.528	55.528	55.528	55.528	55.528
31/03/16	55.528	55.528	55.528	55.528	55.528	55.528	55.528	55.528	55.528

DAILY STAGE MEASUREMENT FOR OFU RIVER									
Location: Oforachi Bridge			Gage Locations:		Gage1:				
Gage2:					Gage3:				
Date	Morning				Evening				Stage (m) asl
	Gage1	Gage2	Gage3	Average (m)	Gage1	Gage2	Gage3	Average (m)	
01/04/16	55.528	55.528	55.528	55.528	55.528	55.528	55.528	55.528	55.528
02/04/16	55.528	55.528	55.528	55.528	55.528	55.528	55.528	55.528	55.528
03/04/16	55.528	55.528	55.528	55.528	55.528	55.528	55.528	55.528	55.528
04/04/16	55.528	55.528	55.528	55.528	55.528	55.528	55.528	55.528	55.528
05/04/16	55.528	55.528	55.528	55.528	55.528	55.528	55.528	55.528	55.528
06/04/16	55.528	55.528	55.528	55.528	55.528	55.528	55.528	55.528	55.528
07/04/16	55.528	55.528	55.528	55.528	55.528	55.528	55.528	55.528	55.528
08/04/16	55.528	55.528	55.528	55.528	55.528	55.528	55.528	55.528	55.528
09/04/16	55.528	55.528	55.528	55.528	55.528	55.528	55.528	55.528	55.528
10/04/16	55.539	55.550	55.539	55.543	55.539	55.550	55.539	55.543	55.543
11/04/16	55.539	55.550	55.539	55.543	55.539	55.550	55.539	55.543	55.543
12/04/16	55.539	55.550	55.539	55.543	55.539	55.550	55.539	55.543	55.543
13/04/16	55.539	55.550	55.539	55.543	55.539	55.550	55.539	55.543	55.543
14/04/16	55.539	55.550	55.539	55.543	55.539	55.550	55.539	55.543	55.543
15/04/16	55.565	55.553	55.576	55.565	55.565	55.553	55.576	55.565	55.565
16/04/16	55.568	55.558	55.646	55.591	55.578	55.581	55.656	55.605	55.598
17/04/16	55.574	55.568	55.706	55.616	55.577	55.629	55.726	55.644	55.630
18/04/16	55.585	55.623	55.626	55.611	55.585	55.633	55.626	55.615	55.613
19/04/16	55.590	55.633	55.626	55.616	55.590	55.633	55.626	55.616	55.616
20/04/16	55.540	55.543	55.556	55.546	55.540	55.543	55.556	55.546	55.546
21/04/16	55.540	55.533	55.540	55.538	55.540	55.533	55.540	55.538	55.538
22/04/16	55.520	55.523	55.520	55.521	55.520	55.523	55.520	55.521	55.521
23/04/16	55.520	55.523	55.526	55.523	55.530	55.523	55.530	55.528	55.525
24/04/16	55.530	55.523	55.530	55.528	55.520	55.513	55.526	55.520	55.524
25/04/16	55.530	55.513	55.536	55.526	55.520	55.513	55.526	55.520	55.523
26/04/16	55.520	55.513	55.536	55.523	55.520	55.513	55.536	55.523	55.523
27/04/16	55.515	55.509	55.536	55.520	55.515	55.509	55.536	55.520	55.520
28/04/16	55.545	55.543	55.566	55.551	55.550	55.553	55.576	55.560	55.556
29/04/16	55.540	55.553	55.566	55.553	55.540	55.553	55.566	55.553	55.553
30/04/16	55.540	55.513	55.566	55.540	55.540	55.513	55.566	55.540	55.540

DAILY STAGE MEASUREMENT FOR OFU RIVER									
Location: Oforachi Bridge			Gage Locations:		Gage1:				
Gage2:					Gage3:				
Date	Morning				Evening				Stage (m) asl
	Gage1	Gage2	Gage3	Average (m)	Gage1	Gage2	Gage3	Average (m)	
01/05/16	55.540	55.535	55.576	55.550	55.540	55.543	55.576	55.553	55.552
02/05/16	55.535	55.533	55.566	55.545	55.525	55.528	55.566	55.540	55.542
03/05/16	55.530	55.523	55.556	55.536	55.530	55.523	55.556	55.536	55.536
04/05/16	55.540	55.543	55.566	55.550	55.540	55.543	55.566	55.550	55.550
05/05/16	55.530	55.523	55.556	55.536	55.520	55.513	55.546	55.526	55.531
06/05/16	55.510	55.503	55.536	55.516	55.510	55.503	55.536	55.516	55.516
07/05/16	55.520	55.513	55.546	55.526	55.520	55.513	55.546	55.526	55.526
08/05/16	55.525	55.523	55.556	55.535	55.530	55.523	55.556	55.536	55.536
09/05/16	55.530	55.533	55.566	55.543	55.530	55.523	55.556	55.536	55.540
10/05/16	55.560	55.573	55.616	55.583	55.570	55.583	55.636	55.596	55.590
11/05/16	55.610	55.613	55.656	55.626	55.605	55.603	55.646	55.618	55.622
12/05/16	55.600	55.603	55.636	55.613	55.600	55.603	55.636	55.613	55.613
13/05/16	55.590	55.593	55.626	55.603	55.580	55.593	55.636	55.603	55.603
14/05/16	55.580	55.573	55.616	55.590	55.600	55.603	55.646	55.616	55.603
15/05/16	55.600	55.613	55.656	55.623	55.600	55.613	55.656	55.623	55.623
16/05/16	55.620	55.623	55.676	55.640	55.608	55.603	55.656	55.622	55.631
17/05/16	55.605	55.603	55.626	55.611	55.603	55.601	55.636	55.613	55.612
18/05/16	55.600	55.593	55.616	55.603	55.600	55.593	55.616	55.603	55.603
19/05/16	55.590	55.583	55.590	55.588	55.540	55.543	55.540	55.541	55.564
20/05/16	55.580	55.578	55.586	55.581	55.580	55.578	55.586	55.581	55.581
21/05/16	55.585	55.633	55.656	55.625	55.090	55.633	55.656	55.460	55.542
22/05/16	55.585	55.633	55.656	55.625	55.600	55.643	55.666	55.636	55.631
23/05/16	55.580	55.563	55.586	55.576	55.586	55.603	55.646	55.612	55.594
24/05/16	55.600	55.613	55.626	55.613	55.600	55.613	55.626	55.613	55.613
25/05/16	55.605	55.633	55.656	55.631	55.640	55.648	55.696	55.661	55.646
26/05/16	55.640	55.643	55.676	55.653	55.640	55.643	55.664	55.649	55.651
27/05/16	55.620	55.613	55.656	55.630	55.610	55.613	55.646	55.623	55.626
28/05/16	55.620	55.603	55.636	55.620	55.610	55.603	55.636	55.616	55.618
29/05/16	55.610	55.593	55.626	55.610	55.610	55.603	55.626	55.613	55.611
30/05/16	55.610	55.593	55.626	55.610	55.610	55.603	55.626	55.613	55.611
31/05/16	55.605	55.583	55.616	55.601	55.600	55.573	55.606	55.593	55.597

DAILY STAGE MEASUREMENT FOR OFU RIVER									
Location: Oforachi Bridge			Gage Locations:		Gage1:				
Gage2:					Gage3:				
Date	Morning				Evening				Stage (m) asl
	Gage1	Gage2	Gage3	Average (m)	Gage1	Gage2	Gage3	Average (m)	
01/06/16	55.600	55.593	55.616	55.603	55.600	55.593	55.616	55.603	55.603
02/06/16	55.643	55.643	55.643	55.643	55.640	55.643	55.640	55.641	55.642
03/06/16	55.620	55.623	55.626	55.623	55.615	55.633	55.626	55.625	55.624
04/06/16	55.590	55.633	55.616	55.613	55.585	55.543	55.586	55.571	55.592
05/06/16	55.600	55.593	55.600	55.598	55.590	55.583	55.590	55.588	55.593
06/06/16	55.580	55.573	55.616	55.590	55.580	55.573	55.616	55.590	55.590
07/06/16	55.580	55.573	55.616	55.590	55.575	55.593	55.626	55.598	55.594
08/06/16	55.580	55.593	55.626	55.600	55.570	55.583	55.626	55.593	55.596
09/06/16	55.590	55.583	55.636	55.603	55.590	55.583	55.636	55.603	55.603
10/06/16	55.600	55.613	55.656	55.623	55.600	55.603	55.646	55.616	55.620
11/06/16	55.550	55.533	55.596	55.560	55.550	55.533	55.596	55.560	55.560
12/06/16	55.550	55.543	55.606	55.566	55.555	55.553	55.601	55.570	55.568
13/06/16	55.580	55.593	55.636	55.603	55.580	55.593	55.636	55.603	55.603
14/06/16	55.643	55.643	55.666	55.651	55.643	55.643	55.666	55.651	55.651
15/06/16	55.625	55.613	55.641	55.626	55.620	55.608	55.636	55.621	55.624
16/06/16	55.643	55.643	55.666	55.651	55.643	55.643	55.666	55.651	55.651
17/06/16	55.620	55.613	55.656	55.630	55.620	55.613	55.656	55.630	55.630
18/06/16	55.610	55.608	55.646	55.621	55.610	55.606	55.646	55.621	55.621
19/06/16	55.600	55.603	55.656	55.620	55.600	55.603	55.636	55.613	55.616
20/06/16	55.590	55.583	55.626	55.600	55.590	55.573	55.626	55.596	55.598
21/06/16	55.620	55.603	55.656	55.626	55.620	55.603	55.656	55.626	55.626
22/06/16	55.610	55.598	55.651	55.620	55.610	55.603	55.646	55.620	55.620
23/06/16	55.783	55.783	55.946	55.837	55.783	55.783	55.946	55.837	55.837
24/06/16	55.803	55.803	55.876	55.827	55.803	55.803	55.946	55.851	55.839
25/06/16	55.743	55.743	55.746	55.744	55.723	55.723	55.726	55.724	55.734
26/06/16	55.683	55.683	55.706	55.691	55.673	55.673	55.673	55.673	55.682
27/06/16	55.663	55.663	55.663	55.663	55.663	55.663	55.663	55.663	55.663
28/06/16	55.643	55.643	55.666	55.651	55.643	55.643	55.666	55.651	55.651
29/06/16	55.628	55.623	55.656	55.636	55.623	55.623	55.656	55.634	55.635
30/06/16	55.620	55.618	55.646	55.628	55.618	55.613	55.636	55.622	55.625

DAILY STAGE MEASUREMENT FOR OFU RIVER									
Location: Oforachi Bridge			Gage Locations:		Gage1:				
Gage2:					Gage3:				
Date	Morning				Evening				Stage (m) asl
	Gage1	Gage2	Gage3	Average (m)	Gage1	Gage2	Gage3	Average (m)	
01/07/16	55.610	55.603	55.636	55.616	55.595	55.573	55.631	55.600	55.608
02/07/16	55.610	55.593	55.611	55.605	55.600	55.593	55.600	55.598	55.601
03/06/16	55.600	55.588	55.600	55.596	55.600	55.593	55.600	55.598	55.597
04/07/16	55.600	55.593	55.600	55.598	55.600	55.593	55.600	55.598	55.598
05/07/16	55.640	55.633	55.640	55.637	55.635	55.623	55.635	55.631	55.634
06/07/16	55.630	55.623	55.630	55.628	55.620	55.613	55.620	55.618	55.623
07/07/16	55.600	55.613	55.600	55.604	55.600	55.613	55.600	55.604	55.604
08/07/16	55.590	55.583	55.590	55.588	55.580	55.578	55.580	55.579	55.584
09/07/16	55.595	55.583	55.595	55.591	55.595	55.583	55.595	55.591	55.591
10/07/16	55.610	55.593	55.610	55.604	55.615	55.603	55.646	55.621	55.613
11/07/16	55.610	55.593	55.610	55.604	55.610	55.593	55.610	55.604	55.604
12/07/16	55.600	55.583	55.600	55.594	55.620	55.633	55.620	55.624	55.609
13/07/16	55.643	55.643	55.646	55.645	55.653	55.653	55.653	55.653	55.649
14/07/16	55.653	55.653	55.653	55.653	55.653	55.653	55.653	55.653	55.653
15/07/16	55.643	55.643	55.643	55.643	55.643	55.643	55.643	55.643	55.643
16/07/16	55.620	55.603	55.656	55.626	55.615	55.593	55.656	55.621	55.624
17/07/16	55.630	55.613	55.630	55.624	55.620	55.623	55.646	55.630	55.627
18/07/16	55.620	55.623	55.646	55.630	55.620	55.623	55.646	55.630	55.630
19/07/16	55.610	55.593	55.636	55.613	55.608	55.583	55.626	55.606	55.609
20/07/16	55.602	55.573	55.621	55.599	55.600	55.563	55.616	55.593	55.596
21/07/16	55.600	55.563	55.616	55.593	55.600	55.563	55.616	55.593	55.593
22/07/16	55.600	55.563	55.616	55.593	55.610	55.573	55.616	55.600	55.596
23/07/16	55.673	55.673	55.673	55.673	55.673	55.673	55.673	55.673	55.673
24/07/16	55.683	55.683	55.683	55.683	55.683	55.683	55.683	55.683	55.683
25/07/16	55.653	55.653	55.656	55.655	55.653	55.653	55.656	55.655	55.655
26/07/16	55.620	55.623	55.626	55.623	55.620	55.623	55.626	55.623	55.623
27/07/16	55.615	55.623	55.626	55.621	55.610	55.623	55.626	55.620	55.621
28/07/16	55.610	55.623	55.626	55.620	55.600	55.613	55.600	55.604	55.612
29/07/16	55.610	55.593	55.610	55.604	55.610	55.593	55.610	55.604	55.604
30/07/16	55.590	55.593	55.590	55.591	55.590	55.593	55.590	55.591	55.591
31/07/16	55.610	55.603	55.611	55.608	55.610	55.603	55.610	55.608	55.608

DAILY STAGE MEASUREMENT FOR OFU RIVER									
Location: Oforachi Bridge			Gage Locations:		Gage1:				
Gage2:					Gage3:				
Date	Morning				Evening				Stage (m) asl
	Gage1	Gage2	Gage3	Average (m)	Gage1	Gage2	Gage3	Average (m)	
01/08/16	55.743	55.743	55.743	55.743	55.743	55.743	55.743	55.743	55.743
02/08/16	55.743	55.743	55.743	55.743	55.743	55.743	55.743	55.743	55.743
03/08/16	55.743	55.743	55.743	55.743	55.743	55.743	55.743	55.743	55.743
04/08/16	56.265	56.265	56.265	56.265	56.265	56.265	56.265	56.265	56.265
05/08/16	56.308	56.308	56.308	56.308	56.308	56.308	56.308	56.308	56.308
06/08/16	56.308	56.308	56.308	56.308	56.308	56.308	56.308	56.308	56.308
07/08/16	56.308	56.308	56.308	56.308	56.308	56.308	56.308	56.308	56.308
08/08/16	56.308	56.308	56.308	56.308	56.308	56.308	56.308	56.308	56.308
09/08/16	56.304	56.304	56.304	56.304	56.304	56.304	56.304	56.304	56.304
10/08/16	56.304	56.304	56.304	56.304	56.304	56.304	56.304	56.304	56.304
11/08/16	56.304	56.304	56.304	56.304	56.304	56.304	56.304	56.304	56.304
12/08/16	56.304	56.304	56.304	56.304	56.304	56.304	56.304	56.304	56.304
13/08/16	56.304	56.304	56.304	56.304	56.304	56.304	56.304	56.304	56.304
14/08/16	56.304	56.304	56.304	56.304	56.304	56.304	56.304	56.304	56.304
15/08/16	56.305	56.305	56.305	56.305	56.305	56.305	56.305	56.305	56.305
16/08/16	56.121	56.121	56.121	56.121	56.121	56.121	56.121	56.121	56.121
17/08/16	56.201	56.201	56.201	56.201	56.201	56.201	56.201	56.201	56.201
18/08/16	56.201	56.201	56.201	56.201	56.201	56.201	56.201	56.201	56.201
19/08/16	56.308	56.308	56.308	56.308	56.308	56.308	56.308	56.308	56.308
20/08/16	56.308	56.308	56.308	56.308	56.308	56.308	56.308	56.308	56.308
21/08/16	56.308	56.308	56.308	56.308	56.308	56.308	56.308	56.308	56.308
22/08/16	56.308	56.308	56.308	56.308	56.308	56.308	56.308	56.308	56.308
23/08/16	56.308	56.308	56.308	56.308	56.308	56.308	56.308	56.308	56.308
24/08/16	56.308	56.308	56.308	56.308	56.308	56.308	56.308	56.308	56.308
25/08/16	56.308	56.308	56.308	56.308	56.308	56.308	56.308	56.308	56.308
26/08/16	56.310	56.310	56.310	56.310	56.310	56.310	56.310	56.310	56.310
27/08/16	56.302	56.302	56.302	56.302	56.302	56.302	56.302	56.302	56.302
28/08/16	56.303	56.303	56.303	56.303	56.303	56.303	56.303	56.303	56.303
29/08/16	56.301	56.301	56.301	56.301	56.301	56.301	56.301	56.301	56.301
30/08/16	56.302	56.302	56.302	56.302	56.302	56.302	56.302	56.302	56.302
31/08/16	56.302	56.302	56.302	56.302	56.302	56.302	56.302	56.302	56.302

DAILY STAGE MEASUREMENT FOR OFU RIVER									
Location: Oforachi Bridge			Gage Locations:		Gage1:				
Gage2:					Gage3:				
Date	Morning				Evening				Stage (m) asl
	Gage1	Gage2	Gage3	Average (m)	Gage1	Gage2	Gage3	Average (m)	
01/09/16	56.304	56.304	56.304	56.304	56.304	56.304	56.304	56.304	56.304
02/09/16	56.304	56.304	56.304	56.304	56.304	56.304	56.304	56.304	56.304
03/09/16	56.304	56.304	56.304	56.304	56.304	56.304	56.304	56.304	56.304
04/09/16	56.304	56.304	56.304	56.304	56.304	56.304	56.304	56.304	56.304
05/09/16	56.304	56.304	56.304	56.304	56.304	56.304	56.304	56.304	56.304
06/09/16	56.304	56.304	56.304	56.304	56.304	56.304	56.304	56.304	56.304
07/09/16	55.954	55.954	55.954	55.954	55.954	55.954	55.954	55.954	55.954
08/09/16	55.954	55.954	55.954	55.954	55.954	55.954	55.954	55.954	55.954
09/09/16	55.954	55.954	55.954	55.954	55.954	55.954	55.954	55.954	55.954
10/09/16	56.304	56.304	56.304	56.304	56.304	56.304	56.304	56.304	56.304
11/09/16	56.304	56.304	56.304	56.304	56.304	56.304	56.304	56.304	56.304
12/09/16	56.304	56.304	56.304	56.304	56.304	56.304	56.304	56.304	56.304
13/09/16	56.304	56.304	56.304	56.304	56.304	56.304	56.304	56.304	56.304
14/09/16	56.106	56.106	56.106	56.106	56.106	56.106	56.106	56.106	56.106
15/09/16	56.106	56.106	56.106	56.106	56.106	56.106	56.106	56.106	56.106
16/09/16	56.106	56.106	56.106	56.106	56.106	56.106	56.106	56.106	56.106
17/09/16	56.106	56.106	56.106	56.106	56.106	56.106	56.106	56.106	56.106
18/09/16	56.321	56.321	56.321	56.321	56.321	56.321	56.321	56.321	56.321
19/09/16	56.321	56.321	56.321	56.321	56.321	56.321	56.321	56.321	56.321
20/09/16	56.321	56.321	56.321	56.321	56.321	56.321	56.321	56.321	56.321
21/09/16	56.321	56.321	56.321	56.321	56.321	56.321	56.321	56.321	56.321
22/09/16	56.321	56.321	56.321	56.321	56.321	56.321	56.321	56.321	56.321
23/09/16	56.387	56.387	56.387	56.387	56.387	56.387	56.387	56.387	56.387
24/09/16	56.363	56.363	56.363	56.363	56.363	56.363	56.363	56.363	56.363
25/09/16	56.334	56.334	56.334	56.334	56.334	56.334	56.334	56.334	56.334
26/09/16	56.334	56.334	56.334	56.334	56.334	56.334	56.334	56.334	56.334
27/09/16	56.334	56.334	56.334	56.334	56.334	56.334	56.334	56.334	56.334
28/09/16	56.334	56.334	56.334	56.334	56.334	56.334	56.334	56.334	56.334
29/09/16	56.334	56.334	56.334	56.334	56.334	56.334	56.334	56.334	56.334
30/09/16	56.312	56.312	56.312	56.312	56.312	56.312	56.312	56.312	56.312

DAILY STAGE MEASUREMENT FOR OFU RIVER									
Location: Oforachi Bridge			Gage Locations:		Gage1:				
Gage2:					Gage3:				
Date	Morning				Evening				Stage (m) asl
	Gage1	Gage2	Gage3	Average (m)	Gage1	Gage2	Gage3	Average (m)	
01/10/16	55.743	55.743	55.743	55.743	55.743	55.743	55.743	55.743	55.743
02/10/16	55.743	55.743	55.743	55.743	55.723	55.723	55.726	55.724	55.734
03/10/16	55.723	55.723	55.726	55.725	55.723	55.723	55.726	55.724	55.724
04/10/16	55.733	55.733	55.746	55.740	55.733	55.733	55.746	55.737	55.738
05/10/16	55.713	55.713	55.716	55.715	55.703	55.703	55.711	55.706	55.710
06/10/16	55.683	55.683	55.706	55.695	55.683	55.683	55.706	55.691	55.693
07/10/16	55.663	55.663	55.696	55.680	55.683	55.683	55.701	55.689	55.684
08/10/16	55.673	55.673	55.706	55.690	55.663	55.663	55.696	55.674	55.682
09/10/16	55.663	55.663	55.696	55.680	55.663	55.663	55.696	55.674	55.677
10/10/16	55.683	55.683	55.706	55.695	55.703	55.703	55.703	55.703	55.699
11/10/16	55.703	55.703	55.726	55.715	55.703	55.703	55.726	55.711	55.713
12/10/16	55.703	55.703	55.726	55.715	55.703	55.703	55.726	55.711	55.713
13/10/16	55.703	55.703	55.726	55.715	55.683	55.683	55.706	55.691	55.703
14/10/16	55.673	55.673	55.696	55.685	55.678	55.678	55.706	55.687	55.686
15/10/16	55.693	55.693	55.716	55.705	55.693	55.693	55.716	55.701	55.703
16/10/16	55.883	55.883	55.896	55.890	55.793	55.793	55.836	55.807	55.848
17/10/16	55.753	55.753	55.796	55.775	55.743	55.743	55.743	55.743	55.759
18/10/16	55.733	55.733	55.733	55.733	55.733	55.733	55.733	55.733	55.733
19/10/16	55.733	55.733	55.733	55.733	55.735	55.735	55.735	55.735	55.734
20/10/16	55.743	55.743	55.743	55.743	55.734	55.734	55.734	55.734	55.739
21/10/16	55.733	55.733	55.733	55.733	55.753	55.753	55.796	55.767	55.750
22/10/16	55.763	55.763	55.763	55.763	55.753	55.753	55.796	55.767	55.765
23/10/16	55.755	55.755	55.755	55.755	55.743	55.743	55.743	55.743	55.749
24/10/16	55.703	55.703	55.726	55.715	55.703	55.703	55.726	55.711	55.713
25/10/16	55.673	55.673	55.696	55.685	55.673	55.673	55.696	55.681	55.683
26/10/16	55.673	55.673	55.696	55.685	55.663	55.663	55.691	55.672	55.678
27/10/16	55.643	55.643	55.666	55.655	55.643	55.643	55.666	55.651	55.653
28/10/16	55.663	55.663	55.666	55.665	55.663	55.663	55.666	55.664	55.664
29/10/16	55.668	55.668	55.696	55.682	55.668	55.668	56.696	56.011	55.846
30/10/16	55.673	55.673	55.696	55.685	55.673	55.673	55.696	55.681	55.683
31/10/16	55.673	55.673	55.696	55.685	55.673	55.673	55.696	55.681	55.683

DAILY STAGE MEASUREMENT FOR OFU RIVER									
Location: Oforachi Bridge			Gage Locations:		Gage1:				
Gage2:					Gage3:				
Date	Morning				Evening				Stage (m) asl
	Gage1	Gage2	Gage3	Average (m)	Gage1	Gage2	Gage3	Average (m)	
01/11/16	55.673	55.673	55.676	55.674	55.668	55.668	55.676	55.671	55.672
02/11/16	55.663	55.663	55.671	55.666	55.663	55.663	55.676	55.667	55.667
03/11/16	55.663	55.663	55.676	55.667	55.663	55.663	55.676	55.667	55.667
04/11/16	55.663	55.663	55.676	55.667	55.637	55.637	55.676	55.650	55.659
05/11/16	55.643	55.643	55.656	55.647	55.643	55.643	55.676	55.654	55.651
06/11/16	55.643	55.643	55.656	55.647	55.640	55.633	55.640	55.638	55.643
07/11/16	55.640	55.623	55.640	55.634	55.640	55.623	55.640	55.634	55.634
08/11/16	55.640	55.623	55.640	55.634	55.640	55.623	55.640	55.634	55.634
09/11/16	55.640	55.623	55.640	55.634	55.640	55.623	55.640	55.634	55.634
10/11/16	55.640	55.623	55.640	55.634	55.640	55.623	55.640	55.634	55.634
11/11/16	55.640	55.623	55.640	55.634	55.640	55.623	55.640	55.634	55.634
12/11/16	55.640	55.623	55.640	55.634	55.640	55.623	55.640	55.634	55.634
13/11/16	55.630	55.623	55.630	55.628	55.624	55.623	55.624	55.624	55.626
14/11/16	55.630	55.613	55.630	55.624	55.620	55.613	55.620	55.618	55.621
15/11/16	55.620	55.613	55.620	55.618	55.620	55.603	55.636	55.620	55.619
16/11/16	55.610	55.603	55.636	55.616	55.620	55.603	55.636	55.620	55.618
17/11/16	55.620	55.603	55.636	55.620	55.620	55.603	55.636	55.620	55.620
18/11/16	55.620	55.603	55.636	55.620	55.620	55.603	55.636	55.620	55.620
19/11/16	55.614	55.603	55.636	55.618	55.613	55.603	55.636	55.617	55.618
20/11/16	55.610	55.593	55.610	55.604	55.600	55.593	55.600	55.598	55.601
21/11/16	55.610	55.593	55.610	55.604	55.610	55.603	55.610	55.608	55.606
22/11/16	55.610	55.603	55.610	55.608	55.610	55.598	55.610	55.606	55.607
23/11/16	55.610	55.598	55.610	55.606	55.610	55.598	55.610	55.606	55.606
24/11/16	55.446	55.446	55.446	55.446	55.446	55.446	55.446	55.446	55.446
25/11/16	55.453	55.453	55.453	55.453	55.453	55.453	55.453	55.453	55.453
26/11/16	55.453	55.453	55.453	55.453	55.453	55.453	55.453	55.453	55.453
27/11/16	55.453	55.453	55.453	55.453	55.453	55.453	55.453	55.453	55.453
28/11/16	55.453	55.453	55.453	55.453	55.453	55.453	55.453	55.453	55.453
29/11/16	55.453	55.453	55.453	55.453	55.453	55.453	55.453	55.453	55.453
30/11/16	55.453	55.453	55.453	55.453	55.453	55.453	55.453	55.453	55.453

DAILY STAGE MEASUREMENT FOR OFU RIVER									
Location: Oforachi Bridge			Gage Locations:		Gage1:				
Gage2:					Gage3:				
Date	Morning				Evening				Stage (m) asl
	Gage1	Gage2	Gage3	Average (m)	Gage1	Gage2	Gage3	Average (m)	
01/12/16	55.453	55.453	55.453	55.453	55.453	55.453	55.453	55.453	55.453
02/12/16	55.453	55.453	55.453	55.453	55.453	55.453	55.453	55.453	55.453
03/12/16	55.453	55.453	55.453	55.453	55.453	55.453	55.453	55.453	55.453
04/12/16	55.453	55.453	55.453	55.453	55.453	55.453	55.453	55.453	55.453
05/12/16	55.453	55.453	55.453	55.453	55.453	55.453	55.453	55.453	55.453
06/12/16	55.453	55.453	55.453	55.453	55.453	55.453	55.453	55.453	55.453
07/12/16	55.451	55.451	55.451	55.451	55.451	55.451	55.451	55.451	55.451
08/12/16	55.451	55.451	55.451	55.451	55.451	55.451	55.451	55.451	55.451
09/12/16	55.451	55.451	55.451	55.451	55.451	55.451	55.451	55.451	55.451
10/12/16	55.451	55.451	55.451	55.451	55.451	55.451	55.451	55.451	55.451
11/12/16	55.451	55.451	55.451	55.451	55.451	55.451	55.451	55.451	55.451
12/12/16	55.451	55.451	55.451	55.451	55.451	55.451	55.451	55.451	55.451
13/12/16	55.451	55.451	55.451	55.451	55.451	55.451	55.451	55.451	55.451
14/12/16	55.451	55.451	55.451	55.451	55.451	55.451	55.451	55.451	55.451
15/12/16	55.451	55.451	55.451	55.451	55.451	55.451	55.451	55.451	55.451
16/12/16	55.451	55.451	55.451	55.451	55.451	55.451	55.451	55.451	55.451
17/12/16	55.451	55.451	55.451	55.451	55.451	55.451	55.451	55.451	55.451
18/12/16	55.451	55.451	55.451	55.451	55.451	55.451	55.451	55.451	55.451
19/12/16	55.451	55.451	55.451	55.451	55.451	55.451	55.451	55.451	55.451
20/12/16	55.445	55.445	55.445	55.445	55.445	55.445	55.445	55.445	55.445
21/12/16	55.445	55.445	55.445	55.445	55.445	55.445	55.445	55.445	55.445
22/12/16	55.445	55.445	55.445	55.445	55.445	55.445	55.445	55.445	55.445
23/12/16	55.444	55.444	55.444	55.444	55.444	55.444	55.444	55.444	55.444
24/12/16	55.444	55.444	55.444	55.444	55.444	55.444	55.444	55.444	55.444
25/12/16	55.444	55.444	55.444	55.444	55.444	55.444	55.444	55.444	55.444
26/12/16	55.444	55.444	55.444	55.444	55.444	55.444	55.444	55.444	55.444
27/12/16	55.444	55.444	55.444	55.444	55.444	55.444	55.444	55.444	55.444
28/12/16	55.444	55.444	55.444	55.444	55.444	55.444	55.444	55.444	55.444
29/12/16	55.444	55.444	55.444	55.444	55.444	55.444	55.444	55.444	55.444
30/12/16	55.444	55.444	55.444	55.444	55.444	55.444	55.444	55.444	55.444
31/12/16	55.444	55.444	55.444	55.444	55.444	55.444	55.444	55.444	55.444

DAILY STAGE MEASUREMENT FOR OFU RIVER									
Location: Oforachi Bridge			Gage Locations:		Gage1:				
Gage2:					Gage3:				
Date	Morning				Evening				Stage (m) asl
	Gage1	Gage2	Gage3	Average (m)	Gage1	Gage2	Gage3	Average (m)	
01/01/17	55.443	55.443	55.443	55.443	55.443	55.443	55.443	55.443	55.443
02/01/17	55.443	55.443	55.443	55.443	55.443	55.443	55.443	55.443	55.443
03/01/17	55.443	55.443	55.443	55.443	55.443	55.443	55.443	55.443	55.443
04/01/17	55.443	55.443	55.443	55.443	55.443	55.443	55.443	55.443	55.443
05/01/17	55.443	55.443	55.443	55.443	55.443	55.443	55.443	55.443	55.443
06/01/17	55.443	55.443	55.443	55.443	55.443	55.443	55.443	55.443	55.443
07/01/17	55.443	55.443	55.443	55.443	55.443	55.443	55.443	55.443	55.443
08/01/17	55.443	55.443	55.443	55.443	55.443	55.443	55.443	55.443	55.443
09/01/17	55.443	55.443	55.443	55.443	55.443	55.443	55.443	55.443	55.443
10/01/17	55.443	55.443	55.443	55.443	55.443	55.443	55.443	55.443	55.443
11/01/17	55.443	55.443	55.443	55.443	55.443	55.443	55.443	55.443	55.443
12/01/17	55.443	55.443	55.443	55.443	55.443	55.443	55.443	55.443	55.443
13/01/17	55.443	55.443	55.443	55.443	55.443	55.443	55.443	55.443	55.443
14/01/17	55.443	55.443	55.443	55.443	55.443	55.443	55.443	55.443	55.443
15/01/17	55.443	55.443	55.443	55.443	55.443	55.443	55.443	55.443	55.443
16/01/17	55.443	55.443	55.443	55.443	55.443	55.443	55.443	55.443	55.443
17/01/17	55.443	55.443	55.443	55.443	55.443	55.443	55.443	55.443	55.443
18/01/17	55.443	55.443	55.443	55.443	55.443	55.443	55.443	55.443	55.443
19/01/17	55.443	55.443	55.443	55.443	55.443	55.443	55.443	55.443	55.443
20/01/17	55.443	55.443	55.443	55.443	55.443	55.443	55.443	55.443	55.443
21/01/17	55.443	55.443	55.443	55.443	55.443	55.443	55.443	55.443	55.443
22/01/17	55.443	55.443	55.443	55.443	55.443	55.443	55.443	55.443	55.443
23/01/17	55.443	55.443	55.443	55.443	55.443	55.443	55.443	55.443	55.443
24/01/17	55.443	55.443	55.443	55.443	55.443	55.443	55.443	55.443	55.443
25/01/17	55.443	55.443	55.443	55.443	55.443	55.443	55.443	55.443	55.443
26/01/17	55.443	55.443	55.443	55.443	55.443	55.443	55.443	55.443	55.443
27/01/17	55.443	55.443	55.443	55.443	55.443	55.443	55.443	55.443	55.443
28/01/17	55.443	55.443	55.443	55.443	55.443	55.443	55.443	55.443	55.443
29/01/17	55.443	55.443	55.443	55.443	55.443	55.443	55.443	55.443	55.443
30/01/17	55.443	55.443	55.443	55.443	55.443	55.443	55.443	55.443	55.443
31/01/17	55.443	55.443	55.443	55.443	55.443	55.443	55.443	55.443	55.443

APPENDIX VIII: SOIL CLASSIFICATION

Table 1.6 Unified Soil Classification Chart (after ASTM, 2005)

Criteria for assigning group symbols and group names using laboratory tests[a]				Soil classification: Group symbol	Soil classification: Group name[b]
Coarse-grained soils More than 50% retained on No. 200 sieve	Gravels More than 50% of coarse fraction retained on No. 4 sieve	Clean Gravels Less than 5% fines[c]	$C_u \geq 4$ and $1 \leq C_c \leq 3^e$	GW	Well-graded gravel[f]
			$C_u < 4$ and/or $1 > C_c > 3^e$	GP	Poorly graded gravel[f]
		Gravels with Fines More than 12% fines[c]	Fines classify as ML or MH	GM	Silty gravel[f,g,h]
			Fines classify as CL or CH	GC	Clayey gravel[f,g,h]
	Sands 50% or more of coarse fraction passes No. 4 sieve	Clean Sands Less than 5% fines[d]	$C_u \geq 6$ and $1 \leq C_c \leq 3^e$	SW	Well-graded sand[i]
			$C_u < 6$ and/or $1 > C_c > 3^e$	SP	Poorly graded sand[i]
		Sand with Fines More than 12% fines[d]	Fines classify as ML or MH	SM	Silty sand[g,h,i]
			Fines classify as CL or CH	SC	Clayey sand[g,h,i]
Fine-grained soils 50% or more passes the No. 200 sieve	Silts and Clays Liquid limit less than 50	Inorganic	PI > 7 and plots on or above "A" line[j]	CL	Lean clay[k,l,m]
			PI < 4 or plots below "A" line[j]	ML	Silt[k,l,m]
		Organic	$\frac{\text{Liquid limit—oven dried}}{\text{Liquid limit—not dried}} < 0.75$	OL	Organic clay[k,l,m,n] / Organic silt[k,l,m,o]
	Silts and Clays Liquid limit 50 or more	Inorganic	PI plots on or above "A" line	CH	Fat clay[k,l,m]
			PI plots below "A" line	MH	Elastic silt[k,l,m]
		Organic	$\frac{\text{Liquid limit—oven dried}}{\text{Liquid limit—not dried}} < 0.75$	OH	Organic clay[k,l,m,p] / Organic silt[k,l,m,q]
Highly organic soils	Primarily organic matter, dark in color, and organic odor			PT	Peat

[a] Based on the material passing the 75-mm. (3-in) sieve.
[b] If field sample contained cobbles or boulders, or both, add "with cobbles or boulders, or both" to group name.
[c] Gravels with 5 to 12% fines require dual symbols: GW-GM well-graded gravel with silt; GW-GC well-graded gravel with clay; GP-GM poorly graded gravel with silt; GP-GC poorly graded gravel with clay.
[d] Sands with 5 to 12% fines require dual symbols: SW-SM well-graded sand with silt; SW-SC well-graded sand with clay; SP-SM poorly graded sand with silt; SP-SC poorly graded sand with clay.
[e] $C_u = D_{60}/D_{10}$ $C_c = \frac{(D_{30})^2}{D_{10} \times D_{60}}$
[f] If soil contains ≥15% sand, add "with sand" to group name.
[g] If fines classify as CL-ML, use dual symbol GC-GM or SC-SM.
[h] If fines are organic, add "with organic fines" to group name.
[i] If soil contains ≥15% gravel, add "with gravel" to group name.
[j] If Atterberg limits plot in hatched area, soil is a CL-ML, silty clay.
[k] If soil contains 15 to 29% plus No. 200, add "with sand" or "with gravel," whichever is predominant.
[l] If soil contains ≥30% plus No. 200, predominantly sand, add "sandy" to group name.
[m] If soil contains ≥30% plus No. 200, predominantly gravel, add "gravelly" to group name.
[n] PI ≥ 4 and plots on or above "A" line.
[o] PI < 4 or plots below "A" line.
[p] PI plots on or above "A" line.
[q] PI plots below "A" line.

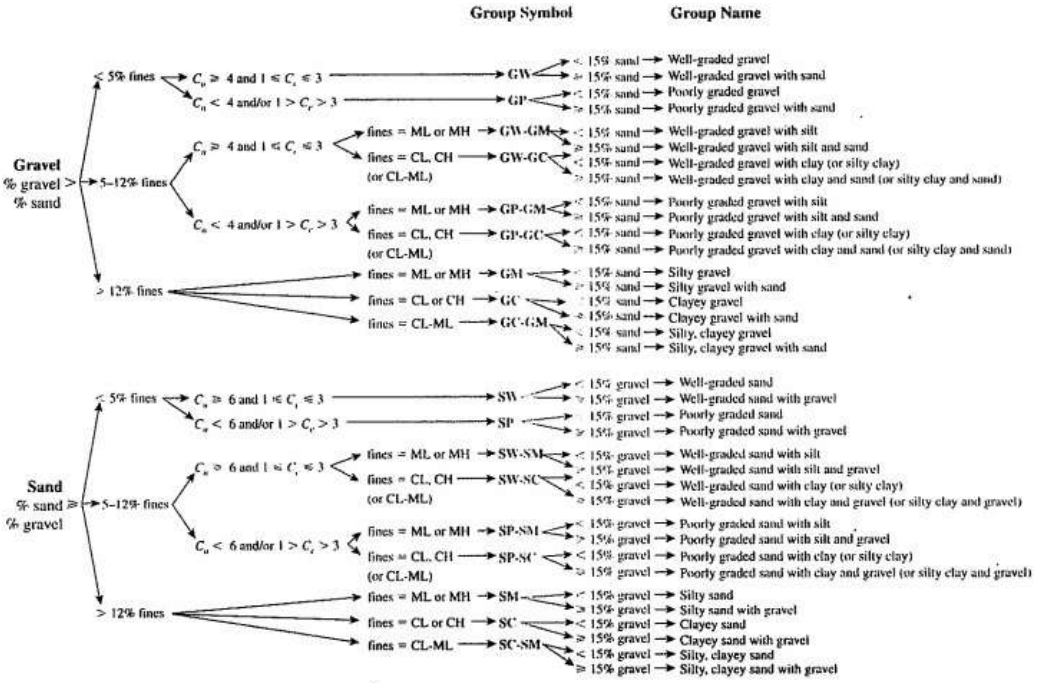


Figure 1.6 Flowchart for classifying coarse-grained soils (more than 50% retained on No. 200 Sieve) (After ASTM, 2005)

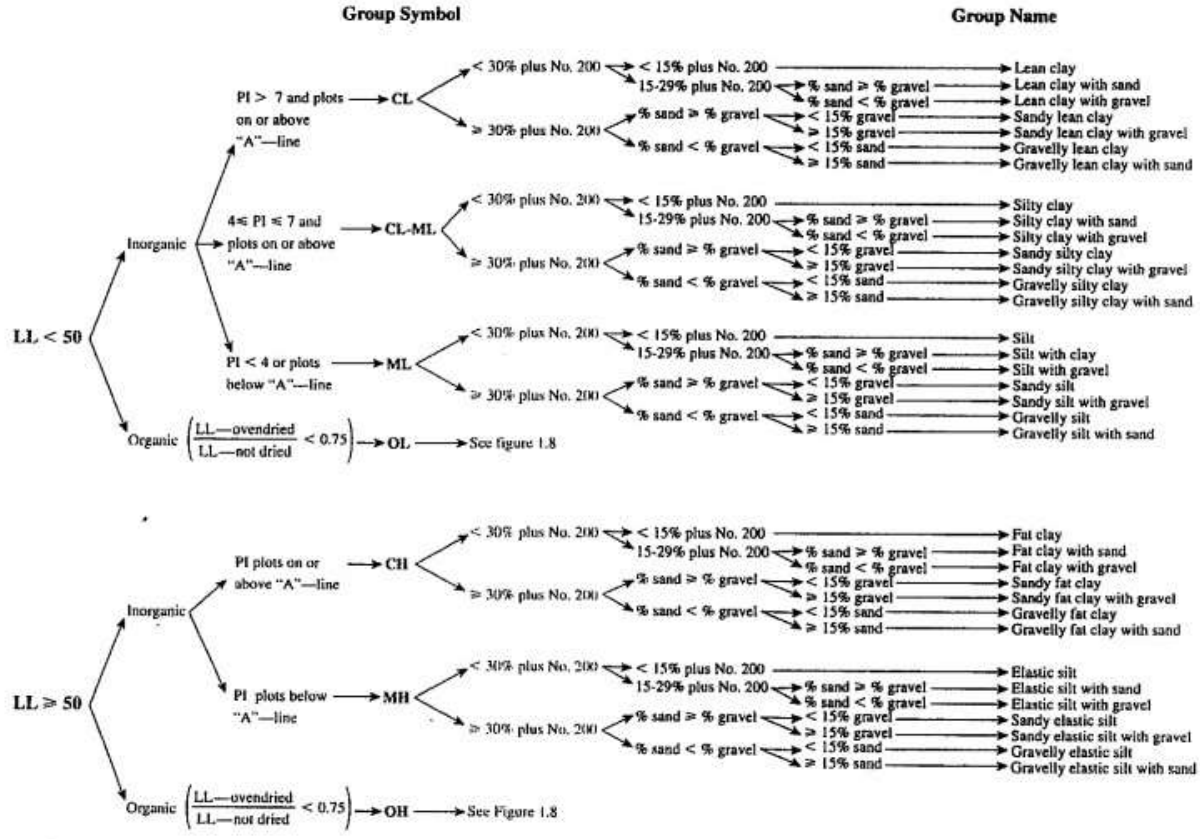


Figure 1.7 Flowchart for classifying fine-grained soil (50% or more passes No. 200 Sieve) (After ASTM, 2005)

Table 1.5 AASHTO Soil Classification System

General classification	Granular materials (35% or less of total sample passing No. 200 sieve)						
Group classification	A-1		A-3	A-2			
	A-1-a	A-1-b		A-2-4	A-2-5	A-2-6	A-2-7
Sieve analysis (% passing)							
No. 10 sieve	50 max						
No. 40 sieve	30 max	50 max	51 min				
No. 200 sieve	15 max	25 max	10 max	35 max	35 max	35 max	35 max
For fraction passing No. 40 sieve							
Liquid limit (LL)				40 max	41 min	40 max	41 min
Plasticity index (PI)	6 max		Nonplastic	10 max	10 max	11 min	11 min
Usual type of material	Stone fragments, gravel, and sand		Fine sand	Silty or clayey gravel and sand			
Subgrade rating	Excellent to good						

General classification	Silt–clay materials (More than 35% of total sample passing No. 200 sieve)			
Group classification	A-4	A-5	A-6	A-7
				A-7-5[a]
				A-7-6[b]
Sieve analysis (% passing)				
No. 10 sieve				
No. 40 sieve				
No. 200 sieve	36 min	36 min	36 min	36 min
For fraction passing No. 40 sieve				
Liquid limit (LL)	40 max	41 min	40 max	41 min
Plasticity index (PI)	10 max	10 max	11 min	11 min
Usual types of material	Mostly silty soils		Mostly clayey soils	
Subgrade rating	Fair to poor			

[a] If PI ≤ LL − 30, the classification is A-7-5.
[b] If PI > LL − 30, the classification is A-7-6.

Table VIII: Soil classification table based on values of saturated hydraulic conductivity K (according to the Czech standard)

Soil (according the relative permeability)	**Approximate range of saturated hydraulic conductivity (m s^{-1})**	**Examples of soil types**
Highly impermeable	< 10^{-10}	clays with low and medium plasticity, clays with high and extremely high plasticity
Impermeable	from 10^{-8} to 10^{-10}	gravel loams, gravel clays and sandy clays, loams with low and medium plasticity
Lowly (poorly) permeable	from 10^{-6} to 10^{-8}	sandy loams, loamy sands and clayey sands, loamy gravels and clayey gravels
Permeable	from 10^{-4} to 10^{-6}	sands and gravels , containing fine-grained fraction(5 – 15 %)
Highly permeable	> 10^{-4}	sands and gravels without or with very low fine grained fraction (<5%)

Source: CSN 721020 (n.d)

APPENDIX IX: SCS RUNOFF CURVE NUMBERS

Table IXa: Runoff curve numbers for urban areas

Cover description: Cover type and hydrologic condition	Average percent impervious area [2]	Curve numbers for hydrologic soil group: A	B	C	D
Fully developed urban areas (vegetation established)					
Open space (lawns, parks, golf courses, cemeteries, etc.) [3]:					
Poor condition (grass cover < 50%)		68	79	86	89
Fair condition (grass cover 50% to 75%)		49	69	79	84
Good condition (grass cover > 75%)		39	61	74	80
Impervious areas:					
Paved parking lots, roofs, driveways, etc. (excluding right-of-way)		98	98	98	98
Streets and roads:					
Paved; curbs and storm sewers (excluding right-of-way)		98	98	98	98
Paved; open ditches (including right-of-way)		83	89	92	93
Gravel (including right-of-way)		76	85	89	91
Dirt (including right-of-way)		72	82	87	89
Western desert urban areas:					
Natural desert landscaping (pervious areas only) [4]		63	77	85	88
Artificial desert landscaping (impervious weed barrier, desert shrub with 1- to 2-inch sand or gravel mulch and basin borders)		96	96	96	96
Urban districts:					
Commercial and business	85	89	92	94	95
Industrial	72	81	88	91	93
Residential districts by average lot size:					
1/8 acre or less (town houses)	65	77	85	90	92
1/4 acre	38	61	75	83	87
1/3 acre	30	57	72	81	86
1/2 acre	25	54	70	80	85
1 acre	20	51	68	79	84
2 acres	12	46	65	77	82
Developing urban areas					
Newly graded areas (pervious areas only, no vegetation) [5]		77	86	91	94
Idle lands (CN's are determined using cover types similar to those in table 2-2c).					

[1] Average runoff condition, and $I_a = 0.2S$.

[2] The average percent impervious area shown was used to develop the composite CN's. Other assumptions are as follows: impervious areas are directly connected to the drainage system, impervious areas have a CN of 98, and pervious areas are considered equivalent to open space in good hydrologic condition. CN's for other combinations of conditions may be computed using figure 2-3 or 2-4.

[3] CN's shown are equivalent to those of pasture. Composite CN's may be computed for other combinations of open space cover type.

[4] Composite CN's for natural desert landscaping should be computed using figures 2-3 or 2-4 based on the impervious area percentage (CN = 98) and the pervious area CN. The pervious area CN's are assumed equivalent to desert shrub in poor hydrologic condition.

[5] Composite CN's to use for the design of temporary measures during grading and construction should be computed using figure 2-3 or 2-4 based on the degree of development (impervious area percentage) and the CN's for the newly graded pervious areas.

Source: TR-55 (1986)

Table IXb: Runoff curve numbers for cultivated agricultural lands

Cover description			Curve numbers for hydrologic soil group			
Cover type	Treatment [2]	Hydrologic condition [3]	A	B	C	D
Fallow	Bare soil	—	77	86	91	94
	Crop residue cover (CR)	Poor	76	85	90	93
		Good	74	83	88	90
Row crops	Straight row (SR)	Poor	72	81	88	91
		Good	67	78	85	89
	SR + CR	Poor	71	80	87	90
		Good	64	75	82	85
	Contoured (C)	Poor	70	79	84	88
		Good	65	75	82	86
	C + CR	Poor	69	78	83	87
		Good	64	74	81	85
	Contoured & terraced (C&T)	Poor	66	74	80	82
		Good	62	71	78	81
	C&T + CR	Poor	65	73	79	81
		Good	61	70	77	80
Small grain	SR	Poor	65	76	84	88
		Good	63	75	83	87
	SR + CR	Poor	64	75	83	86
		Good	60	72	80	84
	C	Poor	63	74	82	85
		Good	61	73	81	84
	C + CR	Poor	62	73	81	84
		Good	60	72	80	83
	C&T	Poor	61	72	79	82
		Good	59	70	78	81
	C&T + CR	Poor	60	71	78	81
		Good	58	69	77	80
Close-seeded or broadcast legumes or rotation meadow	SR	Poor	66	77	85	89
		Good	58	72	81	85
	C	Poor	64	75	83	85
		Good	55	69	78	83
	C&T	Poor	63	73	80	83
		Good	51	67	76	80

[1] Average runoff condition, and I_a=0.2S

[2] Crop residue cover applies only if residue is on at least 5% of the surface throughout the year.

[3] Hydraulic condition is based on combination factors that affect infiltration and runoff, including (a) density and canopy of vegetative areas, (b) amount of year-round cover, (c) amount of grass or close-seeded legumes, (d) percent of residue cover on the land surface (good ≥ 20%), and (e) degree of surface roughness.

Poor: Factors impair infiltration and tend to increase runoff.

Good: Factors encourage average and better than average infiltration and tend to decrease runoff.

Source: TR-55 (1986)

Table IXc: Runoff curve numbers for other agricultural lands

Cover description		Curve numbers for hydrologic soil group			
Cover type	Hydrologic condition	A	B	C	D
Pasture, grassland, or range—continuous forage for grazing. [2]	Poor	68	79	86	89
	Fair	49	69	79	84
	Good	39	61	74	80
Meadow—continuous grass, protected from grazing and generally mowed for hay.	—	30	58	71	78
Brush—brush-weed-grass mixture with brush the major element. [3]	Poor	48	67	77	83
	Fair	35	56	70	77
	Good	30 [4]	48	65	73
Woods—grass combination (orchard or tree farm). [5]	Poor	57	73	82	86
	Fair	43	65	76	82
	Good	32	58	72	79
Woods. [6]	Poor	45	66	77	83
	Fair	36	60	73	79
	Good	30 [4]	55	70	77
Farmsteads—buildings, lanes, driveways, and surrounding lots.	—	59	74	82	86

1 Average runoff condition, and $I_a = 0.2S$.

2 *Poor:* <50%) ground cover or heavily grazed with no mulch.
Fair: 50 to 75% ground cover and not heavily grazed.
Good: > 75% ground cover and lightly or only occasionally grazed.

3 *Poor:* <50% ground cover.
Fair: 50 to 75% ground cover.
Good: >75% ground cover.

4 Actual curve number is less than 30; use CN = 30 for runoff computations.

5 CN's shown were computed for areas with 50% woods and 50% grass (pasture) cover. Other combinations of conditions may be computed from the CN's for woods and pasture.

6 *Poor:* Forest litter, small trees, and brush are destroyed by heavy grazing or regular burning.
Fair: Woods are grazed but not burned, and some forest litter covers the soil.
Good: Woods are protected from grazing, and litter and brush adequately cover the soil.

Source: TR-55 (1986)

Table IXd: Runoff curve numbers for arid and semiarid rangelands

Cover description		Curve numbers for hydrologic soil group			
Cover type	Hydrologic condition [2]	A [3]	B	C	D
Herbaceous—mixture of grass, weeds, and low-growing brush, with brush the minor element.	Poor		80	87	93
	Fair		71	81	89
	Good		62	74	85
Oak-aspen—mountain brush mixture of oak brush, aspen, mountain mahogany, bitter brush, maple, and other brush.	Poor		66	74	79
	Fair		48	57	63
	Good		30	41	48
Pinyon-juniper—pinyon, juniper, or both; grass understory.	Poor		75	85	89
	Fair		58	73	80
	Good		41	61	71
Sagebrush with grass understory.	Poor		67	80	85
	Fair		51	63	70
	Good		35	47	55
Desert shrub—major plants include saltbush, greasewood, creosotebush, blackbrush, bursage, palo verde, mesquite, and cactus.	Poor	63	77	85	88
	Fair	55	72	81	86
	Good	49	68	79	84

[1] Average runoff condition, and $I_a = 0.2S$. For range in humid regions, use table 2-2c.
[2] Poor: <30% ground cover (litter, grass, and brush overstory).
Fair: 30 to 70% ground cover.
Good: > 70% ground cover.
[3] Curve numbers for group A have been developed only for desert shrub.

Source: TR-55 (1986)

Rainfall Groups for Antecedent Soil Moisture Conditions during Growing and Dormant Seasons			
Antecedent Condition	**Description**	**Growing Season** **5-Day Antecedent Rainfall**	**Dormant Season** **5-Day Antecedent Rainfall**
Dry AMC I	An optimum condition of watershed soils, where soils are dry but not to the wilting point, and when satisfactory plowing or cultivation takes pace	Less than 1.4 in. or 35 mm	Less than 0.05 in. or 12 mm
Average AMC II	The average case for annual floods	1.4 in. to 2 in. or 35 to 53 mm	0.5 to 1 in. or 12 to 28 mm
Wet AMC III	When a heavy rainfall, or light rainfall and low temperatures, have occurred during the five days previous to a given storm	Over 2 in. or 53mm	Over 1 in. or 28 mm

Source: TR-55; US. Department of Agricultural Soil Conservation Service (1986)

APPENDIX X: NORMALLY DISTRIBUTED RANDOM NUMBERS

Table Xa: Random Numbers Generated for the Thomas-Fiering Model

	1	2	3	4	5	6	7	8	9	10	11	12
1	-0.112	1.375	0.262	1.043	-1.149	1.212	-0.142	1.929	-1.229	-1.552	-1.989	0.001
2	-1.827	1.025	0.652	0.922	-0.076	0.947	-0.062	1.964	0.935	0.548	0.919	0.038
3	1.151	-0.394	-1.067	-1.942	-0.402	0.360	-1.705	-0.471	-0.151	0.106	-0.154	0.995
4	0.682	2.378	1.160	-0.450	-0.209	-1.656	-0.596	-0.732	1.694	-2.623	0.569	1.810
5	0.490	0.661	-0.105	-0.100	-1.043	-0.954	1.003	-1.165	-0.325	1.375	-0.819	0.434
6	-0.002	-0.852	0.027	1.292	0.177	-1.895	0.830	1.661	1.582	0.279	-1.030	-2.906
7	-0.765	-1.004	-0.432	-1.649	-1.219	1.909	0.534	0.579	-1.282	-2.489	0.361	0.414
8	-0.301	0.621	-1.467	0.190	1.395	0.189	-0.560	-0.296	-1.617	0.527	0.547	0.194
9	0.188	-0.143	0.603	-0.566	0.380	-1.072	-0.464	-1.358	0.024	0.467	0.166	-1.327
10	-0.420	0.000	0.544	-0.426	-0.846	-0.306	1.794	-2.618	-0.023	0.667	0.533	0.104
11	0.720	0.924	-1.046	-1.082	-0.374	-0.371	-0.597	0.452	0.558	-0.652	-1.554	0.249
12	1.029	1.236	0.588	0.943	0.829	-0.482	-1.146	-1.015	-0.010	-0.689	-2.530	-0.763
13	-2.346	-1.730	-1.043	0.192	-0.068	-0.068	-0.795	1.007	0.501	0.149	-0.443	0.150
14	0.781	-0.613	-1.109	0.471	0.746	-0.384	-0.228	-0.519	0.144	-1.469	1.861	0.311
15	-1.122	-0.959	1.610	0.495	-0.039	0.742	-0.986	1.613	-1.355	0.189	0.521	-1.193
16	-0.366	-1.455	-0.361	-0.105	-2.163	-1.309	-1.018	1.426	0.674	-0.099	-0.035	-0.708
17	-1.423	-2.404	-0.956	-0.088	0.911	0.831	1.754	-1.893	-1.327	0.685	0.646	0.854
18	-0.743	0.114	-2.075	-0.748	0.052	1.848	1.277	-2.025	-0.831	0.301	-0.920	0.057
19	0.201	-1.057	0.611	-0.971	0.520	1.036	0.901	-1.041	-0.050	1.419	0.035	0.888
20	0.550	-1.321	1.153	0.711	0.810	2.213	-2.586	-0.642	0.490	1.587	0.526	1.570
21	1.453	0.292	0.896	-0.400	-1.275	-1.368	2.404	-0.447	0.709	0.956	1.549	1.173
22	-1.267	-0.626	1.217	-0.346	-0.346	-0.878	-0.253	0.601	-0.430	1.227	-0.937	0.490
23	1.123	-0.867	-2.166	-0.048	1.040	-0.681	0.286	-1.156	-0.111	-0.476	-0.545	0.824
24	-0.936	-0.363	-0.255	-0.468	-0.083	0.463	-0.121	-0.487	-0.083	-0.144	0.671	2.922
25	0.374	-0.478	0.163	-0.699	0.960	-1.990	0.249	0.973	0.000	-1.262	0.952	0.103
26	0.638	0.373	-0.148	1.791	0.801	-0.576	1.769	0.637	0.193	-0.755	-0.573	-1.259
27	-1.099	0.314	0.569	-0.330	-0.444	-2.018	0.599	-0.475	0.740	-0.803	0.068	-1.598
28	-0.329	-0.721	-0.953	-0.296	-0.286	1.058	-0.562	-0.939	-0.246	-0.737	-1.015	0.863
29	-1.094	-1.158	-0.738	-0.858	-0.021	-0.299	0.866	-0.152	0.638	-2.606	1.743	0.288
30	-0.662	0.126	-0.186	0.663	0.572	-0.874	0.221	0.036	-1.022	-0.933	-0.863	0.447
31	0.730	2.347	-2.409	0.732	1.454	-2.720	-2.745	-1.020	-0.691	1.083	-0.555	1.016

Table Xb: Random Numbers Generated for the Thomas-Fiering Model (Continues)

	1	2	3	4	5	6	7	8	9	10	11	12
32	-1.097	-0.173	-0.216	-0.696	0.755	0.174	-0.859	-0.650	1.007	-0.047	0.648	1.105
33	2.426	2.040	0.940	0.321	-0.228	-0.259	-0.659	-0.855	-0.237	-0.101	-0.269	-0.335
34	-0.187	1.127	0.040	0.428	-0.288	1.404	-1.218	-2.019	0.699	1.175	0.964	0.220
35	-0.588	-0.077	-0.790	-0.925	0.600	-0.936	1.005	-0.225	0.356	0.539	-1.242	-1.623
36	-0.245	-0.348	-0.774	0.266	0.260	0.301	0.327	0.460	-1.697	0.369	0.013	-1.012
37	-0.336	-1.112	-0.127	0.569	0.344	-1.067	-1.493	0.524	0.887	-0.630	0.233	1.293
38	0.158	1.260	-0.911	-0.594	-0.747	1.300	-1.453	-1.215	-0.181	-0.147	-0.723	0.541
39	-0.894	-0.745	0.453	-1.629	1.764	-1.712	-1.519	0.242	0.068	0.641	0.983	0.184
40	-1.431	0.102	-0.232	1.836	-0.070	1.397	0.471	0.298	-1.668	0.907	-0.021	0.024
41	1.084	0.040	-1.039	0.774	0.877	1.303	0.615	-0.096	0.040	-0.106	-0.588	0.014
42	-0.298	0.508	0.169	-1.217	0.616	-0.298	0.230	1.265	-0.191	-0.525	-0.191	1.470
43	1.193	0.857	0.302	-0.975	1.303	-2.097	0.801	-0.476	-0.942	1.231	0.107	0.491
44	1.309	1.481	-0.210	2.429	-0.036	1.180	1.826	0.550	0.125	-1.137	0.439	2.268
45	-0.305	-1.199	0.870	0.378	-1.638	0.135	1.826	-0.570	-0.827	0.519	-0.464	-1.714
46	1.207	-0.046	-0.338	-1.554	-0.441	0.780	-0.707	-1.163	-1.276	0.276	-0.569	0.185
47	0.043	-0.053	-1.687	2.280	0.619	0.777	-0.502	0.425	-0.239	-0.270	-0.344	-0.153
48	-0.361	-0.408	-0.971	1.207	-1.160	0.788	-0.031	-0.235	0.778	-1.287	0.867	-0.655
49	-1.934	-0.384	-2.325	-1.923	0.908	1.477	0.272	0.348	0.165	0.355	0.270	-0.448
50	-0.732	3.401	0.526	0.633	-0.616	-1.399	1.428	0.112	0.788	0.276	-0.159	0.659
51	1.079	0.395	0.248	-1.495	-0.234	0.434	1.814	0.201	-0.020	-0.985	-0.244	-2.844
52	0.015	0.819	1.540	0.737	-1.196	-1.022	0.047	-0.349	-0.297	-1.846	-0.395	1.712
53	1.797	-0.132	1.422	1.231	0.817	-0.816	-0.065	-1.938	-0.972	-0.521	1.357	-0.023
54	0.286	1.233	2.090	1.084	-0.037	-0.877	0.678	-0.514	0.376	-2.635	-1.212	0.575
55	-0.896	-0.765	-0.166	-0.273	0.126	-1.795	-1.940	-0.729	-2.172	-0.957	0.213	-1.533
56	1.183	1.255	-0.666	-1.615	-0.460	-1.125	-0.065	0.845	-0.591	-0.309	-0.589	-1.366
57	-0.537	0.893	-0.971	1.009	0.683	-0.604	-0.682	-0.305	-0.463	-0.123	0.789	-0.343
58	-1.136	-1.446	0.848	0.333	-0.055	-0.444	1.358	-0.523	0.199	-0.421	-1.873	-0.512
59	-1.055	1.640	-1.249	0.763	-0.488	0.376	0.141	-0.258	0.661	0.910	0.104	-0.875
60	-0.335	-0.781	0.644	0.899	0.265	1.046	0.793	1.233	0.111	-1.202	-2.141	-0.332
61	1.561	-0.217	0.500	0.002	-0.139	-1.268	-0.398	-0.216	2.031	1.946	-0.221	1.059

APPENDIX XI: RUNOFF COMPUTATION BY RATIONAL METHOD

Table XIa: Recommended Guide on the Value of Runoff Coefficient in Rural Areas

		Mean Annual Rainfall (mm)		
Component	**Classification**	**<600**	**600-900**	**>900**
Surface slope (C_s)				
	Wet lands and swamps (<3%)	0.01	0.03	0.05
	Flat areas (3 to 10%)	0.06	0.08	0.11
	Hilly (10 to 30%)	0.12	0.16	0.20
	Steep Areas (>30%)	0.22	0.26	0.30
Permeability (C_p)				
	Very permeable	0.03	0.04	0.05
	Permeable	0.06	0.08	0.10
	Semi permeable	0.12	0.16	0.20
	Impermeable	0.21	0.26	0.30
Vegetation (C_v)				
	Thick bush and plantation	0.03	0.04	0.05
	Light bush and farm land	0.07	0.11	0.15
	Grassland	0.17	0.21	0.25
	No vegetation	0.26	0.28	0.30

Table XIb: Guidance on Permeability of Catchment based on soil type

Material	**Permeability rating**
Gravel, coarse sand	Very permeable
Fine sand, sandy loam	Permeable
Silt, loam, clayey sand	Semi permeable
Clay, peat, rock	Impermeable

Source: FMW (2013)

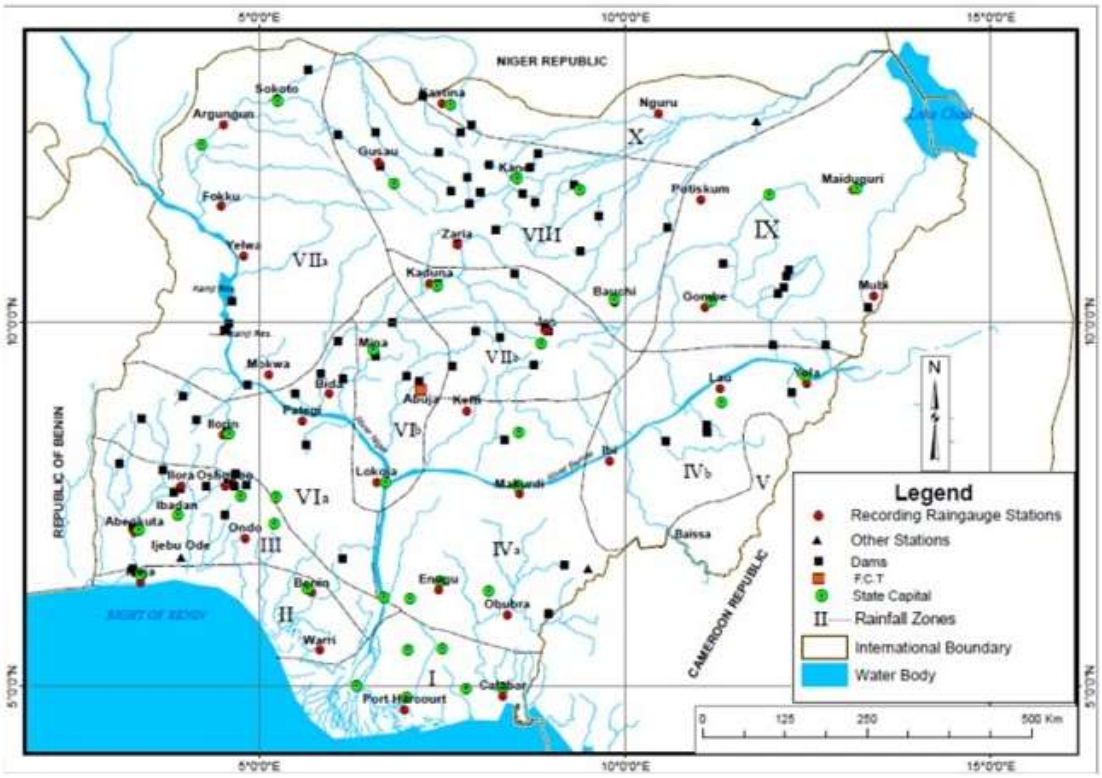


Fig. XI: Map showing the Rainfall Zones of Nigeria (FMW, 2013)

Table XIc: Ranges of characteristics of some Rainfall zones

Zone	A (%)	B (%)	C (%)	Altitude (m)	Annual mean rainfall (mm)	Annual mean no. of rainy days
I	41–46	47–90	43–49	80	2150	170
II	50–54	50–55	50–65	80	1550–2900	125–190
III	52–54	56–57	52–57	225–305	1217–1600	106–151
IVa	48–49	54–55	54–60	113–307	1224–1800	94–109
IVb	50–51	52–54	54–57	150–190	900–1150	75–90

Source: FMW (2013)

Table XId: Estimates of parameters β and 1/α for calculation of Rainfall Intensity

Zone	(1/α), β	0.2 h	0.4 h	1 h	3 h	6 h	12 h	24 h
I	1/α	23.52	19.19	12.10	6.63	3.74	1.87	0.98
	β	118.94	97.43	60.13	26.25	14.48	7.63	4.03
II	1/α	24.83	20.97	14.36	6.29	3.88	2.16	1.26
	β	113.16	85.74	55.06	23.58	13.30	7.03	3.81
III	1/α	19.57	14.99	11.32	5.59	2.94	1.49	0.85
	β	108.78	78.59	43.63	17.43	9.55	4.85	2.61
IVa	1/α	21.42	16.24	12.65	4.69	3.04	1.57	0.89
	β	111.83	83.38	49.13	20.03	10.56	5.61	2.83

APPENDIX XII: ANALYTICAL HIERARCHICAL PROCESS TABLES

Table XIIa: Fundamental Scale for Pair wise Comparison

Intensity of Importance	Definition	Explanation
1	Equal importance	Two elements contribute equally to the objective
3	Moderate importance	Experience and judgment slightly favor one element over another
5	Strong importance	Experience and judgment strongly favor one element over another
7	Very Strong importance	One element is favored very strongly over another; its dominance is demonstrated in practice
9	Extreme importance	The evidence favoring one element over another is of the highest possible order of affirmation
2,4,6, and 8 are intermediate values		

Source: Saaty (1980)

Table XIIb: Random Inconsistency Indices (RI) for N-10

N	1	2	3	4	5	6	7	8	9	10
RI	0	0	0.58	0.89	1.12	1.24	1.32	1.41	1.45	1.49

Source: Saaty (1980)

APPENDIX XIII: RESULTS OF SOIL ANALYSES

Atterberg Limits Data Sheet

ASTM D4318-10

Project Name:	PhD Research	**Tested By:**	M.I. Alfa	**Date:**	18/5/2016
Location:	Oforachi	**Checked By:**	D.B. Adie	**Date:**	30/5/2016
Boring No:	OF 01	**Test Number:**	1	**Depth**	12-24 inches
Coordinate		**Elevation:**			

USCS Soil Classification: **ML**

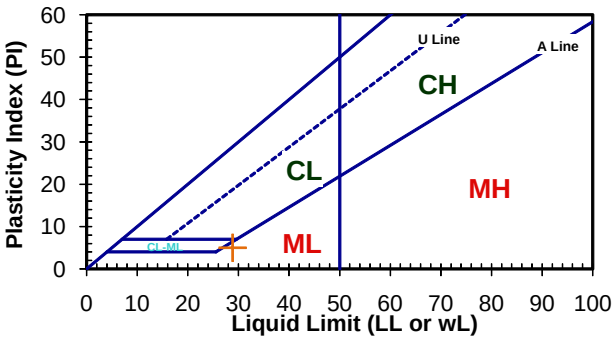
TEST			PLASTIC LIMIT				LIQUID LIMIT				
Variable	**NO**		**1**	**2**	**3**	**4**	**1**	**2**	**3**	**4**	**5**
	Var.	**Units**									
Number of Blows	N	blows					47	36	28	17	13
Can Number	---	---	OF1	OF2	OF3	OF4	OF5	OF6	OF7	OF8	OF8
Mass of Empty Can	M_C	(g)	8.80	8.80	8.80	8.80	9.40	9.40	8.20	8.90	8.90
Mass Can & Soil (Wet)	M_{CMS}	(g)	11.40	11.10	10.60	11.03	21.90	24.50	26.40	27.50	27.90
Mass Can & Soil (Dry)	M_{CDS}	(g)	10.90	10.60	10.30	10.60	18.90	21.00	23.20	23.20	23.40
Mass of Soil	M_S	(g)	2.10	1.80	1.50	1.80	9.50	11.60	15.00	14.30	14.50
Mass of Water	M_W	(g)	0.50	0.50	0.30	0.43	3.00	3.50	3.20	4.30	4.50
Water Content	w	(%)	23.8	27.8	20.0	23.9	31.6	30.2	21.3	30.1	31.0

Liquid Limit (LL or w_L) (%):	**28.86**
Plastic Limit (PL or w_P) (%):	**23.87**
Plasticity Index (PI) (%):	**4.99**
USCS Classification:	**ML**

PI at "A" Line = 0.73(LL-20)

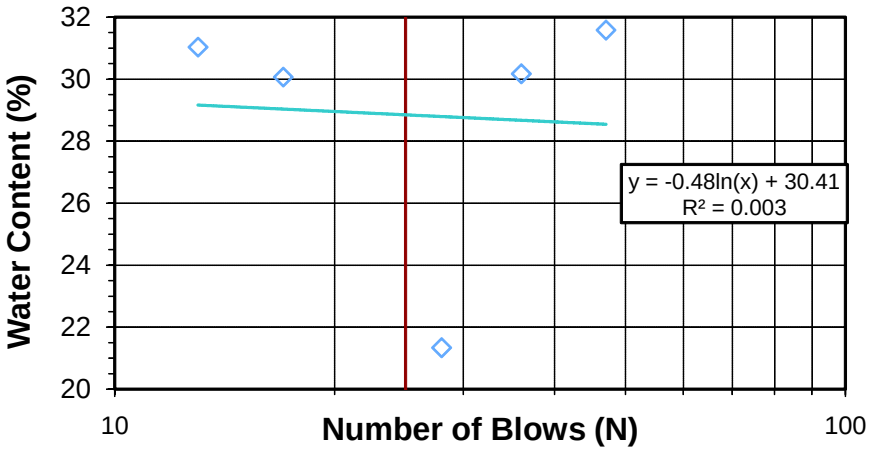
One Point Liquid Limit Calculation:

$LL = w_n (N/25)^{0.12}$



PROCEDURE USED

	Wet Preperation Multipoint
X	**Dry Preperation Multipoint**
	Procedure A Multipoint
	Procedure B One-Point



Atterberg Limits Data Sheet

ASTM D4318-10

Project Name:	PhD Research	**Tested By:**	M.I. Alfa	**Date:**	18/5/2016
Location:	Oforachi	**Checked By:**	D.B. Adie	**Date:**	30/5/2016
Boring No:	OF 02	**Test Number:**	1	**Depth**	12-24 inches
Coordinate		**Elevation:**			

USCS Soil Classification: ML

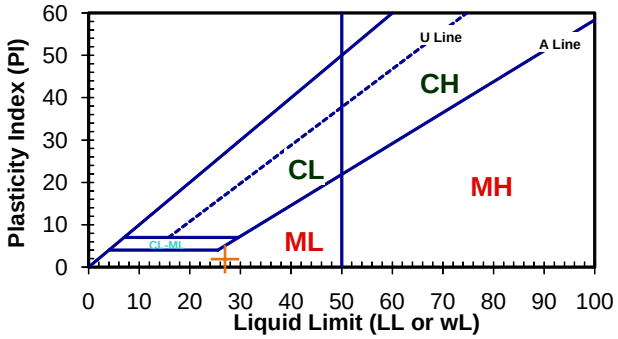
TEST			PLASTIC LIMIT				LIQUID LIMIT				
Variable	NO		1	2	3	4	1	2	3	4	5
	Var.	Units									
Number of Blows	N	blows					48	37	29	19	11
Can Number	---	---	OF1	OF2	OF3	OF4	OF5	OF6	OF7	OF8	OF8
Mass of Empty Can	M_C	(g)	8.80	8.80	9.40	9.00	8.20	8.40	8.90	8.40	9.00
Mass Can & Soil (Wet)	M_{CMS}	(g)	10.70	11.10	12.60	11.47	22.10	20.20	23.20	27.10	30.50
Mass Can & Soil (Dry)	M_{CDS}	(g)	10.40	10.50	12.10	10.93	19.40	17.90	20.10	23.10	25.40
Mass of Soil	M_S	(g)	1.60	1.70	2.70	1.93	11.20	9.50	11.20	14.70	16.40
Mass of Water	M_W	(g)	0.30	0.60	0.50	0.54	2.70	2.30	3.10	4.00	5.10
Water Content	w	(%)	18.7	35.3	18.5	28.0	24.1	24.2	27.7	27.2	31.1

Liquid Limit (LL or w_L) (%):	**26.96**
Plastic Limit (PL or w_P) (%):	**25.14**
Plasticity Index (PI) (%):	**1.82**
USCS Classification:	**ML**

PI at "A" Line = 0.73(LL-20)

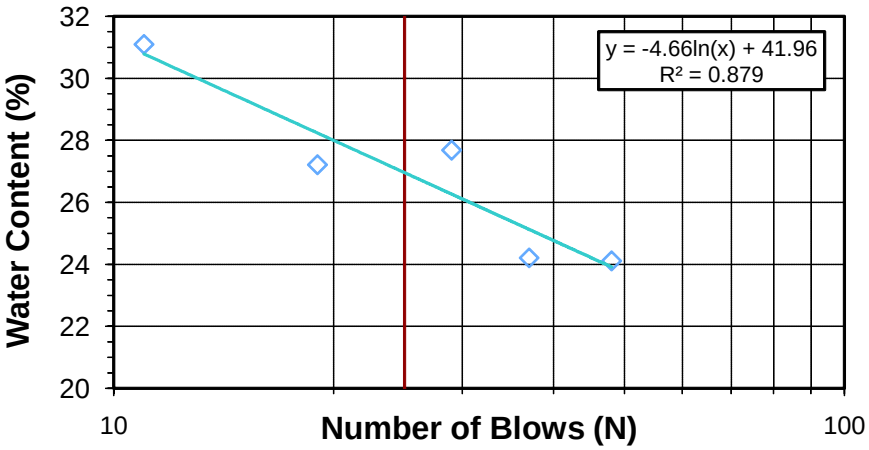
One Point Liquid Limit Calculation:

$LL = w_n (N/25)^{0.12}$



PROCEDURE USED

	Wet Preperation Multipoint
X	**Dry Preperation Multipoint**
	Procedure A Multipoint
	Procedure B One-Point



Atterberg Limits Data Sheet

ASTM D4318-10

Project Name:	PhD Research	**Tested By:**	M.I. Alfa	**Date:**	18/5/2016
Location:	Oforachi	**Checked By:**	D.B. Adie	**Date:**	30/5/2016
Boring No:	OF 03	**Test Number:**	1	**Depth**	12-24 inches
Coordinate		**Elevation:**			

USCS Soil Classification: CL

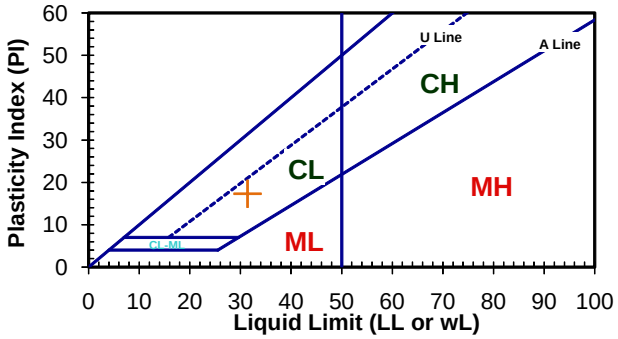
TEST			PLASTIC LIMIT				LIQUID LIMIT				
Variable	**NO**		**1**	**2**	**3**	**4**	**1**	**2**	**3**	**4**	**5**
	Var.	**Units**									
Number of Blows	N	blows					48	37	28	18	13
Can Number	---	---	OF1	OF2	OF3	OF4	OF5	OF6	OF7	OF8	OF8
Mass of Empty Can	M_C	(g)	10.20	14.40	14.50	13.03	8.70	8.60	14.70	14.00	14.00
Mass Can & Soil (Wet)	M_{CMS}	(g)	12.20	16.50	16.90	15.20	20.50	22.60	24.60	35.00	31.10
Mass Can & Soil (Dry)	M_{CDS}	(g)	12.00	16.20	16.60	14.93	18.40	19.90	20.80	31.00	27.60
Mass of Soil	M_S	(g)	1.80	1.80	2.10	1.90	9.70	11.30	6.10	17.00	13.60
Mass of Water	M_W	(g)	0.20	0.30	0.30	0.27	2.10	2.70	3.80	4.00	3.50
Water Content	w	(%)	11.1	16.7	14.3	14.2	21.6	23.9	62.3	23.5	25.7

Liquid Limit (LL or w_L) (%):	**31.40**
Plastic Limit (PL or w_P) (%):	**14.07**
Plasticity Index (PI) (%):	**17.33**
USCS Classification:	**CL**

PI at "A" Line = 0.73(LL-20)

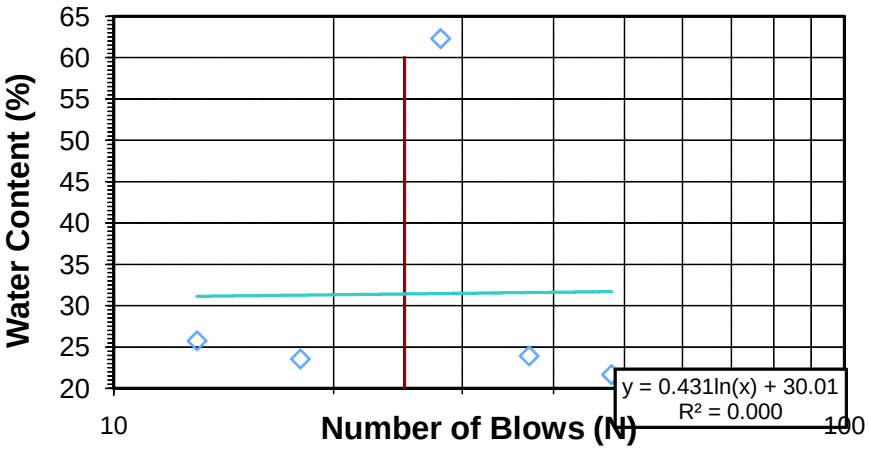
One Point Liquid Limit Calculation:

$LL = w_n (N/25)^{0.12}$



PROCEDURE USED

	Wet Preperation Multipoint
X	**Dry Preperation Multipoint**
	Procedure A Multipoint
	Procedure B One-Point



Atterberg Limits Data Sheet

ASTM D4318-10

Project Name:	PhD Research	**Tested By:**	M.I. Alfa	**Date:**	18/5/2016
Location:	Oforachi	**Checked By:**	D.B. Adie	**Date:**	30/5/2016
Boring No:	OF 04	**Test Number:**	1	**Depth**	12-24 inches
Coordinate		**Elevation:**			

USCS Soil Classification: **Nil**

TEST			PLASTIC LIMIT				LIQUID LIMIT				
Variable	**NO**		**1**	**2**	**3**	**4**	**1**	**2**	**3**	**4**	**5**
	Var.	**Units**									
Number of Blows	N	blows									
Can Number	---	---									
Mass of Empty Can	M_C	(g)									
Mass Can & Soil (Wet)	M_{CMS}	(g)									
Mass Can & Soil (Dry)	M_{CDS}	(g)									
Mass of Soil	M_S	(g)									
Mass of Water	M_W	(g)									
Water Content	w	(%)									

Liquid Limit (LL or w_L) (%):	**Nil**
Plastic Limit (PL or w_P) (%):	**Nil**
Plasticity Index (PI) (%):	**Nil**

ASTM D4318-10

Project Name:	PhD Research	**Tested By:**	M.I. Alfa	**Date:**	18/5/2016
Location:	Oforachi	**Checked By:**	D.B. Adie	**Date:**	30/5/2016
Boring No:	OF 05	**Test Number:**	1	**Depth**	12-24 inches
Coordinate		**Elevation:**			

USCS Soil Classification: ML

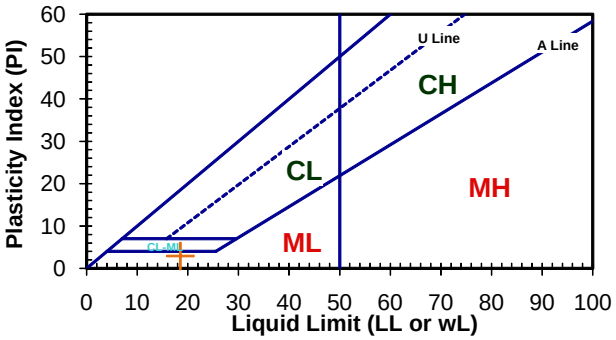
TEST			PLASTIC LIMIT				LIQUID LIMIT				
Variable	**NO**		**1**	**2**	**3**	**4**	**1**	**2**	**3**	**4**	**5**
	Var.	**Units**									
Number of Blows	N	blows					47	37	28	17	13
Can Number	---	---	OF1	OF2	OF3	OF4	OF5	OF6	OF7	OF8	OF8
Mass of Empty Can	M_C	(g)	14.20	13.70	15.60	14.50	14.60	11.30	15.00	13.70	13.80
Mass Can & Soil (Wet)	M_{CMS}	(g)	15.90	15.70	17.20	16.27	27.10	25.50	31.00	32.40	32.40
Mass Can & Soil (Dry)	M_{CDS}	(g)	15.60	15.50	17.00	16.03	25.10	23.20	28.20	29.10	30.40
Mass of Soil	M_S	(g)	1.40	1.80	1.40	1.53	10.50	11.90	13.20	15.40	16.60
Mass of Water	M_W	(g)	0.30	0.20	0.20	0.24	2.00	2.30	2.80	3.30	2.00
Water Content	w	(%)	21.4	11.1	14.3	15.7	19.0	19.3	21.2	21.4	12.0

Liquid Limit (LL or w_L) (%):	**18.54**
Plastic Limit (PL or w_P) (%):	**15.63**
Plasticity Index (PI) (%):	**2.91**
USCS Classification:	**ML**

PI at "A" Line = 0.73(LL-20)

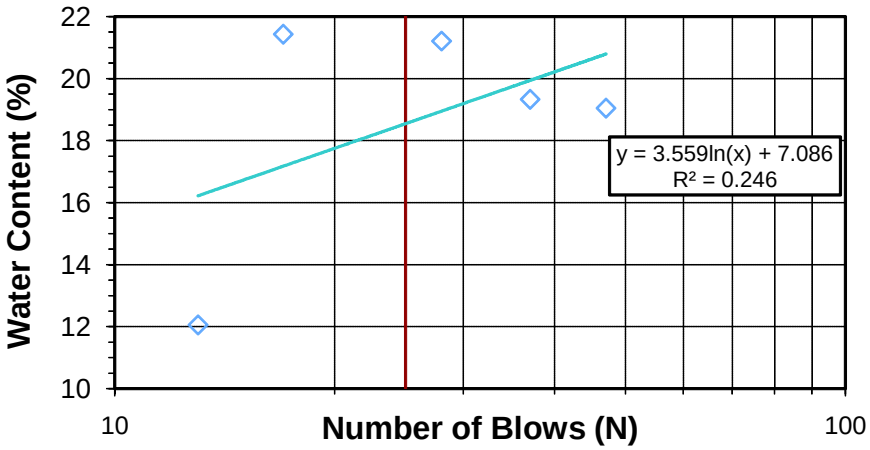
One Point Liquid Limit Calculation:

$LL = w_n (N/25)^{0.12}$



PROCEDURE USED

	Wet Preperation Multipoint
X	**Dry Preperation Multipoint**
	Procedure A Multipoint
	Procedure B One-Point



Atterberg Limits Data Sheet

ASTM D4318-10

Project Name:	PhD Research	**Tested By:**	M.I. Alfa	**Date:**	18/5/2016
Location:	Oforachi	**Checked By:**	D.B. Adie	**Date:**	30/5/2016
Boring No:	OF 06	**Test Number:**	1	**Depth**	12-24 inches
Coordinate		**Elevation:**			

USCS Soil Classification: **ML-MH**

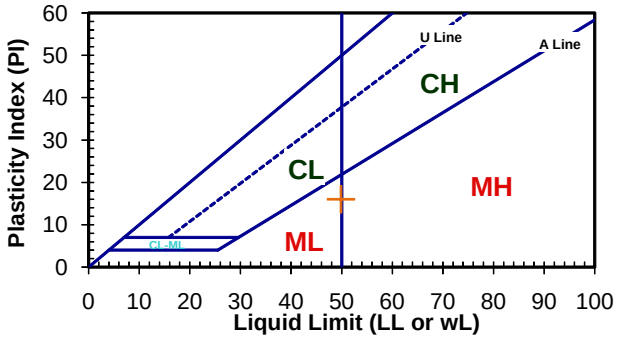
TEST			PLASTIC LIMIT				LIQUID LIMIT				
Variable	**NO**		**1**	**2**	**3**	**4**	**1**	**2**	**3**	**4**	**5**
	Var.	**Units**									
Number of Blows	N	blows					47	36	28	17	13
Can Number	---	---	OF1	OF2	OF3	OF4	OF5	OF6	OF7	OF8	OF8
Mass of Empty Can	M_C	(g)	8.90	8.90	8.90	8.90	8.90	8.60	8.70	9.50	9.00
Mass Can & Soil (Wet)	M_{CMS}	(g)	11.10	11.50	11.20	11.27	21.50	20.70	24.50	28.60	26.70
Mass Can & Soil (Dry)	M_{CDS}	(g)	10.60	10.80	10.60	10.67	17.50	16.50	19.40	22.20	20.70
Mass of Soil	M_S	(g)	1.70	1.90	1.70	1.77	8.60	7.90	10.70	12.70	11.70
Mass of Water	M_W	(g)	0.50	0.70	0.60	0.60	4.00	4.20	5.10	6.40	6.00
Water Content	w	(%)	29.4	36.8	35.3	33.9	46.5	53.2	47.7	50.4	51.3

Liquid Limit (LL or w_L) (%):	**49.84**
Plastic Limit (PL or w_P) (%):	**33.86**
Plasticity Index (PI) (%):	**15.98**
USCS Classification:	**ML-MH**

PI at "A" Line = 0.73(LL-20)

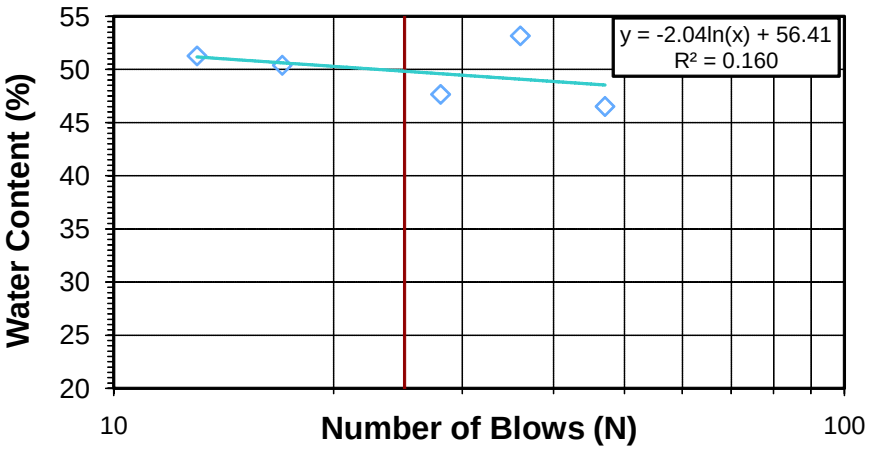
One Point Liquid Limit Calculation:

$LL = w_n (N/25)^{0.12}$



PROCEDURE USED

	Wet Preperation Multipoint
X	**Dry Preperation Multipoint**
	Procedure A Multipoint
	Procedure B One-Point



Atterberg Limits Data Sheet

ASTM D4318-10

Project Name:	PhD Research	**Tested By:**	M.I. Alfa	**Date:**	18/5/2016
Location:	Oforachi	**Checked By:**	D.B. Adie	**Date:**	30/5/2016
Boring No:	OF 07	**Test Number:**	1	**Depth**	12-24 inches
Coordinate		**Elevation:**			

USCS Soil Classification: **Nil**

TEST			PLASTIC LIMIT				LIQUID LIMIT				
Variable	**NO**		**1**	**2**	**3**	**4**	**1**	**2**	**3**	**4**	**5**
	Var.	**Units**									
Number of Blows	N	blows									
Can Number	---	---									
Mass of Empty Can	M_C	(g)									
Mass Can & Soil (Wet)	M_{CMS}	(g)									
Mass Can & Soil (Dry)	M_{CDS}	(g)									
Mass of Soil	M_S	(g)									
Mass of Water	M_W	(g)									
Water Content	w	(%)									

Liquid Limit (LL or w_L) (%):	**Nil**
Plastic Limit (PL or w_P) (%):	**Nil**
Plasticity Index (PI) (%):	**Nil**

Atterberg Limits Data Sheet

ASTM D4318-10

Project Name:	PhD Research	**Tested By:**	M.I. Alfa	**Date:**	18/5/2016
Location:	Oforachi	**Checked By:**	D.B. Adie	**Date:**	30/5/2016
Boring No:	OF 08	**Test Number:**	1	**Depth**	12-24 inches
Coordinate		**Elevation:**			

USCS Soil Classification: ML

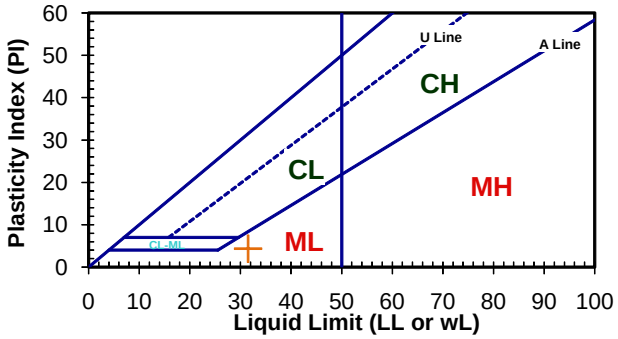
TEST			PLASTIC LIMIT				LIQUID LIMIT				
Variable	**NO**		**1**	**2**	**3**	**4**	**1**	**2**	**3**	**4**	**5**
	Var.	**Units**									
Number of Blows	N	blows					48	37	26	15	12
Can Number	---	---	OF1	OF2	OF3	OF4	OF5	OF6	OF7	OF8	OF8
Mass of Empty Can	M_C	(g)	8.40	8.70	8.90	8.67	8.50	9.10	8.50	8.80	9.10
Mass Can & Soil (Wet)	M_{CMS}	(g)	10.40	10.70	11.00	10.70	19.20	24.50	26.70	31.30	31.40
Mass Can & Soil (Dry)	M_{CDS}	(g)	9.90	10.30	10.60	10.27	16.80	20.90	22.30	25.60	25.90
Mass of Soil	M_S	(g)	1.50	1.60	1.70	1.60	8.30	11.80	13.80	16.80	16.80
Mass of Water	M_W	(g)	0.50	0.40	0.40	0.43	2.40	3.60	4.40	5.70	5.50
Water Content	w	(%)	33.3	25.0	23.5	26.9	28.9	30.5	31.9	33.9	32.7

Liquid Limit (LL or w_L) (%):	**31.52**
Plastic Limit (PL or w_P) (%):	**27.18**
Plasticity Index (PI) (%):	**4.34**
USCS Classification:	**ML**

PI at "A" Line = 0.73(LL-20)

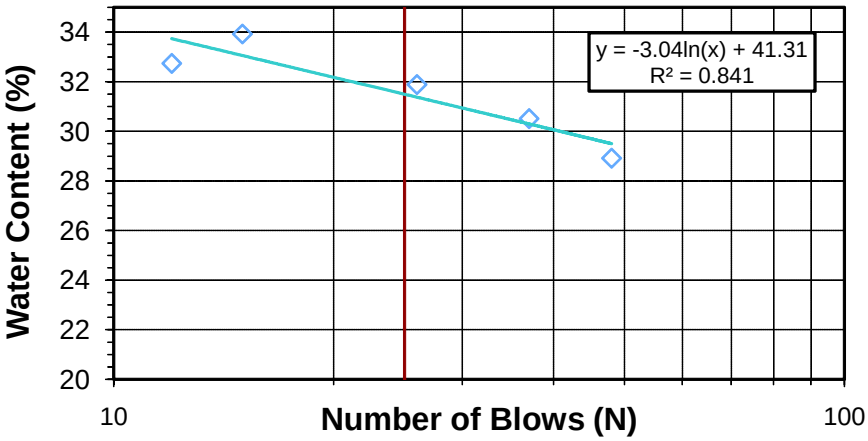
One Point Liquid Limit Calculation:

$LL = w_n (N/25)^{0.12}$



PROCEDURE USED

	Wet Preperation Multipoint
X	**Dry Preperation Multipoint**
	Procedure A Multipoint
	Procedure B One-Point



Atterberg Limits Data Sheet

ASTM D4318-10

Project Name:	PhD Research	**Tested By:**	M.I. Alfa	**Date:**	18/5/2016
Location:	Oforachi	**Checked By:**	D.B. Adie	**Date:**	30/5/2016
Boring No:	OF 09	**Test Number:**	1	**Depth**	12-24 inches
Coordinate		**Elevation:**			

USCS Soil Classification: CL-ML

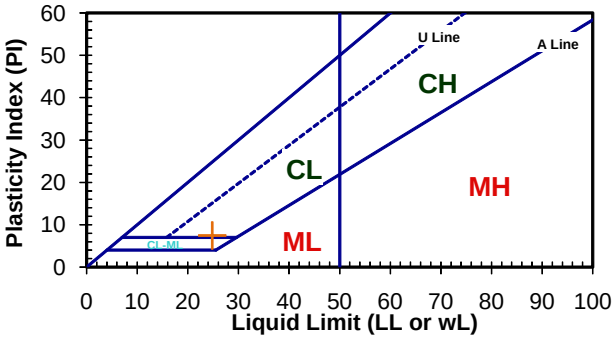
TEST			PLASTIC LIMIT				LIQUID LIMIT				
Variable	NO		1	2	3	4	1	2	3	4	5
	Var.	Units									
Number of Blows	N	blows					48	37	27	19	12
Can Number	---	---	OF1	OF2	OF3	OF4	OF5	OF6	OF7	OF8	OF8
Mass of Empty Can	M_C	(g)	8.90	8.50	8.30	8.57	8.60	8.60	8.40	8.90	9.10
Mass Can & Soil (Wet)	M_{CMS}	(g)	10.40	10.50	10.20	10.37	24.20	22.60	23.70	27.40	34.00
Mass Can & Soil (Dry)	M_{CDS}	(g)	10.20	10.20	9.90	10.10	21.20	19.80	20.70	23.70	28.90
Mass of Soil	M_S	(g)	1.30	1.70	1.60	1.53	12.60	11.20	12.30	14.80	19.80
Mass of Water	M_W	(g)	0.20	0.30	0.30	0.27	3.00	2.80	3.00	3.70	5.10
Water Content	w	(%)	15.4	17.6	18.7	17.6	23.8	25.0	24.4	25.0	25.8

Liquid Limit (LL or w_L) (%):	**24.82**
Plastic Limit (PL or w_P) (%):	**17.36**
Plasticity Index (PI) (%):	**7.46**
USCS Classification:	**CL-ML**

PI at "A" Line = 0.73(LL-20)

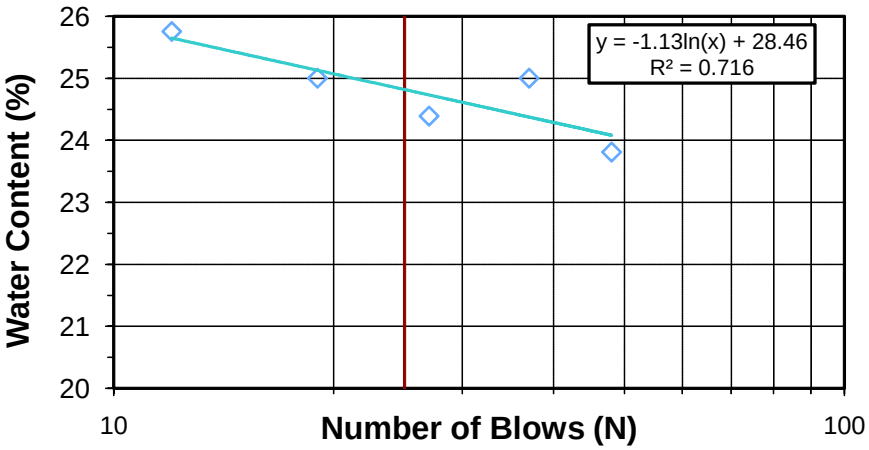
One Point Liquid Limit Calculation:

$LL = w_n (N/25)^{0.12}$



PROCEDURE USED

- [ ] **Wet Preperation Multipoint**
- [x] **Dry Preperation Multipoint**
- [ ] **Procedure A Multipoint**
- [ ] **Procedure B One-Point**



Atterberg Limits Data Sheet

ASTM D4318-10

Project Name:	PhD Research	**Tested By:**	M.I. Alfa	**Date:**	18/5/2016
Location:	Oforachi	**Checked By:**	D.B. Adie	**Date:**	30/5/2016
Boring No:	OF 10	**Test Number:**	1	**Depth**	12-24 inches
Coordinate		**Elevation:**			

USCS Soil Classification: CL-ML

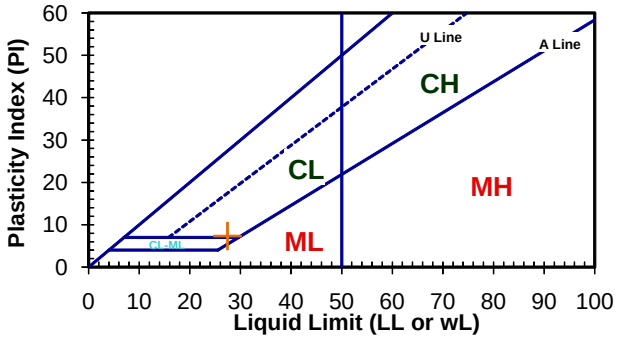
TEST			PLASTIC LIMIT				LIQUID LIMIT				
Variable	**NO**		**1**	**2**	**3**	**4**	**1**	**2**	**3**	**4**	**5**
	Var.	**Units**									
Number of Blows	N	blows					48	37	26	18	13
Can Number	---	---	OF1	OF2	OF3	OF4	OF5	OF6	OF7	OF8	OF8
Mass of Empty Can	M_C	(g)	8.40	8.70	9.00	8.70	8.50	9.10	9.00	9.20	8.90
Mass Can & Soil (Wet)	M_{CMS}	(g)	10.60	11.30	10.80	10.90	22.60	27.70	28.60	25.90	27.10
Mass Can & Soil (Dry)	M_{CDS}	(g)	10.20	10.90	10.50	10.53	19.70	23.80	24.40	22.20	23.00
Mass of Soil	M_S	(g)	1.80	2.20	1.50	1.83	11.20	14.70	15.40	13.00	14.10
Mass of Water	M_W	(g)	0.40	0.40	0.30	0.37	2.90	3.90	4.20	3.70	4.10
Water Content	w	(%)	22.2	18.2	20.0	20.2	25.9	26.5	27.3	28.5	29.1

Liquid Limit (LL or w_L) (%):	**27.45**
Plastic Limit (PL or w_P) (%):	**20.16**
Plasticity Index (PI) (%):	**7.29**
USCS Classification:	**CL-ML**

PI at "A" Line = 0.73(LL-20)

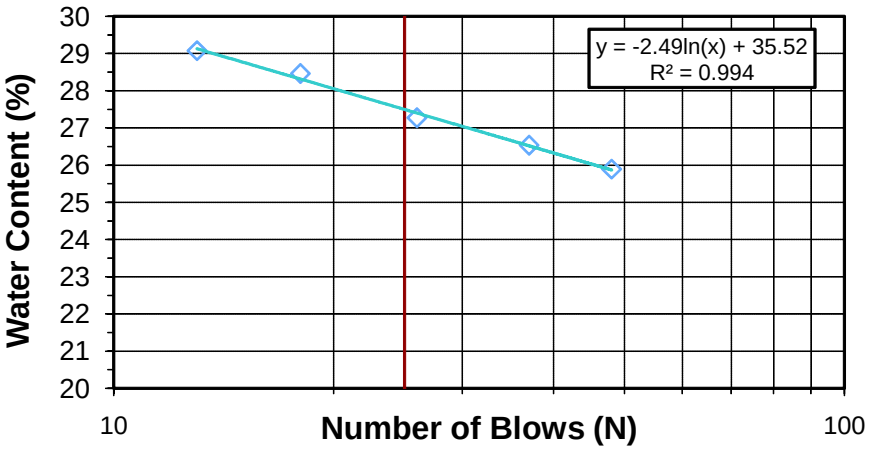
One Point Liquid Limit Calculation:

$LL = w_n (N/25)^{0.12}$



PROCEDURE USED

- [ ] **Wet Preperation Multipoint**
- [X] **Dry Preperation Multipoint**
- [ ] **Procedure A Multipoint**
- [ ] **Procedure B One-Point**



Sieve Analysis Data Sheet

ASTM D422-63(2007)

Project Name: PhD Research | **Tested By:** M.I. Alfa | **Date:** 18/5/2016

Location: Oforachi | **Checked By:** D.B. Adie | **Date:** 30/5/2016

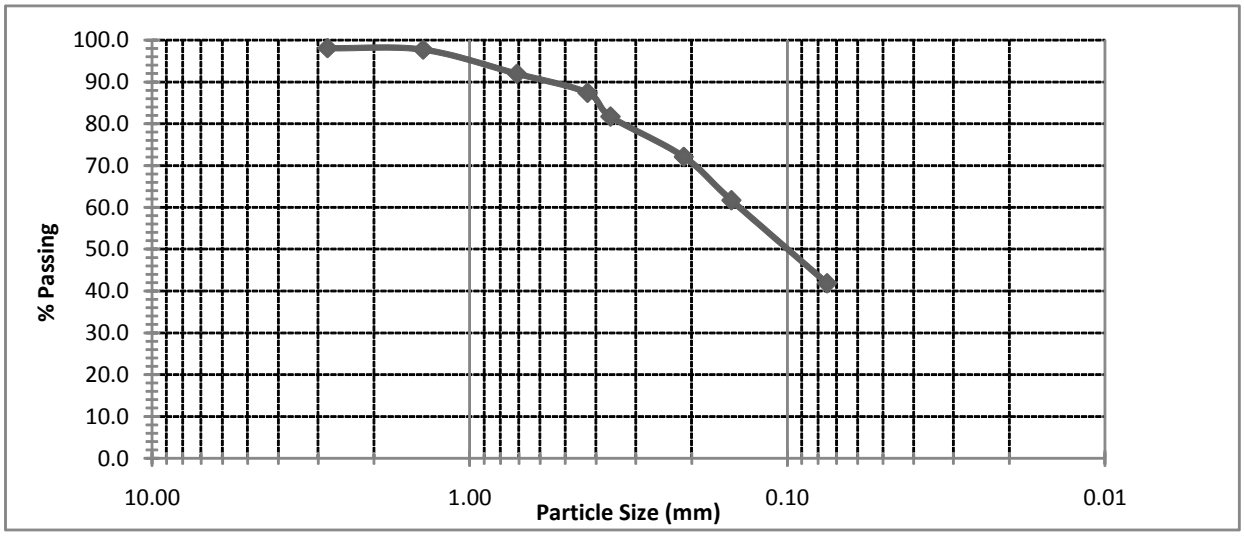
Boring No: OF 01 | **Test Number:** 1

Sample Depth: 12-24 inches | **Elevation:**

USCS Soil Classification:

AASHTO Soil Classification:

Sieve Number	Diameter (mm)	Mass of Sieve (g)	Mass of Sieve & Soil (g)	Soil Retained (g)	Soil Retained (%)	Soil Passing (%)
#7	2.80	512.38	516.18	3.8	1.9	98.1
#14	1.40	464.38	465.08	0.7	0.3	97.8
#25	0.71	411.99	423.49	11.5	5.8	92.0
#36	0.43	368.57	377.77	9.2	4.6	87.4
#52	0.36	528.66	540.06	11.4	5.7	81.7
#72	0.21	340.89	359.99	19.1	9.6	72.2
#100	0.15	347.23	368.13	20.9	10.5	61.7
#200	0.075	378.07	417.77	39.7	19.9	41.9
Pan	0	374.07	457.77	83.7	41.9	0.0
			TOTAL:	**200**	**100.0**	



Grain Size Distribution Curve Results:

% Gravel:	0.00	**D_{10}:**	0.025	**C_u:**	5.60
% Sand:	58.15	**D_{30}:**	0.055	**C_c:**	0.86
% Fines:	41.85	**D_{60}:**	0.14		

Sieve Analysis Data Sheet

ASTM D422-63(2007)

Project Name: PhD Research | **Tested By:** M.I. Alfa | **Date:** 18/5/2016

Location: Oforachi | **Checked By:** D.B. Adie | **Date:** 30/5/2016

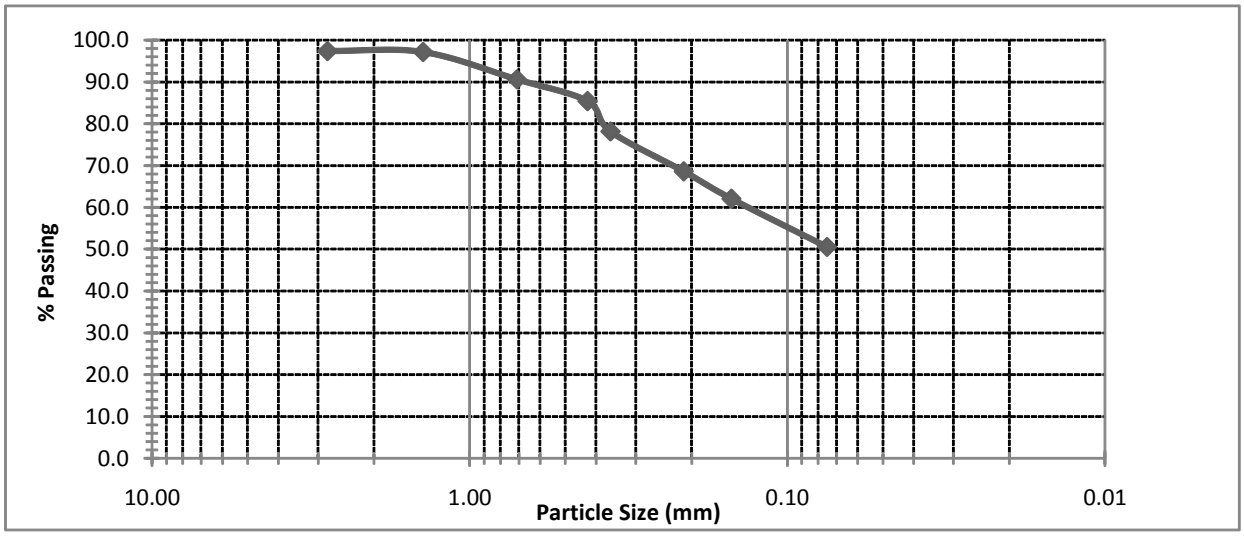
Boring No: OF 02 | **Test Number:** 1

Sample Depth: 12-24 inches | **Elevation:**

USCS Soil Classification:

AASHTO Soil Classification:

Sieve Number	Diameter (mm)	Mass of Sieve (g)	Mass of Sieve & Soil (g)	Soil Retained (g)	Soil Retained (%)	Soil Passing (%)
#7	2.80	512.38	517.58	5.2	2.6	97.4
#14	1.40	464.38	464.88	0.5	0.3	97.2
#25	0.71	411.99	424.99	13.0	6.5	90.7
#36	0.43	368.57	379.07	10.5	5.3	85.4
#52	0.36	528.66	543.06	14.4	7.2	78.2
#72	0.21	340.89	360.09	19.2	9.6	68.6
#100	0.15	347.23	360.33	13.1	6.6	62.1
#200	0.075	378.07	401.07	23.0	11.5	50.6
Pan		374.07	475.17	101.1	50.6	0.0
			TOTAL:	**200**	**100.0**	



Grain Size Distribution Curve Results:

% Gravel:	0.00	**D_{10}:**	0.0045	**C_u:**	31.11
% Sand:	49.45	**D_{30}:**	0.026	**C_c:**	1.07
% Fines:	50.55	**D_{60}:**	0.14		

Sieve Analysis Data Sheet

ASTM D422-63(2007)

Project Name: PhD Research | **Tested By:** M.I. Alfa | **Date:** 18/5/2016

Location: Oforachi | **Checked By:** D.B. Adie | **Date:** 30/5/2016

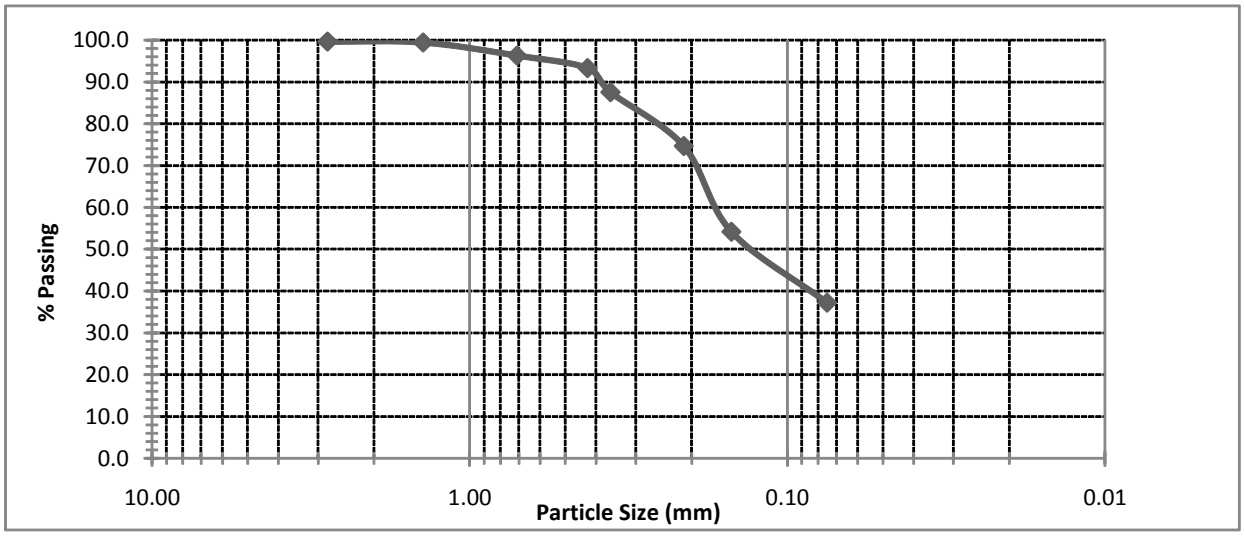
Boring No: OF 03 | **Test Number:** 1

Sample Depth: 12-24 inches | **Elevation:**

USCS Soil Classification:

AASHTO Soil Classification:

Sieve Number	Diameter (mm)	Mass of Sieve (g)	Mass of Sieve & Soil (g)	Soil Retained (g)	Soil Retained (%)	Soil Passing (%)
#7	2.80	512.38	513.08	0.7	0.3	99.7
#14	1.40	464.38	464.78	0.4	0.2	99.5
#25	0.71	411.99	418.29	6.3	3.1	96.3
#36	0.43	368.57	374.57	6.0	3.0	93.3
#52	0.36	528.66	540.16	11.5	5.7	87.6
#72	0.21	340.89	366.69	25.8	12.9	74.7
#100	0.15	347.23	388.33	41.1	20.5	54.2
#200	0.075	378.07	411.97	33.9	16.9	37.3
Pan		374.07	448.77	74.7	37.3	0.0
			TOTAL:	**200.4**	**100.0**	



Grain Size Distribution Curve Results:

% Gravel:	0.00	**D_{10}:**	0.013	**C_u:**	13.08
% Sand:	62.72	**D_{30}:**	0.055	**C_c:**	1.37
% Fines:	37.28	**D_{60}:**	0.17		

Sieve Analysis Data Sheet

ASTM D422-63(2007)

Project Name: PhD Research | **Tested By:** M.I. Alfa | **Date:** 18/5/2016

Location: Oforachi | **Checked By:** D.B. Adie | **Date:** 30/5/2016

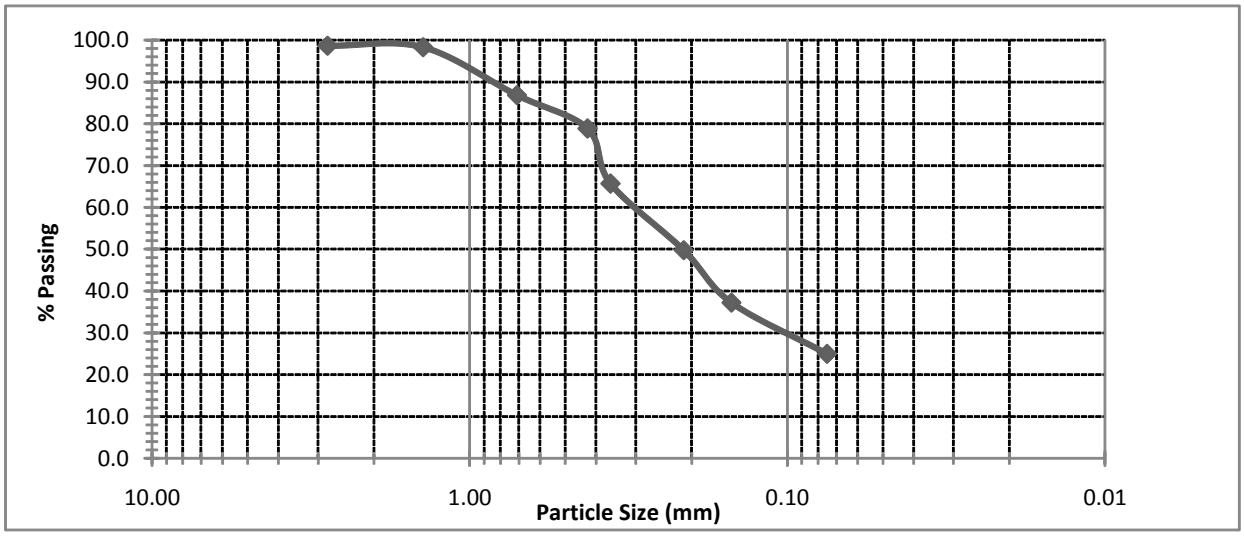
Boring No: OF 04 | **Test Number:** 1

Sample Depth: 12-24 inches | **Elevation:**

USCS Soil Classification: SP - Poorly Graded Sand

AASHTO Soil Classification: A-3 (Fine Sand)

Sieve Number	Diameter (mm)	Mass of Sieve (g)	Mass of Sieve & Soil (g)	Soil Retained (g)	Soil Retained (%)	Soil Passing (%)
#7	2.80	512.38	515.08	2.7	1.4	98.7
#14	1.40	464.38	465.08	0.7	0.3	98.3
#25	0.71	411.99	434.89	22.9	11.5	86.9
#36	0.43	368.57	384.57	16.0	8.0	78.9
#52	0.36	528.66	554.96	26.3	13.2	65.7
#72	0.21	340.89	372.69	31.8	15.9	49.8
#100	0.15	347.23	372.33	25.1	12.6	37.3
#200	0.075	378.07	402.57	24.5	12.3	25.0
Pan		374.07	424.07	50.0	25.0	0.0
			TOTAL:	**200**	**100.0**	



Grain Size Distribution Curve Results:

% Gravel:	0.00	**D_{10}:**	0.028	**C_u:**	11.07
% Sand:	75.00	**D_{30}:**	0.12	**C_c:**	1.66
% Fines:	25.00	**D_{60}:**	0.31		

Sieve Analysis Data Sheet

ASTM D422-63(2007)

Project Name: PhD Research | **Tested By:** M.I. Alfa | **Date:** 18/5/2016

Location: Oforachi | **Checked By:** D.B. Adie | **Date:** 30/5/2016

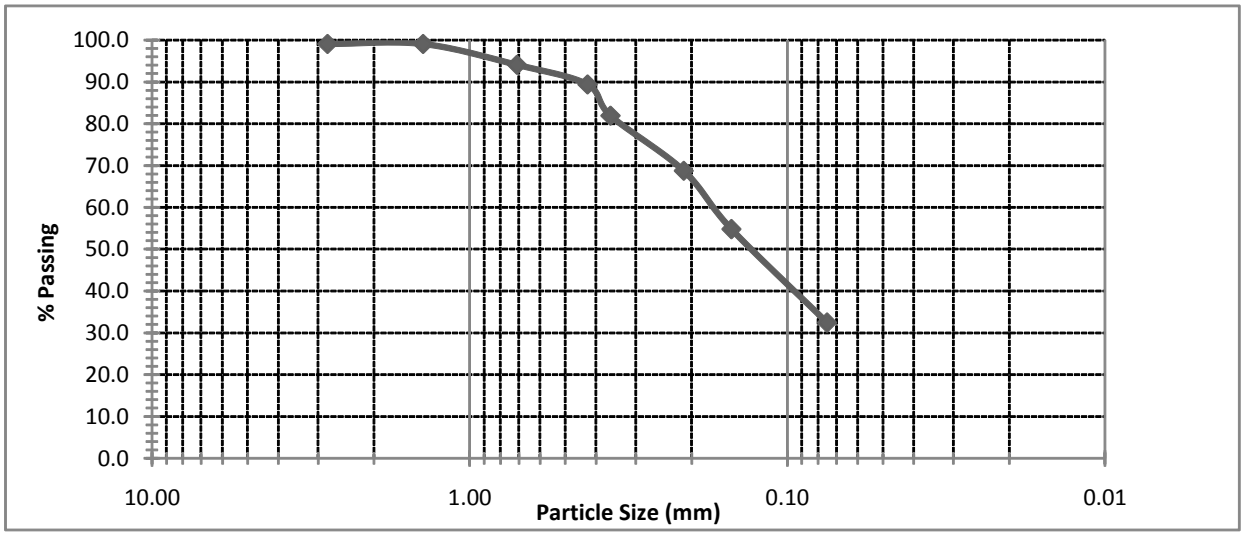
Boring No: OF 05 | **Test Number:** 1

Sample Depth: 12-24 inches | **Elevation:**

USCS Soil Classification:

AASHTO Soil Classification:

Sieve Number	Diameter (mm)	Mass of Sieve (g)	Mass of Sieve & Soil (g)	Soil Retained (g)	Soil Retained (%)	Soil Passing (%)
#7	2.80	512.38	514.18	1.8	0.9	99.1
#14	1.40	464.38	464.38	0.0	0.0	99.1
#25	0.71	411.99	421.99	10.0	5.0	94.1
#36	0.43	368.57	377.97	9.4	4.7	89.4
#52	0.36	528.66	543.56	14.9	7.4	82.0
#72	0.21	340.89	367.19	26.3	13.2	68.8
#100	0.15	347.23	375.23	28.0	14.0	54.8
#200	0.075	378.07	422.77	44.7	22.4	32.5
Pan		374.07	438.97	64.9	32.5	0.0
			TOTAL:	**200**	**100.0**	



Grain Size Distribution Curve Results:

% Gravel:	0.00	**D_{10}:**	0.037	**C_u:**	4.59
% Sand:	67.55	**D_{30}:**	0.07	**C_c:**	0.78
% Fines:	32.45	**D_{60}:**	0.17		

Sieve Analysis Data Sheet

ASTM D422-63(2007)

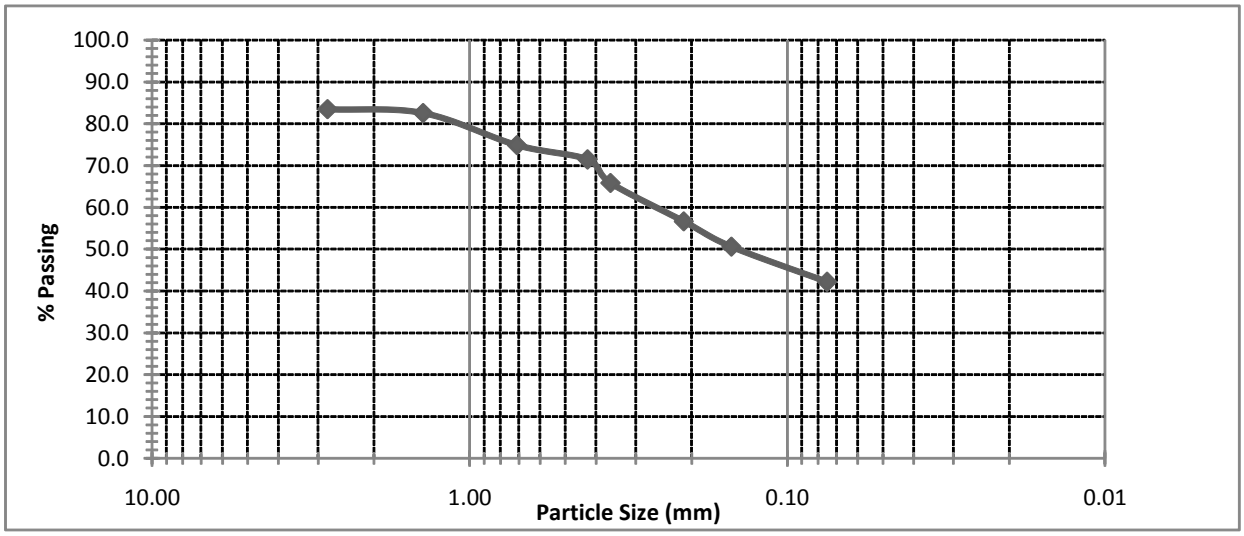
Project Name: PhD Research
Location: Oforachi
Boring No: OF 06
Sample Depth: 12-24 inches

Tested By: M.I. Alfa
Checked By: D.B. Adie
Test Number: 1
Elevation:

Date: 18/5/2016
Date: 30/5/2016

USCS Soil Classification:
AASHTO Soil Classification:

Sieve Number	Diameter (mm)	Mass of Sieve (g)	Mass of Sieve & Soil (g)	Soil Retained (g)	Soil Retained (%)	Soil Passing (%)
#7	2.80	512.38	545.38	33.0	16.5	83.5
#14	1.40	464.38	466.18	1.8	0.9	82.6
#25	0.71	411.99	427.39	15.4	7.7	74.9
#36	0.43	368.57	375.47	6.9	3.4	71.5
#52	0.36	528.66	539.86	11.2	5.6	65.9
#72	0.21	340.89	359.19	18.3	9.2	56.7
#100	0.15	347.23	359.33	12.1	6.1	50.7
#200	0.075	378.07	394.97	16.9	8.4	42.2
Pan		374.07	458.47	84.4	42.2	0.0
			TOTAL:	**200**	**100.0**	



Grain Size Distribution Curve Results:

% Gravel:	0.00	**D_{10}:**	0.002	**C_u:**	135.00
% Sand:	57.80	**D_{30}:**	0.038	**C_c:**	2.67
% Fines:	42.20	**D_{60}:**	0.27		

Sieve Analysis Data Sheet

ASTM D422-63(2007)

Project Name: PhD Research | **Tested By:** M.I. Alfa | **Date:** 18/5/2016

Location: Oforachi | **Checked By:** D.B. Adie | **Date:** 30/5/2016

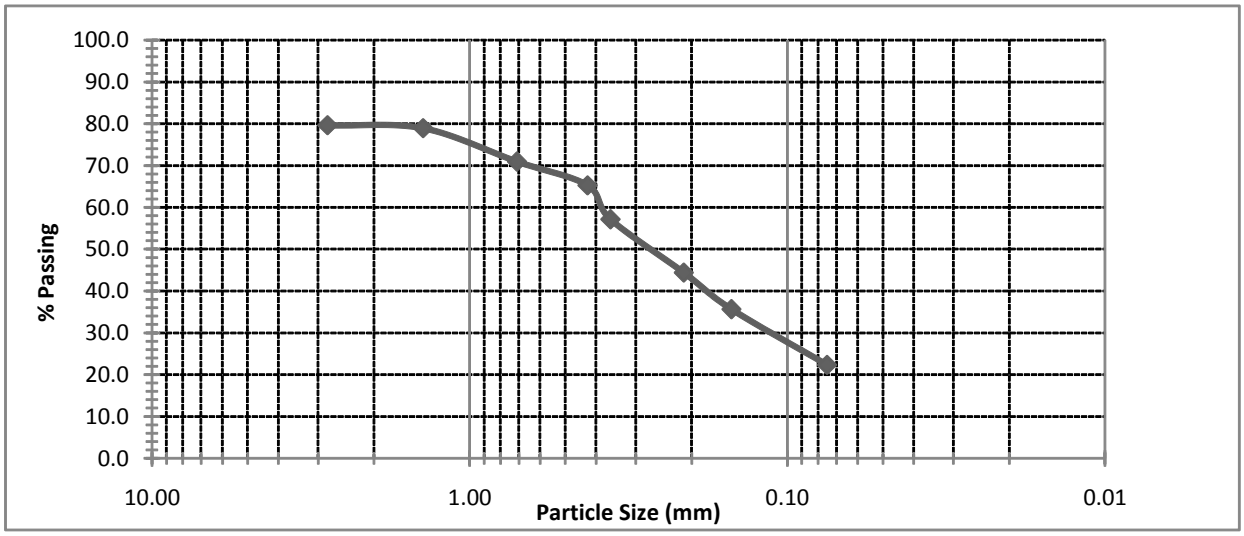
Boring No: OF 07 | **Test Number:** 1

Sample Depth: 12-24 inches | **Elevation:**

USCS Soil Classification: SP - Poorly Graded Sand

AASHTO Soil Classification: A-3 (Fine Sand)

Sieve Number	Diameter (mm)	Mass of Sieve (g)	Mass of Sieve & Soil (g)	Soil Retained (g)	Soil Retained (%)	Soil Passing (%)
#7	2.80	512.38	553.08	40.7	20.4	79.7
#14	1.40	464.38	465.78	1.4	0.7	79.0
#25	0.71	411.99	427.99	16.0	8.0	71.0
#36	0.43	368.57	379.87	11.3	5.7	65.3
#52	0.36	528.66	544.96	16.3	8.1	57.2
#72	0.21	340.89	366.29	25.4	12.7	44.5
#100	0.15	347.23	364.83	17.6	8.8	35.7
#200	0.075	378.07	404.57	26.5	13.3	22.4
Pan		374.07	418.87	44.8	22.4	0.0
			TOTAL:	**200**	**100.0**	



Grain Size Distribution Curve Results:

% Gravel:	0.00	**D_{10}:**	0.036	**C_u:**	8.06
% Sand:	77.60	**D_{30}:**	0.12	**C_c:**	1.38
% Fines:	22.40	**D_{60}:**	0.29		

Sieve Analysis Data Sheet

ASTM D422-63(2007)

Project Name: PhD Research | **Tested By:** M.I. Alfa | **Date:** 18/5/2016

Location: Oforachi | **Checked By:** D.B. Adie | **Date:** 30/5/2016

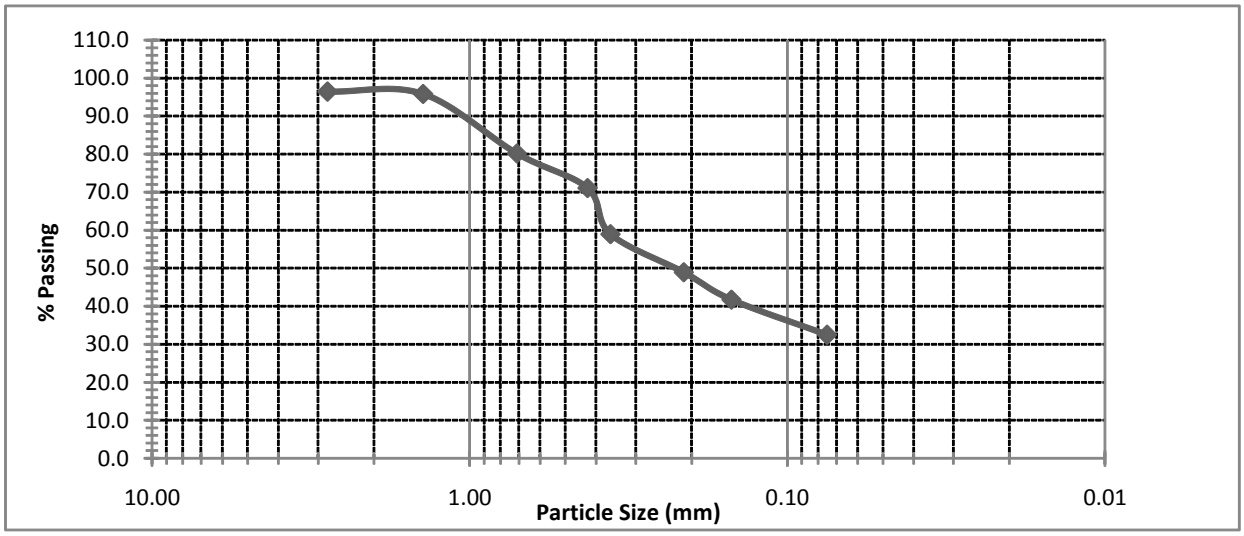
Boring No: OF 08 | **Test Number:** 1

Sample Depth: 12-24 inches | **Elevation:**

USCS Soil Classification:

AASHTO Soil Classification:

Sieve Number	Diameter (mm)	Mass of Sieve (g)	Mass of Sieve & Soil (g)	Soil Retained (g)	Soil Retained (%)	Soil Passing (%)
#7	2.80	512.38	519.48	7.1	3.6	96.5
#14	1.40	464.38	465.58	1.2	0.6	95.9
#25	0.71	411.99	443.29	31.3	15.7	80.2
#36	0.43	368.57	386.77	18.2	9.1	71.1
#52	0.36	528.66	552.86	24.2	12.1	59.0
#72	0.21	340.89	360.99	20.1	10.1	49.0
#100	0.15	347.23	361.63	14.4	7.2	41.8
#200	0.075	378.07	396.57	18.5	9.3	32.5
Pan		374.07	439.07	65.0	32.5	0.0
			TOTAL:	**200**	**100.0**	



Grain Size Distribution Curve Results:

% Gravel:	0.00	**D_{10}:**	0.015	**C_u:**	25.33
% Sand:	67.50	**D_{30}:**	0.06	**C_c:**	0.63
% Fines:	32.50	**D_{60}:**	0.38		

Sieve Analysis Data Sheet

ASTM D422-63(2007)

Project Name: PhD Research | **Tested By:** M.I. Alfa | **Date:** 18/5/2016

Location: Oforachi | **Checked By:** D.B. Adie | **Date:** 30/5/2016

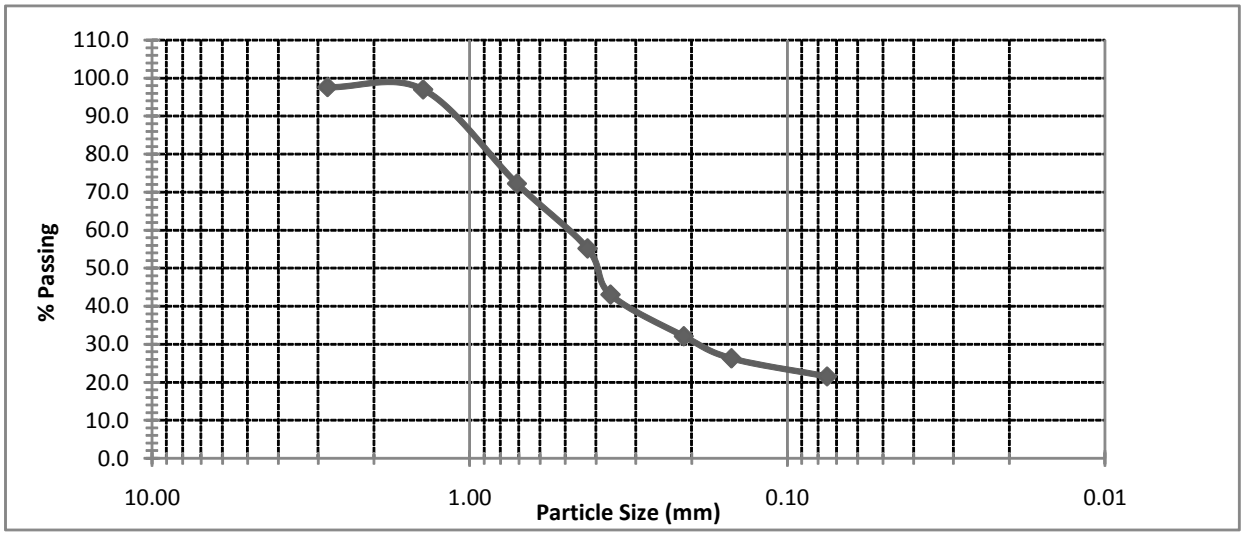
Boring No: OF 09 | **Test Number:** 1

Sample Depth: 12-24 inches | **Elevation:**

USCS Soil Classification:

AASHTO Soil Classification:

Sieve Number	Diameter (mm)	Mass of Sieve (g)	Mass of Sieve & Soil (g)	Soil Retained (g)	Soil Retained (%)	Soil Passing (%)
#7	2.80	512.38	517.08	4.7	2.4	97.7
#14	1.40	464.38	465.58	1.2	0.6	97.1
#25	0.71	411.99	461.49	49.5	24.8	72.3
#36	0.43	368.57	402.77	34.2	17.1	55.2
#52	0.36	528.66	552.96	24.3	12.2	43.1
#72	0.21	340.89	362.79	21.9	11.0	32.1
#100	0.15	347.23	358.83	11.6	5.8	26.3
#200	0.075	378.07	387.57	9.5	4.8	21.6
Pan		374.07	417.17	43.1	21.6	0.0
			TOTAL:	**200**	**100.0**	



Grain Size Distribution Curve Results:

% Gravel:	0.00	**D_{10}:**	0.011	**C_u:**	44.55
% Sand:	78.45	**D_{30}:**	0.2	**C_c:**	7.42
% Fines:	21.55	**D_{60}:**	0.49		

Sieve Analysis Data Sheet

ASTM D422-63(2007)

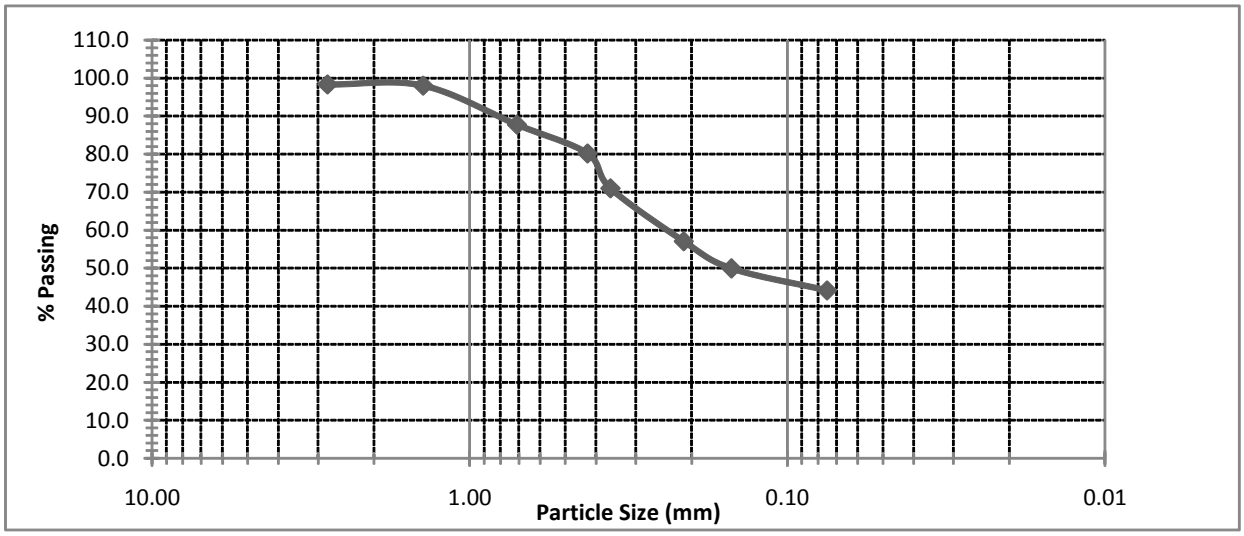
Project Name: PhD Research
Location: Oforachi
Boring No: OF 10
Sample Depth: 12-24 inches

Tested By: M.I. Alfa
Checked By: D.B. Adie
Test Number: 1
Elevation:

Date: 18/5/2016
Date: 30/5/2016

USCS Soil Classification:
AASHTO Soil Classification:

Sieve Number	Diameter (mm)	Mass of Sieve (g)	Mass of Sieve & Soil (g)	Soil Retained (g)	Soil Retained (%)	Soil Passing (%)
#7	2.80	512.38	515.68	3.3	1.6	98.4
#14	1.40	464.38	464.98	0.6	0.3	98.1
#25	0.71	411.99	432.49	20.5	10.3	87.8
#36	0.43	368.57	383.77	15.2	7.6	80.2
#52	0.36	528.66	546.96	18.3	9.1	71.1
#72	0.21	340.89	368.79	27.9	14.0	57.1
#100	0.15	347.23	361.53	14.3	7.2	50.0
#200	0.075	378.07	389.57	11.5	5.8	44.2
Pan		374.07	462.47	88.4	44.2	0.0
			TOTAL:	**200**	**100.0**	



Grain Size Distribution Curve Results:

% Gravel:	0.00	**D_{10}:**	0.0014	**C_u:**	171.43
% Sand:	55.80	**D_{30}:**	0.015	**C_c:**	0.67
% Fines:	44.20	**D_{60}:**	0.24		

Infiltration Test

Project Name: PhD Research
Location: Oforachi (Okobu)
Coordinate
Boring No: OF01
Initial Water level: 2.00 cm

Tested By: M.I. Alfa **Date:** 9/10/16
Checked By: D.B. Adie **Date:**
Test Number: 1
Soil Type
Start Time: 8:34 **End Time:** 12:34

S/No	Clock Reading	Time elapse (min)	Cum. Time (min)	Water level (cm)	Infiltration (cm)	Infiltration Rate		Cum. Infiltration (cm)	Infiltration (cm)	SSE
					Measured	(cm/min)	(cm/hr)		Calculated	
1	8:34	0	0	2.00	0.00		0.00		0	0
2	8:36	2	2	2.20	0.20	0.10	6.00	0.20	0.21037762	0.000108
3	8:39	3	5	2.20	0.20	0.07	4.00	0.40	0.31785096	0.013889
4	8:44	5	10	2.30	0.30	0.06	3.60	0.70	0.42594464	0.015862
5	8:54	10	20	2.50	0.50	0.05	3.00	1.20	0.55524767	0.003052
6	9:04	10	30	2.50	0.50	0.05	3.00	1.70	0.63574584	0.018427
7	9:19	15	45	2.70	0.70	0.05	2.80	2.40	0.71219012	0.000149
8	9:34	15	60	2.60	0.60	0.04	2.40	3.00	0.75769336	0.024867
9	10:04	30	90	3.10	1.10	0.04	2.20	4.10	0.79510837	0.092959
10	10:34	30	120	3.00	1.00	0.03	2.00	5.10	0.78876614	0.04462
11	11:04	30	150	2.90	0.90	0.03	1.80	6.00	0.75446062	0.021182
12	11:34	30	180	2.60	0.60	0.02	1.20	6.60	0.70029192	0.010058
13	12:04	30	210	2.50	0.50	0.02	1.00	7.10	0.63107186	0.01718
14	12:34	30	240	2.50	0.50	0.02	1.00	7.60	0.54993562	0.002494
						S	A			0.264846
						0.02067365	-0.00013409	K =	-0.0002011	cm/s
									-0.0120681	cm/min
									-2.011E-06	m/s

Infiltration Test

Project Name: PhD Research
Location: Oforachi (Okobu)
Coordinate
Boring No: OF02
Initial Water level: 2.00 cm

Tested By: M.I. Alfa **Date:** 9/10/16
Checked By: D.B. Adie **Date:**
Test Number: 1
Soil Type
Start Time: 12:40 **End Time:** 16:40

S/No	Clock Reading	Time elapse (min)	Cum. Time (min)	Water level (cm)	Infiltration (cm)	Infiltration Rate		Cum. Infiltration (cm)	Infiltration (cm)	SSE
					Measured	(cm/min)	(cm/hr)		Calculated	
1	12:40	0	0	2.00	0.00				0	0
2	12:42	2	2	2.20	0.20	0.10	6.00	0.20	0.253166922	0.002827
3	12:45	3	5	2.20	0.20	0.07	4.00	0.40	0.382954128	0.033472
4	12:50	5	10	2.20	0.20	0.04	2.40	0.60	0.513946018	0.098562
5	13:00	10	20	2.60	0.60	0.06	3.60	1.20	0.671563625	0.005121
6	13:10	10	30	2.50	0.50	0.05	3.00	1.70	0.770556418	0.073201
7	13:25	15	45	2.80	0.80	0.05	3.20	2.50	0.865828491	0.004333
8	13:40	15	60	2.70	0.70	0.05	2.80	3.20	0.923933922	0.050146
9	14:10	30	90	3.50	1.50	0.05	3.00	4.70	0.975770271	0.274817
10	14:40	30	120	3.40	1.40	0.05	2.80	6.10	0.975045052	0.180587
11	15:10	30	150	3.30	1.30	0.04	2.60	7.40	0.940730094	0.129075
12	15:40	30	180	2.60	0.60	0.02	1.20	8.00	0.882555306	0.079838
13	16:10	30	210	2.60	0.60	0.02	1.20	8.60	0.8063007	0.04256
14	16:40	30	240	2.60	0.60	0.02	1.20	9.20	0.715732276	0.013394
						S	A			0.987933
						0.02483336	-0.00015724	K =	-0.00023586	cm/s
									-0.01415169	cm/min
									-2.3586E-06	m/s

Infiltration Test

Project Name: PhD Research **Tested By:** M.I. Alfa **Date:** 10/10/16
Location: Oforachi **Checked By:** D.B. Adie **Date:**
Coordinate **Test Number:** 1
Boring No: OF03 **Soil Type**
Initial Water level: 2.00 cm **Start Time:** 8:30 **End Time:** 12:30

S/No	Clock Reading	Time elapse (min)	Cum. Time (min)	Water level (cm)	Infiltration (cm)	Infiltration Rate		Cum. Infiltration (cm)	Infiltration (cm)	SSE
					Measured	(cm/min)	(cm/hr)		Calculated	
1	8:30	0	0	2.00	0.00				0	0
2	8:32	2	2	2.30	0.30	0.15	9.00	0.30	0.3215404	0.000464
3	8:35	3	5	2.40	0.40	0.13	8.00	0.70	0.48413609	0.007079
4	8:40	5	10	2.70	0.70	0.14	8.40	1.40	0.64600037	0.002916
5	8:50	10	20	2.90	0.90	0.09	5.40	2.30	0.83623958	0.004065
6	9:00	10	30	2.90	0.90	0.09	5.40	3.20	0.95149483	0.002652
7	9:15	15	45	3.00	1.00	0.07	4.00	4.20	1.05631046	0.003171
8	9:30	15	60	2.90	0.90	0.06	3.60	5.10	1.11358817	0.04562
9	10:00	30	90	3.40	1.40	0.05	2.80	6.50	1.14580549	0.064615
10	10:30	30	120	3.20	1.20	0.04	2.40	7.70	1.11079403	0.007958
11	11:00	30	150	3.20	1.20	0.04	2.40	8.90	1.03281968	0.027949
12	11:30	30	180	2.60	0.60	0.02	1.20	9.50	0.92432747	0.105188
13	12:00	30	210	2.80	0.80	0.03	1.60	10.30	0.7927103	5.31E-05
14	12:30	30	240	2.70	0.70	0.02	1.40	11.00	0.64278507	0.003274
						S	A			0.275004
						0.03176306	-0.00022005	K =	-0.00033008	cm/s
									-0.01980489	cm/min
									-3.3008E-06	m/s

Infiltration Test

Project Name: PhD Research **Tested By:** M.I. Alfa **Date:** 10/10/16
Location: Oforachi **Checked By:** D.B. Adie **Date:**
Coordinate **Test Number:** 1
Boring No: OF04 **Soil Type**
Initial Water level: 2.00 cm **Start Time:** 12:40 **End Time:** 16:40

S/No	Clock Reading	Time elapse (min)	Cum. Time (min)	Water level (cm)	Infiltration (cm)	Infiltration Rate		Cum. Infiltration (cm)	Infiltration (cm)	SSE
					Measured	(cm/min)	(cm/hr)		Calculated	
1	12:40	0	0	2.00	0.00				0	0
2	12:42	2	2	2.40	0.40	0.20	12.00	0.40	0.35845111	0.001726
3	12:45	3	5	2.40	0.40	0.13	8.00	0.80	0.54080702	0.019827
4	12:50	5	10	2.60	0.60	0.12	7.20	1.40	0.72345166	0.01524
5	13:00	10	20	3.10	1.10	0.11	6.60	2.50	0.9403852	0.025477
6	13:10	10	30	3.00	1.00	0.10	6.00	3.50	1.07398403	0.005474
7	13:25	15	45	3.40	1.40	0.09	5.60	4.90	1.19873453	0.040508
8	13:40	15	60	3.30	1.30	0.09	5.20	6.20	1.27065295	0.000861
9	14:10	30	90	3.40	1.40	0.05	2.80	7.60	1.3229819	0.005932
10	14:40	30	120	3.20	1.20	0.04	2.40	8.80	1.30059498	0.010119
11	15:10	30	150	3.10	1.10	0.04	2.20	9.90	1.2304605	0.01702
12	15:40	30	180	3.00	1.00	0.03	2.00	10.90	1.12640946	0.015979
13	16:10	30	210	3.00	1.00	0.03	2.00	11.90	0.99665809	1.12E-05
14	16:40	30	240	3.00	1.00	0.03	2.00	12.90	0.84655974	0.023544
						S	A			0.181718
						0.03530043	-0.00023538	K =	-0.0003531	cm/s
									-0.0211843	cm/min
									-3.531E-06	m/s

Infiltration Test

Project Name: PhD Research
Location: Oforachi
Coordinate
Boring No: OF05
Initial Water level: 2.00 cm

Tested By: M.I. Alfa **Date:** 11/10/16
Checked By: D.B. Adie **Date:**
Test Number: 1
Soil Type
Start Time: 8:35 **End Time:** 12:35

S/No	Clock Reading	Time elapse (min)	Cum. Time (min)	Water level (cm)	Infiltration (cm)	Infiltration Rate		Cum. Infiltration (cm)	Infiltration (cm)	SSE
					Measured	(cm/min)	(cm/hr)		Calculated	
1	8:35	0	0	2.00	0.00				0	0
2	8:37	2	2	2.20	0.20	0.10	6.00	0.20	0.07372925	0.015944
3	8:40	3	5	2.20	0.20	0.07	4.00	0.40	0.12149254	0.006163
4	8:45	5	10	2.30	0.30	0.06	3.60	0.70	0.17965203	0.014484
5	8:55	10	20	2.10	0.10	0.01	0.60	0.80	0.26973759	0.028811
6	9:05	10	30	2.20	0.20	0.02	1.20	1.00	0.34508726	0.02105
7	9:20	15	45	2.50	0.50	0.03	2.00	1.50	0.44473515	0.003054
8	9:35	15	60	2.60	0.60	0.04	2.40	2.10	0.53504085	0.00422
9	10:04	30	90	2.50	0.50	0.02	1.00	2.60	0.69947113	0.039789
10	10:35	30	120	2.90	0.90	0.03	1.80	3.50	0.85068957	0.002432
11	11:05	30	150	3.20	1.20	0.04	2.40	4.70	0.99346491	0.042657
12	11:35	30	180	3.10	1.10	0.04	2.20	5.80	1.13024286	0.000915
13	12:05	30	210	3.30	1.30	0.04	2.60	7.10	1.26247629	0.001408
14	12:35	30	240	3.30	1.30	0.04	2.60	8.40	1.3911118	0.008301
						S	A			0.189227
						0.0062421	4.45875E-05	K =	6.6881E-05	cm/s
									0.00401288	cm/min
									6.6881E-07	m/s

Infiltration Test

Project Name: PhD Research
Location: Oforachi
Coordinate
Boring No: OF06
Initial Water level: 2.00 cm

Tested By: M.I. Alfa **Date:** 11/10/16
Checked By: D.B. Adie **Date:**
Test Number: 1
Soil Type
Start Time: 12:40 **End Time:** 16:40

S/No	Clock Reading	Time elapse (min)	Cum. Time (min)	Water level (cm)	Infiltration (cm)	Infiltration Rate		Cum. Infiltration (cm)	Infiltration (cm)	SSE
					Measured	(cm/min)	(cm/hr)		Calculated	
1	12:40	0	0	2.00	0.00				0	0
2	12:42	2	2	2.30	0.30	0.15	9.00	0.30	0.14749347	0.023258
3	12:45	3	5	2.30	0.30	0.10	6.00	0.60	0.22233835	0.006031
4	12:50	5	10	2.40	0.40	0.08	4.80	1.00	0.29711059	0.010586
5	13:00	10	20	2.60	0.60	0.06	3.60	1.60	0.38553118	0.045997
6	13:10	10	30	2.50	0.50	0.05	3.00	2.10	0.43961712	0.003646
7	13:25	15	45	2.40	0.40	0.03	1.60	2.50	0.48957849	0.008024
8	13:40	15	60	2.30	0.30	0.02	1.20	2.80	0.51777256	0.047425
9	14:10	30	90	2.40	0.40	0.01	0.80	3.20	0.53645864	0.018621
10	14:40	30	120	2.60	0.60	0.02	1.20	3.80	0.52436112	0.005721
11	15:10	30	150	2.50	0.50	0.02	1.00	4.30	0.49259117	5.49E-05
12	15:40	30	180	2.40	0.40	0.01	0.80	4.70	0.44684729	0.002195
13	16:10	30	210	2.40	0.40	0.01	0.80	5.10	0.39051465	9E-05
14	16:40	30	240	2.40	0.40	0.01	0.80	5.50	0.32579887	0.005506
						S	A			0.177156
						0.01454409	-9.8576E-05	K =	-0.00014786	cm/s
									-0.00887183	cm/min
									-1.4786E-06	m/s

Infiltration Test

Project Name: PhD Research
Location: Oforachi
Coordinate
Boring No: OF07
Initial Water level: 2.00 cm

Tested By: M.I. Alfa **Date:** 12/10/16
Checked By: D.B. Adie **Date:**
Test Number: 1
Soil Type
Start Time: 8:34 **End Time:** 12:34

S/No	Clock Reading	Time elapse (min)	Cum. Time (min)	Water level (cm)	Infiltration (cm)	Infiltration Rate		Cum. Infiltration (cm)	Infiltration (cm)	SSE
					Measured	(cm/min)	(cm/hr)		Calculated	
1	8:34	0	0	2.00	0.00				0	0
2	8:36	2	2	2.50	0.50	0.25	15.00	0.50	0.27896955	0.048854
3	8:39	3	5	2.50	0.50	0.17	10.00	1.00	0.42130677	0.006193
4	8:44	5	10	2.50	0.50	0.10	6.00	1.50	0.5642882	0.004133
5	8:54	10	20	2.80	0.80	0.08	4.80	2.30	0.73496494	0.00423
6	9:04	10	30	2.70	0.70	0.07	4.20	3.00	0.84088288	0.019848
7	9:19	15	45	2.80	0.80	0.05	3.20	3.80	0.94097451	0.019874
8	9:34	15	60	2.70	0.70	0.05	2.80	4.50	1.0000107	0.090006
9	10:04	30	90	3.20	1.20	0.04	2.40	5.70	1.046973	0.023417
10	10:34	30	120	3.30	1.30	0.04	2.60	7.00	1.03587415	0.069762
11	11:04	30	150	3.30	1.30	0.04	2.60	8.30	0.98767103	0.097549
12	11:34	30	180	2.70	0.70	0.02	1.40	9.00	0.9131116	0.045417
13	12:04	30	210	2.70	0.70	0.02	1.40	9.70	0.81858063	0.014061
14	12:34	30	240	2.70	0.70	0.02	1.40	10.40	0.70823818	6.79E-05
						S	A			0.443413
						0.02743171	-0.00017941	K =	-0.0002691	cm/s
									-0.0161473	cm/min
									-2.691E-06	m/s

Infiltration Test

Project Name: PhD Research
Location: Oforachi
Coordinate
Boring No: OF08
Initial Water level: 2.00 cm

Tested By: M.I. Alfa **Date:** 12/10/16
Checked By: D.B. Adie **Date:**
Test Number: 1
Soil Type
Start Time: 12:40 **End Time:** 16:40

S/No	Clock Reading	Time elapse (min)	Cum. Time (min)	Water level (cm)	Infiltration (cm)	Infiltration Rate		Cum. Infiltration (cm)	Infiltration (cm)	SSE
					Measured	(cm/min)	(cm/hr)		Calculated	
1	12:40	0	0	2.00	0.00				0	0
2	12:42	2	2	2.20	0.20	0.10	6.00	0.20	0.231799083	0.001011
3	12:45	3	5	2.20	0.20	0.07	4.00	0.40	0.350577561	0.022674
4	12:50	5	10	2.30	0.30	0.06	3.60	0.70	0.470404207	0.029038
5	13:00	10	20	2.50	0.50	0.05	3.00	1.20	0.614477339	0.013105
6	13:10	10	30	2.50	0.50	0.05	3.00	1.70	0.704860961	0.041968
7	13:25	15	45	2.80	0.80	0.05	3.20	2.50	0.791699333	6.89E-05
8	13:40	15	60	2.70	0.70	0.05	2.80	3.20	0.84449992	0.02088
9	14:10	30	90	3.30	1.30	0.04	2.60	4.50	0.891145919	0.167162
10	14:40	30	120	3.20	1.20	0.04	2.40	5.70	0.88965522	0.096314
11	15:10	30	150	3.00	1.00	0.03	2.00	6.70	0.857402518	0.020334
12	15:40	30	180	2.60	0.60	0.02	1.20	7.30	0.803298614	0.04133
13	16:10	30	210	2.60	0.60	0.02	1.20	7.90	0.732636934	0.017593
14	16:40	30	240	2.60	0.60	0.02	1.20	8.50	0.648866437	0.002388
						S	A			0.473865
						0.02274278	-0.00014446	K =	-0.000216694	cm/s
									-0.013001668	cm/min
									-2.16694E-06	m/s

Infiltration Test

Project Name: PhD Research
Location: Oforachi
Coordinate
Boring No: OF09
Initial Water level: 2.00 cm

Tested By: M.I. Alfa **Date:** 13/10/16
Checked By: D.B. Adie **Date:**
Test Number: 1
Soil Type
Start Time: 8:34 **End Time:** 12:34

S/No	Clock Reading	Time elapse (min)	Cum. Time (min)	Water level (cm)	Infiltration (cm)	Infiltration Rate		Cum. Infiltration (cm)	Infiltration (cm)	SSE
					Measured	(cm/min)	(cm/hr)		Calculated	
1	8:34	0	0	2.00	0.00				0	0
2	8:36	2	2	2.30	0.30	0.15	9.00	0.30	0.21739108	0.006824
3	8:39	3	5	2.30	0.30	0.10	6.00	0.60	0.33015841	0.00091
4	8:44	5	10	2.50	0.50	0.10	6.00	1.10	0.44529154	0.002993
5	8:54	10	20	2.70	0.70	0.07	4.20	1.80	0.58649141	0.012884
6	9:04	10	30	2.60	0.60	0.06	3.60	2.40	0.6776607	0.006031
7	9:19	15	45	2.70	0.70	0.05	2.80	3.10	0.768999	0.004761
8	9:34	15	60	2.60	0.60	0.04	2.40	3.70	0.82861918	0.052267
9	10:04	30	90	3.10	1.10	0.04	2.20	4.80	0.89292215	0.042881
10	10:34	30	120	3.00	1.00	0.03	2.00	5.80	0.91236893	0.007679
11	11:04	30	150	2.90	0.90	0.03	1.80	6.70	0.90315013	9.92E-06
12	11:34	30	180	2.80	0.80	0.03	1.60	7.50	0.87356929	0.005412
13	12:04	30	210	2.80	0.80	0.03	1.60	8.30	0.82855907	0.000816
14	12:34	30	240	2.80	0.80	0.03	1.60	9.10	0.77133341	0.000822
						S	A			0.14429
						0.02119286	-0.00012304	K =	-0.00018456	cm/s
									-0.01107381	cm/min
									-1.8456E-06	m/s

Infiltration Test

Project Name: PhD Research
Location: Oforachi
Coordinate
Boring No: OF10
Initial Water level: 2.00 cm

Tested By: M.I. Alfa **Date:**
Checked By: D.B. Adie **Date:**
Test Number: 1
Soil Type
Start Time: 12:40 **End Time:** 16:40

S/No	Clock Reading	Time elapse (min)	Cum. Time (min)	Water level (cm)	Infiltration (cm)	Infiltration Rate		Cum. Infiltration (cm)	Infiltration (cm)	SSE
					Measured	(cm/min)	(cm/hr)		Calculated	
1	12:40	0	0	2.00	0.00			0.00	0	0
2	12:42	2	2	2.30	0.30	0.15	9.00	0.30	0.26205261	0.00144
3	12:45	3	5	2.30	0.30	0.10	6.00	0.60	0.39523437	0.00907
4	12:50	5	10	2.40	0.40	0.08	4.80	1.00	0.52849307	0.01651
5	13:00	10	20	2.70	0.70	0.07	4.20	1.70	0.68649661	0.000182
6	13:10	10	30	2.60	0.60	0.06	3.60	2.30	0.78354547	0.033689
7	13:25	15	45	2.80	0.80	0.05	3.20	3.10	0.87378671	0.005444
8	13:40	15	60	2.70	0.70	0.05	2.80	3.80	0.92538424	0.050798
9	14:10	30	90	3.40	1.40	0.05	2.80	5.20	0.96164643	0.192154
10	14:40	30	120	3.30	1.30	0.04	2.60	6.50	0.94325816	0.127265
11	15:10	30	150	2.80	0.80	0.03	1.60	7.30	0.88994524	0.00809
12	15:40	30	180	2.70	0.70	0.02	1.40	8.00	0.81182425	0.012505
13	16:10	30	210	2.60	0.60	0.02	1.20	8.60	0.71490492	0.013203
14	16:40	30	240	2.60	0.60	0.02	1.20	9.20	0.60310292	9.63E-06
						S	A			0.47036
						0.02582028	-0.00017329	K =	-0.00025993	cm/s
									-0.01559582	cm/min
									-2.5993E-06	m/s

Moisture Contents

Project Name:	PhD Research	**Tested By:**	M.I. Alfa	**Date:**	09-10-16
Location:	Oforachi	**Checked By:**	D.B. Adie	**Date:**	
Boring No:	OF 01	**Depth**	12-24 inches		
Coordinate		**Elevation:**			

Sample No.	Can No.	Mass of Can (g)	Mass of Can + Wet Soil (g)	Mass of Can + Dry Soil (g)	Mass of Dry Soil (g)	Mass of Water (g)	Moisture Content (%)	Average Moisture Content (%)
1	OF01	8.30	42.11	33.30	25.00	8.81	35.24	**34.19**
2	OF02	9.30	44.58	35.80	26.50	8.78	33.13	

Moisture Contents

Project Name:	PhD Research	**Tested By:**	M.I. Alfa	**Date:**	09-10-16
Location:	Oforachi	**Checked By:**	D.B. Adie	**Date:**	
Boring No:	OF 02	**Depth**	12-24 inches		
Coordinate		**Elevation:**			

Sample No.	Can No.	Mass of Can (g)	Mass of Can + Wet Soil (g)	Mass of Can + Dry Soil (g)	Mass of Dry Soil (g)	Mass of Water (g)	Moisture Content (%)	Average Moisture Content (%)
1	OF03	8.90	39.40	32.45	23.55	6.95	29.51	**29.66**
2	OF04	9.10	44.80	36.60	27.50	8.20	29.82	

Moisture Contents

Project Name:	PhD Research	**Tested By:**	M.I. Alfa	**Date:**	10-10-16
Location:	Oforachi	**Checked By:**	D.B. Adie	**Date:**	
Boring No:	OF 03	**Depth**	12-24 inches		
Coordinate		**Elevation:**			

Sample No.	Can No.	Mass of Can (g)	Mass of Can + Wet Soil (g)	Mass of Can + Dry Soil (g)	Mass of Dry Soil (g)	Mass of Water (g)	Moisture Content (%)	Average Moisture Content (%)
1	OF05	8.50	37.80	32.45	23.95	5.35	22.34	**22.51**
2	OF06	9.10	44.80	38.20	29.10	6.60	22.68	

Moisture Contents

Project Name:	PhD Research	**Tested By:**	M.I. Alfa	**Date:**	10-10-16
Location:	Oforachi	**Checked By:**	D.B. Adie	**Date:**	
Boring No:	OF 04	**Depth**	12-24 inches		
Coordinate		**Elevation:**			

Sample No.	Can No.	Mass of Can (g)	Mass of Can + Wet Soil (g)	Mass of Can + Dry Soil (g)	Mass of Dry Soil (g)	Mass of Water (g)	Moisture Content (%)	Average Moisture Content (%)
1	OF07	9.00	39.00	34.10	25.10	4.90	19.52	**19.69**
2	OF08	9.00	41.00	35.70	26.70	5.30	19.85	

Moisture Contents

Project Name:	PhD Research	**Tested By:**	M.I. Alfa	**Date:**	11-10-16
Location:	Oforachi	**Checked By:**	D.B. Adie	**Date:**	
Boring No:	OF 05	**Depth**	12-24 inches		
Coordinate		**Elevation:**			

Sample No.	Can No.	Mass of Can (g)	Mass of Can + Wet Soil (g)	Mass of Can + Dry Soil (g)	Mass of Dry Soil (g)	Mass of Water (g)	Moisture Content (%)	Average Moisture Content (%)
1	OF09	8.60	52.30	39.70	31.10	12.60	40.51	**40.69**
2	OF10	9.00	45.20	34.70	25.70	10.50	40.86	

Moisture Contents

Project Name:	PhD Research	**Tested By:**	M.I. Alfa	**Date:**	11-10-16
Location:	Oforachi	**Checked By:**	D.B. Adie	**Date:**	
Boring No:	OF 06	**Depth**	12-24 inches		
Coordinate		**Elevation:**			

Sample No.	Can No.	Mass of Can (g)	Mass of Can + Wet Soil (g)	Mass of Can + Dry Soil (g)	Mass of Dry Soil (g)	Mass of Water (g)	Moisture Content (%)	Average Moisture Content (%)
1	OF11	9.10	35.20	27.40	18.30	7.80	42.62	**42.48**
2	OF12	9.30	28.80	23.00	13.70	5.80	42.34	

Moisture Contents

Project Name:	PhD Research	**Tested By:**	M.I. Alfa	**Date:**	12-10-16
Location:	Oforachi	**Checked By:**	D.B. Adie	**Date:**	
Boring No:	OF 07	**Depth**	12-24 inches		
Coordinate		**Elevation:**			

Sample No.	Can No.	Mass of Can (g)	Mass of Can + Wet Soil (g)	Mass of Can + Dry Soil (g)	Mass of Dry Soil (g)	Mass of Water (g)	Moisture Content (%)	Average Moisture Content (%)
1	OF13	9.00	38.40	32.75	23.75	5.65	23.79	**23.85**
2	OF14	8.80	34.20	29.30	20.50	4.90	23.90	

Moisture Contents

Project Name:	PhD Research	**Tested By:**	M.I. Alfa	**Date:**	12-10-16
Location:	Oforachi	**Checked By:**	D.B. Adie	**Date:**	
Boring No:	OF 08	**Depth**	12-24 inches		
Coordinate		**Elevation:**			

Sample No.	Can No.	Mass of Can (g)	Mass of Can + Wet Soil (g)	Mass of Can + Dry Soil (g)	Mass of Dry Soil (g)	Mass of Water (g)	Moisture Content (%)	Average Moisture Content (%)
1	OF15	9.10	40.40	32.90	23.80	7.50	31.51	**31.61**
2	OF16	9.00	43.90	35.50	26.50	8.40	31.70	

Moisture Contents

Project Name:	PhD Research	**Tested By:**	M.I. Alfa	**Date:**	13-10-16
Location:	Oforachi	**Checked By:**	D.B. Adie	**Date:**	
Boring No:	OF 09	**Depth**	12-24 inches		
Coordinate		**Elevation:**			

Sample No.	Can No.	Mass of Can (g)	Mass of Can + Wet Soil (g)	Mass of Can + Dry Soil (g)	Mass of Dry Soil (g)	Mass of Water (g)	Moisture Content (%)	Average Moisture Content (%)
1	OF17	8.90	44.00	36.20	27.30	7.80	28.57	**28.80**
2	OF18	8.40	44.01	36.00	27.60	8.01	29.02	

Moisture Contents

Project Name:	PhD Research	**Tested By:**	M.I. Alfa	**Date:**	13-10-16
Location:	Oforachi	**Checked By:**	D.B. Adie	**Date:**	30/5/2016
Boring No:	OF 10	**Depth**	12-24 inches		
Coordinate		**Elevation:**			

Sample No.	Can No.	Mass of Can (g)	Mass of Can + Wet Soil (g)	Mass of Can + Dry Soil (g)	Mass of Dry Soil (g)	Mass of Water (g)	Moisture Content (%)	Average Moisture Content (%)
1	OF19	9.20	39.50	32.90	23.70	6.60	27.85	**27.63**
2	OF20	8.90	44.70	37.00	28.10	7.70	27.40	

APPENDIX XIV: CURVE NUMBER ESTIMATION

Table XIVa: 1987 Curve Number Estimation for all HSGs by landcover type

Landcover	Area, A (km^2)	CN							
		A		B		C		D	
		CN	A*CN	CN	A*CN	CN	A*CN	CN	A*CN
Vegetation	711.23	33	23470.63	56	39828.95	70	49786.19	77	54764.81
Bare Surface/light Grassland	415.12	55.5	23039.29	70.5	29266.12	80	33209.78	84.5	35077.83
Built up Areas	478.15	77	36817.43	85	40642.61	90	43033.36	92	43989.65
Total	1604.50		83327.35		109737.69		126029.33		133832.30
		51.93		68.39		78.55		83.41	

Table XIVb: 1987 Composite Curve Number Estimation for Ofu River Catchment

SMU	FAOSOIL Symbol	Name	Textured Class	Area, A (km^2)	HSG	CN	A*CN
1021	Af13-1a	Ferric Acrisols	Sandy loam	975.61	A	51.93	50666.73
1567	Nd5-1a	Dystric Nitosols	Loam	259.77	B	68.39	17766.63
1193	G2-2/3a	Gleysols	Clay Loam	366.61	D	83.41	30579.41
677	Jd3-2a	Calcaric Fluvisols	Sandy Clay Loam	2.59	C	78.55	203.13
				1604.58			99215.90
Catchment Composite CN						61.83	

Table XIVc: 2001 Curve Number Estimation for all HSGs by landcover type

Landcover	Area, A (km^2)	CN							
		A		B		C		D	
		CN	A*CN	CN	A*CN	CN	A*CN	CN	A*CN
Vegetation	651.9942	33	21515.81	56	36511.68	70	45639.59	77	50203.55
Bare Surface/light Grassland	402.2163	55.5	22323.00	70.5	28356.25	80	32177.30	84.5	33987.28
Built up Areas	550.2915	77	42372.45	85	46774.78	90	49526.24	92	50626.82
Total	1604.50		86211.26		111642.70		127343.13		134817.65
		53.73		69.58		79.37		84.02	

Table XIVd: 2001 Composite Curve Number Estimation for Ofu River Catchment

SMU	FAOSOIL Symbol	Name	Textured Class	Area, A (km^2)	HSG	CN	A*CN
1021	Af13-1a	Ferric Acrisols	Sandy loam	975.61	A	53.73	52420.28
1567	Nd5-1a	Dystric Nitosols	Loam	259.77	B	69.58	18075.05
1193	G2-2/3a	Gleysols	Clay Loam	366.61	D	84.02	30804.55
677	Jd3-2a	Calcaric Fluvisols	Sandy Clay Loam	2.59	C	79.37	205.25
				1604.58			101505.13
Catchment Composite CN						63.26	

Table XIVe: 2016 Curve Number Estimation for all HSGs by landcover type

Landcover	Area, A (km^2)	CN							
		A		B		C		D	
		CN	A*CN	CN	A*CN	CN	A*CN	CN	A*CN
Vegetation	869.10	33	28680.28	56	48669.57	70	60836.96	77	66920.65
Bare Surface	122.84	76	9335.92	85	10441.49	90	11055.69	92	11301.37
Built up Areas	612.56	77	47167.24	85	52067.74	90	55130.54	92	56355.67
Total	1604.50		85183.44		111178.79		127023.19		134577.69
		53.09		69.29		79.17		83.88	

Table XIVf: 2016 Composite Curve Number Estimation for Ofu River Catchment

SMU	FAOSOIL Symbol	Name	Textured Class	Area, A (km^2)	HSG	CN	A*CN
1021	Af13-1a	Ferric Acrisols	Sandy loam	975.61	A	53.09	51795.32
1567	Nd5-1a	Dystric Nitosols	Loam	259.77	B	69.29	17999.94
1193	G2-2/3a	Gleysols	Clay Loam	366.61	D	83.88	30749.73
677	Jd3-2a	Calcaric Fluvisols	Sandy Clay Loam	2.59	C	79.17	204.73
				1604.58			100749.72
Catchment Composite CN						62.79	

APPENDIX XV: SYNTHETIC STREAM FLOW RESULTS

Table XVa: Generated Synthetic Stream flow Data (1974-2016) for Ofu River at Oforachi Using T-F Model

Year	Discharge (m^3/s)												
	Jan	Feb	Mar	Apr	May	Jun	Jul	Aug	Sep	Oct	Nov	Dec	Total
1974	3.52	1.67	2.48	8.95	17.49	67.97	147.34	219.71	404.76	91.96	5.31	4.02	**975.18**
1975	4.00	1.61	1.79	17.47	22.41	139.80	66.09	231.15	499.89	178.00	6.89	13.69	**1182.78**
1976	6.00	3.79	3.48	15.20	3.79	15.26	235.06	448.35	492.03	132.09	11.62	11.57	**1378.25**
1977	1.23	1.13	1.33	9.27	8.36	20.49	101.93	431.06	361.53	118.68	3.17	2.96	**1061.14**
1978	5.77	2.35	0.77	7.87	27.19	22.77	124.40	261.70	417.86	61.09	3.80	4.61	**940.18**
1979	1.64	1.46	0.99	7.48	10.45	47.30	123.93	327.37	410.44	70.06	7.19	59.12	**1067.43**
1980	2.75	1.84	1.41	8.16	25.41	10.04	105.99	497.86	400.09	41.40	8.17	3.11	**1106.24**
1981	4.32	3.28	2.11	31.07	22.26	24.38	206.93	608.77	412.23	53.29	3.73	0.49	**1372.86**
1982	1.87	2.04	1.79	10.96	7.69	10.05	119.15	322.67	515.37	61.59	5.23	0.41	**1058.82**
1983	3.00	1.75	0.91	7.72	8.79	68.82	114.43	270.71	401.07	52.63	2.96	4.25	**937.05**
1984	1.51	1.02	0.61	4.82	11.01	29.32	158.14	411.07	487.26	26.07	12.13	4.59	**1147.55**
1985	1.93	1.93	1.30	14.42	18.28	20.30	119.24	383.46	311.44	39.87	3.17	2.82	**918.18**
1986	4.60	7.38	1.94	18.45	38.78	6.32	35.78	152.45	379.22	115.23	3.87	5.71	**769.72**
1987	1.46	1.48	1.02	6.85	21.33	39.04	93.51	271.39	565.70	93.03	7.18	8.50	**1110.48**
1988	11.16	10.52	8.78	34.58	9.27	30.15	95.43	255.65	404.74	70.70	4.41	1.44	**936.83**
1989	2.87	3.54	2.42	18.11	8.79	85.46	95.55	172.74	547.50	158.02	8.62	3.61	**1107.26**
1990	2.07	1.85	1.01	6.16	18.69	19.52	153.90	395.98	452.89	102.77	2.69	0.29	**1157.81**
1991	3.27	2.13	1.15	11.28	14.01	42.54	141.26	479.27	252.20	61.47	5.08	0.75	**1014.41**
1992	2.81	1.45	1.03	12.18	15.05	18.04	65.79	341.83	532.94	68.30	5.72	9.30	**1074.44**
1993	2.92	3.76	1.82	9.81	5.94	80.59	87.39	217.27	418.78	71.02	3.48	3.27	**906.06**
1994	1.75	1.30	1.15	4.81	50.33	11.83	60.42	298.58	432.30	103.99	8.58	3.47	**978.49**
1995	1.27	1.52	1.04	21.61	10.59	84.86	167.93	492.14	253.44	78.74	5.04	2.26	**1120.43**
1996	5.80	3.37	1.58	16.79	23.71	79.01	173.95	438.12	410.56	71.28	3.74	1.93	**1229.83**
1997	2.61	2.64	1.95	7.70	18.96	29.11	127.68	599.68	371.62	54.74	4.55	10.04	**1231.28**
1998	5.32	4.43	3.24	11.29	34.07	9.34	125.82	330.96	323.78	109.53	5.45	3.85	**967.09**
1999	6.27	6.19	3.64	55.47	10.93	74.04	257.80	655.65	401.13	43.89	6.27	27.51	**1548.79**
2000	1.99	1.16	1.21	12.19	2.78	39.31	229.91	425.71	324.66	79.46	4.00	0.32	**1122.70**
2001	7.60	3.77	2.23	7.12	7.70	57.95	105.68	241.80	306.29	68.13	3.77	2.32	**814.36**
2002	3.14	2.33	0.90	24.47	19.05	57.05	112.87	426.17	381.45	62.64	4.22	1.71	**1096.01**
2003	2.55	1.82	0.93	15.37	4.18	58.78	132.86	368.30	512.82	49.27	7.87	1.36	**1156.11**
2004	1.03	1.13	0.38	2.31	24.24	88.09	158.18	486.72	419.72	89.34	5.89	1.47	**1278.51**
2005	2.08	7.29	5.47	30.82	6.66	14.84	168.75	463.22	500.85	98.36	4.73	4.30	**1307.38**
2006	5.41	3.73	2.73	8.15	9.19	46.53	236.08	559.08	392.66	46.29	4.40	0.10	**1314.35**
2007	4.24	3.87	4.46	28.95	4.06	18.93	111.09	325.71	387.24	31.00	4.01	12.22	**935.79**
2008	7.43	3.60	4.01	34.13	22.56	20.98	109.01	188.89	342.45	51.58	10.17	3.02	**797.84**
2009	3.52	4.12	5.74	38.76	10.90	20.43	139.12	342.47	463.08	24.78	2.60	2.94	**1058.46**
2010	1.76	1.29	0.92	7.84	12.49	11.47	52.20	200.84	244.62	32.94	5.52	0.45	**572.34**
2011	7.23	6.12	3.06	8.21	7.59	17.58	105.57	475.92	341.93	56.74	3.70	0.44	**1034.09**
2012	2.64	3.09	1.49	18.13	20.10	24.00	90.86	300.83	373.35	65.92	7.63	1.87	**909.92**
2013	1.60	0.94	0.99	10.73	10.72	26.80	183.42	388.83	434.75	64.49	1.91	0.79	**1125.97**
2014	1.83	3.41	1.48	16.13	7.41	45.02	134.09	367.03	496.89	130.32	5.47	0.90	**1209.98**
2015	2.76	1.64	1.51	17.36	14.09	67.81	179.61	696.47	396.83	42.28	1.63	0.89	**1422.88**
2016	8.43	3.72	2.98	16.73	9.99	16.01	92.87	313.17	737.07	279.86	4.75	6.61	**1492.18**
Average	3.65	2.99	2.12	15.72	15.29	39.95	131.33	374.11	416.68	79.14	5.36	5.47	**1091.80**

TableXVb: Adjusted Synthetic Stream flow Data (1974-2016) for Ofu River at Oforachi Using T-F Model

Year	Discharge (m^3/s)												
	Jan	Feb	Mar	Apr	May	Jun	Jul	Aug	Sep	Oct	Nov	Dec	Total
1974	3.55	3.28	1.84	13.30	19.07	36.56	135.26	370.79	443.72	76.42	5.98	3.89	**1113.67**
1975	3.24	3.31	2.16	13.55	21.65	9.98	135.96	372.80	440.47	63.72	5.95	3.39	**1076.17**
1976	1.92	2.28	1.36	13.48	11.88	56.08	134.51	411.02	440.73	70.50	5.86	3.50	**1153.12**
1977	5.04	3.54	2.38	13.31	14.28	54.14	135.65	407.98	445.20	72.48	6.03	3.95	**1163.96**
1978	2.07	2.96	2.64	13.27	24.17	53.30	135.46	378.17	443.27	80.98	6.01	3.86	**1146.18**
1979	4.77	3.38	2.54	13.26	15.37	44.22	135.46	389.73	443.52	79.66	5.95	1.03	**1138.90**
1980	4.05	3.21	2.34	13.28	23.23	58.01	135.61	419.73	443.88	83.89	5.93	3.94	**1197.10**
1981	3.02	2.52	2.01	13.93	21.58	52.70	134.75	439.25	443.46	82.13	6.02	4.08	**1205.45**
1982	4.63	3.11	2.16	13.36	13.93	58.01	135.50	388.90	439.94	80.91	5.98	4.08	**1150.50**
1983	3.89	3.25	2.58	13.27	14.50	36.25	135.54	379.76	443.84	82.23	6.03	3.88	**1125.02**
1984	4.86	3.59	2.72	13.19	15.67	50.87	135.17	404.46	440.90	86.15	5.84	3.86	**1167.29**
1985	4.59	3.16	2.39	13.46	19.49	54.21	135.50	399.60	446.91	84.11	6.03	3.96	**1173.40**
1986	2.84	0.58	2.09	13.57	30.25	59.39	136.22	358.95	444.59	72.99	6.01	3.81	**1131.29**
1987	4.89	3.38	2.53	13.24	21.09	47.27	135.72	379.88	438.22	76.26	5.95	3.66	**1132.09**
1988	0.00	0.00	0.00	14.03	14.76	50.57	135.70	377.11	443.72	79.56	6.00	4.03	**1125.48**
1989	3.97	2.40	1.86	13.57	14.51	30.09	135.70	362.52	438.84	66.67	5.92	3.91	**1079.95**
1990	4.50	3.20	2.53	13.23	19.70	54.50	135.20	401.80	442.07	74.83	6.04	4.09	**1161.68**
1991	3.71	3.07	2.46	13.37	17.25	45.98	135.31	416.46	448.93	80.93	5.99	4.06	**1177.52**
1992	4.01	3.39	2.52	13.40	17.79	55.05	135.96	392.27	439.34	79.92	5.97	3.62	**1153.23**
1993	3.94	2.29	2.15	13.33	13.01	31.89	135.77	370.36	443.24	79.52	6.02	3.93	**1105.45**
1994	4.71	3.46	2.46	13.19	36.32	57.35	136.01	384.66	442.78	74.65	5.92	3.92	**1165.41**
1995	5.02	3.35	2.52	13.66	15.45	30.31	135.08	418.72	448.89	78.38	5.99	3.99	**1161.37**
1996	2.06	2.48	2.26	13.53	22.34	32.48	135.03	409.22	443.52	79.48	6.02	4.00	**1152.41**
1997	4.14	2.83	2.09	13.27	19.84	50.95	135.43	437.65	444.85	81.92	6.00	3.58	**1202.54**
1998	2.37	1.98	1.48	13.37	27.78	58.27	135.44	390.36	446.49	73.83	5.98	3.90	**1161.24**
1999	1.75	1.14	1.29	14.63	15.62	34.32	134.31	447.50	443.84	83.52	5.96	2.67	**1186.56**
2000	4.55	3.52	2.43	13.40	11.35	47.17	134.55	407.04	446.46	78.27	6.01	4.09	**1158.83**
2001	0.88	2.29	1.95	13.25	13.93	40.27	135.62	374.67	447.08	79.94	6.01	3.98	**1119.89**
2002	3.80	2.97	2.58	13.75	19.89	40.61	135.56	407.11	444.51	80.75	6.01	4.01	**1161.55**
2003	4.18	3.22	2.57	13.49	12.08	39.97	135.38	396.93	440.02	82.73	5.93	4.03	**1140.53**
2004	5.17	3.54	2.83	13.12	22.62	29.12	135.17	417.77	443.21	76.81	5.97	4.03	**1159.34**
2005	4.49	0.62	0.43	13.93	13.38	56.23	135.08	413.64	440.43	75.48	6.00	3.88	**1163.58**
2006	2.31	2.31	1.72	13.28	14.71	44.50	134.50	430.50	444.13	83.17	6.00	4.10	**1181.23**
2007	3.08	2.24	0.90	13.87	12.02	54.72	135.57	389.44	444.32	85.42	6.01	3.47	**1151.06**
2008	0.99	2.37	1.12	14.02	21.73	53.96	135.59	365.36	445.85	82.39	5.88	3.95	**1133.20**
2009	3.55	2.12	0.30	14.15	15.61	54.16	135.33	392.39	441.72	86.34	6.04	3.95	**1155.67**
2010	4.70	3.46	2.57	13.27	16.44	57.48	136.08	367.47	449.19	85.14	5.98	4.08	**1145.86**
2011	1.12	1.18	1.56	13.28	13.87	55.22	135.62	415.87	445.87	81.62	6.02	4.08	**1175.31**
2012	4.13	2.61	2.30	13.57	20.44	52.84	135.74	385.06	444.79	80.27	5.94	4.01	**1151.70**
2013	4.80	3.63	2.54	13.36	15.51	51.81	134.95	400.54	442.69	80.48	6.05	4.06	**1160.43**
2014	4.65	2.46	2.31	13.51	13.78	45.06	135.37	396.71	440.57	70.76	5.98	4.06	**1135.22**
2015	4.04	3.30	2.29	13.54	17.29	36.62	134.98	454.68	443.99	83.76	6.06	4.06	**1204.61**
2016	0.33	2.31	1.60	13.53	15.13	55.80	135.73	387.23	432.36	48.68	5.99	3.76	**1102.45**
Average	3.50	2.68	2.03	13.50	17.91	46.94	135.40	397.95	443.31	78.32	5.98	3.82	**1151.34**

APPENDIX XVI: RESULTS OF NRCS-CN RAINFALL-RUNOFF MODELLING

Table XVI: Annual Daily Peak Runoff (m^3/s)

Year	P(mm)	P-Ia	$(P-Ia)^2$	(P-Ia)+S	Q (mm)	$Q(m^3s)$
1979	99.54	69.43	4820.45	219.96	21.92	1506.56
1980	99.48	69.37	4812.56	219.90	21.88	1504.49
1981	47.71	17.61	310.05	168.14	1.84	126.77
1982	79.52	49.41	2441.35	199.94	12.21	839.41
1983	98.72	68.62	4708.05	219.15	21.48	1476.90
1984	85.58	55.48	3077.79	206.01	14.94	1027.06
1985	116.65	86.55	7490.60	237.08	31.60	2172.04
1986	63.38	33.27	1107.11	183.80	6.02	414.08
1987	61.21	31.10	967.50	181.63	5.33	366.18
1988	74.92	44.81	2007.95	195.34	10.28	706.65
1989	70.75	40.64	1651.58	191.17	8.64	593.91
1990	82.81	52.70	2777.43	203.23	13.67	939.50
1991	95.19	65.09	4236.55	215.62	19.65	1350.73
1992	49.66	19.55	382.25	170.08	2.25	154.50
1993	92.64	62.53	3910.14	213.06	18.35	1261.63
1994	57.99	27.88	777.28	178.41	4.36	299.50
1995	95.78	65.68	4313.41	216.21	19.95	1371.50
1996	71.53	41.42	1715.79	191.95	8.94	614.49
1997	60.88	30.77	946.97	181.30	5.22	359.07
1998	76.42	46.31	2144.70	196.84	10.90	749.02
1999	89.18	59.08	3490.14	209.61	16.65	1144.67
2000	20.93	-9.18	84.27	141.35	0.00	0.00
2001	34.89	4.78	22.85	155.31	0.15	10.11
2002	90.84	60.73	3688.36	211.26	17.46	1200.20
2003	77.96	47.85	2289.64	198.38	11.54	793.44
2004	90.08	59.97	3596.32	210.50	17.08	1174.49
2005	40.31	10.21	104.15	160.74	0.65	44.54
2006	53.82	23.71	562.32	174.24	3.23	221.85
2007	95.90	65.79	4328.93	216.32	20.01	1375.68
2008	114.06	83.96	7048.68	234.49	30.06	2066.49
2009	107.51	77.40	5991.50	227.93	26.29	1807.04
2010	47.44	17.34	300.63	167.87	1.79	123.11
2011	51.50	21.40	457.91	171.93	2.66	183.09
2012	70.30	40.19	1615.37	190.72	8.47	582.26
2013	60.28	30.18	910.72	180.71	5.04	346.46

APPENDIX XVII: ESTIMATION OF RUNOFF COEFFICIENT

Slope Class	Area, A (km^2)	Runoff Coefficient (C)	A*C
<3%	850.31	0.05	42.52
3-10%	675.86	0.11	74.34
10-30%	60.18	0.20	12.04
>30%	17.96	0.30	5.39
	1604.31		134.28
C_s		0.08	

Name	Textured Class	Permeability	Area, A (km^2)	Runoff Coefficient (C)	A*C
Ferric Acrisols	Sandy loam	Permeable	975.61	0.10	97.56
Dystric Nitosols	Loam	Semi-permeable	259.77	0.20	51.95
Gleysols	Clay Loam	Semi-permeable	366.61	0.20	73.32
Calcaric Fluvisols	Sandy Clay Loam	Semi-permeable	2.59	0.20	0.52
			1604.58		223.35
C_p				0.14	

Landcover	Area	RC	A*RC
Vegetation	869.10	0.05	43.45
Bare Surface	122.84	0.15	18.43
Built up Areas	612.56	0.30	183.77
	1604.50		245.65
C_v		0.15	

APPENDIX XVIII: FLOOD FREQUENCY ANALYSIS RESULTS

Table XVIIIa: Flood Frequency Calculations using log-Pearson Type III Analysis

Rank	Year	Q_{max} (m^3/s)	logQ	(log Q -avg(logQ))^2	(log Q -avg(logQ))^3	Return Period, Tr = [(n+1)/m]	Exceedence Probability (1/Tr)
1	1964	723.30	2.859	0.045	0.009459	63.00	0.0159
2	1956	588.40	2.770	0.015	0.001809	31.50	0.0317
3	1958	578.70	2.762	0.013	0.001506	21.00	0.0476
4	1962	578.10	2.762	0.013	0.001488	15.75	0.0635
5	1961	555.10	2.744	0.009	0.000900	12.60	0.0794
6	1967	516.90	2.713	0.004	0.000282	10.50	0.0952
7	1970	498.10	2.697	0.002	0.000121	9.00	0.1111
8	1965	486.00	2.687	0.002	0.000058	7.88	0.1270
9	1971	482.00	2.683	0.001	0.000044	7.00	0.1429
10	1973	476.30	2.678	0.001	0.000027	6.30	0.1587
11	1969	457.30	2.660	0.000	0.000002	5.73	0.1746
12	2015	454.68	2.658	0.000	0.000001	5.25	0.1905
13	2010	449.19	2.652	0.000	0.000000	4.85	0.2063
14	1991	448.93	2.652	0.000	0.000000	4.50	0.2222
15	1995	448.89	2.652	0.000	0.000000	4.20	0.2381
16	1999	447.50	2.651	0.000	0.000000	3.94	0.2540
17	2001	447.08	2.650	0.000	0.000000	3.71	0.2698
18	1985	446.91	2.650	0.000	0.000000	3.50	0.2857
19	1998	446.49	2.650	0.000	0.000000	3.32	0.3016
20	2000	446.46	2.650	0.000	0.000000	3.15	0.3175
21	2011	445.87	2.649	0.000	0.000000	3.00	0.3333
22	2008	445.85	2.649	0.000	0.000000	2.86	0.3492
23	1977	445.20	2.649	0.000	0.000000	2.74	0.3651
24	1997	444.85	2.648	0.000	0.000000	2.63	0.3810
25	2012	444.79	2.648	0.000	0.000000	2.52	0.3968
26	1986	444.59	2.648	0.000	0.000000	2.42	0.4127
27	2002	444.51	2.648	0.000	0.000000	2.33	0.4286
28	2007	444.32	2.648	0.000	0.000000	2.25	0.4444
29	2006	444.13	2.648	0.000	0.000000	2.17	0.4603
30	1980	443.88	2.647	0.000	0.000000	2.10	0.4762
31	1983	443.84	2.647	0.000	0.000000	2.03	0.4921
32	1988	443.72	2.647	0.000	0.000000	1.97	0.5079
33	1974	443.72	2.647	0.000	0.000000	1.91	0.5238
34	1979	443.52	2.647	0.000	0.000000	1.85	0.5397
35	1996	443.52	2.647	0.000	0.000000	1.80	0.5556
36	1981	443.46	2.647	0.000	0.000000	1.75	0.5714
37	1978	443.27	2.647	0.000	0.000000	1.70	0.5873
38	1993	443.24	2.647	0.000	0.000000	1.66	0.6032
39	2004	443.21	2.647	0.000	0.000000	1.62	0.6190
40	1994	442.78	2.646	0.000	0.000000	1.58	0.6349
41	2013	442.69	2.646	0.000	0.000000	1.54	0.6508
42	1990	442.07	2.645	0.000	0.000000	1.50	0.6667
43	2009	441.72	2.645	0.000	0.000000	1.47	0.6825
44	1984	440.90	2.644	0.000	0.000000	1.43	0.6984
45	1976	440.73	2.644	0.000	0.000000	1.40	0.7143
46	2014	440.57	2.644	0.000	0.000000	1.37	0.7302
47	1975	440.47	2.644	0.000	0.000000	1.34	0.7460
48	2005	440.43	2.644	0.000	0.000000	1.31	0.7619
49	2003	440.02	2.643	0.000	0.000000	1.29	0.7778
50	1982	439.94	2.643	0.000	0.000000	1.26	0.7937
51	1992	439.34	2.643	0.000	0.000000	1.24	0.8095
52	1989	438.84	2.642	0.000	0.000000	1.21	0.8254
53	1987	438.22	2.642	0.000	0.000000	1.19	0.8413
54	1957	435.50	2.639	0.000	-0.000001	1.17	0.8571
55	2016	432.36	2.636	0.000	-0.000002	1.15	0.8730
56	1955	399.90	2.602	0.002	-0.000097	1.13	0.8889
57	1959	362.10	2.559	0.008	-0.000705	1.11	0.9048
58	1968	334.10	2.524	0.015	-0.001905	1.09	0.9206
59	1960	328.50	2.517	0.017	-0.002263	1.07	0.9365
60	1963	322.90	2.509	0.019	-0.002672	1.05	0.9524
61	1972	318.20	2.503	0.021	-0.003057	1.03	0.9683
62	1966	298.80	2.475	0.030	-0.005128	1.02	0.9841
	Sum	**27817**	**164.165**	**0.219**	**0.000**		
	Average	**449**	**2.648**	**0.004**	**-0.0000021**		

Table XVIIIb: Estimated Discharge Values using log-Pearson Type III Analysis

Variance	0.0036				
standard deviation	0.0599				
skew coefficient	-0.0104				
Tr	**K(-0.1)**	**K(0)**	**slope**	**K(-0.0104)**	**Q (m^3/s)**
2	0.017	0.000	-0.17	0.002	444.57
5	0.846	0.842	-0.04	0.842	499.23
10	1.270	1.282	0.12	1.281	530.35
25	1.716	1.751	0.35	1.747	565.61
50	2.000	2.054	0.54	2.048	589.59
100	2.252	2.326	0.74	2.318	611.96
200	2.482	2.576	0.94	2.566	633.25
1000	2.950	3.090	1.4	3.075	679.33

APPENDIX XIX: ESTIMATION OF FLOOD VULNERABLE POPULATION

Table XIXa: Population at Risk for 1995 and 2000 Flood Scenarios

State	LGA	Population (Persons)			Area (km^2)	Population density		Area inundated		Persons affected	
		1991	1995	2000		1995	2000	1995	2000	1995	2000
	Dekina	177513	196969	224313	2487.55	79.18	90.17	2.03	2.02	161	183
	Ofu	108095	125840	152172	1670.27	75.34	91.11	6.38	6.37	481	581
Kogi	Igalamela/Odolu							78.88	78.75	5245	6085
	Idah	224692	253340	294339	3809.91	66.49	77.26	0.00	0.00	0	0
	Ibaji							163.75	163.71	10889	12648
Enugu	Uzo-Uwani	127150	139962	157806	855.00	163.70	184.57	0.95	0.95	156	176
		637450	716109	828630	8822.73			251.98	251.80	16932	19673

Table XIXb: Population at Risk for 100-year and 200-year Return Periods

State	LGA	Population (Persons)			Area (km^2)	Population density (persons/km^2)		Area inundated (km^2)		Persons affected	
		2006	100 Years	200 Years	100 Years	200 Years	100 Years	200 Years	100 Years	200 Years	100 Years
	Dekina	260968	932993	12561575	2487.55	375.07	5049.78	2.21	2.23	828	11269
	Ofu	191480	1232480	55093299	1670.27	737.89	32984.67	6.97	7.04	5147	232184
Kogi	Igalamela/Odolu	147048	639546	12845631	2250.85	284.14	5707.01	91.93	92.37	26120	527132
	Idah	79755	346873	6967135	39.79	8717.60	175097.65	0.00	0.00	0	0
	Ibaji	127572	554841	11144272	1519.27	365.20	7335.28	164.78	164.78	60179	1208741
Enugu	Uzo-Uwani	127150	412142	4543112	855.00	482.04	5313.58	0.95	0.95	459	5051
		933973	4118875	103155024	8822.73			266.84	267.37	92733	1984377

Table XIXc: Age Distribution of Population for 1995 and 2000

State	LGA	Persons affected		Under 15 Years				Above 65 Years				15 - 65 Years			
				1995		2000		1995		2000		1995		2000	
		1995	2000	WD	ND	WD	ND	WD	ND	WD	ND	WD	ND	WD	ND
	Dekina	161	183	1	73	1	83	0	5	0	6	1	81	1	92
	Ofu	481	581	3	216	3	262	0	14	0	17	3	245	4	295
Kogi		5245	6085	36	2350	41	2727	2	144	3	166	41	2672	47	3101
	Idah	0	0	0	0	0	0	0	0	0	0	0	0	0	0
		10889	12648	70	4882	81	5671	4	298	5	346	79	5556	92	6453
Enugu	Uzo-Uwani	156	176	1	55	1	62	0	8	0	8	2	90	2	103
		16932	19673	110	7577	128	8804	7	468	8	543	126	8644	146	10044

***WD-With disability, ND-No disability**

Table XIXd: Age Distribution of Population for 100 years and 200 years Return Periods

State	LGA	Persons affected		Under 15 Years				Above 65 Years				15 - 65 Years			
				100 Years		200 Years		100 Years		200 Years		100 Years		200 Years	
		2055	2155	WD	ND	WD	ND	WD	ND	WD	ND	WD	ND	WD	ND
	Dekina	828	11269	6	371	75	5050	0	23	5	308	6	422	85	5746
	Ofu	5147	232184	29	2312	1329	104256	2	141	81	6353	34	2629	1512	118653
Kogi	Igalamela/Odolu	26120	527132	177	11701	3567	235144	11	713	218	14389	202	13316	4091	269723
	Idah	0	0	0	0	0	0	0	0	0	0	0	0	0	0
	Ibaji	60179	1208741	385	26982	7730	541940	23	1645	471	33024	438	30706	8797	616779
Enugu	Uzo-Uwani	459	5051	3	161	35	1763	0	21	4	223	5	269	59	2967
		92733	1984377	600	41527	12735	888154	37	2542	779	54297	685	47342	14545	1013867

***WD-With disability, ND-No disability**

Table XIXe: 1995 and 2000 Affected Population Distributed by Poverty Line

State	LGA	Persons affected		Poverty			
				1995		2000	
		1995	2000	In poverty	Above poverty	In poverty	Above poverty
	Dekina	161	183	118	43	134	49
	Ofu	481	581	353	128	426	155
Kogi	Igalamela/Odolu	5245	6085	3850	1395	4466	1619
	Idah	0	0	0	0	0	0
	Ibaji	10889	12648	7993	2896	9284	3364
Enugu	Uzo-Uwani	156	176	115	41	129	47
		16932	19673	12428	4504	14440	5233

Table XIXf: Affected Population Distributed by Poverty Line for 100-Years and 200-Years Return Periods

State	LGA	Persons affected		Poverty			
				100 Years		200 Years	
		100 Years	200 Years	In poverty	Above poverty	In poverty	Above poverty
	Dekina	828	11269	571	257	7776	3493
	Ofu	5147	232184	3551	1596	160207	71977
Kogi	Igalamela/Odolu	26120	527132	18023	8097	363721	163411
	Idah	0	0	0	0	0	0
	Ibaji	60179	1208741	41524	18655	834031	374710
Enugu	Uzo-Uwani	459	5051	317	142	3485	1566
		92733	1984377	63986	28747	1369220	615157

Table XIXg: 1995 and 2000 Affected Population Distributed by Gender

State	LGA	Persons affected		Gender			
				1995		2000	
		1995	2000	Male	Female	Male	Female
	Dekina	161	183	78	83	88	95
	Ofu	481	581	233	248	281	300
Kogi	Igalamela/Odolu	5245	6085	2539	2706	2946	3139
	Idah	0	0	0	0	0	0
	Ibaji	10889	12648	5272	5617	6123	6525
Enugu	Uzo-Uwani	156	176	74	82	84	92
		16932	19673	8195	8737	9522	10151

Table XIXh: Affected Population Distributed by Gender for 100-Years and 200-Years Return Periods

State	LGA	Persons affected		Gender			
		100 Years	200 Years	100 Years		200 Years	
				Male	Female	Male	Female
	Dekina	828	11269	417	411	5674	5595
	Ofu	5147	232184	2599	2548	117221	114963
Kogi	Igalamela/Odolu	26120	527132	13231	12889	267025	260107
	Idah	0	0	0	0	0	0
	Ibaji	60179	1208741	30390	29789	610406	598335
Enugu	Uzo-Uwani	459	5051	230	229	2533	2518
		92733	1984377	46867	45866	1002859	981518

APPENDIX XX: ELEMENTS AT RISK

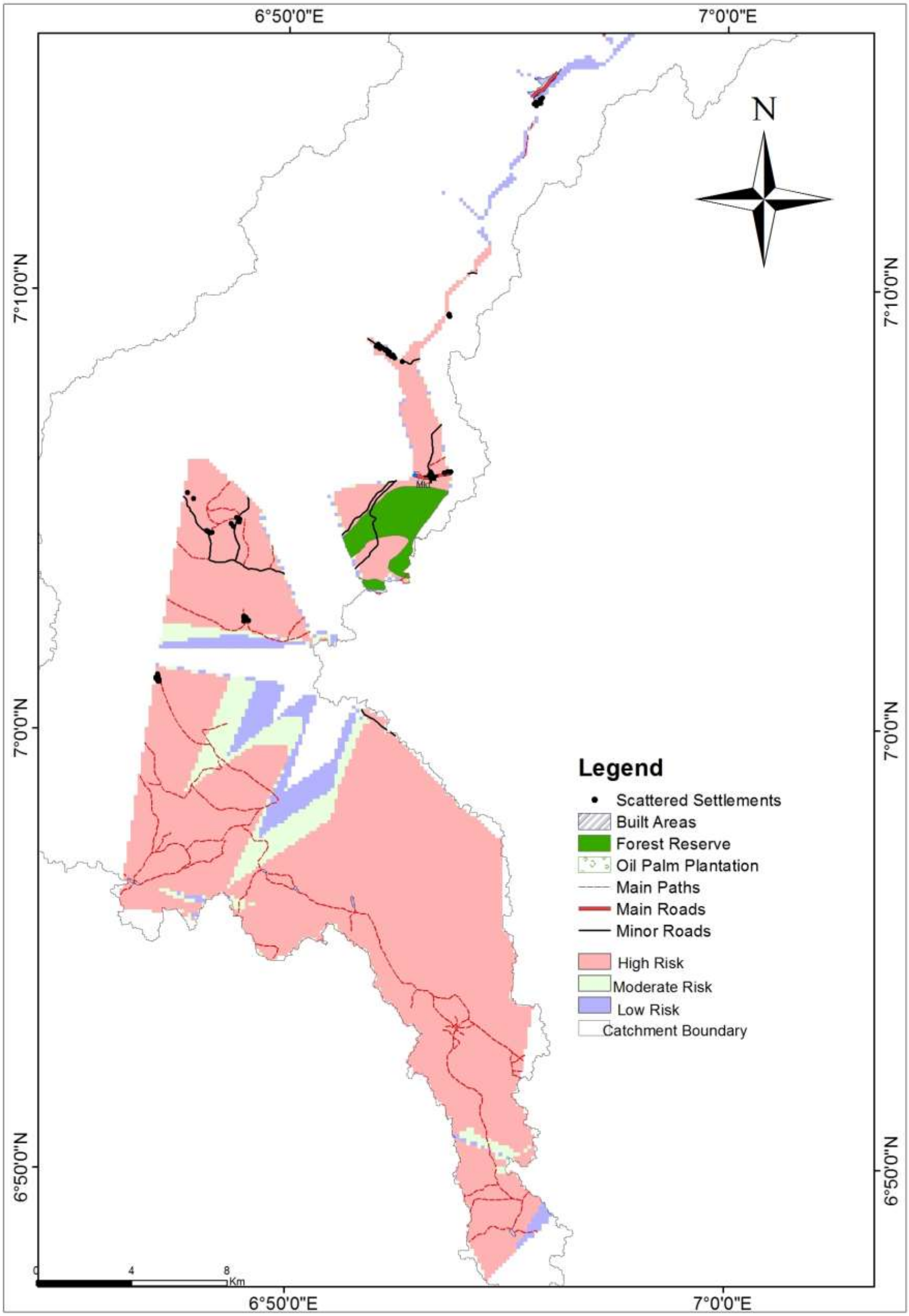


Fig. XXa: Elements at Risk of the 1995 Flood

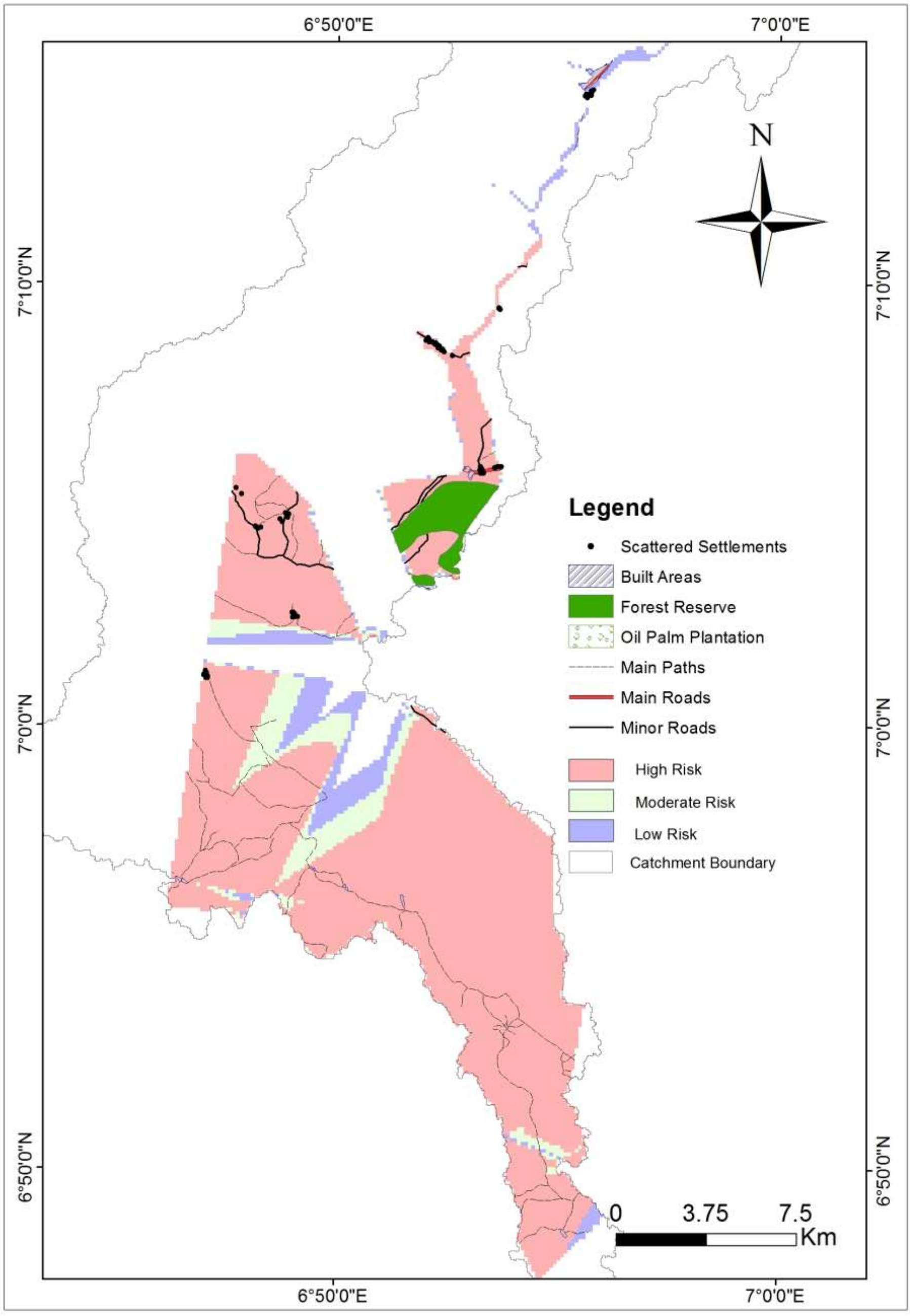


Fig. XXb: Elements at Risk of the 2000 Flood

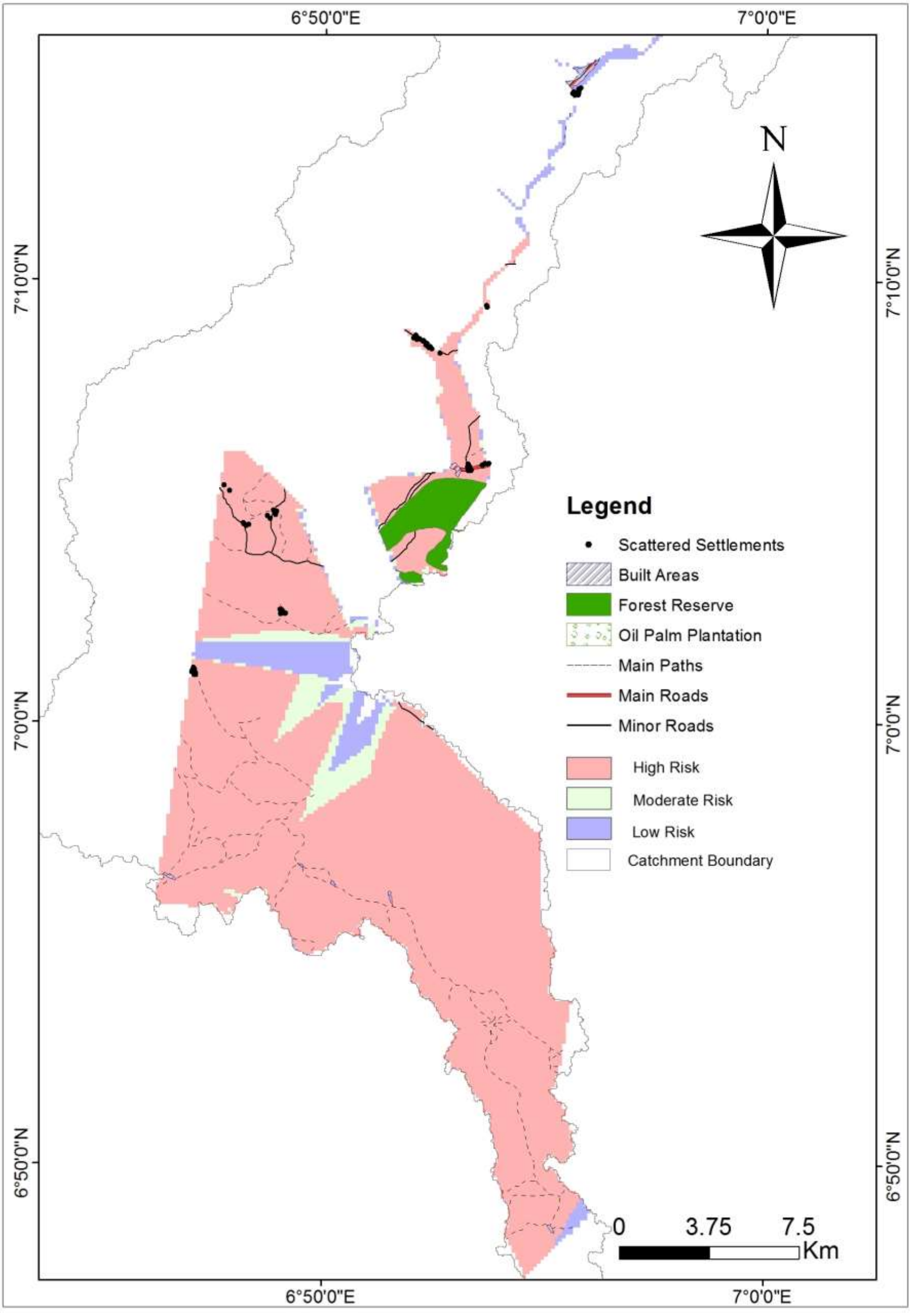


Fig. XXc: Elements at Risk of the 100-Year Flood

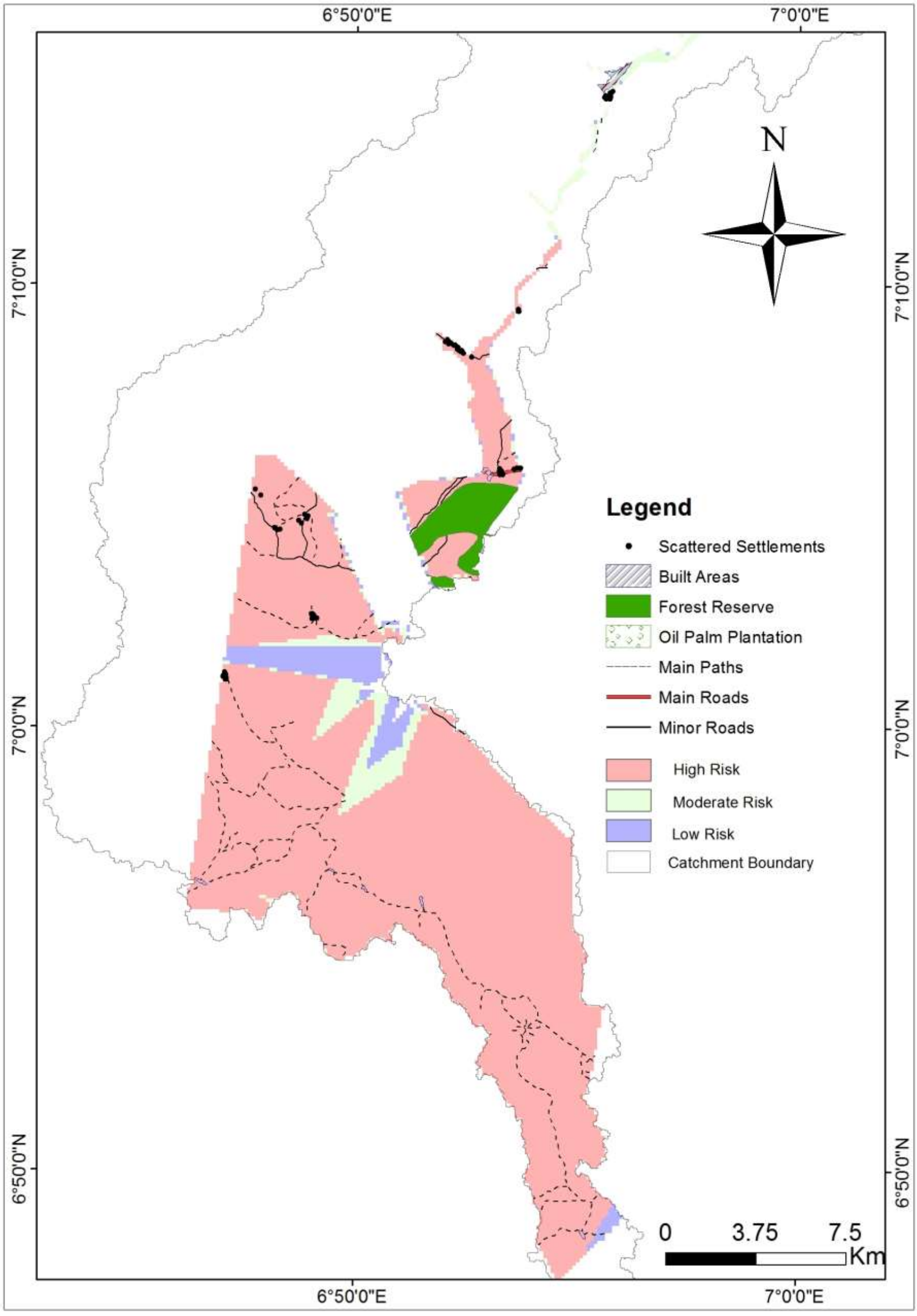


Fig. XXd: Elements at Risk of the 200-Year Flood